

SYNTHESIS AND CHARACTERIZATION OF NOVEL Pincer Ligands and
Triarylaminium Oxidants

A Dissertation

by

JILLIAN JORDAN DAVIDSON

Submitted to the Office of Graduate and Professional Studies of
Texas A&M University
in partial fulfillment of the requirements for the degree of

DOCTOR OF PHILOSOPHY

Chair of Committee,	Oleg V. Ozerov
Committee Members,	John A. Gladysz
	François Gabbai
	Mahmoud El-Halwagi
Head of Department,	David Russell

December 2014

Major Subject: Chemistry

Copyright 2014 Jillian Jordan Davidson

ABSTRACT

Diarylamido-based tridentate pincer ligands have become an important archetype in transition-metal chemistry and their reactivity has been widely explored. The diarylamido backbone offers rigidity and can be easily tuned to change the steric and electronic properties of the ligand. Motivated by previous successes, efforts were made to expand the scope of pincer ligands developed within the Ozerov group, which historically have been limited to C_{2v} symmetric ligands bearing either two phosphine donor arms or two imine donor arms. New ligands synthesized for this purpose include C_s symmetric ligands PNP and PNN ligands.

In an effort to categorize pincer ligands commonly employed in the Ozerov group we set out to compare the redox properties of the ligands and their donor ability towards a metal center. This was a two part endeavor where we (a) obtained cyclic voltammograms for (pincer)MCl compounds of Group 10 metals and (b) measured the IR stretching frequencies of (pincer)RhCO compounds. Our underlying assumptions were that the cyclic voltammograms report on how easy it is to oxidize the ligand (approximates the electron-richness of the ligand) and that the IR stretching frequencies give insight into the “electron-richness” of the metal center (a reflection on the basicity of the pincer ligand). The results of this study suggest that changes to the ligand framework directly affect the level of conjugation and in turn affect the redox potentials and the $\nu(\text{CO})$ values in a nearly linear fashion. The more electron-rich a ligand is, (due to direct conjugation from donor substituents on the diarylamido-backbone and from the

influence of the donor arms) the more readily it is oxidized and the stronger donor it becomes.

Chemical oxidations have become a rising field of interest. Triarylamminium oxidants are advantageous since they boast modest oxidation potentials and generate chemically neutral amines upon reduction. Our goal was to expand the scope of triarylamminium oxidants bearing non-coordinating carborane anions. A series of oxidizing triarylamminium radical cations were synthesized and isolated as $[\text{NAr}_3]^+[\text{CRB}_{11}\text{Cl}_{11}]^-$ salts (R = H, CH₃). These salts were prepared by treatment of a neutral amine, Me₃SiX (X = OTf, Cl), and Na[CRB₁₁Cl₁₁] (R = H, CH₃) with half an equivalent of PhI(OAc)₂.

DEDICATION

To my parents.

Thank you for giving me a stellar education and a strong work ethic. I may have hated the process, but it definitely paid off.

ACKNOWLEDGEMENTS

First, I would like to thank my advisor, Dr. Oleg Ozerov, who has always kept a fire lit under my feet and whose patience with me showed no bounds. I would like to thank you for your time, consideration, and dedication to my development as a chemist and as a writer.

Secondly, I would like to thank my parents. Although I get most of the credit for this dissertation, you also deserve some. Your support, love, and criticism have been critical in ensuring my success. In addition, from a very early age you taught me perseverance and the definition of hard-work. Without these values it is unlikely that I would be typing this acknowledgements page today. Lastly, from the bottom of my heart I want to thank you for stressing education and ensuring I had a stellar one. I can't imagine the sacrifices you both had to make along the way to do so.

Next I would like to thank my co-workers and friends in the department. Graduate school would have been miserable without your support and friendship. Thank god the bars are within walking distance! I would especially like to thank Dr. David Herbert, Dr. Yanjun Zhu, and Chun-I Lee. You were each great friends and coworkers. In addition, I would like to thank Dr. Amanda Pitts, Dr. Lisa Perez, and the Laboratory for Molecular Simulation.

Dr. Samuel Timpa, you get your own paragraph since you have been my pillar the last five years. I have no idea why you put up with me, but I am so glad you have. Maybe someday you will change your mind about baby Ping.

I would also like to acknowledge my committee members, Dr. John A. Gladysz, Dr. François Gabbai, and Dr. Mahmoud El-Halwagi. Thank you for your continued support throughout the past few years.

NOMENCLATURE

AGUI	Ampac Graphical User Interface
BArF ₂₄	tetrakis(3,5-bis(trifluoromethyl)phenyl)borate
CH ₂ Cl ₂	dichloromethane
CV	cyclic voltammetry
DCM	dichloromethane
DFT	density functional theory
DMF	<i>N,N</i> -dimethylformamide
ECP	effective core potential
Et ₂ O	diethyl ether
EPR	electron paramagnetic resonance
Fc	ferrocene
Fc ⁺	ferrocenium
h	hour
HOMO	highest occupied molecular orbital
IR	infrared
MALDI	matrix assisted laser desorption/ionization
min	minutes
NaOCMe ₂ Et	sodium <i>tert</i> -pentoxide
NBS	<i>N</i> -bromosuccinimide
NMR	nuclear magnetic resonance
LUMO	lowest occupied molecular orbital

Redox	oxidation-reduction
SET	single electron transfer
SDD	Stuttgart/Dresden triple- ζ quality basis set
SOMO	singly occupied molecular orbital
THF	tetrahydrofuran
UV	ultraviolet
vt	virtual triplet
WCA	weakly coordinating anion

TABLE OF CONTENTS

	Page
ABSTRACT	ii
DEDICATION	iv
ACKNOWLEDGEMENTS	v
NOMENCLATURE	vii
TABLE OF CONTENTS	ix
LIST OF FIGURES	xiii
LIST OF TABLES	xxiii
LIST OF SCHEMES	xxiv
CHAPTER I INTRODUCTION AND LITERATURE REVIEW	1
1.1 Background and Significance of Pincer Ligands	1
1.2 Development of π -Accepting Pincer Ligands	5
1.3 Non-innocent Ligands	7
1.3.1 Brønsted Acid-base non-innocent ligands	10
1.3.2 Redox non-innocent ligands	11
1.4 Weakly Coordinating Anions	18
1.5 Triarylamminium Radical Cations	20
1.6 Synthesis of Triarylamminium Radical Cations Paired with Carborane Anions	22
1.7 Overview of the Work Presented in this Dissertation	24
CHAPTER II SYNTHESIS, CHARACTERIZATION, AND APPLICATION OF TRIARYLAMMINIUM OXIDANTS	25
2.1 Introduction	25
2.2 Triarylamine Synthesis	26
2.3 Synthesis of Electron-Poor Triarylamines	32
2.4 Cyclic Voltammetry	34

	Page
2.5 Synthesis of Aminium Salts	35
2.6 Stoichiometric Reactions with the Aminium Salts.	41
2.6.1 Stoichiometric reaction of aminium with hexamethylbenzene	41
2.6.2 Reaction of hexamethylbenzene with Na[CHB ₁₁ Cl ₁₁], Me ₃ SiX reagents, and PhI(OAc) ₂	43
2.6.3 DFT investigation of the hexamethylbenzene radical cation	44
2.6.4 Reactions with Au(I) salts	47
2.7 Conclusion.....	49
2.8 Experimental.	50
2.8.1 General experimental considerations.	50
2.8.2 Computation methodology	51
2.8.3 Synthesis of 2-5 and 2-6.....	52
2.8.4 Synthesis and characterization of triaryl amines.....	53
2.8.5 Reactions with tris(4-bromophenyl)amine	71
2.8.6 Coupling reactions targeting diaryl amines and the synthesis of 2-16.....	73
2.8.7 Unsuccessful coupling reactions targeting triaryl amines	75
2.8.8 Synthesis of oxidant salts.	76
2.8.9 Reactions with hexamethylbenzene.	80
2.8.10 Reactions with Au	83
2.8.11 X-Ray data collection, solution, and refinement for 2-31[CHB ₁₁ Cl ₁₁].....	85
 CHAPTER III COMPARISON OF ELECTRONIC PROPERTIES OF DIARYLAMIDO-BASED PN _X Pincer Ligands: Redox Activity at THE Ligand and Donor Ability Towards the Metal.....	86
3.1 Introduction	86
3.2 Ligand Synthesis and Characterization	89
3.2.1 Synthesis of C _{2v} symmetric PNP ligands.	89
3.2.2 Synthesis of C _s symmetric PNP and PNN ligands	91
3.3.3 NMR characterization of the pincer ligands.....	93
3.3 Synthesis of Group 10 Pincer Complexes.....	94
3.4 Synthesis of (Pincer)RhCO Complexes	98
3.5 Characterization of RhCO and Pd Pincer Complexes.....	99
3.6 Structural Analysis of Neutral Pincer Complexes in the Solid State	103
3.7 Solid-State Structure of 3-5NiCl and its Radical Cation [3-5NiCl][CHB ₁₁ Cl ₁₁]	105
3.8 Analysis of the Electronic Properties	107
3.8.1 Investigation into the redox properties of group 10 metals.....	107
3.8.2 Basicity trends	109
3.8.3 Relationship between $\nu(\text{CO})$ values for (pincer)RhCO complexes and E _{1/2} values for (pincer)PdCl complexes.....	111

	Page
3.9 Analysis of 3-4PdCl and its Radical Cations [3-4PdCl][CHB ₁₁ Cl ₁₁] and [3-4PdCl][CHB ₁₁ Cl ₁₁] ₂	114
3.9.1 Solid-state structures of 3-4PdCl and its radical cation [3-4PdCl][CHB ₁₁ Cl ₁₁].....	114
3.9.2 Towards the synthesis and characterization of [3-4PdCl][CHB ₁₁ Cl ₁₁] ₂	117
3.9.3 DFT Analysis of the oxidation products of 3-4PdCl.....	117
3.10 Conclusion.....	121
3.11 Experimental.	122
3.11.1 General considerations.	122
3.11.2 Computation methodology	124
3.11.3 Synthesis of 3-1H and its metal complexes.....	125
3.11.4 Synthesis of complexes of 3-2H.....	128
3.11.5 Metal complexes of 3-3H.....	133
3.11.6 Synthesis of 3-4Me and its complexes	134
3.11.7 Synthesis of complexes of 3-5Me.	150
3.11.8 Synthesis of 3-F.....	151
3.11.9 Synthesis of 3-6H and its complexes.	153
3.11.10 Synthesis of 3-G	163
3.11.11 Synthesis of 3-7H and its complexes	165
3.11.12 Synthesis of 3-9H and its complexes	183
3.11.13 Synthesis of 3-10H and its complexes	190
3.11.14 Synthesis of 3-11H and its complexes	199
3.11.15 X-Ray data collection, solution, and refinement.....	208
 CHAPTER IV PALLADIUM COMPLEXES OF A NEW PHOSPHINE-AMIDO-SILOXIDE PINCER LIGAND WITH VARIABLE DEGREES OF PROTONATION	 219
4.1 Introduction.....	219
4.2 Results and Discussion.....	222
4.2.1 Synthesis and characterization of 4-5.....	222
4.2.2 Synthesis of Pd complexes of 4-5	223
4.2.3 Solid state structures of 4-8 and 4-13	228
4.3 Conclusion.....	231
4.4 Experimental Section.	231
4.4.1 General considerations.	231
4.4.2 Synthesis of 4-1 and 4-5.....	232
4.4.3 Synthesis of palladium complexes of 4-5.....	235
4.4.4 X-Ray data collection, solution and refinement.....	253
 CHAPTER V CONCLUSION	 257

	Page
REFERENCES	260
APPENDIX A	272
APPENDIX B	281
APPENDIX C	286

LIST OF FIGURES

	Page
Figure 1.1 (Top) General representation of a pincer ligand where M = metal center and X, E = donor atoms. (Bottom) Potential modification sites (Z, E, X, R, Y) in two generic pincer ligands.	2
Figure 1.2 Metal complexes bearing neutral, monoanionic, and trianionic pincer ligand motifs.	4
Figure 1.3 Electron-poor pincer ligands.	6
Figure 1.4 Generic complexes of Brønsted acid-base non-innocent ligands. Cooperative ligand sites where protonation can occur are highlighted in red.	10
Figure 1.5 Select weakly coordinating anions.	18
Figure 2.1 Triarylamines 2-1-2-6 and their $E_{1/2}$ potentials referenced vs Fc/Fc ⁺ in dichloromethane.	28
Figure 2.2 Selected orbital depictions of the hexamethylbenzene radical cation. C(Ar)–C(Ar) bond lengths for hexamethylbenzene and hexamethylbenzene radical cation are also shown.	46
Figure 2.3 POV-Ray ¹⁰³ rendition of the ORTEP ¹⁰⁴ drawing (50% probability ellipsoids) of 2-31[CHB ₁₁ Cl ₁₁]. Hydrogen atoms have been omitted for clarity. More data for this structure can be found in Appendix C.	49
Figure 2.4 ¹ H NMR spectrum of 2-6 (CDCl ₃ , 500 MHz). Trace quantities of silicone grease are observed.	53
Figure 2.5 ¹ H NMR spectrum (C ₆ D ₆ , 500 MHz) of 2-7. Water is observed in the NMR spectrum.	54
Figure 2.6 ¹ H NMR spectrum of 2-20 (C ₆ D ₆ , 500 MHz). Trace amounts of water, dichloroethane, and toluene are observed.	56
Figure 2.7 ¹ H NMR spectrum of 2-9 (C ₆ D ₆ , 500 MHz). Trace quantities of hexanes and water are observed.	57
Figure 2.8 ¹ H NMR spectrum of 2-22 (C ₆ D ₆ , 500 MHz). The sample is contaminated with water and grease. These can be successfully removed via sublimation.	59

	Page
Figure 2.9 ^1H NMR spectrum (C_6D_6 , 500 MHz) of 2-8. Trace quantities of water and hexanes are observed in addition to biphenyl (< 5% impurity).	60
Figure 2.10 ^1H NMR spectrum of 2-25 (C_6D_6 , 500 MHz) with greater than 97% purity. Trace quantities of hexanes are observed. Silicone grease is also observed in the spectrum.	62
Figure 2.11 ^1H NMR spectrum (C_6D_6 , 500 MHz) of 2-21 with greater than 97% purity. Trace quantities of silicone grease, diethyl ether, and hexanes are observed.	64
Figure 2.12 ^1H NMR spectrum of 2-11 (C_6D_6 , 500 MHz). Trace quantities of diphenylamine, water and silicone grease are observed.	65
Figure 2.13 ^1H NMR spectrum (C_6D_6 , 500 MHz) of 2-26. Acetone, water, silicone grease, and dichloromethane are observed.	66
Figure 2.14 ^1H NMR spectrum of 2-24 (C_6D_6 , 500 MHz). Trace quantities of water and silicone grease are observed.	68
Figure 2.15 ^1H NMR spectrum of 2-10 (C_6D_6 , 500 MHz). Minor quantities of hexanes, silicone grease, and water are observed.	69
Figure 2.16 ^1H NMR spectrum of 2-23 (C_6D_6 , 500 MHz). Dichloromethane and trace quantities of hexanes are observed.	71
Figure 2.17 ^1H NMR spectrum of 2-16 (C_6D_6 , 95% pure, 500 MHz). Trace quantities of 3,5-trifluoromethylphenylamine are observed. In addition silicone grease and trace quantities of hexanes are observed.	74
Figure 2.18 ^1H NMR analysis of the reaction of 2-24[$\text{CHB}_{11}\text{Cl}_{11}$] with ferrocene in the presence of C_6F_6 in C_6D_6 (500 MHz). The spectrum is contaminated with silicone grease, diethyl ether, hexanes and dichloromethane.	79
Figure 2.19 ^1H NMR (CD_2Cl_2 , 500 MHz) of 2-31[$\text{CHB}_{11}\text{Cl}_{11}$] (<95%). Trace quantities of pentane, diethyl ether and 2-31[Cl] are observed.	84
Figure 3.1 Redox active pincer ligands denoted by their three donor atoms and showing the charge of the closed-shell form.	88
Figure 3.2 Generic complexes of pincer ligands under study in this work.	89

Figure 3.3 POV-Ray renditions ¹⁰³ of the ORTEP drawings ¹⁰⁴ (50% probability ellipsoids) of 3-8PdOAc, 3-8PdCl, 3-7PdCl, 3-11RhCO, and 3-6RhCO. Hydrogen atoms are omitted for clarity. Top left: 3-8PdOAc. Top center: 3-8PdCl·CH ₂ Cl ₂ (A molecule of dichloromethane was observed in the asymmetric unit cell and has been removed.) Top right: 3-7PdCl. Bottom left: 3-11RhCO. Bottom right: 3-6RhCO.	102
Figure 3.4 ORTEP drawing ¹⁰⁴ (50% probability ellipsoids) of 3-5NiCl and [3-5NiCl][CHB ₁₁ Cl ₁₁] showing selected atom labeling. Hydrogen atoms are omitted for clarity. Selected bond distances (Å) and angles (deg) are reported in Table 3.4.	106
Figure 3.5 $\nu(\text{CO})$ Values (cm ⁻¹) for a series of (pincer)RhCO Complexes.	111
Figure 3.6 A plot of $\nu(\text{CO})$ values (cm ⁻¹) in (pincer)RhCO vs E _{1/2} values (V) for (pincer)PdCl complexes. The scan rate was 100 mV/s in the positive direction.	113
Figure 3.7. POV-Ray renditions of ORTEP ¹⁰⁴ drawings (50% probability ellipsoids) of 3-4PdCl (left) and [3-4PdCl][CHB ₁₁ Cl ₁₁] (right). Hydrogen atoms in all structures and cocrystallized toluene in the structure of 3-4PdCl are omitted for clarity. For the structures of 3-4PdCl and [3-4PdCl][CHB ₁₁ Cl ₁₁], only one of the two independent molecules or cation/anion pairs is shown.	116
Figure 3.8 HOMO and HOMO-1 of 3-4PdCl.	118
Figure 3.9 Selected orbital pictures for [3-4PdCl][CHB ₁₁ Cl ₁₁].	119
Figure 3.10 HOMO and LUMO orbitals of doubly oxidized 3-4PdCl in the singlet form.	121
Figure 3.11 ¹ H NMR spectrum of 3-1H (C ₆ D ₆ , 500 MHz).	126
Figure 3.12 ¹ H NMR spectrum of 3-1PdCl (500 MHz, C ₆ D ₆). Trace quantities of diethyl ether, pentane and dichloromethane are observed.	128
Figure 3.13 ¹ H NMR spectrum of 3-2PdOAc (500 MHz, C ₆ D ₆). Impurities include dichloromethane, pentane and diethyl ether.	129

	Page
Figure 3.14 ^1H NMR spectrum of 3-2PdOTf (C_6D_6 , 500 MHz). Pentane and diethyl ether are observed in the spectrum	131
Figure 3.15 ^1H NMR spectrum of 2-RhCO (500 MHz, C_6D_6). Less than 2% of free ligand is observed in the spectrum.....	133
Figure 3.16 ^1H NMR spectrum of 3-B (500 MHz, C_6D_6). Trace quantities of dichloromethane are observed.	135
Figure 3.17 ^1H NMR spectrum of 3-C (500 MHz, C_6D_6). Silicone grease was observed in the NMR solvent.	136
Figure 3.18 ^1H NMR spectrum of 3-D (500 MHz, C_6D_6). Trace quantities of hexane and silicone grease are observed.	138
Figure 3.19 ^1H NMR spectrum of 3-4Me (500 MHz, C_6D_6). Trace quantities of pentane and diethyl ether are observed.....	140
Figure 3.20 ^1H NMR spectrum of 3-4H (500 MHz, C_6D_6). Trace quantities of pentane are observed.....	142
Figure 3.21 ^1H NMR spectrum of 3-4PdCl (500 MHz, C_6D_6). Trace quantities of pentane and toluene are observed.	144
Figure 3.22 ^1H NMR spectrum of 3-4PdOAc (500 MHz, C_6D_6). Acetic acid is observed.	146
Figure 3.23 ^1H NMR spectrum of 3-4Rh(CH_3)Cl (500 MHz, C_6D_6). Trace quantities of pentane, toluene, and diethyl ether are observed.	148
Figure 3.24 ^1H NMR spectrum of 3-4RhCO (500 MHz, C_6D_6). Trace quantities of diethyl ether and pentane are observed.....	149
Figure 3.25 ^1H Spectrum of 3-5NiCl (500 MHz, C_6D_6).	151
Figure 3.26 ^1H NMR spectrum of 3-F (500 MHz, C_6D_6). Trace quantities of dichloromethane, pentane and diethyl ether are observed.....	153
Figure 3.27 ^1H NMR spectrum of 3-6H (500 MHz, C_6D_6). Residual toluene and water are observed.	155
Figure 3.28 ^1H NMR spectrum of 3-6PdCl (500 MHz, C_6D_6). Trace amounts of hexanes and silicone grease are observed.....	157

Figure 3.29 ^1H NMR spectrum of 3-6PdOAc (500 MHz, CDCl_3). Residual toluene and trace amounts of silicone grease are observed.	159
Figure 3.30 ^1H NMR spectrum of 3-6RhCO (500 MHz, C_6D_6). Trace amounts of dichloromethane, and cyclooctadiene. Silicone grease is also present.	161
Figure 3.31 ^1H NMR spectrum of 3-6PtCl (500 MHz, C_6D_6). Dichloromethane, pentane, 2,6-lutidine, silicone grease, and diethyl ether are observed in the NMR solvent.	163
Figure 3.32 ^1H NMR spectrum of 3-G as observed in C_6D_6 . Trace quantities of diethyl ether and water are observed.	165
Figure 3.33 ^1H NMR spectrum of 3-7H (500 MHz, C_6D_6).	167
Figure 3.34 ^1H NMR spectrum of 3-7PdOAc (500 MHz, C_6D_6). Trace quantities of dichloromethane and pentane are observed.	169
Figure 3.35 ^1H NMR spectrum of 3-7PdCl (500 MHz, CDCl_3). Trace quantities of diethyl ether, silicone grease, and pentane are observed.	171
Figure 3.36 ^1H NMR spectrum of 3-7RhCO (500 MHz, C_6D_6). Trace quantities of diethyl ether, dichloromethane, and pentane are observed along with some residual silicone grease.	173
Figure 3.37 ^1H NMR spectrum of 3-8H (500 MHz, C_6D_6). Trace quantities of silicone grease are observed.	175
Figure 3.38 ^1H NMR spectrum of 3-8PdOAc (500 MHz, C_6D_6). Residual solvent impurities are observed that include dichloromethane, pentane, toluene, silicone grease, and diethyl ether.	177
Figure 3.39 ^1H NMR spectrum of 3-8PdCl (500 MHz, C_6D_6). Residual silicone grease is observed.	179
Figure 3.40 ^1H NMR spectrum of 3-8PdOTf (toluene- d_8 , 500 MHz).	180
Figure 3.41 ^1H NMR spectrum of 3-8RhCO (500 MHz, C_6D_6). Trace quantities of dichloromethane, silicone grease, and pentane are observed in the spectrum.	182
Figure 3.42 ^1H NMR spectrum of 3-H (500 MHz, C_6D_6). Trace quantities of diethyl ether, silicone grease, and pentane are observed.	184

	Page
Figure 3.43 ^1H NMR spectrum of 3-9H (500 MHz, C_6D_6). Trace quantities of diethyl ether are observed.....	186
Figure 3.44 ^1H NMR spectrum of 3-9RhCO (500 MHz, C_6D_6). Trace quantities of diethyl ether and pentane are observed.....	188
Figure 3.45 ^1H NMR spectrum of 3-10H (500 MHz, C_6D_6). Trace quantities of diethyl ether, 3-9H, silicone grease, and pentane are observed.....	191
Figure 3.46 ^1H NMR spectrum 3-10RhCO (500 MHz, C_6D_6). Trace quantities of pentane, 2,6-lutidine and diethyl ether are observed. Silicone grease is also observed.	193
Figure 3.47 ^1H NMR spectrum of 3-10Rh(Me)(I)(OAc) (C_6D_6 , 500 MHz). Trace quantities of dichloromethane and diethyl ether are observed.	195
Figure 3.48 ^1H NMR spectrum of 3-10PdCl (500 MHz, C_6D_6). Residual diethyl ether, silicone grease, HOCH_2CF_3 and pentane are observed.	197
Figure 3.49 ^1H NMR spectrum of 3-11H (500 MHz, $(\text{CF}_3)_2\text{CHOH}$, was “referenced” by first running a pure sample of C_6D_6). Four equivalents of dimethylamine are observed along with diethyl ether. The ligand was never isolated cleanly.	200
Figure 3.50 ^1H NMR spectrum of 3-11PdOAc \cdot $(\text{CF}_3)_2\text{CHOH}$ (500 MHz, C_6D_6). Trace quantities of pentane and silicone grease are observed.	202
Figure 3.51 ^1H NMR spectrum of 3-11PdCl as observed (500 MHz, C_6D_6). Trace quantities of pentane and silicone grease are observed.	204
Figure 3.52 ^1H NMR spectrum (C_6D_6 , 500 MHz) of 3-11PdOTf. Trace amounts of silicone grease are observed.	206
Figure 3.53 ^1H NMR spectrum of 3-11RhCO (500 MHz, C_6D_6). Minor impurities of diethyl ether, 2,6-lutidine and pentane are observed.....	208
Figure 4.1 Representation of various PNP, PNN, NNN, SNS, and ONO pincer complexes.	220
Figure 4.2 POV-Ray renditions ¹⁰³ of the ORTEP drawings ¹⁰⁴ of complexes 4-8 (left) and 4-13 (right) (50% thermal ellipsoids). Select hydrogen atoms are omitted for clarity.	230

	Page
Figure 4.3 ¹ H NMR spectrum of 4-5 (500 MHz, C ₆ D ₆). Minor quantities of pentane and diethyl ether are observed.....	235
Figure 4.4 ¹ H NMR spectrum of 4-6 (C ₆ D ₆ , 500 MHz). The product was observed in situ and therefore residual 1,2-pentadione and diethyl ether are observed.....	237
Figure 4.5 ¹ H NMR spectrum of 4-7 (CD ₂ Cl ₂ , 500 MHz). Trace quantities of pentane are observed.....	239
Figure 4.6 ¹ H NMR spectrum (C ₆ D ₆ , 500 MHz) of 4-8. Trace impurities of diethyl ether and dichloromethane are observed.	241
Figure 4.7 ¹ H NMR spectrum of 4-9 (C ₆ D ₆ , 500 MHz). Trace quantities of diethyl ether, isooctane, and dichloromethane are observed.	243
Figure 4.8 ¹ H NMR spectrum (CD ₂ Cl ₂ , 500 MHz) of 4-11. Minor quantities of pentane and diethyl ether are observed.....	247
Figure 4.9 ¹ H NMR spectrum of 4-12 (C ₆ D ₆ , 500 MHz). Residual trimethylsilyl trifluoromethanesulfonate, pentane and grease are observed.....	249
Figure 4.10 ¹ H NMR spectrum of 4-13 (CD ₂ Cl ₂ , 500 MHz). Trace quantities of diethyl ether and acetic acid observed. NOTE: the solubility of this compound in C ₆ D ₆ and CDCl ₃ is minimal.	251
Figure 4.11 ¹ H NMR (C ₆ D ₆ , 500 MHz) of 4-14. Trace quantities of diethyl ether, dichloromethane, pentane and trimethylphosphine are observed.....	253
Figure A-1 Cyclic voltammogram of 3-1PdCl in CH ₂ Cl ₂ at 27 °C. The scan rate was 100 mV/s in the positive direction. The cyclic voltammogram was obtained with 0.3 M [Bu ₄ N][PF ₆] as the supporting electrolyte and resulted in a measured potential (E _{1/2}) equal to -0.05 V.	272
Figure A-2 Cyclic voltammogram of 3-10PdCl in CH ₂ Cl ₂ at 27 °C. The scan rate was 100 mV/s in the positive direction. The cyclic voltammogram was obtained with 0.3 M [Bu ₄ N][PF ₆] as the supporting electrolyte and resulted in a measured potential (E _{1/2}) equal to 0.13 V.....	273
Figure A-3 Cyclic voltammogram of 3-5NiCl in CH ₂ Cl ₂ at 27 °C. The scan rate was 100 mV/s in the positive direction. The cyclic voltammogram was obtained with 0.3 M [Bu ₄ N][PF ₆] as the supporting electrolyte and resulted in a measured potential (E _{1/2}) equal to -0.01 V.	273

- Figure A-4 Cyclic voltammogram of 3-5PdCl in CH₂Cl₂ at 27 °C. The scan rate was 100 mV/s in the positive direction. The cyclic voltammogram was obtained with 0.3 M [Bu₄N][PF₆] as the supporting electrolyte and resulted in a measured potential (E_{1/2}) equal to 0.11 V.....274
- Figure A-5 Cyclic voltammogram of 3-5PtCl in CH₂Cl₂ at 27 °C. The scan rate was 100 mV/s in the positive direction. The cyclic voltammogram was obtained with 0.3 M [Bu₄N][PF₆] as the supporting electrolyte and resulted in a measured potential (E_{1/2}) equal to 0.09 V.....274
- Figure A-6 Cyclic voltammogram of 3-6PdCl in CH₂Cl₂ at 27 °C. The scan rate was 100 mV/s in the positive direction. The cyclic voltammogram was obtained with 0.3 M [Bu₄N][PF₆] as the supporting electrolyte and resulted in a measured potential (E_{1/2}) equal to -0.02 V.275
- Figure A-7 Cyclic voltammogram of 3-6PtCl in CH₂Cl₂ at 27 °C. The scan rate was 100 mV/s in the positive direction. The cyclic voltammogram was obtained with 0.3 M [Bu₄N][PF₆] as the supporting electrolyte and resulted in a measured potential (E_{1/2}) equal to -0.05 V.275
- Figure A-8 Cyclic voltammogram of 3-3NiCl in CH₂Cl₂ at 27 °C. The scan rate was 100 mV/s in the positive direction. The cyclic voltammogram was obtained with 0.3 M [Bu₄N][PF₆] as the supporting electrolyte and resulted in a measured potential (E_{1/2}) equal to -0.19 V.276
- Figure A-9 Cyclic voltammogram of 3-3PdCl in CH₂Cl₂ at 27 °C. The scan rate was 100 mV/s in the positive direction. The cyclic voltammogram was obtained with 0.3 M [Bu₄N][PF₆] as the supporting electrolyte and resulted in a measured potential (E_{1/2}) equal to -0.07 V.276
- Figure A-10 Cyclic voltammogram of 3-3PtCl in CH₂Cl₂ at 27 °C. The scan rate was 100 mV/s in the positive direction. The cyclic voltammogram was obtained with 0.3 M [Bu₄N][PF₆] as the supporting electrolyte and resulted in a measured potential (E_{1/2}) equal to -0.11 V.277
- Figure A-11 Cyclic voltammogram of 3-7PdCl in CH₂Cl₂ at 27 °C. The scan rate was 100 mV/s in the positive direction. The cyclic voltammogram was obtained with 0.3 M [Bu₄N][PF₆] as the supporting electrolyte and resulted in a measured potential (E_{1/2}) equal to 0.09 V.....277

- Figure A-12 Cyclic voltammogram of 3-8PdCl in CH₂Cl₂ at 27 °C. The scan rate was 100 mV/s in the positive direction. The cyclic voltammogram was obtained with 0.3 M [Bu₄N][PF₆]₆ as the supporting electrolyte and resulted in a measured potential (E_{1/2}) equal to 0.04 V.....278
- Figure A-13 Cyclic voltammogram of 3-11PdCl in CH₂Cl₂ at 27 °C. The scan rate was 100 mV/s in the positive direction. The cyclic voltammogram was obtained with 0.3 M [Bu₄N][PF₆] as the supporting electrolyte and resulted in a measured potential (E_{1/2}) equal to 0.32 V.....278
- Figure A-14 Cyclic voltammogram of 3-6PdCl in CH₂Cl₂ at 27 °C. The scan rate was 100 mV/s in the positive direction. The cyclic voltammogram was obtained with 0.3 M [Bu₄N][PF₆] as the supporting electrolyte and resulted in a measured potential (E_{1/2}) equal to 0.04 V.....279
- Figure A-15 Cyclic voltammogram of 3-12PdCl in CH₂Cl₂ at 27 °C. The scan rate was 100 mV/s in the positive direction. The cyclic voltammogram was obtained with 0.3 M [Bu₄N][PF₆] as the supporting electrolyte and resulted in a measured potential (E_{1/2}) equal to 0.69 V.....279
- Figure A-16 Cyclic voltammogram of 3-4PdCl in CH₂Cl₂ at 27 °C. The scan rate was 100 mV/s in the positive direction. The cyclic voltammogram was obtained with 0.3 M [Bu₄N][PF₆] as the supporting electrolyte and resulted in a measured potential (E_{1/2}) equal to -0.24V and 0.82 V.....280
- Figure B.1 UV-Vis spectrum of 3-3NiCl. The spectrum was obtained using a 7.65 × 10⁻³ M sample of 3-3NiCl in dichloromethane. λ_{max} was determined to be 646 nm. This corresponds to an ε value of 297 cm⁻¹M⁻¹.281
- Figure B.2 UV-Vis spectrum of 3-10RhCO. The spectrum was obtained using a 2.48 × 10⁻³ M sample of 3-10RhCO in dichloromethane. λ_{max} was determined to be 513 nm. This corresponds to an ε value of 107 cm⁻¹M⁻¹. ...282
- Figure B.3 UV-Vis spectrum of 3-6PdOAc. The spectrum was obtained using a 2.17 × 10⁻³ M sample of 3-6PdOAc in dichloromethane. λ_{max} was determined to be 522 nm. This corresponds to an ε value of 1343 cm⁻¹M⁻¹282
- Figure B.4 UV-Vis spectrum of 3-2PdOAc. The spectrum was obtained using a 2.36 × 10⁻³ M sample of 3-2PdOAc in dichloromethane. λ_{max} was determined to be 547 nm. This corresponds to an ε value of 718 cm⁻¹M⁻¹. ...283

- Figure B.5 UV-Vis spectrum of 3-3PdCl. The spectrum was obtained using a 2.22×10^{-3} M sample of 3-3PdCl in dichloromethane. λ_{max} was determined to be 512 nm. This corresponds to an ϵ value of $1310 \text{ cm}^{-1}\text{M}^{-1}$283
- Figure B.6 UV-Vis spectrum of 3-10PdCl. The spectrum was obtained using a 1.51×10^{-3} M sample of 3-10PdCl in dichloromethane. λ_{max} was determined to be 447 and 522 nm. These values correspond to ϵ values of 1205 and $1150 \text{ cm}^{-1}\text{M}^{-1}$ respectively.284
- Figure B.7 UV-Vis spectrum of 3-5PdCl. The spectrum was obtained using a 2.13×10^{-3} M sample of 3-5PdCl in dichloromethane. λ_{max} was determined to be 506 nm. This corresponds to an ϵ value of $977 \text{ cm}^{-1}\text{M}^{-1}$284
- Figure B.8 UV-Vis spectrum of 3-7PdCl. The spectrum was obtained using a 4.26×10^{-4} M sample of 3-7PdCl in dichloromethane. λ_{max} was determined to be 429 and 537 nm. These correspond to ϵ values of 429 and $537 \text{ cm}^{-1}\text{M}^{-1}$ respectively.285
- Figure B.9 UV-Vis spectrum of 3-5PtCl. The spectrum was obtained using a 3.36×10^{-4} M sample of 3-5PtCl in dichloromethane. λ_{max} was determined to be 375 and 460 nm. These values correspond to ϵ value of 3492 and $4473 \text{ cm}^{-1}\text{M}^{-1}$ respectively.285

LIST OF TABLES

	Page
Table 2.1 Buchwald-Hartwig coupling to generate triarylamines.	30
Table 2.2 Reactions to produce secondary amines.....	31
Table 2.3 $E_{1/2}$ (V) vs Fc/Fc^+ values.	35
Table 3.1 NMR data for PNP and PNN pincer ligands in C_6D_6	94
Table 3.2 NMR features of (pincer)RhCO and (pincer)PdX complexes.	101
Table 3.3 Comparison of the metric parameters associated with group 10 pincer complexes.	104
Table 3.4 Selected bond lengths of 3-5NiCl and $[3-5NiCl][CHB_{11}Cl_{11}]$	106
Table 3.5 $E_{1/2}$ (V) for (pincer)MCl complexes.	108
Table 3.6 $\nu(CO)$ values (cm^{-1}) in (pincer)RhCO vs $E_{1/2}$ values (V) for (pincer)PdCl complexes.	114
Table 3.7 Selected bond distances (\AA) and angles ($^\circ$) from the solid-state X-ray studies of 3-4PdCl and $[3-4PdCl][CHB_{11}Cl_{11}]$	116
Table 3.8 Computed metric parameters associated with 3-4PdCl and $[3-4PdCl][CHB_{11}Cl_{11}]$	120
Table 4.1 Crystallographic Data for 4-8 and 4-13.	230
Table B.1 Tabulated data regarding UV-Vis spectra of various pincer metal complexes. Each experiment was run in dichloromethane. Individual concentrations of each sample are given as well as the absorbance value at λ_{max}	281

LIST OF SCHEMES

	Page
Scheme 1.1 Binding modes of a dithiolene ligand.....	8
Scheme 1.2 Ligands which act as spectators (top) compared to ligands which act in a non-innocent fashion (middle and bottom).....	9
Scheme 1.3 Activation of water by a (PNN)Ru(II) complex.....	11
Scheme 1.4 Redox-switch oxidation of dihydrogen.	13
Scheme 1.5 [2+2] cycloaddition of 1,5-hexadiene via oxidation and reduction of a 2,6-dimininepyridine ligand.	15
Scheme 1.6 “Oxidative addition” at a Zr(IV) d ⁰ metal center.	17
Scheme 1.7 Oxidation of the [NNN] ³⁻ backbone by two electrons to generate the Zirconium-imido complex with a [NNN] ¹⁻ ligand.....	17
Scheme 1.8 Synthesis of fullerenium cations.....	22
Scheme 1.9 Synthesis of aminium carborane salts.	23
Scheme 2.1 Reactions of triarylaminines with an excess of Br ₂	33
Scheme 2.2 Synthesis of 2-25, 2-26, and 2-27 with NBS.	34
Scheme 2.3 Generation of a triarylaminium radical cation.....	36
Scheme 2.4 Synthesis and reactivity of 2-27[CHB ₁₁ Cl ₁₁].	38
Scheme 2.5 Synthesis of 2-21[CHB ₁₁ Cl ₁₁].	39
Scheme 2.6 Synthesis of 2-24[CRB ₁₁ Cl ₁₁].	40
Scheme 2.7 Proposed synthetic route to aminium salts using SO ₂ Cl ₂ as an oxidant.	41
Scheme 2.8 Synthesis of 2-31[CHB ₁₁ Cl ₁₁].	48
Scheme 3.1 Synthetic routes to C _{2v} symmetric ligands.	91
Scheme 3.2 Synthetic routes to C _s symmetric pincer ligands.....	92
Scheme 3.3 N-H cleavage by Pd(II).....	96

	Page
Scheme 3.4 N–Me cleavage.....	97
Scheme 3.5 Synthetic route to (pincer)RhCO complexes.....	99
Scheme 4.1 Indirect formation of a phosphine-amido-siloxide pincer complex.	221
Scheme 4.2 Synthesis of 4-5.	223
Scheme 4.3 Reaction of 4-5 with common Pd(II) precursors.	224
Scheme 4.4 Reaction of 4-8 with Me ₃ SiX reagents.	226
Scheme 4.5 Formation of Pd(II) complexes with dianionic pincer ligands.	228

CHAPTER I

INTRODUCTION AND LITERATURE REVIEW

1.1 Background and Significance of Pincer Ligands

The ability to control the steric and electronic properties of a metal center by a well-defined ligand system is of great importance with respect to stability, reactivity, and catalysis. Pincer ligands, tridentate ligands that bind to a metal center in a meridional fashion, are one of the most well defined ligand sets. Since their introduction by Shaw in the 1970's,¹ pincer ligands have become popular tools for organometallic synthesis due to the extreme stability of their transition metal complexes and relative ease with which modular variations can be imparted while preserving the overall binding mode. Pincer ligands have demonstrated versatile reactivity in a number of different applications including catalysis² and in the development of material science as sensors and switches.³

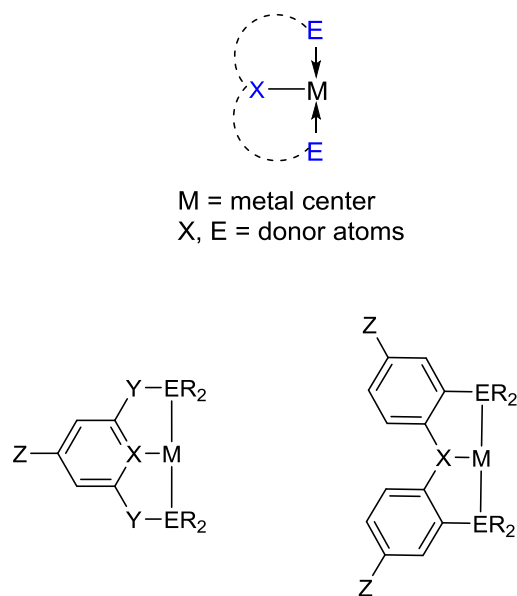
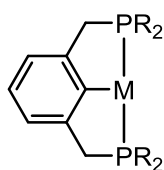


Figure 1.1 (Top) General representation of a pincer ligand where M = metal center and X, E = donor atoms. (Bottom) Potential modification sites (Z, E, X, R, Y) in two generic pincer ligands.

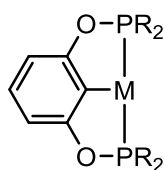
Pincer ligands are commonly categorized by the nature of their donor atoms and are given the general abbreviations EXE (side arm donors, E; central donor, X) (Figure 1.1). Pincer ligands are frequently derived from pyridine, aryl, or diarylamido skeletons.^{2a} Modification of various parameters associated with these backbones allows for a refined adjustment of the electronic and steric properties of a metal center. Two generic depictions of these bonding motifs are shown in Figure 1.1. The sites denoted X, E, Z, R and Y represent locations at which modifications can be readily achieved. The facility with which different functionalities can be incorporated onto the pincer framework has resulted in the production of a large number of ligands with varying

electronic and steric properties. Monoanionic pincer ligands with a central anionic (X-type) donor flanked by two neutral (L-type) donors are by far the most common type in the literature and are found with a great variety of LXL combinations (Figure 1.2).^{2a,2g,3-4} Representative examples of monoanionic pincer ligands include Shaw's PCP ligand (Figure 1.2 **A**),¹ PCP ligands based on resorcinol (Figure 1.2 **B**),^{1,5} diarylamido-based PNP ligands (Figure 1.2 **C**),⁶ Fryzuk's PNP ligand (Figure 1.2 **D**),^{4a} and aryl amine NCN ligands (Figure 1.2 **E**).⁷ Neutral (LLL-type) pincer ligands have also been reported. These ligands are commonly based on a pyridine⁸ (Figure 1.2 **F**) or carbene⁹ backbone (Figure 1.3 **G**). Recently trianionic pincer ligands have also emerged. These include the two diarylamino-based $[\text{NNN}]^{3-}$ and $[\text{ONO}]^{3-}$ ligands reported by Heyduk (Figure 1.2 **H** and **I**),^{10,11} the aryl $[\text{NCN}]^{3-}$ ligand (Figure 1.2 **J**) published by Veige,¹² and Bercaw's $[\text{OCO}]^{3-}$ ligand (Figure 1.2 **H**).¹³ It is also noteworthy to mention that there are prominent ligand frameworks in the literature that could be viewed as falling under the definition of a pincer ligand, but are not commonly referred to as such. Representative examples include pybox (pybox = bis(oxazolinyl)pyridine), which catalyzes asymmetric Negishi cross-coupling reactions¹⁴ and ligands based on a terpyridine scaffold such as the tpy' ligand (tpy' = 4,4',4''-tri-*tert*-butylterpyridine).¹⁵

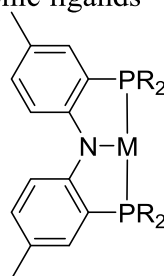
Metal complexes with monoanionic ligands



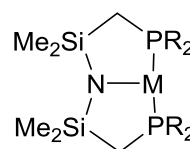
A PCP
Shaw



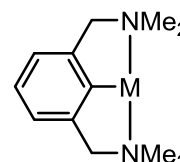
B POCOP
Morales-Morales



C PNP
Ozerov

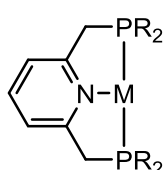


D PNP
Fryzuk

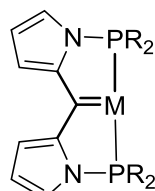


E NCN
Herdtweck

Metal complexes with neutral ligands

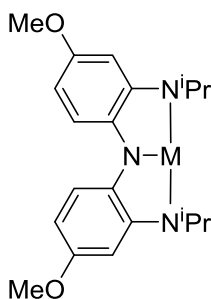


F PNP
Milstein

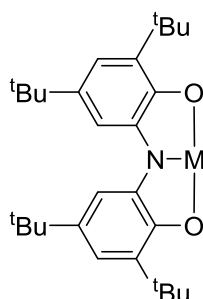


G PCP
Ozerov

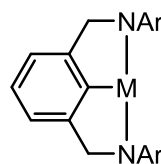
Metal complexes with trianionic ligands



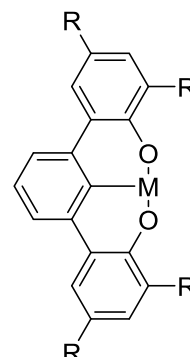
H [NNN]³⁻
Heyduk



I [ONO]³⁻
Heyduk



J [NCN]³⁻
Veige



K [OCO]³⁻
Bercaw

Figure 1.2 Metal complexes bearing neutral, monoanionic, and trianionic pincer ligand motifs.

1.2 Development of π -Accepting Pincer Ligands

Traditionally, pincer ligands have been prepared through incorporation of donating substituents such as aryl (Ph) or alkyl donors (ⁱPr, ^tBu) on the phosphines. In an endeavor to further tune electronic parameters, the phosphines of pincer ligands have recently been substituted with less electron-donating substituents such as OR,¹⁶ C₆F₅, CF₃, and pyrrolyl groups.¹⁷ The π -acceptor character of these phosphines decrease in the following order: P(fluoroalkyl)₃ > P(pyrrolyl)₃ \approx P(C₆F₅)₃ > P(OPh)₃.¹⁸ These systems are of interest because back donation from the metal to the phosphine will effectively decrease the electron density at the metal center. In order to monitor the effect of these (and other) modifications, it is common to prepare (pincer)RhCO compounds and analyze the CO stretching frequency by infrared spectroscopy.¹⁸⁻¹⁹ The electron density at Rh can be correlated to the donating ability of each ligand and the extent of backbonding to the CO. It is expected that more electron-donating ligands will promote backbonding into the CO π^* orbital ultimately weakening the CO bond and resulting in a decrease in the $\nu(\text{CO})$.²⁰ Figure 1.3 demonstrates that less electron donating groups on the phosphines result in less basic ligands.^{1,21}

In 2005, the syntheses of perfluoroaryl (Figure 1.3 **A**) and pyrrolyl-substituted (Figure 1.3 **B**) PCP ligands were reported by van Koten and Milstein.^{17a,17d} Shortly thereafter, Roddick and co-workers published the synthesis and characterization of a CF₃ substituted PCP (Figure 1.3 **C**) ligand.^{17b} More recently, our group dedicated a considerable amount of effort towards the synthesis of a PNP ligand with pyrrolyl substituted phosphines (Figure 1.3 **D**).^{17c} Of additional relevance are the perfluoroaryl

POCOP (Figure 1.3 E) and POCCP (Figure 1.3 F) ligands reported in 2014 by Spencer.²² Although no catalytic reactivity with these ligands has been reported, the electron-poor nature of their corresponding pincer complexes gives them the potential to be quite useful in organometallic transformations.

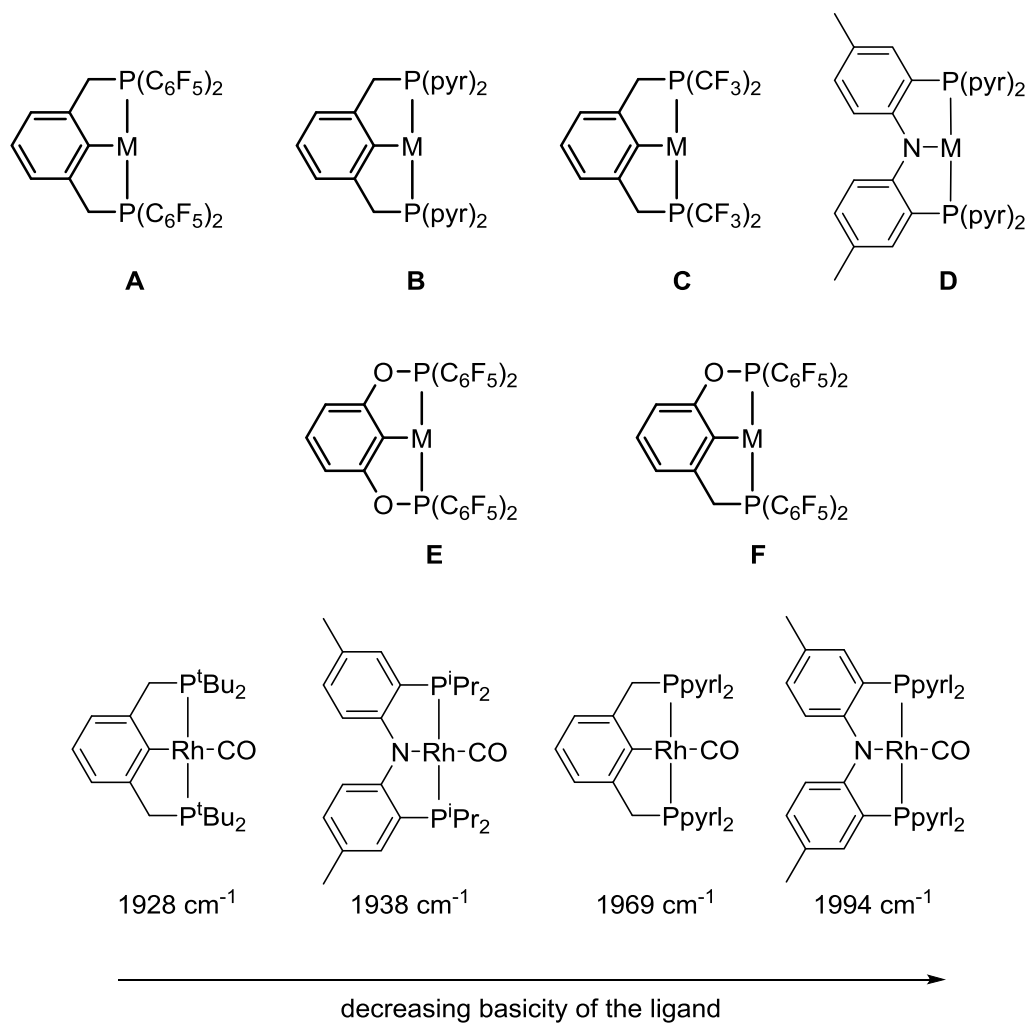
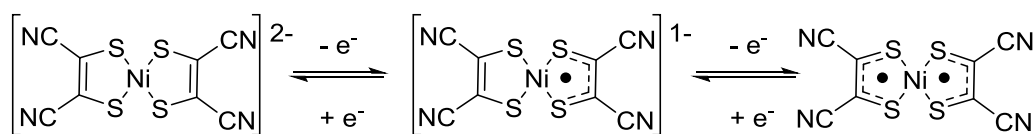


Figure 1.3 Electron-poor pincer ligands.

1.3 Non-innocent Ligands

The reactivity of a metal complex as a whole is derived from the interactions between the metal center and its surrounding ligands. In classical organometallic transformations bond cleavage or formation steps take place at the metal center, with the ancillary ligands acting solely as bystanders. These processes do not result in changes to the connectivity, charge, or composition of the ancillary ligands. Recently, a new approach to organometallic synthesis has emerged in which a ligand remains bound to the metal center, but is directly involved in elementary organometallic transformations. These ligands are often referred to as non-innocent. The term “non-innocent” was first coined in 1966 by Jørgensen in order to define the oxidation state ambiguity of redox-active molecules. According to this early definition ligands are “innocent when they allow oxidation states of the central atoms to be defined.”²³ In contrast, non-innocent ligands provide a certain amount of ambiguity and often times make it difficult to define the oxidation state of a metal. An early example where the term non-innocent was applied is in the case of bis(maleonitriledithiolate)Ni complexes which possess three possible binding modes as seen in Scheme 1.1.²⁴ Through EPR and X-ray diffraction studies these systems were eventually determined to exist as Ni(II) complexes bearing two ligand radical anions.²⁴

Scheme 1.1 Binding modes of a dithiolene ligand.

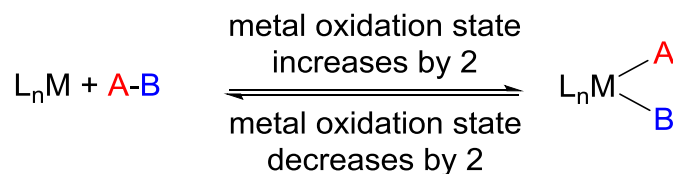


Since the 1960s new technologies and advances in computation chemistry have emerged which make assignment of redox events to the metal or the ligand less arbitrary.²⁵ In light of these advancements, over the past five decades the study of non-innocent ligands has moved from investigations into electronic structure, to a diverse field of chemistry in which reactions depend on the non-innocent character to the ligand. Non-innocent ligands have found application in catalysis, group-transfer chemistry, energy storage, and in biological applications.²⁶ As a result, Jørgensen's definition of non-innocence has expanded to define ligands which undergo chemical changes during the course of a reaction. These ligands assist the metal center in carrying out desired transformations, most commonly by accepting or losing protons²⁷ or electrons. Three different routes to cleave a bond by a transition metal complex are illustrated in Scheme 1.2. In the first reaction an example of classical oxidative addition and reductive elimination is shown. In oxidative addition the A–B bond of a substrate is cleaved at the metal center resulting in formation of a M–A bond and a M–B bond and an increase in the metal's oxidation state by 2. In the second reaction A–B bond cleavage is facilitated by a complex bearing a redox non-innocent ligand. In this case the metal's oxidation state is unchanged and the ligand is oxidized. In the final reaction H–B bond cleavage is

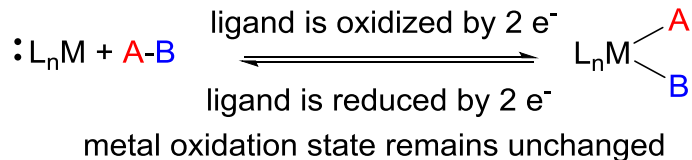
mediated by a complex bearing a Brønsted acid-base non-innocent ligand. In this case the ligand is directly involved in the activation step through protonation of the ligand backbone.

Scheme 1.2 Ligands which act as spectators (top) compared to ligands which act in a non-innocent fashion (middle and bottom).

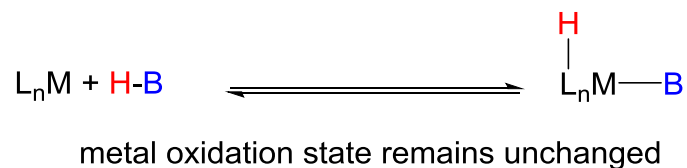
Oxidative Addition (ligand is a spectator)



Redox Non-Innocence



Brønsted Acid-Base Non-innocence



1.3.1 Brønsted Acid-base non-innocent ligands

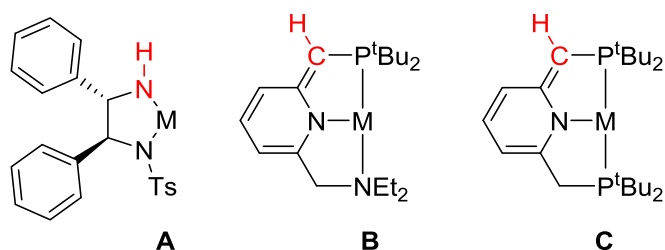
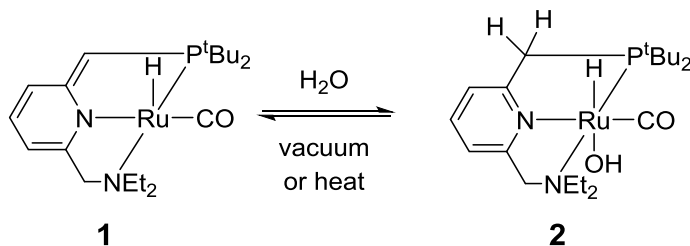


Figure 1.4 Generic complexes of Brønsted acid-base non-innocent ligands. Cooperative ligand sites where protonation can occur are highlighted in red.

Brønsted acid-base non-innocent ligands are those which undergo reversible protonation in order to activate a substrate and facilitate product formation.²⁸ Examples of some generic complexes that undergo Brønsted acid-base reactions that have been reported in the literature are given in Figure 1.4.^{2g,29} These complexes have shown versatility for a number of catalytic processes. For example Ru(II) complexes bearing chiral *N*-sulfonylated 1,2-diamide ligands (Figure 1.4 A) have been used for asymmetric transfer hydrogenation of ketones.³⁰ This process was mediated by reversible protonation/deprotonation of the amide.^{29,31} The Milstein group commonly employs pyridine-based PNP and PNN ligands which undergo deprotonation at the sp³-C of the pincer, resulting in dearomatization of the pyridine backbone (B and C Figure 1.4). The dearomatized complexes have demonstrated a proclivity for activating N–H,³² sp² and sp³ C–H,³³ and O–H bonds.^{2g,34} To demonstrate the reactivity of these complexes an overview of the activation of a water molecule by a (PNN)Ru(II) complex is outlined in

Scheme 1.3. Treatment of a non-aromatic (PNN)Ru(II) complex (Scheme 1.3 **1**) with one equivalent of water led to ligand aromatization in conjunction with formation of a *trans* hydrido-hydroxo complex (Scheme 1.3 **2**). Presumably this complex was formed by coordination of the water molecule in an L-type fashion to Ru, followed by proton migration to the olefinic bond of the sidearm. Further studies on this system revealed that it promoted thermal H₂ and light-induced O₂ evolution in the presence of an excess of water.³⁵ In addition to water oxidation the non-aromatic (PNN)Ru(II) complex (Scheme 1.2 **1**) also catalyzes the coupling of alcohols to form esters^{28c} and the dehydrogenative coupling of alcohols with amines to produce amides.³⁶

Scheme 1.3 Activation of water by a (PNN)Ru(II) complex.



1.3.2 Redox non-innocent ligands

Redox non-innocent ligands, also commonly referred to as redox active ligands, can undergo oxidation or reduction events.³⁷ As a result redox non-innocent ligands can access two or more charge states when bound to a metal. Common redox non-innocent ligands include dithiolates,³⁸ semiquinones,^{10a,39} amido phenolates,⁴⁰ diimines,⁴¹ terpyridines,⁴² and bis(amino)pyridines.^{37a} These ligands have the potential to redefine

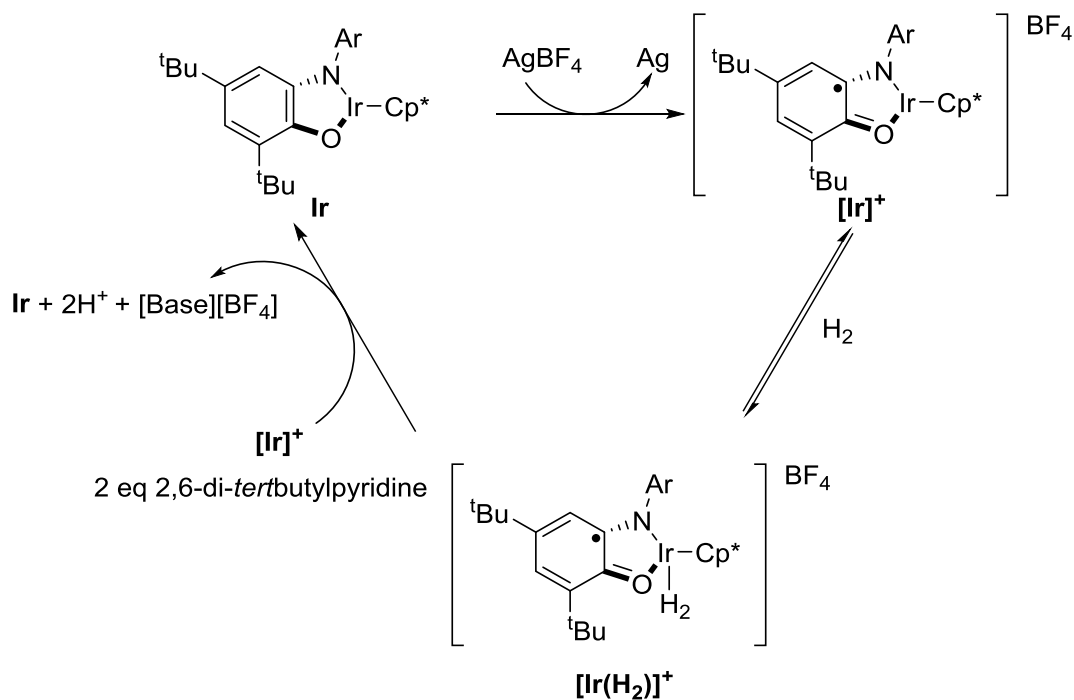
many of the ways we accomplish reactions since they provide a site for redox events to take place other than the metal center and can also serve as electron or hole reservoirs.^{26,37a} There are three general ways to exploit redox non-innocent ligand complexes to promote bond activation and formation: 1) The first strategy involves oxidation or reduction of the ligand in order to tune the electronics at the metal center. 2) The second strategy is to use the ligand as an electron or hole reservoir. This allows the metal to store electrons on the ligand during transformations which generate electron density at the metal center and to abstract electrons from the ligand when a step results in a deficiency of electron density at the metal. 3) The third application of redox non-innocent ligand complexes involves generation of ligand-centered radicals which can actively participate in chemical transformations. In this case the ligand is directly involved in the cleavage and formation of chemical bonds. These three applications have been discussed extensively in a review by de Bruin.²⁵

1.3.2.1 Redox-active ligands which are used to tune the electronic properties of a metal center.

The electronic properties of a metal center are vital in controlling reactivity and selectivity. Traditionally the electronic properties of a metal center are modified by changing the electron-donating or withdrawing ability of its ligand set. A second way to modify the electronics is to oxidize or reduce the ligand backbone using an external reagent. This allows for the modification the electronics of a metal complex without producing large steric changes or affecting the original oxidation state of the metal

center. The oxidation of dihydrogen using the redox switch behavior of a 3,5-di-*tert*-butylamidophenolate ligand exemplifies this technique (Scheme 1.4).^{40a,40b} Oxidation of **Ir** (Scheme 1.4) with AgBF₄ resulted in the formation of **[Ir]⁺**, which is characterized by a ligand centered radical. **[Ir]⁺** is sufficiently Lewis acidic enough to allow coordination of a molecule of dihydrogen to yield **[Ir(H₂)⁺**. (Dihydrogen does not coordinate to the reduced species). In the presence of a base, such as 2,6-di-*tert*-butylpyridine, **[Ir(H₂)⁺** activated dihydrogen resulting in the production of two protons and two electrons, which were ultimately taken up by the ligand to reform the neutral **Ir** species.

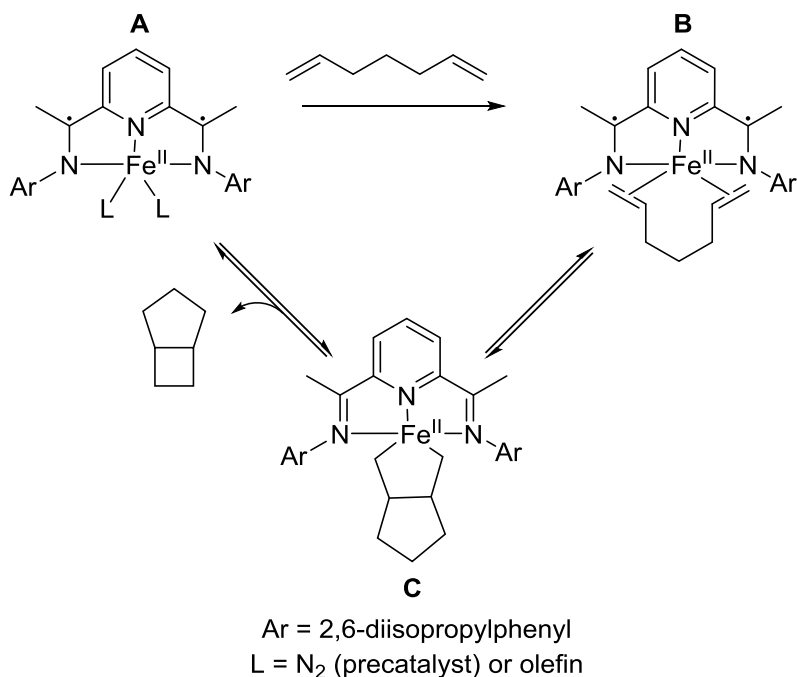
Scheme 1.4 Redox-switch oxidation of dihydrogen.



1.3.3.2 Ligands which act as electron reservoirs.

From an organometallic chemist's perspective complexes of precious metals such as rhodium, iridium, palladium, and platinum are by far the most active and versatile catalysts.^{19b,43} The high cost of these metals; however, has inspired researchers to try and access alternative catalysts employing earth abundant and inexpensive metals such as iron and copper.^{25-26,41a,44} One of the challenges associated with this quest is earth-abundant base metals commonly undergo one electron redox processes.²⁶ This presents a problem since many important organometallic transformations, such as oxidative addition and reductive elimination, are based on a two electron redox process. Redox non-innocent ligands are seen as a promising tool in enabling two-electron reactivity in the 3d metal series.²⁶ A prominent example of this approach is Fe complexes of the redox non-innocent 2,6-diiminepyridine ligand,^{41a} which catalyze ethylene polymerization,⁴⁵ [2+2] cycloadditions,⁴⁶ enyne cyclizations,⁴⁷ hydrogenation of olefins, alkynes and aryl azides,^{46a,48} and hydrosilylation.⁴⁹ In each of these catalytic reactions the ligand acts as an electron reservoir and the iron metal center maintains an oxidation state of +2. For instance, in the [2+2]-cycloaddition of 1,5-hexadiene the 2,6-diiminepyridine ligand framework served as a reservoir for two electrons eliminating the necessity of accessing Fe(IV) (Scheme 1.5).⁵⁰ In this process coordination of the diene resulted in displacement of dinitrogen from complex **A** and formation of **B**. Oxidative cyclization then resulted in formation of **C** with concurrent oxidation of the ligand backbone. Reductive elimination from **C** and reduction of the ligand backbone yielded the bicyclic product.

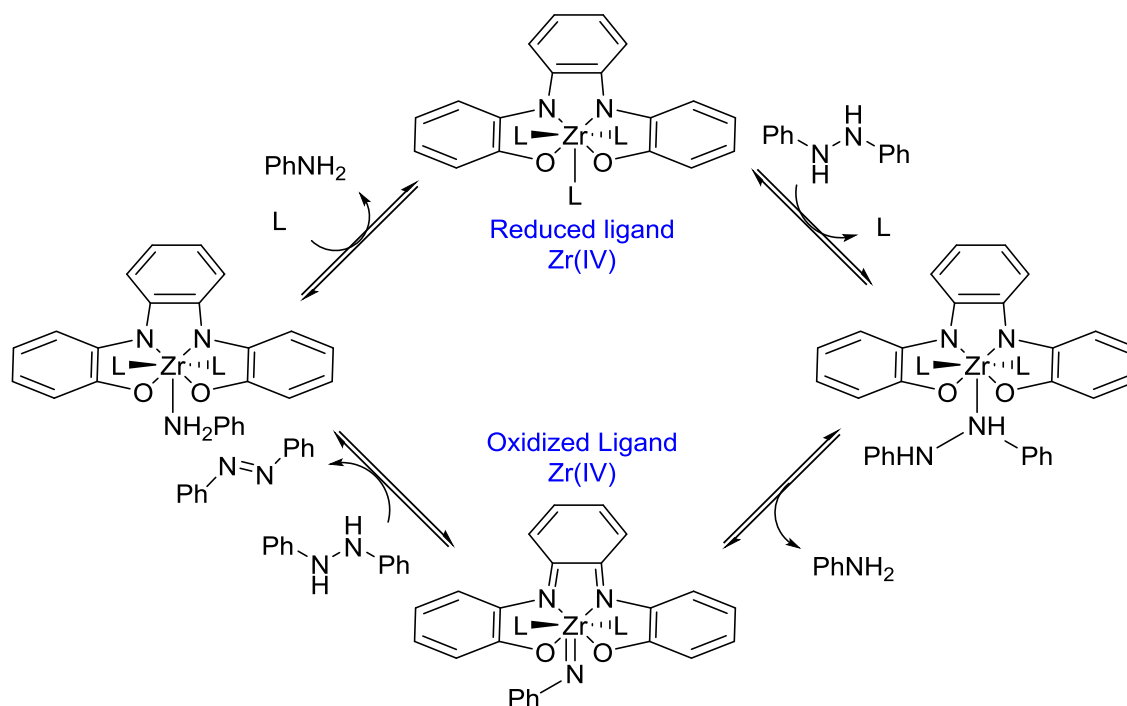
Scheme 1.5 [2+2] cycloaddition of 1,5-hexadiene via oxidation and reduction of a 2,6-diminepyridine ligand.



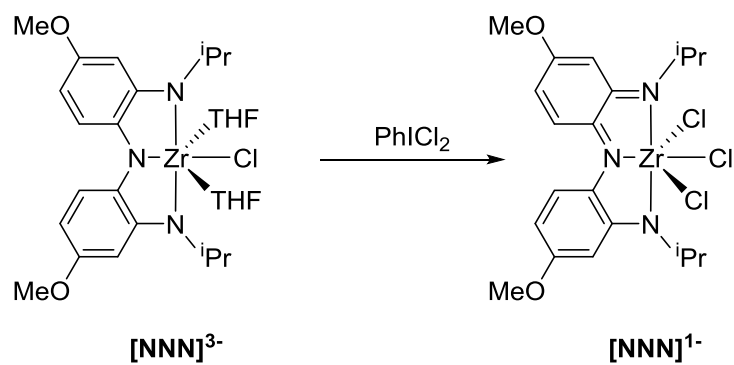
In the previous example catalytic activity was promoted by reduction of the 2,6-diiminepyridine backbone. Redox non-innocent ligands can also undergo oxidation. This approach has promise for application in early metal catalysis; by providing a foundation from which d^0 metals can undergo oxidative addition with an external substrate.^{10b} As in the previous example with iron, the electrons required for these transformations stem from the ligand backbone rather than the metal center. One example of this reactivity is the disproportionation of diphenyl hydrazine into aniline and azobenzene (Scheme 1.6).^{40c} This process was catalyzed by a Zr(IV) *ortho*-diimine complex by coordination of diphenyl hydrazine and elimination of aniline via oxidation of the ligand backbone by

two electrons. In the absence of a redox non-innocent ligand this step would not have been feasible since the Zr(IV) was a d^0 metal site. In the next step, the reaction with a second molecule of diphenyl hydrazine resulted in elimination of azobenzene and formation of the aniline adduct. This process occurred via reduction of the ligand back into the *ortho*-diamide species. Completion of the catalytic cycle was met by elimination of a second equivalent of aniline. Pincer ligands have also emerged as players in this chemistry. Heyduk *et al.* have developed the chemistry of redox non-innocent trianionic diarylamido-based $[\text{ONO}]^{3-}$ (Figure 1.3 **I**) and $[\text{NNN}]^{3-}$ (Figure 1.3 **H**) ligands. Early metal complexes of these pincer ligands facilitate oxidative addition⁵¹ (Scheme 1.7) and reductive elimination at non-redox active metal sites.⁵² In addition, catalysis which takes advantage of the redox properties of the $[\text{NNN}]^{3-}$ ligand have begun to emerge.^{10b}

Scheme 1.6 “Oxidative addition” at a Zr(IV) d^0 metal center.



Scheme 1.7 Oxidation of the $[\text{NNN}]^{3-}$ backbone by two electrons to generate the Zirconium-imido complex with a $[\text{NNN}]^{1-}$ ligand.



1.4 Weakly Coordinating Anions

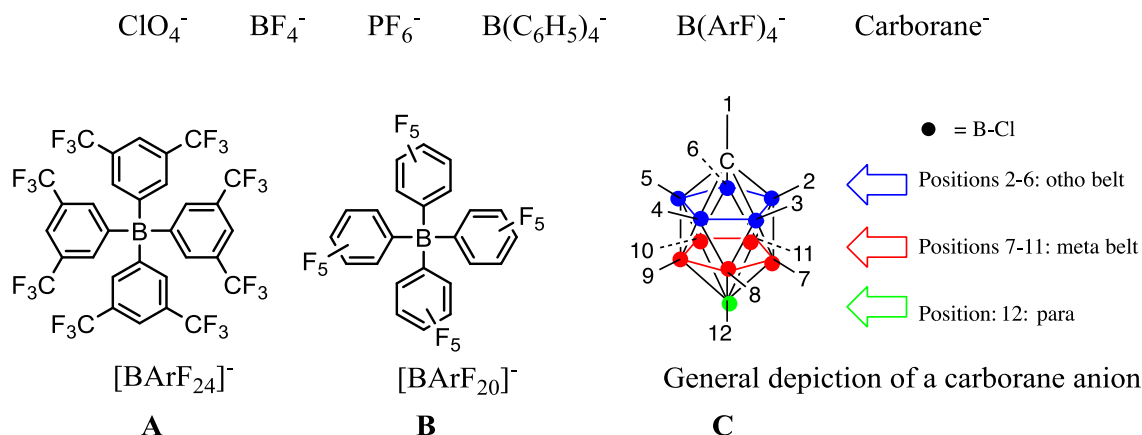


Figure 1.5 Select weakly coordinating anions.

While classical anions such as a ClO_4^- ,⁵³ OTf^- (SO_3CF_3^-),⁵⁴ BF_4^- ,⁵³ SbF_6^- ,⁵⁵ and PF_6^- ⁵⁵ were once considered “non-coordinating,” developments over the past four decades have disabused this notion.⁵⁵⁻⁵⁶ In light of this discovery, efforts were taken to synthesize new weakly coordinating anions (WCA), which are useful when attempting to observe, isolate or do chemistry with maximally “free” cations in solution or the solid state. Examples of some weakly coordinating anions are $[\text{Al}(\text{OR}^F)_4]^-$,⁵⁷ $[\text{Sb}(\text{OTeF}_5)_6]^-$,⁵⁸ $[\text{BArF}_{24}]^-$ (Figure 1.5 **A**),⁵⁹ $[\text{BArF}_{20}]^-$ (Figure 1.5 **B**),⁵⁹ and carborane derived anions (Figure 1.5 **C**).⁶⁰ The weakly coordinating ability of these anions is a result of delocalization of a negative charge over a large area of non-nucleophilic and chemically robust moieties. In addition to being weakly coordinating, other desirable characteristics

of weakly coordinating anions include low nucleophilicity, chemical inertness, and solubility in hydrocarbon solvents. As a result of these characteristics, weakly coordinating anions have many applications, including use as anions for olefin polymerization with cationic metallocenes,⁶¹ Li ion catalyzed Diels-Alder reactions,^{59b} electrolytes for Li-ion batteries,⁶² and supporting electrolytes for electrochemistry.⁶³

Carborane anions (Figure 1.5 C) exemplify the term weakly coordinating.⁶⁴ In addition, halogenated derivatives of the parent carborane $[\text{CHB}_{11}\text{H}_{11}]^-$ are some of the most chemically robust anions to date and have demonstrated an unsurpassed stability towards electrophiles and oxidizing agents.^{64a,65} Carborane salts of the free Brønsted acid,⁶⁶ silylium ion,^{65a} protonated benzene and toluene, and of oxidized fullerenium radical cations have been reported.^{60a,64b,66-67} One disadvantage of carborane anions is they have limited solubility in hydrocarbon solvents. Substitution of the icosahedral cage of the parent carborane, $[\text{CHB}_{11}\text{H}_{11}]^-$, is used to target more soluble anions. The parent carborane anion contains somewhat hydridic B–H bonds, which are susceptible towards electrophilic substitution. As a result modification of the cage is feasible and chlorinated,⁶⁸ fluorinated,⁶⁹ brominated,⁷⁰ iodinated,⁷¹ hydroxylated,⁷² methylated⁷³ and trifluoromethylated⁷⁴ analogs have also been reported. The C–H bond, on the other hand, is relatively acidic. Treatment of $[\text{CHB}_{11}\text{Cl}_{11}]^-$ with strong bases and subsequent reaction with electrophiles, such as alkyl halides, results in C-alkylation to form $[\text{CRB}_{11}\text{Cl}_{11}]^-$ derivatives.⁷⁵ C-alkylation allows for variable solubility. Longer alkyl chains for instance increase the solubility of the anions and their component salts.

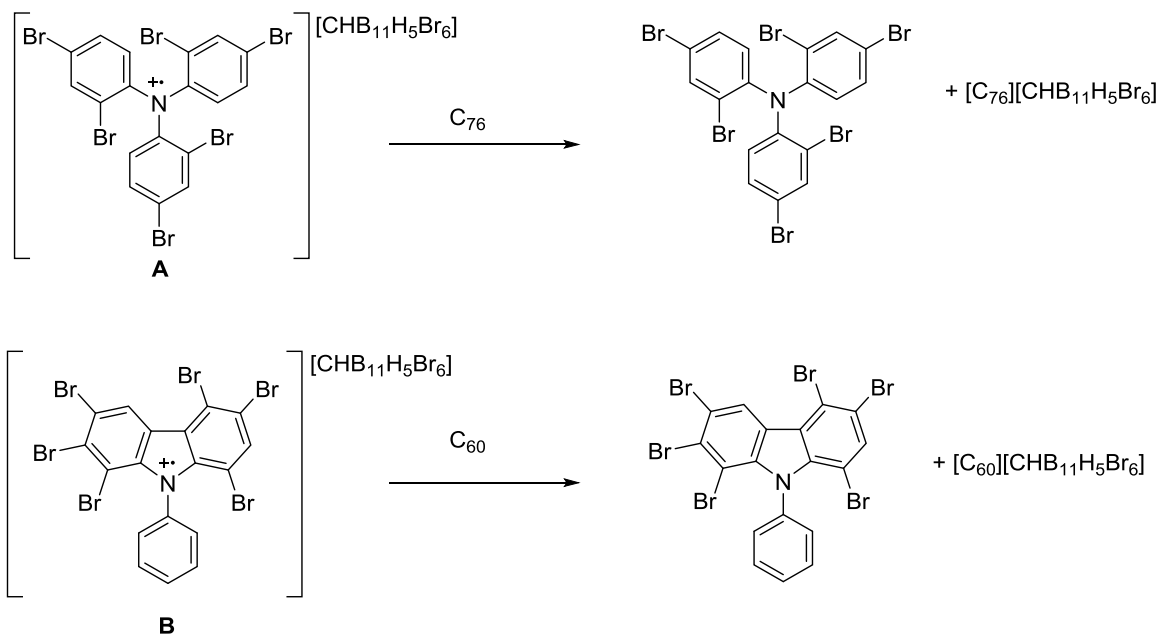
1.5 Triarylaminium Radical Cations

An oxidant is a substance that accepts electrons and is reduced in an oxidation-reduction reaction. Triarylaminium ($[\text{N}(\text{Ar})_3]^{+\cdot}$) radical cations are an important class of organic oxidants.⁷⁶ First reported in the 1950's as intermediates in the synthesis of N-methylgranatanine,⁷⁷ triarylaminium radical cations have become useful single electron transfer reagents and catalysts for a number of processes including oxidative cyclization of tertiary amines,⁷⁸ Diels-Alder reactions,⁷⁹ cyclopropanations,⁸⁰ and oxidation reactions.⁸¹ In addition, when paired with a weakly coordinating carborane anion, the reduction of a triarylaminium radical cation has resulted in the stabilization of some highly unusual and reactive cations. The success of the triarylaminium carborane salts is a result of two features, the weakly coordinating ability of the carborane anion and the low nucleophilicity of the amine by-product that forms upon reduction of the aminium radical cation. The Reed group has pioneered this chemistry with their investigation into the isolation of stable fullerenium salts.^{67b,67d} The challenge associated with isolating fullerenium salts was the deficiency of stable oxidant salts which had the oxidizing power to facilitate the desired transformations and additionally did not bear an anion which would react with the cation. For instance, treatment of C_{76} ($E_{1/2} = 0.81 \text{ V vs Fc/Fc}^+$) with [tris(2,4-dibromopheny)aminium][SbCl_6] resulted in oxidation of the fullerene. However, the lifetime of $[\text{C}_{76}^{+\cdot}][\text{SbCl}_6]$ in solution was limited to a number of hours.^{67b} The authors suggest that one explanation for the decomposition of $[\text{C}_{76}^{+\cdot}][\text{SbCl}_6]$ is chloride ion abstraction by C_{76}^+ . Isolation of the desired fullerenium radical cation was found to be feasible upon exchange of the $[\text{SbCl}_6]^-$ anion with the

more robust $[\text{CHB}_{11}\text{H}_5\text{Br}_6]^-$ anion. The authors attribute this success to the weaker nucleophilicity of $[\text{CHB}_{11}\text{H}_5\text{Br}_6]^-$ and to its greater stability.^{67b} Treatment of C_{76} with $[\text{tris}(2,4\text{-dibromophenyl})\text{aminium}][\text{CHB}_{11}\text{H}_5\text{Br}_6]$ (Figure 1.8 A) in a weakly nucleophilic solvent resulted in the formation of $[\text{C}_{76}][\text{CHB}_{11}\text{H}_5\text{Br}_6]$ as a brown solid in conjunction with one equivalent of tris(2,4-dibromophenyl)amine (Scheme 1.8).^{67b} Fortuitously, the neutral amine is a poor nucleophile and did not compromise the stability of the resulting cation. In addition, the oxidation product is much less soluble in non-polar hydrocarbon solvents than the amine by-product, making purification straightforward. The amine was readily removed by washing the brown solid with hexanes.

A third advantage of using aminium radical cations as chemical oxidizing agents is that their oxidation potential can be readily tuned by varying the degree of halogenation of the aryl ligands. In order to isolate salts of lower fullerenes (which have higher oxidation potentials) Reed and coworkers synthesized the $[\text{HBPC}][\text{CHB}_{11}\text{H}_5\text{Br}_6]$ salt (HBPC = hexabromo(phenyl)carbazole, Scheme 1.8 B) ($E_{1/2} = 1.34 \text{ V vs Fc/Fc}^+$), which is sufficiently more oxidizing than $[\text{tris}(2,4\text{-dibromophenyl})\text{aminium}][\text{CB}_{11}\text{H}_6\text{Br}_6]$. $[\text{HBPC}][\text{CHB}_{11}\text{H}_5\text{Br}_6]$ was used to isolate salts of $[\text{C}_{60}][\text{CHB}_{11}\text{H}_5\text{Br}_6]$ ($E_{1/2}$ of $\text{C}_{60} = 1.26 \text{ V vs Fc/Fc}^+$) (Scheme 1.10).^{66a} In addition this salt was also used to synthesize an isoelectronic heterofullerenium ion, C_{59}N^+ .⁸²

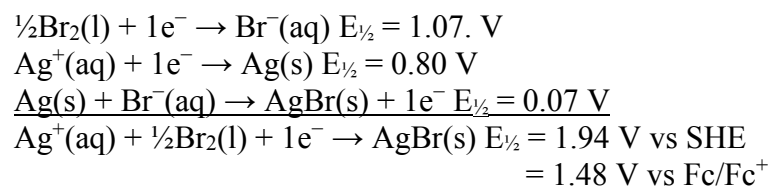
Scheme 1.8 Synthesis of fullerenium cations.



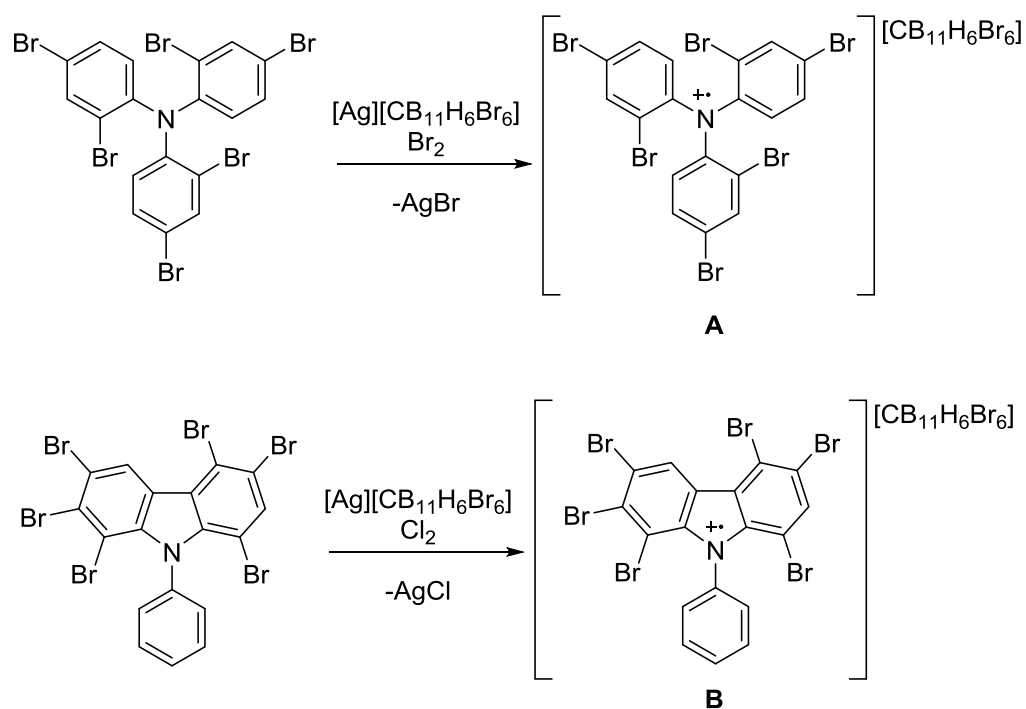
1.6 Synthesis of Triarylamminium Radical Cations Paired with Carborane Anions

Isolation of [tris(2,4-dibromophenyl)aminium][CB₁₁H₆Br₆] (Scheme 1.9 A) was accomplished by Reed et al., by treatment of [Ag][CB₁₁H₆Br₆] with tris(2,4-dibromophenyl)amine ($E_{1/2} = 1.14$ V vs Fc/Fc⁺) and an excess of Br₂ (Scheme 1.9).^{67b} The oxidation occurs by reduction of Br₂ and subsequent formation of AgBr. This process has potential equal to 1.48 V vs Fc/Fc⁺ in dichloromethane (Equation 1.1).⁷⁶ The [HBPC][CHB₁₁H₅Br₆] salt (Figure 1.9 B) was procured by treatment of hexabrominated 9-phenylcarbazole with one equivalent of [Ag][CHB₁₁H₅Br₆] and an excess of Cl₂. Cl₂ was used in this case since reduction of Cl₂ and subsequent formation of AgCl has a higher reduction potential, which was required to oxidize HBPC.

Equation 1.1



Scheme 1.9 Synthesis of aminium carborane salts.



1.7 Overview of the Work Presented in this Dissertation

The work described in the preceding sections is meant to be an introduction to the studies contributing to this thesis. In Chapter II the synthesis and characterization of strongly oxidizing aminium carborane salts and their reactivity will be presented. Chapter III is an overview of the synthesis and characterization of new redox non-innocent PNP and PNN pincer ligands based on the diarylamido backbone. In addition, the synthesis of group 10 and Rh complexes of these ligands is presented. This chapter then culminates in a comparison of the electronic properties of these ligands by investigating the redox activity of (pincer)MCl complexes and the donating ability of the pincer ligands towards a Rh metal center. In Chapter IV palladium complexes of a new phosphine-amido-siloxide pincer ligand with variable degrees of protonation will be presented. Lastly, a summary of this work is presented in Chapter V.

CHAPTER II
SYNTHESIS, CHARACTERIZATION, AND APPLICATION OF
TRIARYLAMINIUM OXIDANTS

2.1 Introduction

Triarylaminiium radical cations are an important class of organic oxidants and their applications to catalysis and electrosynthesis have been studied extensively.⁸³ Electron-poor triarylaminiium salts bearing robust, weakly coordinating anions can also be used as organic oxidants when targeting the isolation of salts of unstable cations.^{67b,67d} A strategic characteristic of these oxidants is that for electronic and steric reasons the triarylamine by-products that are formed upon reduction of the aminium radical cations are weak Lewis bases. In addition, the free amines are more soluble in organic solvents than the product salts. A final key benefit of triarylaminiium radical cations is that their potentials can be readily varied across a large range by systematically substituting the *ortho* and *para* positions of the aryl rings.⁷⁶ For instance, tris(4-bromophenyl)amine (**2-1**) corresponds to a formal potential of 0.70 V vs a ferrocene/ferrocenium redox couple (Fc/Fc⁺). However, one can readily generate more oxidizing amines by increasing the degree of bromination.^{76,84} Tris(2,4-dibromophenyl)amine (**2-2**) and the nonabrominated analog, tris(2,4,6-tribromophenyl)amine (**2-3**), exhibit much higher potentials of 1.14 V and 1.36 V respectively (vs Fc/Fc⁺).^{84b}

Equation 2.1 Oxidation of C₇₆.^{67b}



Intrigued by previously reported applications^{60b,67d,83} of triarylaminium radical cations, we set out to synthesize new triarylaminium salts bearing weakly coordinating carborane anions. For the purpose of this study we chose to use the undecachlorinated carborane anions [CRB₁₁Cl₁₁]⁻ (R = H, Me) to stabilize the radical cations. The benefit of these anions is that they are very weakly coordinating and nucleophilic, which increases the potential for the carborane anion to remain chemically innocent with respect to undesired reactivity. In addition, [CRB₁₁Cl₁₁]⁻ anions have demonstrated a propensity for stabilizing highly unusual and reactive species.⁸⁵ Finally, [CRB₁₁Cl₁₁]⁻ anions are also useful tools for this chemistry since they are stable towards strong oxidants.^{60a} In this chapter, our preliminary findings regarding the synthesis, electrochemical behavior, and reactivity of highly oxidizing redox systems is delineated.

2.2 Triarylamine Synthesis

Three main characteristics were considered when choosing a triarylamine precursor for the synthesis of highly oxidizing triarylaminium salts: the oxidation potential of the neutral amine, its solubility, and the ease of its synthesis. An ideal amine would have a high oxidation potential, be soluble in non-polar hydrocarbon solvents, and additionally could be synthesized in a timely and reproducible fashion. At the onset of

this study we targeted the synthesis of **2-3**. Unfortunately, in our hands the bromination step was not selective.^{84b} Br₂ was added to a dichloromethane solution of **2-1** at various rates and concentrations and did not result in an increase in the selectivity. In addition the reactions between **2-1** with Br₂ in the presence of FeBr₃, as well as treatment of **2-1** with a Br₂/SbCl₅ mixture did not result in selective halogenation.

Discouraged by these results, we targeted the synthesis of halogenated derivatives of 9-phenylcarbazole. This work was inspired by previous results by the Reed group in which they used carborane salts of a hexabrominated 9-phenylcarbazole radical cation ($E_{1/2} = 1.34$ V vs Fc/Fc⁺) to oxidize C₆₀ to C₆₀^{•+}.^{67d} The treatment of 9-phenylcarbazole with a Br₂/SbCl₅ mixture in dichloromethane resulted in the formation of the heptahalogenated product **2-4**, which exhibited an $E_{1/2}$ value equal to 1.66 V vs Fc/Fc⁺ (Figure 2.1) . In addition, **2-5** ($E_{1/2} = 1.24$ V vs Fc/Fc⁺) was synthesized by the reaction of 9-phenylcarbazole with three equivalents of *N*-bromosuccinimide. Although both **2-4** and **2-5** exhibit high potentials and therefore fit one of our criteria, their solubility in hydrocarbon solvents was found to be quite low.

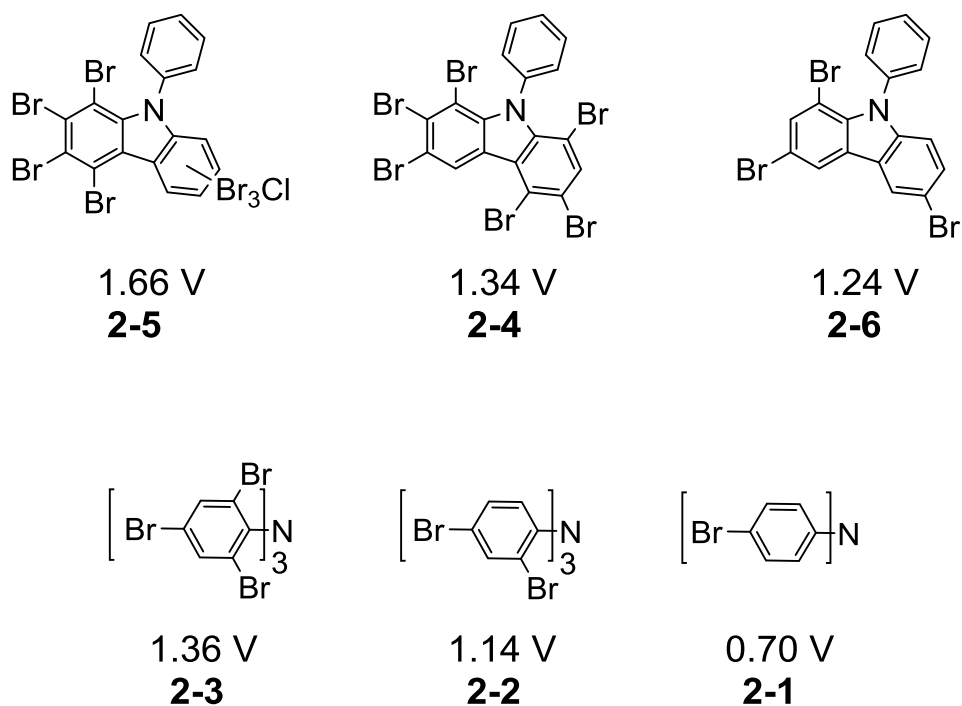


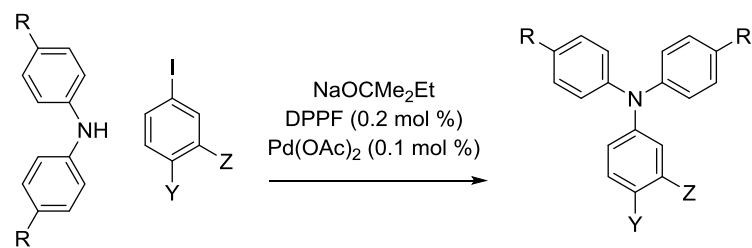
Figure 2.1 Triarylamines **2-1-2-6** and their $E_{1/2}$ potentials referenced vs Fc/Fc^+ in dichloromethane.

In light of these shortcomings we set out to synthesize new electron-poor triarylamines. This was a two part synthesis where we first synthesized triarylamine precursors that incorporated one or more fluorine or trifluoromethyl groups. The strategic use of these substituents provides a fluorine nuclei for ^{19}F NMR analysis and also helps to increase the solubility.⁸⁶ There are two common methods for the synthesis of triarylamines; Ullman couplings and Buchwald-Hartwig aminations.⁸⁷ Here we report the synthesis and characterization of a number triarylamines via Buchwald-Hartwig aminations of a secondary amine and an aryl iodide using $Pd(OAc)_2/DPPF$ ($DPPF = 1,1'$ -bis(diphenylphosphino)ferrocene) and sodium *tert*-pentoxide as the base. The

results of this study are collected in Table 2.1. Tris(4-fluorophenyl)amine (**2-7**),⁸⁸ bis(4-fluorophenyl)(phenyl)amine (**2-8**), and bis(4-fluorophenyl)(4-trifluoromethylphenyl)amine (**2-9**) were procured from the coupling reaction between one equivalent of bis(4-fluorophenyl)amine and the corresponding aryl iodide. Diphenyl(3-trifluoromethylphenyl)amine (**2-10**) and diphenyl(4-trifluoromethylphenyl)amine (**2-11**)^{87c} were synthesized in an analogous manner starting from diphenylamine. It is noteworthy to mention that the low yields attributed with these reactions are in part associated with formation of a C-C coupled biaryl by-product, which was removed from the desired products via distillation. The reactions with aryl iodides substituted with more than one fluorine or trifluoromethyl group unfortunately did not result in conversion to the desired products (**2-12**, **2-13**, **2-14**, and **2-15**).

A different approach towards generating more substituted amines is to first synthesize multiply substituted diarylamines and then attempt to couple those products with aryl halides (Table 2.2). The coupling reaction between 3,5-trifluoromethylphenylamine and 3-iodobenzotrifluoride did not result in formation of the desired product. In addition, no coupling was observed between 4-trifluoromethylphenylamine with 4-iodobenzotrifluoride or 3-iodobenzotrifluoride. The coupling reaction between 3,5-trifluoromethylphenylamine and 4-iodobenzotrifluoride; however, yielded (3,5-trifluoromethylphenyl)(4-trifluoromethylphenyl)amine (**2-16**) in a 63% yield. Attempts to couple **2-16** with phenyl iodide to produce the desired triarylamine; however, did not result in the isolation of **2-17**.

Table 2.1 Buchwald-Hartwig coupling to generate triarylamines.



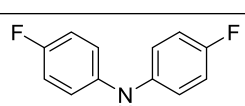
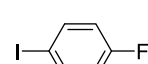
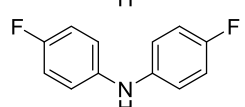
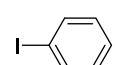
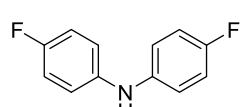
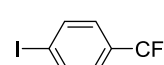
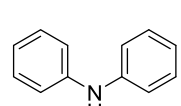
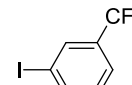
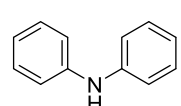
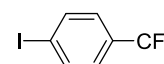
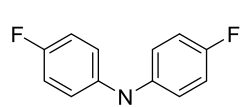
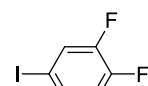
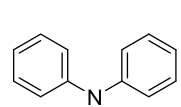
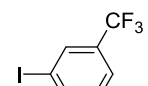
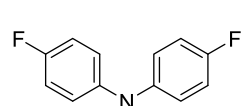
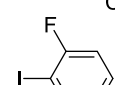
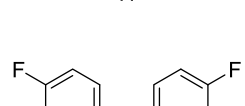
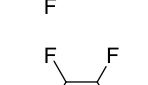
Diarylamine	Aryl Iodide	Yield	¹⁹ F NMR (ppm, C ₆ D ₆)	Product
		25%	-122.3	2-7
		38%	-122.1	2-8
		37%	-63.9 -119.9	2-9
		17%	-66.5	2-10
		45%	-63.8	2-11
		0%		2-12
		0%		2-13
		0%		2-14
		0%		2-15

Table 2.2 Reactions to produce secondary amines.

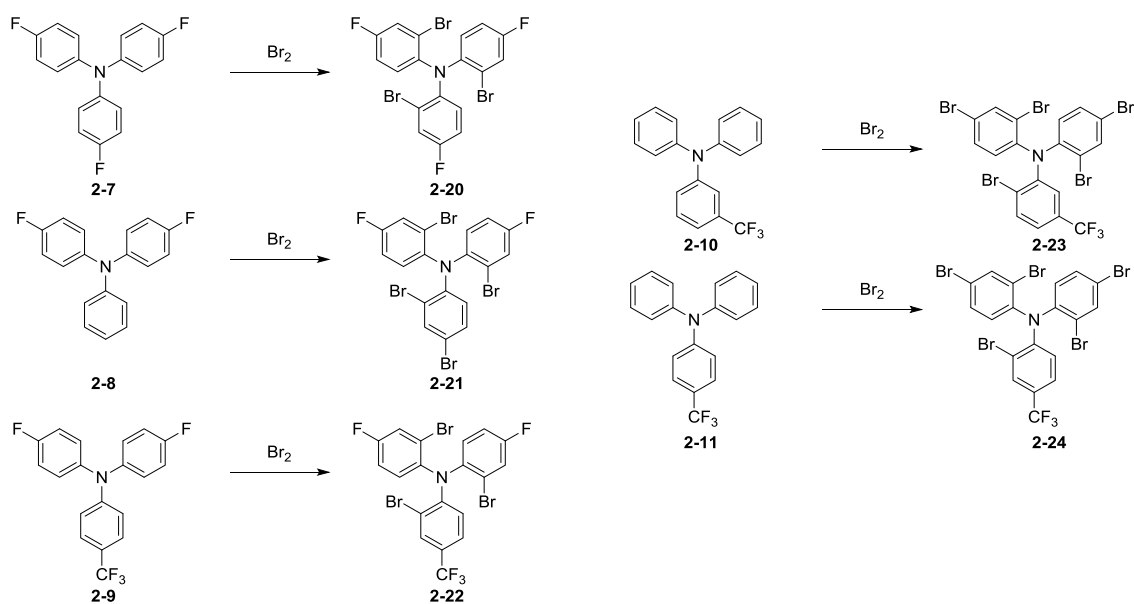
		Yield	¹⁹ F NMR Handle (ppm, C ₆ D ₆)	Product
Amine	Aryl Iodide			
		63%	-65.3, -65.5	2-16
		0%		2-17
		0%		2-18
		0%		2-19

2.3 Synthesis of Electron-Poor Triarylamines

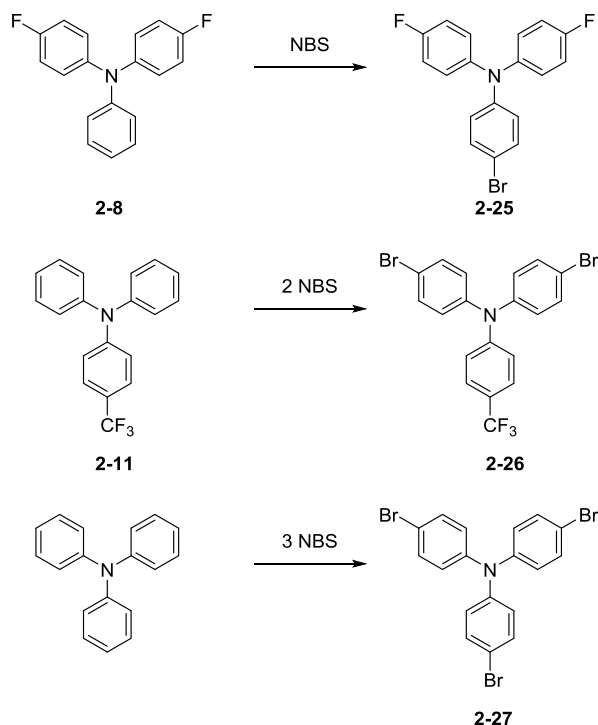
With **2-7**, **2-8**, **2-9**, **2-10**, and **2-11** in hand, we were able to brominate selectively at the *ortho* and *para* positions by treatment of the amine precursors with an excess of Br₂ (Scheme 2.1). Tris(2-bromo-4-fluorophenyl)amine (**2-20**) was synthesized in this manner from **2-7** and was isolated as a colorless powder in a 95% yield. Treatment of **2-8** with an excess of Br₂ resulted in the formation of bis(2-bromo-4-fluorophenyl)(2,4-dibromophenyl)amine (**2-21**), which was isolated from a concentrated hexanes solution as dark crystals. The crystals were then sublimed while being heated under vacuum to give **2-21** as a colorless solid with a 68% yield. Exposure of **2-21** to air for extended periods of time or to wet solvents resulted in a color change back to dark green. Bis(2-bromo-4-fluorophenyl)(2-bromo-4-trifluoromethylphenyl)amine (**2-22**) was produced from the reaction of **2-9** with Br₂ and was isolated as a colorless solid with a 49% yield after recrystallization. Bis(2,4-dibromophenyl)(2-bromo-3-trifluoromethylphenyl)amine (**2-23**) and bis(2,4-dibromophenyl)(2-bromo-4-trifluoromethylphenyl)amine (**2-24**) were synthesized in a similar manner from **2-10** and **2-11** and were isolated upon workup with yields of 17% and 55% respectively. It is interesting to note that in all of the above reactions no further bromination was observed even though the reactions were done in the presence of a large excess of Br₂. Less halogenated amines can be synthesized with *N*-bromosuccinimide (Scheme 2.2). Bis(4-fluorophenyl)(4-bromophenyl)amine (**2-25**) was synthesized by treatment of **2-8** with one equivalent of *N*-bromosuccinimide in dichloromethane. Bis(4-bromophenyl)(4-trifluoromethylphenyl)amine (**2-26**)^{87c} was synthesized by treatment of a solution of **2-11** in dichloromethane with two equivalents

of *N*-bromosuccinimide. Tris(4-bromophenyl)amine (**2-27**) (also commercially available) was synthesized from the reaction of triphenylamine with three equivalents of *N*-bromosuccinimide. Addition of an excess of *N*-bromosuccinimide to **2-27** did not result in selective bromination at the *ortho*-position of the arene rings.

Scheme 2.1 Reactions of triarylamines with an excess of Br₂.



Scheme 2.2 Synthesis of **2-25**, **2-26**, and **2-27** with NBS.



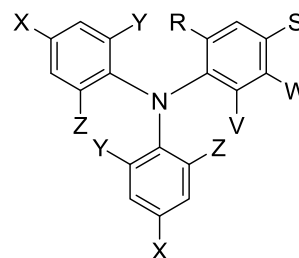
2.4 Cyclic Voltammetry

Cyclic voltammetry was used to determine the $E_{1/2}$ values of the amines analyzed within this work. Electroanalytical data was obtained using a CH Instruments Model 700 D Series Electrochemical Analyzer and Workstation in conjunction with a three electrode cell. The cyclic voltammetry experiments were conducted in dichloromethane with 0.3 M $[\text{Bu}_4\text{N}][\text{PF}_6]$ as the supporting electrolyte at a scan rate of 100 mV/s. The concentration of the analyte solutions were approximately 0.001 M. The observed potentials were referenced to a Fc/Fc^+ redox couple as recommended by IUPAC.^{76,89} The amines analyzed by cyclic voltammetry and their corresponding $E_{1/2}$ values are tabulated

in Table 2.3. In each case, a quasi-reversible one-electron redox event was observed. The potentials listed in Table 2.3 range from 0.64 V to 1.39 V, demonstrating that the formal potential of an amine can be modified by varying substituents at the *ortho* and *para* positions of the arene rings.

Table 2.3 $E_{1/2}$ (V) vs Fc/Fc^+ values.

	X	Y	Z	R	W	V	S	$E_{1/2}$ (V) vs Fc/Fc^+
2-24	Br	Br	H	Br	H	H	CF_3	1.39
2-3	Br	Br	Br	Br	H	Br	Br	1.36
2-22	F	Br	H	Br	H	H	CF_3	1.26
2-23	Br	Br	H	Br	CF_3	H	H	1.19
2-21	F	Br	H	Br	H	H	Br	1.11
2-9	F	H	H	H	H	H	CF_3	0.78
2-27	Br	H	H	H	H	H	Br	0.70
2-20	F	Br	H	Br	H	H	F	0.67
2-7	F	H	H	H	H	H	F	0.64

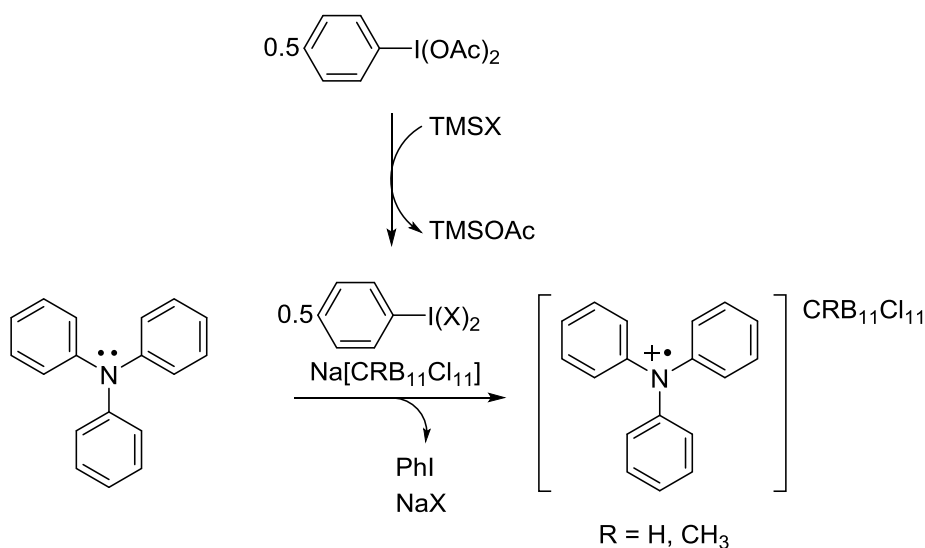


2.5 Synthesis of Aminium Salts

Hypervalent iodine(III) reagents are well-known for their ability to act as powerful single electron transfer (SET) reagents and have garnered popularity as stoichiometric oxidants for organic synthesis⁹⁰ and for transition metal mediated oxidative functionalization reactions.^{90a} These processes are often accompanied by the addition of Lewis acids such as $\text{BF}_3 \cdot \text{Et}_2\text{O}$ ⁹¹ and Me_3SiOTf ,^{90b,92} which enhance the SET oxidizing ability of hypervalent iodine(III) reagents.^{90e} We envisioned that hypervalent iodine(III) reagents would be a viable oxidant for generation of triarylamminium radical

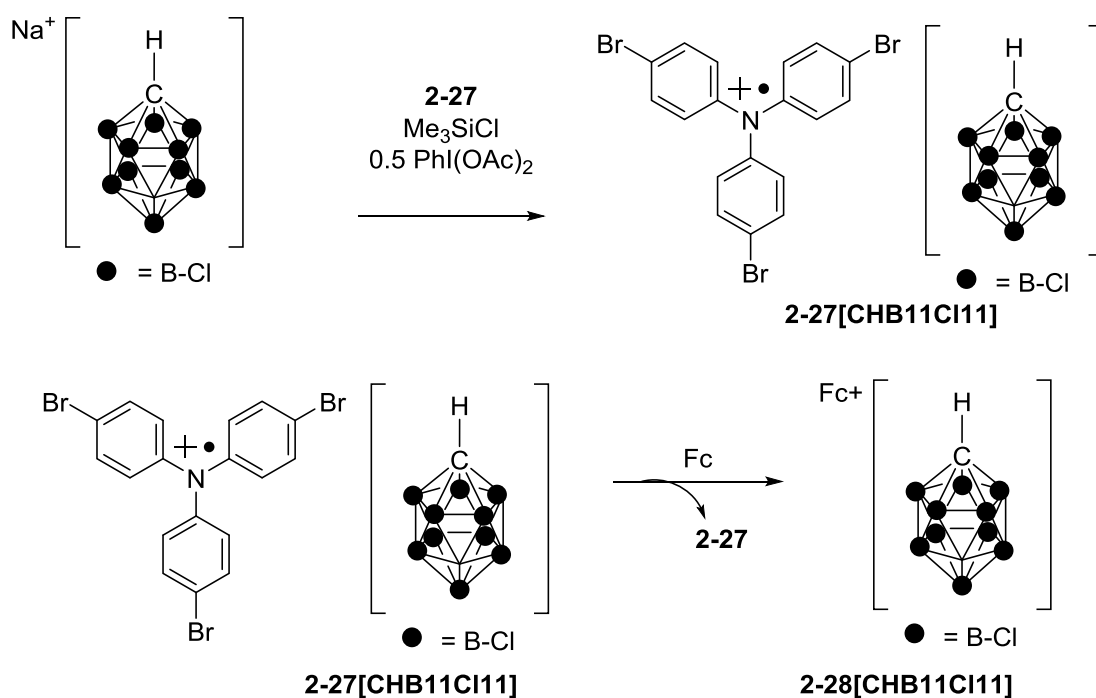
cations and in practice we observed that this was true. Treatment of a solution composed of a triarylamine and Na[CRB₁₁Cl₁₁] (R = H, Me) in dichloromethane with half an equivalent of PhI(OAc)₂ and one equivalent of Me₃SiX (X = OTf, Cl) resulted in conversion to the corresponding triarylaminium salts. Addition of Na[CRB₁₁Cl₁₁] serves two purposes. The first is to provide the product cation with a non-coordinating counter anion. The second purpose is to deliver a Lewis acid (Na⁺) to consume X⁻ (X = OAc⁻, Cl⁻, or OTf⁻). The addition of Me₃SiOTf and Me₃SiCl enhanced the SET oxidizing ability of the iodine(III) reagent, by providing a Lewis acid to consume OAc⁻ and by generating a more reactive iodine(III) center. We observed that the SET oxidizing ability increased in the following manner: PhI(OAc)₂ in the presence of Me₃SiCl < PhI(OAc)₂ in the presence of Me₃SiOTf.

Scheme 2.3 Generation of a triarylaminium radical cation.



[Tris(4-bromophenyl)aminium][CHB₁₁Cl₁₁] (**2-27**[CHB₁₁Cl₁₁]) was prepared by treatment of solution composed of Na[CHB₁₁Cl₁₁] and **2-27** with one equivalent of Me₃SiCl and half an equivalent of PhI(OAc)₂. After 30 min the resulting blue solution was filtered through a pad of Celite and the volatiles were removed under vacuum. The resulting blue residue was dissolved in a minimal amount of dichloromethane and layered with pentane. Slow diffusion of pentane resulted in precipitation of **2-27**[CHB₁₁Cl₁₁] as a NMR silent blue solid in a 69% yield. **2-27**[CHB₁₁Cl₁₁] was subjected to an elemental analysis study, from which the resulting experimental values were in good agreement with the calculated values. In addition, the stoichiometric reaction of **2-27**[CHB₁₁Cl₁₁] with one equivalent of ferrocene in the presence of an internal standard resulted in formation of one equivalent of **2-27** and [Fc⁺][CHB₁₁Cl₁₁] (**2-28**[CHB₁₁Cl₁₁]). **2-28**[CHB₁₁Cl₁₁] was prepared independently from the reaction between Na[CHB₁₁Cl₁₁], ferrocene, Me₃SiCl, and 0.5 equivalents of PhI(OAc)₂. **2-28**[CHB₁₁Cl₁₁] was isolated as a blue powder in a 40% yield. The analogous [Fc⁺][BArF₂₀] salt (**2-28**[BArF₂₀]) was procured in a similar manner by treatment of **2-27**, Na[BArF₂₀], and Me₃SiCl with 0.5 equivalents of PhI(OAc)₂.

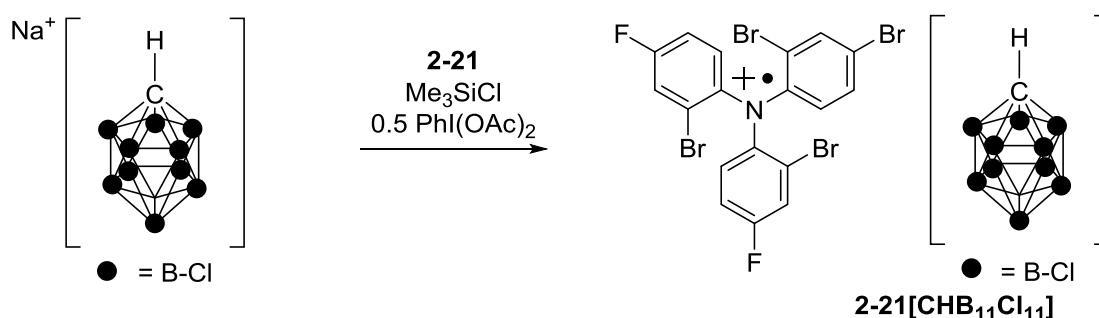
Scheme 2.4 Synthesis and reactivity of **2-27**[CHB₁₁Cl₁₁].



Treatment of **2-21** with Na[CHB₁₁Cl₁₁], Me₃SiCl, and half an equivalent of PhI(OAc)₂ in dichloromethane resulted in formation of a brilliant green solution (Scheme 2.5). After stirring the reaction mixture for 30 min the solution was passed through a pad of Celite and then the volatiles were removed under vacuum. The resulting blue residue was washed with pentane (3 × 5 mL) and then dried under vacuum for an extended period of time to give [bis(2-bromo-4-fluorophenyl)(2,4-dibromophenyl)aminium][CHB₁₁Cl₁₁] (**2-21**[CHB₁₁Cl₁₁]) as a green powder in a 90% yield. Elemental analysis of **2-21**[CHB₁₁Cl₁₁] demonstrated good agreement between the experimental and calculated values. **2-21**[CHB₁₁Cl₁₁] was not stable in dichloromethane for extended periods of time. Failure to completely remove the

volatiles and attempts to recrystallize the salt resulted in the formation of a brown oil; whose identity is not known. Treatment of the brown oil with ferrocene did not result in formation of **2-21** or **2-29**[CHB₁₁Cl₁₁].

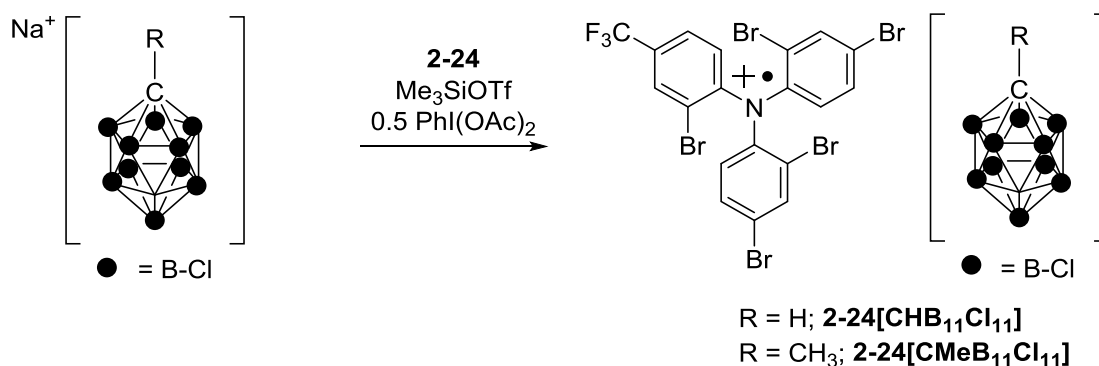
Scheme 2.5 Synthesis of **2-21**[CHB₁₁Cl₁₁].



Isolation of [bis(2,4-dibromophenyl)(2-bromo-4-trifluoromethylphenyl)-aminium][CHB₁₁Cl₁₁] (**2-24**[CHB₁₁Cl₁₁]) was also achieved via a slightly modified procedure. Treatment of a dichloromethane solution of **2-24**, Na[CHB₁₁Cl₁₁], and Me₃SiCl with half an equivalent of PhI(OAc)₂ did not result in oxidation of the amine. However, we found that treatment of a dichloromethane solution of **2-24** with Na[CHB₁₁Cl₁₁], Me₃SiOTf, and half an equivalent of PhI(OAc)₂ did result in oxidation of the amine to form **2-24**[CHB₁₁Cl₁₁] (Scheme 2.6). This was evidenced by multinuclear NMR spectroscopy by the disappearance of diamagnetic signals associated with **2-24** and by the drastic color change to blue observed upon addition of PhI(OAc)₂. **2-24**[CHB₁₁Cl₁₁] was isolated as brilliant blue solid with a 95% yield after workup.

2-[CHB₁₁Cl₁₁] was subjected to an elemental analysis study from which good agreement between the calculated and experimental values was observed. Upon treatment of **2-24[CHB₁₁Cl₁₁]** with one equivalent of ferrocene in the presence of an internal standard, one equivalent of **2-24** was observed by NMR spectroscopy. The similar salt, [bis(2,4-dibromophenyl)(2-bromo-4-trifluoromethylphenyl)aminium][CMeB₁₁Cl₁₁] (**2-24[CMeB₁₁Cl₁₁]**) was prepared by treatment of a dichloromethane solution of **2-24** with Na[CMeB₁₁Cl₁₁], Me₃SiOTf, and half an equivalent of PhI(OAc)₂. **2-24[CMeB₁₁Cl₁₁]** was isolated as a blue powder in a 75% yield.

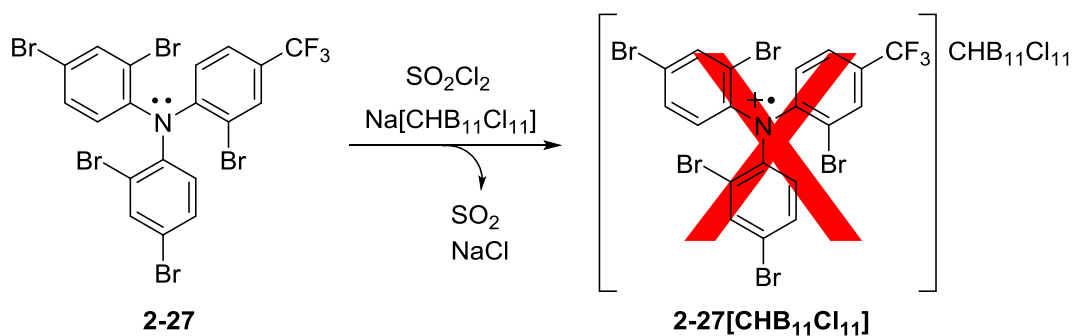
Scheme 2.6 Synthesis of **2-24[CRB₁₁Cl₁₁]**.



We also hypothesized that SO₂Cl₂ might be a viable SET reagent for generation of triarylaminium radical cations (Scheme 2.7). We envisioned that treatment of a solution composed of a triarylamine and Na[CRB₁₁Cl₁₁] (R = H, Me) in dichloromethane with SO₂Cl₂ could result in conversion to the corresponding triarylaminium salts through reduction of SO₂Cl₂, and formation of NaCl and SO₂. Na[CHB₁₁Cl₁₁] was added to

provide the product cation with a non-coordinating counter anion and to consume Cl^- . Unfortunately, treatment a solution of **2-24** and $\text{Na}[\text{CHB}_{11}\text{Cl}_{11}]$ with excess SO_2Cl_2 resulted in a mixture of diamagnetic products. At this time we have no evidence to suggest that **2-24** $[\text{CHB}_{11}\text{Cl}_{11}]$ was formed from this reaction.

Scheme 2.7 Proposed synthetic route to aminium salts using SO_2Cl_2 as an oxidant.



2.6 Stoichiometric Reactions with the Aminium Salts

2.6.1 Stoichiometric reaction of aminium with hexamethylbenzene

We chose to investigate the reactivity of the aminium salts reported in the previous section through stoichiometric reactions with hexamethylbenzene (C_6Me_6). The hexamethylbenzene radical cation has been studied considerably in the literature;⁹³ however its structural characterization has been elusive. The aminium salt **2-24** $[\text{CHB}_{11}\text{Cl}_{11}]$ is a viable oxidant for targeting stable salts of the hexamethylbenzene radical cation. In addition to being a powerful enough oxidant (analysis of

hexamethylbenzene by cyclic voltammetry showed an irreversible oxidation event at 1.24 V vs Fc/Fc⁺), **2-24**[CHB₁₁Cl₁₁] also incorporates a weakly coordinating carborane anion. Carborane anions have been used to stabilize highly reactive cations.^{67c,67d} Treatment **2-24**[CHB₁₁Cl₁₁] with a stoichiometric equivalent of hexamethylbenzene resulted in the formation of brown crystals. Analysis of the reaction mixture by ¹H NMR spectroscopy revealed formation of **2-24**. Separation of the free amine from the crystals was accomplished by washing the brown crystals multiple times with pentane. The brown solid was then taken up in a variety of different solvents in attempt to isolate X-ray quality crystals for single crystal X-ray diffraction. In most cases a brown oily solid was isolated rather than quality crystals. Frustrated with these results, we attempted to collect X-ray diffraction quality crystals by changing the anion to [CMeB₁₁Cl₁₁]⁻. Upon treatment of a solution of Na[CMeC₁₁B₁₁], **2-24**, and Me₃SiOTf with half an equivalent of PhI(OAc)₂, a brilliant blue solution formed. Addition of one equivalent of hexamethylbenzene to this solution resulted in copious precipitation of a purple solid. Isolation of the solid was achieved by washing it with pentane. The purple solid was then recrystallized via slow diffusion of pentane into a dichloromethane solution. The resultant purple solid is very soluble in dichloromethane and acetonitrile. It is also slightly soluble in diethyl ether and aromatic solvents; however, exposure of the product to these solvents resulted in the formation of a brown oil over time. ¹H NMR analysis of the purple solid revealed no signals corresponding to hexamethylbenzene. At this time the identity of the product is still unknown and we have no concrete evidence suggesting

that the target hexamethylbenzene radical cation salts are being formed; however, it is promising that we see reduction of the aminium.

2.6.2 Reaction of hexamethylbenzene with Na[CHB₁₁Cl₁₁], Me₃SiX reagents, and PhI(OAc)₂

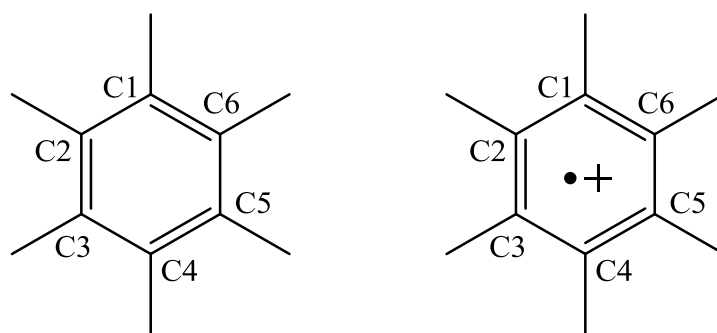
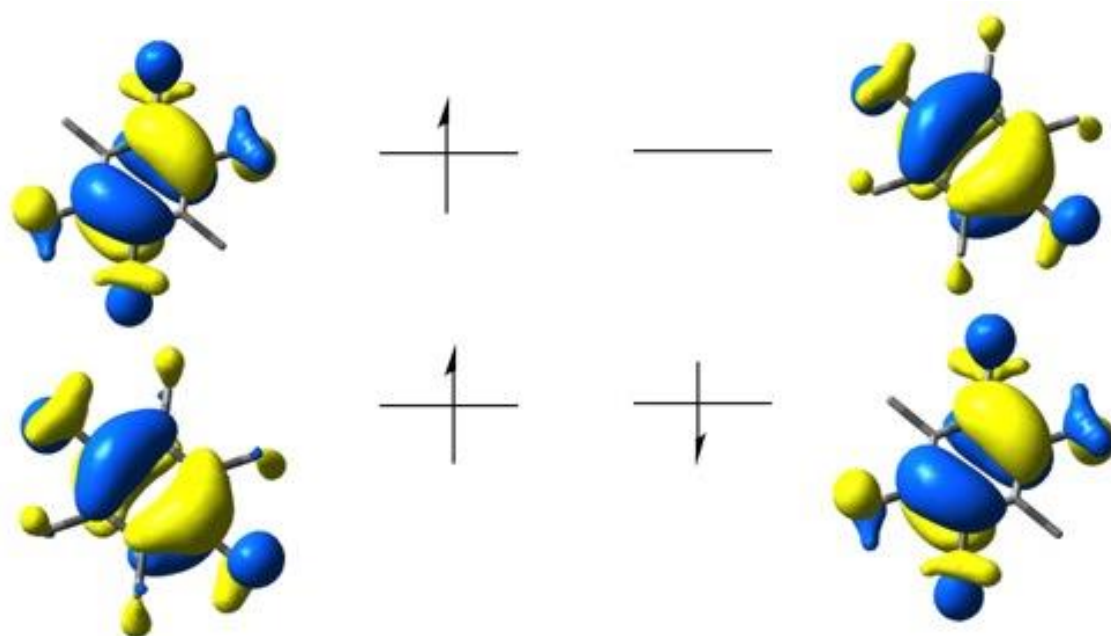
The direct oxidation of hexamethylbenzene was also investigated employing the same synthetic procedure used to produce the aminium salts. Treatment of a dichloromethane solution of hexamethylbenzene, Na[CHB₁₁Cl₁₁], and Me₃SiCl with half an equivalent of PhI(OAc)₂ did not result in a color change or disappearance of the hexamethylbenzene signals by ¹H NMR spectroscopy. On the other hand, treatment of hexamethylbenzene with Na[CHB₁₁Cl₁₁], Me₃SiOTf, and half an equivalent of PhI(OAc)₂ resulted in an immediate color change to purple. Removal of the volatiles under vacuum gave a purple oil. The oil was then dissolved in dichloromethane and filtered through a pad of Celite. Concentration of the dichloromethane solution and slow diffusion of pentane resulted in precipitation of a red solid. Analysis of the solid by ¹H NMR spectroscopy revealed a small amount of hexamethylbenzene and a broad singlet at 13.6 ppm, which appeared to increase in intensity over time. Two similar reactions were also conducted using Na[CMeB₁₁Cl₁₁], which suggest that the identity of the product may vary depending on the number of equivalents of hexamethylbenzene added. Treatment of one equivalent of hexamethylbenzene with stoichiometric equivalents of Na[CMeB₁₁Cl₁₁] and Me₃SiOTf and half an equivalent of PhI(OAc)₂ resulted in the formation of a red solid. On the other hand, if two equivalents of hexamethylbenzene

were reacted, a purple solid formed. The identities of the products from these reactions still remain unknown.

2.6.3 DFT investigation of the hexamethylbenzene radical cation

In order to gain insight into the nature of the hexamethylbenzene radical cation we turned to density functional theory (DFT) and performed electronic structural calculations to depict the HOMO/LUMO orbital compositions and to approximate metric changes (Figure 2.2). These results were first calculated using B3LYP⁹⁴ and then repeated with no symmetry added at the onset of the calculation. The two different methods produced the same theoretical metric parameters. For comparative purposes the structure of hexamethylbenzene was also calculated and the metrics were compared to the experimental values determined by Robertson.⁹⁵ In the calculated structure, hexamethylbenzene was observed as a planar molecule with a C_{6h} point group symmetry. The calculated C(Ar)–C(Ar) bonds were all found to be equal to 1.41 Å; only slightly elongated compared to the experimental value of 1.39 Å observed by Robertson.⁹⁵ Figure 2.2 depicts selected orbitals of the hexamethylbenzene radical cation

and the computed bond lengths associated with the neutral and cationic species. In the oxidation product, one electron has been removed from an e_{1g} orbital and the static structure is distorted to a C_{2h} point group symmetry. The loss of symmetry is attributed to a slight distortion of two of the methyl groups out of the plane consisting of C_1 - C_6 . The methyl groups at C_1 and C_4 were found to be distorted by 0.27 Å above and below the plane. Oxidation led to modest changes in the magnitudes of the C(Ar)-C(Ar) bond lengths. The (C_1 - C_2), (C_3 - C_4), (C_4 - C_5) and (C_6 - C_1) bond lengths are increased by 0.03 Å upon oxidation; while the (C_2 - C_3) and (C_5 - C_6) bond lengths decreased by 0.03 Å. These results mimic similar calculations regarding the oxidation of benzene to benzene radical cation.⁹⁶



1.41	C1-C2	1.44
1.41	C2-C3	1.38
1.41	C3-C4	1.44
1.41	C4-C5	1.44
1.41	C5-C6	1.38
1.41	C6-C1	1.44

Figure 2.2 Selected orbital depictions of the hexamethylbenzene radical cation. Calculated C(Ar)–C(Ar) bond lengths for hexamethylbenzene and hexamethylbenzene radical cation are also shown.

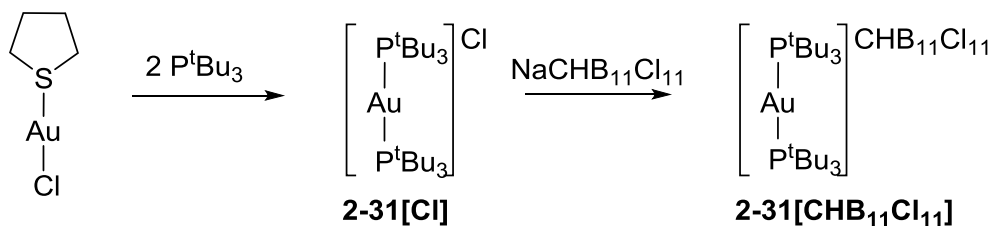
2.6.4 Reactions with Au(I) salts

In a recent, unprecedented study in the Ozerov group Dr. Morgan Macinnis discovered that the oxidation of $M(P^tBu_3)_2$ ($M = Pd, Pt$) with $[Ph_3C][CHB_{11}Cl_{11}]$ resulted in the isolation of $[(^tBu_3P)_2M][HCB_{11}Cl_{11}]$ ($M = Pd$ (**2-29**), Pt (**2-30**)) salts. Pd(I) and Pt(I) dimeric complexes have been widely reported in the literature.⁹⁷ However, prior to the discovery of **2-29** and **2-30** isolated mononuclear Pd(I) and Pt(I) complexes had yet to be reported, but had been proposed as intermediates in catalysis.⁹⁸ Inspired by these results we turned our attention to the possibility of isolating an isoelectronic Au(II) complex. The cationic $[Au(P^tBu_3)_2]Cl$ complex,⁹⁹ $Pd(P^tBu_3)_2$,¹⁰⁰ and $Pt(P^tBu_3)_2$ ¹⁰⁰ have been structurally characterized and were found to exhibit similar molecule structures. Each structure contained a linear configuration about the metal center and the phosphines were found to be in staggered conformations.⁹⁹ We hoped to isolate $[(^tBu_3P)_2Au][CHB_{11}Cl_{11}]_2$ salts so that an analogous structural comparison with the Pd(I) and Pt(I) isoelectronic complexes could be made. In addition, Au(II) complexes are most commonly found as Au(II)-Au(II) dimers.¹⁰⁶ Mononuclear Au(II) complexes consistent with a d^9 configuration are less common and as of yet 2-coordinate linear Au(II) complexes have not been reported in the literature.¹⁰¹

The reaction of one equivalent of chloro(tetrahydrothiophene)gold(I) with two equivalents of triphenylphosphine resulted in quantitative conversion to $[Au(P^tBu_3)_2]Cl$ (**2-31[Cl]**). $[Au(P^tBu_3)_2]X$ salts have been reported ($X = BF_4$,¹⁰² Cl ⁹⁹). Metathesis of **2-31[Cl]** with one equivalent of $Na[CHB_{11}Cl_{11}]$ in dichloromethane resulted in ion exchange to give $[Au(P^tBu_3)_2][CHB_{11}Cl_{11}]$ (**2-31[CHB₁₁Cl₁₁]**) as a colorless solid (70%

yield) (Scheme 2.8). The ^1H NMR spectrum of **2-31**[CHB₁₁Cl₁₁] is characterized by a singlet at δ 3.26 (C-H of the carborane) and a multiplet at δ 1.56 that is coupled to a $^{31}\text{P}\{^1\text{H}\}$ NMR singlet at δ 97.2. To establish the geometry about the Au(I) center we turned to single crystal X-ray diffraction (Figure 2.3). Slow diffusion of pentane into a dichloromethane solution of **2-31**[CHB₁₁Cl₁₁] resulted in the isolation of colorless crystals, which crystallized in the Pnma space group. The crystal lattice is composed of a non-coordinating carborane anion and the cationic gold species, which has a crystallographic three-fold axis running parallel to the Au–P bonds. The geometry about the Au metal center was perfectly linear (P–Au–P = 180.00°). The two Au–P distances were both experimentally observed to be 2.3361(9) Å. This distance is slightly elongated compared to the Au–P bond lengths observed for [Au(P^tBu₃)₂]X (X = BF₄,¹⁰² Cl⁹⁹) which were found to be ca 2.32 Å. The geometry about the metal center in **2-31**[CHB₁₁Cl₁₁] was similar to the geometries observed in Pd(P^tBu₃)₂, Pt(P^tBu₃)₂, **2-29**, and **2-30**. All five structures are characterized by a linear configuration about the metal center and a staggered conformation about the phosphine ligands.

Scheme 2.8 Synthesis of **2-31**[CHB₁₁Cl₁₁].



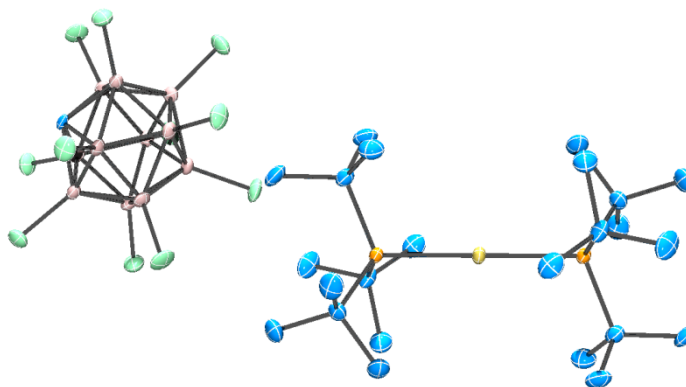


Figure 2.3 POV-Ray¹⁰³ rendition of the ORTEP¹⁰⁴ drawing (50% probability ellipsoids) of **2-31[CHB₁₁Cl₁₁]**. Hydrogen atoms have been omitted for clarity. More data for this structure can be found in Appendix C.

Analysis of **2-31[CHB₁₁Cl₁₁]** by cyclic voltammetry in acetonitrile revealed an irreversible redox event at 1.23 V (vs the Fc/Fc⁺ couple). Treatment of **2-31[CHB₁₁Cl₁₁]** with **2-24[CHB₁₁Cl₁₁]** in dichloromethane resulted in reduction of the amine (as observed by ¹H and ¹⁹F NMR spectroscopy) and a sharp color change from blue to brown. Dark brown crystals were isolated upon filtration of the solution through a pad of Celite and slow diffusion of pentane into the dichloromethane solution. NMR analysis of the crystals did not reveal any diamagnetic NMR signals. The isolated solid therefore does not contain **2-24** or **2-31[CHB₁₁Cl₁₁]**. The identity of the NMR inactive product (or products) is still under investigation.

2.7 Conclusion

In summary, a series of oxidizing triarylaminium radical cations were formed and isolated as [NAr₃]⁺[CRB₁₁Cl₁₁]⁻ salts (R = H, CH₃). These salts were prepared by

treatment of a neutral amine, Me_3SiX ($\text{X} = \text{OTf}, \text{Cl}$), and $\text{Na}[\text{CRB}_{11}\text{Cl}_{11}]$ ($\text{R} = \text{H}, \text{CH}_3$) with half an equivalent of $\text{PhI}(\text{OAc})_2$. Preliminary studies regarding stoichiometric reactions with $[\text{NAr}_3]^+[\text{CRB}_{11}\text{Cl}_{11}]^-$ salts were also presented. At this juncture, the identity of the products formed from the stoichiometric reactions of $[\text{NAr}_3]^+[\text{CRB}_{11}\text{Cl}_{11}]^-$ salts with hexamethylbenzene and $[\text{Au}(\text{I})(\text{P}^t\text{Bu}_3)_2][\text{CHB}_{11}\text{Cl}_{11}]$ are still unknown.

2.8 Experimental

2.8.1 General experimental considerations

Unless otherwise specified all manipulations were performed under an atmosphere of Ar using a standard Schlenk line or a glovebox. Toluene, diethyl ether, hexanes, tetrahydrofuran, dichloromethane, Me_3SiCl , Me_3SiOTf , C_6D_6 , 2,6-lutidine, CD_3CN , and CD_2Cl_2 were all dried over CaH_2 , distilled or vacuum transferred, and then stored over molecular sieves in an Ar filled glove box. $\text{CHB}_{11}\text{H}_{11}$ was purchased from Katchem. All other chemicals used were received from commercial vendors. NMR spectra were recorded on a Varian Inova 500 (^1H , ^{13}C , ^{31}P , ^{19}F), or a Varian 500 (^1H , ^{13}C , ^{31}P , ^{19}F) spectrometer. ^{31}P and ^{19}F NMR spectra were referenced externally using H_3PO_4 (85%, 0 ppm) and CF_3COOH (-78.5 ppm) respectively. Electrochemical studies were carried out using a CH Instruments Model 700 D Series Electrochemical Analyzer and Workstation in conjunction with a three electrode cell. The working electrode was a CHI 104 glassy-carbon disk with a 3.0 mm diameter and the auxiliary electrode was

composed of platinum wire. The third electrode, the reference electrode, was a Ag/AgNO₃ electrode. This was separated from solution by a fine porosity frit. CVs were conducted in dichloromethane with 0.3 M [Bu₄N][PF₆] as the supporting electrolyte at scan rate of 100 mV/s. The concentration of the analyte solutions were approximately 1.00×10^{-3} M. CVs were referenced to the Fc/Fc⁺ redox couple. Low-temperature X-ray data were obtained on a Bruker APEXII CCD based diffractometer (Mo sealed X-ray tube, K_α = 0.71073 Å). All diffractometer manipulations, including data collection, integration and scaling were carried out using the Bruker APEXII software. Elemental analyses were performed by CALI Laboratories, Parsippany, NJ. FT-IR spectra were collected using a Bruker ALPHA-P FT-IR Spectrometer with a diamond ATR head.

2.8.2 Computation methodology

Geometry optimizations and frequency calculations were performed utilizing the B3LYP⁹⁴ functional with a 3-21G¹⁰⁵ basis set on C, H. Where possible the geometries were compared to the values determined experimentally by X-ray crystallography and were found to closely match. The Ampac Graphical User Interface (AGUI) program was used to extract geometric data.

2.8.3 Synthesis of **2-5** and **2-6**

2-5. A Schlenk flask was charged with 9-phenylcarbazole (0.22 g, 0.91 mmol), SbCl₅ (1 mL), 1,2-dichloroethane (5 mL), and Br₂ (2 mL) which was added last in a drop-wise fashion. The reaction was stirred for 18 h resulting in precipitation of an orange solid. The solution was decanted and the resulting solid washed with pentane. ¹H NMR (CDCl₃): δ 7.95 (m, 2H), 7.76 (m, 1H), 7.70 (m, 2H). The solid was also analyzed by MALDI MS which showed the isotopic pattern for **2-5**. The cyclic voltammogram of **2-5** was obtained with 0.3 M [Bu₄N][BARF₂₀] as the supporting electrolyte and resulted in a measured potential (E_{1/2}) equal to 1.55 V vs Fc/Fc⁺.

2-6. In a 50 mL Schlenk flask, 1.25 g (6.91 mmol) of 9-phenylcarbazole was dissolved in dichloromethane. 4.92 g (27.6 mmol) of *N*-bromosuccinimide was added to the solution in 10 portions over the course of 30 minutes. The solution was stirred for 18 h at room temperature. The resulting precipitate was collected on a medium frit and washed with distilled water (2 × 20 mL) and with methanol (2 × 5 mL). The solid was then collected, dissolved in hot chloroform and the remaining succinimide was extracted with water. Upon removal of the volatiles a colorless powder was collected (0.78 g, 1.88 mmol, 27%). ¹H NMR (CDCl₃, Figure 2.4): δ 8.14 (dd, *J* = 2 Hz, *J* = 1 Hz, 2H), 7.57 (m, 2H), 7.44 (m, 4H), 7.20 (dd, *J* = 8 Hz, *J* = 1 Hz, 2H). The cyclic voltammogram of **2-6** was obtained using 0.3 M [Bu₄N][PF₆] as the supporting electrolyte and resulted in a measured potential (E_{1/2}) equal to 1.37 V vs Fc/Fc⁺.

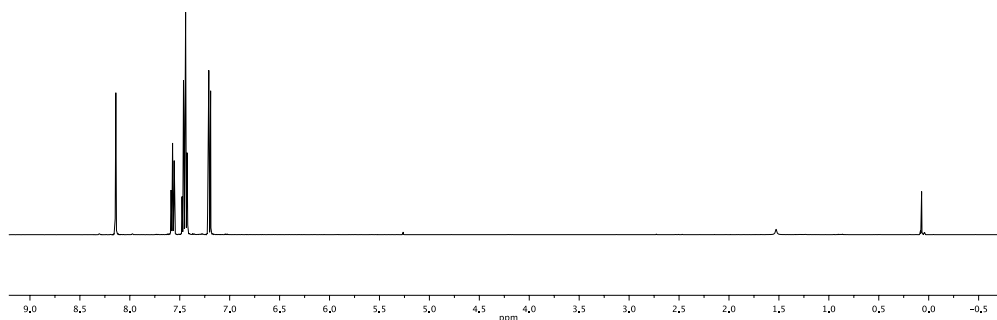


Figure 2.4 ^1H NMR spectrum of **2-6** (CDCl_3 , 500 MHz). Trace quantities of silicone grease are observed.

2.8.4 Synthesis and characterization of triarylaminines

2-7. A Schlenk flask was charged with bis(*p*-fluorophenyl)amine (0.95 g, 4.6 mmol), 4-fluoroiodobenzene (0.58 mL, 4.6 mmol), DPPF (76 mg, 0.14 mmol), $\text{Pd}(\text{OAc})_2$ (10 mg, 0.045 mmol), sodium *tert*-pentoxide (0.56 g, 5.1 mmol), a stir bar, and toluene (25 mL). The reaction mixture was then placed in a 120 °C oil bath and refluxed for 24 h. After cooling the solution to room temperature the volatiles were removed under *vacuo* and the resulting brown oil was taken up in hexanes and filtered through a pad of silica gel. Concentration of the hexane solution and recrystallization at -35 °C resulted in the formation of colorless crystals which were collected and dried

under vacuum to yield **2-7** (0.35 g, 1.2 mmol, 25%). ^1H NMR (C_6D_6 , Figure 2.5): δ 6.67 (m, 6H, Ar-*H*), 6.62 (m, 6H, Ar-*H*). $^{13}\text{C}\{^1\text{H}\}$ NMR (C_6D_6): δ 151.1 (d, $J_{\text{CF}} = 242$ Hz, Ar CF), 144.3 (d, $J_{\text{CF}} = 3$ Hz, Ar CN), 125.5 (d, $J_{\text{CF}} = 8$ Hz, Ar CH), 116.4 (d, $J_{\text{CF}} = 22$ Hz, Ar CH). ^{19}F NMR (C_6D_6): δ -122.3 (tt, $J_{\text{HF}} = 8$ Hz, $J_{\text{HF}} = 5$ Hz). $E_{1/2} = 0.64$ V vs Fc/Fc^+ .

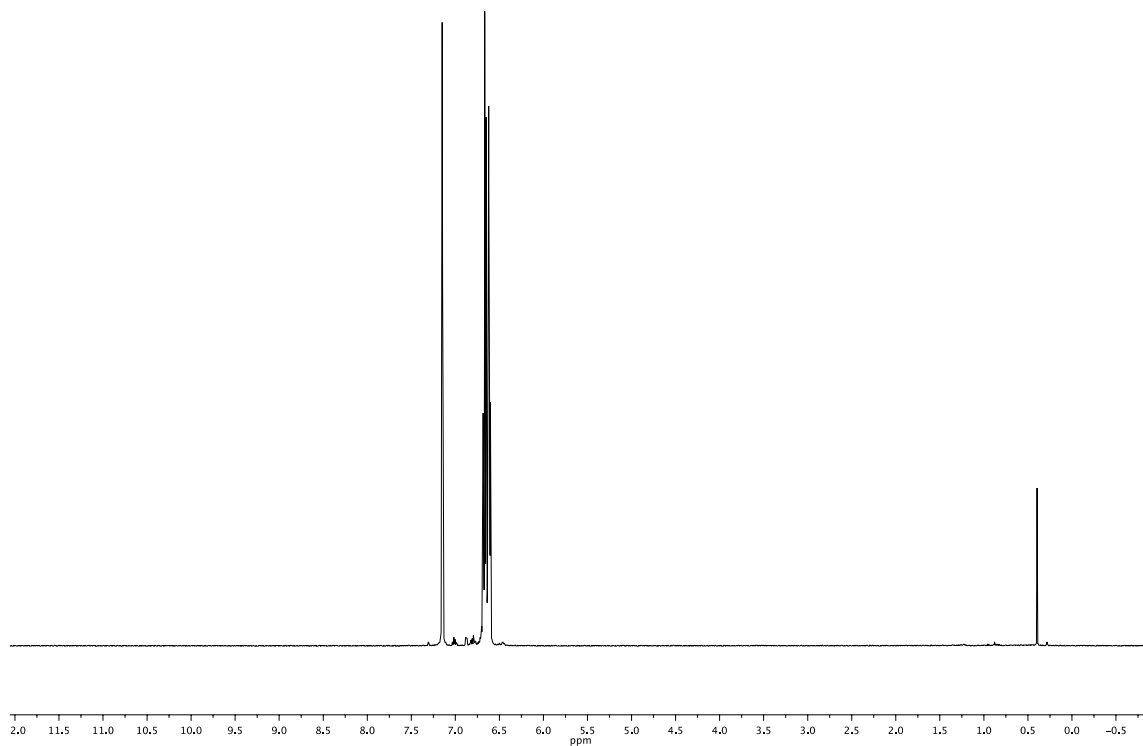


Figure 2.5 ^1H NMR spectrum (C_6D_6 , 500 MHz) of **2-7**. Water is observed in the NMR spectrum.

2-20. A Schlenk flask was charged with **2-7** (84 mg, 0.28 mmol), a stir bar, and dichloromethane (5.0 mL). Br₂ (0.30 mL) was then added drop-wise. The reaction mixture was then stirred for 3 h prior to removal of the volatiles. The resulting tan solid was then dissolved in a minimal amount of hexanes and recrystallized to yield **2-20** as colorless needles (0.14 g, 0.27 mmol, 95%). ¹H NMR (C₆D₆, Figure 2.6): δ 7.08 (dd, 3H, *J*_{HF} = 7 Hz, *J*_{HH} = 3 Hz, Ar-*H*), 6.50 (m, 3H, Ar-*H*), 6.32 (m, 3H, Ar-*H*). ¹H{¹⁹F δ -118.2} NMR (C₆D₆): δ 7.08 (d, 3H, *J*_{HH} = 3 Hz, Ar-*H*), 6.50 (dd, *J*_{HH} = 8 Hz, *J*_{HF} = 3 Hz, 3H, Ar-*H*), 6.32 (d, *J*_{HH} = 8 Hz, 3H, Ar-*H*). ¹³C{¹H} NMR (C₆D₆): δ 159.5 (d, *J*_{CF} = 245 Hz, CF), 142.2 (s), 127.6 (m), 122.1 (d, *J*_{CF} = 25 Hz), 115.1 (d, *J*_{CF} = 22 Hz), 107.9 (s). ¹⁹F NMR (C₆D₆): δ -118.2 (q, *J*_{HF} = 7 Hz). E_{1/2} = 0.67 V vs Fc/Fc⁺.

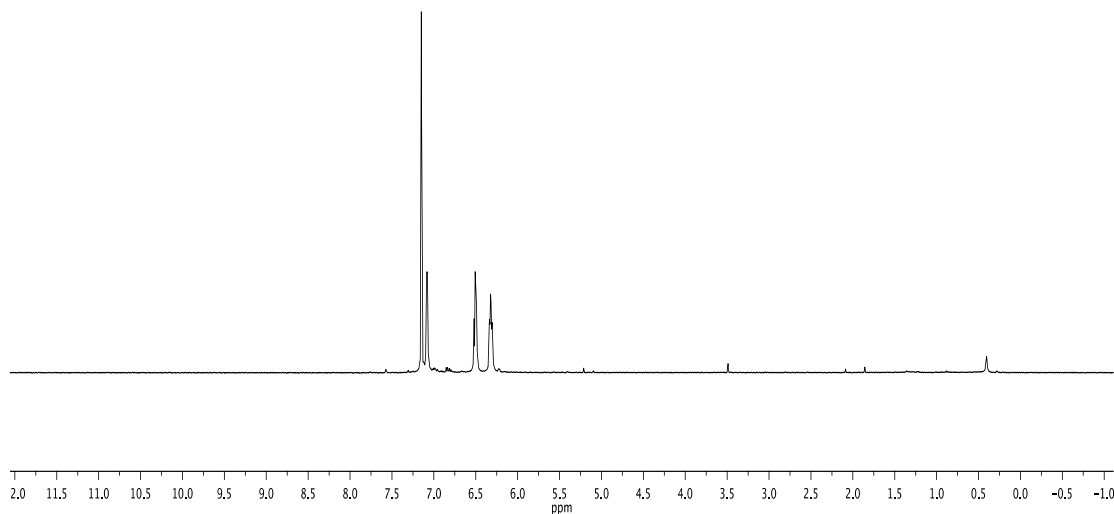


Figure 2.6 ^1H NMR spectrum of **2-20** (C_6D_6 , 500 MHz). Trace amounts of water, dichloroethane, and toluene are observed.

2-9. A Schlenk flask was charged with bis(4-fluorophenyl)amine (1.1 g, 5.3 mmol), 4-iodobenzotrifluoride (0.78 mL, 5.3 mmol), DPPF (88 mg, 0.16 mmol), $\text{Pd}(\text{OAc})_2$ (12 mg, 0.053 mmol), sodium *tert*-pentoxide (0.64 g, 5.8 mmol), a stir bar, and toluene (20 mL). The reaction was refluxed for 24 h and prior to removing the volatiles under vacuum. The resulting brown oil was taken up in hexanes and filtered through a pad of Celite and then a pad of silica gel. The colorless solution was concentrated and stored at $-35\text{ }^\circ\text{C}$. Colorless crystals were then collected and dried to yield **2-9** and a small amount of residual 4,4-bis(trifluoromethyl)-1,1-biphenyl. The biphenyl product was then removed via vacuum distillation. **2-9** was isolated as a

colorless powder (0.68 g, 1.9 mmol, 37%). ^1H NMR (C_6D_6 , Figure 2.7): δ 7.23 (d, $J_{\text{HF}} = 9$ Hz, 2H), 6.68-6.63 (m, 4H), 6.61-6.56 (m, 6H). $^{13}\text{C}\{^1\text{H}\}$ NMR (C_6D_6): δ 160.0 (d, $J_{\text{CF}} = 244$ Hz, CF), 151.1 (s), 142.9 (s), 127.4 (d, $J_{\text{CF}} = 8$ Hz), 126.7 (d, $J_{\text{CF}} = 4$ Hz), 125.6 (d, $J_{\text{CF}} = 284$ Hz, CF_3), 123.0 (d, $J_{\text{CF}} = 32$ Hz, CCF_3), 120.3 (s), 116.7 (d, $J_{\text{CF}} = 23$ Hz). ^{19}F NMR (C_6D_6): δ -63.9 (CF_3), -119.9 (CF). $E_{1/2} = 0.78$ V vs Fc/Fc^+ .

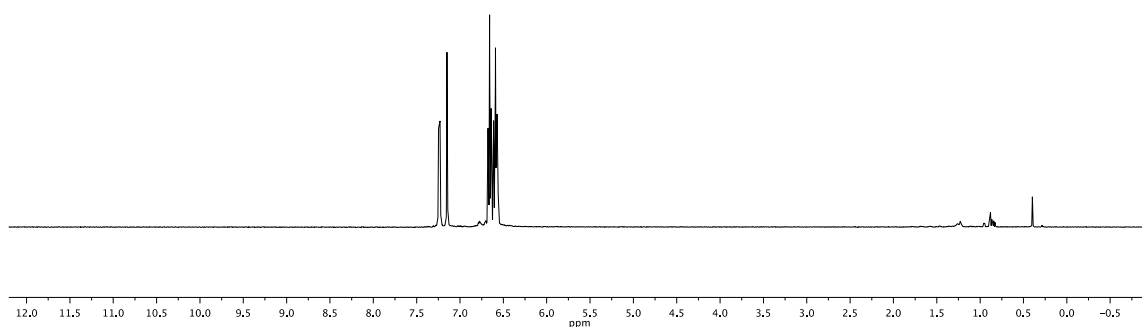


Figure 2.7 ^1H NMR spectrum of **2-9** (C_6D_6 , 500 MHz). Trace quantities of hexanes and water are observed.

2-22. A Schlenk flask was charged with **2-9** (0.16 g, 0.47 mmol), dichloromethane (10 mL) and a stir bar. Br₂ (0.30 mL) was then added drop-wise to the solution while vigorously stirring. The reaction vessel was capped with a glass stopper and stirred for an additional 18 h. The volatiles were next removed under vacuum and the resulting brown solution was washed with cold hexanes (3 × 5 mL). **2-22** was isolated as a tan powder (0.14 g, 0.23 mmol, 49%). ¹H NMR (C₆D₆, Figure 2.8): δ 7.74 (d, *J*_{HH} = 2 Hz, 1H), 7.08 (dd, *J*_{HH} = 9 Hz, *J*_{HH} = 2 Hz, 1H), 7.06-7.04 (m, 2H), 6.50-6.47 (m, 2H), 6.36 (dd, *J*_{HH} = 9 Hz, *J*_{HF} = 1 Hz, 1H), 6.31 (dd, *J*_{HH} = 9 Hz, *J*_{HF} = 5 Hz, 1H), 6.32 (dd, *J*_{HH} = 9 Hz, *J*_{HF} = 5 Hz, 1H). ¹H{¹⁹F δ -117.0} NMR (C₆D₆): δ 7.74 (d, *J*_{HH} = 2 Hz, 1H), 7.08 (dd, *J*_{HH} = 9 Hz, *J*_{HH} = 2 Hz, 1H), 7.06 (d, *J*_{HH} = 9 Hz, 2H), 6.50 (s, 1H), 6.48 (s, 1H), 6.36 (dd, *J*_{HH} = 9 Hz, *J*_{HF} = 1 Hz, 1H), 6.31 (d, *J*_{HH} = 9 Hz, 1H), 6.32 (d, *J*_{HH} = 9 Hz, 1H). ¹H{¹⁹F δ -64.4} NMR (C₆D₆): δ 7.74 (d, *J*_{HH} = 2 Hz, 1H), 7.08 (dd, *J*_{HH} = 9 Hz, *J*_{HH} = 2 Hz, 1H), 7.06-7.04 (m, 2H), 6.50-6.47 (m, 2H), 6.36 (d, *J*_{HH} = 9 Hz, 1H), 6.31 (dd, *J*_{HH} = 9 Hz, *J*_{HF} = 5 Hz, 1H), 6.32 (dd, *J*_{HH} = 9 Hz, *J*_{HF} = 5 Hz, 1H). ¹³C{¹H} NMR (C₆D₆): δ 159.9 (d, *J*_{CF} = 250 Hz, CF), 149.0 (s), 141.7 (d, *J*_{CF} = 3 Hz), 141.3 (s), 132.3 (q, *J*_{CF} = 4 Hz), 127.5 (q, *J*_{CF} = 34 Hz, CCF₃), 126.3 (s), 125.3 (q, *J*_{CF} = 4 Hz), 123.6 (q, *J*_{CF} = 273 Hz, CF₃), 122.7-122.5 (m), 122.1 (m, *J*_{CF} = 27 Hz), 120.9 (d, *J*_{CF} = 27 Hz), 115.3 (dd, *J*_{CF} = 8 Hz *J*_{CF} = 22 Hz). ¹⁹F NMR (C₆D₆): δ -64.4 (s, CF₃), -117.0 (s, F). E_{1/2} = 1.26 V vs Fc/Fc⁺.

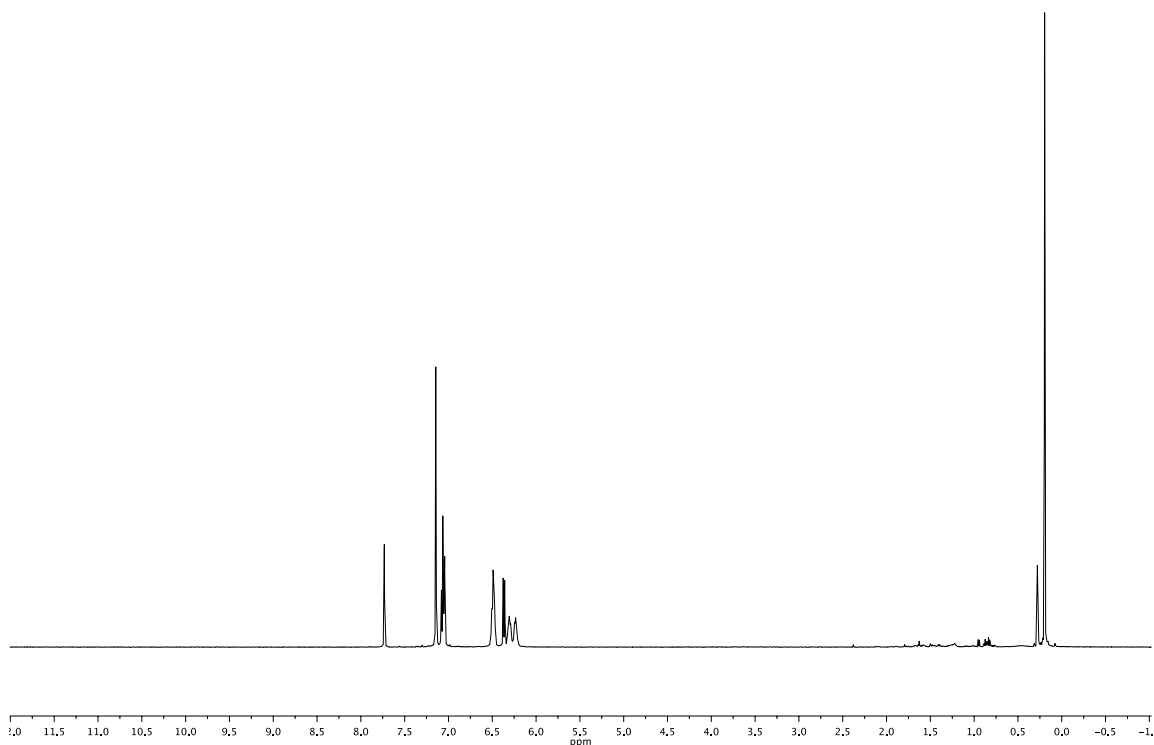


Figure 2.8 ^1H NMR spectrum of **2-22** (C_6D_6 , 500 MHz). The sample is contaminated with water and grease. These can be successfully removed via sublimation.

2-8. A Schlenk flask was charged with bis(4-fluorophenyl)amine (2.9 g, 14 mmol), phenyl iodide (1.6 mL, 14 mmol), DPPF (77 mg, 0.14 mmol), $\text{Pd}(\text{OAc})_2$ (16 mg, 0.070 mmol), sodium *tert*-pentoxide (1.7 g, 15 mmol), a stir bar, and toluene (20 mL). The reaction was then refluxed for 18 h and then the volatiles were removed under vacuum. The resulting brown oil was taken up in hexanes and filtered through a pad of Celite and then a pad of silica gel. The colorless solution was concentrated and stored at $-35\text{ }^\circ\text{C}$. The resulting colorless crystals were then collected and dried to yield **2-8** and a small amount of residual biphenyl. The biphenyl product was removed via vacuum

distillation. **2-8** was then isolated as a colorless solid (1.5 g, 5.3 mmol, 38%). ^1H NMR (C_6D_6 , Figure 2.9): δ 7.02 (t, $J_{\text{HH}} = 8$ Hz, 2H), 6.88 (d, $J_{\text{HH}} = 8$ Hz, 2H), 6.81 (t, $J_{\text{HH}} = 7$ Hz, 1H), 6.72-6.64 (m, 8H). $^{13}\text{C}\{^1\text{H}\}$ NMR (C_6D_6): δ 159.2 (d, $J_{\text{CF}} = 245$ Hz, CF), 148.4 (s), 144.3 (s), 129.6 (s), 126.2 (d, $J_{\text{CF}} = 8$ Hz), 123.3 (s), 122.7 (s), 116.3 (d, $J_{\text{CF}} = 23$ Hz). ^{19}F NMR (C_6D_6): δ -122.1 (m).

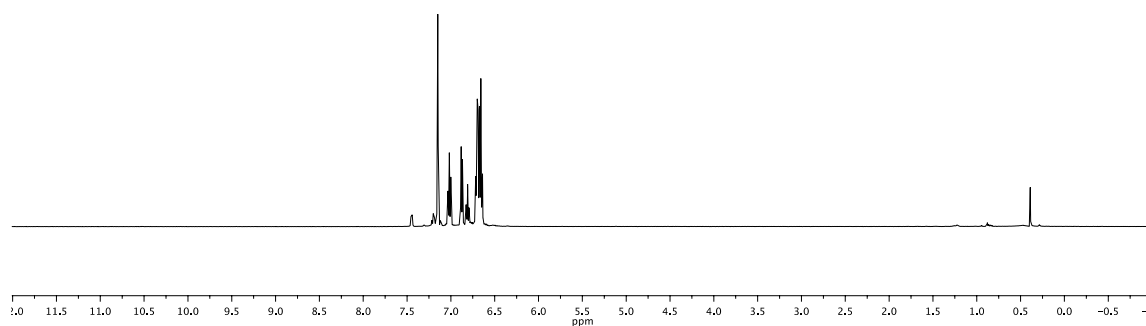


Figure 2.9 ^1H NMR spectrum (C_6D_6 , 500 MHz) of **2-8**. Trace quantities of water and hexanes are observed in addition to biphenyl (< 5% impurity).

2-25. A Schlenk flask was charged with **2-8** (342 mg, 1.22 mmol), *N*-bromosuccinimide (217 mg, 1.22 mmol), a stir bar, and dichloromethane (10 mL). The reaction mixture was stirred for 18 h and then the volatiles were removed under vacuum. The resulting solid was dissolved in hexanes and passed through a pad of silica gel. The volatiles were again removed and the solid was dissolved in a minimal amount of hexamethyldisiloxane and stored at -35 °C. The resulting colorless crystals were then collected and dried to yield **2-25** (199 mg, 0.553 mmol, 45%). ¹H NMR (C₆D₆, Figure 2.10): δ 7.11 (d, *J*_{HH} = 9 Hz, 2H), 6.65 (m, 4H), 6.59 (m, 4H), 6.51 (d, *J*_{HH} = 9 Hz, 2H). ¹H{¹⁹F δ -121.3} NMR (C₆D₆): δ 7.11 (d, *J*_{HH} = 9 Hz, 2H), 6.65 (d, *J*_{HH} = 9 Hz, 4H), 6.59 (d, *J*_{HH} = 9 Hz, 4H), 6.51 (d, *J*_{HH} = 9 Hz). ¹³C{¹H} NMR (C₆D₆): δ 159.4 (d, *J*_{CF} = 245 Hz, CF), 147.3 (s, CN), 143.7 (d, *J*_{CF} = 3 Hz, CN), 132.6 (s), 126.3 (d, *J*_{CF} = 8 Hz), 124.3 (s), 116.5 (d, *J*_{CF} = 22 Hz), 114.9 (s). ¹⁹F NMR (C₆D₆): δ -121.3 (m).

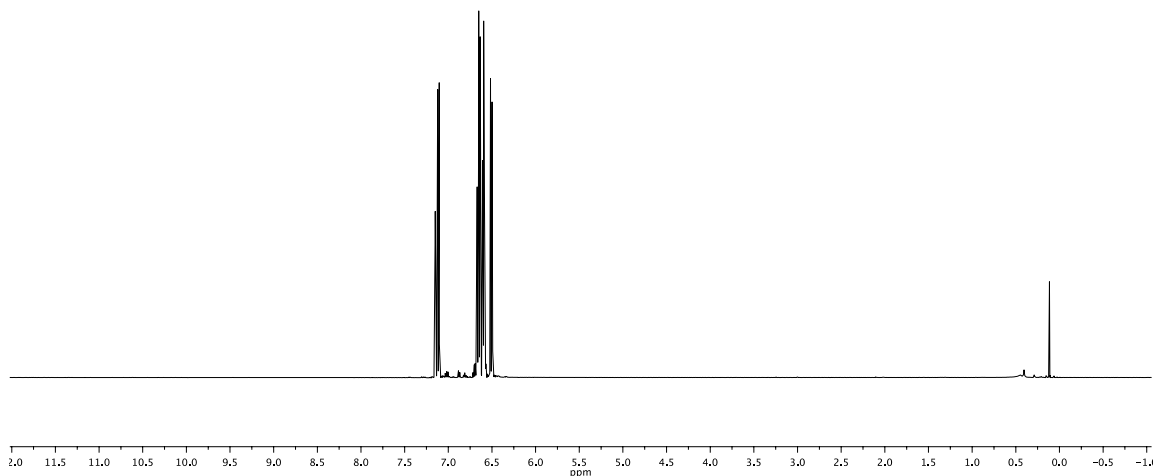


Figure 2.10 ^1H NMR spectrum of **2-25** (C_6D_6 , 500 MHz) with greater than 97% purity. Trace quantities of hexanes are observed. Silicone grease is also observed in the spectrum.

2-21. A Schlenk flask was charged with **2-8** (3.77 g, 13.4 mmol), dichloromethane (10 mL), and a stir bar. The reaction was stirred for 18 h after adding Br_2 (1.00 mL) in a drop-wise fashion. Removal of a small aliquot and analysis by ^{19}F NMR spectroscopy revealed a mixture of products. Br_2 (1.00 mL) was added a second time. The reaction was stirred for another 18 h. ^{19}F NMR analysis of a small aliquot of the reaction mixture revealed only one product at -117.7 ppm. The volatiles were next

removed under vacuum and the resulting oil was taken up in hexanes and passed through a pad of silica gel. Concentration of the solution and storage at -35 °C resulted in the formation of green needles. Sublimation of the green crystals, while being heated under vacuum, gave **2-21** as a colorless solid (5.45 mg, 9.22 mmol, 68%). ^1H NMR (C_6D_6 , Figure 2.11): δ 7.57 (d, $J_{\text{HH}} = 2$ Hz, 1H), 7.06 (dd, $J_{\text{HF}} = 8$ Hz, $J_{\text{HH}} = 3$ Hz, 2H), 6.98 (dd, $J_{\text{HH}} = 9$ Hz, $J_{\text{HH}} = 2$ Hz, 1H), 6.50 (m, 2H), 6.29 (dd, $J_{\text{HH}} = 9$ Hz, $J_{\text{HF}} = 5$ Hz, 2H), 6.22 (d, $J_{\text{HH}} = 9$ Hz, 1H). $^1\text{H}\{^{19}\text{F} \delta -117.7\}$ NMR (C_6D_6): δ 7.57 (d, $J_{\text{HH}} = 2$ Hz, 1H), 7.06 (d, $J_{\text{HH}} = 3$ Hz, 2H), 6.98 (dd, $J_{\text{HH}} = 9$ Hz, $J_{\text{HH}} = 2$ Hz, 1H), 6.50 (m, 2H), 6.29 (d, $J_{\text{HH}} = 9$ Hz, 2H), 6.22 (d, $J_{\text{HH}} = 9$ Hz, 1H). $^{13}\text{C}\{^1\text{H}\}$ NMR (C_6D_6): δ 159.7 (d, $J_{\text{CF}} = 249$ Hz, CF), 145.1 (s, CN), 142.0 (s), 141.8 (s), 137.4 (s), 137.3 (s), 131.4 (m, overlapping signals), 118.1 (s), 115.2 (d, $J_{\text{CF}} = 22$ Hz). ^{19}F NMR (C_6D_6): δ -117.7 (m). $E_{1/2} = 1.11$ V vs Fc/Fc $^+$.

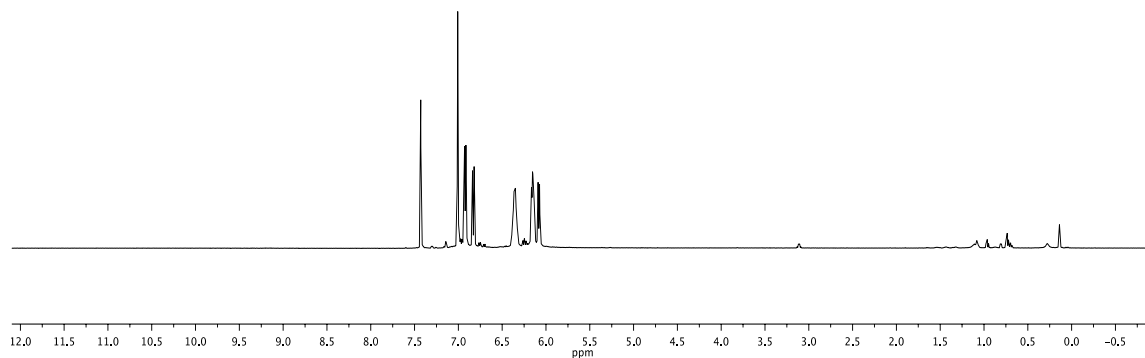


Figure 2.11 ^1H NMR spectrum (C_6D_6 , 500 MHz) of **2-21** with greater than 97% purity. Trace quantities of silicone grease, diethyl ether, and hexanes are observed.

2-11. A Schlenk flask was charged with diphenylamine (7.9 g, 0.46 mol), 4-iodobenzotrifluoride (6.7 mL, 0.46 mol), $\text{Pd}(\text{OAc})_2$ (31 mg, 0.14 mmol), DPPF (0.10 g, 0.18 mmol), sodium *tert*-pentoxide (5.0 g, 0.46 mol), a stir bar, and toluene (25 mL). The reaction was then refluxed for 24 h after which time a small aliquot was analyzed by ^{19}F NMR analysis. Two products were observed at -63.8 and -65.2 ppm. The reaction was allowed to continue refluxing for an additional 24 hours. ^{19}F NMR analysis revealed the same reaction mixture. The volatiles were removed under vacuum. The residual diarylamine and 4,4-trifluoromethyl-1,1-biphenyl were removed via distillation. The remaining brown oil was then dissolved in hexanes and passed through a pad of Celite and then a pad of silica gel. Concentration of the hexanes solution and storage at $-35\text{ }^\circ\text{C}$

resulted in copious precipitation of **2-11** as a colorless solid (7.9 g, 0.21 mol, 45%). ^1H NMR (C_6D_6 , Figure 2.12): δ 7.21 (d, $J = 9$ Hz, 2H, Ar-H), 7.02-6.99 (m, 4H, Ar-H), 6.92-6.90 (m, 4H, Ar-H), 6.84 (t, $J = 7$ Hz, 2H, Ar-H), 6.79 (d, $J = 8$ Hz, 2H, Ar-H). $^{13}\text{C}\{^1\text{H}\}$ NMR (C_6D_6): δ 151.2 (s), 147.3 (s), 129.8 (s), 129.6 (s), 129.6 (q, $J_{\text{CF}} = 4$ Hz), 125.7 (s), 124.4 (s), 121.6 (s), 118.2 (s). ^{19}F NMR (C_6D_6): δ -63.8 (CF_3).

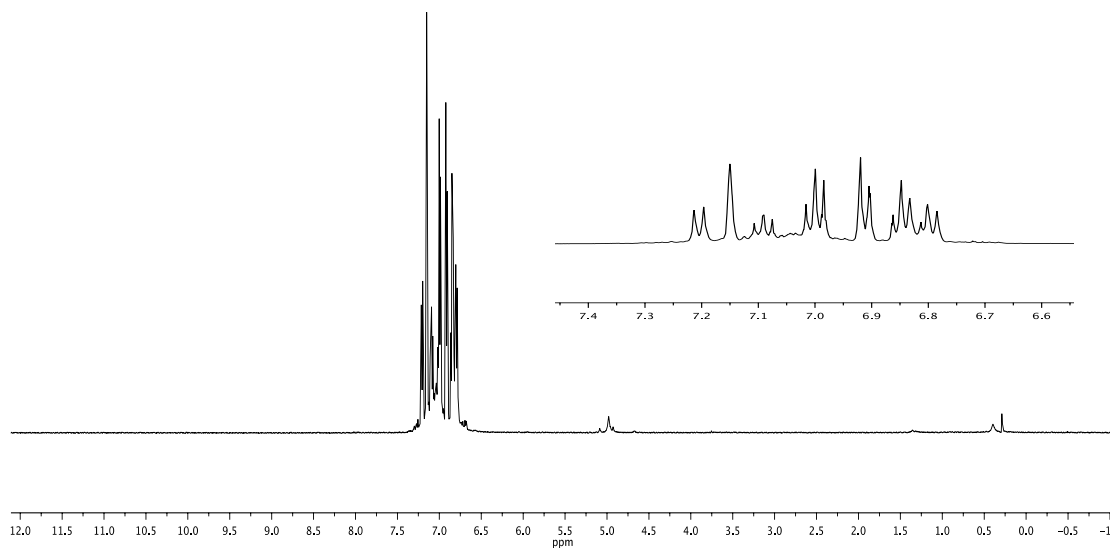


Figure 2.12 ^1H NMR spectrum of **2-11** (C_6D_6 , 500 MHz). Trace quantities of diphenylamine, water and silicone grease are observed.

2-26. A Schlenk flask was charged with **2-11** (186 mg, 0.618 mmol), dichloromethane (5 mL), and a stir bar. *N*-bromosuccinimide (219 mg, 1.30 mmol) was then added slowly. After 30 min the volatiles were removed and the resulting solid was

dissolved in hexanes and passed through a pad of Celite. The solution was then concentrated and stored at $-35\text{ }^{\circ}\text{C}$ to yield colorless crystals. ^1H NMR (C_6D_6 , Figure 2.13): δ 7.22 (d, $J = 8\text{ Hz}$, 2H, Ar-H), 7.10 (d, $J = 9\text{ Hz}$, 4H, Ar-H), 6.58 (d, $J = 8\text{ Hz}$, 2H, Ar-H), 6.41 (d, $J = 8\text{ Hz}$, 4H, Ar-H). $^{13}\text{C}\{^1\text{H}\}$ NMR (C_6D_6): δ 150.1 (s, CN), 145.7 (s, CN), 133.0 (s), 126.8 (s), 124.2 (q, $J_{\text{CF}} = 44\text{ Hz}$, CCF_3), 124.2 (d, $J_{\text{CF}} = 33\text{ Hz}$), 122.2 (s), 117.4 (s). ^{19}F NMR (C_6D_6): δ -64.0 (CF_3).

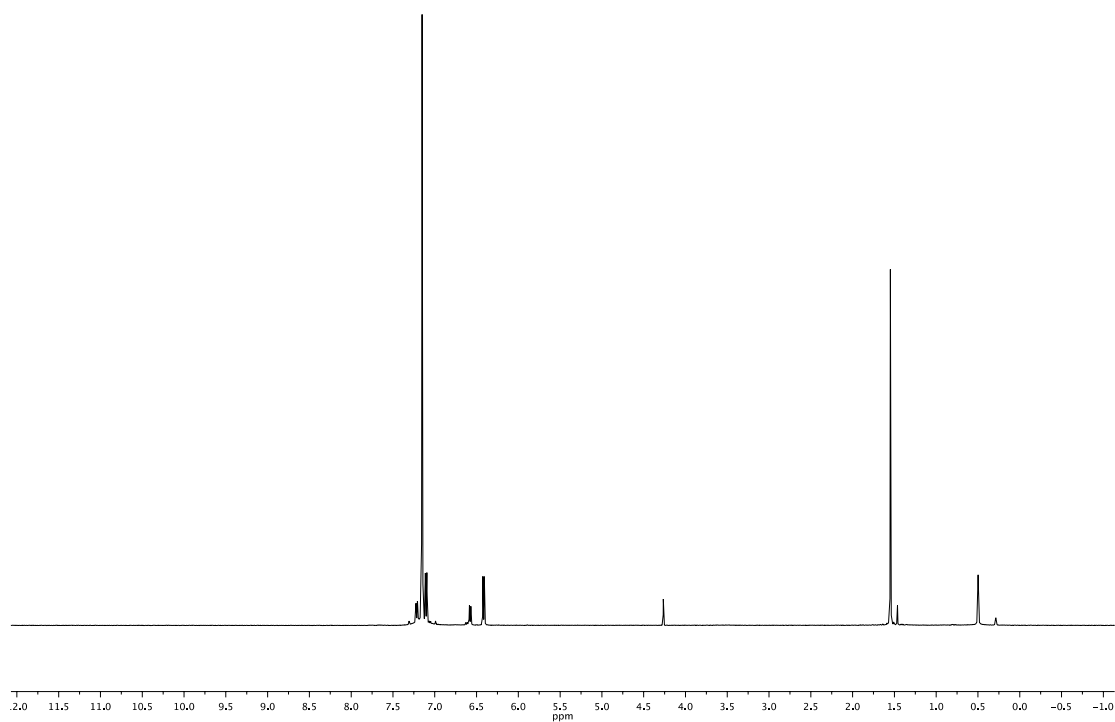


Figure 2.13 ^1H NMR spectrum (C_6D_6 , 500 MHz) of **2-26**. Acetone, water, silicone grease, and dichloromethane are observed.

2-24. A Schlenk flask was charged with **2-11** (7.90 g, 20.7 mmol), dichloromethane (25 mL) and a stir bar. Br₂ (6.00 mL, 117 mmol) was then added in a drop-wise fashion in 6 portions. The reaction was capped and stirred for 1 h. The volatiles were then removed under vacuum and the resulting brown solid was dissolved in diethyl ether and filtered through a pad of Celite. The ethereal solution was then evaporated to dryness and the resulting brown solid was taken up in a 1:6 mixture (v/v) of diethyl ether and hexanes and stored at -35 °C. The resulting solid was isolated and dried under vacuum to yield a brown solid. Sublimation of the solid gave **2-24** as a colorless solid. (8.07 g, 11.4 mmol, 55%). ¹H NMR (C₆D₆, Figure 2.14): δ 7.71 (s, 1H, Ar-H), 7.54 (s, 2H, Ar-H), 7.07 (d, *J* = 7 Hz, 1H, Ar-H), 6.96 (dd, *J* = 8 Hz, *J* = 2 Hz, 2H, Ar-H), 6.32 (d, *J* = 8 Hz, 1H, Ar-H), 6.18 (d, *J* = 8 Hz, 1H, Ar-H), 6.10 (d, *J* = 8 Hz, Ar-H). ¹³C{¹H} NMR (C₆D₆): δ 148.1 (s, CN), 143.8 (d, *J*_{CF} = 16 Hz, CN), 137.4 (s), 137.2 (s), 134.9 (s), 132.2 (d, *J*_{CF} = 4 Hz), 131.5 (d, *J*_{CF} = 4 Hz), 126.7 (s), 125.4 (q, *J*_{CF} = 4 Hz), 123.9 (q, *J*_{CF} = 270 Hz, CF₃), 122.9 (m, *J*_{CF} = 15 Hz, CCF₃), 119.2 (s), 118.9 (s). ¹⁹F NMR (C₆D₆): δ -65.8 (m).

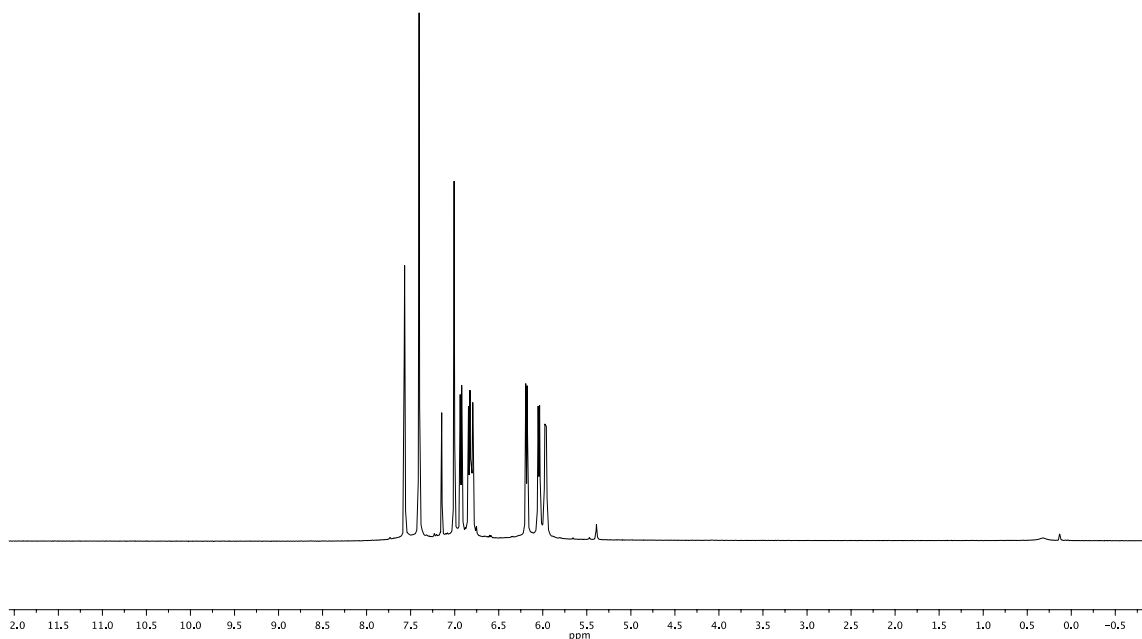


Figure 2.14 ^1H NMR spectrum of **2-24** (C_6D_6 , 500 MHz). Trace quantities of water and silicone grease are observed.

2-10. A Schlenk flask was charged with diphenylamine (0.59 g, 3.5 mmol), 3-iodobenzotrifluoride (0.50 mL, 3.5 mmol), $\text{Pd}(\text{OAc})_2$ (8.0 mg, 0.036 mmol), DPPF (58 mg, 0.10 mmol), sodium *tert*-pentoxide (0.38 g, 3.5 mmol), a stir bar, and toluene (10 mL). The reaction was then refluxed for 3 d and then the volatiles were removed under vacuum. The remaining brown oil was then dissolved in hexanes and passed through a pad of silica gel. The solution was concentrated and recrystallized at $-35\text{ }^\circ\text{C}$ to give a pale yellow oil. ^1H NMR (C_6D_6 , Figure 2.15): δ 7.47 (s, 1H), 6.98 (m, 6H), 6.91 (m, 4H), 6.81 (m, 3H). $^{13}\text{C}\{^1\text{H}\}$ NMR (C_6D_6): δ 149.0 (s, CN), 147.5 (s, CN), 132.00 (q, J_{CF}

= 32 Hz, CCF₃), 130.1 (s), 129.9 (s), 126.0 (s), 125.2 (s), 124.1 (s), 119.0 (q, $J_{CF} = 104$ Hz, CF₃). ¹⁹F NMR (C₆D₆): δ -66.5 (s).

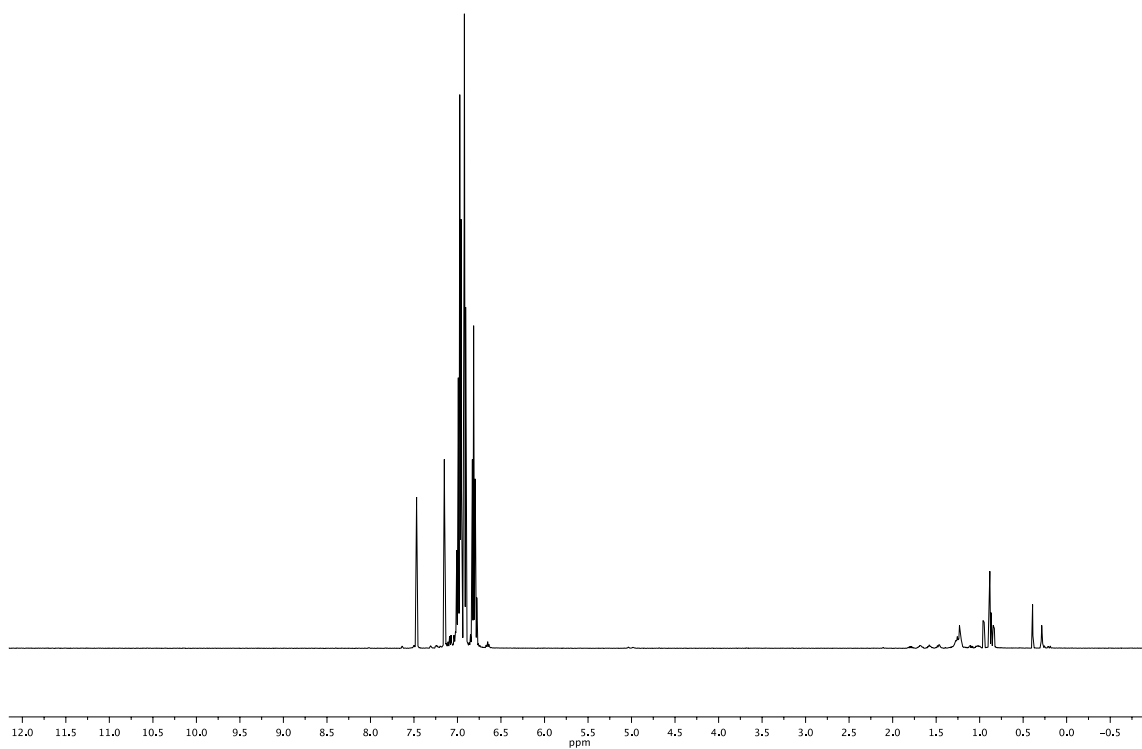


Figure 2.15 ¹H NMR spectrum of **2-10** (C₆D₆, 500 MHz). Minor quantities of hexanes, silicone grease, and water are observed.

2-23. A Schlenk flask was charged with diphenylamine (0.59 mg, 3.5 mmol), 3-iodobenzotrifluoride (0.50 mL, 3.5 mmol), Pd(OAc)₂ (8.0 mg, 0.036 mmol), DPPF (58 mg, 0.10 mmol), sodium *tert*-pentoxide (0.38 g, 3.5 mmol), a stir bar, and toluene (10

mL). The reaction was then refluxed for 3 d and then the volatiles were removed under vacuum. The remaining brown oil was dissolved in hexanes and passed through a pad of silica gel. The solution was concentrated and recrystallized at -35 °C to give a pale yellow oil (^{19}F NMR (C_6D_6): δ 66.5 (s)). No further steps to purify the compound were taken. The oil was next dissolved in dichloromethane (10 mL) and Br_2 (0.30 mL) was added drop-wise. The reaction was stirred for 1 h and then the volatiles were removed under vacuum and the resulting brown solid was washed with cold hexanes (3×10 mL). The hexane washes were then collected and dried under vacuum to yield **2-23** as a pale brown solid (0.42 g, 0.59 mmol, 17%). ^1H NMR (C_6D_6 , Figure 2.16): δ 7.47 (m, 2H), 7.20 (d, $J = 20$ Hz, 1 H), 7.04 (m, 1H), 6.92 (m, 2H), 6.38 (m, 2H). ^{19}F NMR (C_6D_6): δ -65.1 (s). $E_{1/2} = 1.17$ V vs Fc/Fc^+ .

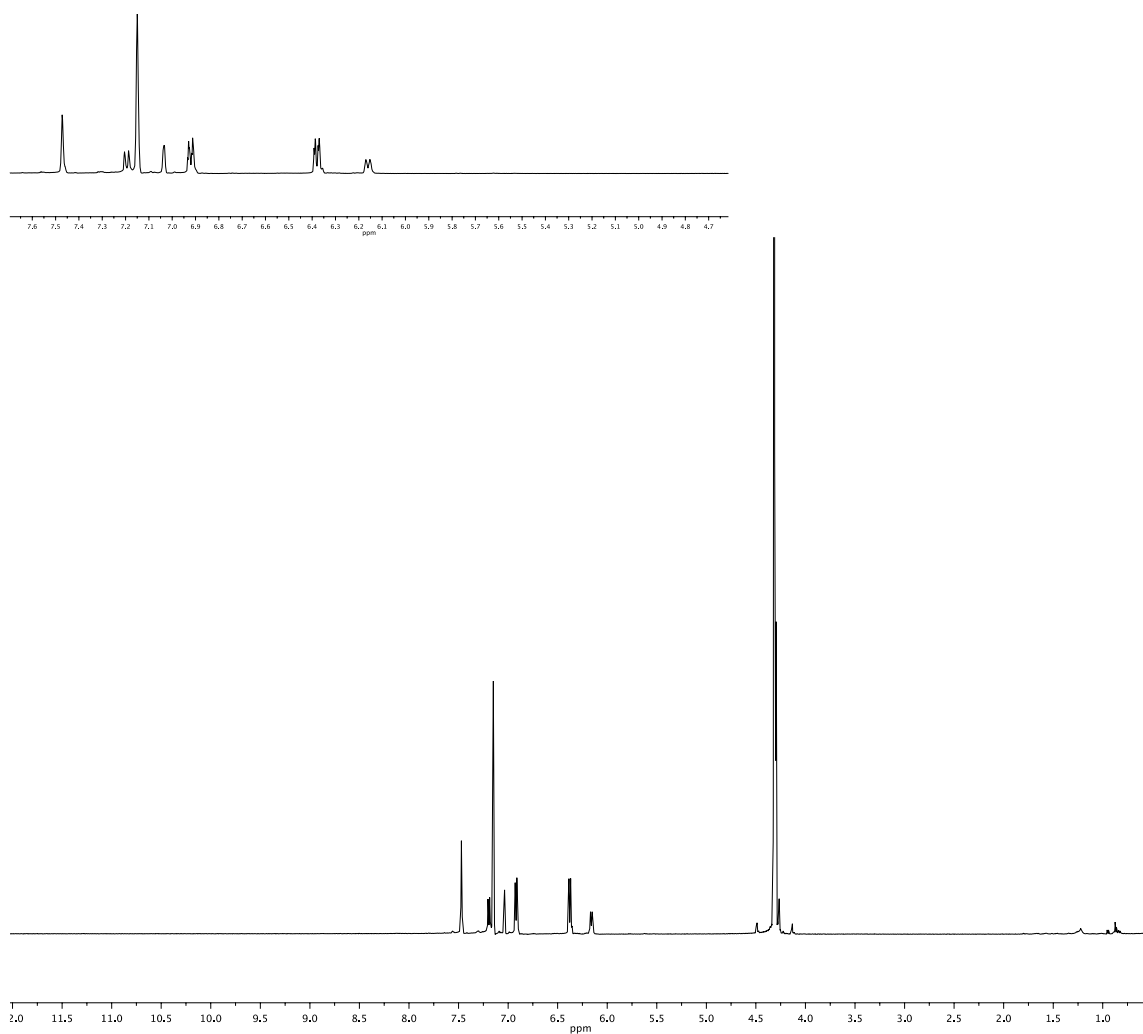


Figure 2.16 ^1H NMR spectrum of **2-23** (C_6D_6 , 500 MHz). Dichloromethane and trace quantities of hexanes are observed.

2.8.5 Reactions with tris(4-bromophenyl)amine

Reaction of 2-27 with 3 equivalents *N*-bromosuccinimide. A Schlenk flask was charged with **2-27** (110 mg, 0.228 mmol), a stir bar, and dichloromethane (5 mL). *N*-bromosuccinimide (122 mg, 0.685 mmol) was then added slowly to the solution while

stirring vigorously. After 18 h the solution was passed over a pad of Celite and the volatiles were removed under vacuum. NMR analysis of the resulting colorless solid revealed a mixture of products.

Reaction of 2-27 with Br₂. A Schlenk flask was charged with **2-27** (0.15 g, 0.31 mmol), a stir bar, and chloroform (5 mL). Br₂ (50 mg, 0.31 mmol) was then added drop-wise to the solution while stirring vigorously. After 18 h ethanol was added to the reaction mixture resulting in copious precipitation. NMR analysis of the resulting colorless solid revealed a mixture of products.

Reaction of 2-27 with Br₂ and FeBr₃. A Schlenk flask was charged with **2-27** (0.41 g, 0.86 mmol), a stir bar, FeBr₃ (20 mg), and a chloroform/trifluoroacetic acid mixture (5 mL:5 mL). Br₂ (0.89 mg, 5.6 mmol) was then added drop-wise to the solution while stirring vigorously. The reaction was then refluxed for 1 week at 100 °C resulting in a colorless precipitate. NMR analysis of the precipitate revealed a mixture of products.

Reaction of 2-27 with Br₂ and SbCl₅. A Schlenk flask was charged with **2-27** (82 mg, 0.17 mmol), a stir bar, and chloroform (5 mL). A Br₂ (0.50 ml, 9.7 mmol)/SbCl₅(1 mL) solution in dichloromethane was then added drop-wise to the solution while stirring vigorously. After 3 d the volatiles were removed and the resulting solid was dissolved in chloroform. Addition of ethanol to the chloroform solution resulted in copious precipitation. The solid was collected and washed with ethanol (3 × 5 mL). NMR analysis of the resulting colorless solid revealed a mixture of products.

2.8.6 Coupling reactions targeting diarylamines and the synthesis of **2-16**

Attempted synthesis of 2-12. A Schlenk flask was charged with bis(4-fluorophenyl)amine (1.0 g, 4.9 mmol), 3,4-difluoriodobenzene (0.56 mL, 4.9 mmol), DPPF (54 mg, 0.10 mmol), Pd(OAc)₂ (11 mg, 0.050 mmol), sodium *tert*-pentoxide (0.54 g, 4.9 mmol), a stir bar, and toluene (10 mL). The reaction mixture was then subjected to reflux for 24 h, after which a small aliquot of the reaction mixture was removed, dried under vacuum and subjected to ¹⁹F NMR analysis. Less than 10% consumption of 3,4-difluoriodobenzene is observed. Heating the reaction mixture in a 130 °C oil bath for an additional 4 d does not result in any further reactivity based on ¹⁹F NMR spectroscopy.

2-16. A Schlenk flask was charged with 3-iodobenzotrifluoride (0.92 mL, 6.4 mmol), 3,5-trifluoromethylphenylamine (1.0 mL, 6.4 mmol), Pd(OAc)₂ (14 mg, 0.064 mmol), DPPF (0.11 g, 0.19 mmol), sodium *tert*-pentoxide (0.78 mg, 7.1 mmol), a stir bar, and toluene (10 mL). The reaction was then refluxed for 5 d and then the volatiles were removed under vacuum. The remaining brown oil was then dissolved in hexanes and passed through a pad of silica gel. The solution was then concentrated and stored at -35 °C. A brown oil crashed out. The hexanes were decanted and the oil was dried under vacuum to yield **2-16** (1.5 g, 4.0 mmol, 63%) as a brown oil. ¹H NMR (C₆D₆, Figure 2.17): δ 7.33 (s, 1H), 6.98 (d, *J* = 8 Hz, 1H), 6.88 (m, 3H), 6.75 (t, *J* = 8 Hz, 1H), 6.66 (d, *J* = 7 Hz, 1H), 4.64 (s, 1H, *N-H*). ¹³C{¹H} NMR (C₆D₆): δ 144.1 (s, CN), 141.4 (s, CN), 133.0 (q, *J*_{CF} = 32 Hz, CCF₃), 132.2 (q, *J*_{CF} = 32 Hz, CCF₃), 130.3 (s), 125.2 (d, *J*_{CF} = 91 Hz, CF₃), 123.1 (d, *J*_{CF} = 91 Hz, CF₃), 125.1 (s), 120.6 (s), 119.6 (d, *J*_{CF} = 4 Hz), 116.3 (s), 114.0 (s). ¹⁹F NMR (C₆D₆): δ -65.3 (s, 3F, CF₃), -65.5 (s, 6F, CF₃).

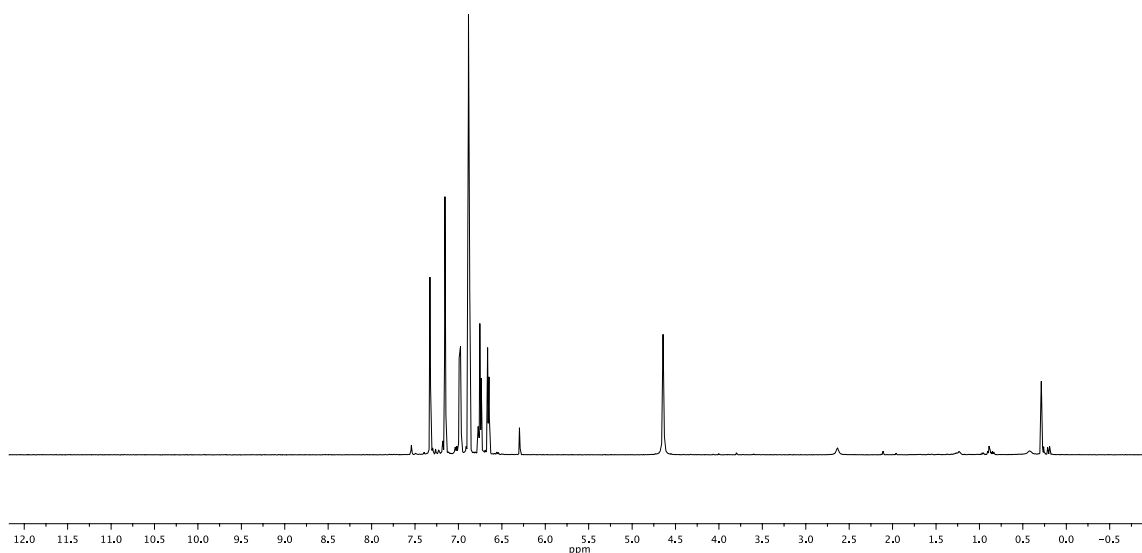


Figure 2.17 ^1H NMR spectrum of **2-16** (C_6D_6 , 95% pure, 500 MHz). Trace quantities of 3,5-trifluoromethylphenylamine are observed. In addition silicone grease and trace quantities of hexanes are observed.

Attempt to synthesize 2-18. A Schlenk flask was charged with 4-trifluoromethylphenylamine (2.0 mL, 16 mmol), 4-iodobenzotrifluoride (2.3 mL, 16 mmol), DPPF (44 mg, 0.080 mmol), $\text{Pd}(\text{OAc})_2$ (11 mg, 0.048 mmol), sodium *tert*-pentoxide (1.6 g, 16 mmol), a stir bar, and toluene (10 mL). The reaction mixture was then subjected to reflux for 18 h, after which a small aliquot of the reaction mixture was removed, dried under vacuum and subjected to ^{19}F NMR analysis. Only starting materials were observed.

Attempted synthesise 2-19. A Schlenk flask was charged with 4-trifluoromethylphenylamine (0.20 mL, 1.6 mmol), 3-iodobenzotrifluoride (0.23 mL, 1.6 mmol), DPPF (0.26 g, 0.48 mmol), Pd(OAc)₂ (36 mg, 0.16 mmol), sodium *tert*-pentoxide (0.17 g, 1.6 mmol), a stir bar, and toluene (10 mL). The reaction mixture was subjected to reflux for 5 d and then a small aliquot of the reaction mixture was subjected to ¹⁹F NMR analysis. Only starting materials were observed.

2.8.7 Unsuccessful coupling reactions targeting triarylamines

Attempted synthesis of 2-15. A Schlenk flask was charged with bis(4-fluorophenyl)amine (0.79 g, 3.8 mmol), 2,3,4,5,6-fluoroiodobenzene (0.51 mL, 3.8 mmol), DPPF (42 mg, 0.080 mmol), Pd(OAc)₂ (9.0 mg, 0.040 mmol), sodium *tert*-pentoxide (0.42 g, 3.5 mmol), a stir bar, and toluene (10 mL). The reaction mixture was then refluxed for 3 d, after which time a small aliquot of the reaction mixture was removed and subjected to ¹⁹F NMR analysis. Only starting material was observed.

Attempted synthesis of 2-14. A Schlenk flask was charged with bis(4-fluorophenyl)amine (0.93 g, 4.5 mmol), 2,6-difluoroiodobenzene (1.1 g, 4.5 mmol), DPPF (49 mg, 0.090 mmol), Pd(OAc)₂ (10 mg, 0.050 mmol), sodium *tert*-pentoxide (0.50 g, 4.5 mmol), a stir bar, and toluene (10 mL). The reaction mixture was then refluxed for 3 d, after which a small aliquot of the reaction mixture was removed and subjected to ¹⁹F NMR analysis. Only starting material was observed.

Attempted isolation of 2-17. A Schlenk flask was charged with 3,5-bis(trifluoromethyl)-*N*-(3-trifluoromethyl)phenyl)aniline (1.5 g, 4.0 mmol), phenyl

iodide (0.45 mL, 4.0 mmol), DPPF (67 mg, 0.12 mmol), Pd(OAc)₂ (45 mg, 0.20 mmol), sodium *tert*-pentoxide (0.49 g, 4.4 mmol), and toluene (30 mL). The reaction was refluxed for 5d at which time a small aliquot was removed for NMR analysis. No conversion to the desired product was observed.

Attempted synthesis of 2-12. A Schlenk flask was charged with diphenylamine (0.97 g, 5.7 mmol), 3,5-trifluoromethyliodobenzene (1.0 mL, 5.7 mmol), DPPF (64 mg, 0.12 mmol), Pd(OAc)₂ (13 mg, 0.060 mmol), sodium *tert*-pentoxide (0.63 g, 5.7 mmol), a stir bar, and toluene (10 mL). The reaction mixture was then refluxed for 24 h, after which a small aliquot of the reaction mixture was removed, dried under vacuum and subjected to ¹⁹F NMR analysis revealing a mixture of products. The reaction was refluxed for an additional 4 d, after which time the reaction was quenched with H₂O (1 mL). ¹⁹F NMR analysis revealed a mixture of product. No purification methods were attempted.

2.8.8 Synthesis of oxidant salts

2-28[CHB₁₁Cl₁₁]. A Schlenk flask was charged with Na[CHB₁₁Cl₁₁] (0.185 g, 0.34 mmol), ferrocene (62 mg, 0.34 mmol), PhI(OAc)₂ (54 mg, 0.17 mmol), and dichloromethane (10 mL). Me₃SiCl (43 μL, 0.34 mmol) was then added to the colorless solution resulting in a color change to royal blue. The solution was stirred for 30 min and then the volatiles were removed extensively under vacuum. The resulting blue powder was dissolved in dichloromethane and filtered through a pad of Celite. The solution was then layered with pentane and slow diffusion at -35 °C resulted in the isolation of

2-28[CHB₁₁Cl₁₁] (55 mg, 0.078 mmol) as a paramagnetic blue powder. No steps to further purify the material was taken.

2-28[BArF₂₀]. A Schlenk flask was charged with K[BArF₂₀] (0.49 g, 0.68 mmol), ferrocene (0.13 g, 0.68 mmol), PhI(OAc)₂ (0.11 g, 0.34 mmol) and dichloromethane (10 mL). Me₃SiCl (87 μ L, 0.68 mmol) was then added to the colorless solution resulting in a color change to royal blue. The solution was stirred for 30 min and then the volatiles were removed extensively under vacuum. The resulting blue powder was then dissolved in dichloromethane and filtered through a pad of Celite. The solution was then layered with pentane and slow diffusion at -35 °C resulted in the isolation of **2-28[BArF₂₀]** (0.41 g, 0.47 mmol) as a paramagnetic blue powder. No steps to further purify the material was taken.

2-27[CHB₁₁Cl₁₁]. A Schlenk flask was charged with Na[CHB₁₁Cl₁₁] (628 mg, 1.15 mmol), **2-27** (555 mg, 1.15 mmol), PhI(OAc)₂ (185 mg, 0.575 mmol), and dichloromethane (10 mL). Me₃SiCl (209 μ L, 1.15 mmol) was then added to the colorless solution resulting in a color change to royal blue. The solution was stirred for 30 min and then the volatiles were removed extensively under vacuum. The resulting blue powder was dissolved in dichloromethane and filtered through a pad of Celite. The solution was then layered with pentane and slow diffusion at -35 °C resulted in the isolation of **2-27[CHB₁₁Cl₁₁]** (457 mg, 40%) as a paramagnetic blue powder. Elemental Analysis Calculated: C, 22.73; H, 1.31. Found C, 22.87; H, 1.17.

2-21[CHB₁₁Cl₁₁]. A Schlenk flask was charged with Na[CHB₁₁Cl₁₁] (0.25 g, 0.46 mmol), **2-21** (0.27 g, 0.46 mmol), PhI(OAc)₂ (74 mg, 0.23 mmol), and

dichloromethane (7 mL). Me₃SiCl (58 μL, 0.46 mmol) was then added to the colorless solution resulting in a color change to green. The solution was then stirred for 30 min and then the volatiles were removed extensively under vacuum. The resulting green powder was then dissolved in dichloromethane and filtered through a pad of Celite. The solution was then layered with pentane and slow diffusion at -35 °C resulted in the isolation of a green powder. Multinuclear NMR analysis (¹H and ¹⁹F) did not reveal the characteristic peaks of **2-21** suggesting the oxidation has occurred. Elemental Analysis Calculated: C, 20.60; H, 0.91; N, 1.48, Found: C, 20.40; H, 0.90; N, 1.25.

2-24[CHB₁₁Cl₁₁]. A Schlenk flask was charged with Na[CHB₁₁Cl₁₁] (400 mg, 0.734 mmol), **2-24** (523 mg, 0.734 mmol), PhI(OAc)₂ (118 mg, 0.367 mmol), and dichloromethane (10 mL). Me₃SiOTf (132 μL, 0.734 mmol) was then added to the colorless solution resulting in a color change to royal blue. The solution was stirred for 30 min and then the volatiles were removed extensively under vacuum. The resulting blue powder was then dissolved in dichloromethane and filtered through a pad of Celite. The solution was then layered with pentane and slow diffusion at -35 °C resulted in the isolation of **2-24[CHB₁₁Cl₁₁]** (864 mg, 0.700 mmol, 95%) as a blue powder. Elemental Analysis Calculated: C, 19.54; H, 0.82; N, 1.14, Found: C, 19.87; H, 0.75; N, 1.03.

Reaction of 2-24[CHB₁₁Cl₁₁] with ferrocene. A J. Young tube was charged with **2-24[CHB₁₁Cl₁₁]** (32 mg, 0.029 mmol), ferrocene (6.2 mg, 0.033 mmol), C₆F₆ (4.0 μL, 0.034 mmol), and C₆D₆ (1.2 mL). An immediate solution color change from blue to yellow is observed in conjunction with formation of blue crystals. ¹H NMR analysis demonstrates formation of one equivalent of **2-24** (Figure 2.18). A signal corresponding

to ferrocene was still observed but was shifted to 4.23 ppm and was very broad. By ^{19}F NMR analysis approximately one equivalent of amine was observed relative to the C_6F_6 .

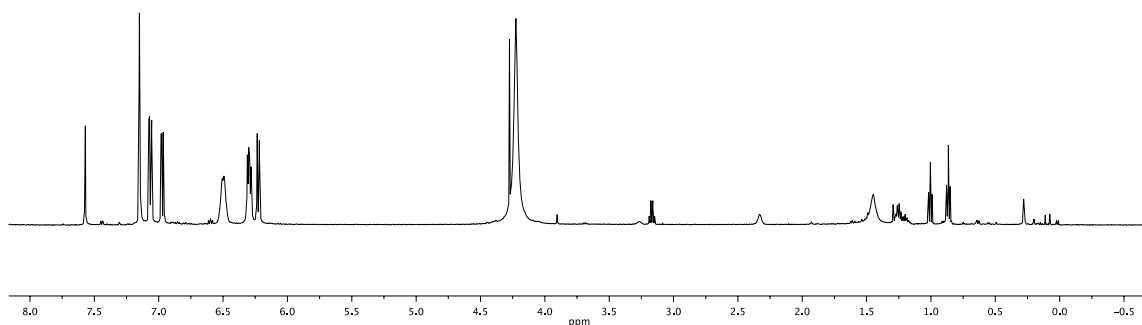


Figure 2.18 ^1H NMR analysis of the reaction of **2-24**[**CHB₁₁Cl₁₁**] with ferrocene in the presence of C_6F_6 in C_6D_6 (500 MHz). The spectrum is contaminated with silicone grease, diethyl ether, hexanes and dichloromethane.

2-24[**CMeB₁₁Cl₁₁**]. A Schlenk flask was charged with $\text{Na}[\text{CMeB}_{11}\text{Cl}_{11}]$ (65 mg, 0.12 mmol), **2-24** (84 mg, 0.12 mmol), $\text{PhI}(\text{OAc})_2$ (19 mg, 0.058 mmol), and dichloromethane (4 mL). Me_3SiOTf (22 μL , 0.12 mmol) was then added to the colorless solution resulting in a color change to royal blue. The solution was stirred for 30 min and then the volatiles were removed extensively under vacuum. The resulting blue powder was then dissolved in dichloromethane and filtered through a pad of Celite. The solution was layered with pentane and slow diffusion at $-35\text{ }^\circ\text{C}$ resulted in the isolation of **2-24**[**CMeB₁₁Cl₁₁**] (0.11 g) as a blue powder.

Attempted isolation of 2-24[CHB₁₁Cl₁₁] with Me₃SiCl. A Schlenk flask was charged with Na[CHB₁₁Cl₁₁] (0.13 g, 0.24 mmol), **2-24** (0.17 mg, 0.24 mmol), PhI(OAc)₂ (39 mg, 0.12 mmol), and dichloromethane (5 mL). Me₃SiCl (39 μ L, 0.24 mmol) was then added to the colorless solution. No color change was observed. The solution was stirred for 1 h and then the volatiles were removed extensively under vacuum. The neutral amine is observed by multinuclear NMR analysis (¹H and ¹⁹F) suggesting the oxidation has not occurred.

Attempted isolation of 2-24[CHB₁₁Cl₁₁] using SO₂Cl₂ as the oxidant. A Schlenk flask was charged with Na[CHB₁₁Cl₁₁] (94 mg, 0.17 mmol), **2-24** (0.12 g, 0.17 mmol), and dichloromethane (5 mL). SO₂Cl₂ (8.5 μ L, 0.17 mmol) was then added to the colorless solution. No color change was observed. An excess of SO₂Cl₂ (40 μ L, 0.82 mmol) was added and the reaction was stirred for 1 h, resulting in a blue solution. The volatiles were removed extensively under vacuum. The resulting blue powder was then dissolved in dichloromethane and filtered through a pad of Celite. The solution was then layered with pentane and slow diffusion at -35 °C resulted in the isolation of blue crystals. Multiple diamagnetic signals were observed by ¹⁹F signals (δ -64.32 (s), -64.36 (s), -64.56 (s), -64.66 (s), -64.81 (s)).

2.8.9 Reactions with hexamethylbenzene

Reaction hexamethylbenzene with 2-24[CHB₁₁Cl₁₁]. A Schlenk flask was charged with **2-24[CHB₁₁Cl₁₁]** (0.21 g, 0.17 mmol), C₆Me₆ (23 mg, 0.17 mmol), and dichloromethane (5 mL). The reaction was stirred for 20 min resulting in a brown

solution. The solution was then concentrated and layered with pentane. Slow diffusion resulted in the formation of brown crystals that were collected and washed with pentane (2×5 mL). The solid was then dried to yield 0.10 g. IR: 3023 (CH of carborane), 2962 (broad cluster), 1689, 1591, 1464, 1296, 814 cm^{-1} .

Reaction of hexamethylbenzene with 2-24[CM₆B₁₀Cl₁₁]. A Schlenk flask was charged with **2-24** (86 mg, 0.12 mmol), Na[CM₆B₁₀Cl₁₁] (66 mg, 0.12 mmol), PhI(OAc)₂ (19 mg, 0.060 mmol), and dichloromethane (5 mL). Me₃SiCl (15 μL , 0.12 mmol) was then added to the colorless solution resulting in a color change to royal blue. The reaction was stirred for 30 min and then C₆Me₆ (19 mg, 0.12 mmol) was added to the flask resulting in an immediate color change from blue to purple. The volatiles were then removed and the resulting purple oil was washed with pentane (3×5 mL). The solid was then dried to yield 53 mg of purple powder.

Reaction of hexamethylbenzene with Me₃SiCl, Na[CHB₁₀Cl₁₁], and PhI(OAc)₂. A Schlenk flask was charged with Na[CHB₁₀Cl₁₁] (0.16 mg, 0.30 mmol), C₆Me₆ (48 mg, 0.30 mmol), PhI(OAc)₂ (48 mg, 0.15 mmol) and dichloromethane (4 mL). Me₃SiCl (37 μL , 0.30 mmol) was then added to the colorless solution. No reaction is observed (indicated by the observation of the tris(4-bromophenyl)amine by ¹H NMR spectroscopy and by the lack of a color change).

Reaction of hexamethylbenzene with Me₃SiOTf, Na[CHB₁₀Cl₁₁], and PhI(OAc)₂. A Schlenk flask was charged with Na[CHB₁₀Cl₁₁] (71 mg, 0.13 mmol), C₆Me₆ (21 mg, 0.13 mmol), PhI(OAc)₂ (21 mg, 0.064 mmol), and dichloromethane (4 mL). Me₃SiOTf (23 μL , 0.13 mmol) was then added to the colorless solution resulting in

a color change to red. The solution was stirred for 30 min, the volatiles were removed under vacuum. The resulting red oil was dissolved in dichloromethane and filtered through a pad of Celite. Removal of the volatiles resulted in the isolation of a red oil. Hexamethylbenzene is not observed by ^1H NMR analysis, but a broad signal at 13.6 was observed to form over time.

Reaction of hexamethylbenzene with Me_3SiOTf , $\text{Na}[\text{CMeB}_{11}\text{Cl}_{11}]$, and $\text{PhI}(\text{OAc})_2$. A J. Young tube was charged with $\text{Na}[\text{CMeB}_{11}\text{Cl}_{11}]$ (50 mg, 0.089 mmol), C_6Me_6 (17 mg, 0.089 mmol), $\text{PhI}(\text{OAc})_2$ (14 mg, 0.045 mmol), and CD_2Cl_2 (1 mL). Me_3SiOTf (16 μL , 0.08 mmol) was then added to the colorless solution resulting in a solution color change to red. Within minutes a red oil also appeared. The solution was then filtered through a pad of Celite and then the volatiles were removed under vacuum to yield a brown solid. Analysis of the solid by ^1H NMR revealed signals corresponding to coordinated diethyl ether (which is indicative of $\text{Na}[\text{CMeB}_{11}\text{Cl}_{11}]$), and hexamethylbenzene.

Reaction of two equivalents of hexamethylbenzene with Me_3SiOTf , $\text{Na}[\text{CMeB}_{11}\text{Cl}_{11}]$, and $\text{PhI}(\text{OAc})_2$. A J. Young tube was charged with $\text{Na}[\text{CMeB}_{11}\text{Cl}_{11}]$ (50 mg, 0.089 mmol), C_6Me_6 (33 mg, 0.18 mmol), $\text{PhI}(\text{OAc})_2$ (14 mg, 0.045 mmol), and CD_2Cl_2 (1 mL). Me_3SiOTf (16 μL , 0.08 mmol) was then added to the colorless solution resulting in a solution color change to purple. The solution was then filtered through a pad of Celite and then the volatiles were removed under vacuum to yield a purple oil. Analysis of the oil by ^1H NMR revealed signals corresponding to phenyl iodide and a broad signal at 13.6 ppm.

2.8.10 Reactions with Au

[Au(P^tBu₃)₂]Cl (2-31[Cl]).⁹⁹ A Schlenk flask was charged with chloro(tetrahydrothiophene)gold(I) (108 mg, 0.270 mmol), a stir bar, and diethyl ether (5.0 mL). Tri-*tert*-butylphosphine (109 mg, 0.540 mmol) was then added to the ethereal solution and stirred for 1 h. The volatiles were then removed under vacuum and the resulting colorless solid was washed with cold pentane (3 × 2 mL). The solid was then dried under vacuum to yield **2-31[Cl]** (147 mg, 0.231 mmol). No attempts at further purification were undertaken. ¹H NMR (C₆D₆): δ 0.99 (d, *J*_{PH} = 14 Hz, ^tBu). ³¹P{¹H} NMR (C₆D₆): δ 89.2 (m).

[Au(P^tBu₃)₂][CHB₁₁Cl₁₁] (2-31[CHB₁₁Cl₁₁]). A Schlenk flask was charged with **2-29[Cl]** (126 mg, 0.198 mmol), Na[CHB₁₁Cl₁₁] (108 mg, 0.198 mmol) and dichloromethane (4 mL). The solution was stirred for 1 h, and then analysis of a small aliquot by ³¹P{¹H} NMR spectroscopy revealed only one product. The solution was then filtered through a pad of Celite and the volatiles were removed under vacuum. **2-31[CHB₁₁Cl₁₁]** was isolated a colorless powder (160 mg, 0.139 mmol). No attempts to purify the powder were taken. ¹H NMR (CD₂Cl₂, Figure 2.19): δ 3.26 (s, CHB₁₁Cl₁₁), 1.56 (m, ^tBu). ¹H{³¹P δ 97.2} NMR (C₆D₆, Figure 2.19): δ 3.26 (s, CHB₁₁Cl₁₁), 1.5 (s, ^tBu). ³¹P{¹H} NMR (C₆D₆): δ 97.2 (s).

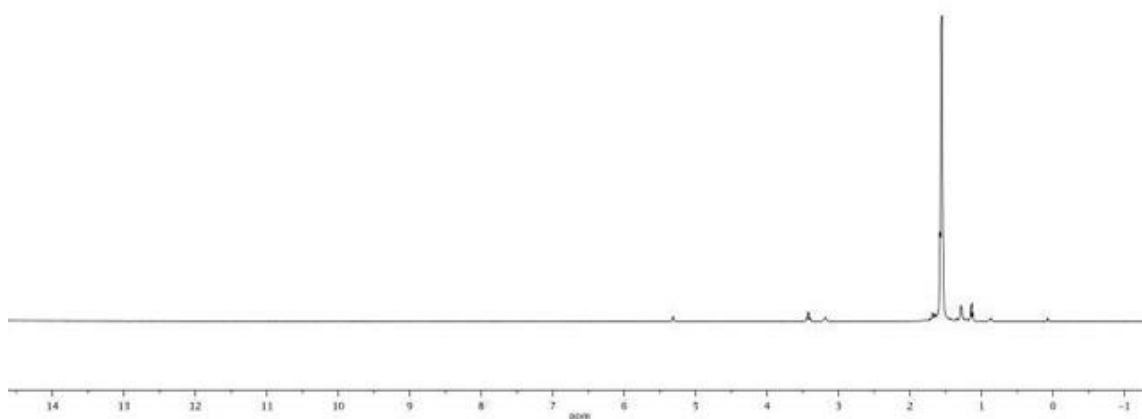


Figure 2.19 ^1H NMR (CD_2Cl_2 , 500 MHz) of **2-31[CHB₁₁Cl₁₁]** (<95%). Trace quantities of pentane, diethyl ether and **2-31[Cl]** are observed.

Reaction of 2-31[CHB₁₁Cl₁₁] with 2-24[CHB₁₁Cl₁₁]. A J. Young tube was charged in **2-29[Cl]** (31 mg, 0.054 mmol), Na[CHB₁₁Cl₁₁] (29 mg, 0.054 mmol) and CD_2Cl_2 (1 mL). The reaction was placed in a 50 °C oil bath for 1 hr. ^1H NMR analysis revealed complete conversion to **2-31[CHB₁₁Cl₁₁]**. $^{31}\text{P}\{^1\text{H}\}$ NMR (C_6D_6): δ 97.2 (s). **2-24[CHB₁₁Cl₁₁]** (66 mg, 0.054 mmol) was then added to the J. Young tube resulting in a color change to brown. ^{19}F NMR analysis reveals a signal at δ -63.4 ppm corresponding to the reduced amine. The reaction mixture was then filtered through a pad of Celite and layered with pentane. Storage of the dichloromethane/pentane solution

at -35 °C for 2 h resulted in the formation brown needles which were collected and washed two times with pentane. (76 mg).

2.8.11 X-Ray data collection, solution, and refinement for 2-31[CHB₁₁Cl₁₁]

X-Ray data collection, solution, and refinement for 2-31[CHB₁₁Cl₁₁]. X-ray quality crystals of 2-31[CHB₁₁Cl₁₁] were obtained from slow diffusion of pentane into a dichloromethane solution of 2-31[CHB₁₁Cl₁₁] stored at -35 °C. A colorless, multi-faceted block of suitable size (0.32 × 0.20 × 0.1 mm) was selected from a representative sample of crystals of the same habit using an optical microscope and mounted onto a nylon loop. Low temperature (110 K) X-ray data were obtained on a Bruker APEXII CCD based diffractometer (Mo sealed X-ray tube, K_α = 0.71073 Å). All diffractometer manipulations, including data collection, integration and scaling were carried out using the Bruker APEXII software.¹⁰⁷ An absorption correction was applied using SADABS.¹⁰⁷ The space group was determined on the basis of systematic absences and intensity statistics and the structure was solved by direct methods and refined by full-matrix least squares on F^2 . The structure was solved in the monoclinic Pnma space group using XS¹⁰⁸ (incorporated in SHELXTL). All non-hydrogen atoms were refined with anisotropic thermal parameters. The structure was brought to convergence by weighted full-matrix least-squares refinement on $|F|^2$, and the final structure converged to $R_1 = 0.0352$ and $wR_2 = 0.0976$.

CHAPTER III
COMPARISON OF ELECTRONIC PROPERTIES OF DIARYLAMIDO-BASED
PNX PINCER LIGANDS: REDOX ACTIVITY AT THE LIGAND AND DONOR
ABILITY TOWARDS THE METAL

3.1 Introduction

The reactivity of a metal complex as a whole is derived from the interactions between the metal center and its surrounding ligands. It is common to employ supporting, ancillary ligands to define the coordination sphere of the reactive transition metal site. In the traditional approach, the steric and electronic nature of the ancillary ligands is taken advantage of to modulate the reactivity at the metal center, but the ancillary ligands themselves remain “spectators”^{19b} and preserve their connectivity, composition, and charge. Recently, another approach to the utilization of supporting ligands has emerged in which they are designed to remain bound to the metal center, but undergo chemical changes over the course of reactions. These ligands are often referred to as non-innocent and assist the metal center in carrying out desired transformations, most commonly by accepting or losing protons²⁷ or electrons.

Redox-active non-innocent ligands have attracted significant attention.^{37a} These ligands provide a site other than the metal center for redox events to occur, serve as electron or hole reservoirs, and can be used to modify the electronic properties of the metal center. Common redox non-innocent ligand scaffolds include dithiolates,³⁸ semiquinones,^{10a,39} amido phenolates,⁴⁰ diimines,⁴¹ and terpyridines.⁴² Redox non-

innocent ligands are seen as a promising tool in enabling two-electron reactivity in the 3d metal series, a process necessary for organometallic catalysis.²⁶ Arguably the most prominent example of this approach is the use of Fe complexes of 2,6-bis(imino)pyridine ligands (**A**, Figure 3.1) which catalyze ethylene polymerization,⁴⁵ [2+2] cycloadditions,⁴⁶ enyne cyclizations,⁴⁷ hydrogenation of olefins, alkynes and aryl azides,^{46a,48} and hydrosilylation.⁴⁹ Ligand **A** is an example of a non-innocent ligand capable of undergoing reduction vs its closed-shell (neutral) form. As a tridentate, meridionally chelating ligand, it can also be characterized as a pincer ligand. Pincer ligands that are oxidizable have largely been based on the diarylamido backbone. Heyduk has reported the NNN^{10b,109} (**B**, Figure 3.1) and ONO¹¹ (**C**, Figure 3.1) redox non-innocent trianionic ligands, the former of which promotes catalytic nitrene transfer by complexes of a redox-inactive d⁰ metal.^{10b} Our own group in collaboration with Nocera et al.,¹¹⁰ as well as Mindiola, Szilagy, and Meyer investigated the redox non-innocence of the PNP (**D**, Figure 3.1) ligand,¹¹¹ while Hu and Vicic reported on the non-innocence of [NNN]⁻ pincer ligands such as **E** (Figure 3.1).^{112,113}

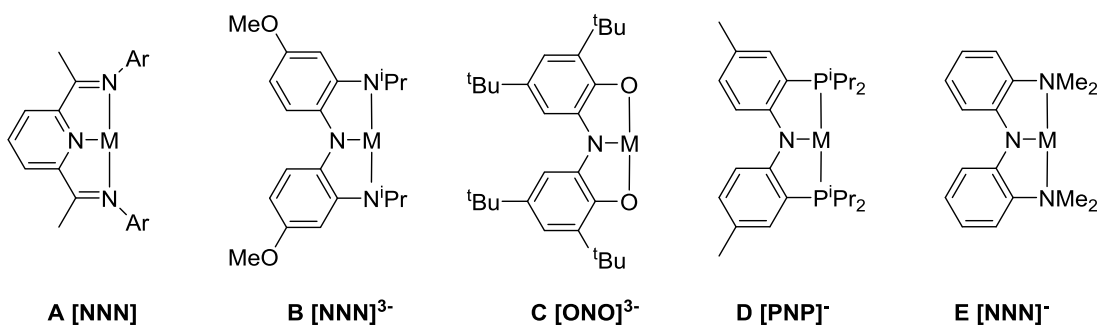


Figure 3.1 Redox active pincer ligands denoted by their three donor atoms and showing the charge of the closed-shell form.

Owing to the convenient modularity of the diarylamido scaffold, a large number of derived pincer ligands have been reported including various PNP,^{6,114-115} SNS,¹¹⁶ NNN,¹¹⁷ and PNN¹¹⁸ ligands. In this report we aimed to analyze an array of diarylamido-based pincer complexes in order to systematically examine the effects of various substituents on the redox properties and on the overall donating ability of the pincer ligand toward the metal in group 10 and rhodium complexes. In this chapter, analysis of three classes of ligands (Figure 3.2) is presented: C_{2v} symmetric PNP pincer ligands (contain two identical phosphine arms), C_s symmetric PNN ligands, and C_s symmetric PNP' ligands (contain two different phosphine arms). The PNP' ligands containing phosphines substituted with fluorinated alkoxy groups were inspired by the reports of Milstein,^{21a} Roddick,^{17b} and van Koten^{17a} describing aryl(bisphosphine) PCP pincer ligands with electron-withdrawing substituents on the phosphorus atoms.

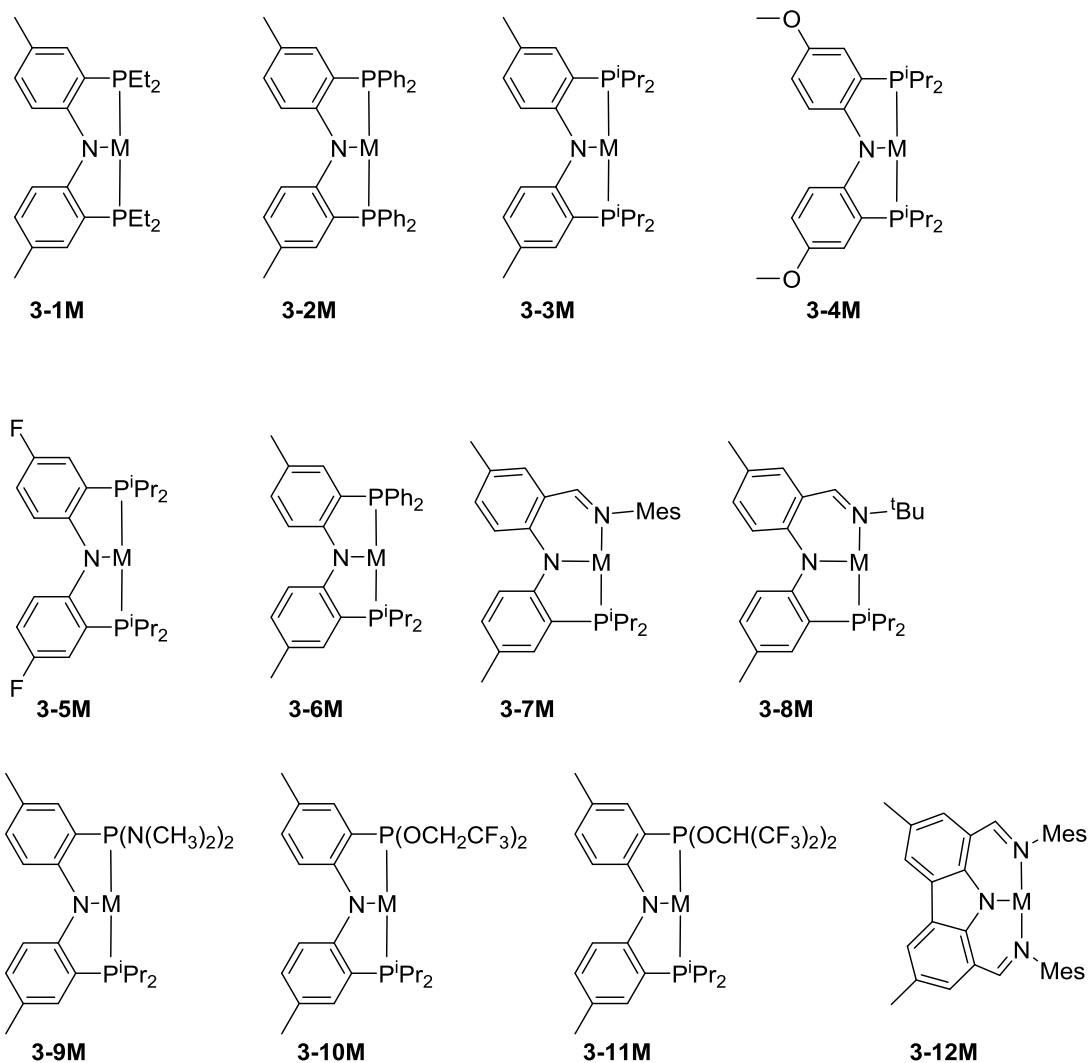


Figure 3.2 Generic complexes of pincer ligands under study in this work.

3.2 Ligand Synthesis and Characterization

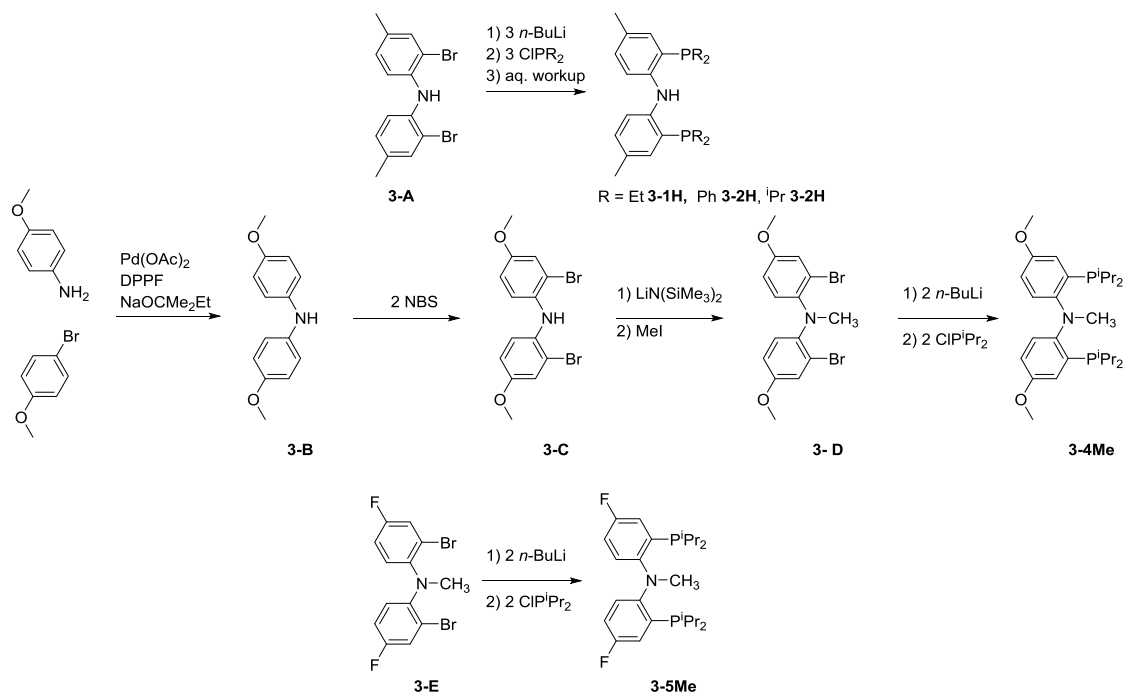
3.2.1 Synthesis of C_{2v} symmetric PNP ligands

PNP ligands can be prepared in their NH form (i.e., **3-1H**, **3-2H**, **3-3H**⁶), or the NMe form (i.e., **3-4Me**, **3-5Me**^{114c}). We have previously reported that N-methylated

PNP ligands with two PⁱPr₂ arms can give rise to group 9 and 10 PNP complexes via N–Me cleavage at the metal center.^{114b-c} Jessica DeMott found that the synthesis of the new ligand **3-1H** closely followed our previous syntheses of **3-2H** and **3-3H** (Scheme 3.1). Trilithiation of a common precursor **3-A** with three equivalents of *n*-butyllithium followed by reaction with three equivalents ClPEt₂ yielded **3-1H** as a yellow oil upon hydrolytic workup (Scheme 3.1). Analysis of the oil by ¹H NMR spectroscopy revealed that it was a mixture that contained 87% composition of **3-1H**; however, the crude ligand without further purification was adequate for the synthesis of **3-1PdCl** (*vide infra*).

The preparation of **3-4Me** was carried out analogously to the synthesis of **3-5Me** (Scheme 3.1). Buchwald-Hartwig coupling of *p*-anisidine and *p*-bromoanisole produced bis(*p*-methoxyphenyl)amine (**3-B**).^{87f-i} *Ortho*-bromination of **3-B** with two equivalents of *N*-bromosuccinimide followed by *N*-methylation gave the key precursor **3-D**. Addition of two equivalents of *n*-butyllithium and subsequent quenching with ⁱPr₂PCl gave **3-4Me** in a 93% yield. It is possible to make **3-4H** via trilithiation of **3-C** and subsequent quenching with ClPⁱPr₂; however, we found that this route was subject to poor yields (24%); a result of multiple product formation.

Scheme 3.1 Synthetic routes to C_{2v} symmetric ligands.

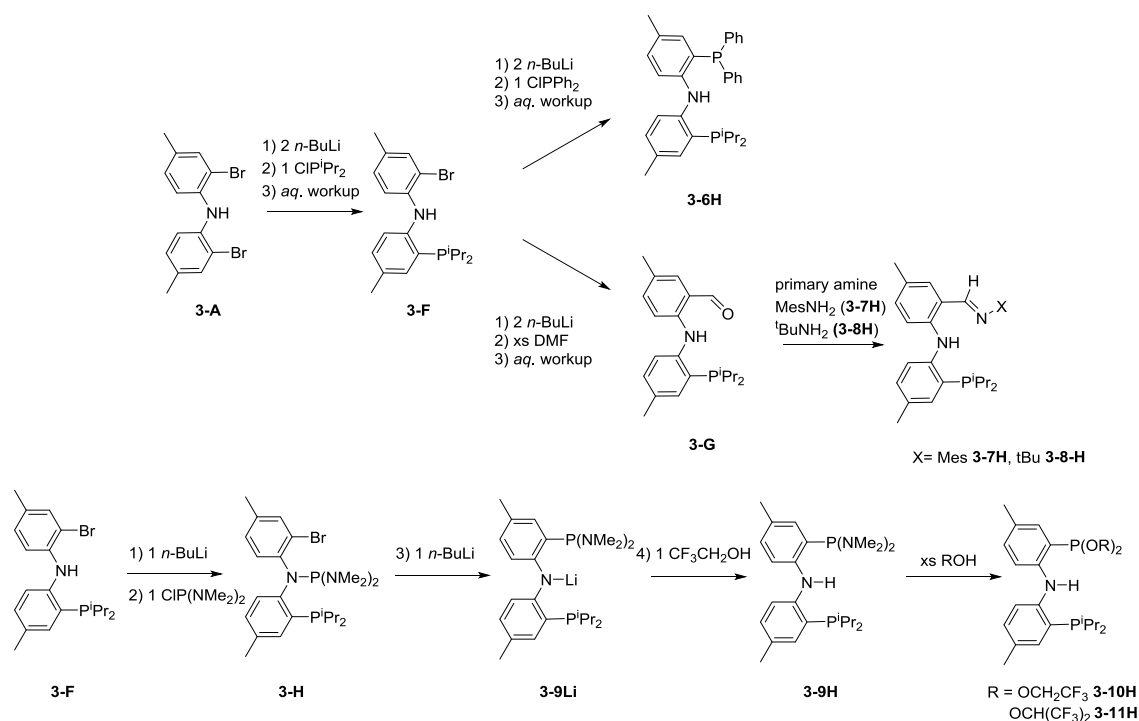


3.2.2 Synthesis of C_s symmetric PNP and PNN ligands

Our syntheses of the C_s -symmetric PNP and PNN ligands (Scheme 3.2) rely on the conveniently accessible common precursor **3-F**. Its preparation by selective lithiation/phosphination of **3-A** was previously reported by our group in 2011 when we used it for the synthesis of binucleating PNN ligands via **3-G**.^{118a} The new monomeric PNN ligands **3-7H** and **3-8H** were synthesized analogously, via Schiff-base condensation between **3-G** and a primary amine (2,4,6-trimethylaniline or *tert*-butylamine) in the presence of an acid catalyst (Scheme 3.2). **3-7H** and **3-8H** were isolated as yellow solids in 71% and 87% yields respectively.

3-6H was produced by dilithiation of **3-F** with two equivalents of *n*-butyllithium, followed by addition of one equivalent of ClPPh₂. Aqueous workup and recrystallization in a pentane/toluene mixture yielded **3-6H** as a colorless solid with a moderate yield of 62%. Our synthesis of **3-6H** closely follows the synthesis of a related C_s-symmetric PNP' ligand differing from **3-6H** only in the absence of the Me groups *para* to the nitrogen on the diarylamine backbone by Liang et al.¹¹⁹ **3-6H** itself was previously reported by Goldberg et al.^{118b}

Scheme 3.2 Synthetic routes to C_s symmetric pincer ligands.



The synthesis of **3-10H** and **3-11H** was envisaged to proceed via alcoholysis of **3-9H** (Scheme 3.2). **3-9H** could not be synthesized from **3-F** in the exact manner used for **3-6H**, where dilithiation of **3-F** was followed by selective C-phosphination. Instead, the synthesis of **3-9H** was carried out in a stepwise manner. Deprotonation of **3-F** with one equivalent of *n*-butyllithium, followed by N-phosphination with one equivalent of ClP(NMe₂)₂ produced **3-H**. The net migration of the P(NMe₂)₂ group to the *ortho*-carbon of the aryl ring to give **3-9Li** was then observed upon addition of a second equivalent of *n*-butyllithium. Controlled protolysis of **3-9Li** with trifluoroethanol occurs readily and can be monitored via the disappearance of the yellow color of the reaction mixture. It is imperative that only one equivalent of trifluoroethanol is added to the reaction, because **3-9H** is susceptible to excess trifluoroethanol. **3-9H** was isolated as a white powder in a 78% yield. **3-10H** and **3-11H** were then formed by treatment of **3-9H** with an excess of trifluoroethanol or hexafluoroisopropanol, respectively. **3-10H** was obtained in greater than 98% yields as a colorless oil (>95% purity) upon removal of volatiles *in vacuo*. Isolation of **3-11H** by simple exposure to vacuum was not possible as formation of side products was evident by NMR spectroscopy. This was circumvented by producing the ligand *in situ* and then reacting it directly with a metal precursor (*vide infra*).

3.3.3 NMR characterization of the pincer ligands

All of the ligands synthesized above were characterized in solution by multinuclear NMR spectroscopy. Table 3.1 reports the corresponding chemical shifts of their ³¹P NMR and ¹H NMR (N–H or N–Me) resonances, as well as the symmetry observed by NMR spectroscopy at ambient temperature. Free ligands with two different

PR₂ groups displayed no discernible spin-spin coupling between the two inequivalent ³¹P nuclei. The N–H hydrogens of PNP and PNN ligands resonate at chemical shifts similar to those previously reported for similar pincer ligands.^{114c,118b,114d} Other spectroscopic details for the individual ligands can be found in the experimental section of this chapter.

Table 3.1 NMR data for PNP and PNN pincer ligands in C₆D₆.

pincer	δ, ³¹ P NMR	δ, ¹ H NMR	Symmetry in solution
3-F	-13.9 P ⁱ Pr ₂	7.69 (d, NH 10 Hz)	C _s
3-6H	-16.1 PPh ₂ -14.2 P ⁱ Pr ₂	Overlapping with Ar signals	C _s
3-G	-8.0 P ⁱ Pr ₂	10.69 (s, NH)	C _s
3-7H	-5.8 P ⁱ Pr ₂	11.33 (s, NH)	C _s
3-8H	-7.3 P ⁱ Pr ₂	11.80 (s, NH)	C _s
3-9H	98.2 P(NMe ₂) ₂ -13.1 P ⁱ Pr ₂	8.55 (d, NH, 8 Hz)	C _s
3-10H	166.3 P(OCH ₂ CF ₃) ₂ -15.0 P ⁱ Pr ₂	7.43 (d, NH, 5 Hz)	C _s
3-11H	215.2 P(OCH(CF ₃) ₂) ₂ 35.9 P ⁱ Pr ₂ (CF ₃) ₂ CHOH)	NA ^a	C _s
3-1H	-36.5 PEt ₂	7.87 (t, NH, 8 Hz)	C _{2v}
3-2H	-18.9 PPh ₂	7.08 (t, NH, 6 Hz)	C _{2v}
3-3H	-12.9 P ⁱ Pr ₂	8.23 (t, NH, 8 Hz)	C _{2v}
3-4Me	-6.3 P ⁱ Pr ₂	3.48 (s, NCH ₃)	C _{2v}
3-5Me	-6.2 P ⁱ Pr ₂	3.27 (s, NCH ₃)	C _{2v}

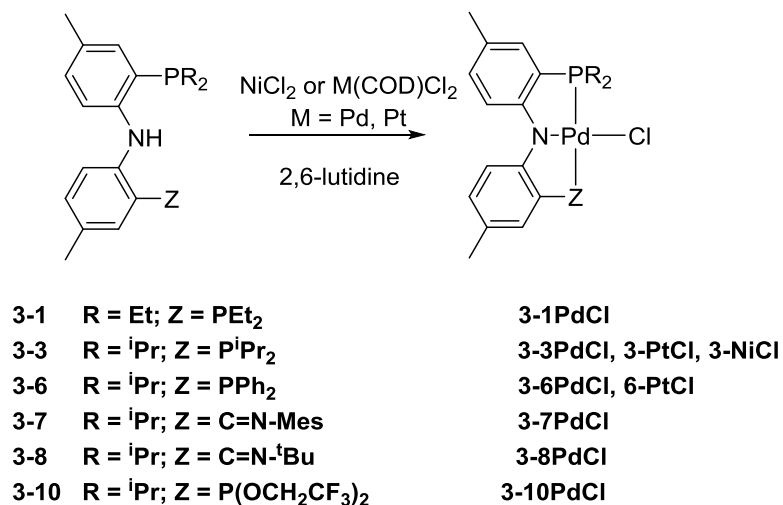
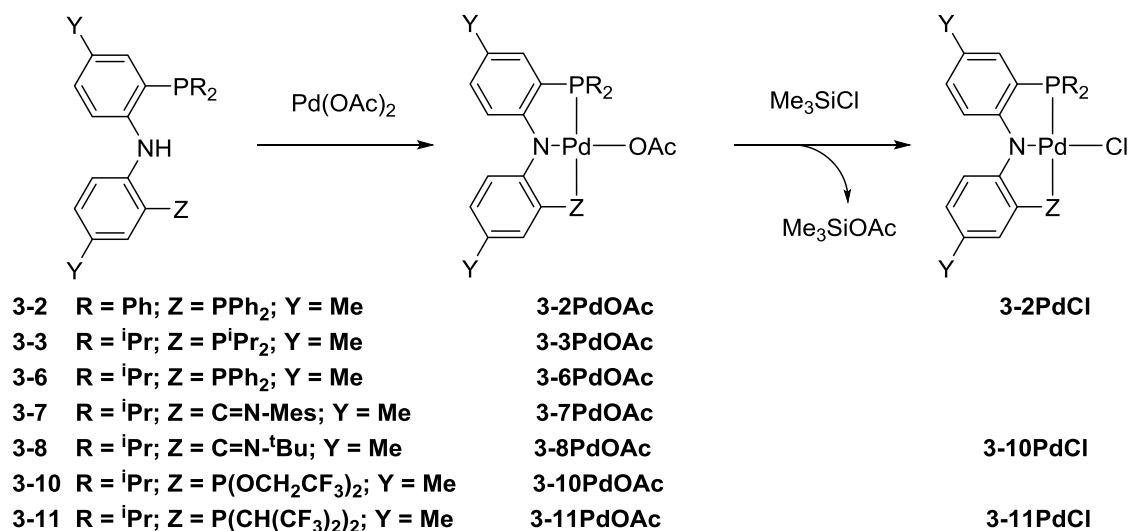
^a **3-11H** was not isolated; the spectra were collected in the reaction mixture in hexafluoroisopropanol.

3.3 Synthesis of Group 10 Pincer Complexes

The PNP and PNN ligands discussed in this publication are ideally suited to support a variety of square-planar pincer complexes of the general formula (PNZ)MX

(M = Ni, Pd, Pt; Z = P, N; X = OAc, Cl). Two forms of the ligand precursor (N–H or N–Me) were used to introduce the amido-PNX ligand into the coordination sphere of a group 10 metal. In the case of the (PNZ)H form of the ligand, the direct reaction of the neutral pincer with a group 10 metal halide (Pd(COD)Cl₂, NiCl₂ or Pt(COD)Cl₂) or acetate (Pd(OAc)₂) precursor generated (PNZ)MX. When a group 10 metal halide was the reagent, addition of a base such as 2,6-lutidine was necessary to remove the net HCl by-product observed in the formation of (PNZ)MCl. In the case of Pd(OAc)₂, the addition of a base was not necessary and the reaction produced (PNZ)PdOAc in conjunction with an equivalent of acetic acid as a by-product. Compounds **3-1PdCl**, **3-3PdCl**,^{114b} **3-6PdCl**,^{118b} **3-7PdCl**, **3-8PdCl**, and **3-10PdCl** were prepared by stirring one equivalent of the corresponding free ligand, with one equivalent of both 2,6-lutidine and Pd(COD)Cl₂ in diethyl ether. The colorless solution immediately became red demonstrating conversion to the desired complexes with concomitant formation of a lutidinium chloride salt and free 1,5-cyclooctadiene. **3-6PtCl** and **3-3PtCl**^{114b} were prepared in an analogous manner by treatment of one equivalent of the corresponding free ligand with one equivalent of both Pt(COD)Cl₂ and 2,6-lutidine. Compound **3-3NiCl** was synthesized by heating a benzene solution of **3-3H** with one equivalent of anhydrous NiCl₂ and one equivalent of 2,6-lutidine for 18 h.^{114b} Compounds **3-2PdOAc**,^{114c} **3-6PdOAc**, **3-7PdOAc**, **3-8PdOAc**, **3-10PdOAc**, and **3-11PdOAc** were all synthesized by stirring the corresponding free ligand and Pd(OAc)₂ in diethyl ether for 1 h. These reactions are demonstrated graphically in Scheme 3.3.

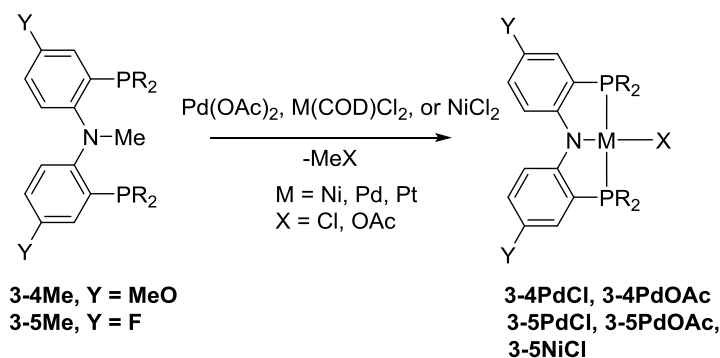
Scheme 3.3 N-H cleavage by Pd(II).



In the case of (PNP)Me precursors **3-4Me** and **3-5Me**, the free ligand was reacted with a group 10 metal halide precursor (Pd(COD)Cl₂, NiCl₂ or Pt(COD)Cl₂) to produce (PNP)MCl and an equivalent of MeCl by N–C cleavage (Scheme 3.4).^{114c}

3-4PdCl was prepared from the reaction of **3-4Me** and Pd(COD)Cl₂ in toluene. The reaction mixture was heated in an 80 °C oil bath for 3 d. Upon workup **3-4PdCl** was isolated as a green powder in a 41% yield. The analogous compound **3-4PdOAc** was synthesized from the reaction of **3-4Me** and Pd(OAc)₂. **3-5PdCl**, **3-5PtCl**, and **3-5NiCl** were prepared by heating a benzene solution of **3-5Me** with Pd(COD)Cl₂, Pt(COD)Cl₂ or NiCl₂ for 18 h.^{114c} The acetate ligand in (PNZ)PdOAc can be conveniently exchanged for chloride by reaction with Me₃SiCl, resulting in the formation of (PNZ)PdCl and expulsion of one equivalent of Me₃SiOAc. This synthetic route was used to prepare compounds **3-3PdCl**, **3-4PdCl**, **3-8PdCl**, and **3-11PdCl**. In addition the acetate ligand in (PNZ)PdOAc can also be sometimes exchanged for a triflate by treatment with Me₃SiOTf, resulting in the formation of (PNZ)PdOTf and expulsion of one equivalent of Me₃SiOAc. This synthetic route was used to prepare compounds **3-2PdOTf**, **3-8PdOTf**, and **3-11PdOTf**.

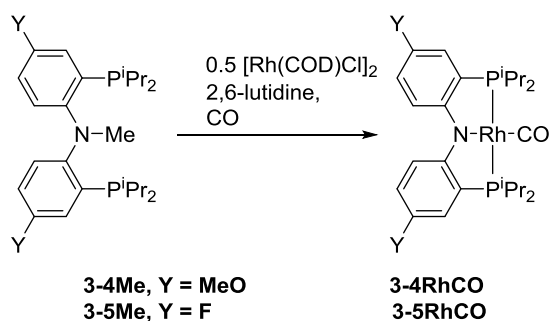
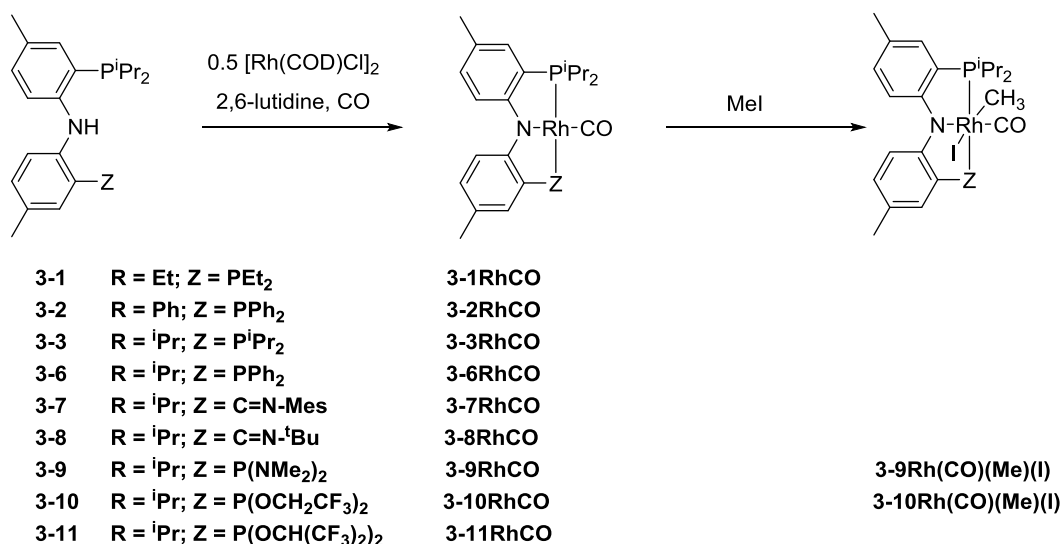
Scheme 3.4 N–Me cleavage



3.4 Synthesis of (Pincer)RhCO Complexes

(Pincer)RhCO complexes were all synthesized through the reaction of a pincer ligand with 0.5 equivalents of $[\text{Rh}(\text{COD})\text{Cl}]_2$ in the presence of one equivalent of 2,6-lutidine under 1 atm of carbon monoxide (Scheme 3.5). The (pincer)Rh-CO complexes **3-1RhCO**, **3-2RhCO**, **3-3RhCO**,^{21b} **3-4RhCO**, **3-5RhCO**,^{21b} **3-6RhCO**, **3-7RhCO**, **3-8RhCO**, **3-9RhCO**, **3-10RhCO**, and **3-11RhCO** were all synthesized by the given route. These complexes were all isolated as brown, yellow, or orange powders and have been fully characterized by infrared and multinuclear NMR spectroscopy. Treatment of **3-10RhCO** with an excess of methyl iodide resulted in a drastic color change from blue to red and formation of the Rh(III) complex **3-10Rh(CO)(Me)(I)** (Scheme 3.5). **3-10Rh(CO)(Me)(I)** was isolated as a 6-coordinate complex, evidenced by the observation of a CO stretching frequency at 2052 cm^{-1} by infrared spectroscopy. Attempts to remove the CO ligand were not successful. **3-10Rh(CO)(Me)(OAc)** was isolated by treatment of **3-10Rh(CO)(Me)(I)** with AgOAc. This reactivity closely mimicked the reactivity observed for **3-9RhCO**, which also formed a Rh(III) 6-coordinate complex (**3-9Rh(CO)(Me)(I)**) in the presence of MeI. However, in this case the CO ligand was found to be labile and could be removed under vacuum when being irradiated with light from a 500 W halogen lamp.

Scheme 3.5 Synthetic route to (pincer)RhCO complexes.



3.5 Characterization of RhCO and Pd Pincer Complexes

Spectroscopic and experimental data associated with the pincer complexes prepared in this work can be found in Table 3.2 and the experimental section of this chapter. It can be generally noted that metallation was accompanied by a downfield shift of the $^{31}\text{P}\{^1\text{H}\}$ NMR signal. In the case of the C_s symmetric (PNP')M complexes large $^2J_{\text{PP}}$ values were observed, characteristic for spin-spin coupling between two

inequivalent *trans*-phosphines. These $^2J_{PP}$ values were generally greater for PdCl complexes (>400 Hz) than for RhCO complexes (<350 Hz) and were largest for complexes of ligands **3-10H** and **3-11H**. The fluoroalkoxy-substituted phosphorus atoms also displayed the largest $^1J_{Rh-P}$ values.

The NMR spectra of **3-1PdCl**, **3-1PdOAc**, **3-2PdCl**, **3-2RhCO**, **3-3RhCO**, **3-3PdCl**, **3-3PdOAc**, **3-4PdCl**, **3-4PdOAc**, and **3-4RhCO** were consistent with C_{2v} symmetry on the NMR timescale. **3-6PdCl**, **3-6RhCO**, **3-6PdOAc**, **3-9RhCO**, **3-10PdCl**, **3-10PdOAc**, **3-10RhCO**, **3-11PdCl**, **3-11PdOAc**, and **3-11RhCO** exist as C_s symmetric complexes in solution. On the other hand, **3-7PdCl**, **3-7PdOAc**, **3-7RhCO**, **3-8PdCl**, **3-8PdOAc**, and **3-8RhCO** are consistent with C_1 symmetry on the NMR time scale. The lower symmetry of the PNN pincer complexes suggests that the “flipping” of the two aromatic rings of the diarylamido backbone past each other is significantly slower in the PNN pincer complexes than in the PNP systems. The symmetry of these complexes is reflective of the symmetry observed for the binucleating PNN ligand complexes previously reported.^{118a}

Table 3.2 NMR features of (pincer)RhCO and (pincer)PdX complexes.

Complex	³¹ P NMR (C ₆ D ₆) δ ppm	<i>J</i> _{Rh-P} (Hz)	<i>J</i> _{P-P} (Hz)	Color	Symmetry
3-2RhCO	41.3 (d)	135		Orange	C _{2v}
3-3RhCO	61.5 (d)	131		Yellow	C _{2v}
3-4RhCO	62.0 (d)	135		Brown	C _{2v}
3-5RhCO	61.5 (d)	130		Yellow	C _{2v}
3-6RhCO	64.7 (dd, P ⁱ Pr ₂)	133	270	Red	C ₁
	39.2 (dd, PPh ₂)	134			
3-7RhCO	76.3 (d)	130		Red	C ₁
3-8RhCO	78.7 (d)	154		Yellow	C _s
3-9RhCO	130.9	163	315	Red	C _s
	(dd, P(NMe ₂) ₂)	123			
	58.7 (dd, P ⁱ Pr ₂)				
3-10RhCO	190.7	190	346	Red	C _s
	(dd, P(OCH ₂ CF ₃) ₂)	125			
	60.1 (dd, P ⁱ Pr ₂)				
3-11RhCO	207.5	195	340	Yellow	C _{2v}
	(dd, P(OCH(CF ₃) ₂))	127			
	59.3 (dd, P ⁱ Pr ₂)				
3-1PdCl	33.5 (s)			Red	C _{2v}
3-2PdCl	30.2 (s)			Green	C _{2v}
3-4PdCl	47.9 (s)			Green	C _{2v}
3-6PdCl	54.0 (d, P ⁱ Pr ₂)		438	Red	C _s
	25.9 (d, PPh ₂)				
3-7PdCl	70.3 (s)			Red	C ₁
3-8PdCl	70.4 (s)			Red	C ₁
3-10PdCl	159.2 (d, P(OCH ₂ CF ₃) ₂)		545	Purple	C _s
	53.5 (d, P ⁱ Pr ₂)				
3-11PdCl	172.3 (d, P(OCH(CF ₃) ₂) ₂)		525	Purple	C _s
	57.9 (d, P ⁱ Pr ₂)				
3-2PdOAc	28.9 (s)			Red	C _{2v}
3-4PdOAc	48.1 (s)			Red	C _{2v}
3-6PdOAc	25.8 (d, P ⁱ Pr ₂)		412	Red	C _s
	55.8 (d, PPh ₂)				
3-7PdOAc	65.6 (s)			Red	C ₁
3-8PdOAc	66.3 (s)			Red	C ₁
3-11PdOAc	176.2 (d, P(OCH(CF ₃) ₂) ₂)		517	Purple	C _s
	58.6 (d, P ⁱ Pr ₂)				

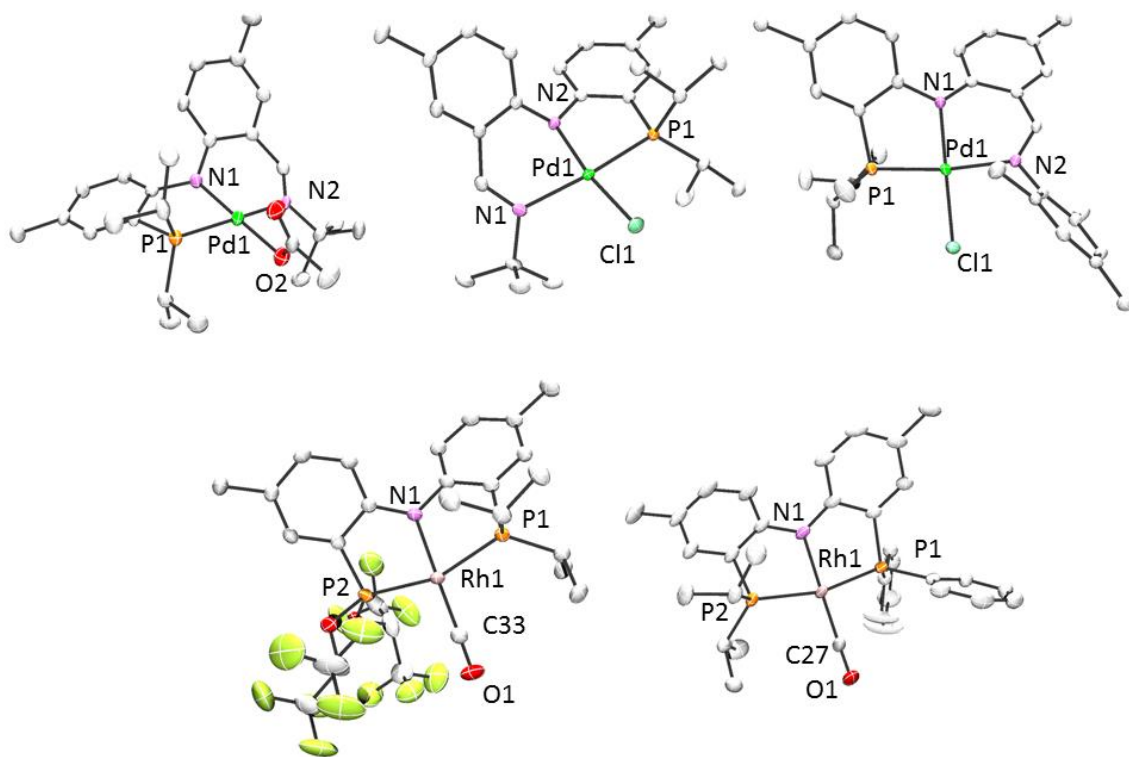


Figure 3.3 POV-Ray renditions¹⁰³ of the ORTEP drawings¹⁰⁴ (50% probability ellipsoids) of **3-8PdOAc**, **3-8PdCl**, **3-7PdCl**, **3-11RhCO**, and **3-6RhCO**. Hydrogen atoms are omitted for clarity. Top left: **3-8PdOAc**. Top center: **3-8PdCl·CH₂Cl₂** (A molecule of dichloromethane was observed in the asymmetric unit cell and has been removed.) Top right: **3-7PdCl**. Bottom left: **3-11RhCO**. Bottom right: **3-6RhCO**.

3.6 Structural Analysis of Neutral Pincer Complexes in the Solid State

The solid-state structures of **3-8PdOAc**, **3-8PdCl·CH₂Cl₂**, **3-7PdCl**, **3-11RhCO**, and **3-6RhCO**, as obtained by single-crystal X-ray diffractometry, are depicted in Figure 3.3 and select metric parameters are tabulated in Table 3.3. In each case the environment about the metal center was found to be approximately square planar. One notable feature is that the pincer bite angles of complexes **3-7H** and **3-8H** are relaxed relative to those observed for the more traditional PNP ligands and closely resemble the bite angles observed in the binucleating PNN type pincer ligand complexes.^{118a} This expansion is related to incorporation of a 6-membered ring containing the metal center. The angle is not as expanded as that observed for the carbazole-based NNN complex, **3-12PdCl**, whose pincer bite angle was observed to be ca 176.8°.^{117a} The bond distances between the donor atoms and Pd resemble those of previously reported similar compounds.^{6,117a,120}

Table 3.3 Comparison of the metric parameters associated with group 10 pincer complexes.

Complex	d(M-X) (Å)	d(M-amido) (Å)	d(M-P₁) (Å)	d(M-1H/N (imine)) (Å)	Pincer bite angle^a (°)
3-8PdOAc	2.0554(3)	2.002(3)	2.2348(13)	2.138(3)	168.21(7)
3-3PdCl^b	2.3157(7)	2.0258(19)	2.2914(4)	2.2914(4)	163.54(3)
3-6PdCl	2.314(4)	2.028(1)	2.300(4)	2.278(4)	163.72(1)
3-8PdCl·CH₂Cl₂	2.3433(7)	2.018(2)	2.2180(6)	2.1543(17)	170.99 (3)
3-7PdCl	2.3224(9)	2.0201(18)	2.2311(10)	2.1022(18)	171.24(5)
3-4PdCl	2.3320(9)	2.039(2)	2.2894(15)	2.2840(15)	169.28(3)
3-12PdCl^c	2.3081(15)	1.989(5)	---	2.060(5)/2.065(5)	176.77(17)

Complex	d(M-CO) /d(C-O) (Å)	d(M-amido) (Å)	d(M-P₁) (Å)	d(M-P₂) (Å)	Bite angle (°)
3-11RhCO	1.829(4)/1.148(5)	2.070(3)	2.3122(10)	2.2184(10)	160.00(3)
3-6RhCO	1.8180(16)/1.149(2)	2.0643(12)	2.2861(4)	2.2777(4)	162.045(14)

^a The term pincer bite angle refers to the angle formed by the two trans donor atoms and the metal center (e.g., P–M–P).

^b Taken from reference 6

^c Taken from reference 117a.

3.7 Solid-State Structure of **3-5NiCl** and its Radical Cation [**3-5NiCl**][**CHB₁₁Cl₁₁**]

Chemical oxidation of **3-5NiCl** with [Ag][**CHB₁₁Cl₁₁**] (work done by Dr. Christos Douvris during his tenure in the Ozerov Group) resulted in the isolation of [**3-5NiCl**][**CHB₁₁Cl₁₁**] as brown crystals. Single crystals of **3-5NiCl** and of [**3-5NiCl**][**CHB₁₁Cl₁₁**] were subjected to an X-ray diffraction study (Figure 3.4, Table 3.4) which allowed for the determination of the solid-state structures. The carborane anion in [**3-5NiCl**][**CHB₁₁Cl₁₁**] is well separated from the cation and can be considered non-coordinating. Both complexes are approximately square planar about Ni. Close inspection of the metric parameters of **3-5NiCl** and [**3-5NiCl**][**CHB₁₁Cl₁₁**] (Table 3.4) revealed little difference between the corresponding bond angles and distances, apart from modest shortening of the Ni–N and Ni–Cl bonds upon oxidation. Szilagyi, Meyer, Mindiola *et al.* undertook a thorough study of the analogous **3-3NiCl** and [**3-3NiCl**][**OTf**] complexes employing NMR, EPR, UV-Vis, and multiedge XAS spectroscopy in addition to structural and theoretical studies.¹¹¹ They also found a similar close correspondence between the structures of the neutral and cationic complexes and concluded that oxidation takes place at the ligand, with no change in the oxidation state of Ni.

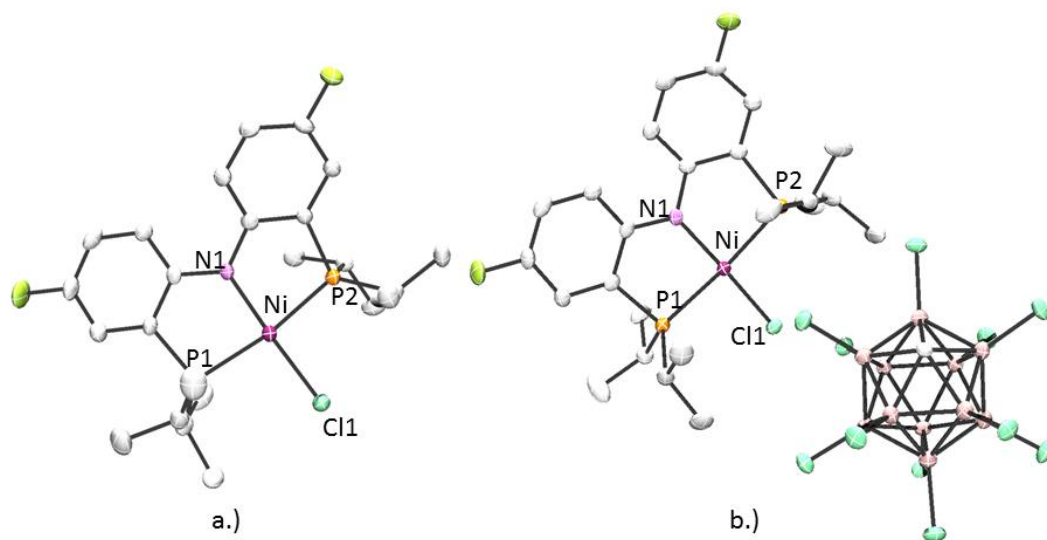


Figure 3.4 ORTEP drawing¹⁰⁴ (50% probability ellipsoids) of **3-5NiCl** and **[3-5NiCl][CHB₁₁Cl₁₁]** showing selected atom labeling. Hydrogen atoms are omitted for clarity. Selected bond distances (Å) and angles (deg) are reported in Table 3.4.

Table 3.4 Selected bond lengths of **3-5NiCl** and **[3-5NiCl][CHB₁₁Cl₁₁]**.

Complex	3-5NiCl	[3-5NiCl][CHB₁₁Cl₁₁]
Ni-Cl (Å)	2.1841(7)	2.1520(7)
Ni-N (Å)	1.8947(19)	1.859(2)
Ni-P (Å)	2.1746(7)	2.1910(7)
Ni-P (Å)	2.1998(7)	2.2158(7)
Cl-Ni-N (°)	175.45(7)	170.08(6)
Cl-Ni-P (°)	92.62(3)	91.66(3)
N-Ni-P (°)	85.33(6)	87.13(6)
P-Ni-P (°)	170.18(2)	168.48(3)

3.8 Analysis of the Electronic Properties

Our investigation of the electronic properties of the pincer ligands discussed within this chapter was a two part endeavor where we (a) obtained cyclic voltammograms for (pincer)MCl compounds of Group 10 metals and (b) measured the IR stretching frequencies of (pincer)RhCO compounds. Our underlying assumptions are that the redox potentials obtained from CV studies report on the ease of oxidation of the pincer ligand (reflects the “electron-richness” of the π -system of the ligand) and that the $\nu(\text{CO})$ IR stretching frequencies give insight into the “electron-richness” of the metal center. The electron-richness of the metal center is a direct reflection of the donating ability of the pincer ligand towards the metal center.

3.8.1 Investigation into the redox properties of group 10 metals

The redox properties of **3-1PdCl**, **3-2PdCl**, **3-3PdCl**, **3-3PtCl**, **3-3NiCl**, **3-4PdCl**, **3-5PdCl**, **3-5PtCl**, **3-5NiCl**, **3-6PdCl**, **3-6PtCl**, **3-7PdCl**, **3-8PdCl**, **3-10PdCl**, **3-11PdCl**, and **3-12PdCl** were investigated by cyclic voltammetry using 0.3 M [Bu₄N][PF₆] as the electrolyte in dichloromethane. Ferrocene was used as an internal standard and the potentials reported in Table 3.5 are referenced vs the ferrocene/ferrocenium redox couple.⁷⁶ It is noteworthy that the redox potentials of the (pincer)PdCl complexes can be varied within a range of about 0.6 V within the framework of diarylamido-based PNZ ligands; this range expands to almost one volt (-0.27 V to 0.69 V) if the carbazole-based ligand (**12-Me**) is included. The cyclic voltammograms of **3-1PdCl**, **3-2PdCl**, **3-3PdCl**, **3-4PtCl**, **3-4NiCl**, **3-5PdCl**, **3-5PtCl**,

3-5NiCl, **3-6PdCl**, **3-6PtCl**, **3-7PdCl**, **3-8PdCl**, **3-10PdCl**, **3-11PdCl**, and **3-12PdCl** exhibit quasi-reversible one-electron redox events. The notable exception to this observation is the cyclic voltammogram obtained for **3-4PdCl**, which is characterized as having two quasi-reversible one-electron redox events. Further studies on the non-innocent character of this ligand are currently under investigation and will be outlined in Section 3.9.

Table 3.5 $E_{1/2}$ (V) for (pincer)MCl complexes.

Ligand	Pd-Cl E/V vs Fc/Fc⁺	Pt-Cl E/V vs Fc/Fc⁺	Ni-Cl E/V vs Fc/Fc⁺
3-4	-0.27 (3-4PdCl) 0.94		
3-3	-0.08 (3-3PdCl)	-0.11 (3-3PtCl)	-0.19 (3-3NiCl)
3-1	-0.05 (3-1PdCl)		
3-6	-0.02 (3-6PdCl)	-0.05 (3-6PtCl)	
3-7	0.04 (3-7PdCl)		
3-2	0.04 (3-2PdCl)		
3-8	0.06 (3-8PdCl)		
3-5	0.11 (3-5PdCl)	0.06 (3-5PdCl)	-0.01 (3-5PdCl)
3-10	0.15 (3-10PdCl)		
3-11	0.32 (3-11PdCl)		
3-12	0.69 (3-12PdCl)		

The data reported in Table 3.5 are consistent with the notion of ligand-based redox events in (pincer)MCl complexes. This is supported by three major observations. 1) The redox potential appears to be affected to a great degree by substituents conjugated with the diarylamido π -system, but are remote from the metal center (*vide infra*). 2) Only small changes in the $E_{1/2}$ values are observed upon varying the identity of the metal (Ex:

3-3PdCl, **3-3PtCl**, and **3-3NiCl**). One would expect that had the redox events been metal based, a large difference in the $E_{1/2}$ values for different metal centers would have been observed. 3) Exchange of the diarylamido backbone for a carbazole unit has the greatest effect on the redox potential. The ionization potential of carbazole is considerably higher than that of diphenylamine, so the greater difficulty in oxidizing **3-12PdCl** is to be expected.¹²¹ Additionally, this is clearly not just a consequence of the nitrogenous side donors in **3-12Me**; the redox potentials for **3-7PdCl** and **3-8PdCl** were not so dramatically different from the PNP analogs. In addition, the reported $E_{1/2}$ value for the (NNN*)NiCl complex by Hu and Vicic (-0.12 V vs Fc/Fc⁺, NNN* = (2-(Me₂N)C₆H₄)₂N) is quite similar to that of **3-3NiCl** reflecting the similarity of the diarylamido backbones.¹¹³

3.8.2 Basicity trends

A comparison of the $\nu(\text{CO})$ frequencies of **3-2RhCO**, **3-3RhCO**,^{21b} **3-4RhCO**, **3-5RhCO**, **3-6RhCO**, **3-7RhCO**, **3-8RhCO**, **3-9RhCO**, **3-10RhCO**, **3-11RhCO**, **3-13RhCO**,¹²² **3-14RhCO**,¹²³ **3-15RhCO**,¹ **3-16RhCO**,¹²⁴ **3-17RhCO**,^{4a} **3-18RhCO**,^{114d} and **3-19RhCO**^{21a} allowed for an assessment of the donor strength of the corresponding pincer ligands towards Rh via the extent of backbonding to CO.^{20,125} It is important to note that the magnitude of $\nu(\text{CO})$ may be influenced by factors other than the “electron-richness” of the metal center; such influences have been discussed in the literature.^{125b,126} However, we expect that within the confines of our study, various other influences on the differences in $\nu(\text{CO})$ are minimal because of the similarity among the

analyzed complexes. A survey of the $\nu(\text{CO})$ values for a series of (pincer)RhCO complexes is summarized in Figure 3.5. The IR spectra of **3-3RhCO**, **3-4RhCO**, **3-5RhCO**, **3-6RhCO**, **3-7RhCO**, **3-8RhCO**, **3-9RhCO**, **3-10RhCO**, and **3-11RhCO** were collected in this work under the same conditions and on the same instrument. The $\nu(\text{CO})$ values for **3-3RhCO**,^{21b} **3-13RhCO**,¹²² **3-14RhCO**,¹²³ **3-15RhCO**,¹ **3-16RhCO**,¹²⁴ **3-17RhCO**,^{4a} **3-18RhCO**,^{114d} and **3-19RhCO**^{21a} come from literature sources and have been obtained on different instruments and in different media, which may cause deviations on the order of a few wavenumbers. The $\nu(\text{CO})$ frequencies of these (pincer)RhCO compounds range from 1900 cm^{-1} to 1980 cm^{-1} , a span of 80 cm^{-1} . The lowest stretching frequency, and thus the most donating pincer ligand in this series, is observed for **3-14RhCO** where the pincer combines trialkylphosphine side arms with the central alkyl donor. The new complex with a bis(hexafluoroisopropoxy) arm (**3-11RhCO**) is the least donating pincer, with the highest $\nu(\text{CO})$ value. Fluoroalkoxy substituents on phosphorus have been recognized as resulting in some of the most strongly π -accepting PX_3 ligands.¹²⁷ Rh complexes of fluoroalkoxy-substituted phosphines have recently been used in the direct coupling of arenes with aryl iodides¹²⁸ and in designs relevant to water and HX photosplitting catalysis.¹²⁹

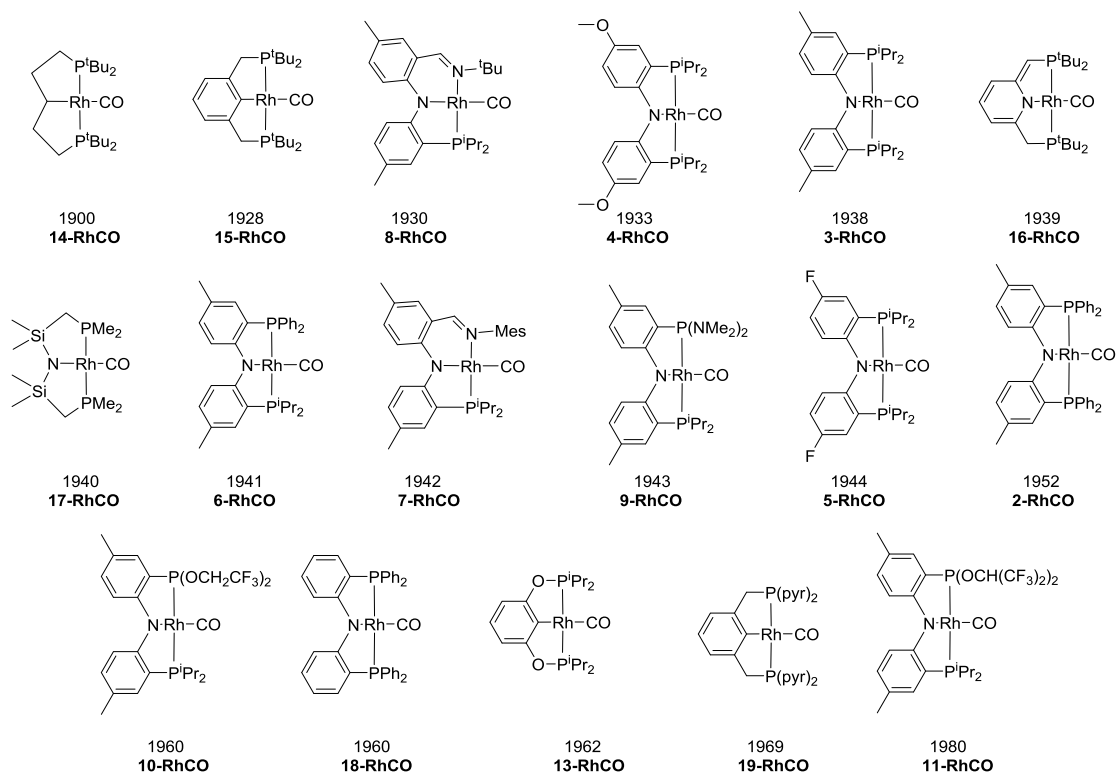


Figure 3.5 $\nu(CO)$ Values (cm^{-1}) for a series of (pincer)RhCO Complexes.

3.8.3 Relationship between $\nu(CO)$ values for (pincer)RhCO complexes and $E_{1/2}$ values for (pincer)PdCl complexes

It is instructive to examine the relationship between $\nu(CO)$ values for (pincer)RhCO complexes and $E_{1/2}$ values for the corresponding (pincer)PdCl complexes as a function of the nature of the pincer ligand. The numerical values are collected in Table 3.6 and Figure 3.6 shows these values plotted in a graphical form. There does not appear to be a smooth relationship between $\nu(CO)$ and $E_{1/2}$ that encompasses the whole set of ligands. For example, it is quite obvious that the ligand responsible for the lowest

$\nu(\text{CO})$ (**3-8RhCO**) does not give rise to the easiest oxidation. On the other hand, there are trends that can be identified within smaller subsets of ligands wherein only substituents at specific sites are varied. The red trendline in Figure 3.6 connects ligands **3-2H**, **3-3H**, **3-6H**, **3-10H**, and **3-11H**. These are all PNP ligands with a constant diarylamido backbone (Me groups *para* to N) with varying substituents on the phosphorus atoms (R in Schemes 3.3). This subset shows a smooth, approximately linear relationship, with the increase in $\nu(\text{CO})$ corresponding to an increase in $E_{1/2}$. The blue trendline connects ligands **3-4Me**, **3-3H**, and **3-5Me**. This subset of PNP ligands shares the same two P^iPr_2 side donors with varying substituents *para* to N in the diarylamine (Y in Scheme 3.3). Here, an increase in $\nu(\text{CO})$ also corresponds to an increase in $E_{1/2}$, but it is clear that the slope of this trendline is very different: the rather large changes in $E_{1/2}$ correspond to relatively small changes in $\nu(\text{CO})$. The (PNP)M complexes can be viewed as a system composed of four fused rings; the two aromatic rings of the diarylamino backbone and the two five-membered metallacycles about the metal center. This four-ring system is constant for (PNP)M complexes with the same M, and the blue and the red trendlines in Figure 3.6 explore the influence of the substituents on this system. The red trendline explores substituents on P, close to the metal, and so for changes across the set there is a more pronounced effect on $\nu(\text{CO})$ than in the blue trendline, where the substituents changing are conjugated with the diarylamido π -system and are relatively remote from the metal. It is understandable that the two PNN ligands (**3-7H** and **3-8H**) do not fall onto either the blue or the red trendline, as the change to PNN involves a change to the four-ring core. While an imine as an N-donor towards Rh is apparently more

donating than a phosphine, the iminyl ($-\text{HC}=\text{NX}$) as a substituent on the diarylamine backbone is probably somewhat π -electron-withdrawing. (R is defined as the substituents on the second phosphine arm. See section on ligand synthesis Scheme 3.2 for a pictorial description.)

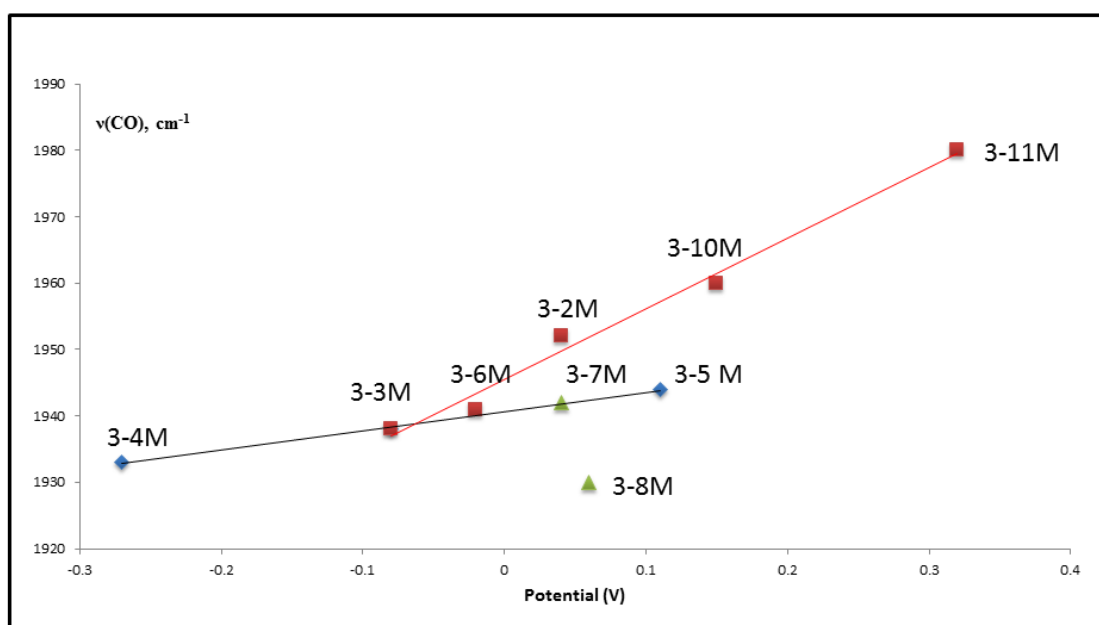


Figure 3.6 A plot of $\nu(\text{CO})$ values (cm^{-1}) in $(\text{pincer})\text{RhCO}$ vs $E_{1/2}$ values (V) for $(\text{pincer})\text{PdCl}$ complexes. The scan rate was 100 mV/s in the positive direction.

Table 3.6 $\nu(\text{CO})$ values (cm^{-1}) in (pincer)RhCO vs $E_{1/2}$ values (V) for (pincer)PdCl complexes.

Ligand	Pd-Cl E/V vs Fc/Fc ⁺	$\nu(\text{CO})$ (cm^{-1})
3-4Me	-0.27 (3-4PdCl) 0.94	1933 (3-4RhCO)
3-3H	-0.08 (3-3PdCl)	1938 (3-3RhCO)
3-1H	-0.05 (3-1PdCl)	
3-6H	-0.02 (3-6PdCl)	1941 (3-10RhCO)
3-7H	0.04 (3-7PdCl)	1942 (3-6RhCO)
3-2H	0.04 (3-2PdCl)	1952 (3-2RhCO)
3-8H	0.06 (3-8PdCl)	1930 (3-8RhCO)
3-5Me	0.11 (3-5PdCl)	1944 (3-5RhCO)
3-10H	0.15 (3-10PdCl)	1960 (3-10RhCO)
3-11H	0.32 (3-11PdCl)	1980 (3-11RhCO)

3.9 Analysis of **3-4PdCl** and its Radical Cations [**3-4PdCl**][**CHB₁₁Cl₁₁**] and [**3-4PdCl**][**CHB₁₁Cl₁₁**]₂

3.9.1 Solid-state structures of **3-4PdCl** and its radical cation [**3-4PdCl**][**CHB₁₁Cl₁₁**]

As previously discussed our pincer frameworks all generate redox non-innocent complexes when chelated to Group 10 metals. In most cases one quasi-reversible redox event was observed at relatively low potentials. The cyclic voltammogram of **3-4PdCl**; however, showed two quasi-reversible anodic waves at -0.27 and 0.94 V. Intrigued by this result, we targeted the chemical oxidation of **3-4PdCl**. Questions we hope to address in this study are 1) whether or not both oxidation events occur on the ligand scaffold and 2) determine if there are metric changes associated with the oxidation of this compound.

It is noteworthy to mention that other methoxy substituted diarylamido-based pincer ligand have been reported which also engender two electron redox events.^{109,130}

The chemical oxidation of **3-4PdCl** with [tris(4-bromophenyl)aminium][CHB₁₁Cl₁₁] resulted in a rapid color change from purple to brown. The neutral amine was extracted from the reaction mixture with pentane. Slow diffusion of pentane into a dichloromethane solution of crude **[3-4PdCl][CHB₁₁Cl₁₁]** resulted in precipitation of orange crystals of **[3-4PdCl][CHB₁₁Cl₁₁]** with a 95% yield. To elucidate the connectivity of **[3-4PdCl][CHB₁₁Cl₁₁]**, we used single-crystal X-ray diffraction techniques. The geometry of **[3-4PdCl][CHB₁₁Cl₁₁]** was observed to be a distorted square planar palladium complex bearing a non-coordinating carborane anion (Figure 3.7). Close inspection of the metrical parameters of **3-4PdCl** and **[3-4PdCl][CHB₁₁Cl₁₁]** reveal similar structural features about the metal center (Table 3.7). This lack of deviation supports our conclusion that the oxidation event is ligand based rather than metal based. The close correspondence between the structures of the neutral and cationic complexes is reflective of the small metric changes observed by Mindiola¹¹¹ and in the case of **3-5NiCl** and **[3-5NiCl][CHB₁₁Cl₁₁]**.

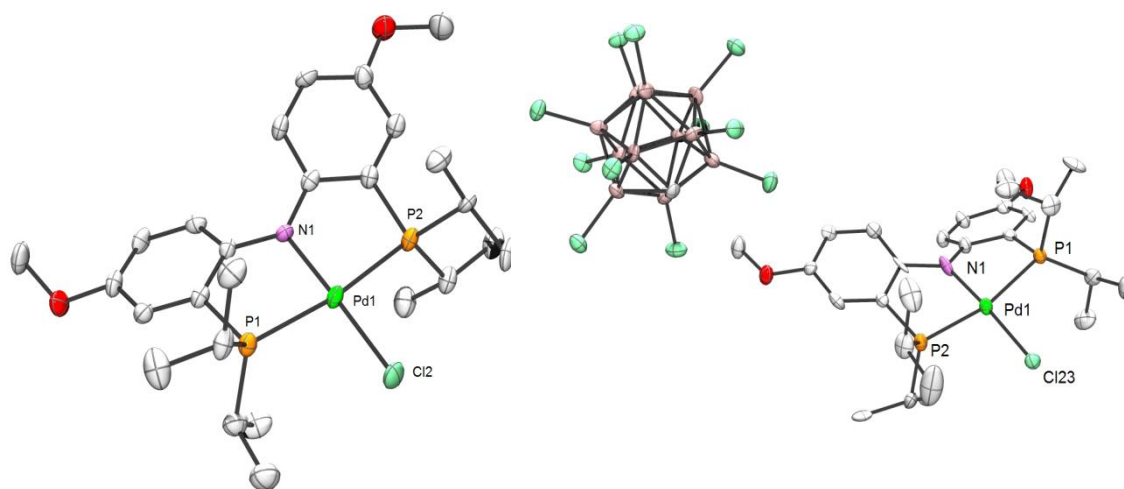


Figure 3.7. POV-Ray renditions of ORTEP¹⁰⁴ drawings (50% probability ellipsoids) of **3-4PdCl** (left) and **[3-4PdCl][CHB₁₁Cl₁₁]** (right). Hydrogen atoms in all structures and cocrystallized toluene in the structure of **3-4PdCl** are omitted for clarity. For the structures of **3-4PdCl** and **[3-4PdCl][CHB₁₁Cl₁₁]**, only one of the two independent molecules or cation/anion pairs is shown.

Table 3.7 Selected bond distances (Å) and angles (°) from the solid-state X-ray studies of **3-4PdCl** and **[3-4PdCl][CHB₁₁Cl₁₁]**.

Metric (Å or °)	3-4PdCl	[3-4PdCl][CHB₁₁Cl₁₁]
Pd1-N1	2.039(2)	2.013(6)
Pd1-P1	2.2923(9)	2.300(2)
Pd1-P2	2.2998(9)	2.2845(19)
O1-C3	1.393(3)	1.354(8)
O2-C12	1.384(3)	1.356(9)
Pd1-Cl1	2.3320(9)	2.299(2)
N1-Pd-P1	84.78(7)	83.11(17)
N1-Pd-P2	84.71(7)	84.59(17)
P1-Pd1-P2	169.28(3)	166.39(8)
N1-Pd1-Cl1	178.09(7)	172.01(18)
P1-Pd1-Cl1	94.00(4)	97.99(7)
P2-Pd1-Cl1	96.45(4)	95.00(7)

3.9.2 Towards the synthesis and characterization of **[3-4PdCl][CHB₁₁Cl₁₁]₂**

The formal potential associated with the oxidation of **[3-4PdCl][CHB₁₁Cl₁₁]** to **[3-4PdCl][CHB₁₁Cl₁₁]₂** was observed at 0.94 V (vs Fc/Fc⁺) by cyclic voltammetry. To determine the nature of the dication, we set out to synthesize it via chemical means. Treatment of **[3-4PdCl][CHB₁₁Cl₁₁]** with one equivalent of [bis(2,4-dibromophenyl)(2-bromo-4-trifluoromethyl)aminium][CHB₁₁Cl₁₁] ($E_{1/2} = 1.39$ V vs Fc/Fc⁺) resulted in an immediate color change from orange to purple and reduction of bis(2,4-dibromophenyl)(2-bromo-4-trifluoromethyl)aminium was evidenced by the presence of bis(2,4-dibromophenyl)(2-bromo-4-trifluoromethyl)amine in the ¹H and ¹⁹F NMR spectra of the reaction mixture. The amine was more soluble than the product salt and was readily separated from the crude oxidation product by removing the volatiles and washing the purple residue with pentane. The solid was then dissolved in dichloromethane. Slow diffusion of pentane resulted in precipitation of purple crystals with no observable NMR signature. At this juncture we have not been able to isolate X-ray quality crystals to establish the connectivity of the product and its identity remains unknown.

3.9.3 DFT Analysis of the oxidation products of **3-4PdCl**

In order to corroborate our hypothesis that both oxidation events will be ligand based in nature we turned to density functional theory (DFT) and performed electronic structural calculations to depict the orbital compositions for **3-4PdCl**, **[3-4PdCl]⁺** and **[3-4PdCl]²⁺**. Geometry optimizations and frequency calculations were performed

utilizing the B3LYP⁹⁴ functional with a 6-311G(d')^{131,132} basis set on C, H, and O; a 6-311G(d) basis set on N;^{133,131a} a 6-31G(d)¹³⁴ basis set on P and Cl, and a Stuttgart/Dresden triple- ζ quality basis set (SDD) with an effective core potential (ECP)¹³⁵ on Pd. Figure 3.8 depicts the HOMO, the HOMO-1, and the atomic compositions of **3-4PdCl**. As expected the HOMO orbital resides predominately on the conjugated arene ligand backbone. The Pd 3d_{yz} and chloride 3p_z orbital contributions are small in the HOMO (10%). The HOMO-1 orbital also shows considerable PNP orbital character.

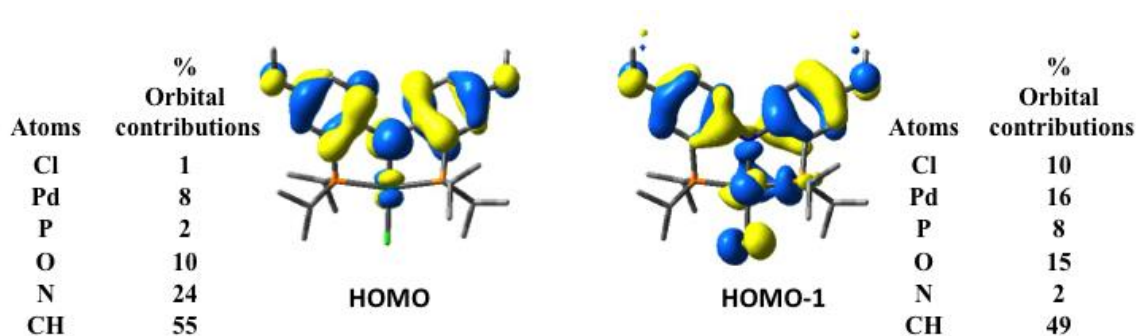


Figure 3.8 HOMO and HOMO-1 of **3-4PdCl**.

Based on DFT results for the neutral **3-4PdCl**, one would expect that oxidation would result in an electron hole centered on the ligand π -system. The α -SOMO of [**3-4PdCl**]⁺ supports this conclusion. Again considerable PNP character is observed with the majority of the electron density lying in N and O p-orbitals and the π -system of the

aromatic backbone. The SOMO, HOMO, and LUMO of $[3-4PdCl]^+$ are depicted Figure 3.9. In addition tabulated metrics corresponding to $3-4PdCl$ and $[3-4PdCl]^+$ are reported in Table 3.8. As observed experimentally, only small metric changes are associated with the first oxidation event. A structural analysis of the calculated geometries of $3-4PdCl$ and $[3-4PdCl]^+$ demonstrate good agreement with the experimental values determined by single crystal X-ray diffraction.

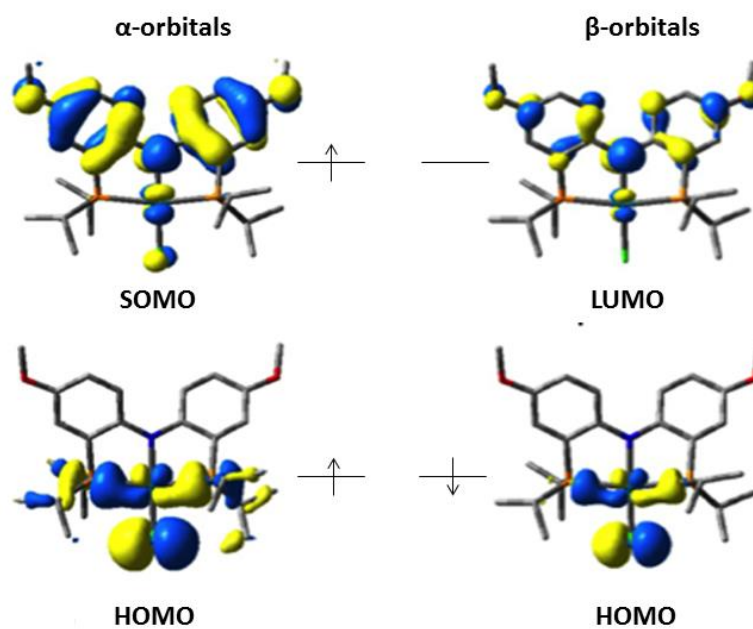
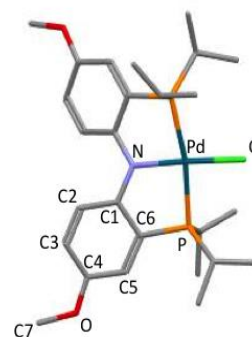


Figure 3.9 Selected orbital pictures for $[3-4PdCl][CHB_{11}Cl_{11}]$.

Table 3.8 Computed metric parameters associated with **3-4PdCl** and **[3-4PdCl][CHB₁₁Cl₁₁]**.

Metric	DFT (neutral)	DFT (oxidized)	DFT (dication)
Pincer bite angle ^a	165.81	167.50	169.55
Pd-P	2.357	2.348	2.366
Pd-N	2.055	2.049	2.044
Pd-Cl	2.367	2.327	2.298
C1-C2	1.425	1.434	1.432
C2-C3	1.398	1.387	1.376
C3-C4	1.399	1.413	1.419
C4-C5	1.399	1.406	1.427
C5-C6	1.395	1.388	1.376
C6-C1	1.413	1.417	1.446
C4-O	1.371	1.342	1.313
C7-O	1.415	1.430	1.449
N-Cl	1.396	1.388	1.370



^a The term pincer bite angle refers to the angle formed by the two trans donor atoms and the M center (e.g., P–Pd–P).

Based on the above analysis, the second oxidation event to form **[3-4PdCl]²⁺** can occur at either the α -SOMO (predominantly ligand based) or the β -HOMO (predominantly metal based) of **[3-4PdCl]⁺**. A singlet state would result from the first possibility and a triplet from the latter. The singlet state of **[3-4PdCl]²⁺** was found to be 18.8 kcal/mol more stable. B3LYP tends to favor the triplet state, suggesting the triplet-singlet gap is likely even larger.¹³⁶ Figure 3.10 shows the HOMO and LUMO orbitals of the singlet **[3-4PdCl]²⁺**. The DFT results predict that upon removal of a second electron from the PNP backbone, metric changes will be observed (Table 3.8). The C(4)-O and C(2)-C(3) bond lengths decreased by 0.06 Å and 0.018 Å respectively from the bond lengths observed in the neutral structure. At the same time an increase in the bond lengths between C(1)-C(2), C(3)-C(4), C(4)-C(5) and C(6)-C(1) relative to the bonds in

the neutral structure was observed. There are only small calculated changes in the bond lengths about the metal center. Based on the results of this analysis DFT predicts that both oxidation events are predominantly ligand based in nature. This conclusion is also supported by the electrochemical analysis results. Had the second oxidation event been metal based in character, one would expect that a second redox event would have also been observed for **3-3PdCl**, which is supported by a similar ligand. In the case of **3-4PdCl** we propose that the second oxidation event is observed within the range of the CV window because the methoxy group can help to stabilize the electron poor structure via an increase in the level of conjugation of the π -system.

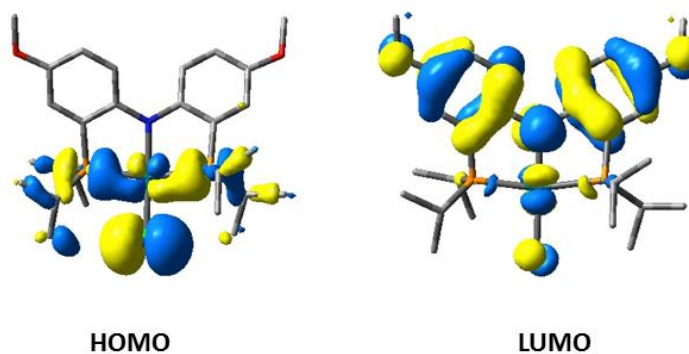


Figure 3.10 HOMO and LUMO orbitals of doubly oxidized **3-4PdCl** in the singlet form.

3.10 Conclusion

In summary, a series of new pincer ligands based on the diarylamido backbone have been prepared which incorporate a variety of substituents that change the stereo and

electronic properties of the ligand. In the context of this work, we were especially interested in exploring the relationship between the redox activity of the metal-bound pincer ligand and the electronic effect of the pincer on the metal center. The electronic properties of a series of pincer ligands were analyzed on the basis of redox potentials observed for group 10 metal complexes (PNZ)MCl (P = phosphine, Z = phosphine or imine) and $\nu(\text{CO})$ values in the corresponding (PNZ)RhCO complexes. Overall, this analysis is consistent with the oxidation of (PNZ)MCl being ligand-based as it is more affected by substituents on the diarylamine backbone, whereas the $\nu(\text{CO})$ in (PNZ)RhCO and thus the donor ability of the pincer ligand towards the metal is more strongly affected by the nature of the donors directly attached to the metal. As a final note, the metal and the oxidizable pincer ligand are directly connected and their electronic properties cannot be modified completely independently. However, judicious choice of the donor atoms and the nature of their substituents as well as modifications to the diarylamido framework allows for some control of the degree to which the redox activity of the ligand and the electronic effect of the ligand on a metal center are influenced.

3.11 Experimental

3.11.1 General considerations

Unless otherwise specified all manipulations were performed under an atmosphere of Ar using a standard Schlenk line or a glovebox. Toluene, diethyl ether, hexanes, tetrahydrofuran, dichloromethane, trimethylsilylchloride (Gelest), C_6D_6 , 2,6-lutidine (Aldrich), CIP^iPr_2 (Dalchem), $\text{CIP}(\text{NMe}_2)_2$ (Dalchem), and toluene- d_8 were all

dried over CaH₂, distilled or vacuum transferred and then stored over molecular sieves in an Ar filled glove box. Pd(COD)Cl₂,¹³⁷ **3-A**,¹³⁸ **3-3H**,⁶ **3-5Me**,^{114c} **3-3PdCl**,⁶ **3-3PdOAc**,^{114c} **3-5PdCl**,^{114c} **3-5PdOAc**,^{114c} **3-2PdCl**,^{114c} **3-3NiCl**,^{114b} **3-3NiOAc**,^{114b} **3-G**,^{118a} and **3-F**^{118a} were prepared according to the published procedures. The synthesis of [tris(4-bromophenyl)aminium][CHB₁₁Cl₁₁] is reported in Chapter 2 of this dissertation. 2,6-lutidine and DMF were dried over CaH₂ and distilled prior to use. All other chemicals used were received from commercial vendors. NMR spectra were recorded on a Varian Inova 300 (¹H, ¹³C, ³¹P), Varian Inova 500 (¹H, ¹³C, ³¹P, ¹⁹F), or a Varian 500 (¹H, ¹³C, ³¹P, ¹⁹F) spectrometer. ³¹P and ¹⁹F NMR spectra were referenced externally using H₃PO₄ (85%, 0 ppm) and CF₃COOH (-78.5 ppm) respectively. Single frequency phosphorus decoupled proton spectrum were recorded on the Varian Inova 500 (¹H, ¹³C, ³¹P, ¹⁹F), or Varian 500 (¹H, ¹³C, ³¹P, ¹⁹F) spectrometers. The frequency at which the spectrum was decoupled is referenced at the beginning of each data set. Electrochemical studies were carried out using a CH Instruments Model 700 D Series Electrochemical Analyzer and Workstation in conjunction with a three electrode cell. The working electrode was a CHI 104 glassy carbon disk with a 3.0 mm diameter and the auxiliary electrode was composed of platinum wire. The third electrode, the reference electrode, was a Ag/AgNO₃ electrode. This was separated from solution by a fine porosity frit. CVs were conducted in dichloromethane with 0.3 M [Bu₄N][PF₆] as the supporting electrolyte at scan rate of 100 mV/s. The concentration of the analyte solutions were approximately 1.00 × 10⁻³ M. CVs were referenced to Fe(Cp)₂/Fe(Cp)₂⁺ redox couple. Low-temperature X-ray data were obtained on a Bruker APEXII CCD

based diffractometer (Mo sealed X-ray tube, $K_{\alpha} = 0.71073 \text{ \AA}$). All diffractometer manipulations, including data collection, integration and scaling were carried out using the Bruker APEXII software. Elemental analyses were performed by CALI Laboratories, Parsippany, NJ. FT-IR spectra were collected using a Bruker ALPHA-P FT-IR Spectrometer with a diamond ATR.

3.11.2 Computation methodology

Geometry optimizations and frequency calculations were performed utilizing the B3LYP⁹⁴ functional with a 6-311(d')^{131,132} basis set on C, H, and O; a 6-311G(d) basis set on N;^{133,131a} a 6-31G(d)¹³⁴ basis set on P and Cl and finally, a Stuttgart/Dresden triple- ζ quality basis set (SDD) with an effective core potential (ECP)¹³⁵ on Pd. Where possible the geometries were compared to the values determined experimentally by X-ray crystallography and were found to closely match. The Ampac Graphical User Interface (AGUI) program was used to extract geometric data.

3-A. A 3000 mL 3-necked flask was charged with bis(*p*-tolyl)amine (142 g, 0.400 mol), a stir bar and CH_2Cl_2 (1.50 L). *N*-bromosuccinimide (142 g, 0.800 mol) was subsequently added to the reaction mixture in 10 portions over the course of 2.5 h. The reaction was vigorously stirred at ambient temperature for 48 h. To ensure quantitative conversion to the desired product a 1 mL aliquot was removed and dried *in vacuo* in a J. Young tube. A ^1H NMR experiment was conducted in CDCl_3 concluding that 99% conversion to the desired product had occurred. The volatiles were then removed *in vacuo* and the resulting black solid was dissolved in pentane (1.20 L), stirred vigorously

over silica gel for 30 min and then filtered through a pad of Celite. Removal of the volatiles *in vacuo* and recrystallization in cold pentane at -35 °C resulted in the isolation of pure product as a white solid. An additional fraction was obtained by again washing the black residue with pentane (4 × 200 mL). The pentane solution was then concentrated under vacuum and the resulting solution was recrystallized at -35 °C to obtain a second crop of **3-A** (181.6 g, 0.51 mmol, 71%). ¹H NMR (CDCl₃): δ 7.38 (s, 2H, Ar H), 7.09 (d, 2H, *J*_{HH} = 8 Hz, Ar H), 6.98 (d, 2H, *J*_{HH} = 8 Hz, Ar H), 6.16 (s, 1H, NH), 2.26 (s, 6H, Ar CH₃).

3.11.3 Synthesis of **3-1H** and its metal complexes

3-1H. In a 25 mL Schlenk flask under Ar, **3-A** (0.42 g, 1.2 mmol) was dissolved in diethyl ether. The solution was placed in freezer for 1 h at -35°C. *n*-Butyllithium (1.6 mL of 2.5 M solution in hexanes, 3.9 mmol) was then added and the solution was stirred overnight. The solution was cooled to -35°C in freezer for 1 h, then ClPEt₂ (0.53 mL, 4.4 mmol) was added. The mixture immediately became bright yellow-orange. After 3 h, the reaction was quenched with 30 μL degassed H₂O/MeOH soln. The solution was stirred for 20 min and then the volatiles were removed. The product was extracted with pentane and toluene then filtered over Celite and silica gel yielding a pale yellow solution. The volatiles were reduced leaving a yellow oil. The oil was found to be a mixture containing approximately 87% desired ligand by ³¹P NMR. This mixture was used without further purification for the synthesis of **3-1PdCl**. ¹H NMR (C₆D₆, Figure 3.11): δ 7.87 (t, *J*_{PH} = 8 Hz, 1H, NH), 7.28 (dd, *J* = 4 Hz, *J* = 8 Hz, 2H, Ar H), 7.19 (br s, 2H, Ar H), 6.93 (dd,

$J = 2$ Hz, $J = 8$ Hz, 2H, Ar H), 2.21 (s, 6H, Ar CH_3), 1.60 (m, 8H, CH_2CH_3), 1.02 (m, 12H, CH_2CH_3). $^{13}C\{^1H\}$ NMR (C_6D_6): δ 146.3 (m), 131.4 (s), 130.5 (s), 129.9 (s), 126.8 (m), 117.4 (s), 20.9 (s), 19.7 (d, $J_{PC} = 8$ Hz), 10.3 (m). $^{31}P\{^1H\}$ NMR (C_6D_6): δ -36.5.

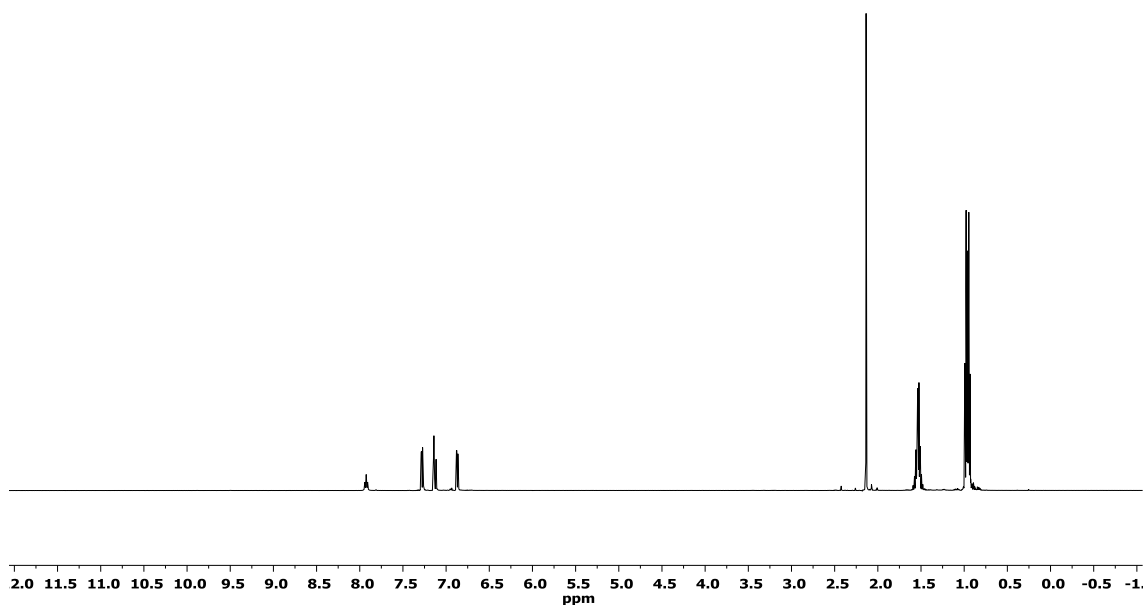


Figure 3.11 1H NMR spectrum of **3-1H** (500 MHz, C_6D_6).

3-1PdCl. In 25 mL Schlenk flask, under Ar, Pd(COD)Cl₂ (86 mg, 0.3 mmol) was added to a toluene solution of **3-1H** (0.12 g, 0.33 mmol). The solution became a dark red and was stirred overnight at RT. After 12 h, solution was filtered through Celite and silica gel. The volatiles were removed and red oily solid was dissolved in toluene. Product was recrystallized from a toluene solution layered with pentane to yield red crystals of **3-1PdCl** (114 mg, 0.22 mmol, 73% isolated yield). ¹H NMR (C₆D₆, Figure 3.12): δ 7.72 (dvt, *J*_{HH} = 8 Hz, *J*_{PH} = 3 Hz, 2H, Ar *H*), 6.77 (d, *J*_{HH} = 8.5 Hz, 2H, Ar *H*), 6.73 (vt, *J*_{PH} = 6 Hz, 2H, Ar *H*), 2.10 (s, 6H, Ar *CH*₃), 1.86 (m, 4H, *CH*₂*CH*₃), 1.49 (m, 4H, *CH*₂*CH*₃), 1.25 (m, 12H, *CH*₂*CH*₃). ¹³C{¹H} NMR (C₆D₆): δ 161.6 (vt, *J*_{PC} = 11.5 Hz), 132.7 (s), 131.5 (s), 126.3 (vt, *J*_{PC} = 4 Hz), 120.9 (vt, *J*_{PC} = 20 Hz), 116.2 (vt, *J*_{PC} = 7 Hz), 20.2 (s), 19.1 (vt, *J*_{PC} = 14 Hz), 8.9 (s). ³¹P{¹H} NMR (C₆D₆): δ 33.5.

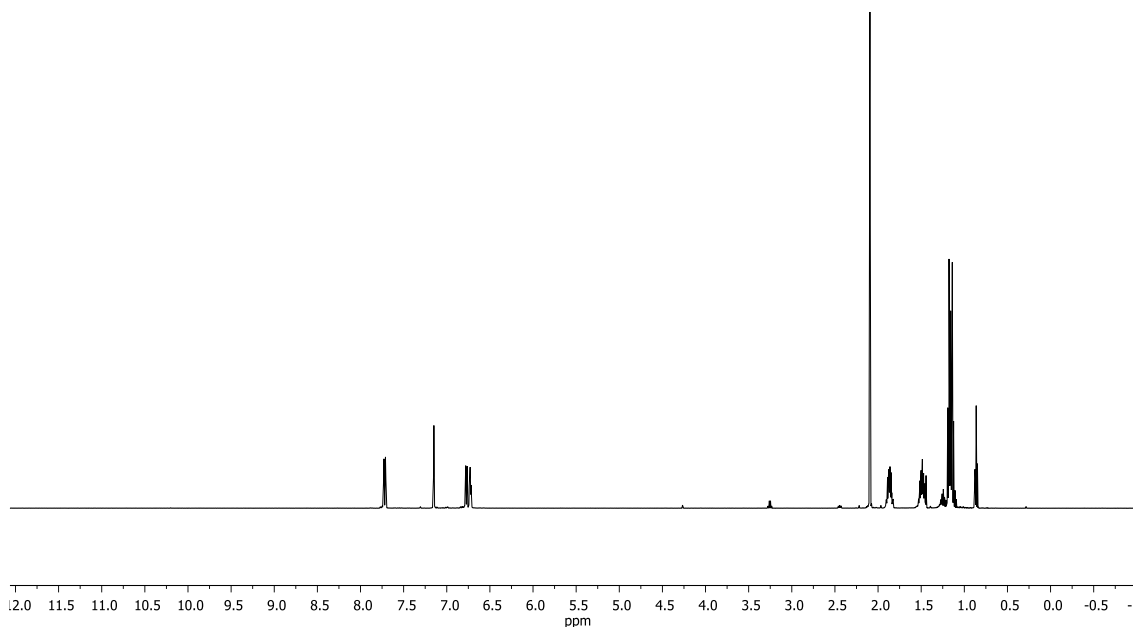


Figure 3.12 ^1H NMR spectrum of **3-1PdCl** (500 MHz, C_6D_6). Trace quantities of diethyl ether, pentane and dichloromethane are observed.

3.11.4 Synthesis of complexes of **3-2H**

3-2PdOAc. A Schlenk flask was charged with **3-2H** (1.00 g, 1.76 mmol), $\text{Pd}(\text{OAc})_2$ (396 mg, 1.76 mmol) and toluene (5 mL). The reaction mixture was stirred for 18 h and then the resulting solid was taken up in additional toluene and recrystallized at $-35\text{ }^\circ\text{C}$ to yield **3-2PdOAc** as a red solid (0.906 g, 1.24 mmol 69%). ^1H NMR (C_6D_6 , Figure 3.13): δ 8.01 (m, 8H, Ar *H*), 7.65 (d, 2H, $J = 11$ Hz, Ar *H*), 7.05-6.97 (m, 14H, 8 Hz), 6.67 (d, 2H, $J_{\text{HH}} = 8$ Hz, Ar *H*), 1.93 (s, 3H, CH_3), 1.89 (s, 6H, CH_3). $^{31}\text{P}\{^1\text{H}\}$ NMR

(C₆D₆): δ 29.6. ¹H NMR (CDCl₃): δ 7.82-7.78 (m, 8H, Ar H), 7.47-7.42 (m, 14H, Ar H), 6.86 (d, 2H, J = 8 Hz, Ar H), 6.83 (m, 2H, Ar H), 2.13 (s, 6H, Ar CH₃), 1.68 (s, 3H, CH₃). ¹³C{¹H} NMR (CDCl₃): δ 176.0 (OAc), 160.2 (d, J_{CP} = 27 Hz, Ar CN), 133.9 (s, Ar CH), 133.8 (s, Ar CH), 132.7 (s, Ar CH), 131.1 (s, Ar C), 130.9 (s, Ar CH), 130.7 (s, Ar CH), 129.2 (s, Ar C), 128.8 (s, Ar CH), 127.0 (s, Ar C), 121.8 (s, Ar C), 116.8 (s, Ar CH), 23.6 (s, OAc), 20.3 (s, Ar CH₃). ³¹P{¹H} NMR (CDCl₃): δ 28.9.

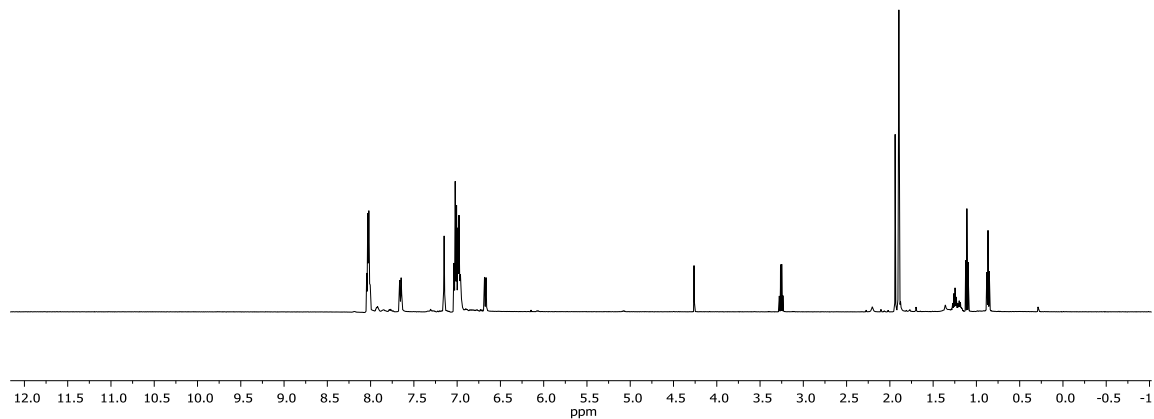


Figure 3.13 ¹H NMR spectrum of **3-2PdOAc** (500 MHz, C₆D₆). Impurities include dichloromethane, pentane and diethyl ether.

3-2PdCl.^{114c} A Schlenk flask was charged with **3-2PdOAc** (117 mg, 0.160 mmol), a stir bar, diethyl ether (5 mL) and Me₃SiCl (100 μL, 0.801 mmol) and stirred for 12 h at room temperature. The volatiles were then removed *in vacuo* while being warmed in a 100 °C oil bath, resulting in a green powder. The solid was then recrystallized in pentane to yield **3-2PdCl** as a green powder (83.0 mg, 0.127 mmol, 80%).

3-2PdOTf. A vial was charged with **3-2PdOAc** (30 mg, 41 μmol), diethyl ether (1 mL) and Me₃SiOTf (0.10 mL). An immediate color change to blue is observed and green crystals are observed to precipitate out of solution. After 2 d the brown solution was decanted and the resulting green crystals were dried *in vacuo* to yield **3-2PdOTf** (26 mg, 32 μmol, 78%). ¹H NMR (C₆D₆, Figure 3.14) δ 7.86 (m, 8H, Ar H), 7.55 (d, *J* = 6.8 Hz, 2H, Ar H), 7.00 (m, 12H, Ar H), 6.85 (s, 2H, Ar H), 6.63 (d, *J* = 8.0 Hz, 2H, Ar H), 1.83 (s, 6H, Ar CH₃). ¹⁹F NMR (C₆D₆): δ -78.4 (s). ³¹P{¹H} NMR (C₆D₆) δ 32.5 (s).

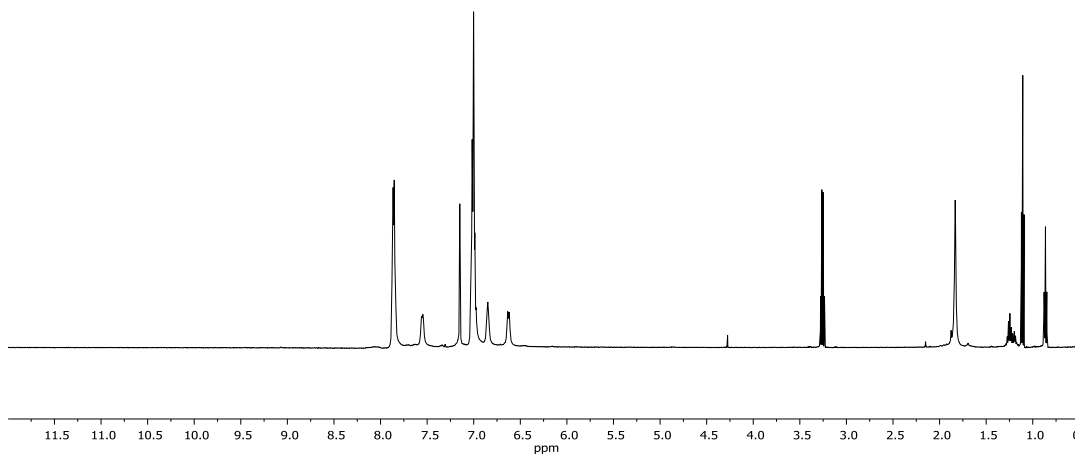


Figure 3.14 ^1H NMR spectrum of **3-2PdOTf** (500 MHz, C_6D_6). Pentane and diethyl ether are observed in the spectrum

3-2RhCO. A Schlenk flask was charged with **3-2H** (0.30 g, 0.53 mmol), $[\text{Rh}(\text{COD})\text{Cl}]_2$ (0.13 mg, 0.27 mmol), 2,6-lutidine (61 μL , 0.53 mmol), diethyl ether (10 mL) and a stir bar. Exposure to CO (1 atm) resulted in the formation of an orange solution. The reaction mixture was stirred for 12 h and then the volatiles were removed *in vacuo*. The resulting solid was taken up in dichloromethane and passed through a pad of Celite. The solution was then concentrated and layered with diethyl ether. Recrystallization at $-35\text{ }^\circ\text{C}$ resulted in the isolation of **3-2RhCO** as an orange solid (0.17 g, 0.25 mmol, 46%). ^1H NMR (CDCl_3 , Figure 3.15): δ 8.12 (m, 10H, Ar H), 7.44 (s, 2H,

Ar H), 7.34 (t, $J_{PH} = 3$ Hz, 2H, Ar H), 7.26 (m, 10H, Ar H), 7.06 (d, $J_{HH} = 9$ Hz, 2H, Ar H), 2.24 (s, 6H, CH_3). $^1H\{^{31}P \delta 41.3\}$ NMR ($CDCl_3$): δ 8.12 (m, 10H, Ar H), 7.44 (s, 2H, Ar H), 7.34 (s, 2H, Ar H), 7.26 (m, 10H, Ar H), 7.06 (d, $J_{HH} = 9$ Hz, 2H, Ar H), 2.24 (s, 6H, CH_3). $^{13}C\{^1H\}$ NMR ($CDCl_3$): δ 196.3 (d, $J = 13$ Hz, CO), 161.2 (t, $J_{CP} = 14$ Hz, Ar C), 135.2 (s, Ar C), 135.0 (s, Ar C), 134.8 (s, Ar C), 134.7 (s, Ar C), 134.6 (s, Ar C), 134.6 (s, Ar C), 133.3 (s, Ar C), 131.2 (s, Ar C), 129.7 (t, $J_{CP} = 5$ Hz, Ar C), 128.9 (s, Ar C), 126.9 (s, Ar C), 123.7 (t, $J_{CP} = 23$ Hz, Ar C), 116.7 (d, $J_{CP} = 21$ Hz, Ar C), 21.4 (s, CH_3). $^{31}P\{^1H\}$ NMR ($CDCl_3$): δ 41.1 (d, $J_{RHP} = 136$ Hz). 1H NMR (C_6D_6): δ 7.82 (m, 9H, Ar H), 7.04 (m, 3H, Ar H), 6.97 (m, 12H, Ar H), 6.77 (d, $J_{HH} = 9$ Hz, 2H, Ar H), 1.95 (s, 6H, CH_3). $^{31}P\{^1H\}$ NMR (C_6D_6): δ 41.3 (d, $J_{RHP} = 135$ Hz). IR $\nu(CO) = 1952$ cm^{-1} .

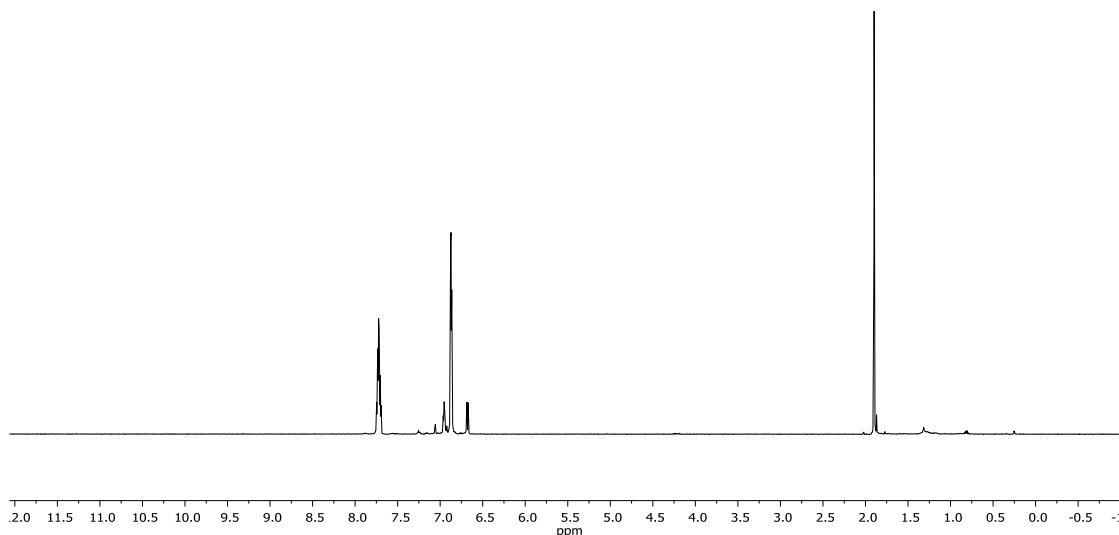


Figure 3.15 ^1H NMR spectrum of **2-RhCO** (500 MHz, C_6D_6). Less than 2% of free ligand is observed in the spectrum.

3.11.5 Metal complexes of **3-3H**

3-3NiCl. A C_6D_6 solution of **3-3NiOAc** (55 mg, 0.10 μmol) was charged with Me_3SiCl (3.8 μl , 0.30 μmol). The reaction's progress was monitored by ^{31}P NMR spectroscopy. After 1 h the sample was analyzed by ^{31}P NMR spectroscopy, which revealed complete conversion one product (signified by a singlet at 34.2 pp[m]). The volatiles were then removed *in vacuo* to yield a green powder (43 mg, 0.082 mmol, 81%).

3.11.6 Synthesis of **3-4Me** and its complexes

3-B. In the glove box a Schlenk flask was charged with *p*-anisidine (20.0 g, 162 mmol), Pd(OAc)₂ (200 mg, 0.892 mmol), DPPF (640 mg, 1.16 mmol), and toluene (250 mL). Degassed 4-bromoanisole (20.4 mL, 162 mmol) and sodium *tert*-pentoxide (20.6 g, 187 mmol) were quickly added to the reaction mixture under an atmosphere of Ar. The reaction was refluxed for 36 h and then cooled to ambient temperature. A 1 mL aliquot was removed from the reaction mixture and dried in a J. Young tube. ¹H NMR analysis revealed conversion to the coupled product. The reaction was quenched with 3.3 mL of degassed H₂O and stirred for an additional 40 min prior to removing the volatiles *in vacuo*. The resulting solid was then dissolved in dichloromethane, stirred over silica gel and then filtered through a pad of Celite. The solution was then concentrated and stored at -35 °C for 12 hours. The resulting precipitate was then collected and dried *in vacuo* to yield **3-B** as a colorless solid (25.3 g, 110 mmol, 69%). ¹H NMR (C₆D₆, Figure 3.16): δ 6.81 (d, *J* = 7 Hz, 4H, Ar *H*), 6.76 (d, *J* = 7 Hz, 4H, Ar *H*), 4.77 (s, 1H, NH), 3.35 (s, 6H, CH₃). ¹³C{¹H} NMR (C₆D₆): δ 154.8 (s, Ar C), 138.4 (s, Ar C), 119.9 (s, Ar CH), 115.0 (s, Ar CH), 55.2 (s, OCH₃).

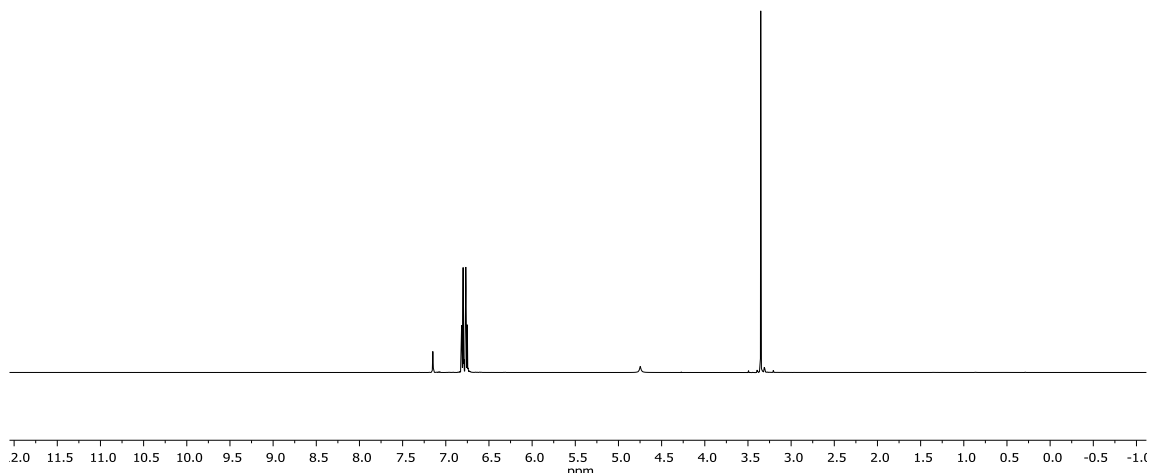


Figure 3.16 ^1H NMR spectrum of **3-B** (500 MHz, C_6D_6). Trace quantities of dichloromethane are observed.

3-C. A Schlenk flask was charged with **3-B** (5.05 g, 22.1 mmol), a stir bar, and dichloromethane (250 mL). *N*-bromosuccinimide (7.85 g, 44.1 mmol) was then added to the reaction vessel in small portions over the course of 10 m. The reaction mixture was then stirred for 24 h under a steady flow of Ar and then a small aliquot was removed and dried *in vacuo*. ^1H NMR analysis revealed 99% conversion to **3-C**. The volatiles were removed and the resulting solid was dissolved in tetrahydrofuran, filtered through a pad of Celite and dried. The solution was then concentrated, layered with pentane and stored at $-35\text{ }^\circ\text{C}$ to yield purple crystals. Removal of the volatiles a second time resulted in the isolation of **3-C** (7.73 g, 20.1 mmol, 91%) as a colorless solid. ^1H NMR (C_6D_6 , Figure

3.17): δ 7.09 (d, 2H, $J_{\text{HH}} = 3$ Hz, Ar H), 6.82 (d, 2H, $J_{\text{HH}} = 9$ Hz, Ar H), 6.56 (dd, 2H, $J_{\text{HH}} = 3$ Hz, $J_{\text{HH}} = 9$ Hz, Ar H), 6.00 (s, 1H, NH), 3.13 (s, 6H, CH₃). $^{13}\text{C}\{^1\text{H}\}$ NMR (C₆D₆): δ 155.4 (s, Ar CN), 135.4 (s, Ar CP), 120.4 (s, Ar C), 118.3 (s, Ar C), 115.7 (s, Ar CCH₃), 115.0 (s, Ar C), 55.3 (s, CH₃).

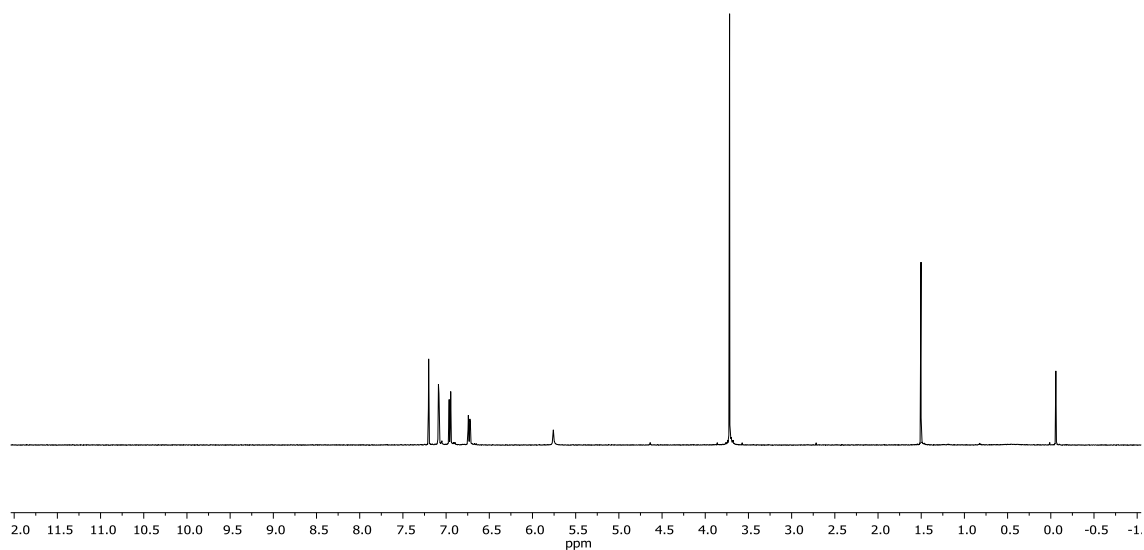


Figure 3.17 ^1H NMR spectrum of **3-C** (500 MHz, C₆D₆). Silicone grease was observed in the NMR solvent.

3-D. A Schlenk flask was charged with hexamethyldisilazane (1.0 mL, 5.0 mmol), *n*-butyllithium (2.0 mL of a 2.5 M solution in hexanes, 5.0 mmol) and tetrahydrofuran (5 mL). The reaction mixture was stirred for 20 min and then **3-C** (1.7 g, 4.5 mmol) was added. After 5 min of continued stirring CH₃I (0.42 mL, 6.7 mmol) was added to the solution. The reaction mixture was stirred overnight and then the volatiles were removed *in vacuo*. The resulting colorless solid was taken up in diethyl ether and filtered through a bed of silica gel. Addition of pentane to the ethereal solution resulted in copious precipitation. The precipitation was collected to yield **3-D** as a colorless powder (0.80 g, 2.0 mmol, 44%). ¹H NMR (C₆D₆, Figure 3.18): δ 7.16 (d, *J*_{HH} = 3 Hz, 2H, Ar *H*), 6.70 (d, *J*_{HH} = 9 Hz, 2H, Ar *H*), 6.62 (dd, *J*_{HH} = 9 Hz, *J*_{HH} = 3 Hz, 2H, Ar *H*), 3.13 (s, 6H, OCH₃), 2.93 (s, 3H, NCH₃). ¹³C{¹H} NMR (C₆D₆): δ 156.6 (s), 142.9 (s), 124.6 (s), 121.5 (s), 119.5 (s), 114.5 (s).

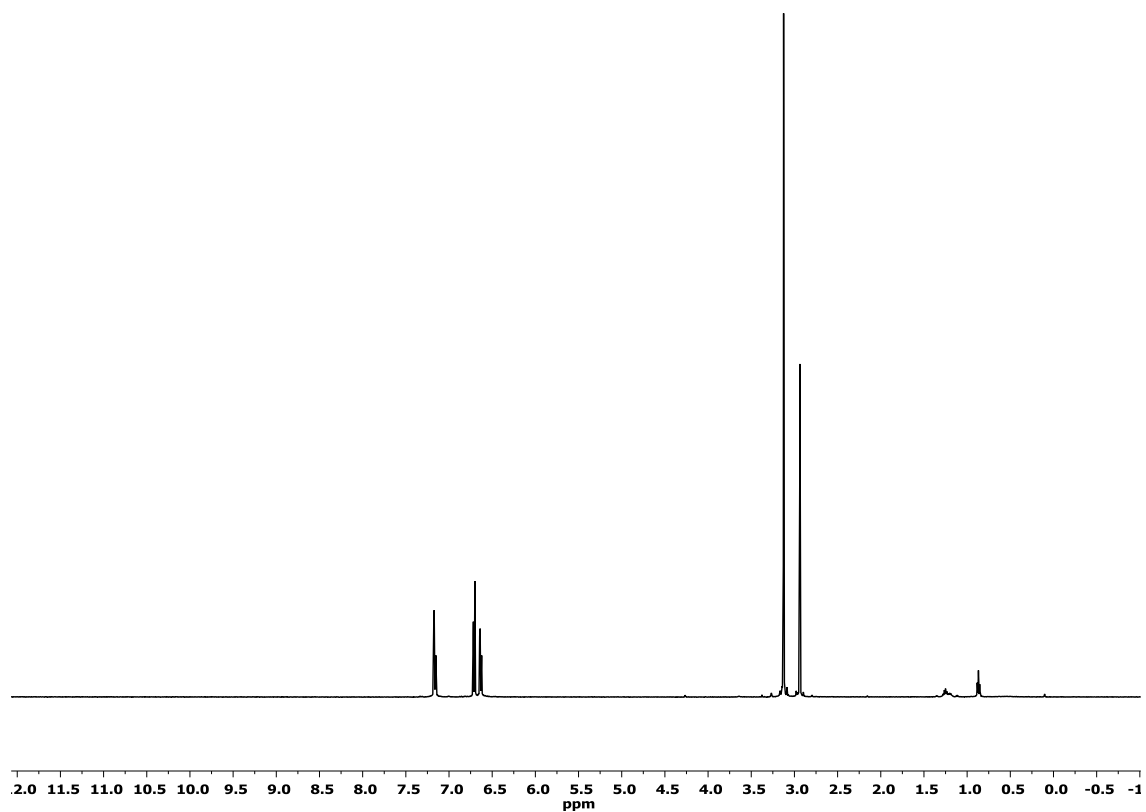


Figure 3.18 ¹H NMR spectrum of **3-D** (500 MHz, C₆D₆). Trace quantities of hexane and silicone grease are observed.

3-4Me. A Schlenk flask was charged with **3-D** (0.68 g, 1.7 mmol), a stir bar, diethyl ether (10 mL), and *n*-butyllithium (1.4 mL, 2.5 M solution in hexanes, 3.4 mmol). After 1 h ClPⁱPr₂ (0.54 mL, 3.4 mmol) was added to the ethereal solution via syringe. The reaction was stirred for 2 h and then filtered through a pad of silica gel. Removal of the volatiles under vacuum and recrystallization in pentane gave **3-4Me** as a colorless powder (0.75 mg, 1.6 mmol, 93%). ¹H NMR (C₆D₆, Figure 3.19): δ 7.17 (dd, *J*_{HH} = 3 Hz, *J*_{PH} = 2 Hz, 2H, Ar *H*), 6.90 (dd, *J*_{HH} = 9 Hz, *J*_{PH} = 3 Hz, 2H, Ar *H*), 6.68 (dd, *J*_{HH} = 9 Hz, *J*_{HH} = 3 Hz, 2H, Ar *H*), 3.48 (s, 3H, NCH₃), 3.38 (s, 6H, OCH₃), 2.13 – 1.97 (m, 4H, CH(CH₃)₂), 1.18 (dd, *J*_{PH} = 13 Hz, *J*_{HH} = 8 Hz, 12H, CH(CH₃)₂), 1.01 (dd, *J*_{PH} = 12 Hz, *J*_{HH} = 7 Hz, 12H, CH(CH₃)₂). ¹H{³¹P δ -6.2} NMR (C₆D₆): δ 7.17 (dd, *J*_{HH} = 3 Hz, 2H, Ar *H*), 6.90 (dd, *J*_{HH} = 9 Hz, 2H, Ar *H*), 6.68 (dd, *J*_{HH} = 9 Hz, *J*_{HH} = 3 Hz, 2H, Ar *H*), 3.48 (s, 3H, NCH₃), 3.38 (s, 6H, OCH₃), 2.13 – 1.97 (m, 4H, CH(CH₃)₂), 1.18 (dd, *J*_{HH} = 8 Hz, 12H, CH(CH₃)₂), 1.01 (dd, *J*_{HH} = 7 Hz, 12H, CH(CH₃)₂). ¹³C{¹H} NMR (C₆D₆): δ 155.7 (s, C, Ar CN), 152.4 (d, *J*_{CP} = 5 Hz, C, Ar C), 134.3 (d, *J*_{CP} = 10 Hz, C, Ar C), 124.8 (s, Ar C), 120.0 (s, Ar C), 114.2 (s, Ar C), 55.0 (s, OCH₃), 25.0 (d, *J*_{CP} = 1 Hz, CH(CH₃)₂), 21.1 (s, CH₃), 20.3 (s, CH₃). ³¹P{¹H} NMR (C₆D₆): δ -6.2 (s)

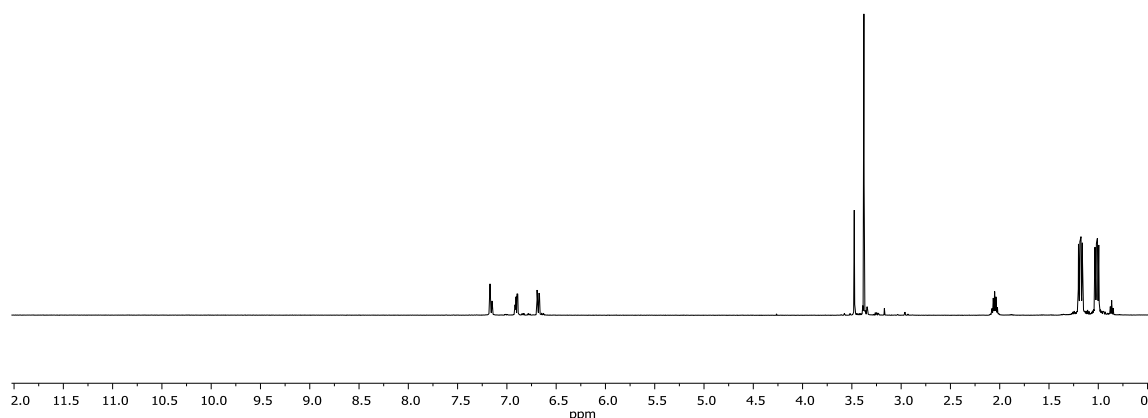


Figure 3.19 ^1H NMR spectrum of **3-4Me** (500 MHz, C_6D_6). Trace quantities of pentane and diethyl ether are observed.

3-4H. A 25 mL Schlenk flask was charged with **3-D** (0.13 g, 0.34 mmol), diethyl ether (10 mL) and a stir bar. *n*-Butyllithium (0.54 mL, 1.4 mmol, 2.5 M in hexanes) was then added drop-wise to the stirring solution at ambient temperature. The reaction mixture was stirred for 45 min and prior to addition of ClPP^iPr_2 (0.16 mL, 1.0 mmol). The reaction underwent an immediate color change from yellow to red, however stirring overnight gave in a colorless solution. The reaction was quenched with degassed H_2O (200 μL) and stirred for 1 h at ambient temperature. The volatiles were removed *in vacuo* and the resulting oil was dissolved in diethyl ether and filtered through silica gel.

The light brown oil which was observed after removal of the volatiles was taken up in pentane. Colorless crystals were formed after this solution was concentrated and stored at -35 °C for 2 wks (31 mg, 83 μmol, 24%). The ligand was used without any further purification. ^1H NMR (C_6D_6 , Figure 3.20): δ 7.90 (t, 1H, $J_{\text{PH}} = 8$ Hz, NH), 7.30 (dd, 2H, $J_{\text{PH}} = 4$ Hz, $J_{\text{HH}} = 9$ Hz, Ar H), 7.10 (s, 2H, Ar H), 6.72 (dd, 2H, $J_{\text{HH}} = 3$ Hz, $J_{\text{HH}} = 9$ Hz, Ar H), 3.40 (s, 6H, CH_3O), 2.00-1.91 (m, 2H, $\text{CH}(\text{CH}_3)_2$), 1.11 (dd, 12H, $J_{\text{PH}} = 15$ Hz, $J_{\text{HH}} = 7$ Hz, $\text{CH}(\text{CH}_3)_2$), 0.97 (dd, 12H, $J_{\text{PH}} = 12$ Hz, $J_{\text{HH}} = 7$ Hz, $\text{CH}(\text{CH}_3)_2$). $^1\text{H}\{^{31}\text{P}$ δ -11.7} NMR (C_6D_6): δ 7.90 (s, 1H, NH), 7.30 (d, 2H, $J_{\text{HH}} = 9$ Hz, Ar H), 7.10 (s, 2H, Ar H), 6.72 (dd, 2H, $J_{\text{HH}} = 3$ Hz, $J_{\text{HH}} = 9$ Hz, Ar H), 3.40 (s, 6H, CH_3O), 2.00-1.91 (m, 2H, $\text{CH}(\text{CH}_3)_2$), 1.11 (d, 12H, $J_{\text{HH}} = 7$ Hz, $\text{CH}(\text{CH}_3)_2$), 0.97 (d, 12 H, $J_{\text{HH}} = 7$ Hz, $\text{CH}(\text{CH}_3)_2$). $^{13}\text{C}\{^1\text{H}\}$ NMR (CDCl_3): δ 153.9 (s, Ar CN), 143.6 (d, $J_{\text{CP}} = 20$ Hz, Ar CN), 125.3 (d, $J_{\text{CP}} = 18$ Hz, Ar C), 119.4 (s, Ar C), 118.5 (s, Ar C), 115.3 (s, Ar C), 55.2 (s, CH_3O), 23.7 (d, $J_{\text{CP}} = 12$ Hz, $\text{CH}(\text{CH}_3)_2$), 20.4 (d, $J_{\text{CP}} = 19$ Hz, $\text{CH}(\text{CH}_3)_2$), 19.3 (d, $J_{\text{CP}} = 8$ Hz, $\text{CH}(\text{CH}_3)_2$). $^{31}\text{P}\{^1\text{H}\}$ NMR (C_6D_6): δ -11.7.

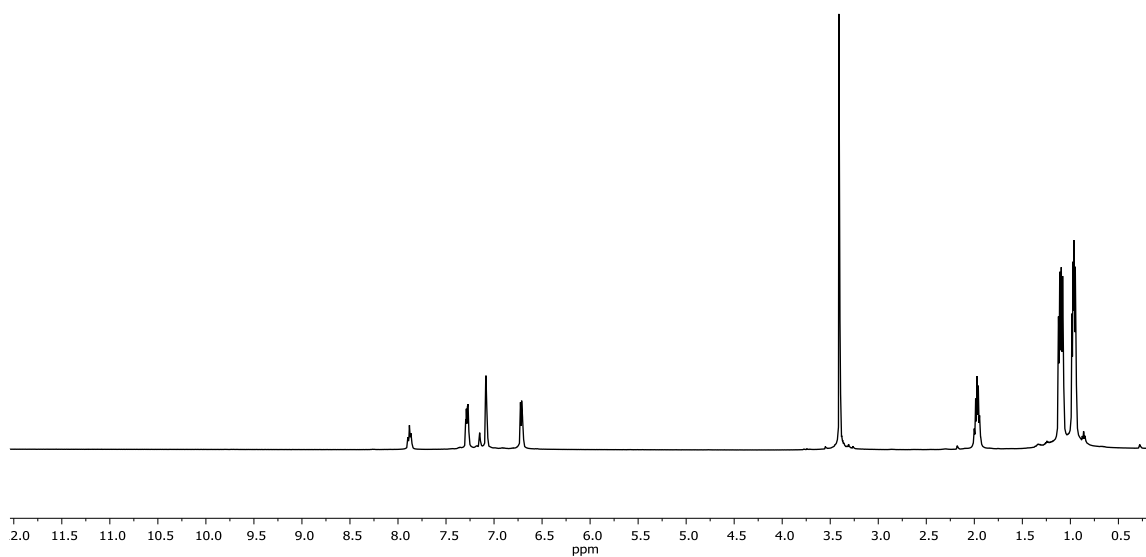


Figure 3.20 ^1H NMR spectrum of **3-4H** (500 MHz, C_6D_6). Trace quantities of pentane are observed.

3-4PdCl. A Teflon stoppered Schlenk flask was charged with toluene (10 mL), a stir bar, **3-4Me** (541 mg, 1.14 mmol), and Pd(COD)Cl₂ (324 mg, 1.14 mmol). The reaction vessel was then placed in an 80 °C oil bath for 3 d. After warming the reaction vessel to room temperature the toluene solution was passed through a pad of silica gel and washed with diethyl ether. Removal of the volatiles and recrystallization at -35 °C in toluene gave **3-4PdCl** as a green powder (281 mg, 467 μmol, 41%). ¹H NMR (C₆D₆, Figure 3.21): δ 7.61 (d, 2H, *J*_{HH} = 9 Hz, Ar *H*), 6.71 (s, 2H, Ar *H*), 6.62 (d, 2H, *J*_{HH} = 9 Hz, Ar *H*), 3.38 (s, 6H, *MeO*), 2.27-2.24 (m, 4H, *CH*(CH₃)₂), 1.42 (dvt, 12H, *J*_{PH} = 16 Hz, *J*_{HH} = 7 Hz, CH(CH₃)₂), 1.11 (dvt, 12H, *J*_{PH} = 15 Hz, *J*_{HH} = 7 Hz, CH(CH₃)₂). ¹H{³¹P δ 47.9} NMR (C₆D₆): δ 7.61 (d, 2H, *J*_{HH} = 9 Hz, Ar *H*), 6.71 (s, 2H, Ar *H*), 6.62 (d, 2H, *J*_{HH} = 9 Hz, Ar *H*), 3.38 (s, 6H, *CH*₃O), 2.27-2.24 (m, 4H, *CH*(CH₃)₂), 1.42 (d, 12H, *J*_{HH} = 7 Hz, CH(CH₃)₂), 1.11 (d, 12H, *J*_{HH} = 7 Hz, CH(CH₃)₂). ¹³C{¹H} NMR (C₆D₆): δ 159.0 (s, Ar CN), 151.4 (s, Ar C), 119.2 (s, Ar C), 117.7 (m, Ar CH, appears to be two overlapping peaks), 116.0 (s, Ar CH), 55.7 (s, OCH₃), 25.1 (t, *J*_{CP} = 12 Hz, CH(CH₃)₂), 18.69 (s, CH₃), 18.0 (s, CH₃). ³¹P{¹H} NMR (C₆D₆): δ 47.9. Elemental Analysis Calculated: C, 51.84; H, 6.69. Found: C, 51.76; H, 6.74.

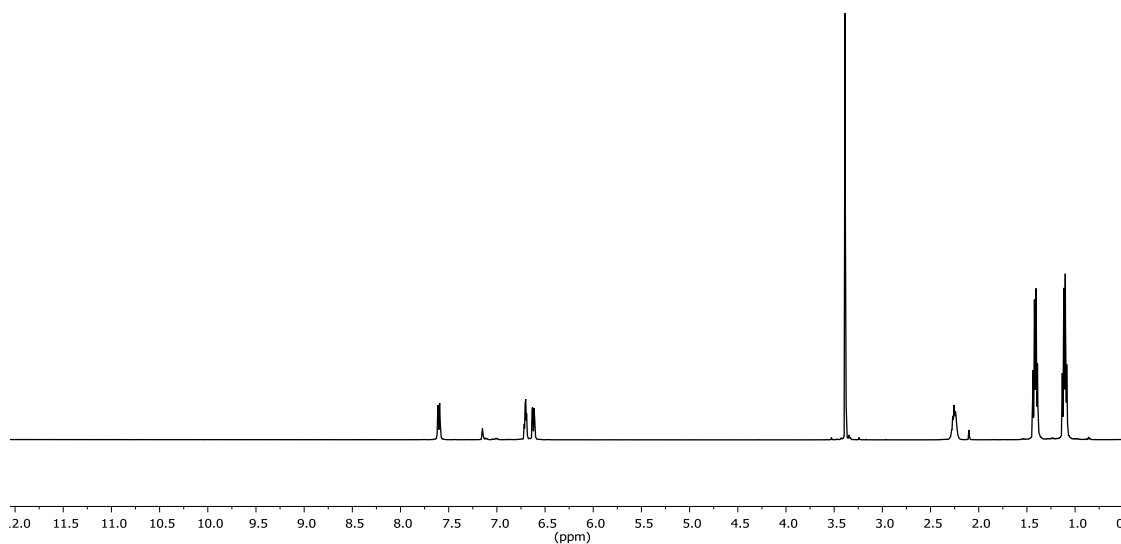


Figure 3.21 ^1H NMR spectrum of **3-4PdCl** (500 MHz, C_6D_6). Trace quantities of pentane and toluene are observed.

[3-4PdCl][CHB₁₁Cl₁₁]. A Schlenk flask was charged with **3-4PdCl** (85 mg, 0.14 mmol), [tris(4-bromophenyl)aminium][CHB₁₁Cl₁₁] (0.14 g, 0.14 mmol), a stir bar, and dichloromethane (5 mL). An immediate color change to brown is observed and a brown precipitate forms. After 30 min the volatiles were removed under vacuum and the resulting brown precipitate was washed with diethyl ether. The solid was then dissolved in a minimal amount of dichloromethane and stored at $-35\text{ }^\circ\text{C}$ for 36 h. The resulting brown crystals were then collected by decanting off the solvent. ^1H NMR analysis revealed that the amine has been completely removed and no signals corresponding to a

diamagnetic complex were observed. Elemental Analysis Calculated: C, 28.82; H3.76. Found: C, 28.76; H 3.62.

3-4PdOAc. A J. Young tube was charged with **3-4Me** (40 mg, 0.11 mmol), Pd(OAc)₂ (25 mg, 0.11 mmol), and C₆D₆ (1 mL). The reaction mixture immediately turned a deep red color. The volatiles were removed *in vacuo* and the resulting red solid was taken up in diethyl ether and filtered through a pad of silica gel. The volatiles were again removed while heating at 100 °C to yield **3-4PdOAc** as a red powder (20 mg, 32 μmol, 30%). ¹H NMR (C₆D₆, Figure 3.22): δ 7.57 (d, 2H, *J* = 9 Hz, Ar *H*), 6.68 (s, 2H, Ar *H*), 6.61 (d, *J* = 3 Hz, Ar *H*), 3.39 (s, 6H, Ar CH₃), 2.26-2.24 (m, 4H, CH(CH₃)₂), 2.23 (s, 3H, OAc), 1.36 (dvt, 12H, *J*_{PH} = 17 Hz, *J*_{HH} = 8 Hz, CH(CH₃)₂), 1.09 (dvt, 12H, *J*_{PH} = 15 Hz, *J*_{HH} = 8 Hz, CH(CH₃)₂). ¹³C {¹H} NMR (C₆D₆): δ 175.8 (CO), 159.0 (t, *J*_{CP} = 11 Hz, CN), 151.2 (t, *J*_{CP} = 4 Hz), 119.6 (t, *J*_{CP} = 19 Hz), 117.8 (s), 117.6 (s), 116.3 (t, *J*_{CP} = 8 Hz), 55.7 (s, OCH₃), 24.7 (t, *J*_{CP} = 11 Hz, CH(CH₃)₂), 23.3 (s, OAc), 18.4 (CH(CH₃)₂), 17.7 (CH(CH₃)₂). ³¹P {¹H} NMR (C₆D₆): δ 48.1.

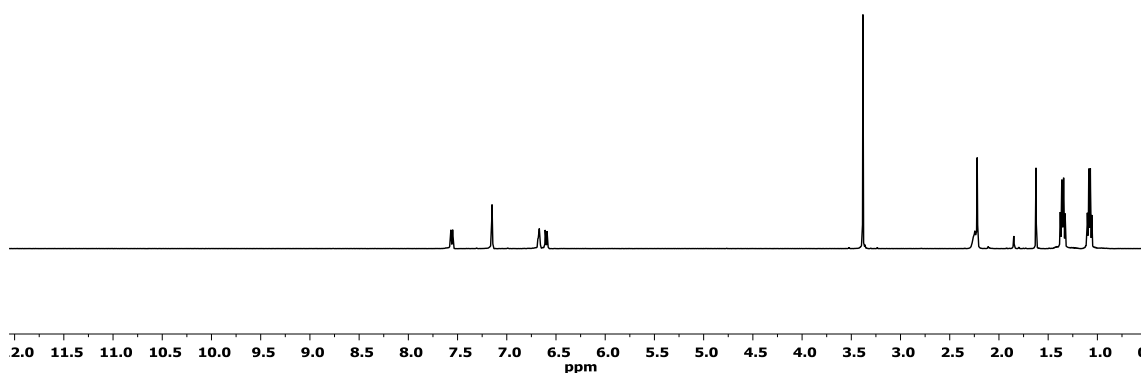


Figure 3.22 ^1H NMR spectrum of **3-4PdOAc** (500 MHz, C_6D_6). Acetic acid is observed.

3-4Rh(CH₃)(Cl). A J. Young tube was charged with **3-4Me** (0.18 g, 0.38 mmol), $[\text{Rh}(\text{COD})\text{Cl}]_2$ (93 mg, 0.19 mmol) and C_6D_6 (1.5 mL). After the reaction mixture at 90 °C for 18 h a color change from red to green was observed. The solution was then passed through a pad of silica gel, using diethyl ether to ensure quantitative transfer. The volatiles were removed *in vacuo* and the resulting solid was washed three times with toluene. The volatiles were again removed and the oil was taken up in a 1:1 mixture (v/v) of pentane and diethyl ether and recrystallized at 35 °C to yield **3-4Rh(CH₃)(Cl)** as

a green powder (66 mg, 0.11 mmol, 29%). ^1H NMR (C_6D_6 , Figure 3.23): δ 7.76 (dt, $J_{\text{HH}} = 9$ Hz, $J_{\text{PH}} = 2$ Hz, 2H, Ar *H*), 6.82 (dvt, $J_{\text{PH}} = 8$ Hz, $J_{\text{HH}} = 4$ Hz, 2H, Ar *H*), 6.64 (dd, $J_{\text{HH}} = 9$ Hz, $J_{\text{HH}} = 3$ Hz, 2H, Ar *H*), 3.43 (s, 6H, OCH_3), 2.61 (m, $J = 7$ Hz, 2H, $\text{CH}(\text{CH}_3)_2$), 2.38 – 2.34 (m, 2H, $\text{CH}(\text{CH}_3)_2$), 2.33 (m, 3H, Rh CH_3), 1.49 (dvt, $J_{\text{PH}} = 15$ Hz, $J_{\text{HH}} = 7$ Hz, 6H, $\text{CHCH}_3)_2$), 1.15 (dvt, $J_{\text{PH}} = 15$ Hz, $J_{\text{HH}} = 7$ Hz, 12H, $\text{CHCH}_3)_2$), 0.98 (dvt, $J_{\text{PH}} = 15$ Hz, $J_{\text{HH}} = 7$ Hz, 6H, $\text{CHCH}_3)_2$). $^1\text{H}\{^{31}\text{P}$ δ 36.5} NMR (C_6D_6): δ 7.76 (d, $J_{\text{HH}} = 9$ Hz 2H, Ar *H*), 6.82 (d, $J_{\text{HH}} = 4$ Hz, 2H, Ar *H*), 6.64 (dd, $J_{\text{HH}} = 9$ Hz, $J_{\text{HH}} = 3$ Hz, 2H, Ar *H*), 3.43 (s, 6H, OCH_3), 2.61 (m, 2H, $\text{CH}(\text{CH}_3)_2$), 2.38 – 2.34 (m, 2H, $\text{CH}(\text{CH}_3)_2$), 2.33 (d, $J_{\text{RhH}} = 3$ Hz, 3H, Rh CH_3), 1.49 (d, $J_{\text{HH}} = 7$ Hz, 6H, $\text{CHCH}_3)_2$), 1.15 (d, $J_{\text{HH}} = 7$ Hz, 12H, $\text{CHCH}_3)_2$), 0.98 (d, $J_{\text{HH}} = 7$ Hz, 6H, $\text{CHCH}_3)_2$). $^{13}\text{C}\{^1\text{H}\}$ NMR (C_6D_6): δ 158.1 (s, Ar *C*), 151.2 (s, Ar *C*), 121.0 (s, Ar *C*), 118.0 (s, Ar *CH*), 117.8 (s, Ar *CH*), 117.1 (s, Ar *CH*), 55.7 (s, OCH_3), 27.0 (d, $J_{\text{CP}} = 11$ Hz, $\text{CH}(\text{CH}_3)_2$), 24.2 (d, $J_{\text{CP}} = 12$ Hz, $\text{CH}(\text{CH}_3)_2$), 19.4 (d, $J_{\text{CP}} = 33$ Hz, $\text{CH}(\text{CH}_3)_2$), 18.1 (d, $J_{\text{CP}} = 17$ Hz, $\text{CH}(\text{CH}_3)_2$), 2.0 (d, $J_{\text{RhC}} = 33$ Hz, Rh CH_3). $^{31}\text{P}\{^1\text{H}\}$ NMR (C_6D_6): δ 36.5 (d, $J_{\text{Rhp}} = 109$ Hz).

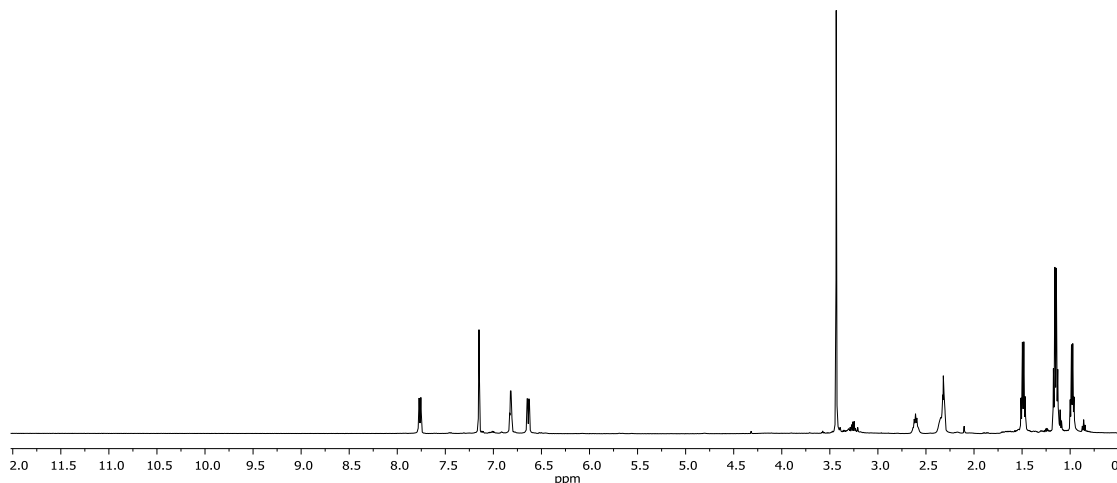


Figure 3.23 ^1H NMR spectrum of **3-4Rh(CH₃)Cl** (500 MHz, C₆D₆). Trace quantities of pentane, toluene, and diethyl ether are observed.

3-4RhCO. A J. Young tube was charged with **3-4Rh(CH₃)Cl** (44.0 mg, 71.8 μmol), CO (1 atm), and C₆D₆ (1 mL). The J. Young tube was placed in a 70 °C oil bath for 18 h. Crystals were then obtained by layering the benzene solution with diethyl ether. The brown crystals were collected by decanting the solvent layer and drying the resulting orange blocks under vacuum. **3-4RhCO** was isolated as an orange powder. (10.0 mg, 17.0 μmol , 24%). ^1H NMR (C₆D₆, Figure 3.24): δ 7.64 (d, $J_{\text{HH}} = 9$ Hz, 2H, Ar *H*), 6.80 (q, $J_{\text{PH}} = 4$ Hz, 2H, Ar *H*), 6.64 (dd, $J_{\text{HH}} = 9$ Hz, $J_{\text{HH}} = 3$ Hz, 2H, Ar *H*), 3.44 (s, 6H, OCH₃), 2.14 – 2.06 (m, 4H, CH(CH₃)₂), 1.24 (dvt, $J_{\text{PH}} = 15$ Hz, $J_{\text{HH}} = 7$ Hz, 12H,

$\text{CH}(\text{CH}_3)_2$), 1.03 (dvt, $J_{\text{PH}} = 15 \text{ Hz}$, $J_{\text{HH}} = 7 \text{ Hz}$, 12H, $\text{CH}(\text{CH}_3)_2$). $^1\text{H}\{^{31}\text{P} \delta 62.0\}$ NMR (C_6D_6 , Figure 3.24): δ 7.64 (d, $J_{\text{HH}} = 9 \text{ Hz}$, 2H, Ar H), 6.80 (s, 2H, Ar H), 6.64 (dd, $J_{\text{HH}} = 9 \text{ Hz}$, $J_{\text{HH}} = 3 \text{ Hz}$, 2H, Ar H), 3.44 (s, 6H, OCH_3), 2.10 (hept, $J_{\text{HH}} = 7 \text{ Hz}$, 4H, $\text{CH}(\text{CH}_3)_2$), 1.24 (d, $J_{\text{HH}} = 7 \text{ Hz}$, 12H, $\text{CH}(\text{CH}_3)_2$), 1.03 (d, $J_{\text{HH}} = 7 \text{ Hz}$, 12H, $\text{CH}(\text{CH}_3)_2$). $^{13}\text{C}\{^1\text{H}\}$ NMR (C_6D_6): δ 198.2 (d, $J_{\text{RhC}} = 65 \text{ Hz}$, CO), 159.1 (d, $J_{\text{CP}} = 15 \text{ Hz}$, Ar C), 150.9 (s, Ar C), 122.2 (t, $J_{\text{CP}} = 17 \text{ Hz}$, Ar C), 118.1 (s, Ar CH), 116.9 (s, Ar CH), 115.1 (s, Ar CH), 55.8 (s, OCH_3), 25.8 (s, $\text{CH}(\text{CH}_3)_2$), 19.5 (s, CH_3), 18.5 (s, CH_3). $^{31}\text{P}\{^1\text{H}\}$ NMR (C_6D_6): δ 62.0 (d, $J_{\text{RHP}} = 135 \text{ Hz}$). IR (ν_{CO}): 1933 cm^{-1} .

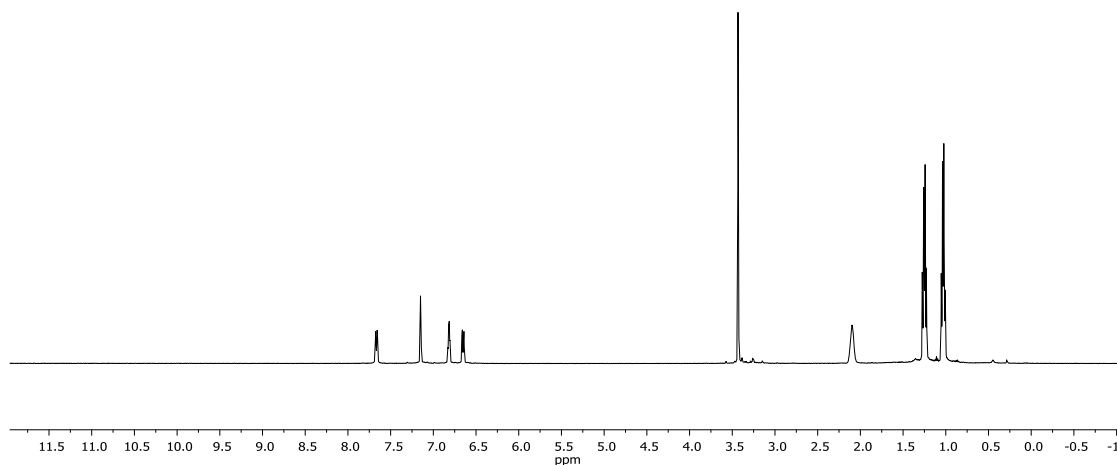


Figure 3.24 ^1H NMR spectrum of **3-4RhCO** (500 MHz, C_6D_6). Trace quantities of diethyl ether and pentane are observed.

3.11.7 Synthesis of complexes of **3-5Me**

3-5NiCl. A Schlenk flask was charged with **3-5Me** (3.00 g, 6.65 mmol), $\text{NiCl}_2(\text{H}_2\text{O})_6$ (1.90 g, 7.98 mmol), toluene (25 mL) and a stir bar. The reaction mixture was then refluxed under a flow of Ar for 6 h. The solution was then passed through a pad of Celite. The volatiles were removed under vacuum and the resulting green solid was washed with pentane to yield **3-5NiCl** (2.58 g, 73%). ^1H NMR (C_6D_6 , Figure 3.25): δ 7.13 (ddt, $J_{\text{HH}} = 9$ Hz, $J_{\text{HH}} = 4$ Hz, $J_{\text{PH}} = 2$ Hz, 2H, Ar H), 6.75 (dq, $J_{\text{HH}} = 7$ Hz, $J_{\text{HH}} = 4$ Hz, 2H, Ar H), 6.57 (td, $J_{\text{HF}} = 8$ Hz, $J_{\text{HH}} = 3$ Hz, 2H, Ar H), 2.03 (m, 4H, $\text{CH}(\text{CH}_3)_2$), 1.41 (dvt, $J_{\text{PH}} = 15$ Hz, $J_{\text{HH}} = 7$ Hz, 12H, $\text{CH}(\text{CH}_3)_2$), 1.10 (dvt, $J_{\text{PH}} = 15$ Hz, $J_{\text{HH}} = 7$ Hz, 12H, $\text{CH}(\text{CH}_3)_2$). $^1\text{H}\{^{31}\text{P}$ δ 32.7} NMR (C_6D_6): δ 7.13 (dd, $J = 9$ Hz, $J = 4$ Hz, 2H), 6.75 (dd, $J = 7$ Hz, $J = 4$ Hz, 2H), 6.57 (td, $J = 8$ Hz, $J = 3$ Hz, 1H), 2.03 (hept, $J = 7$ Hz, 4H), 1.41 (d, $J = 7$ Hz, 12H), 1.10 (d, $J = 7$ Hz, 12H). $^{13}\text{C}\{^1\text{H}\}$ NMR (C_6D_6): δ 160.5 (t, $J_{\text{CP}} = 13$ Hz, Ar C), 155.4 (s, Ar C), 153.5 (s, Ar C), 121.8 (t, $J_{\text{CP}} = 18$ Hz, Ar C), 117.9 (dd, $J_{\text{CF}} = 101$ Hz, $J_{\text{CP}} = 22$ Hz, Ar C), 116.4 (d, $J_{\text{CP}} = 9$ Hz, Ar C), 24.0 (t, $J_{\text{CP}} = 12$ Hz, $\text{P}(\text{CH}(\text{CH}_3)_2)_2$), 18.4 (s, $\text{P}(\text{CH}(\text{CH}_3)_2)_2$), 17.5 (s, $\text{P}(\text{CH}(\text{CH}_3)_2)_2$). ^{19}F NMR (C_6D_6): δ -128.6 (q, $J_{\text{HF}} = 8$ Hz). $^{31}\text{P}\{^1\text{H}\}$ NMR (C_6D_6): δ 32.7 (s). Elemental Analysis Calculated: C, 60.11; H, 6.39. Found: C, 60.06; H, 6.42.

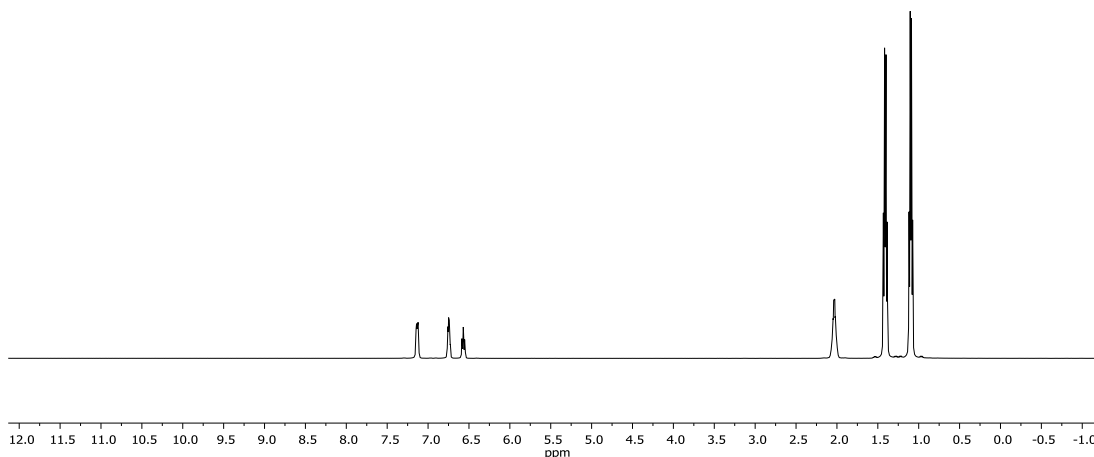


Figure 3.25 ¹H Spectrum of **3-5NiCl** (500 MHz, C₆D₆).

3.11.8 Synthesis of **3-F**

3-F.^{118a} **3-A** (13 g, 36 mmol) was dissolved in anhydrous diethyl ether (100 ml) and cooled with a dry ice/acetone bath. The amine solution was then treated with *n*-butyllithium (29 mL, 2.5 M in hexanes) in a drop-wise fashion via an addition funnel. The reaction was then stirred for 30 min before being warmed to room temperature to yield a yellow solution. The reaction was again cooled with a dry ice/acetone bath and ClPⁱPr₂ (112 mL, 73 mmol) was added in a drop-wise fashion via syringe resulting in an immediate color change from yellow to orange. The reaction was stirred for 12 h before being hydrolyzed with a 1:1 ethanol/H₂O solution (2.5 mL). Stirring was commenced for

an additional 1 h before removing the volatiles *in vacuo*. The resulting colorless solid was then extracted in a pentane/diethyl ether solution (10:1) and stirred vigorously over silica gel for 30 min before being filtered through a pad of Celite. The volatiles were removed and the resulting white solid was washed with 3 × 5 mL portions of pentane to yield pure product as a white solid (12 g, 87%). ¹H NMR (C₆D₆, Figure 3.26): δ 7.69 (d, 1H, *J* = 10 Hz, *NH*), 7.23 (m, 3H, *Ar H*), 7.17 (m (overlapping with solvent), 1H, *Ar H*), 6.90 (d, 1H, *J* = 8 Hz, *Ar H*), 6.71 (d, 1H, *J* = 9 Hz, *Ar H*), 2.18 (s, 3H, *Ar CH*₃), 1.96 (m, 2H, *CH(CH*₃*)*₂), 1.93 (s, 3H, *Ar CH*₃), 1.06 (dd, 6H, *J*_{PH} = 16 Hz, *J*_{HH} = 7 Hz, *CH(CH*₃*)*₂), 0.92 (dd, 6H, *J*_{PH} = 11 Hz, *J*_{HH} = 7 Hz, *CH(CH*₃*)*₂). ¹³C{¹H} NMR (C₆D₆): δ 146.1 (d, *J*_{CP} = 19 Hz, *CN*), 139.7 (s, *Ar C*), 133.9 (s, *Ar C*), 133.9 (d, *J*_{CP} = 2 Hz, *Ar CH*), 131.0 (s, *Ar C*), 130.7 (s, *Ar C*), 130.0 (s, *Ar C*), 128.9 (s, *Ar C*), 128.3 (s, *Ar C*), 118.5 (d, *J*_{CP} = 3 Hz, *Ar CH*), 116.5 (s, *Ar C*), 114.1 (s, *Ar C*), 23.2 (d, *J*_{CP} = 11 Hz, *CH(CH*₃*)*₂), 20.9 (s, *Ar CH*₃), 20.4 (s, *Ar CH*₃), 20.2 (d, *J*_{CP} = 10 Hz, *CH(CH*₃*)*₂), 18.9 (d, *J*_{CP} = 8 Hz, *CH(CH*₃*)*₂). ³¹P{¹H} NMR (C₆D₆): δ -13.9.

Note: Often times a small amount of **3-3H** is formed. This can be readily removed by washing the solid with a small amount of pentane. ¹H NMR (C₆D₆): δ 8.28 (t, 1H, *J*_{PH} = 8 Hz, *N H*), 7.38 (d, 2H, *J* = 6 Hz, *Ar H*), 7.19 (s, 2H, *Ar H*), 6.91 (d, 2H, *J* = 8 Hz, *Ar H*), 2.18 (s, 6H, *Ar CH*₃), 2.01 (m, 4H, *CH(CH*₃*)*₂), 1.12 (dd, 12H, *J*_{PH} = 15 Hz, *J*_{HH} = 7 Hz, *CH(CH*₃*)*₂), 0.97 (dd, *J*_{PH} = 12 Hz, *J*_{HH} = 7 Hz, 12H, *CH(CH*₃*)*₂). ³¹P{¹H} NMR (C₆D₆): δ -12.9.

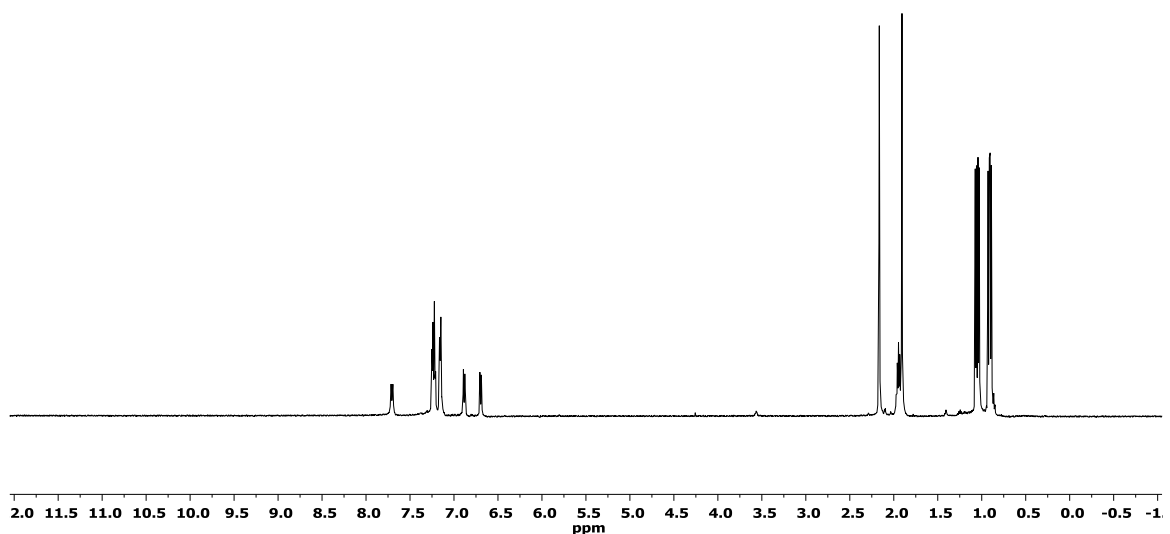


Figure 3.26 ^1H NMR spectrum of **3-F** (500 MHz, C_6D_6). Trace quantities of dichloromethane, pentane and diethyl ether are observed.

3.11.9 Synthesis of **3-6H** and its complexes

3-6H. A Schlenk flask was charged with **3-F** (0.98 g, 2.5 mmol) and a stir bar. The solid was then dissolved in diethyl ether (30 mL) and the resulting solution was cooled to $-35\text{ }^\circ\text{C}$ in the glove box freezer. *n*-Butyllithium (2.0 mL, 0.80 mmol, 2.5 M in hexanes) was then added slowly to the reaction flask via syringe, resulting in a bright yellow solution. The reaction mixture was then stirred for 2 h at ambient temperature. ClPPh_2 (0.50 mL, 2.5 mmol) was added slowly via syringe resulting in a red solution.

The reaction mixture was stirred overnight and then quenched with degassed H₂O (0.20 mL). Stirring was commenced for an additional hour resulting in a colorless solution. The volatiles were then removed *in vacuo* and the flask was brought into the glovebox where it was dissolved in diethyl ether and stirred vigorously over silica gel. The resultant mixture was then filtered through a pad of Celite and the diethyl ether was removed *in vacuo*. The resulting colorless solid was then dissolved in a 1:1 mixture (v/v) of pentane and toluene and recrystallized at -35 °C to yield **3-6H** as a colorless solid (0.78 g, 1.6 mmol, 62%). ¹H NMR (C₆D₆, Figure 3.27): δ 7.65 (dd, 1H, *J*_{PH} = 11 Hz, *J*_{HH} = 3 Hz), 7.49-7.46 (m, 4H), 7.39 (dd, 1H, *J* = 5 Hz, *J* = 9 Hz), 7.23 (dd, 1H, *J* = 5 Hz, *J* = 9 Hz), 7.11 (s, 1H), 7.08-6.99 (m, 6H), 6.95 (d, 1H, *J* = 4 Hz), 6.88 (dd, 2H, *J*_{HH} = 8 Hz, *J*_{PH} = 20 Hz), 2.15 (s, 3H, Ar CH₃), 1.95 (s, 3H, Ar CH₃), 1.87 (m, 2H, CH(CH₃)₂), 1.01 (dd, 6H, *J*_{HH} = 7 Hz, *J*_{PH} = 15 Hz, CH(CH₃)₂), 0.87 (dd, 6H, *J*_{HH} = 7 Hz, *J*_{PH} = 12 Hz, CH(CH₃)₂). ¹³C{¹H} NMR (CDCl₃): δ 147.2 (d, *J*_{CP} = 19 Hz, quaternary CN), 144.4 (d, *J*_{CP} = 20 Hz, quaternary CN), 136.4 (d, *J*_{CP} = 10 Hz, Ar C), 134.3 (s, Ar C), 134.2 (s, Ar C), 134.1 (s, Ar C), 133.6 (s, Ar C), 131.2 (s, Ar C), 130.4 (s, Ar C), 130.2 (s, Ar C), 128.8 (s, Ar C), 128.7 (s, Ar C), 128.6 (s, Ar C), 128.5 (s, Ar C), 128.4 (s, Ar C), 121.8 (d, *J*_{CP} = 16 Hz, Ar C), 119.2 (s, Ar C), 116.5 (s, Ar C), 23.1 (d, *J*_{CP} = 11 Hz, CH(CH₃)₂), 20.9 (s, Ar CH₃), 20.8 (s, Ar CH₃), 20.1 (d, *J*_{CP} = 19 Hz, CH(CH₃)₂), 19.0 (d, *J*_{CP} = 9 Hz, CH(CH₃)₂). ³¹P{¹H} NMR (C₆D₆): δ -16.1 (s), -14.2 (br s).

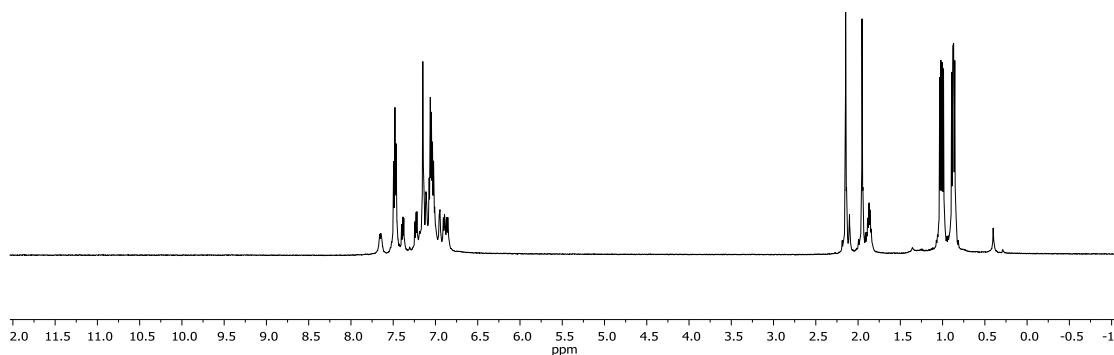


Figure 3.27 ^1H NMR spectrum of **3-6H** (500 MHz, C_6D_6). Residual toluene and water are observed.

3-6PdCl. A Schlenk flask was charged with a stir bar, **3-6H** (0.27 g, 0.54 mmol) and $\text{Pd}(\text{COD})\text{Cl}_2$ (0.15 g, 0.55 mmol). The solids were dissolved in toluene (10 mL) resulting in a dark red solution. 2,6-lutidine (63 μL , 0.54 mmol) was added to the mixture via syringe. The resulting solution was stirred for 12 h and then filtered through a pad of silica gel. The volatiles were removed *in vacuo* and the resulting red oil was dissolved in a 1:1 mixture (v/v) of pentane and toluene and then stored at $-35\text{ }^\circ\text{C}$. The resulting precipitate was dried *in vacuo* and recrystallized in benzene to yield **3-6PdCl** as a red powder (0.23 mg, 62%) ^1H NMR (C_6D_6 , Figure 3.28): δ 8.00-7.95 (m, 4H, Ar H), 7.77 (dd, 1H, $J = 8\text{ Hz}$, $J = 5\text{ Hz}$, Ar H), 7.67 (dd, 1H, $J = 9\text{ Hz}$, $J = 4\text{ Hz}$, Ar H),

7.03-6.98 (m, 7H, Ar *H*), 6.80 (d, 1H, $J = 9$ Hz, Ar *H*), 6.76-6.73 (m, 2H, Ar *H*), 2.31-2.23 (m, 2H, $\text{CH}(\text{CH}_3)_2$), 2.10 (s, 3H, Ar CH_3), 1.90 (s, 3H, Ar CH_3), 1.42 (dd, 6H, $J_{\text{PH}} = 17$ Hz, $J_{\text{HH}} = 7$ Hz, $\text{CH}(\text{CH}_3)_2$), 1.06 (dd, 6H, $J_{\text{PH}} = 16$ Hz, $J_{\text{HH}} = 7$ Hz, $\text{CH}(\text{CH}_3)_2$).

$^{31}\text{P}\{^1\text{H}\}$ NMR (C_6D_6): δ 54.0 (d, $J_{\text{PP}} = 438$ Hz), 25.9 (d, $J_{\text{PP}} = 438$ Hz). ^1H NMR (CDCl_3): δ 7.77-7.73 (m, 4H, Ar *H*), 7.49 (dd, 1H, $J = 9$ Hz, $J = 5$ Hz, Ar *H*), 7.45-7.40 (m, 7H, Ar *H*), 6.92 (d, 1H, $J = 9$ Hz, Ar *H*), 6.88 (t, 2H, $J = 7$ Hz, Ar *H*), 6.82 (d, 1H, $J = 10$ Hz, Ar *H*), 2.60 (m, 2H, $\text{CH}(\text{CH}_3)_2$), 2.22 (s, 3H, Ar CH_3), 2.14 (s, 3H, Ar CH_3), 1.48 (dd, 6H, $J_{\text{PH}} = 17$ Hz, $J_{\text{HH}} = 7$ Hz, $\text{CH}(\text{CH}_3)_2$), 1.31 (dd, 6H, $J_{\text{PH}} = 16$ Hz, $J_{\text{HH}} = 7$ Hz, $\text{CH}(\text{CH}_3)_2$).

$^{13}\text{C}\{^1\text{H}\}$ NMR (CDCl_3): δ 161.2 (d, $J_{\text{CP}} = 21$ Hz, Ar CN), 160.8 (d, $J_{\text{CP}} = 26$ Hz, Ar CN), 137.8 (s, Ar C), 133.7 (d, $J_{\text{CP}} = 2$ Hz, Ar CH), 133.6 (d, $J_{\text{CP}} = 2$ Hz, Ar CH), 132.8 (d, $J_{\text{CP}} = 2$ Hz, Ar CH), 132.4 (s, Ar C), 132.3 (d, $J_{\text{CP}} = 2$ Hz, Ar CH), 130.8 (d, $J_{\text{CP}} = 4$ Hz, Ar CH), 130.7 (d, $J_{\text{CP}} = 2$ Hz, Ar CH), 130.5 (d, $J_{\text{CP}} = 3$ Hz, Ar CH), 129.2 (s, Ar C), 128.8 (d, $J_{\text{CP}} = 11$ Hz, Ar CH), 128.3 (s, Ar C), 126.7 (d, $J_{\text{CP}} = 7$ Hz, Ar CH), 126.5 (d, $J_{\text{CP}} = 7$ Hz, Ar CH), 125.4 (s, Ar C), 120.9 (d, $J_{\text{CP}} = 3$ Hz, Ar C), 120.5 (d, $J_{\text{CP}} = 3$ Hz, Ar C), 118.7 (d, $J_{\text{CP}} = 3$ Hz, Ar C), 118.4 (d, $J_{\text{CP}} = 3$ Hz, Ar C), 116.4 (d, $J_{\text{CP}} = 13$ Hz, Ar CH), 116.1 (d, $J_{\text{CP}} = 14$ Hz, Ar CH), 25.1 (d, $J_{\text{CP}} = 4$ Hz, $\text{CH}(\text{CH}_3)_3$), 24.9 (d, $J_{\text{CP}} = 4$ Hz, $\text{CH}(\text{CH}_3)_3$), 20.4 (s, Ar CH_3), 20.3 (s, Ar CH_3), 18.7 (d, $J_{\text{CP}} = 5$ Hz, $\text{CH}(\text{CH}_3)_3$), 18.1 (d, $J_{\text{CP}} = 2$ Hz, $\text{CH}(\text{CH}_3)_3$).

$^{31}\text{P}\{^1\text{H}\}$ NMR (CDCl_3): δ 55.6 (d, $J_{\text{PP}} = 433$ Hz), 27.2 (d, $J_{\text{PP}} = 433$ Hz). Elemental Analysis Calculated: C, 60.20; H, 5.68; N, 2.19. Found: C, 60.13; H, 5.63; N, 2.04.

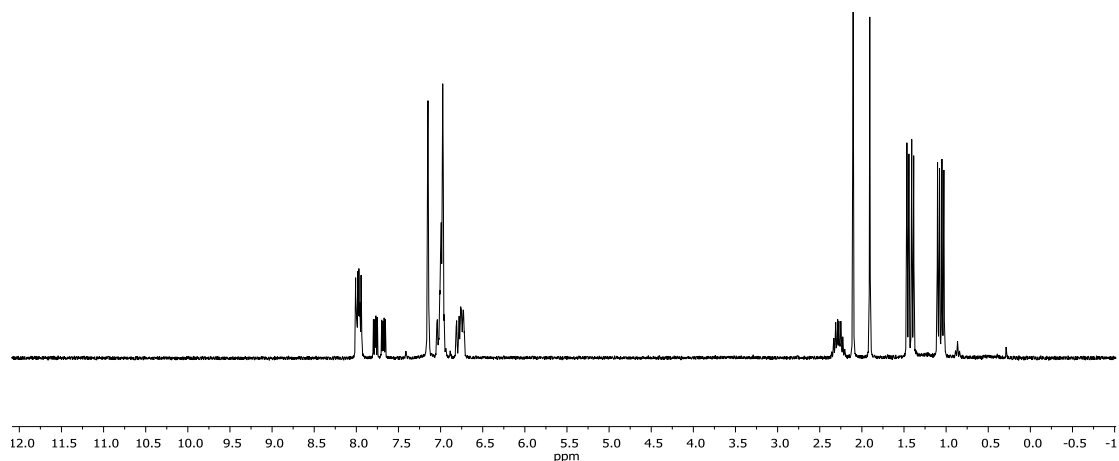


Figure 3.28 ^1H NMR spectrum of **3-6PdCl** (500 MHz, C_6D_6). Trace amounts of hexanes and silicone grease are observed.

3-6PdOAc. A Schlenk flask was charged with a stir bar, **3-6H** (306 mg, 0.616 mmol) and $\text{Pd}(\text{OAc})_2$ (138 mg, 0.616 mmol). The solids were dissolved in toluene (10 mL) resulting in a dark red solution. The resulting solution was stirred for 4 h and then filtered through a pad of silica gel. The volatiles were removed *in vacuo* and the resulting red solid was washed with 3×5 mL portions of toluene to yield **3-6Pd(OAc)** as a red powder (365 mg, 69%). ^1H NMR (CDCl_3 , Figure 3.29): δ 7.79-7.74 (m, 4H, Ar *H*), 7.46-7.40 (m, 7H, Ar *H*), 7.37 (dd, 1H, $J = 9$ Hz, $J = 4$ Hz, Ar *H*), 6.89-6.80 (m, 4H, Ar *H*), 2.60 (m, 2H, $\text{CH}(\text{CH}_3)_2$), 2.22 (s, 3H, Ar CH_3), 2.12 (s, 3H, Ar CH_3), 1.78 (s, 3H,

CH_3), 1.41 (dd, 6H, $J_{\text{PH}} = 18 \text{ Hz}$, $J_{\text{HH}} = 7 \text{ Hz}$, $\text{CH}(\text{CH}_3)_2$), 1.23 (dd, 6H, $J_{\text{PH}} = 15 \text{ Hz}$, $J_{\text{HH}} = 7 \text{ Hz}$, $\text{CH}(\text{CH}_3)_2$). $^{13}\text{C}\{^1\text{H}\}$ NMR (CDCl_3): δ 176.5 (s, CO), 161.1 (d, $J_{\text{CP}} = 21 \text{ Hz}$, Ar CN), 160.8 (d, $J_{\text{CP}} = 26 \text{ Hz}$, Ar CN), 134.2 (s, Ar CH), 133.6 (d, $J_{\text{CP}} = 2 \text{ Hz}$, Ar CH), 133.5 (d, $J_{\text{CP}} = 2 \text{ Hz}$, Ar CH), 132.7 (d, $J_{\text{CP}} = 3 \text{ Hz}$, Ar CH), 132.4 (s, Ar CH), 132.1 (d, $J_{\text{CP}} = 2 \text{ Hz}$, Ar CH), 131.1 (d, $J_{\text{CP}} = 3 \text{ Hz}$, Ar CH), 130.7 (d, $J_{\text{CP}} = 3 \text{ Hz}$, Ar CH), 129.2 (s, Ar CH), 128.8 (d, $J_{\text{CP}} = 10 \text{ Hz}$, Ar CH), 128.3 (s, Ar CH), 126.7 (s, Ar CH), 126.4 (s, Ar CH), 126.3 (s, Ar CH), 126.3 (s, Ar CH), 125.4 (s, Ar CH), 121.2 (d, $J_{\text{CP}} = 3 \text{ Hz}$, Ar C), 120.8 (d, $J_{\text{CP}} = 3 \text{ Hz}$, Ar C), 118.8 (d, $J_{\text{CP}} = 3 \text{ Hz}$, Ar C), 118.5 (d, $J_{\text{CP}} = 3 \text{ Hz}$, Ar C), 116.9 (d, $J_{\text{CP}} = 13 \text{ Hz}$, Ar C), 116.0 (d, $J_{\text{CP}} = 13 \text{ Hz}$, Ar C), 24.5 (d, $J_{\text{CP}} = 4 \text{ Hz}$, $\text{CH}(\text{CH}_3)_3$), 24.4 (d, $J_{\text{CP}} = 4 \text{ Hz}$, $\text{CH}(\text{CH}_3)_3$), 23.0 (s, CH_3), 20.4 (s, Ar CH_3), 20.3 (s, Ar CH_3), 18.4 (d, $J_{\text{CP}} = 6 \text{ Hz}$, $\text{CH}(\text{CH}_3)_3$), 17.7 (d, $J_{\text{CP}} = 3 \text{ Hz}$, $\text{CH}(\text{CH}_3)_3$). $^{31}\text{P}\{^1\text{H}\}$ NMR (CDCl_3): δ 55.8 (d, $J_{\text{PP}} = 412 \text{ Hz}$), 25.8 (d, $J_{\text{PP}} = 412 \text{ Hz}$).

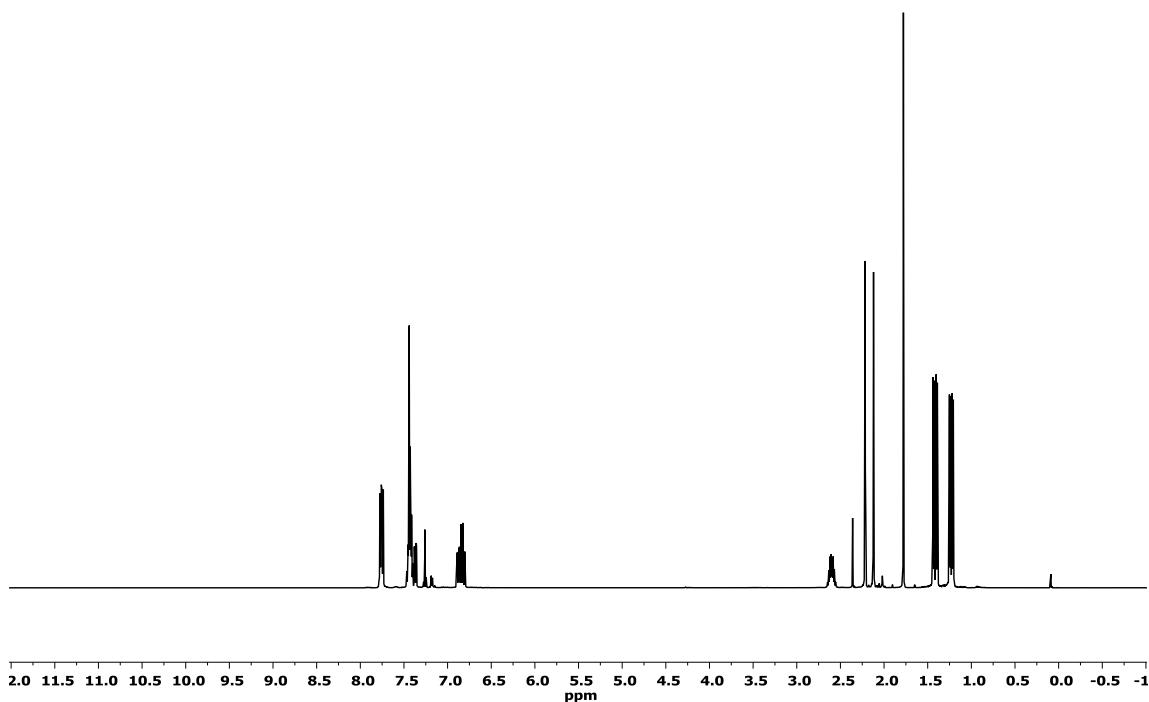


Figure 3.29 ^1H NMR spectrum of **3-6PdOAc** (500 MHz, CDCl_3). Residual toluene and trace amounts of silicone grease are observed.

3-6RhCO. A J. Young tube was charged with **3-6H** (24 mg, 48 μmol), $[\text{Rh}(\text{COD})\text{Cl}]_2$ (24 mg, 48 μmol), 2,6-lutidine (5.5 μL , 48 μmol) and C_6D_6 (1 mL). The mixture was then degassed and then CO (1 atm) was added resulting in a red color change. The volatiles were then removed and the resulting solid was filtered through a pad of silica gel with fluorobenzene. Removal of the fluorobenzene *in vacuo* resulting in pure **3-6RhCO** which was isolated as a yellow solid after washing with 3 mL portions of

toluene (25 mg, 40 μmol , 60%). ^1H NMR (C_6D_6 , Figure 3.30): δ 7.92-7.85 (m, 4H, Ar H), 7.80 (dd, 1H, $J_{\text{PH}} = 9$ Hz, $J_{\text{HH}} = 5$ Hz, Ar H), 7.74 (dd, 1H, $J_{\text{PH}} = 8$ Hz, $J_{\text{HH}} = 4$ Hz, Ar H), 7.07 (d, 1H, $J_{\text{PH}} = 10$ Hz, Ar H), 7.00-6.97 (m, 6H, Ar H), 6.89 (d, 1H, $J_{\text{PH}} = 8$ Hz, Ar H), 6.82-6.78 (m, 3H, Ar H), 2.20-2.13 (m, 2H, $\text{CH}(\text{CH}_3)_2$), 2.17 (s, 3H, Ar CH_3), 1.95 (s, 3H, Ar CH_3), 1.27 (dd, 6H, $J_{\text{PH}} = 17$ Hz, $J_{\text{HH}} = 7$ Hz, $\text{CH}(\text{CH}_3)_2$), 0.98 (dd, 6H, $J_{\text{PH}} = 15$ Hz, $J_{\text{HH}} = 7$ Hz, $\text{CH}(\text{CH}_3)_2$). $^{13}\text{C}\{^1\text{H}\}$ NMR (C_6D_6): δ 197.2 (s, CO), 162.6 (t, $J_{\text{CP}} = 22$ Hz, CN), 135.3 (s, Ar C), 135.0 (s, Ar C), 134.9 (s, Ar C), 134.1 (d, $J_{\text{CP}} = 13$ Hz, Ar C), 133.2 (s, Ar C), 132.6 (d, $J_{\text{CP}} = 13$ Hz, Ar C), 130.4 (s, Ar C), 129.2 (d, $J_{\text{CP}} = 11$ Hz, Ar C), 126.2 (d, $J_{\text{CP}} = 7$ Hz, Ar C), 125.8 (d, $J_{\text{CP}} = 7$ Hz, Ar C), 123.6 (d, $J_{\text{CP}} = 44$ Hz, Ar C), 121.8 (d, $J_{\text{CP}} = 37$ Hz, Ar C), 116.8 (d, $J_{\text{CP}} = 12$ Hz, Ar C), 115.9 (d, $J_{\text{CP}} = 13$ Hz, Ar C), 25.9 (d, $J_{\text{CP}} = 23$ Hz, $\text{CH}(\text{CH}_3)_2$), 20.9 (s, Ar CH_3), 20.6 (s, Ar CH_3), 20.0 (d, $J_{\text{CP}} = 6$ Hz, $\text{CH}(\text{CH}_3)_2$), 18.9 (s, $\text{CH}(\text{CH}_3)_2$). $^{31}\text{P}\{^1\text{H}\}$ NMR (C_6D_6): δ 64.7 (dd, $J_{\text{PP}} = 270$ Hz, $J_{\text{RHP}} = 133$ Hz), 39.2 (dd, $J_{\text{PP}} = 270$ Hz, $J_{\text{RHP}} = 134$ Hz). IR: 1941 cm^{-1} .

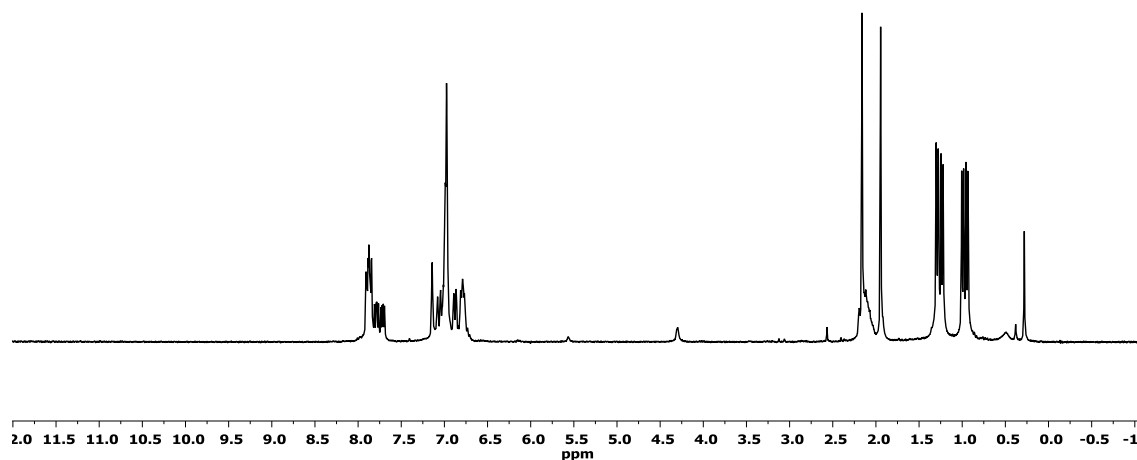


Figure 3.30 ^1H NMR spectrum of **3-6RhCO** (500 MHz, C_6D_6). Trace amounts of dichloromethane, and cyclooctadiene. Silicone grease is also present.

3-6PtCl. A vial was charged with **3-6H** (52 mg, 0.10 mmol), $\text{Pt}(\text{COD})\text{Cl}_2$ (39 mg, 0.10 mmol) and toluene (3 mL). 2,6-lutidine (12 μL , 0.10 mmol) was added to the solution via microsyringe. The reaction was allowed to react for 30 min and then the volatiles were removed *in vacuo*. The resulting yellow solid was filtered through a pad of silica gel with toluene and a small amount of diethyl ether. NMR analysis after removal of the volatiles revealed a slight impurity. The solid was again filtered through silica gel using CH_2Cl_2 and the volatiles were again removed under vacuum to yield pure

product as a yellow solid (56 mg, 77 μmol , 71%). Crystals were obtained by dissolving the solid in dichloromethane and storing the solution at $-35\text{ }^\circ\text{C}$. ^1H NMR (CDCl_3 , Figure 3.31): δ 7.79-7.75 (m, 4H, Ar H), 7.56 (dd, 1H, $J = 6\text{ Hz}$, $J = 9\text{ Hz}$, Ar H), 7.49 (dd, $J = 5\text{ Hz}$, $J = 9\text{ Hz}$, 1H, Ar H), 7.45-7.41 (m, 6H, Ar H), 6.98 (d, 1H, $J = 9\text{ Hz}$, Ar H), 6.90-6.86 (m, 3H, Ar H), 2.80-2.77 (m, 2H, $\text{CH}(\text{CH}_3)_2$), 2.25 (s, 3H, Ar CH_3), 2.17 (s, 3H, Ar CH_3), 1.46 (dd, 6H, $J_{\text{HH}} 7\text{ Hz}$, $J_{\text{PH}} 17\text{ Hz}$, $\text{CH}(\text{CH}_3)_2$), 1.29 (dd, 6H, $J_{\text{HH}} 7\text{ Hz}$, $J_{\text{PH}} 16\text{ Hz}$, $\text{CH}(\text{CH}_3)_2$). $^{13}\text{C}\{^1\text{H}\}$ NMR (CDCl_3): δ 134.7 (s), 133.8 (s), 133.7 (s), 132.6 (s), 132.4 (s), 132.1 (s), 131.2 (s), 130.7 (s), 128.8 (s), 128.7 (s), 127.1 (s), 126.9 (s), 116.4 (s), 116.0 (s), 31.0 (s), 28.2 (s), 25.2 (s), 20.3 (s), 18.4 (s), 18.1 (s). $^{31}\text{P}\{^1\text{H}\}$ NMR (CDCl_3): δ 43.7 (d, $J_{\text{PtP}} = 2751\text{ Hz}$, $J_{\text{PP}} 398\text{ Hz}$), 24.4 (d, $J_{\text{PtP}} = 2668\text{ Hz}$, $J_{\text{PP}} = 398\text{ Hz}$). ^1H NMR (C_6D_6): δ 8.02-7.98 (m, 4H, Ar H), 7.84 (dd, 1H, $J = 6\text{ Hz}$, $J = 9\text{ Hz}$, Ar H), 7.74 (dd, 1H, $J = 4\text{ Hz}$, $J = 9\text{ Hz}$, Ar H), 7.09 (d, 1H, $J = 11\text{ Hz}$, Ar H), 7.02-6.97 (m, 7H, Ar H), 6.68 (d, 1H, $J = 9\text{ Hz}$, Ar H), 6.72 (t, 2H, Ar H), 2.52-2.46 (m, 2H, $\text{CH}(\text{CH}_3)_2$), 2.13 (s, 3H, Ar CH_3), 1.93 (s, 3H, Ar CH_3), 1.42 (dd, 6H, $J_{\text{PH}} = 17\text{ Hz}$, $J_{\text{HH}} = 7\text{ Hz}$, $\text{CH}(\text{CH}_3)_2$), 1.08 (dd, 6H, $J_{\text{PH}} = 16\text{ Hz}$, $J_{\text{HH}} = 7\text{ Hz}$, $\text{CH}(\text{CH}_3)_2$). $^{31}\text{P}\{^1\text{H}\}$ NMR (C_6D_6): δ 43.3 (d, $J_{\text{PtP}} = 2760\text{ Hz}$, $J_{\text{PP}} = 402\text{ Hz}$), 24.6 (d, $J_{\text{PtP}} = 2685\text{ Hz}$, $J_{\text{PP}} = 402\text{ Hz}$).

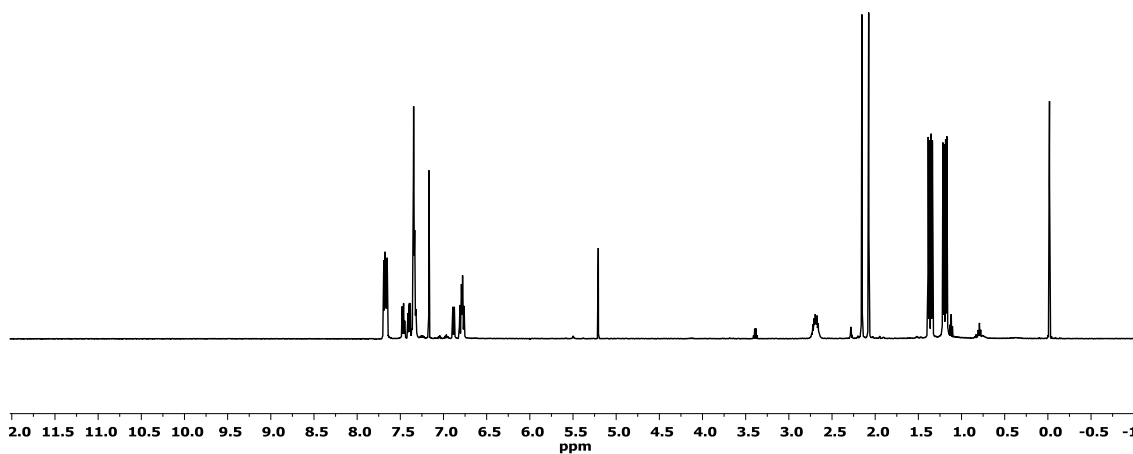


Figure 3.31 ^1H NMR spectrum of **3-6PtCl** (500 MHz, C_6D_6). Dichloromethane, pentane, 2,6-lutidine, silicone grease, and diethyl ether are observed.

3.11.10 Synthesis of **3-G**

3-G. A Schlenk flask was charged with **3-F** (1.2 g, 3.1 mmol), a stir bar and diethyl ether (25 mL). *n*-butyllithium (2.5 mL, 6.1 mmol, 2.5 M in hexanes) was then added drop-wise via addition funnel. The mixture was stirred for 1 h and then DMF (0.50 mL, 6.2 mmol) was added to the reaction vessel. The mixture was stirred for 20 h and then quenched with a degassed solution of ethanol/water (3:1, 1.0 mL). The volatiles were removed *in vacuo* and the resulting yellow solid was dissolved in diethyl ether and

stirred vigorously over silica gel before being passed through a pad of Celite. The ethereal solution was then concentrated *in vacuo* and stored at -35 °C. The resulting yellow precipitate was dried to yield **3-G** as a yellow solid (0.73 g, 2.2 mmol, 71%). If **3-F** is still present in the solid it can be removed via column chromatography (with silica gel) using first pentane to remove **3-F** and then ethyl acetate to wash **3-G** completely off the column. ^1H NMR (C_6D_6 , Figure 3.32): δ 10.69 (s, 1H, NH), 9.71 (s, 1H, (O)CH), 7.30 (dd, 1H, $J_{\text{PH}} = 4$ Hz, $J_{\text{HH}} = 8$ Hz, Ar H), 7.25 (s, 1H, Ar H), 7.05 (d, 1H, $J_{\text{HH}} = 8$ Hz, Ar H), 6.90 (d, 1H, $J_{\text{HH}} = 8$ Hz, Ar H), 6.84-6.80 (m, 2H, Ar H), 2.16 (s, 3H, CH₃), 1.98 (m, 2H, CH(CH₃)₂), 1.97 (s, 3H, CH₃), 1.07 (dd, 6H, $J_{\text{HH}} = 7$ Hz, $J_{\text{PH}} = 15$ Hz, CH(CH₃)₂), 0.92 (dd, 6H, $J_{\text{HH}} = 7$ Hz, $J_{\text{PH}} = 12$ Hz, CH(CH₃)₂). $^1\text{H}\{^{31}\text{P}\}$ NMR (C_6D_6): δ 10.69 (s, 1H, NH), 9.71 (s, 1H, imine CH), 7.30 (d, 1H, $J_{\text{HH}} = 8$ Hz, Ar H), 7.25 (s, 1H, Ar H), 7.05 (d, 1H, $J_{\text{HH}} = 8$ Hz, Ar H), 6.90 (d, 1H, $J_{\text{HH}} = 8$ Hz, Ar H), 6.84 (s, 1H, Ar H), 2.16 (s, 3H, CH₃), 1.98 (m, 2H, CH(CH₃)₂), 1.97 (s, 3H, CH₃), 1.07 (d, 6H, $J_{\text{HH}} = 7$ Hz, CH(CH₃)₂), 0.92 (d, 6H, $J_{\text{HH}} = 7$ Hz, CH(CH₃)₂), $^{13}\text{C}\{^1\text{H}\}$: δ 193.5 (s, (O)CH), 146.3 (s, CC(O)H), 143.7 (d, $J_{\text{CP}} = 23$ Hz, Ar CN), 136.5 (s, Ar CH), 136.2 (s, Ar CH), 134.5 (s, Ar CH), 133.1 (s, Ar C), 130.4 (s, Ar CH), 129.8 (d, $J_{\text{CP}} = 23$ Hz, Ar C), 125.8 (s, Ar C), 124.1 (s, Ar CH), 120.5 (s, Ar C), 113.4 (s, Ar CH), 23.5 (d, $J_{\text{CP}} = 14$ Hz, CH(CH₃)₂), 21.1 (s, Ar CH₃), 20.3 (d, $J_{\text{CP}} = 20$ Hz, CH(CH₃)₂), 20.0 (s, Ar CH₃), 19.2 (d, $J_{\text{CP}} = 10$ Hz, CH(CH₃)₂). $^{31}\text{P}\{^1\text{H}\}$ NMR (C_6D_6): δ -8.0 (s).

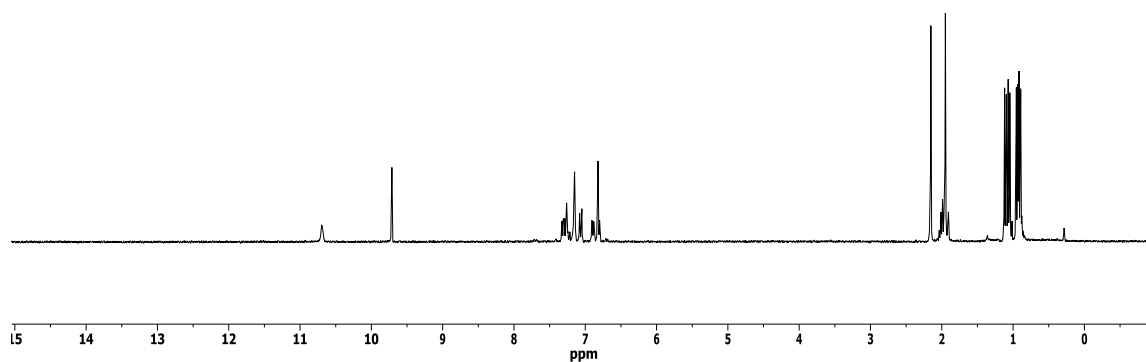


Figure 3.32 ^1H NMR spectrum of **3-G** (500 MHz, C_6D_6). Trace quantities of diethyl ether and water are observed.

3.11.11 Synthesis of **3-7H** and its complexes

3-7H. A Teflon screw cap Schlenk flask was charged with **3-G** (0.16 g, 0.48 mmol), toluene (15 mL), 2,4,6-trimethylaniline (0.14 mL, 0.96 mmol), acetic acid (6.0 μL , 20 mol%), molecular sieves, and a stir bar. The flask was then placed in a 110 $^\circ\text{C}$ oil bath for 72 h and then cooled to ambient temperature and the volatiles were removed *in vacuo*. The remaining yellow solid was extracted in pentane and stirred vigorously over silica gel for 1 h before being filtered through a pad of Celite. The filtrate was

evaporated to dryness and the resulting oil was recrystallized in pentane at $-35\text{ }^{\circ}\text{C}$ to give **3-7H** as a yellow powder (0.17 g, 0.36 mmol, 71%). ^1H NMR (C_6D_6 , Figure 3.33): δ 11.33 (s, 1H, NH), 8.08 (s, 1H, imine CH), 7.49 (dd, 1H, $J_{\text{PH}} = 4\text{ Hz}$, $J_{\text{HH}} = 8\text{ Hz}$, Ar H), 7.33 (d, 1H, $J_{\text{HH}} = 9\text{ Hz}$, Ar H), 7.28 (s, 1H, Ar H), 6.92-6.89 (m, 2H, Ar H), 6.86 (d, 3H, $J_{\text{PH}} = 4\text{ Hz}$, Ar H), 2.28 (s, 6H, *ortho*-CH₃), 2.19 (s, 3H, CH₃), 2.16 (s, 3H, CH₃), 2.10 (s, 3H, CH₃), 1.99 (m, 2H, CH(CH₃)₂), 1.04 (dd, 6H, $J_{\text{PH}} = 15\text{ Hz}$, $J_{\text{HH}} = 7\text{ Hz}$, CH(CH₃)₂), 0.88 (dd, 6H, $J_{\text{PH}} = 12\text{ Hz}$, $J_{\text{HH}} = 7\text{ Hz}$, CH(CH₃)₂). $^1\text{H}\{^3\text{P}\ \delta\ -3.3\}$ NMR (C_6D_6): δ 11.33 (s, 1H, NH), 8.08 (s, 1H, imine CH), 7.49 (d, 1H, $J_{\text{HH}} = 8\text{ Hz}$, Ar H), 7.33 (d, 1H, $J_{\text{HH}} = 9\text{ Hz}$, Ar H), 7.28 (s, 1H, Ar H), 6.92 (m, 2H, Ar H), 6.86 (d, 3H, $J_{\text{PH}} = 4\text{ Hz}$, Ar H), 2.28 (s, 6H, *ortho*-CH₃), 2.19 (s, 3H, CH₃), 2.16 (s, 3H, CH₃), 2.10 (s, 3H, CH₃), 1.99 (m, 2H, CH(CH₃)₂), 1.04 (dd, 6H, $J_{\text{HH}} = 7\text{ Hz}$, $J_{\text{PH}} = 15\text{ Hz}$, CH(CH₃)₂), 0.88 (dd, 6H, $J_{\text{HH}} = 7\text{ Hz}$, $J_{\text{PH}} = 12\text{ Hz}$, CH(CH₃)₂). $^3\text{P}\{^1\text{H}\}$ NMR (C_6D_6): δ -5.8. ^1H NMR (CDCl_3): δ 10.63 (s, 1H, NH), 8.25 (s, 1H, imine CH), 7.35 (dd, 1H, $J_{\text{PH}} = 4\text{ Hz}$, $J_{\text{HH}} = 8\text{ Hz}$, Ar H), 7.24 (m, 1H, Ar H), 7.11 (m, 2H, Ar H), 7.02 (s, 1H, Ar H), 6.88 (s, 1H, $J_{\text{PH}} = 4\text{ Hz}$, Ar H), 2.28 (s, 6H, *ortho*-CH₃), 2.19 (s, 3H, CH₃), 2.16 (s, 3H, CH₃), 2.10 (s, 3H, CH₃), 1.99 (m, 2H, CH(CH₃)₂), 1.04 (dd, 6H, $J_{\text{PH}} = 15\text{ Hz}$, $J_{\text{HH}} = 7\text{ Hz}$, CH(CH₃)₂), 0.88 (dd, 6H, $J_{\text{PH}} = 12\text{ Hz}$, $J_{\text{HH}} = 7\text{ Hz}$, CH(CH₃)₂). $^{13}\text{C}\{^1\text{H}\}$ NMR (CDCl_3): δ 165.5 (s, imine CH), 148.8 (s, Ar C), 145.0 (s, Ar C), 144.1 (d, $J_{\text{CP}} = 18\text{ Hz}$, Ar CN), 140.3 (s, Ar C), 135.0 (s, Ar C), 134.6 (s, Ar C), 132.9 (s, Ar C), 132.5 (d, $J_{\text{CP}} = 11\text{ Hz}$, Ar C), 130.1 (s, Ar C), 129.0 (s, Ar C), 128.7 (s, Ar C), 127.8 (s, Ar C), 127.3 (s, Ar C), 125.6 (s, Ar C), 123.7 (s, Ar C), 122.0 (s, Ar C), 118.7 (s, Ar C), 113.9 (s, Ar C), 23.6 (d, $J_{\text{CP}} = 14\text{ Hz}$,

CH(CH₃)₂), 21.2 (s CH₃), 20.5 (s, CH₃), 20.4 (d, $J_{CP} = 5$ Hz, CH(CH₃)₂), 19.6 (d, $J_{CP} = 10$ Hz, CH(CH₃)₂), 18.77 (s, CH₃), 17.72 (s, CH₃). ³¹P {¹H} NMR (CDCl₃): δ -3.3 (s).

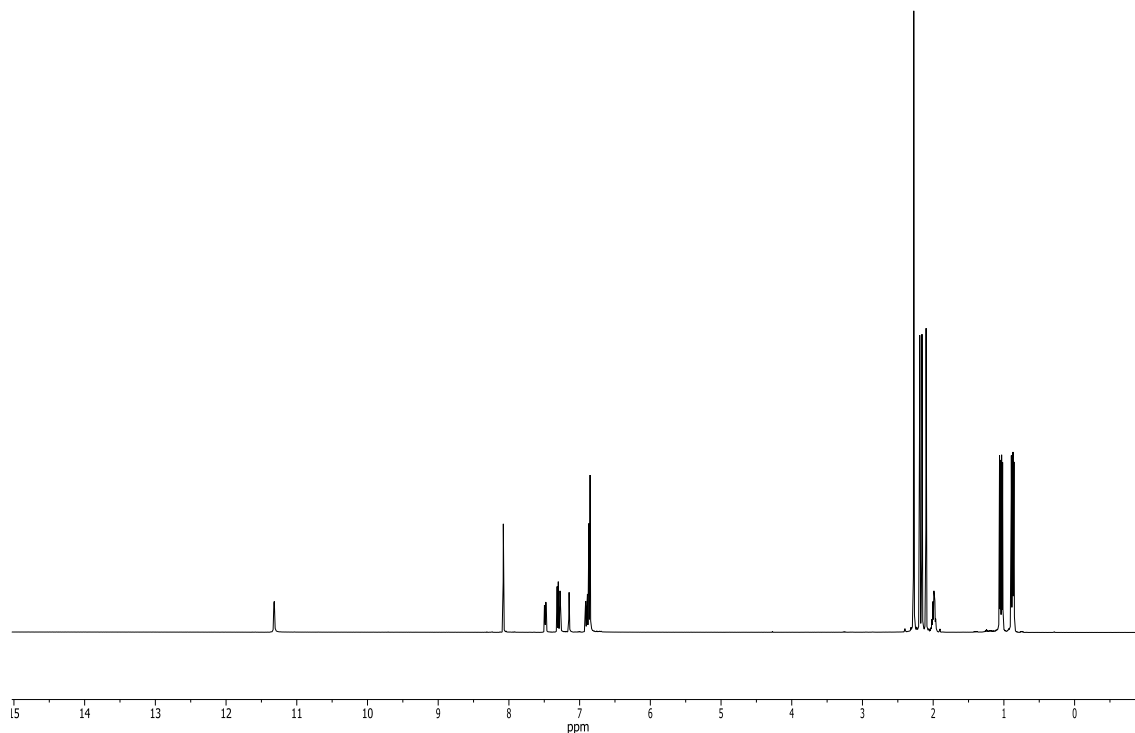


Figure 3.33 ¹H NMR spectrum of **3-7H** (500 MHz, C₆D₆).

3-7PdOAc. A 25 ml Schlenk flask was charged with **3-7H** (0.15 g, 33 μmol) and dissolved in toluene (3 ml) under ambient temperature. Pd(OAc)₂ (76 mg, 0.34 mmol) was then added to the reaction mixture resulting in an immediate color change from yellow to purple. The reaction mixture was stirred for 12 h and then the volatiles were removed *in vacuo*. The resulting red solid was then washed two times with cold pentane

and dried to yield a red powder (0.15 g, 76%). ^1H NMR (C_6D_6 , Figure 3.34): δ 7.63 (d, 1H, $J_{\text{HH}} = 9$ Hz, imine CH), 7.38 (dd, 1H, $J_{\text{PH}} = 4$ Hz, $J_{\text{HH}} = 9$ Hz, Ar H), 7.13 (d, 1H, $J_{\text{PH}} = 13$ Hz, Ar H), 6.82 (s, 1H, Ar H), 6.80 (d, 1H, $J_{\text{PH}} = 8$ Hz, Ar H), 6.75 (d, 2H, $J_{\text{PH}} = 9$ Hz, Ar H), 6.67 (d, 1H, $J_{\text{HH}} = 9$ Hz, Ar H), 6.62 (s, 1H, Ar H), 2.74 (m, 1H, $\text{CH}(\text{CH}_3)_2$), 2.60 (s, 3H, CH_3), 2.29 (s, 3H, CH_3), 2.15 (s, 3H, CH_3), 2.10 (s, 3H, CH_3), 2.05 (s, 3H, CH_3), 2.03 (s, 3H, CH_3), 1.94 (septet, 1H, $\text{CH}(\text{CH}_3)_2$), 1.51 (dd, 3H, $J_{\text{PH}} = 19$ Hz, $J_{\text{HH}} = 6$ Hz, $\text{CH}(\text{CH}_3)_2$), 1.24 (dd, 3H, $J_{\text{PH}} = 19$ Hz, $J_{\text{HH}} = 6$ Hz, $\text{CH}(\text{CH}_3)_2$), 1.14 (dd, 3H, $J_{\text{PH}} = 15$ Hz, $J_{\text{HH}} = 6$ Hz, $\text{CH}(\text{CH}_3)_2$), 0.87 (dd, 3H, $J_{\text{PH}} = 11$ Hz, $J_{\text{HH}} = 6$ Hz, $\text{CH}(\text{CH}_3)_2$). $^1\text{H}\{^3\text{P}$ δ 65.6} NMR (C_6D_6): δ 7.60 (d, 1H, $J_{\text{HH}} = 9$ Hz, Ar H), 7.35 (d, 1H, $J_{\text{HH}} = 9$ Hz, Ar H), 7.16 (s, 1H, Ar H), 7.08 (s, 1H, Ar H), 6.80 (s, 1H, Ar H), 6.77 (s, 1H, Ar H), 6.73 (s, 1H, Ar H), 6.64 (d, 1H, $J_{\text{HH}} = 9$ Hz, Ar H), 6.60 (s, 1H, Ar H), 2.80 (m, 1H, $\text{CH}(\text{CH}_3)_2$), 2.55 (s, 3H, CH_3), 2.24 (s, 3H, CH_3), 2.13 (s, 3H, CH_3), 2.06 (s, 3H, CH_3), 2.04 (s, 3H, CH_3), 1.90 (m, 1H, $\text{CH}(\text{CH}_3)_2$), 1.50 (d, 3H, $J_{\text{HH}} = 6$ Hz, $\text{CH}(\text{CH}_3)_2$), 1.20 (d, 3H, $J_{\text{HH}} = 6$ Hz, $\text{CH}(\text{CH}_3)_2$), 1.11 (d, 3H, $J_{\text{HH}} = 6$ Hz, $\text{CH}(\text{CH}_3)_2$), 0.91 (d, 3H, $J_{\text{HH}} = 6$ Hz, $\text{CH}(\text{CH}_3)_2$). $^{13}\text{C}\{^1\text{H}\}$ NMR (C_6D_6): δ 176.3 (s, OAc), 163.5 (s, Ar CN), 163.3 (s, Ar CH), 150.6 (s, Ar C), 146.8 (s, Ar C), 135.3 (s, Ar CH), 134.8 (s, Ar CH), 132.7 (s, Ar CH), 132.7 (s, Ar C), 131.5 (s, Ar CH), 130.1 (s, Ar C), 128.8 (s, Ar CH), 127.5 (s, Ar C), 125.7 (s, Ar C), 125.4 (s, Ar CH), 120.8 (s, Ar C), 120.7 (s, Ar C), 120.6 (s, Ar C), 120.1 (s, Ar C), 119.7 (s, Ar CH), 26.8 (d, $J_{\text{CP}} = 24$ Hz, $\text{CH}(\text{CH}_3)_2$), 21.8 (d, $J_{\text{CP}} = 24$ Hz, $\text{CH}(\text{CH}_3)_2$), 20.9 (s, CH_3), 20.5 (s, CH_3), 20.1 (s, CH_3), 19.5 (broad s, CH_3), 18.9 (broad s, CH_3), 18.2 (broad s, CH_3), 16.3 (s, CH_3), 16.2 (broad s, CH_3). $^{31}\text{P}\{^1\text{H}\}$ NMR (C_6D_6): δ 65.6.

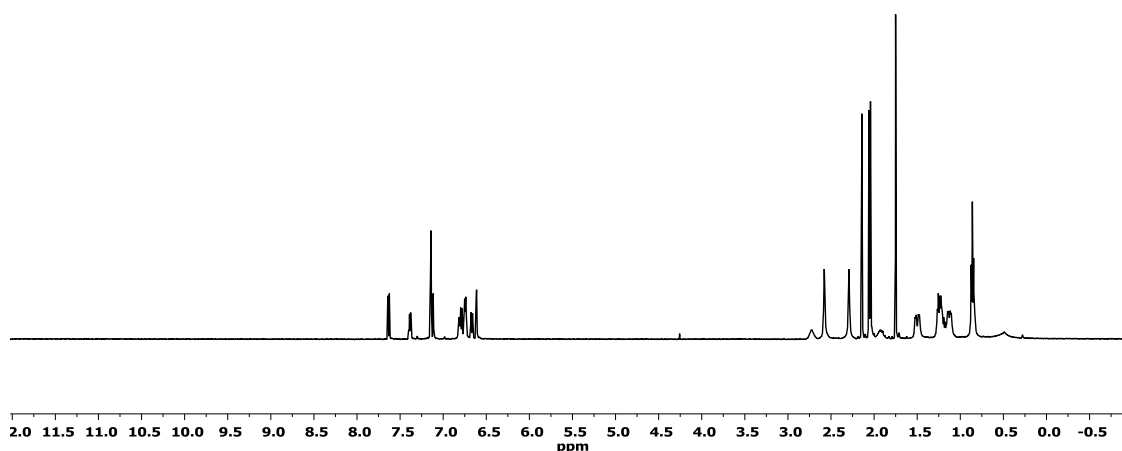


Figure 3.34 ^1H NMR spectrum of **3-7PdOAc** (500 MHz, C_6D_6). Trace quantities of dichloromethane and pentane are observed.

3-7PdCl. A Schlenk flask was charged with **3-7H** (0.12 g, 0.27 mmol), $\text{Pd}(\text{COD})\text{Cl}_2$ (78 mg, 0.27 mmol), 2,6-lutidine (31 μL , 0.27 mmol), toluene (3 mL) and a stir bar. The reaction mixture was stirred for 5 h to yield a red solution. The toluene solution was filtered through a pad of silica gel. To ensure quantitative transfer the silica gel was washed with diethyl ether. The volatiles were then removed *in vacuo*. The resulting red solid was washed with toluene to yield **3-7PdCl** as a red solid (62 mg, 0.10 mmol, 39%). ^1H NMR (C_6D_6 , Figure 3.35): δ 7.59 (d, 1H, $J_{\text{HH}} = 9$ Hz, Ar *H*), 7.38 (dd,

1H, $J_{\text{HH}} = 9$ Hz, $J_{\text{PH}} = 4$ Hz, Ar *H*), 7.21 (d, 1H, $J_{\text{PH}} = 13$ Hz, Ar *H*), 6.87-6.75 (m, 3H, Ar *H*), 6.70 (d, 1H, $J_{\text{PH}} = 9$ Hz, Ar *H*), 6.12 (s, 1H, Ar *H*), 2.58 (s, 3H, CH_3), 2.46 (m, 2H, $\text{CH}(\text{CH}_3)_2$), 2.36 (s, 3H, CH_3), 2.14 (s, 3H, CH_3), 2.07 (s, 3H, CH_3), 2.03 (s, 3H, CH_3), 1.40 (d, 3H, $J_{\text{PH}} = 14$ Hz, $\text{CH}(\text{CH}_3)_2$), 1.29 (d, 3H, $J_{\text{PH}} = 14$ Hz, $\text{CH}(\text{CH}_3)_2$), 1.16 (d, 3H, $J_{\text{PH}} = 10$ Hz, $\text{CH}(\text{CH}_3)_2$), 0.93 (d, 3H, $J_{\text{PH}} = 9$ Hz, $\text{CH}(\text{CH}_3)_2$). $^1\text{H}\{^{31}\text{P} \delta 70.3\}$ NMR (C_6D_6): δ 7.59 (d, 1H, $J_{\text{HH}} = 9$ Hz, Ar *H*), 7.38 (d, 1H, $J_{\text{HH}} = 9$ Hz, Ar *H*), 7.21 (s, 1H, Ar *H*), 6.87-6.75 (m, 3H, Ar *H*), 6.70 (s, 1H, Ar *H*), 6.12 (s, 1H, Ar *H*), 2.58 (s, 3H, CH_3), 2.46 (m, 2H, $\text{CH}(\text{CH}_3)_2$), 2.36 (s, 3H, CH_3), 2.14 (s, 3H, CH_3), 2.07 (s, 3H, CH_3), 2.03 (s, 3H, CH_3), 1.40 (s, 3H, $\text{CH}(\text{CH}_3)_2$), 1.29 (s, 3H, $\text{CH}(\text{CH}_3)_2$), 1.16 (s, 3H, $\text{CH}(\text{CH}_3)_2$), 0.93 (s, 3H, $\text{CH}(\text{CH}_3)_2$). $^{13}\text{C}\{^1\text{H}\}$ NMR (C_6D_6): δ 163.4 (s, Ar C), 163.1 (d, $J_{\text{CP}} = 19$ Hz, Ar CN), 150.7 (s, Ar C), 147.9 (s, Ar C), 135.1 (s, Ar C), 134.8 (s, Ar C), 134.7 (s, Ar C), 132.9 (s, Ar C), 132.3 (s, Ar C), 131.3 (s, Ar C), 129.3 (s, Ar C), 128.8 (s, Ar C), 125.9 (s, Ar C), 125.5 (s, Ar C), 121.1 (s, Ar C), 121.0 (s, Ar C), 120.9 (s, Ar C), 119.0 (s, Ar C), 26.9 (d, $J_{\text{CP}} = 23$ Hz, $\text{CH}(\text{CH}_3)_2$), 24.0 (d, $J_{\text{CP}} = 29$ Hz, $\text{CH}(\text{CH}_3)_2$), 21.0 (s, CH_3), 20.5 (s, CH_3), 20.0 (s, CH_3), 19.6 (d, $J_{\text{CP}} = 14$ Hz, $\text{CH}(\text{CH}_3)_2$), 19.0 (s, CH_3), 17.9 (s, CH_3), 17.5 (s, CH_3). $^{31}\text{P}\{^1\text{H}\}$ NMR (C_6D_6): δ 70.3. ^1H NMR (CDCl_3): δ 7.79 (s, 1H, Ar *CH*), 7.55 (s, 1H, Ar *CH*), 7.17 (s, 1H, Ar *CH*), 7.08 (s, 1H, Ar *CH*), 7.00 (s, 1H, Ar *CH*), 6.88 (s, 2H, Ar *CH*), 2.64 (d, $J = 26$ Hz, 4H, $\text{CH}(\text{CH}_3)_2$ overlapping with CH_3), 2.47 (s, 1H, $\text{CH}(\text{CH}_3)$), 2.36 (s, 3H, CH_3), 2.27 (s, 6H, CH_3), 2.19 (s, 3H, CH_3), 1.48 – 1.18 (m, 12H, $\text{CH}(\text{CH}_3)_2$). Elemental Analysis Calculated for **14-PdCl**: C, 60.11; H, 6.39; N. Found: C, 60.06; H, 6.42.

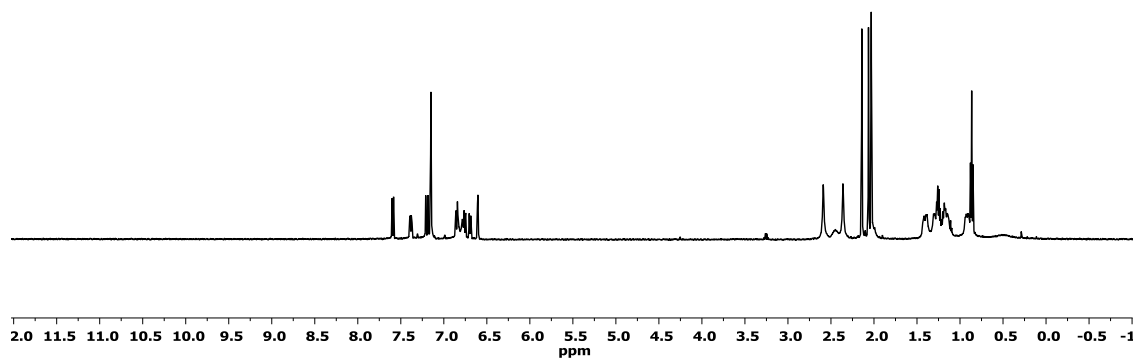


Figure 3.35 ^1H NMR spectrum of **3-7PdCl** (500 MHz, CDCl_3). Trace quantities of diethyl ether, silicone grease, and pentane are observed.

3-7RhCO. A J. Young tube was charged with **3-7H** (41 mg, 89 μmol), $[\text{Rh}(\text{COD})\text{Cl}]_2$ (46 mg, 93 μmol of Rh), 2,6-lutidine (11 μL , 90 μmol) and C_6D_6 (1 mL). The solution was then degassed and exposed to CO (1 atm). A red color change was observed and ^{31}P NMR analysis revealed conversion **3-7RhCO**. The reaction mixture was then filtered through a pad of silica gel and washed with diethyl ether. **3-7RhCO** was obtained as a red solid after removal of the volatiles *in vacuo* and recrystallization by slow diffusion of pentane into dichloromethane (26 mg, 44 μmol , 50%). ^1H NMR

(C₆D₆, Figure 3.36): δ 7.78 (d, 1H, $J = 9$ Hz, Ar H), 7.47 (d, 1H, $J = 9$ Hz, Ar H), 6.94 (d, 1H, $J = 7$ Hz, Ar H), 6.85 (s, 1H, imine CH), 6.80 (d, 1H, $J = 7$ Hz, Ar H), 6.75-6.72 (m, 2H, Ar H), 2.51 (s, 3H, CH_3), 2.41 (m, 1H, $CH(CH_3)_2$), 2.37 (s, 3H, CH_3), 2.15 (s, 3H, CH_3), 2.13 (s, 3H, CH_3), 2.09 (s, 3H, CH_3), 1.90 (m, 1H, $CH(CH_3)_2$), 1.31-1.29 (m, 6H, $CH(CH_3)_2$), 1.11-1.04 (m, 6H, $CH(CH_3)_2$). ¹H NMR (CDCl₃): δ 7.74 (dd, $J = 9.2$ Hz, $J = 2.3$ Hz, 1H, Ar H), 7.56 (d, $J = 8.9$ Hz, 1H, Ar H), 7.28 (dd, $J = 8.6$ Hz, $J = 3.9$ Hz, 1H, Ar H), 7.03 (dd, $J = 7.9$ Hz, $J = 2.2$ Hz, 1H, Ar H), 6.96 (s, 1H, Ar H), 6.94 – 6.86 (m, 3H, Ar H), 2.45 (m, 2H, $CH(CH_3)_2$), 2.38 (s, 3H, CH_3), 2.31 (s, 3H, CH_3), 2.30 – 2.27 (s, 3H, CH_3), 2.25 (s, 3H, CH_3), 2.21 (s, 3H, CH_3), 1.37 – 1.00 (m, 12H, $CH(CH_3)_2$). ¹H{³¹P δ 76.3} NMR (CDCl₃): δ 7.74 (d, $J = 2.3$ Hz, 1H, Ar H), 7.56 (d, $J = 8.9$ Hz, 1H, Ar H), 7.28 (d, $J = 8.6$ Hz, 1H, Ar H), 7.03 (d, $J = 2.2$ Hz, 1H, Ar H), 6.96 (s, 1H, Ar H), 6.94 – 6.86 (m, 3H, Ar H), 2.45 (m, 2H, $CH(CH_3)_2$), 2.38 (s, 3H, CH_3), 2.31 (s, 3H, CH_3), 2.30 – 2.27 (s, 3H, CH_3), 2.25 (s, 3H, CH_3), 2.21 (s, 3H, CH_3), 1.37 – 1.00 (m, 12H, $CH(CH_3)_2$). ¹³C{¹H} NMR (CDCl₃): δ 192.95 – 191.29 (m, CO), 162.5 (s, Ar C), 162.3 (s, Ar C), 162.2 (s, Ar C), 153.60 (s, Ar C), 150.51 (s, Ar C), 134.61 (s, Ar C), 134.08 (s, Ar C), 133.39 (s, Ar C), 131.65 (s, Ar C), 131.15 (s, Ar C), 130.50 (s, Ar C), 128.59 (s, Ar C), 127.74 (s, Ar C), 124.03 (s, Ar C), 123.59 (s, Ar C), 122.91 (s, Ar C), 122.59 (s, Ar C), 119.20 (d, $J_{CP} = 12.1$ Hz, Ar C), 118.88 (s, Ar C), 27.43 (d, $J_{CP} = 27$ Hz, $CH(CH_3)_2$), 23.64 (d, $J_{CP} = 32$ Hz, $CH(CH_3)_2$), 21.04 (s, CH_3), 20.69 (s, CH_3), 20.19 (s, CH_3), 19.59 (s, CH_3), 18.89 (s, CH_3), 18.73 (s, CH_3), 17.95 (s, CH_3). ³¹P{¹H} NMR (CDCl₃): δ 76.3 (d, $J_{RHP} = 130$ Hz). IR ν (CO) = 1942 cm⁻¹.

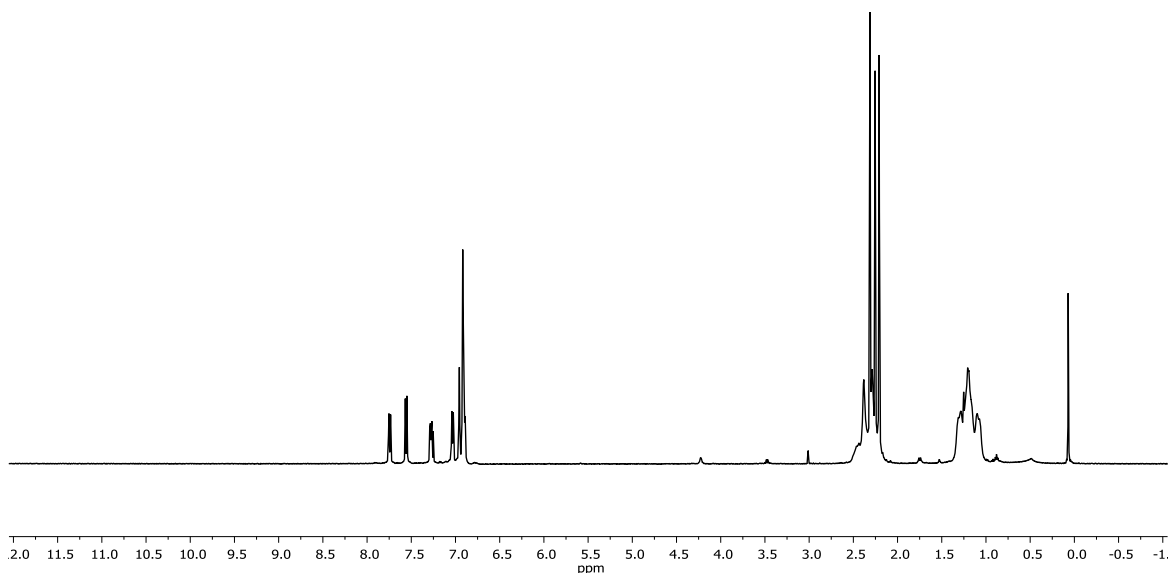


Figure 3.36 ^1H NMR spectrum of **3-7RhCO** (500 MHz, C_6D_6). Trace quantities of diethyl ether, dichloromethane, and pentane are observed along with some residual silicone grease.

3-8H. 3-G (0.396 mg, 1.16 mmol) was dissolved in toluene (15 mL) and treated with *tert*-butylamine (396 μL , 2.32 mmol) and tosylic acid (12.0 mg, 0.070 mmol, 10 mol%) in a Teflon screw-capped Schlenk flask. The reaction mixture was then heated in a 110 $^\circ\text{C}$ oil bath for 10 d while stirring over molecular sieves. The reaction was cooled to ambient temperature, the solution decanted and the volatiles were removed *in vacuo*. The remaining yellow oil was dissolved in pentane and stirred vigorously over silica gel for 5 min before being passed through a pad of Celite. The volatiles were removed and

the resulting yellow oil was recrystallized from fluorobenzene at -35 °C to yield **3-8H** as a yellow solid (398 mg, 1.00 mmol, 87%). ^1H NMR (C_6D_6 , Figure 3.37): δ 11.80 (s, 1H, NH), 8.26 (s, 1H, imine CH), 7.48 (dd, 1H, $J_{\text{PH}} = 4$ Hz, $J_{\text{HH}} = 8$ Hz, Ar H), 7.34 (d, 1H, $J_{\text{HH}} = 9$ Hz, Ar H), 7.24 (s, 1H, Ar H), 6.94 (s, 1H, Ar H), 6.89 (d, 2H, $J_{\text{HH}} = 8$ Hz, Ar H), 2.18 (s, 3H, CH_3), 2.16 (s, 3H, CH_3), 1.99 (m, 2H, $\text{CH}(\text{CH}_3)_2$), 1.34 (s, 9H, CH_3), 1.11 (dd, 6H, $J_{\text{PH}} = 15$ Hz, $J_{\text{HH}} = 7$ Hz, $\text{CH}(\text{CH}_3)_2$), 0.99 (dd, 6H, $J_{\text{PH}} = 11$ Hz, $J_{\text{HH}} = 7$ Hz, $\text{CH}(\text{CH}_3)_2$). $^1\text{H}\{^{31}\text{P} \delta -7.3\}$ NMR (C_6D_6): δ 11.80 (s, 1H, NH), 8.26 (s, 1H, imine CH), 7.48 (dd, 1H, $J_{\text{HH}} = 8$ Hz, Ar H), 7.34 (1H, d, $J_{\text{HH}} = 9$ Hz, Ar H), 7.24 (s, 1H, Ar H), 6.94 (s, 1H, Ar H), 6.89 (d, 2H, $J_{\text{HH}} = 8$ Hz, Ar H), 2.18 (s, 3H, CH_3), 2.16 (s, 3H, CH_3), 1.99 (m, 2H, $\text{CH}(\text{CH}_3)_2$), 1.34 (s, 9H, CH_3), 1.11 (dd, 6H, $J_{\text{HH}} = 7$ Hz, $\text{CH}(\text{CH}_3)_2$), 0.99 (dd, 6H, $J_{\text{HH}} = 7$ Hz, $\text{CH}(\text{CH}_3)_2$). $^{13}\text{C}\{^1\text{H}\}$ NMR (C_6D_6): δ 158.2 (s, imine C), 145.8 (d, $J_{\text{CP}} = 20$ Hz, Ar CN), 145.6 (s, Ar C), 134.6 (s, Ar C), 134.0 (s, Ar C), 131.5 (s, Ar C), 131.4 (s, Ar C), 130.3 (s, Ar C), 128.6 (s, Ar C), 25.4 (s, Ar C), 122.7 (s, Ar C), 120.3 (s, Ar C), 113.5 (s, Ar CH), 57.4 (s, $\text{C}(\text{CH}_3)_3$), 29.9 (s, $\text{C}(\text{CH}_3)_3$), 23.4 (d, $J_{\text{CP}} = 13$ Hz, $\text{CH}(\text{CH}_3)_2$), 21.0 (s, Ar CH_3), 20.5 (d, $J_{\text{CP}} = 20$ Hz, $\text{CH}(\text{CH}_3)_2$), 20.4 (s, Ar CH_3), 19.5 (d, $J_{\text{CP}} = 10$ Hz, $\text{CH}(\text{CH}_3)_2$). $^{31}\text{P}\{^1\text{H}\}$ NMR (C_6D_6): δ -7.3.

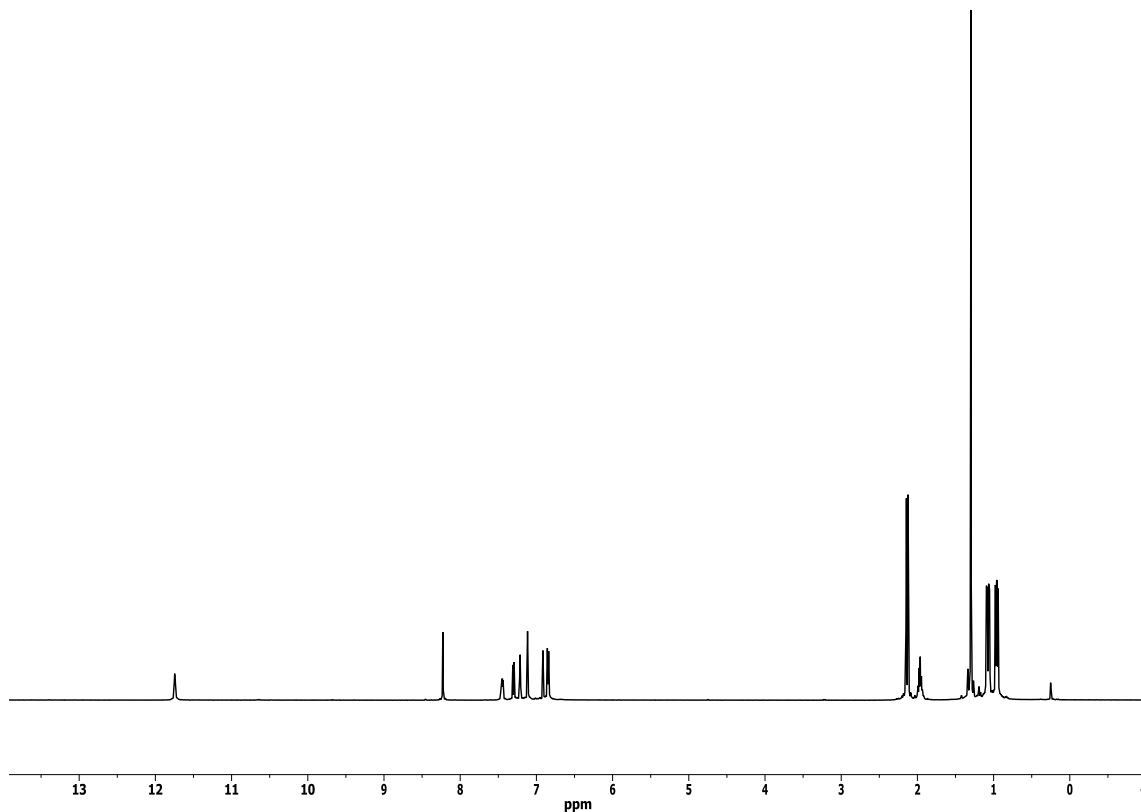


Figure 3.37 ^1H NMR spectrum of **3-8H** (500 MHz, C_6D_6). Trace quantities of silicone grease are observed.

3-8PdOAc. A Schlenk flask was charged with **3-8H** (0.10 g, 0.26 mmol), $\text{Pd}(\text{OAc})_2$ (58 mg, 0.26 μmol), toluene (5 mL), and a stir bar. An immediate color change to a purple solution is observed. The solution was stirred for 1 hour and then passed through a pad of Celite. Removal of the volatiles and washing with 3 \times 5 mL of toluene yielded **3-8PdOAc** as a red powder (0.11 g, 0.20 mmol, 78%). ^1H NMR (C_6D_6 , Figure 3.38): δ 7.41 (d, 1H, $J_{\text{HH}} = 5$ Hz, imine *CH*), 7.39 (s, 1H, Ar *H*), 7.20 (dd, 1H, $J_{\text{PH}} = 9$ Hz, $J_{\text{HH}} = 4$ Hz, Ar *H*), 6.84 (d, 1H, $J = 8$ Hz, Ar *H*), 6.73 (d, 1H, $J_{\text{PH}} = 9$ Hz, $J_{\text{HH}} = 2$

Hz, Ar H), 6.67 (d, 1H, $J = 9$ Hz, Ar H), 6.62 (s, 1H, Ar H), 2.90 (m, 1H, $\text{CH}(\text{CH}_3)_2$), 2.19 (s, 3H, CH_3), 2.07 (s, 3H, CH_3), 2.06 (s, 3H, CH_3), 2.00 (m, 1H, $\text{CH}(\text{CH}_3)_2$), 1.47 (dd, 3H, $J_{\text{PH}} = 20$ Hz, $J_{\text{HH}} = 7$ Hz, $\text{CH}(\text{CH}_3)_2$), 1.44 (s, 9H, $\text{C}(\text{CH}_3)_3$), 1.40 (dd, 3H, $J_{\text{PH}} = 8$ Hz, $J_{\text{HH}} = 7$ Hz, $\text{CH}(\text{CH}_3)_2$), 1.25 (dd, 3H, $J_{\text{PH}} = 16$ Hz, $J_{\text{HH}} = 7$ Hz, $\text{CH}(\text{CH}_3)_2$), 0.85 (dd, 3H, $J_{\text{PH}} = 13$ Hz, $J_{\text{HH}} = 7$ Hz, $\text{CH}(\text{CH}_3)_2$). $^{13}\text{C}\{^1\text{H}\}$ NMR (C_6D_6): δ 175.9 (s, CO), 162.6 (d, $J_{\text{CP}} = 21$ Hz, N C of pincer backbone), 157.7 (s, Ar C), 150.3 (s, Ar C), 134.7 (s, Ar C), 133.9 (s, Ar C), 132.9 (s, Ar C), 131.2 (s, Ar C), 129.3 (s, Ar C), 125.5 (s, Ar C), 122.0 (s, Ar C), 121.9 (s, Ar C), 121.4 (s, Ar C), 118.7 (s, Ar C), 62.7 (s, $\text{C}(\text{CH}_3)_3$), 30.6 (s, $\text{C}(\text{CH}_3)_3$), 27.4 (d, $J_{\text{CP}} = 22$ Hz, $\text{CH}(\text{CH}_3)_2$), 24.1 (s, CH_3), 22.0 (s, CH_3), 21.8 (s, CH_3), 20.2 (s, CH_3), 19.6 (d, $J_{\text{CP}} = 5$ Hz, $\text{CH}(\text{CH}_3)_2$), 18.7 (d, $J_{\text{CP}} = 4$ Hz, $\text{CH}(\text{CH}_3)_2$), 16.3 (s, CH_3), 15.9 (d, $J_{\text{CP}} = 5$ Hz, $\text{CH}(\text{CH}_3)_2$). $^{31}\text{P}\{^1\text{H}\}$ NMR (C_6D_6): δ 66.3.

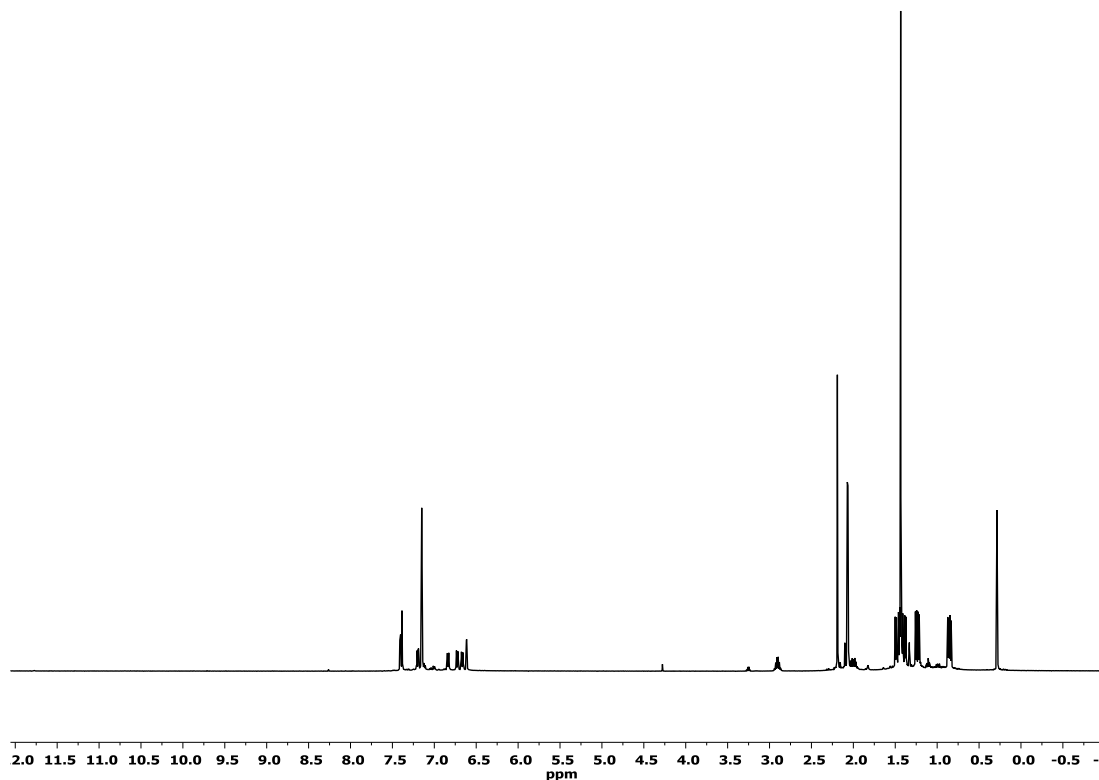


Figure 3.38 ^1H NMR spectrum of **3-8PdOAc** (500 MHz, C_6D_6). Residual solvent impurities are observed that include dichloromethane, pentane, toluene, silicone grease, and diethyl ether.

3-8PdCl. A Schlenk flash was charged with **3-8H** (51 mg, 0.13 mmol), 2,6-lutidine (15 μL , 0.13 mmol), $\text{Pd}(\text{COD})\text{Cl}_2$ (38 mg, 0.13 mmol), toluene (5 mL) and a stir bar. The resulting red solution was then stirred overnight and then filtered through a pad of Celite. The volatiles were then removed *in vacuo* and the solid was recrystallized in toluene to yield **3-8PdCl** as a deep red powder (32 mg, 60 μmol , 50%). ^1H NMR (C_6D_6 , Figure 3.39): δ 7.48 (d, 1H, $J_{\text{PH}} = 13$ Hz, imine CH), 7.32 (d, 1H, $J_{\text{HH}} = 9$ Hz, Ar H), 7.22 (dd, 1H, $J_{\text{PH}} = 5$ Hz, $J_{\text{HH}} = 9$ Hz, Ar H), 6.89 (d, 1H, $J_{\text{PH}} = 8$ Hz, Ar H), 6.76 (d, 1H, $J_{\text{HH}} = 9$ Hz, Ar H), 6.69 (d, 1H $J_{\text{HH}} = 9$ Hz, Ar H), 6.61 (s, 1H, Ar H), 2.52 (m, 1H,

$CH(CH_3)_2$, 2.13 (m, 1H, $CH(CH_3)_2$), 2.10 (s, 3H, Ar CH_3), 2.05 (s, 3H, Ar CH_3), 1.64 (s, 9H, $C(CH_3)_3$), 1.58 (dd, 3H, $J_{PH} = 17$ Hz, $J_{HH} = 9$ Hz, $CH(CH_3)_2$), 1.32 (dd, 3H, $J_{PH} = 17$ Hz, $J_{HH} = 9$ Hz, $CH(CH_3)_2$), 1.26 (dd, 3H, $J_{PH} = 18$ Hz, $J_{HH} = 11$ Hz, $CH(CH_3)_2$), 0.87 (dd, 3H, $J_{PH} = 15$ Hz, $J_{HH} = 8$ Hz, $CH(CH_3)_2$). $^1H\{^{31}P \delta 70.4\}$ NMR (C_6D_6): δ 7.49 (s, 1H, imine CH), 7.32 (d, 1H, $J_{HH} = 9$ Hz, Ar H), 7.22 (dd, 1H, $J_{HH} = 9$ Hz, Ar H), 6.89 (s, 1H, Ar H), 6.76 (d, 1H, $J_{HH} = 9$ Hz, Ar H), 6.69 (d, 1H, $J_{HH} = 9$ Hz, Ar H), 6.61 (s, 1H, Ar H), 2.52 (m, 1H, $CH(CH_3)_2$), 2.13 (m, 1H, $CH(CH_3)_2$), 2.10 (s, 3H, Ar CH_3), 2.05 (s, 3H, Ar CH_3), 1.64 (s, 9H, $C(CH_3)_3$), 1.57 (d, 3H, $J_{HH} = 7$ Hz, $CH(CH_3)_2$), 1.32 (d, 3H, $J_{HH} = 7$ Hz, $CH(CH_3)_2$), 1.26 (d, 3H, $J_{HH} = 7$ Hz, $CH(CH_3)_2$), 0.88 (d, 3H, $J_{HH} = 7$ Hz, $CH(CH_3)_2$). $^{13}C\{^1H\}$ NMR (C_6D_6): δ 162.7 (d, $J_{CP} = 21$ Hz, CN), 158.0 (s, Ar C), 150.7 (s, Ar C), 134.4 (s, Ar C), 133.8 (s, Ar C), 133.2 (s, Ar C), 131.2 (s, Ar C), 129.0 (d, $J_{CP} = 7$ Hz, Ar C), 125.6 (s, Ar C), 122.5 (d, $J_{CP} = 16$ Hz, Ar C), 122.2 (s, Ar C), 121.9 (s, Ar C), 118.1 (s, Ar C), 63.6 (s, $C(CH_3)_3$), 31.5 (s, $C(CH_3)_3$), 26.6 (d, $J_{CP} = 24$ Hz, $CH(CH_3)_2$), 24.4 (d, $J_{CP} = 30$ Hz, $CH(CH_3)_2$), 20.5 (s, Ar CH_3), 2.02 (s, Ar CH_3), 18.9 (d, $J_{CP} = 4$ Hz, $CH(CH_3)_2$), 18.3 (s, $CH(CH_3)_2$), 18.1 (s, $CH(CH_3)_2$), 17.1 (s, $CH(CH_3)_2$). $^{31}P\{^1H\}$ NMR (C_6D_6): δ 70.4. Elemental Analysis Calculated for **3-8PdCl**: C, 55.87; H, 6.60; N, 5.21. Found: C, 55.72; H, 6.88; N, 5.09.

3-8PdCl. A J. Young tube was charged with **3-8PdOAc** (77.4 mg, 13.8 μ mol) and C_6D_6 (1 mL). Me_3SiCl (18.0 μ L, 14.2 μ mol) was added to the reaction mixture via syringe. After 72 h the volatiles were removed *in vacuo* and the resulting solid was washed three times with toluene (1 mL). After the final wash the volatiles were removed *in vacuo* to yield **3-8PdCl** as a purple solid (63.0 mg, 11.7 μ mol, 85%).

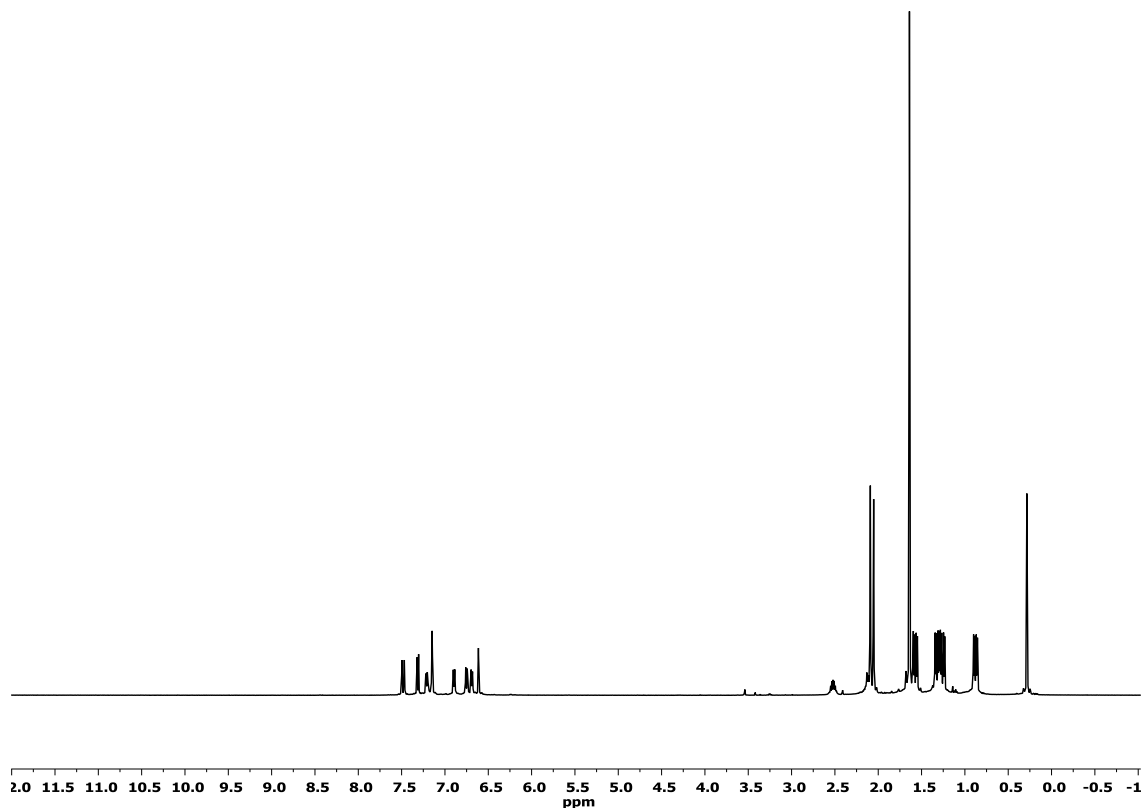


Figure 3.39 ^1H NMR spectrum of **3-8PdCl** (500 MHz, C_6D_6). Residual silicone grease is observed.

3-8PdOTf. A J. Young tube was charged with **3-8PdOAc** (15 mg, 27 μmol), Me_3SiOTf (25 μL , 0.14 mmol) and toluene- d_8 (1 mL). A color change is immediately observed from red to yellow and yellow crystals slowly precipitate out of solution. The solvent was decanted and the crystals were dried *in vacuo*. ^1H NMR (toluene- d_8 , Figure 3.40): δ 8.10 (d, 1H, $J = 15$ Hz, Ar H), 7.84 (dd, 1H, $J = 3$ Hz, $J = 9$ Hz, Ar H), 7.00 (s, 1H, imine CH), 6.88 (d, 1H, $J = 8$ Hz, Ar H), 6.61 (s, 2H, Ar H), 6.07 (d, 1H, $J = 8$ Hz, Ar H), 3.19-3.12 (m, 1H, $CH(\text{CH}_3)_2$), 2.08 (s, 3H, Ar CH_3), 1.81 (s, 3H, Ar CH_3), 1.71

(s, 9H, C(CH₃)₃), 1.67-1.09 (m, 1H, CH(CH₃)₂), 1.12 (dd, 3H, $J_{\text{HH}} = 7$ Hz, $J_{\text{PH}} = 18$ Hz, CH(CH₃)₂), 1.02 (dd, 3H, $J_{\text{HH}} = 7$ Hz, $J_{\text{PH}} = 21$ Hz, CH(CH₃)₂), 0.86 (dd, 3H, $J_{\text{HH}} = 7$ Hz, $J_{\text{PH}} = 21$ Hz, CH(CH₃)₂), 0.79 (dd, 3H, $J_{\text{HH}} = 7$ Hz, $J_{\text{PH}} = 15$ Hz, CH(CH₃)₂). ³¹P {¹H} NMR (toluene-d₈): δ 75.3. ¹⁹F {¹H} NMR (toluene-d₈): δ -77.1. ¹⁹F {¹H} NMR (CD₂Cl₂): δ -79.4.

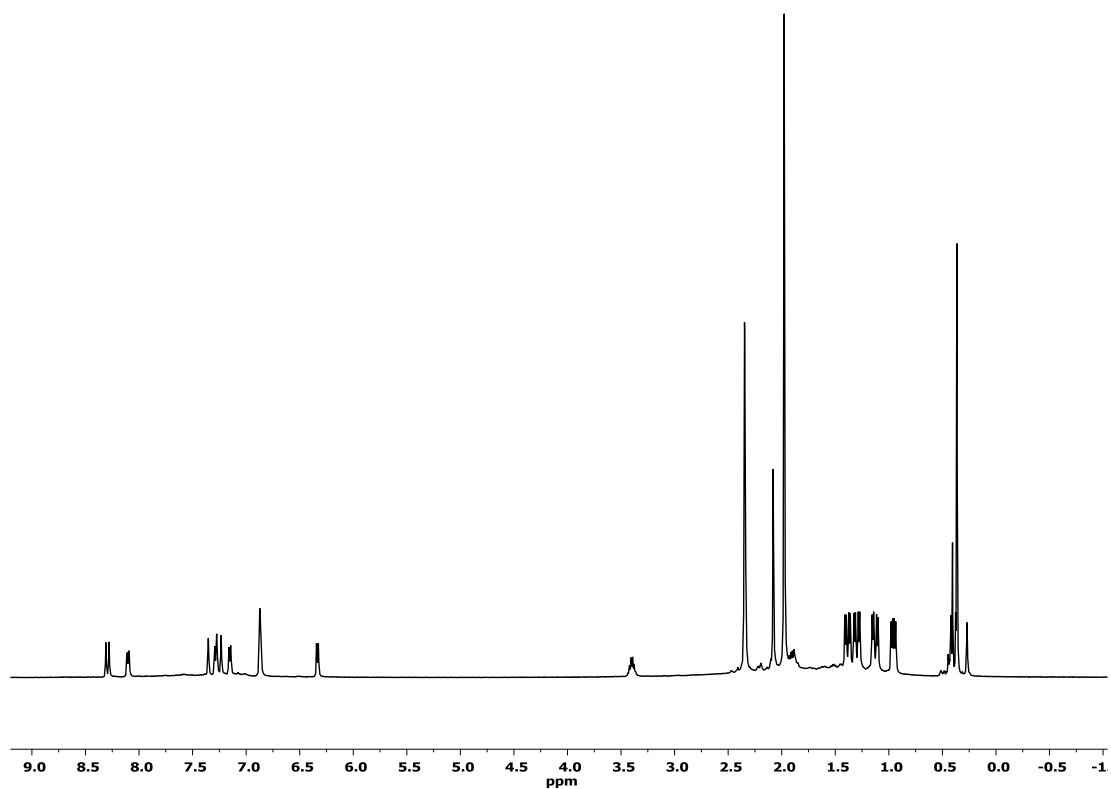


Figure 3.40 ¹H NMR spectrum of **3-8PdOTf** (500 MHz, toluene-d₈). There is overlap with the solvent peak at 2.08 ppm. Silicone grease is still prevalent.

3-8RhCO. A J. Young tube was charged with **3-8H** (42 mg, 0.11 mmol), [Rh(COD)Cl]₂ (52 mg, 0.11 mmol of Rh), 2,6-lutidine (13 μ l, 0.11 mmol) and C₆D₆ (1 mL). Upon addition of CO (1 atm) the solution immediately turns red. The solution was allowed to react overnight and was then passed through a pad of silica gel. The frit was then washed with diethyl ether and the volatiles were removed *in vacuo* to yield a red solid. This was then taken up in dichloromethane and stored at -35 °C to yield red crystals of **3-8RhCO** (47 mg, 0.089 mmol, 84%). ¹H NMR (C₆D₆, Figure 3.41): δ 7.81 (d, 1H, $J_{\text{PH}} = 9$ Hz, imine CH), 7.53 (d, 1H, $J_{\text{HH}} = 8$ Hz, Ar H), 7.30 (dd, 1H, $J_{\text{PH}} = 8$ Hz, $J_{\text{HH}} = 4$ Hz, Ar H), 7.01 (d, 1H, $J_{\text{HH}} = 7$ Hz, Ar H), 6.80 (d, 1H, $J_{\text{HH}} = 9$ Hz, Ar H), 6.76 (s, 1H, Ar H), 6.75 (m, 1H, Ar H), 2.30 (m, 1H, CH(CH₃)₂), 2.14 (s, 3H, CH₃), 2.12 (s, 3H, CH₃), 1.46 (s, 9H, C(CH₃)₃), 1.32-1.19 (m, 9H, CH(CH₃)₂), 0.98 (dd, 3H, $J_{\text{PH}} = 13$ Hz, $J_{\text{HH}} = 7$ Hz, CH(CH₃)₂). ¹H NMR (CDCl₃): δ 8.25 (dd, $J = 9$ Hz, $J = 3$ Hz, 1H, imine CH), 7.50 (d, $J = 3$ Hz, 1H, Ar H), 7.47 (dd, $J = 9$ Hz, $J = 3$ Hz, 1H, Ar H), 7.38 – 7.30 (m, 2H Ar H), 7.17 (s, 1H, Ar H), 7.01 (d, $J = 9$ Hz, 1H, Ar H), 2.81 (m, 1H, CH(CH₃)₂), 2.50 (s, 3H, Ar CH₃), 2.48 (m, 1H, CH(CH₃)₂), 2.41 (s, 3H, Ar CH₃), 1.86 (s, 9H, C(CH₃)₃), 1.57 (dd, $J = 16$ Hz, $J = 7$ Hz, 3H, CH(CH₃)₂), 1.49 (dd, $J = 15$ Hz, $J = 7$ Hz, 6H, CH(CH₃)₃), 1.42 (dd, $J = 14$ Hz, $J = 7$ Hz, 3H, CH(CH₃)₃). ¹³C {¹H} NMR (CDCl₃): δ 194.7 (s, CO), 161.6 (d, $J = 21.7$ Hz, Ar C), 158.2 (s), 150.1 (s), 134.2 (s), 133.1 (s), 132.0 (s), 130.8 (s), 128.6 – 127.3 (m), 124.6 (s), 123.5 (s), 120.50 (d, $J = 13$ Hz), 117.19 (d, $J = 43$ Hz), 63.71 (s (C(CH₃)₃), 31.95 (s, (C(CH₃)₃), 27.46 (d, $J = 26$ Hz, CH(CH₃)₂), 23.99 (d, $J = 34$ Hz, CH(CH₃)₂), 20.79 (s, CH₃), 20.15 (s, CH₃), 19.82 (s,

CH₃), 19.13 (s, CH₃), 18.20 (s, CH₃), 17.68 (s, CH₃). ³¹P{¹H} NMR (C₆D₆): δ 78.7 (d, $J_{\text{RhP}} = 154$ Hz). IR $\nu(\text{CO}) = 1930 \text{ cm}^{-1}$.

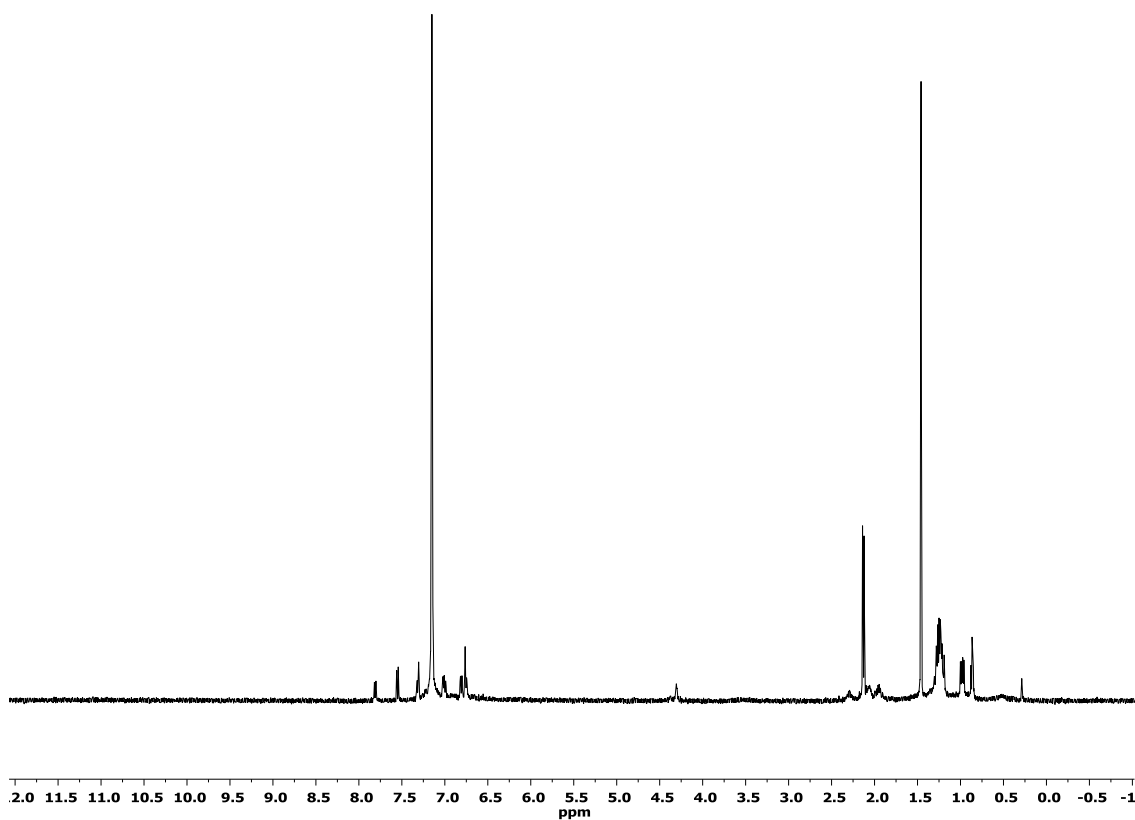


Figure 3.41 ¹H NMR spectrum of **3-8RhCO** (500 MHz, C₆D₆). Trace quantities of dichloromethane, silicone grease, and pentane are observed in the spectrum.

3.11.12 Synthesis of **3-9H** and its complexes

3-H. A Schlenk flask was charged with **3-F** (0.30 g, 0.77 mmol), a stir bar, and diethyl ether. n-Butyllithium (0.31 mL, 0.77 mmol) was then added in a dropwise fashion. After 30 min CIP(NMe₂)₂ (0.11 mL, 0.77 μmol) was added and stirring was commenced for an additional 1.5 h. The ethereal solution was then filtered through a pad of Celite. Removal of the volatiles *in vacuo* and recrystallization in pentane at -35 °C resulted in the isolation of **3-H** as colorless crystals (0.30 g, 0.59 mmol, 77%). ¹H NMR (C₆D₆, Figure 3.42): δ 7.93 (dd, *J*_{HH} = 5 Hz, *J*_{PH} = 10 Hz, 1H, Ar *H*), 7.56 (dd, *J*_{HH} = 5 Hz, *J*_{PH} = 10 Hz, 1H, Ar *H*), 7.31 (m, 1H, Ar *H*), 7.21 (d, *J*_{HH} = 5 Hz, 1H, Ar *H*), 6.99 (d, *J*_{HH} = 5 Hz, 1H, Ar *H*), 6.89 (d, *J*_{HH} = 5 Hz, 1H, Ar *H*), 2.48 (d, *J*_{PH} = 10 Hz, 12H, P(N(CH₃)₂)₂), 2.15 (s, 3H, Ar CH₃), 1.93 (s, 3H, Ar CH₃), 1.90 (m, 2H, CH(CH₃)₂), 1.15 (dd, *J*_{HH} = 7 Hz, *J*_{PH} = 15 Hz, 6H, CH(CH₃)₂), 0.95 (dd, *J*_{HH} = 7 Hz, *J*_{PH} = 15 Hz, 6H, CH(CH₃)₂). ¹H{³¹P δ -9.1} NMR (C₆D₆): δ 7.93 (d, *J*_{HH} = 5 Hz, 1H, Ar *H*), 7.56 (d, *J*_{HH} = 5 Hz, 1H, Ar *H*), 7.31 (m, 1H, Ar *H*), 7.21 (d, *J*_{HH} = 5 Hz, 1H, Ar *H*), 6.99 (d, *J*_{HH} = 5 Hz, 1H, Ar *H*), 6.89 (d, *J*_{HH} = 5 Hz, 1H, Ar *H*), 2.48 (d, *J*_{PH} = 10 Hz, 12H, P(N(CH₃)₂)₂), 2.15 (s, 3H, Ar CH₃), 1.93 (s, 3H, Ar CH₃), 1.90 (m, 2H, CH(CH₃)₂), 1.15 (d, *J*_{HH} = 7 Hz, 6H, CH(CH₃)₂), 0.95 (d, *J*_{HH} = 7 Hz, 6H, CH(CH₃)₂). ¹H{³¹P δ 124.5} NMR (C₆D₆): δ 7.93 (dd, *J*_{HH} = 5 Hz, *J*_{PH} = 10 Hz, 1H, Ar *H*), 7.56 (dd, *J*_{HH} = 5 Hz, *J*_{PH} = 10 Hz, 1H, Ar *H*), 7.31 (m, 1H, Ar *H*), 7.21 (d, *J*_{HH} = 5 Hz, 1H, Ar *H*), 6.99 (d, *J*_{HH} = 5 Hz, 1H, Ar *H*), 6.89 (d, *J*_{HH} = 5 Hz, 1H, Ar *H*), 2.48 (s, 12H, P(N(CH₃)₂)₂), 2.15 (s, 3H, Ar CH₃), 1.93 (s, 3H, Ar CH₃), 1.90 (m, 2H, CH(CH₃)₂), 1.15 (dd, *J*_{HH} = 7 Hz, *J*_{PH} = 15 Hz, 6H, CH(CH₃)₂), 0.95 (dd, *J*_{HH} = 7 Hz, *J*_{PH} = 15 Hz, 6H, CH(CH₃)₂). ¹³C{¹H} NMR (C₆D₆): δ

151.4 (dd, $J = 17$ Hz, $J = 21$ Hz, Ar CN), 143.5 (s, Ar C), 136.4 (s, Ar CH), 135.6 (dd, $J = 4$ Hz, $J = 9$ Hz, Ar C), 134.5 (s, Ar CH), 134.3 (s, Ar CH), 133.8 (d, $J = 22$ Hz, Ar C), 132.4 (s, Ar CH), 130.1 (dd, $J = 6$ Hz, $J = 10$ Hz, Ar C), 129.6 (s, Ar CH), 127.4 (s, Ar CH), 124.6 (s, Ar C), 38.8 (d, $J = 2$ Hz, $N(CH_3)_2$), 38.6 (d, $J = 2$ Hz, $N(CH_3)_2$), 26.8 (d, $J = 5$ Hz, $CH(CH_3)_2$), 26.7 (d, $J = 5$ Hz, $CH(CH_3)_2$), 21.9 (s, CH_3), 21.8 (s, CH_3), 20.9 (s, CH_3), 20.6, 20.4 (s, CH_3), 20.4 (s, CH_3). $^{31}P\{^1H\}$ NMR (C_6D_6): δ 124.5 (s, $P(NCH_3)_2$), -9.1 (s, P, P^iPr_2).

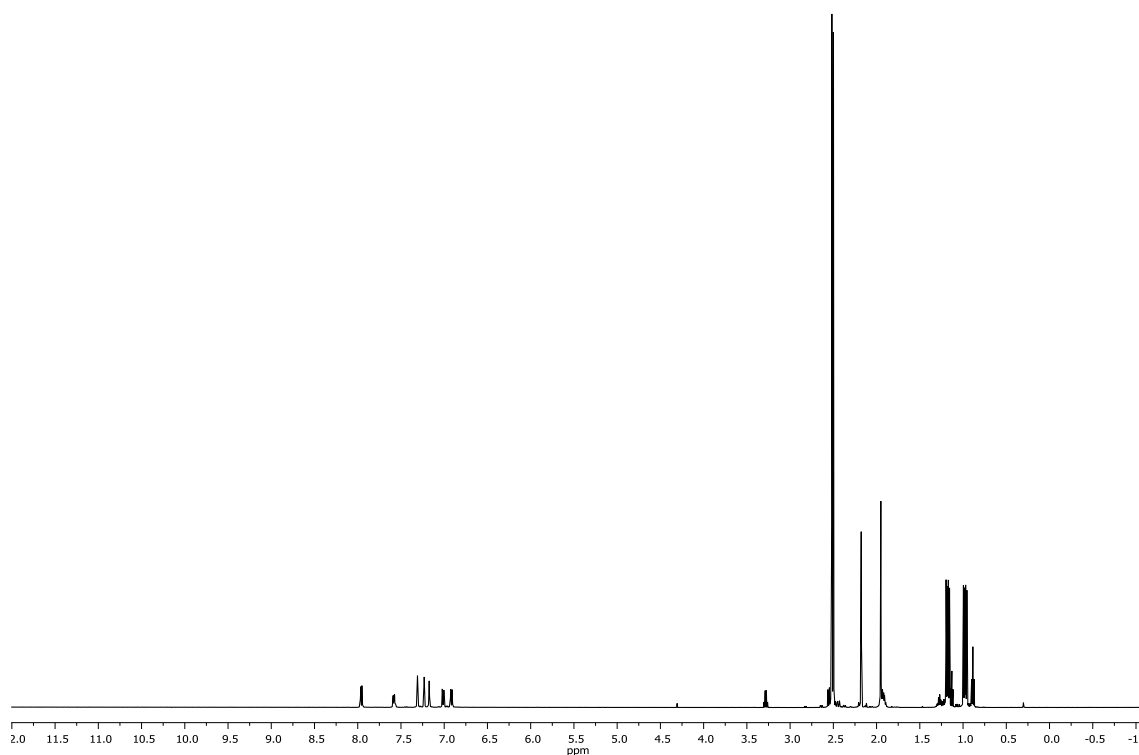


Figure 3.42 ^{13}C -NMR (500 MHz, C_6D_6). Trace quantities of diethyl ether, silicone grease, and pentane are observed.

3-9H. A Schlenk flask was charged with **3-F** (2.67 g, 6.81 mmol), a stir bar, and diethyl ether (100 mL). *n*-Butyllithium (2.72 mL, 6.81 mmol) was then added to the reaction via syringe and allowed to react for 20 min. ClP(NMe₂)₂ (1.00 mL, 6.81 mmol) was then added to the solution. Stirring was continued for 30 min and then a second equivalent of *n*-butyllithium (2.67 mL, 6.81 mmol) was added to the reaction mixture. Removal of a small aliquot and analysis via ³¹P NMR reveal conversion to **3-9Li** as observed by the formation of two singlets at δ 109.5 and -3.4 ppm in diethyl ether. Addition of CF₃CH₂OH (0.49 mL, 6.81 mmol) resulted in immediate precipitation of LiOCH₂CF₃ and formation of a colorless solution. The diethyl ethereal solution was then filtered through a pad of Celite, concentrated and stored at -35 °C. The resulting precipitate was collected and dried *in vacuo* to yield **3-9H** as a colorless powder (2.41 g, 82%). ¹H NMR (C₆D₆, Figure 3.43): δ 8.55 (d, *J*_{PH} = 8 Hz, 1H, *NH*), 7.43 – 7.33 (m, 3H, *Ar H*), 7.13 (s, 1H, *Ar H*), 6.93 (d, *J*_{HH} = 9 Hz, 1H, *Ar H*), 6.84 (d, *J*_{HH} = 8 Hz, 1H, *Ar H*), 2.80 (d, *J*_{PH} = 9 Hz, 12H, P(NCH₃)₂), 2.26 (s, 3H, *Ar CH*₃), 2.18 (s, 3H, *Ar CH*₃), 1.98 – 1.87 (m, 2H, CH(CH₃)₂), 1.09 (dd, *J*_{PH} = 15 Hz, *J*_{HH} = 7 Hz, 6H, CH(CH₃)₂), 0.94 (dd, *J*_{PH} = 12 Hz, *J*_{HH} = 7 Hz, 6H, CH(CH₃)₂). ¹H{³¹P δ -13.1} NMR (C₆D₆): δ 8.54 (s, 1H), 7.44 – 7.32 (m, 3H), 7.13 (s, 1H), 6.93 (d, *J* = 9 Hz, 1H), 6.84 (d, *J* = 8 Hz, 1H), 2.80 (d, *J* = 9 Hz, 12H), 2.26 (s, 3H), 2.18 (s, 3H), 1.95 (m 2H), 1.09 (d, *J* = 7 Hz, 6H), 0.94 (d, 6H). ¹H{³¹P δ 98.2} NMR (C₆D₆): δ 8.55 (d, *J* = 8 Hz, 1H), 7.45 – 7.32 (m, 3H), 7.13 (s, 1H), 6.93 (d, *J* = 8 Hz, 1H), 6.84 (d, *J* = 8 Hz, 1H), 2.80 (d, *J* = 1 Hz, 12H), 2.26 (s, 3H), 2.18 (s, 3H), 1.95 (m, 2H), 1.09 (dd, *J* = 15 Hz, *J* = 7, 6H), 0.94 (dd, *J* = 12 Hz, *J* = 7 Hz, 6H). ¹³C{¹H} NMR (C₆D₆): δ 147.8 (d, *J*_{CP} = 20, *Ar CN*), 143.5 (d, *J*_{CP} = 18

Hz, Ar CN), 133.6 (d, $J_{CP} = 3$ Hz, Ar C), 132.8 (d, $J = 8$ Hz, Ar C), 130.7 (s, Ar C), 130.0 (s, Ar C), 128.8 (s, Ar C), 128.5 (s, Ar C), 127.6 (s, Ar C), 122.80 (s, Ar C), 118.00 (d, $J_{CP} = 3$ Hz, Ar C), 117.09 (s, Ar C), 41.95 (dd, $J_{CP} = 15$ Hz, $J_{CP} = 3$ Hz, P(NCH₃)₂), 23.53 (d, $J_{CP} = 11$ Hz, CH(CH₃)₂), 21.23 (s, Ar CH₃), 20.94 (s, Ar CH₃), 20.48 (d, $J = 19$ Hz, CH(CH₃)₂), 19.28 (d, $J = 9$ Hz, CH(CH₃)₂). ³¹P {¹H} NMR (C₆D₆): δ 98.2 (s, P(NMe₂)₂), -13.1 (s, PⁱPr₂).

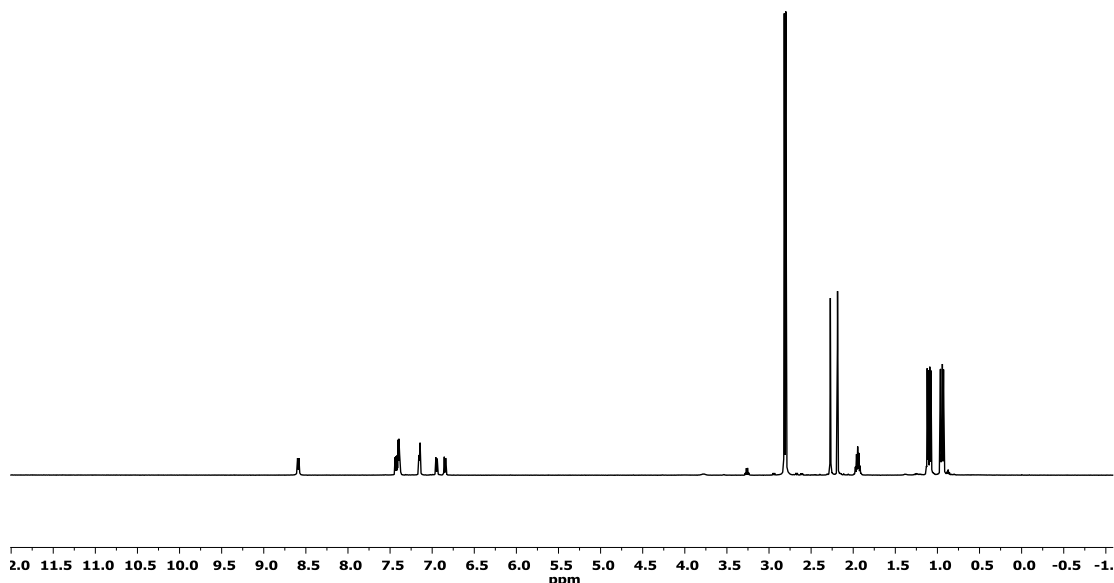


Figure 3.43 ¹H NMR spectrum of **3-9H** (500 MHz, C₆D₆). Trace quantities of diethyl ether are observed.

3-9RhCO. A J. Young tube was charged with **3-9H** (89.0 mg, 206 μmol), $[\text{Rh}(\text{COD})\text{Cl}]_2$ (51.0 mg, 206 μmol), 2,6-lutidine (24.0 μL , 206 μmol), and C_6D_6 (1 mL). The reaction mixture was degassed and then exposed to CO (1 atm). After 30 min the reaction was filtered through a pad of silica gel. The silica gel was washed with diethyl ether and then the volatiles were removed *in vacuo*. Recrystallization of the product in pentane at $-35\text{ }^\circ\text{C}$ resulted in the isolation of **3-9RhCO** as a yellow powder (76.0 mg, 135 μmol , 77%). ^1H NMR (C_6D_6 , Figure 3.44): δ 7.75 – 7.67 (m, 2H, Ar H), 7.23 (d, $J_{\text{PH}} = 9\text{ Hz}$, 1H, Ar H), 6.90 (d, $J_{\text{PH}} = 8\text{ Hz}$, 1H, Ar H), 6.83 (d, $J_{\text{HH}} = 9\text{ Hz}$, 1H, Ar H), 6.79 (d, $J_{\text{HH}} = 9\text{ Hz}$, 1H, Ar H), 2.56 (d, $J_{\text{PH}} = 12\text{ Hz}$, 12H, $\text{N}(\text{CH}_3)_2$), 2.18 (s, 3H, Ar CH_3), 2.16 (s, 3H, Ar CH_3), 2.14 (m, 2H, $\text{CH}(\text{CH}_3)_2$), 1.28 (dd, $J_{\text{PH}} = 17\text{ Hz}$, $J_{\text{HH}} = 7\text{ Hz}$, 6H, $\text{CH}(\text{CH}_3)_2$), 1.05 (dd, $J_{\text{PH}} = 15\text{ Hz}$, $J_{\text{HH}} = 7\text{ Hz}$, 6H, $\text{CH}(\text{CH}_3)_2$). $^1\text{H}\{^{31}\text{P}\}$ NMR (C_6D_6 , Figure 3.44): δ 7.75 – 7.67 (m, 2H, Ar H), 7.23 (d, $J = 9\text{ Hz}$, 1H, Ar H), 6.90 (s, 1H, Ar H), 6.83 (d, $J = 9\text{ Hz}$, 1H, Ar H), 6.79 (d, $J = 9\text{ Hz}$, 1H, Ar H), 2.56 (d, $J = 12\text{ Hz}$, 12H, $\text{N}(\text{CH}_3)_2$), 2.18 (s, 3H, Ar CH_3), 2.16 (s, 3H, Ar CH_3), 2.14 (m, 2H, $\text{CH}(\text{CH}_3)_2$), 1.28 (dd, $J_{\text{PH}} = 17\text{ Hz}$, $J_{\text{HH}} = 7\text{ Hz}$, 6H, $\text{CH}(\text{CH}_3)_2$), 1.05 (dd, $J_{\text{PH}} = 15\text{ Hz}$, $J_{\text{HH}} = 7\text{ Hz}$, 6H, $\text{CH}(\text{CH}_3)_2$). $^1\text{H}\{^{31}\text{P}\}$ NMR (C_6D_6): δ 7.75 – 7.67 (m, 2H, Ar H), 7.23 (s, 1H, Ar H), 6.90 (d, $J = 8\text{ Hz}$, 1H), 6.83 (d, $J = 9\text{ Hz}$, 1H, Ar H), 6.79 (d, $J = 9\text{ Hz}$, 1H, Ar H), 2.56 (s, 12H, $\text{N}(\text{CH}_3)_2$), 2.18 (s, 3H, Ar CH_3), 2.16 (s, 3H, Ar CH_3), 2.14 (m, 2H, $\text{CH}(\text{CH}_3)_2$), 1.28 (dd, $J_{\text{PH}} = 17\text{ Hz}$, $J_{\text{HH}} = 7\text{ Hz}$, 6H), 1.05 (dd, $J_{\text{PH}} = 15\text{ Hz}$, $J_{\text{HH}} = 7\text{ Hz}$, 6H). $^{13}\text{C}\{^1\text{H}\}$ NMR (C_6D_6): δ 140.41 – 139.41 (m), 135.21 (s), 134.11 (s), 134.01 (s), 133.18 (s), 132.72 – 132.59 (m), 132.59 – 132.43 (m), 131.63 – 131.48 (m), 131.25 – 131.14 (m), 130.64 (s), 128.93 (d, $J = 11\text{ Hz}$), 117.32 – 116.76 (m), 116.81 – 116.10

(m), 25.31 – 25.25 (m, $\text{CH}(\text{CH}_3)_2$), 25.07 (s, $\text{CH}(\text{CH}_3)_2$), 20.39 (s, CH_3), 20.13 (s, CH_3), 18.75 (d, $J = 6$ Hz, $\text{CH}(\text{CH}_3)_2$), 17.98 (d, $J_{\text{CP}} = 5$ Hz, $\text{CH}(\text{CH}_3)_2$). $^{31}\text{P}\{^1\text{H}\}$ NMR (C_6D_6): δ 130.9 (dd, $J_{\text{PP}} = 315$ Hz, $J_{\text{RhP}} = 163$ Hz, $\text{P}(\text{NCH}_3)_2$), 58.7 (dd, $J_{\text{PP}} = 315$ Hz, $J_{\text{RhP}} = 123$ Hz, P^{iPr}). IR: $\nu(\text{CO}) = 1943$ cm^{-1} .

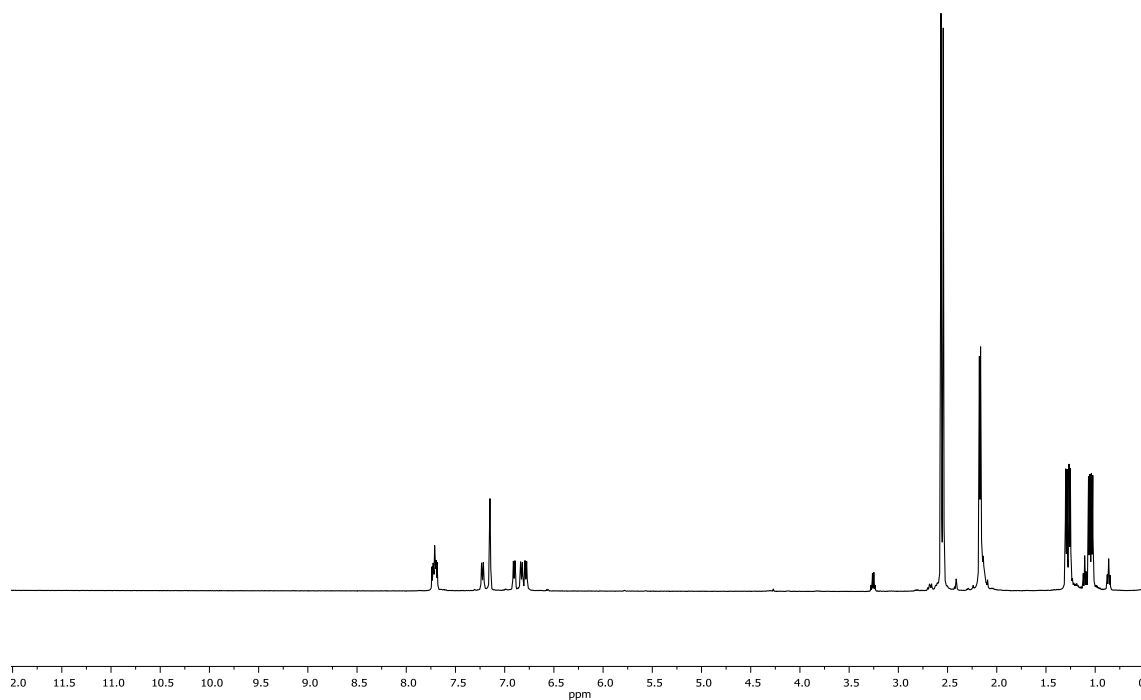


Figure 3.44 ^1H NMR spectrum of **3-9RhCO** (500 MHz, C_6D_6). Trace quantities of diethyl ether and pentane are observed.

Synthesis of **3-9Rh(CO)(Me)(I)** and **3-9Rh(Me)(I)**.

3-9Rh(CO)(Me)(I). A J. Young tube was charged with **3-9Rh(CO)** (18 mg), C₆D₆ (1 mL) and MeI (50 μ L). After 10 min ³¹P NMR analysis revealed conversion to **3-9Rh(CO)(Me)(I)**. The volatiles were removed under vacuum to yield **3-9Rh(CO)(Me)(I)** as a red solid. ¹H NMR (C₆D₆): δ 7.52 – 7.40 (m, 2H, Ar H), 7.07 (d, J = 10 Hz, 1H, Ar H), 6.93 (d, J = 7 Hz, 1H, Ar H), 6.72 (dd, J = 18 Hz, J = 9 Hz, 2H, Ar H), 3.16 (m, J = 17 Hz, 1H, CH(CH₃)₂), 2.77 (d, J = 9 Hz, 6H, CH₃), 2.48 (d, J = 9 Hz, 6H, CH₃), 2.47 – 2.38 (m, 1H, CH(CH₃)₂), 2.14 (s, 3H, Ar CH₃), 2.12 (s, 3H, Ar CH₃), 1.30 (dd, J = 15 Hz, J = 7 Hz, 6H, CH(CH₃)₂), 1.15 (dd, J = 15 Hz, J = 7 Hz, 3H, CH(CH₃)₂), 1.08 (dd, J = 14 Hz, J = 7 Hz, 3H, CH(CH₃)₂), 0.98 (td, J = 5 Hz, J = 2 Hz, 3H, CH₃). ¹³C {¹H} NMR (C₆D₆): δ 192.6 (dt, J = 10 Hz, J = 56 Hz, CO), 159.0 (d, J = 19 Hz, C), 157.8 (d, J = 25 Hz, C), 132.9 (s, Ar C), 132.4 (d, J = 2 Hz, Ar C), 131.9 (d, J = 3 Hz, Ar C), 130.3 (s, Ar C), 128.5 (s, (s, Ar C), 123.0 (s, Ar C), 122.7 (s, Ar C), 118.2 (d, J = 10 Hz, Ar C), 117.5 (d, J = 15 Hz, Ar C), 41.3 (d, J = 5 Hz, N(CH₃)₂), 39.5 (d, J = 4 Hz, N(CH₃)₂), 24.0 (d, J = 19 Hz, CH(CH₃)₂), 21.0 (s, CH₃), 20.9 (s, CH₃), 20.6 (s, CH₃), 20.5 (s, CH₃), 19.1 (s, CH₃). ³¹P {¹H} NMR (C₆D₆): δ 125.2 (dd, J_{RhP} = 110 Hz, J_{PP} = 445 Hz, P(NMe₂)₂), 49.3 (dd, J_{RhP} = 78 Hz, J_{PP} = 445 Hz, PⁱPr₂). IR $\nu(\text{CO})$ = 2079 cm⁻¹. Exposure of the red solid to vacuum while irradiating the sample with a 500 W halogen lamp resulted in the loss of CO and formation of **3-9Rh(Me)(I)**. ¹H NMR (C₆D₆): δ 7.52 – 7.40 (m, 2H, Ar H), 7.07 (d, J = 10 Hz, 1H, Ar H), 6.93 (d, J = 7 Hz, 1H, Ar H), 6.72 (dd, J = 18 Hz, J = 9 Hz, 2H, Ar H), 3.16 (m, J = 17 Hz, 1H, CH(CH₃)₂), 2.77 (d, J = 9 Hz, 6H, NCH₃), 2.48 (d, J = 9 Hz, 6H, NCH₃), 2.47 – 2.38 (m,

1H, CH(CH₃)₂), 2.14 (s, 3H, Ar CH₃), 2.12 (s, 3H, Ar CH₃), 1.30 (dd, $J = 15$ Hz, $J = 7$ Hz, 6H, CH(CH₃)₂), 1.15 (dd, $J = 15$ Hz, $J = 7$ Hz, 3H, CH(CH₃)₂), 1.08 (dd, $J = 14$ Hz, $J = 7$ Hz, 3H, CH(CH₃)₂), 0.98 (td, $J = 5$ Hz, $J = 2$ Hz, 3H, CH₃). ³¹P{¹H} NMR (C₆D₆): δ 125.2 (dd, $J_{\text{RHP}} = 110$ Hz, $J_{\text{PP}} = 445$ Hz, P(NMe₂)₂), 49.3 (dd, $J_{\text{RHP}} = 78$ Hz, $J_{\text{PP}} = 445$ Hz, PⁱPr₂).

3.11.13 Synthesis of **3-10H** and its complexes

3-10H. A Teflon stoppered Schlenk flask was charged with **3-9H** (2.00 g, 4.64 mmol), CF₃CH₂OH (1.70 mL, 23.2 mmol), toluene (15 mL) and a stir bar. The reaction mixture was then refluxed at 100 °C for three days. Cooling the reaction mixture to room temperature and removal of the volatiles *in vacuo* gave a yellow oil. Recrystallization in diethyl ether yielded **3-10H** as a colorless oil (2.47 g, 4.57 mmol, 98%). ¹H NMR (CDCl₃, Figure 3.45): δ 7.43 (d, $J_{\text{PH}} = 5$ Hz, 1H, NH), 7.19-7.17 (m, 4H, Ar H), 7.01 (d, $J_{\text{HH}} = 10$ Hz, 1H, Ar H), 6.89 (dd, $J_{\text{HH}} = 10$ Hz, $J_{\text{PH}} = 5$ Hz, 1H, Ar H), 4.30-4.24 (m, 2H, OCH₂CF₃), 4.19-4.13 (m, 2H, OCH₂CF₃), 2.35 (s, 3H, Ar CH₃), 2.29 (s, 3H, Ar CH₃), 2.17-2.11 (m, 2H, CH(CH₃)₂), 1.13 (dd, $J_{\text{PH}} = 15$ Hz, $J_{\text{HH}} = 5$ Hz, 6H, CH(CH₃)₂), 0.96 (dd, $J_{\text{PH}} = 15$ Hz, $J_{\text{HH}} = 5$ Hz, 6H, CH(CH₃)₂). ¹H{³¹P} NMR (CDCl₃): δ 7.43 (d, $J_{\text{PH}} = 5$ Hz, 1H, NH), 7.19-7.17 (m, 4H, Ar H), 7.01 (d, $J_{\text{HH}} = 10$ Hz, 1H, Ar H), 6.89 (d, $J_{\text{HH}} = 10$ Hz, $J_{\text{PH}} = 5$ Hz, 1H, Ar H), 4.30-4.24 (m, 2H, OCH₂CF₃), 4.19-4.13 (m, 2H, OCH₂CF₃), 2.35 (s, 3H, Ar CH₃), 2.29 (s, 3H, Ar CH₃), 2.17-2.11 (m, 2H, CH(CH₃)₂), 1.13 (d, $J_{\text{HH}} = 5$ Hz, 6H, CH(CH₃)₂), 0.96 (d, $J_{\text{HH}} = 5$ Hz, 6H, CH(CH₃)₂). ¹³C{¹H} NMR (C₆D₆): δ 147.7 (d, $J_{\text{CP}} = 20$ Hz, CN), 144.7 (d, $J_{\text{CP}} = 19$ Hz, CN), 133.7 (d, $J_{\text{CP}} = 5$ Hz,

Ar C), 133.4 (s, Ar C), 132.1 (d, $J_{CP} = 3$ Hz, Ar C), 131.5 (d, $J_{CP} = 13$ Hz, Ar C), 131.0 (s), 129.6 (s, Ar C), 129.5 (s, Ar C), 129.4 (s, Ar C), 121.0 (s, Ar C), 117.5 (d, $J = 3$ Hz, Ar C), 64.1 (m, CH_2), 23.7 (d, $J_{CP} = 10$ Hz, $CH(CH_3)_2$), 20.8 (d, $J_{CP} = 8$ Hz, $CH(CH_3)_2$), 20.4 (s, Ar CH_3), 20.3 (s, Ar CH_3), 19.2 (d, $J_{CP} = 9$ Hz, $CH(CH_3)_2$). ^{31}P NMR (C_6D_6): δ 166.3 (s, $POCH_2CF_3$), -15.0 (s, P^iPr_2). $^{31}P\{^1H\}$ NMR ($CDCl_3$): δ 167.5 (s, $POCH_2CF_3$), -14.7 (s, P^iPr_2). ^{19}F NMR (C_6D_6): δ 75.6.

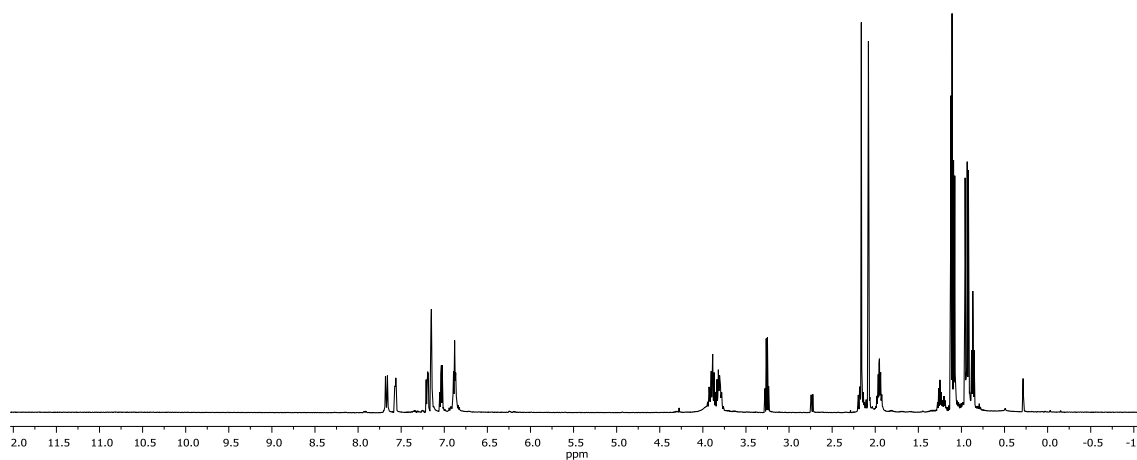


Figure 3.45 1H NMR spectrum of **3-10H** (500 MHz, C_6D_6). Trace quantities of diethyl ether, **3-9H**, silicone grease, and pentane are observed.

3-10RhCO. A J. Young tube was charged with **3-10H** (0.15 g, 0.28 mmol), (Rh(COD)Cl)₂ (65 mg, 0.13 mmol), 2,6-lutidine (32 μ l, 0.28 mmol), and C₆D₆. The mixture was degassed by freeze pump thaw techniques and then exposed to one atmosphere of CO. The volatiles were then removed *in vacuo* and the resulting red oil was taken up in pentane and filtered through a pad of Celite. Removal of the volatiles yielded **3-10RhCO** as a red powder. No additional workup was conducted. (0.12 g, 0.18 mmol, 65%). ¹H NMR (C₆D₆, Figure 3.46): δ 7.60 (dd, $J_{\text{HH}} = 8$ Hz, $J_{\text{PH}} = 4$ Hz, 1H, Ar *H*), 7.53 (t, $J_{\text{HH}} = 8$ Hz, 1H, Ar *H*), 7.24 (d, $J_{\text{PH}} = 11$ Hz, 1H, Ar *H*), 6.83 (d, $J_{\text{PH}} = 8$ Hz, 1H, Ar *H*), 6.78 (d, $J_{\text{HH}} = 9$ Hz, 1H, Ar *H*), 6.75 (d, $J_{\text{HH}} = 9$ Hz, 1H, Ar *H*), 4.57 – 4.20 (m, 2H, OCH₂CF₃), 3.93 (m, 2H, OCH₂CF₃), 2.14 (s, 3H, Ar CH₃), 2.09 – 1.99 (m, 2H, CH(CH₃)₂), 1.98 (s, 3H, Ar CH₃), 1.13 (dd, $J_{\text{PH}} = 17$ Hz, $J_{\text{HH}} = 7$ Hz, 6H, CH(CH₃)₂), 0.92 (dd, $J_{\text{PH}} = 15$ Hz, $J_{\text{HH}} = 7$ Hz, 6H, CH(CH₃)₂). ¹H{³¹P δ 60.1} NMR (C₆D₆): δ 7.60 (d, $J = 9$ Hz, 1H, Ar *H*), 7.53 (t, $J = 8$ Hz, 1H, Ar *H*), 7.24 (d, $J = 11$ Hz, 1H, Ar *H*), 6.83 (s, 1H, Ar *H*), 6.78 (d, $J_{\text{HH}} = 9$ Hz, 1H, Ar *H*), 6.75 (d, $J_{\text{HH}} = 9$ Hz, 1H, Ar *H*), 4.43 – 4.24 (m, 2H, OCH₂CF₃), 4.05 – 3.82 (m, 2H, OCH₂CF₃), 2.14 (s, 3H, Ar CH₃), 2.12 – 1.96 (m, 2H, CH(CH₃)₂), 1.98 (s, 3H, Ar CH₃), 1.13 (d, $J_{\text{HH}} = 6.9$ Hz, 6H, CH(CH₃)₂), 0.92 (d, $J_{\text{HH}} = 6.8$ Hz, 6H, CH(CH₃)₂). ¹H{³¹P δ 190.7} NMR (C₆D₆): δ 7.60 (dd, $J = 8$ Hz, $J = 4$ Hz, 1H, Ar *H*), 7.53 (d, $J = 9$ Hz, 1H, Ar *H*), 7.24 (s, 1H, Ar *H*), 6.83 (d, $J = 8$ Hz, 1H, Ar *H*), 6.78 (d, $J_{\text{HH}} = 9$ Hz, 1H, Ar *H*), 6.75 (d, $J_{\text{HH}} = 9$ Hz, 1H, Ar *H*), 4.36 (m, 1H, OCH₂CF₃), 3.92 (m, 1H, OCH₂CF₃), 2.14 (s, 2H, Ar CH₃), 2.09 – 2.01 (m, 1H, CH(CH₃)₂), 1.98 (s, 1H, CH(CH₃)₂), 1.13 (dd, $J_{\text{PH}} = 17$ Hz, $J_{\text{HH}} = 7$ Hz, 3H, CH(CH₃)),

0.92 (dd, $J_{PH} = 15$ Hz, $J_{HH} = 7$ Hz, 3H, CH(CH₃)). ¹³C{¹H} NMR (C₆D₆): δ 189.3 (d, $J = 71$ Hz, CO), 158.8 (d, $J = 19$ Hz, Ar CN), 157.9 (d, $J = 34$ Hz, Ar CN), 135.1 (s, Ar C), 132.3 (s, Ar C), 132.1 (s, Ar C), 129.6 (s, Ar C), 126.7 (s, Ar C), 125.1 (br, CF₃), 123.0 (br, CF₃), 120.7 (s, Ar C), 120.5 (s, Ar C), 117.4 (s, Ar C), 116.5 (d, $J = 14$ Hz, Ar C), 70.9 – 68.0 (m, CH₂), 34.0 (d, $J = 21$ Hz, CH(CH₃)₂), 29.5 (s, CH₃), 29.0 (s, CH₃), 28.6 (s, CH₃), 27.6 (s, CH₃). ³¹P{¹H} NMR (C₆D₆): δ 190.7 (dd, $J_{PP} = 346$ Hz, $J_{RhP} = 190$ Hz, P^{OCH₂CF₃}), 60.1 (dd, $J_{PP} = 346$ Hz, $J_{RhP} = 125$ Hz, P^{iPr}). ¹⁹F NMR (C₆D₆): δ -75.3 (t, $J_{HF} = 8$ Hz, CF₃). IR ν(CO) = 1960 cm⁻¹.

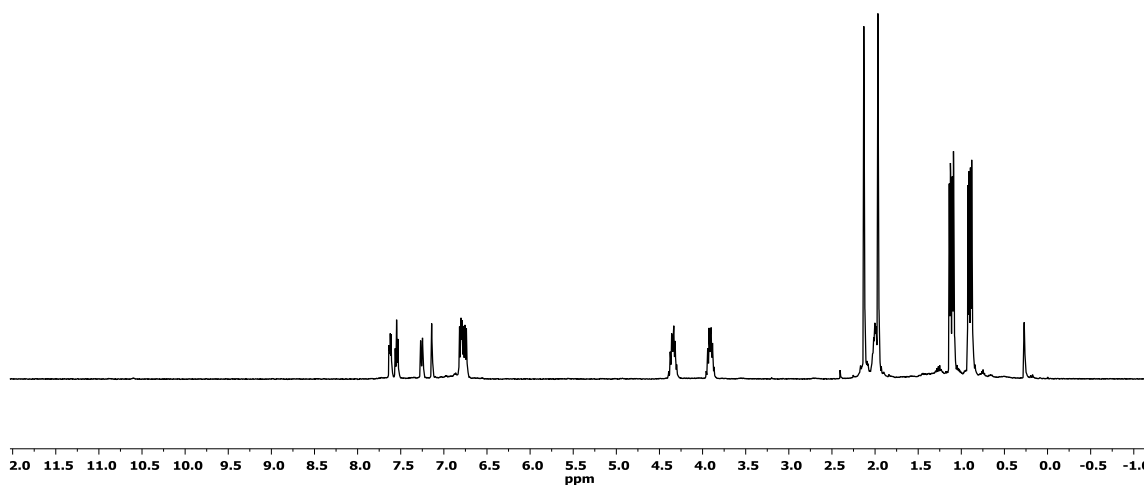


Figure 3.46 ¹H NMR spectrum **3-10RhCO** (500 MHz, C₆D₆). Trace quantities of pentane, 2,6-lutidine and diethyl ether are observed. Silicone grease is also observed.

3-10Rh(Me)(I)(CO). A Schlenk flask was charged with **3-10RhCO** (180 mg, 0.268 mmol), diethyl ether (5 mL), and methyl iodide (100 μ L). The reaction was stirred for 18 h and then the volatiles were removed under vacuum to yield **3-10Rh(Me)(I)(CO)** as an orange powder. ^1H NMR (C_6D_6): δ 7.51 (dd, $J = 8$ Hz, $J = 5$ Hz, 1H, Ar H), 7.45 (m, 1H, Ar H), 7.17 (m, 1H, Ar H), 6.76 (d, $J = 8$ Hz, 1H, Ar H), 6.71 (m, 2H, Ar H), 4.79 (m, 1H, OCH_2), 4.66 (m, 1H, OCH_2), 4.10 (m, 1H, OCH_2), 3.79 (m, 1H, OCH_2), 3.10 (m, 1H, $\text{CH}(\text{CH}_3)_2$), 2.30 (m, 1H, $\text{CH}(\text{CH}_3)_2$), 2.11 (s, 3H, CH_3), 1.98 (s, 3H, CH_3), 1.22 (m, 3H, CH_3), 1.18 (dd, $J_{\text{PH}} = 16$ Hz, $J_{\text{HH}} = 7$ Hz, 3H, $\text{CH}(\text{CH}_3)_2$), 1.08 (dd, $J_{\text{PH}} = 17$ Hz, $J_{\text{HH}} = 7$ Hz, 3H, $\text{CH}(\text{CH}_3)_2$), 0.97 (dd, $J_{\text{PH}} = 15$ Hz, $J_{\text{HH}} = 7$ Hz, 6H, $\text{CH}(\text{CH}_3)_2$). $^{31}\text{P}\{^1\text{H}\}$ NMR (C_6D_6): δ 159.7 (dd, $J_{\text{PP}} = 493$ Hz, $J_{\text{Rhp}} = 131$ Hz, $\text{P}(\text{OCH}_2\text{CF}_3)_2$), 59.7 (dd, $J_{\text{PP}} = 493$ Hz, $J_{\text{Rhp}} = 93$ Hz, P^iPr_2).

3-10Rh(Me)(OAc)(CO). A J. Young tube was charged with **3-10Rh(Me)(I)(CO)** (18 mg, 22 μ mol), and C_6D_6 (1 mL). Upon addition of AgOAc (4.0 mg, 22 μ mol) the orange solution lightens. After 1 h the solution was passed through a pad of silica gel. The volatiles were removed under vacuum to yield **3-10Rh(Me)(OAc)(CO)** as a light orange solid (7.0 mg). ^1H NMR (C_6D_6 , Figure 3.47): δ 7.60 (m, 2H, Ar H), 7.12 (m, 1H, Ar H), 6.74 (m, 2H, Ar H), 6.68 (d, $J = 9$ Hz, 1H, Ar H), 4.86 (m, 1H, OCH_2), 4.48 (m, 1H, OCH_2), 4.10 (m, 1H, OCH_2), 3.82 (m, 1H, OCH_2), 2.25 (m, 1H, $\text{CH}(\text{CH}_3)_2$), 2.19 (m, 1H, $\text{CH}(\text{CH}_3)_2$), 2.11 (s, 3H, CH_3), 1.99 (s, 3H, CH_3), 1.90 (s, 3H, CH_3), 1.21 (dd, $J_{\text{PH}} = 16$ Hz, $J_{\text{HH}} = 7$ Hz, 3H, $\text{CH}(\text{CH}_3)_2$), 1.16

(dd, $J_{\text{PH}} = 17$ Hz, $J_{\text{HH}} = 7$ Hz, 3H, CH(CH₃)₂), (dd, $J_{\text{PH}} = 16$ Hz, $J_{\text{HH}} = 7$ Hz, 3H, CH(CH₃)₂), 0.97 (dd, $J_{\text{PH}} = 15$ Hz, $J_{\text{HH}} = 7$ Hz, 3H, CH(CH₃)₂), 0.91 (dd, $J_{\text{PH}} = 16$ Hz, $J_{\text{HH}} = 7$ Hz, 3H, CH(CH₃)₂), 0.76 (m, 3H, CH₃). ³¹P{¹H} NMR (C₆D₆): δ 167.2 (dd, $J_{\text{PP}} = 501$ Hz, $J_{\text{RHP}} = 134$ Hz, P(OCH₂CF₃)₂), 62.8 (dd, $J_{\text{PP}} = 501$ Hz, $J_{\text{RHP}} = 94$ Hz, PⁱPr₂).

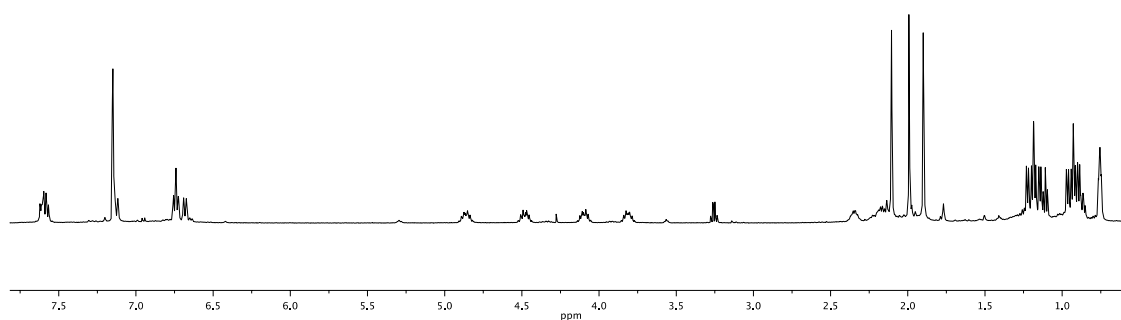


Figure 3.47 ¹H NMR spectrum of **3-10Rh(Me)(I)(OAc)** (500 MHz, C₆D₆). Trace quantities of dichloromethane and diethyl ether are observed.

3-10PdCl. A Schlenk flask was charged with **3-10H** (0.12 g, 0.22 mmol), Pd(COD)Cl₂ (62 g, 0.22 μmol), 2,6-lutidine (25 μL, 0.22 mmol), and diethyl ether. The

reaction mixture was stirred for 12 h and then the solution was filtered through a pad of silica gel with additional diethyl ether. The ethereal solution was then concentrated and stored at $-35\text{ }^{\circ}\text{C}$. The resulting precipitate was collected and the volatiles were removed *in vacuo* to yield **3-10PdCl** as a purple solid (88 mg, 0.13 μmol , 60%). ^1H NMR (C_6D_6 , Figure 3.48): δ 7.56 – 7.49 (m, 2H, Ar H), 7.22 (d, $J_{\text{PH}} = 12\text{ Hz}$, 2H, Ar H), 6.78 – 6.68 (m, 2H, Ar H), 6.66 (d, $J_{\text{HH}} = 9\text{ Hz}$, 1H, Ar H), 4.67 (m, 2H, CH_2CF_3), 4.59 – 4.45 (m, 2H, CH_2CF_3), 2.26 – 2.12 (m, 2H, $\text{CH}(\text{CH}_3)_2$), 2.08 (s, 3H, CH_3), 1.88 (s, 3H, CH_3), 1.30 (dd, $J_{\text{PH}} = 18\text{ Hz}$, $J_{\text{HH}} = 7\text{ Hz}$, 6H, $\text{CH}(\text{CH}_3)_2$), 1.02 (dd, $J_{\text{PH}} = 16\text{ Hz}$, $J_{\text{HH}} = 7\text{ Hz}$, 6H, $\text{CH}(\text{CH}_3)_2$). $^1\text{H}\{^{31}\text{P}\}$ NMR (C_6D_6): δ 7.56 – 7.49 (m, 2H, Ar H), 7.22 (s, 2H), 6.78 – 6.68 (m, 2H), 6.66 (d, $J = 9\text{ Hz}$, 1H, Ar H), 4.67 (m, 2H, CH_2CF_3), 4.59 – 4.45 (m, 2H, CH_2CF_3), 2.26 – 2.12 (m, 2H, $\text{CH}(\text{CH}_3)_2$), 2.08 (s, 3H, CH_3), 1.88 (s, 3H, CH_3), 1.30 (dd, $J = 18\text{ Hz}$, $J = 7\text{ Hz}$, 6H, $\text{CH}(\text{CH}_3)_2$), 1.02 (dd, $J = 16\text{ Hz}$, $J = 7\text{ Hz}$, 6H, $\text{CH}(\text{CH}_3)_2$). $^1\text{H}\{^{31}\text{P}\}$ NMR (C_6D_6): δ 7.56 – 7.49 (m, 2H, Ar H), 7.22 (s, 2H), 6.78 – 6.68 (m, 2H), 6.66 (d, $J = 9\text{ Hz}$, 1H, Ar H), 4.67 (m, 2H, CH_2CF_3), 4.59 – 4.45 (m, 2H, CH_2CF_3), 2.26 – 2.12 (m, 2H, $\text{CH}(\text{CH}_3)_2$), 2.08 (s, 3H, CH_3), 1.88 (s, 3H, CH_3), 1.30 (d, $J_{\text{HH}} = 7\text{ Hz}$, 6H, $\text{CH}(\text{CH}_3)_2$), 1.02 (d, $J_{\text{HH}} = 7\text{ Hz}$, 6H, $\text{CH}(\text{CH}_3)_2$). $^{13}\text{C}\{^1\text{H}\}$ NMR (C_6D_6): δ 161.3 (d, $J_{\text{CP}} = 20\text{ Hz}$, Ar CN), 159.6 (d, $J_{\text{CP}} = 38\text{ Hz}$, Ar CN), 137.9 (s, Ar CH), 136.1 (s, Ar CH), 133.1 (s, Ar CH), 132.5 (s, Ar CH), 130.2 (s, Ar CH), 127.7 (s, Ar CH), 125.8 (d, $J_{\text{CP}} = 60\text{ Hz}$, CF_3), 124.7 (d, $J_{\text{CP}} = 9\text{ Hz}$, Ar C), 122.4 (d, $J_{\text{CP}} = 10\text{ Hz}$, Ar C), 118.1 (d, $J_{\text{CP}} = 42\text{ Hz}$, Ar C), 117.0 (d, $J_{\text{CP}} = 12\text{ Hz}$, Ar CH), 116.4 (d, 12 Hz, Ar CH), 62.5 (m, CH_2CF_3), 25.1 (d, $J_{\text{CP}} = 22\text{ Hz}$, $\text{CH}(\text{CH}_3)_2$), 20.3 (s, CH_3), 19.8 (s, CH_3), 18.5 (s, CH_3), 17.9 (s, CH_3). ^{19}F NMR (C_6D_6): δ 75.6 (d, $J_{\text{FH}} = 8\text{ Hz}$, CH_2CF_3). $^{31}\text{P}\{^1\text{H}\}$ NMR

(C₆D₆): δ 159.2 (dd, $J_{PP} = 545$ Hz, P(OCH₂CF₃)), 53.5 (dd, $J_{PP} = 545$ Hz, P(CH(CH₃)₃).

Elemental Analysis Calculated for **3-10PdCl**: C, 42.25; H, 4.43; N, 2.05. Found: C, 42.32; H, 4.53; N, 1.98.

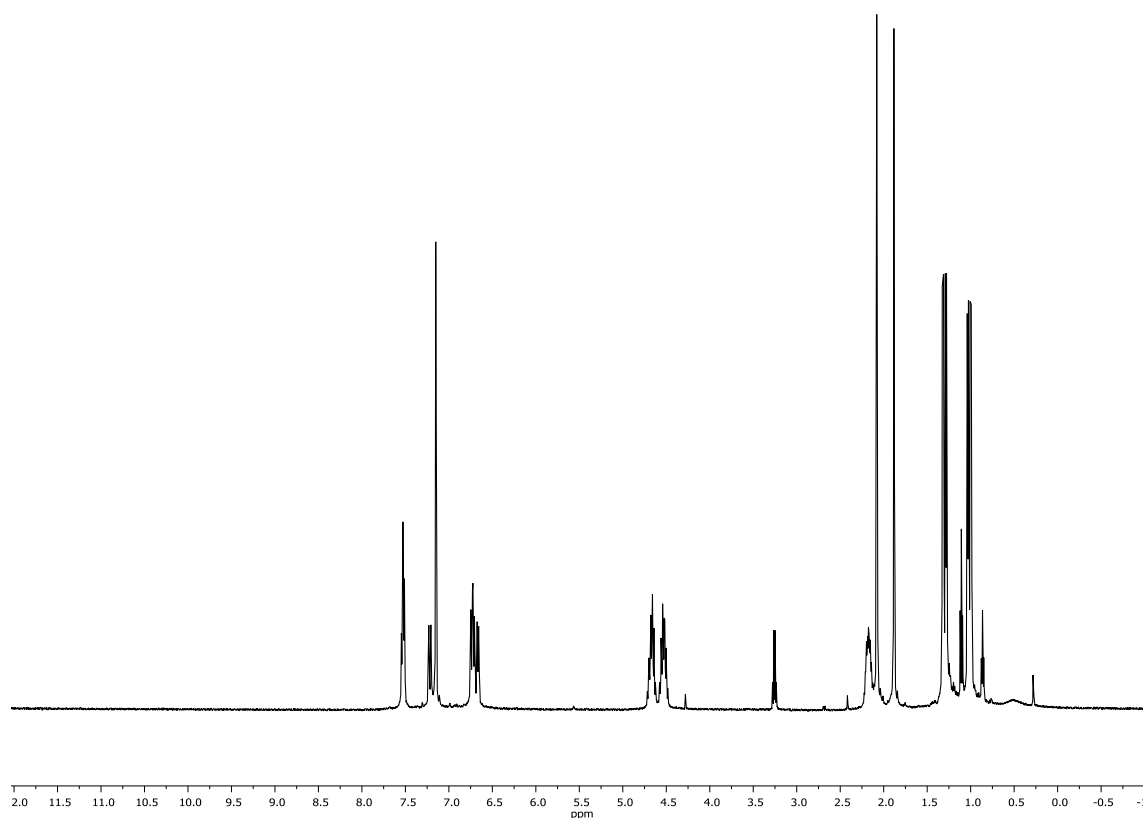


Figure 3.48 ¹H NMR spectrum of **3-10PdCl** (500 MHz, C₆D₆). Residual diethyl ether, silicone grease, HOCH₂CF₃, and pentane are observed.

Reaction of **3-10H** with RhCl₃(H₂O)₃. A J. Young tube was charged with **3-10H** (0.10 mL, 0.17 M in CF₃CH₂OH, 17 μ mol), CF₃CH₂OH (0.25 mL), and RhCl₃(H₂O)₃

(5.0 mg, 17 μmol). The reaction was heated for 18 h at 70 $^{\circ}\text{C}$. No consumption of the ligand was observed by ^{31}P NMR spectroscopy.

Reaction of **3-10H** with $\text{ClRh}(\text{PPh}_3)_3$. A J. Young tube was charged with **3-10H** (63 μL , 0.17 M in $\text{CF}_3\text{CH}_2\text{OH}$, 11 μmol), C_6D_6 (0.25 mL), and $\text{ClRh}(\text{PPh}_3)_3$ (10 mg, 11 μmol). The reaction was heated for 18 h at 80 $^{\circ}\text{C}$. A large mixture of products was observed by ^{31}P NMR spectroscopy.

Reaction of **3-10H** with $[\text{Rh}(\text{OAc})_2]_2$. A J. Young tube was charged with **3-10H** (16 mg, 30 μmol), C_6D_6 (0.25 mL), and $[\text{Rh}(\text{OAc})_2]_2$ (7.0 mg, 15 μmol). The reaction was heated for 18 h at 100 $^{\circ}\text{C}$. A large mixture of products was observed by ^{31}P NMR spectroscopy.

Reaction of **3-10H** with $[\text{Rh}(\text{COD})\text{Cl}]_2$. A Schlenk flask was charged with **3-10H** (2.0 mL, 4.56 M in toluene, 0.91 mmol), $[\text{Rh}(\text{COD})\text{Cl}]_2$ (0.26 g, 0.46 mmol), and diethyl ether (5 mL). The reaction was stirred for 1 h and then filtered through a pad of silica gel using additional diethyl ether to wash the solid off the frit. The solution was then concentrated and stored at -35 $^{\circ}\text{C}$ for 25 h resulting in orange crystals which show *cis*-phosphine coupling $^{31}\text{P}\{^1\text{H}\}$ NMR (C_6D_6): δ 172.7 (dd, $J_{\text{RhP}} = 147$ Hz, $J_{\text{PP}} = 29$ Hz), 172.7 (dd, $J_{\text{RhP}} = 85$ Hz, $J_{\text{PP}} = 29$ Hz). ^{19}F NMR (C_6D_6): δ -73.9, -75.0.

Reaction of **3-10H** with $[\text{Rh}(\text{COD})\text{Cl}]_2$ and *n*-butyllithium. A J. Young tube was charged with **3-10H** (0.55 mL, 0.17 M in $\text{CF}_3\text{CH}_2\text{OH}$, 95 μmol) and $[\text{Rh}(\text{COD})\text{Cl}]_2$ (23 mg, 47 μmol). After 10 min *n*-butyllithium (38 μL , 95 μmol) was added to the mixture.

The reaction was monitored for 18 h over the course of which a large mixture of products was observed.

Reaction of **3-10Rh(CO)(Me)(I)** with PhLi and an aryl chloride. A J. Young tube was charged with **3-10Rh(CO)(Me)(I)** (19 mg, 24 μmol), C_6D_6 (0.50 mL), PhLi (16 μL , 29 μmol), and 4-chlorobenzotrifluoride (7.0 μL , 48 μmol). After 18 h the major product formed was **3-10RhCO** as observed by ^{31}P NMR spectroscopy.

3.11.14 Synthesis of **3-11H** and its complexes

3-11H. A Teflon stoppered Schlenk flask was charged with **3-9H** (82.0 mg, 0.190 mmol) and $(\text{CF}_3)_2\text{CHOH}$ (1 mL). The flask was placed in a 100 °C oil bath for 18 h at which point ^{31}P NMR spectroscopy demonstrated conversion to **3-11H**. The following NMR data was obtained by first referencing a spectrum of pure C_6D_6 . Selected ^1H NMR ($(\text{CF}_3)_2\text{CHOH}$, Figure 3.49): δ 7.79 (d, $J = 8$ Hz, 1H), 7.60 (s, 1H), 7.58 – 7.46 (m, 2H), 7.33 (d, $J = 8$ Hz, 1H), 6.81 (s, 1H), 6.48 (d, $J = 8$ Hz, 1H), 2.64 (s, 3H, CH_3), 2.46 (s, 3H, CH_3), 1.56 (dd, $J_{\text{PH}} = 20$ Hz, $J_{\text{HH}} = 7$ Hz, 6H, $\text{CH}(\text{CH}_3)_2$), 1.43 (dd, $J_{\text{PH}} = 14$ Hz, $J_{\text{HH}} = 7$ Hz, 6H, $\text{CH}(\text{CH}_3)_2$). $^1\text{H}\{^{31}\text{P}\}$ NMR ($(\text{CF}_3)_2\text{CHOH}$): δ 7.79 (d, $J = 8$ Hz, 1H), 7.60 (s, 1H), 7.58 – 7.46 (m, 2H), 7.33 (d, $J = 8$ Hz, 1H), 6.81 (s, 1H), 6.48 (d, $J = 8$ Hz, 1H), 2.64 (s, 3H), 2.46 (s, 3H), 1.56 (d, $J_{\text{HH}} = 7$ Hz, 6H), 1.43 (d, $J_{\text{HH}} = 7$ Hz, 6H). $^{31}\text{P}\{^1\text{H}\}$ NMR ($(\text{CF}_3)_2\text{CHOH}$): δ 215.2 (s, $\text{P}(\text{OCH}(\text{CH}_3)_2)$), 35.9 (s, P^iPr_2).

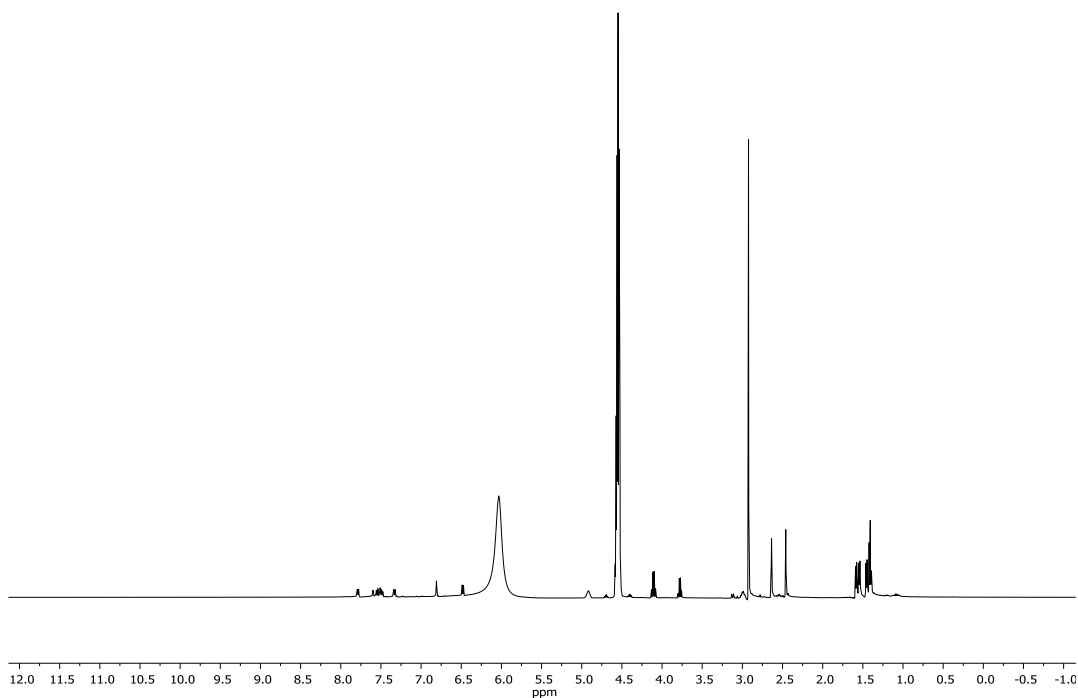


Figure 3.49 ^1H NMR spectrum of **3-11H** (500 MHz, $(\text{CF}_3)_2\text{CHOH}$, was “referenced” by first running a pure sample of C_6D_6). Four equivalents of dimethylamine are observed along with diethyl ether. The ligand was never isolated cleanly.

3-11PdOAc·HOCH(CF₃)₂. A Teflon stoppered round bottom flask was charged with **3-11H** (200 mg, 464 μmol), a stir bar, and $(\text{CF}_3)_2\text{CHOH}$ (5 mL). The reaction mixture was then stirred for 24h in a 100 °C oil bath. $\text{Pd}(\text{OAc})_2$ (113 mg, 464 μmol) was then added to the reaction vessel. Stirring was commenced for 3 d at room temperature. The volatiles were then removed *in vacuo* and the resulting purple solid was filtered through a pad of silica gel with diethyl ether. The volatiles were again removed and the resulting solid was taken up in a minimal amount of pentane and recrystallized at -35 °C to yield **3-11PdOAc·HOCH(CF₃)₂** as dark purple crystals (249 mg, 323 μmol , 64%). ^1H

NMR (C_6D_6 , Figure 3.50): δ 7.40 – 7.34 (m, 2H, Ar *H*), 7.32 (d, $J_{PH} = 12$ Hz, 1H, Ar *H*), 6.65 (d, $J_{HH} = 9$ Hz, 1H, Ar *H*), 6.63 (d, $J_{PH} = 11$ Hz, 1H, Ar *H*), 6.59 (d, $J_{HH} = 9$ Hz, 1H, Ar *H*), 6.42 (m, 2H, P(OCH(CF₃)₂)), 4.73 (s, 1H, OH), 3.77 (m, 1H, HOCH(CF₃)₂), 2.06 (s, 3H, CH₃), 2.02 (s, 3H, CH₃), 2.00 – 1.89 (m, 2H, CH(CH₃)₂), 1.84 (s, 3H, OAc), 1.10 (dd, $J_{PH} = 18$ Hz, $J_{HH} = 7$ Hz, 6H), 0.88 (dd, $J_{PH} = 17$ Hz, $J_{HH} = 7$ Hz, 6H). $^1H\{^{31}P$ δ 176.2} NMR (C_6D_6): δ 7.40 – 7.34 (m, 2H, Ar *H*), 7.32 (d, $J = 12$ Hz, 1H, Ar *H*), 6.65 (d, $J_{HH} = 9$ Hz, 1H, Ar *H*), 6.63 (s, 1H, Ar *H*), 6.59 (d, $J_{HH} = 9$ Hz, 1H, Ar *H*), 6.42 (m, 2H, CH(CF₃)₂), 4.73 (s, 1H, OH), 3.77 (m, 1H, HOCH(CF₃)₂), 2.06 (s, 3H, CH₃), 2.02 (s, 3H, CH₃), 2.00 – 1.89 (m, 2H, CH(CH₃)₂), 1.84 (s, 3H, OAc), 1.10 (dd, $J_{HH} = 7$ Hz, 6H), 0.88 (dd, $J_{HH} = 7$ Hz, 6H). $^1H\{^{31}P$ 58.6} NMR (C_6D_6): δ 7.40 – 7.34 (m, 2H, Ar *H*), 7.32 (s, 1H, Ar *H*), 6.65 (d, $J_{HH} = 9$ Hz, 1H, Ar *H*), 6.63 (d, $J_{PH} = 11$ Hz, 1H, Ar *H*), 6.59 (d, $J_{HH} = 9$ Hz, 1H, Ar *H*), 6.42 (m, 2H, CH(CF₃)₂), 4.73 (s, 1H, OH), 3.77 (m, 1H, HOCH(CF₃)₂), 2.06 (s, 3H, CH₃), 2.02 (s, 3H, CH₃), 2.00 – 1.89 (m, 2H, CH(CH₃)₂), 1.84 (s, 3H, OAc), 1.10 (d, $J_{HH} = 7$ Hz, 6H), 0.88 (d, $J_{HH} = 7$ Hz, 6H). $^{13}C\{^1H\}$ NMR (C_6D_6): δ 178.7 (s, OAc), 161.6 (s, Ar CN), 158.9 (d, $J_{CP} = 40$ Hz, Ar CN), 137.1 (s, Ar C), 133.8 (s, Ar C), 134.1 (s, Ar C), 132.8 (d, $J_{CP} = 38$ Hz, Ar C), 131.4 (s, Ar C), 130.4 (s, Ar C), 126.8 (s), 126.3 (s), 122.8 (s), 120.3 (d, $J_{CP} = 30$ Hz, Ar C), 118.1 (s), 117.3 (d, $J_{CP} = 17$ Hz, Ar C), 116.9 (s), 116.6 (s), 116.2 (s), 116.1 (s), 73.82 (s, OCH(CF₃)₂), 69.53 (s, OCH(CF₃)₂), 24.82 (d, $J = 22$ Hz, CH(CH₃)₂), 21.88 (s, CH₃), 20.27 (s, CH₃), 19.81 (s, CH₃), 17.87 (s, CH₃), 17.36 (s, CH₃). $^{31}P\{^1H\}$ NMR (C_6D_6): δ 176.2 (d, $J_{PP} = 517$ Hz, P(OCH(CF₃)₂), 58.6 (d, $J_{PP} = 517$ Hz, P(CH(CH₃)₂)). ^{19}F NMR (C_6D_6): δ -74.2 (s, CF₃), -74.5 (s, CF₃), -76.5 (m, HOCH(CF₃)₂).

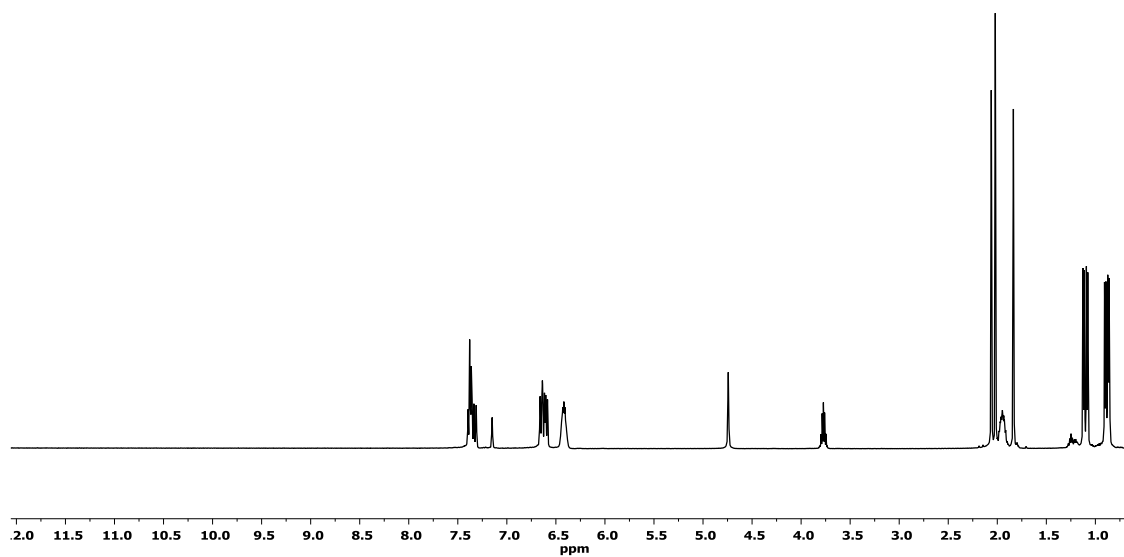


Figure 3.50 ^1H NMR spectrum of **3-11PdOAc·(CF₃)₂CHOH** (500 MHz, C₆D₆). Trace quantities of pentane and silicone grease are observed.

3-11PdCl. A J. Young tube was charged with **3-11PdOAc·HOCH(CF₃)₂** (0.15 mg, 0.18 mmol), C₆D₆ (1 mL), and Me₃SiCl (46 μL , 0.26 mmol). After 72 hours ^{31}P NMR analysis reveal complete conversion to the desired product. The solution was then filtered through a pad of silica gel with diethyl ether. The volatiles were removed *in vacuo* and the product was dissolved in pentane and stored at $-35\text{ }^\circ\text{C}$. After 18 h purple needles were collected by decantation and dried to yield **3-11PdCl** (0.12 g, 87 μmol ,

85%). ^1H NMR (C_6D_6 , Figure 3.51): δ 7.50 – 7.35 (m, 2H, Ar CH), 7.24 (d, $J_{\text{PH}} = 12$ Hz, 1H, Ar H), 6.68 (d, $J_{\text{HH}} = 9$ Hz, 2H, Ar H), 6.60 (d, $J_{\text{PH}} = 9$ Hz, 1H, Ar H), 6.58 – 6.46 (m, 2H, $\text{CH}(\text{CF}_3)_2$), 2.19 – 2.08 (m, 2H, $\text{CH}(\text{CH}_3)_2$), 2.07 (s, 3H, CH_3), 1.80 (s, 3H, CH_3), 1.23 (dd, $J_{\text{PH}} = 18$ Hz, $J_{\text{HH}} = 7$ Hz, 6H, $\text{CH}(\text{CH}_3)_2$), 0.96 (dd, $J_{\text{PH}} = 16$ Hz, $J_{\text{HH}} = 7$ Hz, 6H, $\text{CH}(\text{CH}_3)_2$). $^1\text{H}\{^{31}\text{P}$ δ 57.9} NMR (C_6D_6): δ 7.50 – 7.35 (m, 2H, Ar H), 7.24 (d, $J = 12$ Hz, 1H, Ar H), 6.68 (d, $J = 9$ Hz, 2H, Ar H), 6.60 (s, 1H, Ar H), 6.58 – 6.46 (m, 2H, $\text{CH}(\text{CF}_3)_2$), 2.19 – 2.08 (m, 2H, $\text{CH}(\text{CH}_3)_2$), 2.05 (s, 3H, CH_3), 1.79 (s, 3H, CH_3), 1.22 (d, $J_{\text{HH}} = 7$ Hz, 6H, $\text{CH}(\text{CH}_3)_2$), 0.95 (dd, $J_{\text{HH}} = 7$ Hz, 6H, $\text{CH}(\text{CH}_3)_2$). $^1\text{H}\{^{31}\text{P}$ δ 172.3} NMR (C_6D_6): δ 7.44 (d, $J_{\text{HH}} = 9$ Hz, 1H, Ar H), 7.42 (m, 1H, Ar H), 7.24 (s, 1H, Ar H), 6.68 (d, $J = 9$ Hz, $J_{\text{PH}} = 4$ Hz, 2H, Ar H), 6.60 (d, $J_{\text{PH}} = 9$ Hz, 1H, Ar H), 6.58 – 6.46 (m, 2H, $\text{CH}(\text{CF}_3)_2$), 2.19 – 2.08 (m, 2H, $\text{CH}(\text{CH}_3)_2$), 2.07 (s, 3H, CH_3), 1.80 (s, 3H, CH_3), 1.23 (dd, $J_{\text{PH}} = 18$ Hz, $J_{\text{HH}} = 7$ Hz, 6H, $\text{CH}(\text{CH}_3)_2$), 0.96 (dd, $J_{\text{PH}} = 16$ Hz, $J_{\text{HH}} = 7$ Hz, 6H, $\text{CH}(\text{CH}_3)_2$). $^{31}\text{P}\{^1\text{H}\}$ NMR (C_6D_6): δ 172.3 (d, $J_{\text{PP}} = 525$ Hz, $\text{P}(\text{OCH}(\text{CF}_3)_2)_2$), 57.9 (d, $J_{\text{PP}} = 525$ Hz, P^iPr_2). $^{13}\text{C}\{^1\text{H}\}$ NMR (C_6D_6): δ 161.2 (d, $J_{\text{CP}} = 20$ Hz, Ar CN), 160.0 (d, $J_{\text{CP}} = 40$ Hz, Ar CN), 137.0 (s, Ar C), 133.4 (s, Ar C), 132.3 (s, Ar C), 129.8 (s, Ar C), 124.2 (m, $\text{CH}(\text{CF}_3)_2$), 123.7 (m, $\text{CH}(\text{CF}_3)_2$), 117.9 (d, $J_{\text{CP}} = 3$ Hz, Ar C), 117.6 (d, $J_{\text{CP}} = 3$ Hz, Ar C), 117.2 (d, $J_{\text{CP}} = 3$ Hz, Ar C), 116.9 (s, Ar C), 116.8 (s, Ar C), 116.7 (s, Ar C), 74.0 (m, $\text{CH}(\text{CF}_3)_2$), 25.4 (d, $J_{\text{CP}} = 4$ Hz, $\text{CH}(\text{CH}_3)_2$), 25.2 (d, $J_{\text{CP}} = 4$ Hz, $\text{CH}(\text{CH}_3)_2$), 20.3 (s, CH_3), 19.7 (s, CH_3), 18.2 (d, $J_{\text{CP}} = 4$ Hz, $\text{CH}(\text{CH}_3)_2$), 17.7 (d, $J_{\text{CP}} = 4$ Hz, $\text{CH}(\text{CH}_3)_2$). ^{19}F NMR (C_6D_6): δ -74.0 (s), -74.5 (s). Elemental Analysis Calculated: C 38.16, H 3.45; Found C 38.16, H 3.38.

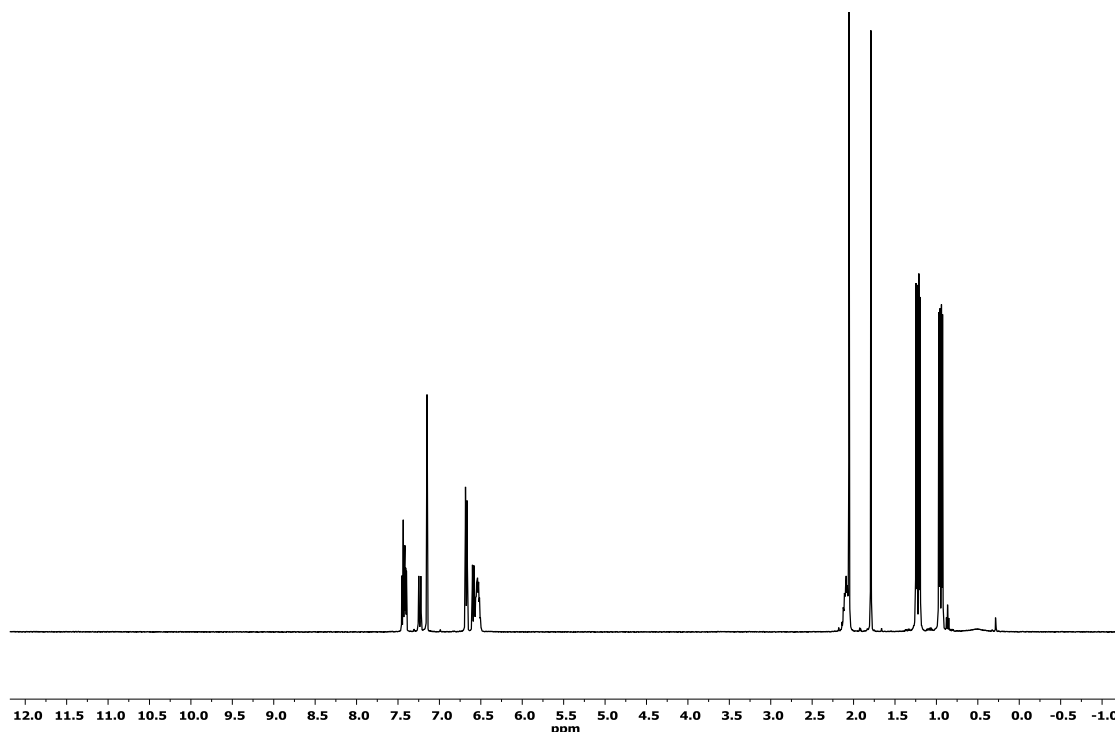


Figure 3.51 ^1H NMR spectrum of **3-11PdCl** as observed (500 MHz, C_6D_6). Trace quantities of pentane and silicone grease are observed.

3-11PdOTf. A J. Young tube was charged with **3-11PdOAc**· $\text{HOCH}(\text{CF}_3)_2$ (53 mg, 62 μmol), C_6D_6 (1 mL), and Me_3SiOTf (22 μL , 0.13 mmol). After 72 h ^{31}P NMR analysis reveal complete conversion to the desired product. The solution was then filtered through a pad of silica gel with diethyl ether. The volatiles were removed *in vacuo* and the product was dissolved in pentane and stored at -35°C . The resulting green crystals were collected and dried to yield **3-11PdOTf** (21 mg, 23 μmol , 51%). ^1H NMR (C_6D_6 , Figure 3.52): δ 7.35 (d, $J = 12$ Hz, 1H, Ar H), 7.27 (t, $J = 8$ Hz, 1H, Ar H), 7.18 (dd, $J = 9$ Hz, $J_{\text{PH}} = 4$ Hz, 1H, Ar H), 6.58 (d, $J_{\text{PH}} = 10$ Hz, 2H, Ar H), 6.52 (d, $J = 9$ Hz,

1H, Ar *H*), 6.33 (m, 2H, CH(CF₃)₂), 2.01 (s, 3H, CH₃), 1.99 – 1.92 (m, 2H, CH(CH₃)₂),
 1.77 (s, 3H, CH₃), 1.12 (dd, *J*_{PH} = 19 Hz, *J*_{HH} = 7 Hz, 6H, CH(CH₃)₃)₂), 0.90 (dd, *J*_{PH} = 17
 Hz, *J*_{HH} = 7 Hz, 6H, CH(CH₃)₃)₂). ¹H {³¹P δ 71.6} NMR (C₆D₆): δ 7.35 (d, *J* = 12 Hz,
 1H, Ar *H*), 7.27 (t, *J* = 8 Hz, 1H, Ar *H*), 7.18 (d, *J* = 9 Hz, 1H, Ar *H*), 6.58 (s, 2H,
 Ar *H*), 6.52 (d, *J* = 9 Hz, 1H, Ar *H*), 6.33 (m, 2H, CH(CF₃)₂), 2.01 (s, 3H, CH₃), 1.99 –
 1.92 (m, 2H, CH(CH₃)₂), 1.77 (s, 3H, CH₃), 1.12 (d, *J* = 7 Hz, 6H, CH(CH₃)₃)₂), 0.90 (d,
J = 7 Hz, 6H, CH(CH₃)₃)₂). ¹H {³¹P δ 171.8} NMR (C₆D₆): δ 7.35 (s, 1H, Ar *H*), 7.27 (d,
J = 9 Hz, 1H, Ar *H*), 7.18 (dd, *J* = 9 Hz, *J* = 4 Hz, 1H, Ar *H*), 6.58 (d, *J* = 10 Hz, 2H, Ar
H), 6.52 (d, *J* = 9 Hz, 1H, Ar *H*), 6.33 (m, 2H, CH(CF₃)₂), 2.01 (s, 3H, CH₃), 1.99 – 1.92
 (m, 2H, CH(CH₃)₂), 1.77 (s, 3H, CH₃), 1.12 (dd, *J* = 19 Hz, *J* = 7 Hz, 6H, CH(CH₃)₃)₂),
 0.90 (dd, *J* = 17 Hz, *J* = 7 Hz, 6H, CH(CH₃)₃)₂). ¹³C {¹H} NMR (C₆D₆): δ 161.6 (d, *J*_{CP} =
 19 Hz, Ar CN), 158.2 (d, *J*_{CP} = 40 Hz, Ar CN), 136.8 (s), 133.8 (s), 131.5 (s), 129.6 (s),
 129.6-129.4 (m), 125.8 (s), 125.3 (s), 122.2 (s), 120.6 (s), 120.0 (s), 118.5 (d, *J*_{CP} = 18
 Hz), 116.5 (d, *J*_{CP} = 14 Hz), 115.6 (s), 115.4 (s), 73.6 (q, CH(CF₃)₂), 25.4 (d, *J*_{CP} = 4 Hz,
 CH(CH₃)₂), 25.2 (d, *J*_{CP} = 4 Hz, CH(CH₃)₂), 20.2 (s, CH₃), 19.7 (s, CH₃), 17.6 (s, CH₃),
 17.3 (s, CH₃). ³¹P {¹H} NMR (C₆D₆): δ 171.8 (d, *J*_{PP} = 480 Hz, P(OCH(CF₃)₂), 71.6 (d,
*J*_{PP} = 480 Hz, PⁱPr₂). ¹⁹F NMR (C₆D₆): δ -74.1 (m, CH(CF₃)₂), -74.5 (m, CH(CF₃)₂), -
 77.6 (s, OTf).

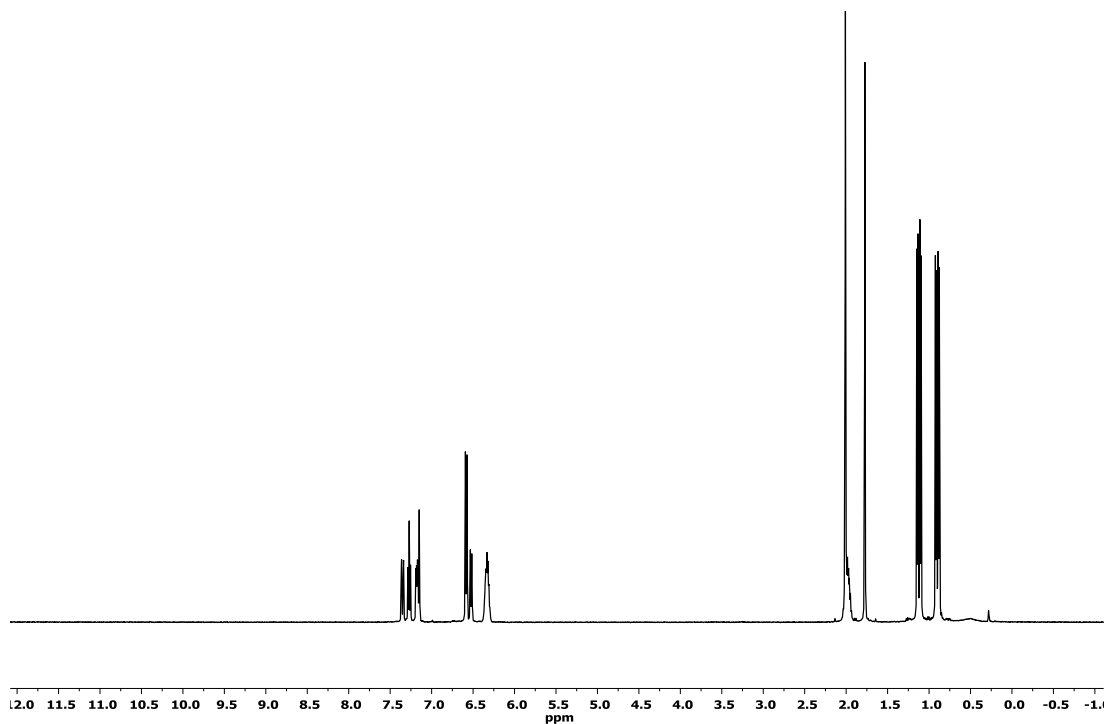


Figure 3.52 ^1H NMR spectrum (500 MHz, C_6D_6) of **3-11PdOTf**. Trace amounts of silicone grease are observed.

3-11RhCO. A Schlenk flask was charged with **3-11H** (304 mg, 0.705 mmol), a stir bar, and hexafluoroisopropanol (4 mL). The flask was heated at 100 °C for 18 h and then cooled to ambient temperature. $[\text{Rh}(\text{COD})\text{Cl}]_2$ (174 mg, 0.353 mmol), 2,6-lutidine (812 μL , 0.705 mmol), and CO (1 atm) were then added to the flask. The reaction mixture was stirred for 2 h and then dried under vacuo. The resulting red solid was taken up in diethyl ether and filtered through a pad of Celite. The volatiles were again removed. **3-11RhCO** was isolated as red crystals after recrystallization at -35 °C in pentane (452 mg, 0.559 mmol, 79%). ^1H NMR (C_6D_6 , Figure 3.53): δ 7.54 (dd, $J_{\text{HH}} = 9$

Hz, $J_{PH} = 4$ Hz, 1H, Ar H), 7.43 (t, $J_{HH} = 8$ Hz, 1H, Ar H), 7.35 (d, $J_{HH} = 2$ Hz, 1H, Ar H), 6.74 (d, $J_{HH} = 10$ Hz, 1H, Ar H), 6.74 (d, $J_{PH} = 10$ Hz, 1H, Ar H), 6.68 (dd, $J_{HH} = 9$ Hz, $J_{HH} = 2$ Hz, 1H, Ar H), 5.75 (m, $J_{PH} = 17$ Hz, $J_{HH} = 6$ Hz, 2H, $CH(CF_3)_2$), 2.11 (s, 3H, CH_3), 1.98 – 1.91 (m, 2H, $CH(CH_3)_2$), 1.88 (s, 3H, CH_3), 1.05 (dd, $J_{PH} = 18$ Hz, $J_{HH} = 7$ Hz, 6H, $CH(CH_3)_2$), 0.83 (dd, $J_{PH} = 16$ Hz, $J_{HH} = 7$ Hz, 6H, $CH(CH_3)_2$). $^1H\{^{31}P$ δ 207.4} NMR (C_6D_6): δ 7.54 (dd, $J_{HH} = 9$ Hz, $J_{PH} = 4$ Hz, 1H, Ar H), 7.43 (t, $J_{HH} = 8$ Hz, 1H, Ar H), 7.35 (d, $J_{HH} = 2$ Hz, 1H, Ar H), 6.74 (d, $J_{HH} = 10$ Hz, 1H, Ar H), 6.74 (d, $J_{PH} = 10$ Hz, 1H, Ar H), 6.68 (dd, $J_{HH} = 9$ Hz, $J_{HH} = 2$ Hz, 1H, Ar H), 5.75 (hept, $J_{HH} = 6$ Hz, 2H, $CH(CF_3)_2$), 2.11 (s, 3H, CH_3), 1.98 – 1.91 (m, 2H, $CH(CH_3)_2$), 1.88 (s, 3H, CH_3), 1.05 (dd, $J_{PH} = 18$ Hz, $J_{HH} = 7$ Hz, 6H, $CH(CH_3)_2$), 0.83 (dd, $J_{PH} = 16$ Hz, $J_{HH} = 7$ Hz, 6H, $CH(CH_3)_2$). $^1H\{^{31}P$ δ 59.3} NMR (C_6D_6): δ 7.54 (d, $J_{HH} = 9$ Hz, 1H, Ar H), 7.43 (t, $J_{HH} = 8$ Hz, 1H, Ar H), 7.35 (d, $J_{HH} = 2$ Hz, 1H, Ar H), 6.74 (d, $J_{HH} = 10$ Hz, 1H, Ar H), 6.74 (s, 1H, Ar H), 6.68 (dd, $J_{HH} = 9$ Hz, $J_{HH} = 2$ Hz, 1H, Ar H), 5.75 (dp, $J_{PH} = 17$ Hz, $J_{HH} = 6$ Hz, 2H, $CH(CF_3)_2$), 2.11 (s, 3H, CH_3), 1.98 – 1.91 (m, 2H, $CH(CH_3)_2$), 1.88 (s, 3H, CH_3), 1.05 (d, $J_{HH} = 7$ Hz, 6H, $CH(CH_3)_2$), 0.83 (d, $J_{HH} = 7$ Hz, 6H, $CH(CH_3)_2$). $^{13}C\{^1H\}$ NMR (C_6D_6): δ 193.8 (m, CO), 161.2 (d, $J = 21$ Hz, Ar C), 160.3 (d, $J = 40$ Hz, Ar C), 136.2 (d, $J = 2$ Hz, Ar C), 132.8 (d, $J = 2$ Hz, Ar C), 132.0 (s, Ar C), 129.2 (s, Ar C), 127.1 (d, $J = 8$ Hz, Ar C), 126.8 (d, $J = 7$ Hz, Ar C), 124.4 (m, CF_3), 122.2 (m, CF_3), 119.9 (m, CF_3), 118.8 (d, $J = 2$ Hz, Ar C), 118.4 (s, Ar C), 117.6 (m, CF_3), 116.0 (d, $J = 12$ Hz, Ar C), 115.4 (d, $J = 18$ Hz, Ar C), 74.6 – 72.8 (m, $CH(CF_3)_2$), 25.1 (d, $J = 25$ Hz, $CH(CH_3)_2$), 20.1 (s, CH_3), 19.6 (s, CH_3), 18.9 (d, $J = 6$ Hz, CH_3), 17.90 (s, CH_3). $^{31}P\{^1H\}$ NMR (C_6D_6): δ 207.4 (dd, $J_{PP} = 340$ Hz, $J_{PRh} = 195$ Hz, $P(OCH(CF_3)_2)$), 59.3 (dd, $J_{PP} =$

340 Hz, $J_{\text{PRh}} = 127$ Hz, P^iPr_2). ^{19}F NMR (C_6D_6): δ -75.0 (s), -74.4 (s). IR $\nu(\text{CO}) = 1980$ cm^{-1} .

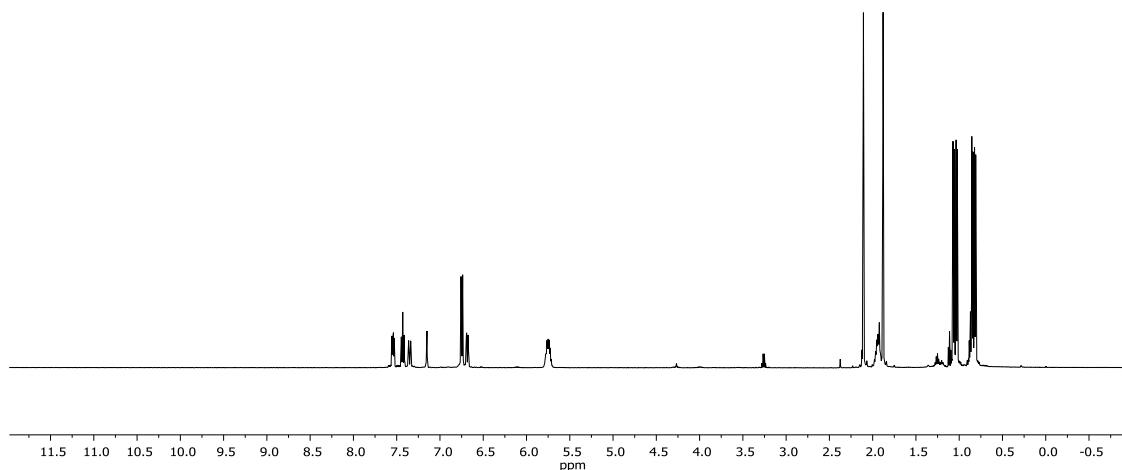


Figure 3.53 ^1H NMR spectrum of **3-11RhCO** (500 MHz, C_6D_6). Minor impurities of diethyl ether, 2,6-lutidine and pentane are observed.

3.11.15 X-Ray data collection, solution, and refinement

X-Ray data collection, solution, and refinement for 3-4PdCl. X-ray quality crystals of **3-4PdCl** were obtained from a concentrated toluene solution of **3-4PdCl** which was stored at -35 $^\circ\text{C}$. The following work was done by Billy McCulloch. An orange, multi-faceted block of suitable size ($0.33 \times 0.21 \times 0.06$ mm) was selected from a

representative sample of crystals of the same habit using an optical microscope and mounted onto a nylon loop. Low temperature (150 K) X-ray data were obtained on a Bruker APEXII CCD based diffractometer (Mo sealed X-ray tube, $K_{\alpha} = 0.71073 \text{ \AA}$). All diffractometer manipulations, including data collection, integration and scaling were carried out using the Bruker APEXII software.¹⁰⁷ An absorption correction was applied using SADABS.¹⁰⁷ The space group was determined on the basis of systematic absences and intensity statistics and the structure was solved by direct methods and refined by full-matrix least squares on F^2 . The structure was solved in the monoclinic $P2_1/n$ space group using XS¹⁰⁸ (incorporated in SHELXTL). All non-hydrogen atoms were refined with anisotropic thermal parameters. The structure was brought to convergence by weighted full-matrix least-squares refinement on $|F|^2$, and the final structure converged to $R_1 = 0.0633$ and $wR_2 = 0.0844$. Structure manipulations were performed with the aid of shelXle.¹³⁹ A check for missed symmetry was run using the ADDSYM program within PLATON,¹⁴⁰ revealing no apparent higher symmetry

X-Ray data collection, solution, and refinement for [3-4PdCl][CHB₁₁Cl₁₁]. X-ray quality crystals of [3-4PdCl][CHB₁₁Cl₁₁] were obtained from a concentrated dichloromethane solution of [3-4PdCl][CHB₁₁Cl₁₁] stored at -35 °C. The following work was done by Chun-I Lee. A Leica MZ 75 microscope was used to identify a suitable orange multifaceted crystal with dimensions (max, intermediate, and min; in mm) $0.30 \times 0.20 \times 0.10$ from a representative sample of crystals of the same habit. The crystal mounted on a nylon loop was then placed in a cold nitrogen stream (Oxford) maintained at 110 K. A BRUKER GADDS X-ray (three-circle) diffractometer was

employed for crystal screening, unit cell determination, and data collection. The goniometer was controlled using the FRAMBO software.¹⁴¹

The sample was optically centered with the aid of a video camera such that no translations were observed as the crystal was rotated through all positions. The detector was set at 5.0 cm from the crystal sample. The X-ray radiation employed was generated from a Cu sealed X-ray tube ($K_{\alpha} = 1.5418 \text{ \AA}$ with a potential of 40 kV and a current of 40 mA) fitted with a graphite monochromator in the parallel mode (175 mm collimator with 0.5 mm pinholes). A total of 180 data frames were taken at widths of 0.5° with an exposure time of 15 s. These reflections were used to determine the unit cell using Cell_Now.¹⁴² A suitable cell was found and refined by nonlinear least-squares and Bravais lattice procedures.

Integrated intensity information for each reflection was obtained by reduction of the data frames with SAINTplus.¹⁴³ The integration method employed a three-dimensional profiling algorithm and all data were corrected for Lorentz and polarization factors, as well as for crystal decay effects. Finally the data was merged and scaled to produce a suitable data set. SADABS¹⁰⁷ was employed to correct the data for absorption effects. The structure was solved in the monoclinic P21/c space group using XS¹⁰⁸ (incorporated in SHELXTL). All non-hydrogen atoms were refined with anisotropic thermal parameters. The hydrogen atoms were placed in idealized positions and refined using riding model.

X-Ray data collection, solution, and refinement for [3-5NiCl][CHB₁₁Cl₁₁]. The following work was done by Dr. Bruce Foxman and Dr. Josh Chen. X-ray quality

crystals of [3-5NiCl][CHB₁₁Cl₁₁] were obtained from slow diffusion of pentane into a concentrated dichloromethane solution of [3-5NiCl][CHB₁₁Cl₁₁] stored at -35 °C. All operations were performed on a Bruker-Nonius Kappa Apex2 diffractometer, using graphite-monochromated MoK α radiation. All diffractometer manipulations, including data collection, integration, scaling, and absorption corrections were carried out using the Bruker Apex2 software.¹⁰⁷ Preliminary cell constants were obtained from three sets of 12 frames. Data collection was carried out at 120K, using a frame time of 20 sec and a detector distance of 60 mm. The optimized strategy used for data collection consisted of five phi scan sets, with 0.5° steps in phi or omega; completeness was 96.9%. A total of 3328 frames were collected. Final cell constants were obtained from the xyz centroids of 9961 reflections after integration.

From the systematic absences, the observed metric constants and intensity statistics, space group $P2_1/c$ was chosen initially; subsequent solution and refinement confirmed the correctness of this choice. The structure was solved using *SIR-92*,¹⁴⁴ and refined (full-matrix-least squares) using the Oxford University *Crystals for Windows* program.¹⁴⁵ All non-hydrogen atoms were refined using anisotropic displacement parameters. After location of H atoms attached to C on electron-density difference maps, the H atoms were initially refined with soft restraints on the bond lengths and angles to regularize their geometry (C---H in the range 0.93--0.98 Å and U_{iso} (H) in the range 1.2-1.5 times U_{eq} of the parent atom), after which the positions were refined with riding constraints.¹⁴⁶ The final least-squares refinement converged to $R_1 = 0.0329$ ($I > 2\sigma(I)$),

6367 data) and $wR_2 = 0.0699$ (F^2 , 8484 data, 487 parameters). The final CIF is available as supporting material.

X-Ray data collection, solution, and refinement for 3-5NiCl. X-ray quality crystals of **3-5NiCl** were obtained from a concentrated pentane solution of **3-5NiCl** stored at $-35\text{ }^\circ\text{C}$. An orange, multi-faceted block of suitable size ($0.30 \times 0.20 \times 0.05\text{ mm}$) was selected from a representative sample of crystals of the same habit using an optical microscope and mounted onto a nylon loop. Low temperature (110 K) X-ray data were obtained on a Bruker APEXII CCD based diffractometer (Mo sealed X-ray tube, $K_\alpha = 0.71073\text{ \AA}$). All diffractometer manipulations, including data collection, integration and scaling were carried out using the Bruker APEXII software.¹⁰⁷ An absorption correction was applied using SADABS.¹⁰⁷ The space group was determined on the basis of systematic absences and intensity statistics and the structure was solved by direct methods and refined by full-matrix least squares on F^2 . The structure was solved in the monoclinic *Pbca* space group using XS¹⁰⁸ (incorporated in SHELXTL). All non-hydrogen atoms were refined with anisotropic thermal parameters. The structure was refined (weighted least squares refinement on F^2) and the final least-squares refinement converged to $R_1 = 0.0360$ ($I > 2\sigma(I)$, 7205 data) and $wR_2 = 0.0611$ (F^2 , 8590 data, 388 parameters, 0 restraints).

X-Ray data collection, solution, and refinement for 3-6RhCO. X-ray quality crystals of **3-6RhCO** were obtained from a concentrated fluorobenzene solution of **3-6RhCO** stored at $-35\text{ }^\circ\text{C}$. The following work was done by Dr. Bruce Foxman and Dr. Josh Chen. All operations were performed on a Bruker-Nonius Kappa Apex2

diffractometer, using graphite-monochromated MoK α radiation. All diffractometer manipulations, including data collection, integration, scaling, and absorption corrections were carried out using the Bruker Apex2 software.¹⁰⁷ Preliminary cell constants were obtained from three sets of 12 frames. Data collection was carried out at 120K, using a frame time of 10 sec and a detector distance of 60 mm. The optimized strategy used for data collection consisted of 9 phi and 1 omega scan sets, with 0.5° steps in phi or omega; completeness was 99.7%. A total of 5721 frames were collected. Final cell constants were obtained from the xyz centroids of 9617 reflections after integration.

From the systematic absences, the observed metric constants and intensity statistics, space group $P2_1/c$ was chosen initially; subsequent solution and refinement confirmed the correctness of this choice. The structures were solved using SIR-92,¹⁴⁴ and refined (full-matrix-least squares) using the Oxford University *Crystals for Windows* program.¹⁴⁵ All ordered non-hydrogen atoms were refined using anisotropic displacement parameters; hydrogen atoms were fixed at calculated geometric positions and allowed to ride on the corresponding carbon atoms.

The solvent structure for **3-6RhCO** contained significant disorder of the pentane solvate molecule, which was resolved successfully. Atoms C(34), C(35), C(36), C(37), and C(38) were disordered, with the occupancy of each fixed at 0.5. The solvate crystallizes unsymmetrically on a center of symmetry, with atom C(36) displaced ca. 0.5 Å from the center. Thus, the occupancies of all solvent atoms were fixed at 0.5, and the atoms were refined by using anisotropic displacement parameters. The distance between C(36) and C(37) was restrained to be 1.54(1) Å. After location of most H atoms on

electron-density difference maps, the H atoms attached to ordered atoms were initially refined with soft restraints on the bond lengths and angles to regularize their geometry (C---H in the range 0.93-0.98 Å and U_{iso} (H) in the range 1.2-1.5 times U_{eq} of the parent atom), after which the positions were refined with riding constraints.¹⁴⁶ The final least-squares refinement converged to $R_1 = 0.0268$ ($I > 2\sigma(I)$, 9233 data) and $wR_2 = 0.0658$ (F^2 , 9569 data, 388 parameters). The final CIF is available as supporting material. Two CheckCIF Alert B items arise from unresolved disorder in the phenyl group attached to P(2); accordingly, validation response items appear in the CIF.

X-Ray data collection, solution, and refinement for 3-7PdCl. X-ray quality crystals of **3-7PdCl** were obtained from a concentrated fluorobenzene solution of **3-7PdCl** stored at -35 °C. A red, multi-faceted block of suitable size (0.30 × 0.09 × 0.20 mm) was selected from a representative sample of crystals of the same habit using an optical microscope and mounted onto a nylon loop. Low temperature (110 K) X-ray data were obtained on a Bruker APEXII CCD based diffractometer (Mo sealed X-ray tube, $K_{\alpha} = 0.71073$ Å). All diffractometer manipulations, including data collection, integration and scaling were carried out using the Bruker APEXII software.¹⁰⁷ An absorption correction was applied using SADABS.¹⁰⁷ The space group was determined on the basis of systematic absences and intensity statistics and the structure was solved by direct methods and refined by full-matrix least squares on F^2 . The structure was solved in the monoclinic P21/c space group using XS¹⁰⁸ (incorporated in SHELXTL). All non-hydrogen atoms were refined with anisotropic thermal parameters. The structure was

refined (weighted least squares refinement on F^2) and the final least-squares refinement converged to $R_1 = 0.0270$ and $wR_2 = 0.0612$.

X-Ray data collection, solution, and refinement for 3-8PdOAc. X-ray quality crystals of **3-8PdOAc** were obtained from a concentrated fluorobenzene solution of **3-8PdOAc** stored at $-35\text{ }^\circ\text{C}$. The following work was done by Dr. David Herbert. A red, block-shaped crystal ($0.12 \times 0.07 \times 0.05\text{ mm}$) was selected from a representative sample of crystals of the same habit using an optical microscope, mounted onto a nylon loop and placed in a cold stream of nitrogen (110 K). Low-temperature X-ray data were obtained on a Bruker APEXII CCD based diffractometer (Mo sealed X-ray tube, $K_\alpha = 0.71073\text{ \AA}$). All diffractometer manipulations, including data collection, integration and scaling were carried out using the Bruker APEXII software.¹⁰⁷ An absorption correction was applied using SADABS.¹⁰⁷ The space group was determined on the basis of systematic absences and intensity statistics and the structure was solved by direct methods and refined by full-matrix least squares on F^2 . The structure was solved in the monoclinic space group $P2_1/c$ using XS¹⁰⁸ (incorporated in SHELXTL). No obvious missed symmetry was reported by PLATON.⁴ All non-hydrogen atoms were refined with anisotropic thermal parameters. Hydrogen atoms were placed in idealized positions and refined using riding model. The structure was refined (weighted least squares refinement on F^2) to convergence. The large solvent accessible void noted in the CHECKCIF report was addressed by using the program SQUEEZE¹⁴⁷ to remove residual electron density.

X-Ray data collection, solution, and refinement for 3-8PdCl·CH₂Cl₂. X-ray quality crystals of **3-8PdCl** were obtained from a concentrated dichloromethane solution

of **3-8PdCl** which was layered with pentane and stored at -35 °C. A purple, multi-faceted block of suitable size (0.30 × 0.56 × 0.05 mm) was selected from a representative sample of crystals of the same habit using an optical microscope and mounted onto a nylon loop. Low temperature (110 K) X-ray data were obtained on a Bruker APEXII CCD based diffractometer (Mo sealed X-ray tube, $K_{\alpha} = 0.71073 \text{ \AA}$). All diffractometer manipulations, including data collection, integration and scaling were carried out using the Bruker APEXII software.¹⁰⁷ An absorption correction was applied using SADABS.¹⁰⁷ The space group was determined on the basis of systematic absences and intensity statistics and the structure was solved by direct methods and refined by full-matrix least squares on F^2 . The structure was solved in the monoclinic $P2_1/c$ space group using XS¹⁰⁸ (incorporated in SHELXTL). All non-hydrogen atoms were refined with anisotropic thermal parameters. The structure was refined (weighted least squares refinement on F^2) and the final least-squares refinement converged to $R_1 = 0.0349$ ($I > 2\sigma(I)$, 7205 data) and $wR_2 = 0.1480$ (F^2 , 8590 data, 388 parameters, 0 restraints).

X-Ray data collection, solution, and refinement for 3-11RhCO. X-ray quality crystals of **3-11RhCO** were obtained from a concentrated pentane solution of **3-11RhCO** stored at -35 °C. The following work was done by Dr. Nattamai Bhuvanesh. A Leica MZ 7s microscope was used to identify a suitable red blocks with very well defined faces with dimensions (max, intermediate, and min) 0.60 mm × 0.04 mm × 0.02 mm from a representative sample of crystals of the same habit. The crystal mounted on a nylon loop was then placed in a cold nitrogen stream (Oxford) maintained at 110 K.

A BRUKER APEX 2 X-ray (three-circle) diffractometer was employed for crystal screening, unit cell determination, and data collection. The goniometer was controlled using the APEX2 software suite, v2008-6.0.¹⁰⁷ The sample was optically centered with the aid of a video camera such that no translations were observed as the crystal was rotated through all positions. The detector was set at 6.0 cm from the crystal sample (APEX2, 512 × 512 pixel). The X-ray radiation employed was generated from a Mo sealed X-ray tube ($K_{\alpha} = 0.70173 \text{ \AA}$ with a potential of 40 kV and a current of 40 mA) fitted with a graphite monochromator in the parallel mode (175 mm collimator with 0.5 mm pinholes).

Sixty data frames were taken at widths of 0.5° . These reflections were used in the auto-indexing procedure to determine the unit cell. A suitable cell was found and refined by nonlinear least squares and Bravais lattice procedures. The unit cell was verified by examination of the $h k l$ overlays on several frames of data. No super-cell or erroneous reflections were observed. After careful examination of the unit cell, a standard data collection procedure was initiated using omega scans.

Integrated intensity information for each reflection was obtained by reduction of the data frames with the program APEX2.¹⁰⁷ The integration method employed a three dimensional profiling algorithm and all data were corrected for Lorentz and polarization factors, as well as for crystal decay effects and were finally merged and scaled to produce a suitable data set. The absorption correction program SADABS¹⁰⁷ was employed to correct the data for absorption effects (as well as systematic errors).

Systematic reflection conditions and statistical tests of the data suggested the space group *P*-1. A solution was obtained readily using SHELXTL (XS).¹⁰⁸ Hydrogen atoms were placed in idealized positions geometrically except for H25 and H22 (which required accurate bond distances from Rh; H25 and H22 were located from difference Fourier maps) and were set riding on the respective parent atoms. All non-hydrogen atoms were refined with anisotropic thermal parameters. The structure was refined (weighted least squares refinement on F^2) to convergence.^{108,148} Olex2 was employed for the final data presentation and structure plots.¹⁴⁸

CHAPTER IV

PALLADIUM COMPLEXES OF A NEW PHOSPHINE-AMIDO-SILOXIDE Pincer LIGAND WITH VARIABLE DEGREES OF PROTONATION

4.1 Introduction

Pincer ligands with a central anionic (X-type) ligand flanked by two neutral (L-type) donors are by far the most common type and a great variety of LXL combinations have been reported in the literature.^{2a,2g,3-4,149,150} Our group has dedicated a considerable amount of effort to the studies of complexes bearing diarylamido/bis(phosphine) PNP ligands,^{6,114a,114c} as have others.^{114d-i,115a,115b} The diarylamido backbone is particularly attractive because donor side arms connected to the *ortho*-positions are prearranged in a semi-rigid meridional binding motif. In addition to a variety of PNP ligands, symmetric monoanionic NNN¹¹⁷ and SNS¹¹⁶ ligands have been utilized (Figure 4.1). Moreover, Veige et al. have developed the robust chemistry of trianionic, diarylamido-based ONO ligands that carry alkoxide donors in place of the phosphines of PNP.¹⁵¹ Of additional relevance are trianionic and redox non-innocent diarylamido-based NNN ligands by Heyduk et al.¹⁰⁹ The ligands of Veige and Heyduk have been applied to early transition metals, which complement the three hard, anionic donors well.

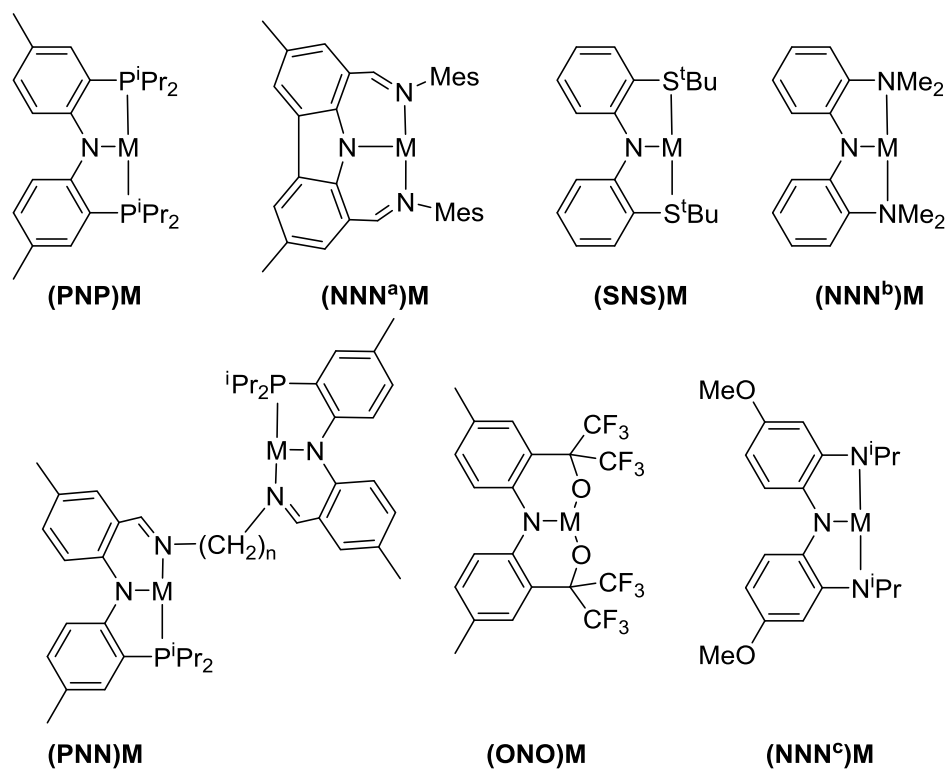
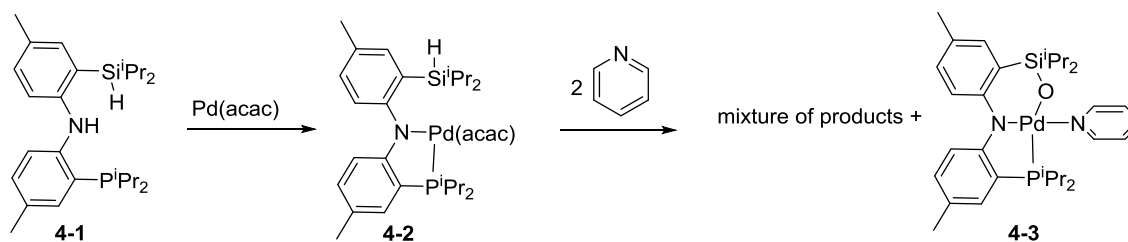


Figure 4.1 Representation of various PNP, PNN, NNN, SNS, and ONO pincer complexes.

We became interested in incorporating a negatively charged side donor into a diarylamido-based pincer, while retaining a phosphine as the other side donor to generate a hybrid ligand which would have more affinity for late transition metals. Over the last few years, convenient synthetic procedures appeared for preparing diarylamido-based pincers with different side donors. Goldberg, Kemp, and co-workers have reported PNP' ligands with different phosphine donors^{118b} and our group disclosed syntheses of monoanionic PNN ligands.^{118a} Utilizing an analogous synthetic approach we have been able to prepare a “PNSiO” ligand, in which one of the phosphines of PNP has been “replaced” with a silanol/siloxide donor. This work was inspired by previous studies in

our group on an analogous “PNSiH” system (**4-1**) by Dr. C. M. Nagaraja and Alyson Christopher. Endeavors to isolate a κ^3 -coordinated complex of **4-1** were all futile and complete Si–H bond activation was never successful. For instance, the reaction of **4-1** with Pd(acac)₂ at room temperature led to isolation of **4-2** (Scheme 4.1). Serendipitously, upon exposure of **4-2** to pyridine Dr. Nagaraja was able to isolate a crystal of **4-3** that was suitable for single-crystal X-ray diffraction. Pincer complexes containing central siloxy donors with flanking phosphines have been previously reported.¹⁵² These P(Si)OP pincer ligands were not synthesized directly but rather arose from reactions of metal-silyl bonds in silyl/bis(phosphine) PSiP complexes with water and or O₂. It is likely that **4-3** forms in a similar manner. Intrigued by **4-3** we set out to independently synthesize the free “PNSiO” ligand. Here, we describe the synthesis of the free ligand and its Pd(II) coordination chemistry, which showcases the capacity of the new ligand to switch between neutral, mono- and dianionic forms.

Scheme 4.1 Indirect formation of a phosphine-amido-siloxide pincer complex.



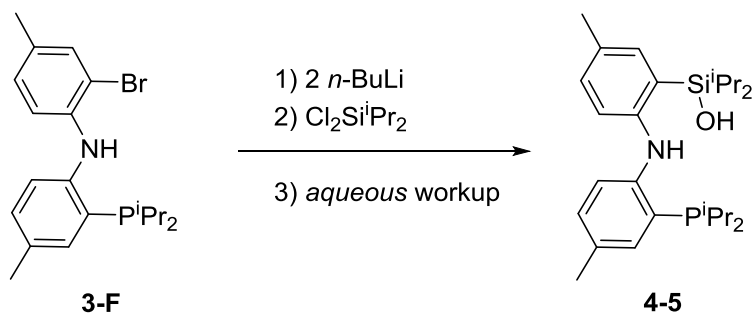
4.2 Results and Discussion

4.2.1 Synthesis and characterization of **4-5**

Compound **3-F** is a convenient precursor from which several types of C_s symmetric PNL ligands have been prepared.^{118a} **3-F** also worked well for the synthesis of the desired PNSiOH ligand (**4-5**) (Scheme 4.2). Treatment of **3-F** with two equivalents of *n*-butyllithium, followed by addition of one equivalent of $Cl_2Si^iPr_2$ and subsequent *aqueous* workup allowed isolation of **4-5** as a colorless solid in a moderate yield of 66% after recrystallization from ether.

Multinuclear NMR analysis of **4-5** indicated C_s symmetry in solution on the NMR timescale. By 1H NMR spectroscopy **4-5** shows a broad singlet at 2.80 ppm for the SiOH proton. Also in evidence were two resonances (each a doublet of doublets) belonging to the methyl groups of the isopropyl arms bound to phosphorus and an additional pair of doublets correspond to the methyl groups of the isopropyl arms bound to silicon. Additionally, six aromatic signals and one singlet corresponding to the amine proton are observed. These features indicate that the two aryl groups are “flipping” faster than the NMR timescale, resulting in time averaged C_s symmetry in solution. A singlet in the $^{31}P\{^1H\}$ NMR spectrum at δ -13.7 ppm was observed, a similar chemical shift to those of free PNP or PNN ligands with a PPr^i_2 group reported previously.^{6,114a,118a}

Scheme 4.2 Synthesis of **4-5**.

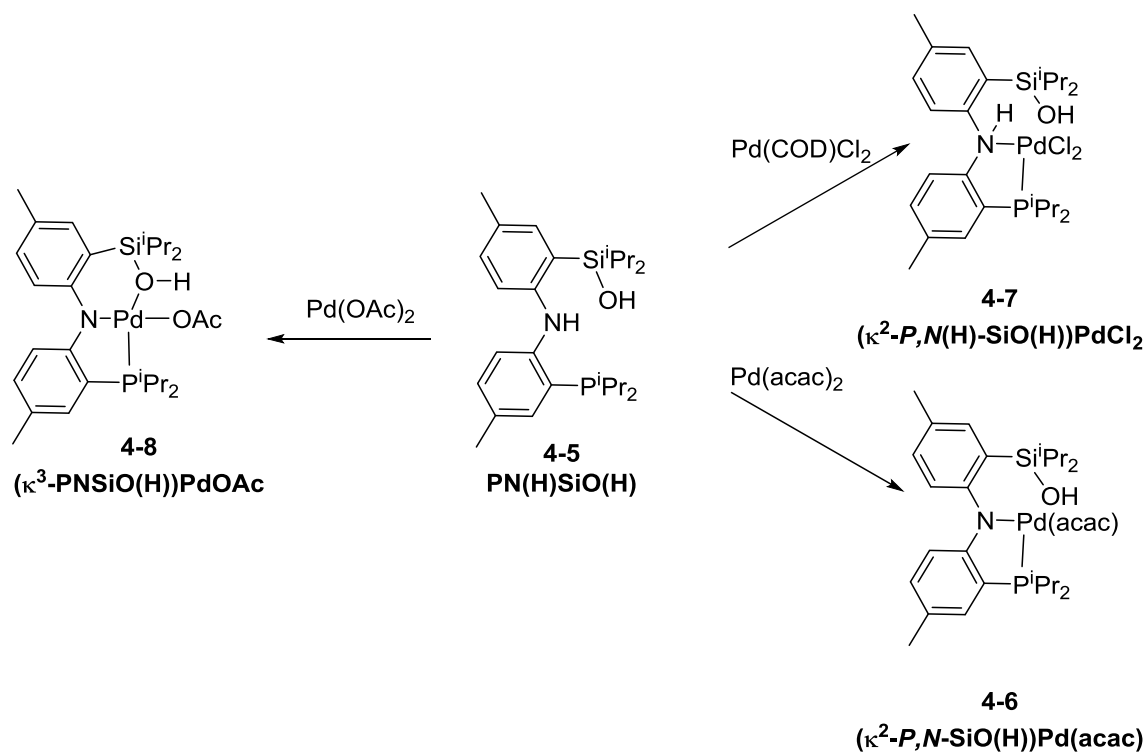


4.2.2 Synthesis of Pd complexes of **4-5**

At first, we set out to investigate the reactions of **4-5** with three common PdX₂ precursors: Pd(acac)₂, (COD)PdCl₂, and Pd(OAc)₂ (COD = 1,4-cyclooctadiene, acac = acetylacetonate) (Scheme 4.3). The reaction between **4-5** and Pd(acac)₂ resulted in N–H bond activation and loss of one equivalent of acetylacetonate to form complex **4-6** with a [κ^2 -*P,N*-SiO(H)] ligand. The NMR spectroscopic features of **4-6** are consistent with the proposed structure. The ¹H NMR spectrum of **4-6** features a broad singlet in ¹H NMR at 5.27 ppm assigned to the silanol proton which differs substantially from the chemical shift of the same proton in **4-5**. It is likely that the SiOH group serves as a hydrogen bond donor to the nitrogen, one of the oxygens of the acac ligand, or perhaps Pd, but we have no firm evidence in support of these interactions.¹⁵³ Treatment of **4-5** with Pd(COD)Cl₂ resulted in the clean formation of a new complex assigned as **4-7** on the basis of spectroscopic data. The ¹H NMR spectrum of **4-7** features singlets at 9.20 ppm and at 4.90 ppm assigned to the NH and SiOH protons, respectively. Complex **4-7** was also observed as the major product in the reaction of **4-5** and Pd(COD)Cl₂ in the

presence of 2,6-lutidine. The non-activation of the NH bond in **4-7** stands in contrast to the reactivity of the PNP and PNN ligands where the central NH is easily cleaved with or even without added base.^{6,114a,114c,118a} **4-7** was isolated as a bright yellow solid with a yield of 45% upon workup.

Scheme 4.3 Reaction of **4-5** with common Pd(II) precursors.

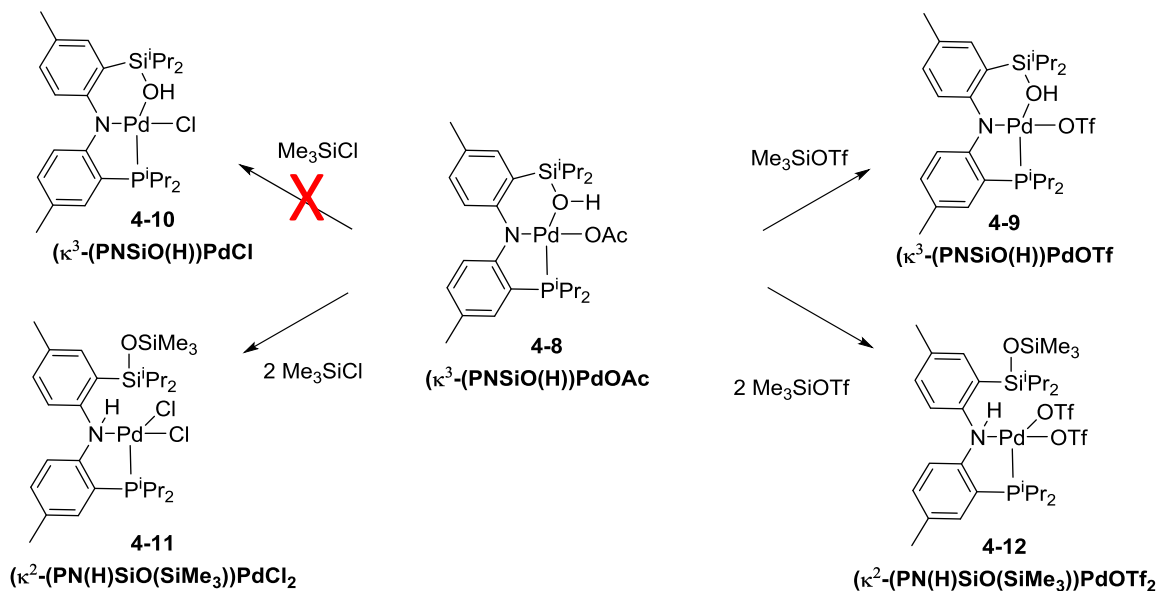


While in both **4-6** and **4-7**, the silanol moiety does not participate in direct bonding to Pd, the reaction of **4-5** with Pd(OAc)₂ produced complex **4-8**, in which **4-5** has been transformed into a monoanionic, tridentate phosphine-amido-silanol ligand. Monoanionic PNO pincer complexes of Pd have been recently reported by Vigalok et al.¹⁵⁴ Complex **4-8** was isolated in 88% yield as an analytically pure purple powder upon workup. The identity of **4-8** was confirmed by solid-state X-ray analysis (*vide infra*), elemental analysis, and with NMR spectroscopic data which is fully consistent with the assignment. The key feature of the ¹H NMR spectrum is the resonance at ca. 14.9 ppm, arising from the SiOH proton. The downfield chemical shift is suggestive of a hydrogen bonding interaction, which is indeed evident in the solid state structure. Interestingly, the NMR spectra of **4-8** are indicative of C₁ symmetry in solution. The ¹H NMR spectrum is characterized by four doublets of doublets and four doublets corresponding to the isopropyl groups on P and Si, respectively. A similar loss of symmetry upon coordination was observed in square-planar PNN complexes and was attributed to the increased barrier for “flipping” of the aryl rings past each other when the ligand is locked about the metal with fused 5- and 6-membered metallacycles.^{118a} In contrast, square-planar complexes of PNP ligands form two 5-membered metallacycles and retain the free ligand’s symmetry.

Next, we wanted to evaluate the potential of **4-8** to serve as a precursor to other PNSiO(H) complexes (Scheme 4.4). Silyl reagents appeared appropriate for metathesis of the acetate with other anionic ligands. This approach was feasible by use of one equivalent of Me₃SiOTf to give complex **4-9** as a purple solid in a moderate yield of

70% upon isolation (Scheme 4). ^{19}F , $^{31}\text{P}\{^1\text{H}\}$, and ^1H NMR analysis of **4-9** are consistent with the formation of a square-planar complex featuring coordination of the [PNSiO(H)] ligand in an κ^3 -fashion to the Pd center. ^{19}F NMR and ^{31}P NMR analysis featured singlets at -79.5 ppm and 88.6 ppm, respectively. Seven aromatic resonances are observed by ^1H NMR spectroscopy, which correspond to the hydroxyl hydrogen and the aromatic protons of the diarylamido backbone. The upfield chemical shift compared to that observed for **4-8** suggests that **4-9** does not exhibit a similar degree of hydrogen bonding between the hydroxyl proton and the adjacent triflate.

Scheme 4.4 Reaction of **4-8** with Me_3SiX reagents.



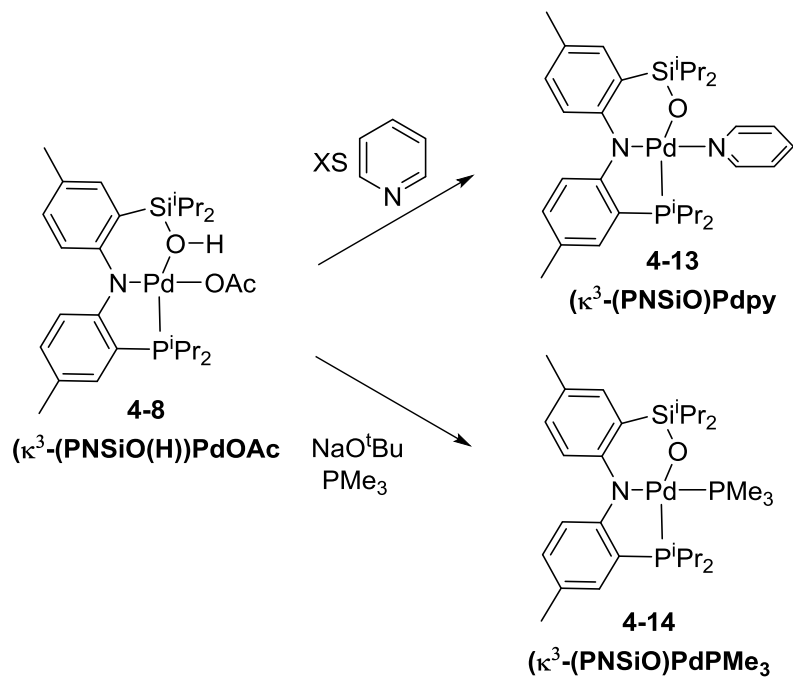
In contrast to the reaction of **4-8** with Me_3SiOTf , the analogous reaction with one equivalent of Me_3SiCl did not lead to the formation of a single product, such as **4-10**.

However, in the presence of an excess of Me_3SiCl , the pincer ligand was transformed by trimethylsilylation of the siloxy oxygen, resulting in **4-11**. Complex **4-11** is formally the product of net addition of Me_3SiCl to complex **4-10**. **4-11** is closely related to complex **4-7**, and exhibits similar NMR spectroscopic features with the exception of SiOH vs SiOSiMe₃ difference. The analogous compound **4-12** can also be isolated upon addition of an excess of Me_3SiOTf to **4-8**. Both **4-11** and **4-12** were isolated as yellow solids.

We surmised that treatment of **4-8** with base in the presence of a neutral donor ligand can result in the net removal of the elements of acetic acid from **4-8** with conversion of silanol to siloxide and formation of complexes of a dianionic, LXX-type PNSiO ligand (Scheme 4.5). Exposure of **4-8** to an excess of pyridine resulted in immediate conversion to complex **4-13**, which was isolated in appreciable yields (59%) as red crystals from cold pentane. $^{31}\text{P}\{^1\text{H}\}$ and ^1H NMR analysis of **4-13** are consistent with the formation of a square-planar complex featuring coordination of a dianionic [PNSiO] ligand in an κ^3 -fashion to the Pd center. The aromatic region of the ^1H NMR spectrum is characterized by 11 proton signals corresponding to the 6 aromatic protons of the diarylamido backbone and to the 5 protons on pyridine. Signals corresponding to a NH or SiOH were not observed. **4-13** was observed as a singlet at 65.1 ppm by $^{31}\text{P}\{^1\text{H}\}$ NMR spectroscopy. A closely related complex **4-14** (first synthesized by Dr. Nagaraja) was isolated upon the reaction of **4-14** with one equivalent of sodium bis(trimethylsilyl)amide in the presence of trimethylphosphine. The $^{31}\text{P}\{^1\text{H}\}$ NMR spectrum of **4-14** featured a pair of doubles at 74.5 and -11.2 ppm corresponding to the isopropyl-bound phosphine and trimethylphosphine respectively. The observed spin-spin

coupling of 29 Hz between the two phosphorus nuclei is consistent with their *cis*-disposition.

Scheme 4.5 Formation of Pd(II) complexes with dianionic pincer ligands.



4.2.3 Solid state structures of **4-8** and **4-13**

The solid-state structure of **4-8** (Figure 4.2, Table 4.1) was confirmed by single-crystal X-ray diffraction analysis and is consistent with our proposal that hydrogen bonding is occurring between the hydroxyl proton and the acetate functionality. The distances between the oxygen atom of the metal κ^1 -bound acetate and the hydroxyl proton and the oxygen of the pincer backbone were found to be 1.594 Å and 2.423 Å

respectively. The structure of **4-8** features a distorted square planar geometry about the Pd metal center.

Complex **4-13** features a tridentate *mer*-coordinating κ^3 -[PNSiO]²⁻ siloxy ligand in a distorted square planar geometry about Pd and is consistent with the NMR data obtained for this complex (*vide supra*). The pyridine ligand is oriented nearly perpendicularly to the plane of the ligand backbone.

The pincer bite angles (P–Pd–O) in **4-8** and **4-13** of around 173-175° are similar to each other and also to those in (PNN)Pd complexes that also feature fused five- and six-membered metallacycles. The Si–O distance of 1.634(3) Å in **4-8** is elongated relative to the Si–O distance of 1.6032(16) Å found for the siloxy group in **4-13**, as might be expected for the silanol vs siloxide binding. The Pd–O–Si angle of 126.84(14)° in **4-8** is less contracted relative to that of **4-13** (118.67(9)°). The sterics associated with the contraction in **4-13** are relieved through distortion of the silicon atom from the plane containing the O and Pd atoms (0.539 Å from the plane in **4-13** compared to 0.198 Å in **4-8**). The distortion of the Si atom seems to have little effect on the nature of the backbone. The dihedral angle between the two aryl rings found in **4-8** is 62.67°, whereas in **4-13** it is only slightly smaller at 60.79°. All other bond lengths and angles are comparable.

Table 4.1 Crystallographic Data for **4-8** and **4-13**.

Metric	4-8	4-13
Pd1–P1	2.225(6)	2.2033(8)
Pd1–O1	2.0281(14)	2.096(2)
Pd1–N1	2.0265(17)	2.005(3)
Pd1–N2 (4-13)	2.0452(17)	
Pd1–O2 (4-8)		2.066(2)
Si1–O1	1.6032(16)	1.634(3)
O1–H1	NA	0.83(5)
P1–Pd1–O1	174.72(5)	173.31(8)
P1–Pd1–N1	83.81(5)	83.80(8)
O1–Pd1–N1	94.80(6)	91.69(10)
N1–Pd–N2 (4-13)	177.56(7)	
N1–Pd–O2 (4-8)		175.76(11)
Pd1–O1–Si1	118.67(9)	126.84(14)
Pd1–O1–H1	NA	98(3)
Si1–O1–H1	NA	134(3)

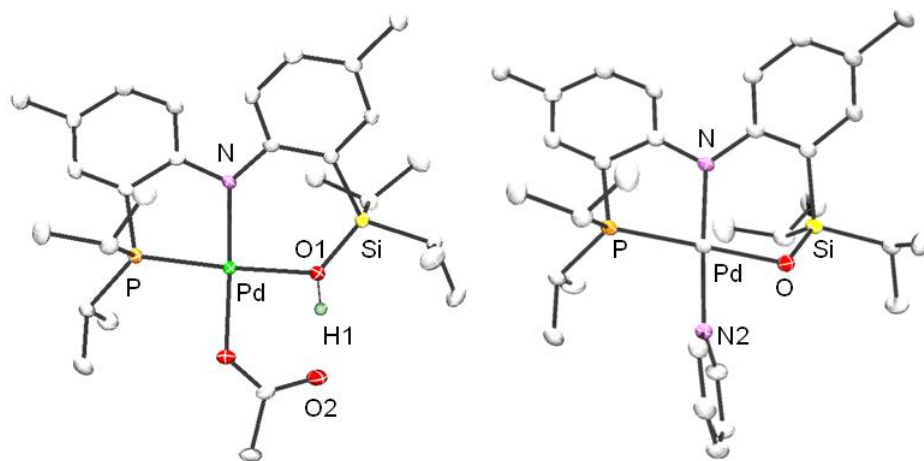


Figure 4.2 POV-Ray renditions¹⁰³ of the ORTEP drawings¹⁰⁴ of complexes **4-8** (left) and **4-13** (right) (50% thermal ellipsoids). Select hydrogen atoms are omitted for clarity.

4.3 Conclusion

Herein we report the synthesis and characterization of a new C_s symmetric pincer ligand of the form $^{\text{Me}}\text{P}^{\text{iPr}}\text{N}(\text{H})\text{Si}^{\text{iPr}}\text{O}(\text{H})$ (**4-5**) and its corresponding Pd complexes. These complexes are characterized by C_1 symmetry and have been analyzed by NMR spectroscopy, elemental analysis, electrochemical analysis, and single crystal X-ray diffraction. The novelty of **4-5** is derived from its ability to coordinate in either a mono- or dianionic fashion ($(\text{L}_2\text{X})\text{Pd}(\text{II})$ vs $\text{LX}_2\text{Pd}(\text{II})$) generating both $\text{Pd}(\text{II})\text{-L}$ and $\text{Pd}(\text{II})\text{-X}$ compounds.

4.4 Experimental Section

4.4.1 General considerations

Unless otherwise specified all manipulations were performed under an atmosphere of Ar using a standard Schlenk line or a glovebox. Toluene, diethyl ether, hexanes, tetrahydrofuran, dichloromethane, pyridine, C_6D_6 , 2,6-lutidine were all dried over CaH_2 , distilled or vacuum transferred and then stored over molecular sieves in an Ar filled glove box. Chlorodiisopropylsilane (Gelest), trimethylsilylchloride (Gelest), trimethylsilyl trifluoromethanesulfonate (Gelest), and dichlorodiisopropylsilane (Gelest) were degassed and stored over molecular sieves. $\text{Pd}(\text{COD})\text{Cl}_2$,¹³⁷ bis(2-bromo-4-methylphenyl)amine,¹³⁸ and **3-F**^{118a} were prepared according to the published procedures. All other chemicals used were received from commercial vendors. NMR spectra were recorded on a Varian Inova 300 (^1H , ^{13}C , ^{31}P), Varian Inova 500 (^1H , ^{13}C ,

³¹P, ¹⁹F), or a Varian 500 (¹H, ¹³C, ³¹P, ¹⁹F) spectrometer. ³¹P and ¹⁹F NMR spectra were referenced externally using H₃PO₄ (85%, 0 ppm) and CF₃COOH (-78.5 ppm) respectively. Single frequency phosphorus decoupled proton spectrum were recorded on the Varian Inova 500 (¹H, ¹³C, ³¹P, ¹⁹F), or Varian 500 (¹H, ¹³C, ³¹P, ¹⁹F) spectrometers. The frequency at which the spectrum was decoupled is referenced at the beginning of each data set. All operations were performed on a Bruker-Nonius Kappa Apex2 diffractometer, using graphite-monochromated MoK α radiation. All diffractometer manipulations, including data collection, integration, scaling, and absorption corrections were carried out using the Bruker Apex2 software.¹⁰⁷ Elemental analyses were performed by CALI Laboratories, Parsippany, NJ.

4.4.2 Synthesis of **4-1** and **4-5**

4-1. A Schlenk flask was charged with **3-F** (0.46 g, 1.8 mmol), diethyl ether (25 mL), and a stir bar. *n*-BuLi (0.95 mL, 2.3 mmol) was added drop-wise via syringe to a stirring solution. Stirred was continued for 1 h and then ClSi(H)ⁱPr₂ (0.20 mL, 0.88 mmol) was added slowly via syringe. The solution became a murky yellow color. The reaction mixture was then stirred for 12 h and prior to being quenched with degassed H₂O (22 μ L). The volatiles were then removed *in vacuo* and the resulting residue was dissolved in pentane and filtered through Celite. Removal of the pentane yielded **4-1** as a colorless powder (0.28 mg, 0.64 mmol, 54%). ¹H NMR (C₆D₆): 7.49-7.46 (m, 2H, Ar *H*, NH), 7.36 (d, 1H, *J*_{HH} = 9 Hz, Ar *H*), 7.18 (dd, 1H, *J*_{HH} = 8 Hz, *J*_{PH} = 5 Hz, Ar *H*), 7.13 (s, 1H, Ar *H*), 6.97 (dd, 1H, *J*_{HH} = 9 Hz, *J*_{HH} = 2 Hz, Ar *H*), 6.88 (dd, 1H, *J*_{HH} = 9 Hz,

$J_{\text{HH}} = 2$ Hz, Ar *H*), 4.46 (t, 1H, $J_{\text{SiH}} = 183$ Hz, $J_{\text{HH}} = 4$ Hz, Si*H*), 2.16 (s, 3H, CH₃), 2.15 (s, 3H, CH₃), 2.00-1.91 (m, 2H, CH(CH₃)₂), 1.48-1.42 (m, 2H, CH(CH₃)₂), 1.19 (d, 6H, $J_{\text{HH}} = 7$ Hz, CHCH₃)₂), 1.13 (d, 6H, $J_{\text{HH}} = 7$ Hz, CHCH₃)₂), 1.08 (dd, 6H, $J_{\text{PH}} = 15$ Hz, $J_{\text{HH}} = 7$ Hz, CHCH₃)₂), 0.95 (dd, 6H, $J_{\text{PH}} = 12$ Hz, $J_{\text{HH}} = 7$ Hz, CHCH₃)₂). ¹H{³¹P} δ -15.4} NMR (C₆D₆): 7.49-7.46 (m, 2H, Ar-*H*, *NH*), 7.36 (d, 1H, $J_{\text{HH}} = 9$ Hz, Ar *H*), 7.18 (d, 1H, $J_{\text{HH}} = 8$ Hz, Ar *H*), 7.13 (s, 1H, Ar *H*), 6.97 (dd, 1H, $J_{\text{HH}} = 9$ Hz, $J_{\text{HH}} = 2$ Hz, Ar *H*), 6.88 (dd, 1H, $J_{\text{HH}} = 9$ Hz, $J_{\text{HH}} = 2$ Hz, Ar *H*), 4.46 (t, 1H, $J_{\text{SiH}} = 183$ Hz, $J_{\text{HH}} = 4$ Hz, Si*H*), 2.16 (s, 3H, CH₃), 2.15 (s, 3H, CH₃), 2.00-1.91 (m, 2H, CH(CH₃)₂), 1.48-1.42 (m, 2H, CH(CH₃)₂), 1.19 (d, 6H, $J_{\text{HH}} = 7$ Hz, CHCH₃)₂), 1.13 (d, 6H, $J_{\text{HH}} = 7$ Hz, CHCH₃)₂), 1.08 (d, 6H, $J_{\text{HH}} = 7$ Hz, CHCH₃)₂), 0.95 (d, 6H, $J_{\text{HH}} = 7$ Hz, CHCH₃)₂). ¹³C{¹H} NMR (C₆D₆): δ 148.9 (d, $J_{\text{CP}} = 19$ Hz, Ar CN), 146.7 (s, Ar CN), 138.4 (s), 133.5 (s), 131.6 (s), 131.5 (s), 131.0 (s), 130.2 (s), 121.0 (s), 120.4 (d, $J_{\text{CP}} = 15$ Hz), 119.2 (s), 115.7 (s), 24.8 (d, $J_{\text{CP}} = 10$ Hz, CH(CH₃)₂), 22.1 (d, $J_{\text{CP}} = 9$ Hz, CH(CH₃)₂), 21.7 (s), 21.6 (s), 20.8 (s), 20.7 (s), 20.48 (d, $J_{\text{CP}} = 9$ Hz, CH(CH₃)₂), 13.0 (s). ³¹P{¹H} NMR (C₆D₆): δ -15.4. Elemental Analysis Calculated: C 70.38, H 9.54, N 3.15; Found C 70.26, H 9.60, N 3.21.

4-5. A Teflon stoppered Schlenk flask was charged with **3-F** (6.2 g, 16 mmol), a stir bar, and diethyl ether (25 mL). *n*-Butyllithium (13 mL, 2.5 M in hexanes, 32 mmol) was then added to the reaction vessel slowly in 4 portions. The reaction was stirred for 1 h and then charged with Cl₂SiⁱPr₂ (2.8 mL, 16 mmol). The reaction was heated at 45 °C for 15 h and then quenched with degassed H₂O (1.0 mL). Removal of the volatiles revealed a colorless solid. This was dissolved in diethyl ether and passed through a pad of silica gel. The solution was concentrated and stored at -35 °C overnight resulting in

colorless crystals. The ethereal solution was decanted and the block crystals dried to yield **4-5** (4.6 g, 11 mmol, 66%). ^1H NMR (C_6D_6 , Figure 4.3): δ 7.77 (d, $J_{\text{PH}} = 10$ Hz, 1H, NH), 7.41 (d, $J_{\text{HH}} = 2$ Hz, 1H, Ar H), 7.30 (d, $J_{\text{HH}} = 8$ Hz, 1H, Ar H), 7.20 (dd, $J_{\text{HH}} = 8$ Hz, $J_{\text{PH}} = 5$ Hz, 1H, Ar H), 7.13 (s, 1H, Ar H), 6.98 (d, $J_{\text{HH}} = 9$ Hz, 1H, Ar H), 6.88 (d, $J_{\text{HH}} = 9$ Hz, 1H, Ar H), 2.80 (s, 1H, OH), 2.18 (s, 3H, CH_3), 2.15 (s, 3H, CH_3), 1.94 (m, 2H, $\text{P}(\text{CH}(\text{CH}_3)_2)_2$), 1.39 – 1.30 (m, 2H, $\text{Si}(\text{CH}(\text{CH}_3)_2)_2$), 1.18 (d, $J_{\text{HH}} = 7$ Hz, 6H, $\text{Si}(\text{CH}(\text{CH}_3)_2)_2$), 1.14 – 1.09 (d, $J_{\text{HH}} = 7$ Hz, 6H, $\text{Si}(\text{CH}(\text{CH}_3)_2)_2$), 1.06 (dd, $J_{\text{PH}} = 16$ Hz, $J_{\text{HH}} = 7$ Hz, 6H, $\text{P}(\text{CH}(\text{CH}_3)_2)_2$), 0.94 (dd, $J_{\text{PH}} = 12$ Hz, $J_{\text{HH}} = 7$ Hz, 6H, $\text{P}(\text{CH}(\text{CH}_3)_2)_2$). ^1H $\{^3\text{1P}\}$ NMR (C_6D_6): δ 7.77 (s, 1H, NH), 7.41 (d, $J_{\text{HH}} = 2$ Hz, 1H, Ar H), 7.30 (d, $J_{\text{HH}} = 8$ Hz, 1H, Ar H), 7.20 (d, $J_{\text{HH}} = 8$ Hz, 1H, Ar H), 7.13 (s, 1H, Ar H), 6.98 (d, $J_{\text{HH}} = 9$ Hz, 1H, Ar H), 6.88 (d, $J_{\text{HH}} = 9$ Hz, 1H, Ar H), 2.80 (s, 1H, OH), 2.18 (s, 3H, CH_3), 2.15 (s, 3H, CH_3), 1.94 (m, 2H, $\text{P}(\text{CH}(\text{CH}_3)_2)_2$), 1.39 – 1.30 (m, 2H, $\text{Si}(\text{CH}(\text{CH}_3)_2)_2$), 1.18 (d, $J = 7$ Hz, 6H, $\text{Si}(\text{CH}(\text{CH}_3)_2)_2$), 1.14 – 1.09 (d, $J = 7$ Hz, 6H, $\text{Si}(\text{CH}(\text{CH}_3)_2)_2$), 1.06 (d, $J = 8$ Hz, 6H, $\text{P}(\text{CH}(\text{CH}_3)_2)_2$), 0.94 (d, $J = 7$ Hz, 6H, $\text{P}(\text{CH}(\text{CH}_3)_2)_2$). ^{13}C $\{^1\text{H}\}$ NMR (C_6D_6): δ 149.2 (d, $J_{\text{CP}} = 19$ Hz, CN), 147.9 (s), 136.7 (s), 133.5 (s), 131.5 (s), 131.1 (s), 131.0 (s), 128.6 (s), 121.5 (s), 121.4 (s), 121.0 (s), 117.3 (s), 23.7 (s, $\text{CH}(\text{CH}_3)_2$), 21.0 (s, CH_3), 20.9 (s, CH_3), 20.4 (d, $J_{\text{CP}} = 23$ Hz, $\text{CH}(\text{CH}_3)_2$), 19.3 (s, CH_3), 18.0 (s, CH_3), 17.7 (s, CH_3), 13.6 (s, CH_3). $^3\text{1P}$ $\{^1\text{H}\}$ NMR (C_6D_6): δ -13.7 (s, $\text{P}(\text{CH}(\text{CH}_3)_2)_2$).

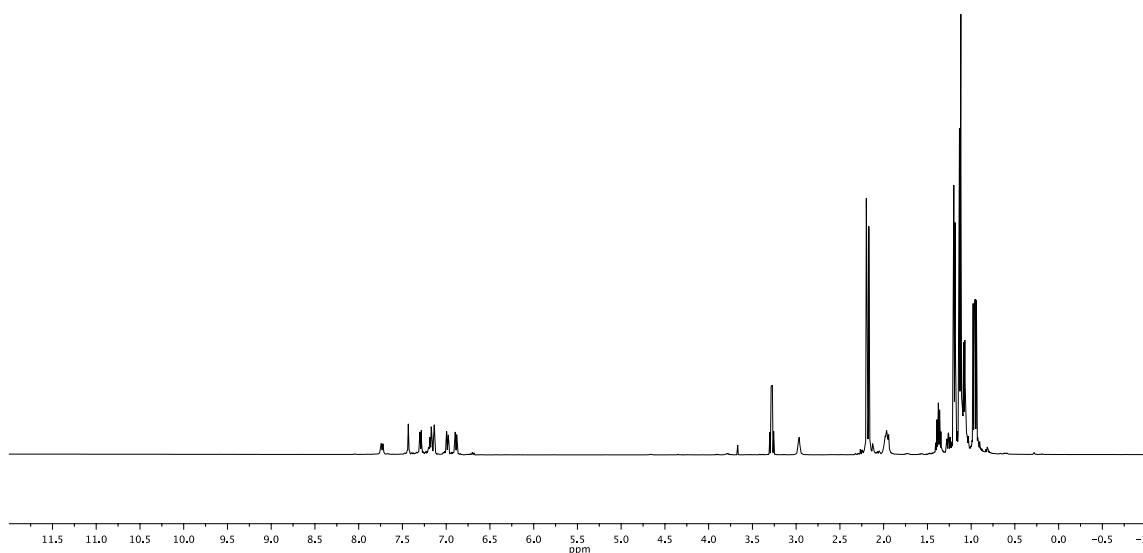


Figure 4.3 ^1H NMR spectrum of **4-5** (500 MHz, C_6D_6). Minor quantities of pentane and diethyl ether are observed.

4.4.3 Synthesis of palladium complexes of **4-5**

4-6. A J. Young tube was charged with **4-5** (35 mg, 0.079 mmol), $\text{Pd}(\text{acac})_2$ (24 mg, 0.079 mmol) and C_6D_6 (0.5 mL). An immediate color change to red is observed in conjunction with formation of one equivalent of free acetylacetonone and **4-6**. ^1H NMR (C_6D_6 , Figure 4.4): δ 7.45 (d, $J_{\text{HH}} = 2$ Hz, 1H, Ar *H*), 7.36 (d, $J_{\text{HH}} = 8$ Hz, 1H, Ar *H*), 7.20 (dd, $J_{\text{HH}} = 8$ Hz, $J_{\text{HH}} = 2$ Hz, 1H, Ar *H*), 7.15 (m, 1H, Ar *H*), 6.73 (dd, $J_{\text{HH}} = 8$ Hz, $J_{\text{HH}} = 2$ Hz, 1H, Ar *H*), 6.67 (d, $J_{\text{PH}} = 9$ Hz, 1H, Ar *H*), 6.49 (dd, $J_{\text{HH}} = 9$ Hz, $J_{\text{PH}} = 5$ Hz, 1H, Ar *H*), 5.27 (br s, 1H, OH), 5.03 (s, 1H, acac), 2.25 (s, 3H, CH_3), 2.14 (m, 2H,

$CH(CH_3)_2$, 2.06 (s, 3H, CH_3), 1.96 (m, 1H, $CH(CH_3)_2$), 1.66 (s, 3H, CH_3), 1.58 (s, 3H, CH_3), 1.41 (d, $J_{HH} = 7$ Hz, 3H, $CH(CH_3)_2$), 1.37 (d, $J_{HH} = 7$ Hz, 3H, $CH(CH_3)_2$), 1.32 (dd, $J_{PH} = 17$ Hz, $J_{HH} = 7$ Hz, 3H, $CH(CH_3)_2$), 1.27 (d, $J_{HH} = 7$ Hz, 6H, $CH(CH_3)_2$), 1.23 (m, 6H, $CH(CH_3)_2$), 1.03 (dd, $J_{PH} = 15$ Hz, $J_{HH} = 7$ Hz, 3H, $CH(CH_3)_2$). $^1H\{^{31}P \delta 72.5\}$ NMR (C_6D_6): δ 7.45 (d, $J_{HH} = 2$ Hz, 1H, Ar H), 7.36 (d, $J_{HH} = 8$ Hz, 1H, Ar H), 7.20 (dd, $J_{HH} = 8$ Hz, $J_{HH} = 2$ Hz, 1H, Ar H), 7.15 (m, 1H, Ar H), 6.73 (dd, $J_{HH} = 8$ Hz, $J_{HH} = 2$ Hz, 1H, Ar H), 6.67 (s, 1H, Ar H), 6.49 (d, $J_{HH} = 9$ Hz, 1H, Ar H), 5.27 (br s, 1H, OH), 5.03 (s, 1H, acac), 2.25 (s, 3H, CH_3), 2.14 (m, 2H, $CH(CH_3)_2$), 2.06 (s, 3H, CH_3), 1.96 (m, 1H, $CH(CH_3)_2$), 1.66 (s, 3H, CH_3), 1.58 (s, 3H, CH_3), 1.41 (d, $J_{HH} = 7$ Hz, 3H, $CH(CH_3)_2$), 1.37 (d, $J_{HH} = 7$ Hz, 3H, $CH(CH_3)_2$), 1.32 (d, $J_{HH} = 7$ Hz, 3H, $CH(CH_3)_2$), 1.27 (d, $J_{HH} = 7$ Hz, 6H, $CH(CH_3)_2$), 1.23 (m, 6H, $CH(CH_3)_2$), 1.03 (d, $J_{HH} = 7$ Hz, 3H, $CH(CH_3)_2$). $^{31}P\{^1H\}$ NMR (C_6D_6): δ 72.5 (s).

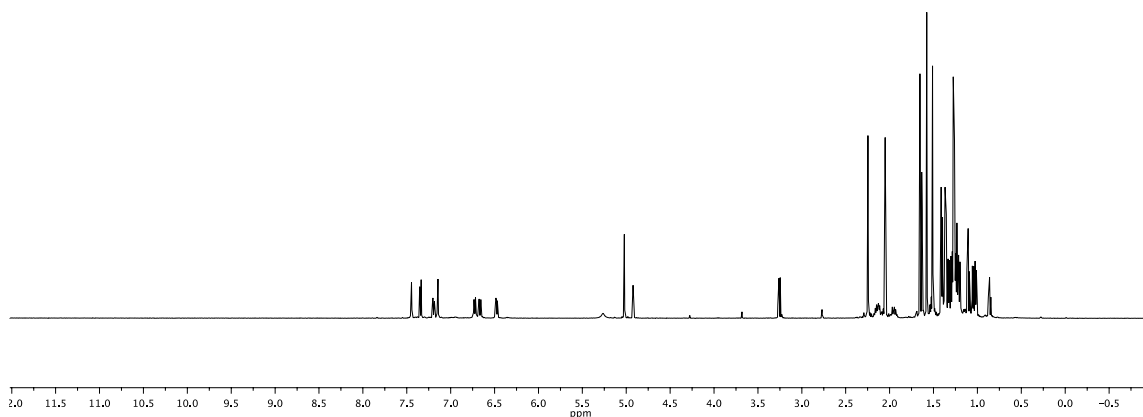


Figure 4.4 ^1H NMR spectrum of **4-6** (500 MHz, C_6D_6). The product was observed *in situ* and therefore residual 1,2-pentadione and diethyl ether are observed.

4-7 A J. Young tube was charged with **4-5** (32 mg, 0.072 μmol), $\text{Pd}(\text{COD})\text{Cl}_2$ (21 mg, 0.072 μmol), 2,6-lutidine (8.4 μL , 0.072 μmol) and C_6D_6 (0.50 mL). The tube was then placed in a 70 $^\circ\text{C}$ oil bath for 18 h. The resulting red solution was filtered through a pad of Celite. Diethyl ether was used to wash the J. Young tube and Celite. The two fractions were then combined and layered with pentane. Slow diffusion resulted in the formation of yellow crystals, which were isolated and washed with pentane (2×5 mL). The yellow crystals were then dried under vacuum to yield **4-7** (20 mg, 0.032 μmol , 45%). ^1H NMR (CD_2Cl_2 , Figure 4.5): δ 9.20 (s, 1H, NH), 7.33 (d, $J_{\text{PH}} = 10$ Hz,

1H, Ar H), 7.27 (d, $J_{\text{HH}} = 9$ Hz, 1H, Ar H), 7.19 (s, 1H, Ar H), 7.15 (d, $J_{\text{HH}} = 9$ Hz, 1H, Ar H), 6.87 (d, $J_{\text{HH}} = 8$ Hz, 2H, Ar H), 4.90 (s, 1H, OH), 2.86 (m, 1H, CH(CH₃)₂), 2.72 (m, 1H, CH(CH₃)₂), 2.40 (s, 3H, CH₃), 2.33 (s, 3H, CH₃), 1.60 (dd, $J_{\text{PH}} = 20$ Hz, $J_{\text{HH}} = 7$ Hz, 3H, CH(CH₃)₂), 1.51 (dd, $J_{\text{PH}} = 18$ Hz, $J_{\text{HH}} = 7$ Hz, 3H, CH(CH₃)₂), 1.46 (dd, $J_{\text{PH}} = 15$ Hz, $J_{\text{HH}} = 7$ Hz, 3H, CH(CH₃)₂), 1.34 (dd, $J_{\text{PH}} = 20$ Hz, $J_{\text{HH}} = 7$ Hz, 3H, CH(CH₃)₂), 1.25 (d, $J_{\text{HH}} = 7$ Hz, 3H, CH(CH₃)₂), 1.16 (m, 6H, CH(CH₃)₂), 1.07 (d, $J_{\text{HH}} = 7$ Hz, 3H, CH(CH₃)₂). ¹H{³¹P δ 71.8} NMR (CD₂Cl₂): δ 9.20 (s, 1H, NH), 7.33 (s, 1H, Ar H), 7.27 (d, $J_{\text{HH}} = 9$ Hz, 1H, Ar H), 7.19 (s, 1H, Ar H), 7.15 (d, $J_{\text{HH}} = 9$ Hz, Ar H), 6.87 (d, $J_{\text{HH}} = 8$ Hz, 2H, Ar H), 4.90 (s, 1H, OH), 2.86 (m, 1H, CH(CH₃)₂), 2.72 (m, 1H, CH(CH₃)₂), 2.40 (s, 3H, CH₃), 2.33 (s, 3H, CH₃), 1.60 (d, $J_{\text{HH}} = 7$ Hz, 3H, CH(CH₃)₂), 1.51 (d, $J_{\text{HH}} = 7$ Hz, 3H, CH(CH₃)₂), 1.46 (d, $J_{\text{HH}} = 7$ Hz, 3H, CH(CH₃)₂), 1.34 (d, $J_{\text{HH}} = 7$ Hz, 3H, CH(CH₃)₂), 1.25 (d, $J_{\text{HH}} = 7$ Hz, 3H, CH(CH₃)₂), 1.16 (m, 6H, CH(CH₃)₂), 1.07 (d, $J_{\text{HH}} = 7$ Hz, 3H, CH(CH₃)₂). ³¹P{¹H} NMR (CD₂Cl₂): δ 76.7 (s). ¹H NMR (C₆D₆): δ 9.65 (s, 1H, NH), 7.24 (s, 1H, Ar H), 6.95 (d, $J = 8$ Hz, 2H Ar H), 6.87 (d, $J = 10$ Hz, 1H, Ar H), 6.82 (d, $J = 8$ Hz, 1H, Ar H), 6.30 (s, 1H, OH), 2.43 (m, 1H, CH(CH₃)₂), 2.28 (m, 1H, CH(CH₃)₂), 2.07 (s, 3H, CH₃), 1.88 (s, 3H, CH₃), 1.56 (m, 1H, CH(CH₃)₂), 1.41 (d, $J_{\text{HH}} = 7$ Hz, 3H, CH(CH₃)₂), 1.36 (dd, $J_{\text{PH}} = 17$ Hz, $J_{\text{HH}} = 7$ Hz, 3H, CH(CH₃)₂), 1.31 (d, $J_{\text{HH}} = 7$ Hz, 3H, CH(CH₃)₂), 1.22 (m, 12H, CH(CH₃)₂), 0.98 (dd, $J_{\text{PH}} = 17$ Hz, $J_{\text{HH}} = 7$ Hz, 3H, CH(CH₃)₂). ³¹P{¹H} NMR (C₆D₆): δ 71.8 (s).

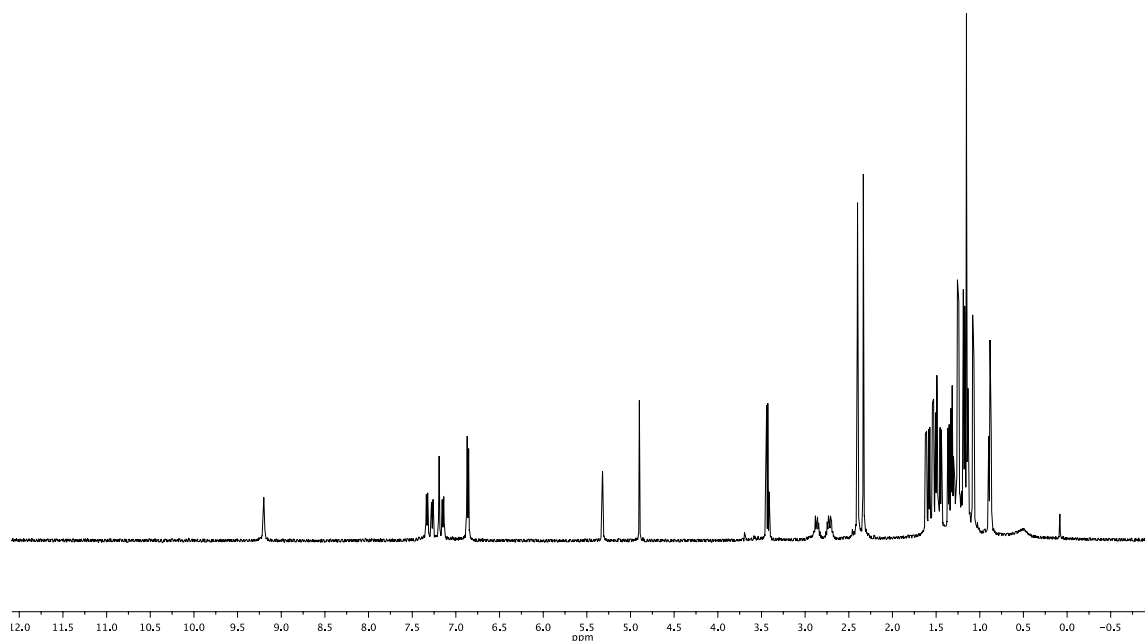


Figure 4.5 ^1H NMR spectrum of **4-7** (500 MHz, CD_2Cl_2). Trace quantities of pentane are observed.

Synthesis of 4-7 in the absence of base. A J. Young tube was charged with **4-5** (180 mg, 0.406 μmol), $\text{Pd}(\text{COD})\text{Cl}_2$ (116 mg, 0.406 μmol) and C_6D_6 (0.50 mL). The tube was then placed in a 70 $^\circ\text{C}$ oil bath for 18 h. The resulting yellow solution was filtered through a pad of Celite. Diethyl ether was used to wash the J. Young tube and Celite. The two fractions were then combined and the volatiles were removed under vacuum to yield **4-7** (176 mg, 0.283 μmol). **4-7** was observed to be the only palladium containing product. COD was also observed via NMR. No further purification steps were taken.

4-8. A Schlenk flask was charged with **4-5** (999 mg, 2.26 mmol), Pd(OAc)₂ (505 mg, 2.26 mmol) and diethyl ether (15 mL). After 3 h ³¹P NMR spectroscopy revealed conversion to one product (δ 79.1 (s)). The solution was filtered through a pad of silica gel with diethyl ether. Removal of the volatiles under vacuum and in pentane at -35 °C yielded **4-8** as a purple powder (1.20 g, 1.97 mmol, 88%). ¹H NMR (C₆D₆, Figure 4.6): δ 14.93 (s, 1H, OH), 7.40 (d, *J*_{HH} = 8 Hz, 1H, Ar *H*), 7.35 (s, 1H, Ar *H*), 7.06 (dd, *J*_{HH} = 9 Hz, *J*_{PH} = 5 Hz, 1H, Ar *H*), 6.97 (d, *J*_{HH} = 6 Hz, 1H, Ar *H*), 6.67 (d, *J*_{HH} = 9 Hz, 1H, Ar *H*), 6.64 (d, *J*_{PH} = 10 Hz, 1H, Ar *H*), 2.15 (s, 3H, CH₃), 2.07 (s, 3H, CH₃), 2.05 – 1.95 (m, 2H, CH(CH₃)₂), 1.94 (s, 3H, CH₃), 1.82 (m, 1H, CH(CH₃)₂), 1.63 – 1.53 (m, 1H, CH(CH₃)₂), 1.51 (d, *J*_{HH} = 6 Hz, 3H, Si(CH(CH₃)₂)₂), 1.34 (d, *J*_{HH} = 6 Hz, 6H, Si(CH(CH₃)₂)₂), 1.25 (d, *J* = 6 Hz, 3H, Si(CH(CH₃)₂)₂), 1.23 (dd, *J*_{PH} = 15 Hz, *J*_{HH} = 7 Hz, 3H, CH(CH₃)₂), 1.22 (dd, *J*_{PH} = 17 Hz, *J*_{HH} = 7 Hz, 3H, CH(CH₃)₂), 1.04 (dd, *J*_{PH} = 18.0 Hz, *J*_{HH} = 7 Hz, 3H, CH(CH₃)₂), 0.81 (dd, *J*_{PH} = 15 Hz, *J*_{HH} = 7 Hz, 3H, CH(CH₃)₂). ¹H {³¹P δ 78.6} NMR (C₆D₆): δ 14.93 (s, 1H, OH), 7.40 (d, *J*_{HH} = 8 Hz, 1H, Ar *H*), 7.35 (s, 1H, Ar *H*), 7.06 (d, *J*_{HH} = 9 Hz, 1H, Ar *H*), 6.97 – 6.93 (d, *J*_{HH} = 6 Hz, 1H, Ar *H*), 6.67 (d, *J*_{HH} = 9 Hz, 1H), 6.67 (s, 1H), 2.15 (s, 3H, CH₃), 2.07 (s, 3H, CH₃), 2.05 – 1.95 (m, 1H, CH(CH₃)₂), 1.94 (s, 3H, CH₃), 1.82 (m, 1H, CH(CH₃)₂), 1.63 – 1.53 (m, 1H, CH(CH₃)₂), 1.51 (d, *J*_{HH} = 6 Hz, 3H, Si(CH(CH₃)₂)₂), 1.42 (m, 1H, CH(CH₃)₂), 1.34 (d, *J*_{HH} = 6 Hz, 6H, Si(CH(CH₃)₂)₂), 1.25 (d, *J*_{HH} = 6 Hz, 3H, Si(CH(CH₃)₂)₂), 1.23 (d, *J*_{HH} = 7 Hz, 3H, CH(CH₃)₂), 1.22 (d, *J*_{HH} = 7 Hz, 3H, CH(CH₃)₂), 1.04 (d, *J*_{HH} = 7 Hz, 3H, CH(CH₃)₂), 0.81 (d, *J*_{HH} = 7 Hz, 3H, CH(CH₃)₂). ¹³C {¹H} NMR (C₆D₆): δ 183.7 ((O)CCH₃), 166.7 (d, *J*_{CP} = 19 Hz, CN),

158.4 (s, CN), 136.4 (s), 133.8 (d, $J_{CP} = 2$ Hz), 132.5 (s), 131.7 (s), 130.5 (s), 129.3 (s), 126.0 (d, $J_{CP} = 8$ Hz), 125.2 (s), 121.1 (d, $J_{CP} = 15$ Hz), 115.8 (s), 26.9 (d, $J = 26$ Hz, $\text{CH}(\text{CH}_3)_2$), 24.22 (s, $\text{CH}(\text{CH}_3)_2$), 22.67 (d, $J_{CP} = 30.5$ Hz, $\text{CH}(\text{CH}_3)_2$), 21.1 (s, $\text{CH}(\text{CH}_3)_2$), 20.33 (s, CH_3), 19.02 (s, CH_3), 18.71 (d, $J_{CP} = 3$ Hz, CH_3), 18.55 (s, CH_3), 18.32 (s, CH_3), 18.14 (s, CH_3), 17.76 (s, CH_3), 16.93 (d, $J_{CP} = 3$ Hz, CH_3), 16.84 (s, CH_3), 13.66 (s, CH_3), 12.80 (s, CH_3). $^{31}\text{P}\{^1\text{H}\}$ NMR (C_6D_6): δ 78.6 (s, $\text{P}(\text{CH}(\text{CH}_3)_2)$).
Elemental Analysis Calculated: C 55.30, H 7.29; Found C 55.25, H 7.29.

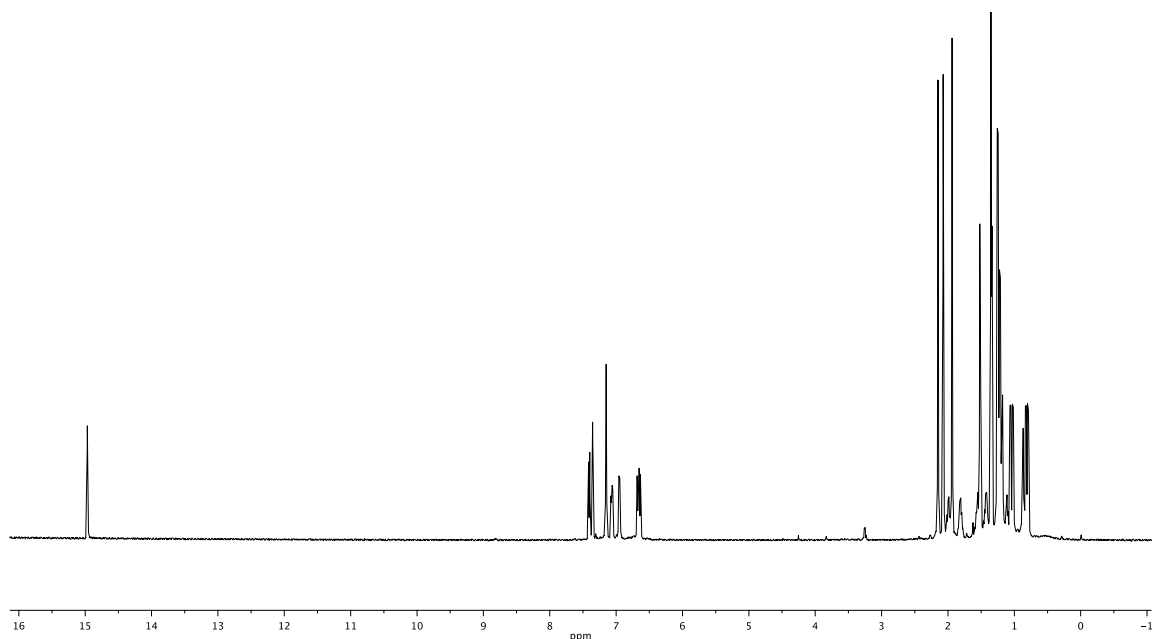


Figure 4.6 ^1H NMR spectrum (500 MHz, C_6D_6) of **4-8**. Trace impurities of diethyl ether and dichloromethane are observed.

4-9. A J. Young tube was charged with **4-8** (38 mg, 63 μmol) and C_6D_6 (1 mL). The tube was then wrapped with aluminum foil to shield the reaction from light. Me_3SiOTf (11 μL , 63 μmol) was then added to the reaction resulting in a deep purple solution. After 20 min multinuclear NMR analysis showed conversion to one product. The reaction was then exposed to light. After 1 h multinuclear NMR analysis evidenced that **4-9** and Me_3SiOAc were the only two products in solution. The solution was then decanted (leaving behind a slight amount of brown oil) and the volatiles were removed under vacuum. The purple solid was then dissolved in a minimal amount of isooctane and stored at $-35\text{ }^\circ\text{C}$. The resulting crystals were isolated by decanting the solution and then drying the solid under vacuum to yield **4-9** as a purple powder (30 mg, 43 μmol , 70%). ^1H NMR (C_6D_6 , Figure 4.7): δ 7.26 (d, $J_{\text{HH}} = 8\text{ Hz}$, 1H, Ar H), 7.21 (s, 1H, Ar H), 7.11 (d, $J_{\text{HH}} = 1\text{ Hz}$, 1H, Ar H), 6.88 (m, 2H, Ar H, OH), 6.62 (d, $J_{\text{HH}} = 9\text{ Hz}$, 1H, Ar H), 6.55 (d, $J_{\text{PH}} = 10\text{ Hz}$, 1H, Ar H), 2.05 (s, 3H, CH_3), 2.01 (s, 3H, CH_3), 1.95 (m, 1H, $\text{CH}(\text{CH}_3)_2$), 1.62 (m, 2H, $\text{CH}(\text{CH}_3)_2$), 1.44 (m, 1H, $\text{CH}(\text{CH}_3)_2$), 1.37 (d, $J_{\text{HH}} = 7\text{ Hz}$, 3H, $\text{CH}(\text{CH}_3)_2$), 1.26 (dd, $J_{\text{PH}} = 18\text{ Hz}$, $J_{\text{HH}} = 7\text{ Hz}$, 3H, $\text{CH}(\text{CH}_3)_2$), 1.12 (m, 12H, $\text{CH}(\text{CH}_3)_2$), 0.93 (m, 6H, $\text{CH}(\text{CH}_3)_2$), 0.69 (dd, $J_{\text{PH}} = 16\text{ Hz}$, $J_{\text{HH}} = 7\text{ Hz}$, 3H, CH_3). $^1\text{H}\{^3\text{P}\}$ NMR (C_6D_6): δ 7.26 (d, $J_{\text{HH}} = 8\text{ Hz}$, 1H, Ar H), 7.21 (s, 1H, Ar H), 7.11 (d, $J_{\text{HH}} = 1\text{ Hz}$, 1H, Ar H), 6.88 (m, 2H, Ar H, O H), 6.62 (d, $J_{\text{HH}} = 9\text{ Hz}$, 1H, Ar H), 6.55 (s, 1H, Ar H), 2.05 (s, 3H, CH_3), 2.01 (s, 3H, CH_3), 1.95 (m, 1H, $\text{CH}(\text{CH}_3)_2$), 1.62 (m, 2H, $\text{CH}(\text{CH}_3)_2$), 1.44 (m, 1H, $\text{CH}(\text{CH}_3)_2$), 1.37 (d, $J_{\text{HH}} = 7\text{ Hz}$, 3H, $\text{CH}(\text{CH}_3)_2$), 1.26 (dd, $J_{\text{PH}} = 18\text{ Hz}$, $J_{\text{HH}} = 7\text{ Hz}$, 3H, $\text{CH}(\text{CH}_3)_2$), 1.12 (m, 9H, $\text{CH}(\text{CH}_3)_2$), 0.93 (m, 6H, $\text{CH}(\text{CH}_3)_2$), 0.69 (d, $J_{\text{HH}} = 7\text{ Hz}$, 3H, $\text{CH}(\text{CH}_3)_2$). $^3\text{P}\{^1\text{H}\}$ NMR (C_6D_6): δ 88.6 (s).

$^{19}\text{F}\{^1\text{H}\}$ NMR (C_6D_6): δ -79.5 (s). Elemental Analysis Calculated: C 46.45, H 5.92;
Found C 46.63, H 5.73.

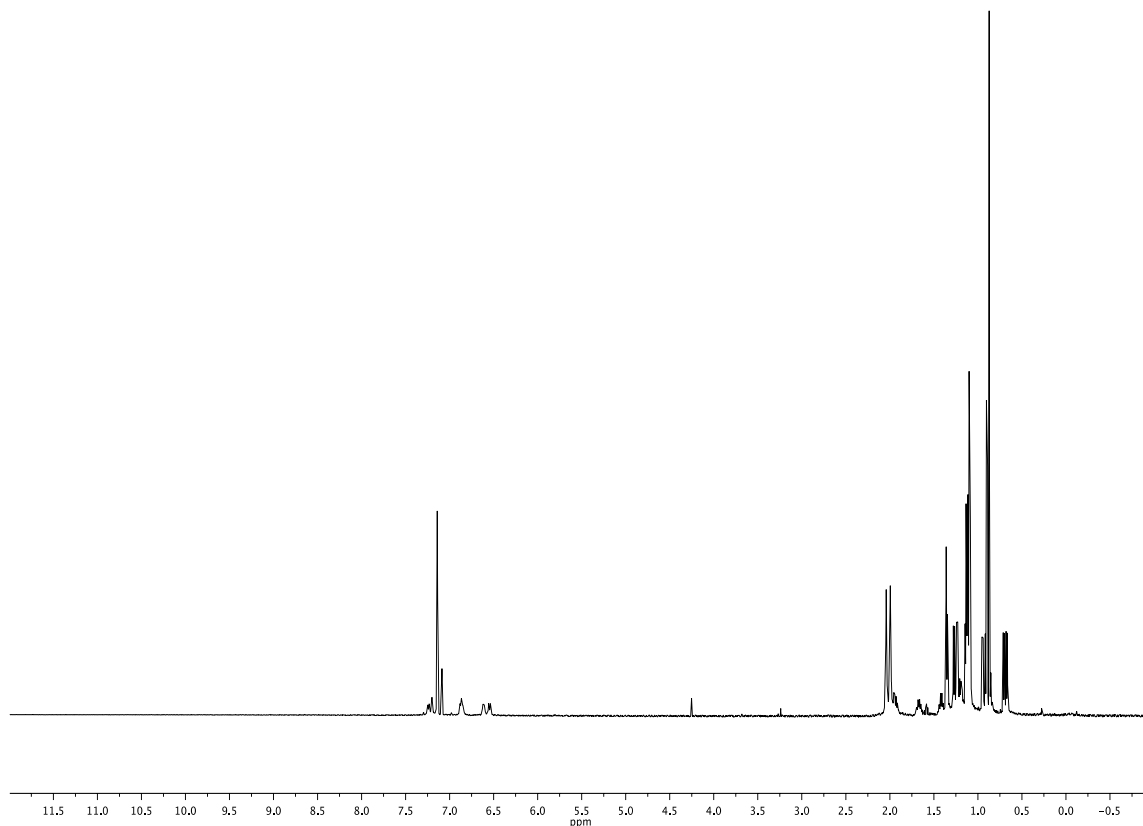


Figure 4.7 ^1H NMR spectrum of **4-9** (500 MHz, C_6D_6). Trace quantities of diethyl ether, isooctane, and dichloromethane are observed.

4-10. A Schlenk tube was charged with **4-8** (59 mg, 0.097 mmol), diethyl ether (5 mL), a stir bar, and trimethylsilyl chloride (12 μL , 0.097 mmol). After stirring 1 h the solution was passed through a pad of Celite and the volatiles were removed under

vacuum. The resulting yellow solid was dissolved in a minimal amount of isooctane and stored at -35 °C. The resulting yellow crystals were then collected and dried under vacuum. $^{31}\text{P}\{^1\text{H}\}$ NMR analysis reveals formation of two products in an approximate 1:1 ratio. $^{31}\text{P}\{^1\text{H}\}$ NMR (C_6D_6): δ 83.4 (s), 68.0 (s).

4-11. A Schlenk flask was charged with **4-8** (124 mg, 0.204 mmol), a stir bar and diethyl ether (5 mL). Me_3SiCl (26.0 μL , 0.204 mmol) was then added drop-wise to the solution. After 10 min the volatiles were removed under vacuum and the resulting solid was analyzed by ^1H and ^{31}P NMR spectroscopy. Two products were observed. The solid was dissolved in diethyl ether (5 mL) and Me_3SiCl (300 μL , 2.36 mmol) was added. The volatiles were again removed under vacuum and the resulting yellow solid was dissolved in a minimal amount of isooctane and stored at -35 °C. The resulting yellow block crystals were isolated and dried under vacuum to yield **4-11** (100 mg, 0.152 mmol, 75%). ^1H NMR (CDCl_3): δ 8.94 (s, 1H, *NH*), 7.45 (d, $J_{\text{PH}} = 7$ Hz, 1H, *Ar H*), 7.40 (d, $J_{\text{HH}} = 7$ Hz, 1H, *Ar H*), 7.31 (dd, $J_{\text{HH}} = 9$ Hz, $J_{\text{PH}} = 3$ Hz, 1H *Ar H*), 7.21 (m, 2H, *Ar H*), 2.96 (m, $J_{\text{HH}} = 21$ Hz, $J_{\text{PH}} = 14$ Hz, $J_{\text{HH}} = 7$ Hz, 2H, $\text{CH}(\text{CH}_3)_2$), 2.55 (s, 3H, CH_3), 2.41 (s, 3H, CH_3), 1.97 (m, 1H, $\text{CH}(\text{CH}_3)_2$), 1.79 (dd, $J_{\text{PH}} = 18$ Hz, $J_{\text{HH}} = 7$ Hz, 3H, $\text{CH}(\text{CH}_3)_2$), 1.68 (dd, $J_{\text{PH}} = 18$ Hz, $J_{\text{HH}} = 7$ Hz, 3H, $\text{CH}(\text{CH}_3)_2$), 1.61 (dd, $J = 18_{\text{PH}}$ Hz, $J_{\text{HH}} = 7$ Hz, 3H, $\text{CH}(\text{CH}_3)_2$), 1.51 (dd, $J_{\text{HH}} = 16$ Hz, $J_{\text{HH}} = 7.0$ Hz, 3H, $\text{CH}(\text{CH}_3)_2$), 1.48 - 1.42 (m, 1H, $\text{CH}(\text{CH}_3)_2$), 1.38 (d, $J_{\text{HH}} = 7$ Hz, 3H, $\text{CH}(\text{CH}_3)_2$), 1.34 (d, $J_{\text{HH}} = 7$ Hz, 3H, $\text{CH}(\text{CH}_3)_2$), 1.33 (d, $J_{\text{HH}} = 7$ Hz, 3H, $\text{CH}(\text{CH}_3)_2$), 1.27 (d, $J_{\text{HH}} = 7$ Hz, 3H, $\text{CH}(\text{CH}_3)_2$), 0.27 (s, 9H, $\text{Si}(\text{CH}_3)_3$). $^1\text{H}\{^{31}\text{P}$ δ 69.1} NMR (CDCl_3): δ 8.94 (s, 1H, *Ar H*), 7.45 (s, 1H, *Ar H*), 7.40 (d, $J_{\text{HH}} = 7$ Hz, 1H, *Ar H*), 7.31 (d, $J_{\text{HH}} = 9$ Hz, 1H *Ar H*), 7.21 (s, 2H, *Ar*

H), 2.96 (m, $J = 21$ Hz, $J = 7$ Hz, 2H, $\text{CH}(\text{CH}_3)_2$), 2.55 (s, 3H, CH_3), 2.41 (s, 3H, CH_3), 1.97 (m, 1H, $\text{CH}(\text{CH}_3)_2$), 1.79 (d, $J_{\text{HH}} = 7$ Hz, 3H, $\text{CH}(\text{CH}_3)_2$), 1.68 (d, $J_{\text{HH}} = 7$ Hz, 3H, $\text{CH}(\text{CH}_3)_2$), 1.61 (d, $J_{\text{HH}} = 7$ Hz, 3H, $\text{CH}(\text{CH}_3)_2$), 1.51 (d, $J_{\text{HH}} = 7.0$ Hz, 3H, $\text{CH}(\text{CH}_3)_2$), 1.48 - 1.42 (m, 1H, $\text{CH}(\text{CH}_3)_2$), 1.38 (d, $J = 7$ Hz, 3H, $\text{CH}(\text{CH}_3)_2$), 1.34 (d, $J = 7$ Hz, 3H, $\text{CH}(\text{CH}_3)_2$), 1.33 (d, $J = 7$ Hz, 3H, $\text{CH}(\text{CH}_3)_2$), 1.27 (d, $J = 7$ Hz, 3H, $\text{CH}(\text{CH}_3)_2$), 0.27 (s, 9H, $\text{Si}(\text{CH}_3)_3$). $^{13}\text{C}\{^1\text{H}\}$ NMR (CDCl_3): δ 153.8 (d, $J_{\text{CP}} = 15$ Hz, Ar C), 151.2 (s, Ar C), 139.1 (d, $J_{\text{CP}} = 5$ Hz, Ar C), 134.5 (s, Ar C), 134.5 (s, Ar C), 131.6 (s, Ar C), 131.2 (s, Ar C), 128.8 (s, Ar C), 128.1 (s, Ar C), 128.0 (s, Ar C), 126.3 (s, Ar C), 107.6 (s, Ar C), 27.4 (d, $J_{\text{CP}} = 13$ Hz, $\text{CH}(\text{CH}_3)_2$), 27.1 (d, $J_{\text{CP}} = 15$ Hz, $\text{CH}(\text{CH}_3)_2$), 21.1 (s, $\text{CH}(\text{CH}_3)_2$), 20.9 (s, $\text{CH}(\text{CH}_3)_2$), 19.3 (s, CH_3), 19.2 (s, CH_3), 18.9 (s, CH_3), 18.7 (s, CH_3), 18.6 (s, CH_3), 18.4 (s, CH_3), 18.3 (s, CH_3), 18.2 (s, CH_3), 16.10 (s, CH_3), 15.1 (s, CH_3), 2.8 (s, $\text{Si}(\text{CH}_3)_3$). $^{31}\text{P}\{^1\text{H}\}$ NMR (CDCl_3): δ 69.1 (s).

^1H NMR (C_6D_6): δ 8.71 (s, 1H, Ar H), 7.34 (d, $J_{\text{PH}} = 24$ Hz, 1H, Ar H), 7.27 (m, 1H, Ar H), 7.18 - 7.08 (m, 4H, Ar H), 2.80 (m, 2H, $\text{CH}(\text{CH}_3)_2$), 2.39 (s, 3H, CH_3), 2.30 (s, 3H, CH_3), 1.75 (m, $J_{\text{HH}} = 7$ Hz, 1H, $\text{CH}(\text{CH}_3)_2$), 1.61 (dd, $J_{\text{PH}} = 18$ Hz, $J_{\text{HH}} = 7$ Hz, 3H, $\text{CH}(\text{CH}_3)_2$), 1.51 (dd, $J_{\text{PH}} = 18$ Hz, $J_{\text{HH}} = 7$ Hz, 3H, $\text{CH}(\text{CH}_3)_2$), 1.45 (dd, $J_{\text{PH}} = 17$, $J_{\text{HH}} = 7$ Hz, 3H, $\text{CH}(\text{CH}_3)_2$), 1.35 (dd, $J_{\text{PH}} = 17$ Hz, $J_{\text{HH}} = 7$ Hz, 3H, $\text{CH}(\text{CH}_3)_2$), 1.24 (d, $J_{\text{HH}} = 7$ Hz, 3H, $\text{CH}(\text{CH}_3)_2$), 1.19 (d, $J_{\text{HH}} = 7$ Hz, 3H, $\text{CH}(\text{CH}_3)_2$), 1.18 (d, $J_{\text{HH}} = 7$ Hz, 3H, $\text{CH}(\text{CH}_3)_2$), 1.13 (d, $J_{\text{HH}} = 7$ Hz, 3H, $\text{CH}(\text{CH}_3)_2$), 0.11 (s, 9H, $\text{Si}(\text{CH}_3)_3$). $^{31}\text{P}\{^1\text{H}\}$ NMR (C_6D_6): δ 67.0 (s).

^1H NMR (CD_2Cl_2 , Figure 4.8): δ 8.71 (s, 1H, Ar H), 7.34 (d, $J_{\text{PH}} = 24$ Hz, 1H, Ar H), 7.27 (d, $J_{\text{HH}} = 9$ Hz, 1H, Ar H), 7.18 - 7.08 (m, 4H, Ar H), 2.80 (m, 2H, $\text{CH}(\text{CH}_3)_2$),

2.39 (s, 3H, CH₃), 2.30 (s, 3H, CH₃), 1.75 (m, $J_{\text{HH}} = 7$ Hz, 1H, CH(CH₃)₂), 1.61 (dd, $J_{\text{PH}} = 18$ Hz, $J_{\text{HH}} = 7$ Hz, 3H, CH(CH₃)₂), 1.51 (dd, $J_{\text{PH}} = 18$ Hz, $J_{\text{HH}} = 7$ Hz, 3H, CH(CH₃)₂), 1.45 (dd, $J_{\text{PH}} = 17$ Hz, $J_{\text{HH}} = 7$ Hz, 3H, CH(CH₃)₂), 1.35 (dd, $J_{\text{PH}} = 17$ Hz, $J_{\text{HH}} = 7$ Hz, 3H, CH(CH₃)₂), 1.24 (d, $J_{\text{HH}} = 7$ Hz, 3H, CH(CH₃)₂), 1.19 (d, $J_{\text{HH}} = 7$ Hz, 3H, CH(CH₃)₂), 1.18 (d, $J_{\text{HH}} = 7$ Hz, 3H, CH(CH₃)₂), 1.13 (d, $J_{\text{HH}} = 7$ Hz, 3H, CH(CH₃)₂), 0.11 (s, 9H, Si(CH₃)₃). $^1\text{H}\{^{31}\text{P} \delta 69.1\}$ NMR (CD₂Cl₂): δ 8.71 (s, 1H, Ar H), 7.34 (s, 1H, Ar H), 7.27 (d, $J_{\text{HH}} = 9$ Hz, 1H, Ar H), 7.18 - 7.08 (m, 4H, Ar H), 2.80 (m, 2H, CH(CH₃)₂), 2.39 (s, 3H, CH₃), 2.30 (s, 3H, CH₃), 1.75 (m, $J_{\text{HH}} = 7$ Hz, 1H, CH(CH₃)₂), 1.61 (d, $J_{\text{HH}} = 7$ Hz, 3H, CH(CH₃)₂), 1.51 (d, $J_{\text{HH}} = 7$ Hz, 3H, CH(CH₃)₂), 1.45 (d, $J_{\text{HH}} = 7$ Hz, 3H, CH(CH₃)₂), 1.35 (dd, $J_{\text{HH}} = 7$ Hz, 3H, CH(CH₃)₂), 1.24 (d, $J_{\text{HH}} = 7$ Hz, 3H, CH(CH₃)₂), 1.19 (d, $J_{\text{HH}} = 7$ Hz, 3H, CH(CH₃)₂), 1.18 (d, $J_{\text{HH}} = 7$ Hz, 3H, CH(CH₃)₂), 1.13 (d, $J_{\text{HH}} = 7$ Hz, 3H, CH(CH₃)₂), 0.11 (s, 9H, Si(CH₃)₃). $^{13}\text{C}\{^1\text{H}\}$ NMR (C₆D₆): δ 153.8 (d, $J_{\text{CP}} = 15$ Hz, Ar CN), 151.7 (s, Ar CN), 139.9 (s), 135.2 (s), 134.9 (s), 131.7 (s), 129.3 (s), 128.3 (m), 126.8 (s), 27.6 (d, $J_{\text{CP}} = 30$ Hz, CH(CH₃)₂), 21.0 (s), 20.9 (s), 19.4 (s), 18.9 (s), 18.7 (s), 18.7 (s), 18.4 (s), 18.3 (s), 16.4 (s), 2.7 (s, SiCH₃).

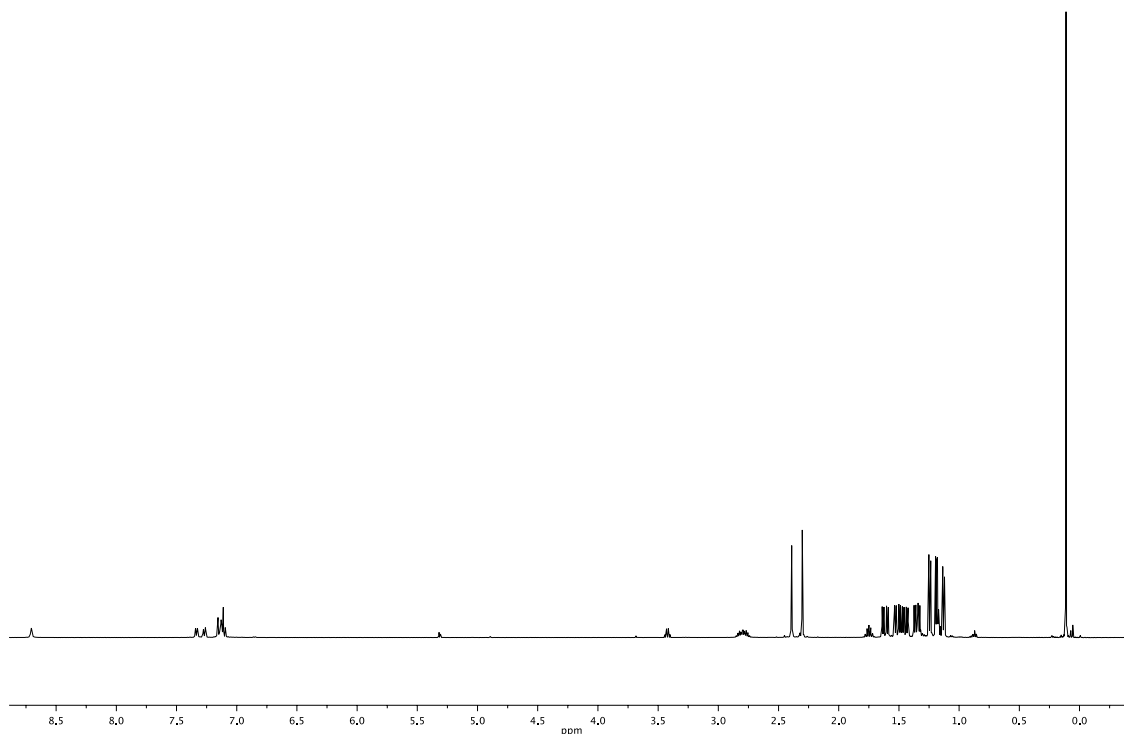


Figure 4.8 ^1H NMR spectrum (500 MHz, CD_2Cl_3) of **4-11**. Minor quantities of pentane and diethyl ether are observed.

4-12. A Schlenk flask was charged with **4-8** (103 mg, 0.169 mmol), a stir bar and diethyl ether (3 mL). Me_3SiOTf (73.0 μmol , 0.330 mmol) was then added slowly via syringe. The reaction mixture immediately turned blue. The volatiles were removed under vacuum and the resulting green oil was washed with pentane (1.0 mL). The oil was then dissolved in diethyl ether, layered with pentane and stored at $-35\text{ }^\circ\text{C}$. The resulting yellow crystals were collected, dried and washed with pentane to yield **4-12**. ^1H NMR (C_6D_6 , Figure 4.9): δ 8.97 (d, $J_{\text{PH}} = 3\text{ Hz}$, 1H, *NH*), 7.95 (d, $J_{\text{HH}} = 8\text{ Hz}$, 1H, Ar *H*), 7.23 (s, 1H, Ar *H*), 7.00 (d, $J_{\text{HH}} = 9\text{ Hz}$, 1H, Ar *H*), 6.79 (d, $J_{\text{PH}} = 8\text{ Hz}$, 1H, Ar *H*),

6.58 (d, $J_{\text{HH}} = 9$ Hz, 1H, Ar *H*), 2.60 (m, 1H, $\text{CH}(\text{CH}_3)_2$), 2.49 (m, 1H, $\text{CH}(\text{CH}_3)_2$), 2.02 (s, 3H, Ar CH_3), 1.90 (m, 1H, $\text{CH}(\text{CH}_3)_2$), 1.85 (s, 3H, Ar CH_3), 1.48 (dd, $J_{\text{PH}} = 20$ Hz, $J_{\text{HH}} = 7$ Hz, 3H, CH_3), 1.34 (m, 10 H, CH_3 , $\text{CH}(\text{CH}_3)_2$), 1.11 (m, 12H, CH_3), 0.06 (s, 9H, CH_3). $^1\text{H}\{^{31}\text{P} \delta 82.7\}$ NMR (C_6D_6): δ 8.97 (s, 1H, Ar *H*), 7.95 (d, $J_{\text{HH}} = 8$ Hz, 1H, Ar *H*), 7.23 (s, 1H, Ar *H*), 7.00 (d, $J_{\text{HH}} = 9$ Hz, 1H, Ar *H*), 6.79 (s, 1H, Ar *H*), 6.58 (d, $J_{\text{HH}} = 9$ Hz, 1H, Ar *H*), 2.60 (m, 1H, $\text{CH}(\text{CH}_3)_2$), 2.49 (m, 1H, $\text{CH}(\text{CH}_3)_2$), 2.02 (s, 3H, CH_3), 1.90 (m, 1H, $\text{CH}(\text{CH}_3)_2$), 1.85 (s, 3H, CH_3), 1.48 (d, $J_{\text{HH}} = 7$ Hz, 3H, CH_3), 1.36 (d, $J_{\text{HH}} = 7$ Hz, 6H, CH_3), 1.32 (d, $J_{\text{HH}} = 7$ Hz, 3H, CH_3), 1.11 (m, 9H, CH_3), 1.06 (d, $J_{\text{HH}} = 7$ Hz, 3H, CH_3), 0.06 (s, 9H, CH_3). $^{31}\text{P}\{^1\text{H}\}$ NMR (C_6D_6): δ 82.7 (s). ^{19}F NMR (C_6D_6): δ -77.5 (m).

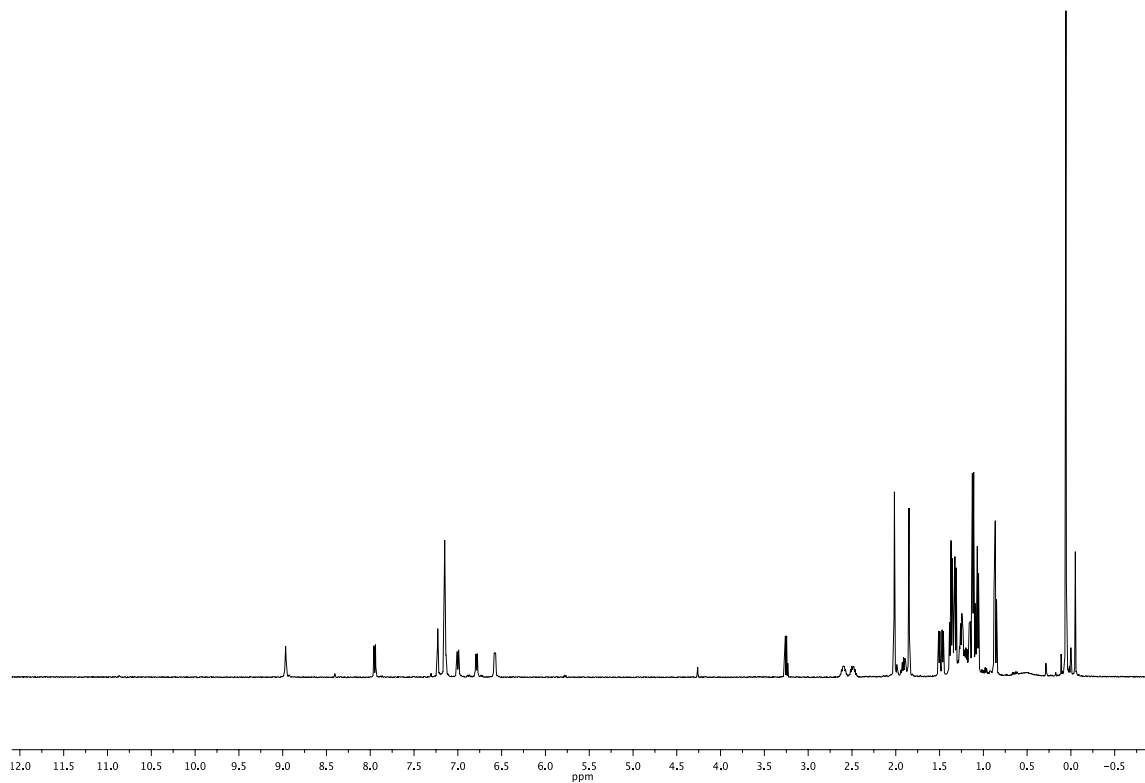


Figure 4.9 ^1H NMR spectrum of **4-12** (500 MHz, C_6D_6). Residual trimethylsilyl trifluoromethanesulfonate, pentane and grease are observed.

4-13. A screw cap vial was charged with **4-8** (50 mg, 0.082 mmol) and diethyl ether (2.0 mL). The solution was then layered with pyridine (0.50 mL) and then stored at $-35\text{ }^\circ\text{C}$. The resulting red crystals were then collected, washed with cold pentane, and dried under vacuum to yield **4-13** (30 mg, 0.048 mmol, 59%). ^1H NMR (500 MHz, CD_2Cl_2 , Figure 4.10): δ 8.72 (d, $J_{\text{HH}} = 5\text{ Hz}$, 2H, Ar *H*), 7.82 (t, $J_{\text{HH}} = 8\text{ Hz}$, 1H, Ar *H*), 7.37 (m, 2H, Ar *H*), 7.15 (d, $J_{\text{HH}} = 2\text{ Hz}$, 1H, Ar *H*), 7.08 (d, $J_{\text{HH}} = 8\text{ Hz}$, 1H, Ar *H*), 6.81 - 6.71 (m, 4H, Ar *H*), 2.33 - 2.22 (m, 2H, $\text{CH}(\text{CH}_3)_2$), 2.17 (s, 3H, Ar CH_3), 2.16 (s, 3H, Ar CH_3), 1.75 (m, 1H, Ar CH_3), 1.38 (dd, $J_{\text{PH}} = 18\text{ Hz}$, $J_{\text{HH}} = 7\text{ Hz}$, 3H, Ar CH_3), 1.25 -

1.16 (m, 9H, CH(CH₃)₂), 1.09 (d, $J = 2$ Hz, 3H, CH(CH₃)₂), 1.00 (m, 3H, CH(CH₃)₂), 0.97 (d, $J_{\text{HH}} = 7$ Hz, 3H), 0.49 (dd, $J_{\text{PH}} = 15$ Hz, $J_{\text{HH}} = 7$ Hz, 3H, CH(CH₃)₂). ¹H{³¹P} δ 65.1} NMR (499 MHz, CD₂Cl₂): δ 8.72 (d, $J_{\text{HH}} = 5$ Hz, 2H, Ar *H*), 7.82 (t, $J_{\text{HH}} = 8$ Hz, 1H), 7.37 (m, 2H, Ar *H*), 7.15 (d, $J_{\text{HH}} = 2$ Hz, 1H, Ar *H*), 7.08 (d, $J_{\text{HH}} = 8$ Hz, 1H, Ar *H*), 6.81 - 6.71 (m, 4H, Ar *H*), 2.33 - 2.22 (m, 2H, CH(CH₃)₂), 2.17 (s, 3H, Ar CH₃), 2.16 (s, 3H, Ar CH₃), 1.75 (m, 1H, Ar CH₃), 1.38 (d, $J_{\text{HH}} = 7$ Hz, 3H, Ar CH₃), 1.25 - 1.16 (m, 9H, CH(CH₃)₂), 1.09 (d, $J = 2$ Hz, 3H, CH(CH₃)₂), 1.00 (m, 3H, CH(CH₃)₂), 0.97 (d, $J_{\text{HH}} = 7$ Hz, 3H), 0.49 (d, $J_{\text{HH}} = 7$ Hz, 3H, CH(CH₃)₂). ¹³C{¹H} NMR (CD₂Cl₂): δ 166.8 (d, $J = 22$ Hz), 157.2 (s), 153.3 (s), 140.8 (s), 138.6 (s), 135.2 (s), 133.2 (s), 131.0 (s), 129.3 (s), 128.0 (s), 125.5 (s), 124.3 (d, $J = 7$ Hz), 123.5 (s), 119.8 (d, $J = 13$ Hz), 113.9 (s), 113.5 (s), 25.7 (d, $J = 22$ Hz), 22.2 (d, $J = 31$ Hz), 21.0 (s), 20.2 (s), 20.0 (s), 19.7 (s), 19.4 (d, $J = 6$ Hz), 18.9 (s), 18.7 (s), 18.7 (s), 16.5 (s), 16.3 (d, $J = 6$ Hz), 14.4 (s). ³¹P{¹H} NMR (202 MHz, CD₂Cl₂): δ 65.1 (s). Elemental Analysis Calculated: C 59.37, H 7.24; Found C 59.19, H 7.24.

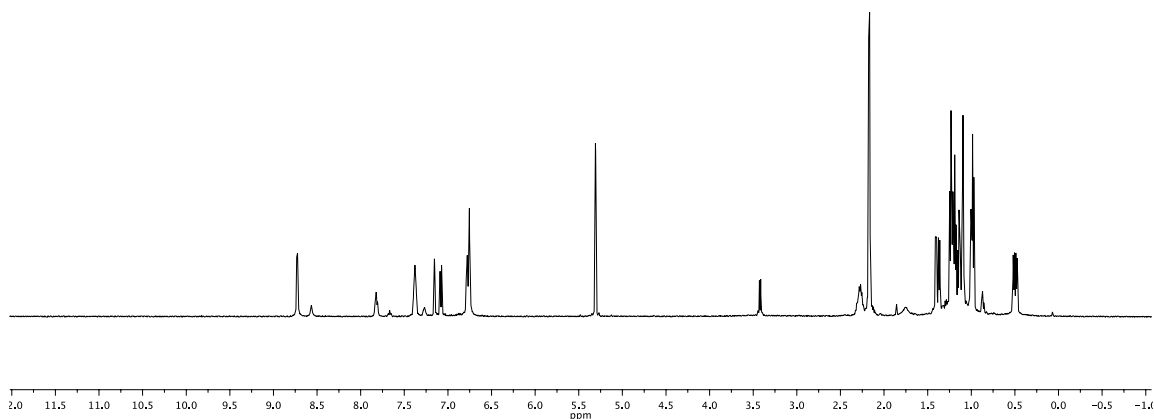


Figure 4.10 ^1H NMR spectrum of **4-13** (500 MHz, CD_2Cl_2). Trace quantities of diethyl ether and acetic acid observed. NOTE: the solubility of this compound in C_6D_6 and CDCl_3 is minimal.

4-14. Under Ar, **4-8** (51 mg, 0.084 mmol) and $\text{P}(\text{CH}_3)_3$ (9.0 μL , 0.084 mmol) were dissolved in C_6D_6 (1 mL). $(\text{Me}_3\text{Si})\text{NNa}$ (11 mg, 0.085 mmol) was added, resulting in a solution changed from purple to orange red. After 1 h the solution was passed through a pad of Celite. The filtrate was collected, and removal of the volatiles *in vacuo* provided a red solid. The solid was dissolved in a minimal amount of pentane and stored at $-35\text{ }^\circ\text{C}$ overnight. The resulting orange powder was collected and dried *in vacuo* to get a fine powder of **4-14** (43 mg, 0.069 mmol, 82%). ^1H NMR (C_6D_6 , Figure 4.11): δ 7.54

(bs, 1H, Ar H), 7.41 (d, 1H, $J_{\text{HH}} = 8$ Hz, Ar H), 6.96 (dd, 1H, $J_{\text{HH}} = 8$ Hz, $J_{\text{HH}} = 2$ Hz, Ar H), 6.77 (m, 2H, Ar H), 6.25 (dd, 1H, $J_{\text{HH}} = 9$ Hz, $J_{\text{PH}} = 4$ Hz, Ar H), 2.15 (s, 3H, CH_3), 2.02 (s, 3H, CH_3), 1.87 (m, 4H, $\text{CH}(\text{CH}_3)_2$), 1.34 (d, 6H, $J_{\text{HH}} = 7$ Hz, $\text{CH}(\text{CH}_3)_2$), 1.29 (dd, 3H, $J_{\text{PH}} = 15$ Hz, $J_{\text{HH}} = 7$ Hz, $\text{CH}(\text{CH}_3)_2$), 1.13 (m, 15H, $\text{CH}(\text{CH}_3)_2$), 1.03 (d, 9H, $J_{\text{PH}} = 10$ Hz, $\text{P}(\text{CH}_3)_3$). $^1\text{H}\{^{31}\text{P} \delta -7.8\}$ NMR (C_6D_6): δ 7.54 (bs, 1H, Ar H), 7.41 (d, 1H, $J = 8$ Hz, Ar H), 6.96 (dd, 1H, $J = 8$ Hz, $J = 2$ Hz, Ar H), 6.77 (m, 2H, Ar H), 6.25 (dd, 1H, $J = 9$ Hz, $J = 4$ Hz, Ar H), 2.15 (s, 3H, CH_3), 2.02 (s, 3H, CH_3), 1.87 (m, 4H, $\text{CH}(\text{CH}_3)_2$), 1.34 (d, 6H, $J_{\text{HH}} = 7$ Hz, $\text{CH}(\text{CH}_3)_2$), 1.29 (dd, 3H, $J_{\text{PH}} = 15$ Hz, $J_{\text{HH}} = 7$ Hz, $\text{CH}(\text{CH}_3)_2$), 1.13 (m, 15H, $\text{CH}(\text{CH}_3)_2$), 1.03 (s, 9H, $\text{P}(\text{CH}_3)_3$). $^1\text{H}\{^{31}\text{P} \delta 74.5\}$ NMR (C_6D_6): δ 7.54 (bs, 1H, Ar H), 7.41 (d, 1H, $J = 8$ Hz, Ar H), 6.96 (dd, 1H, $J = 8$ Hz, $J = 2$ Hz, Ar H), 6.77 (m, 2H, Ar H), 6.25 (d, 1H, $J = 9$ Hz, Ar H), 2.15 (s, 3H, CH_3), 2.02 (s, 3H, CH_3), 1.87 (m, 4H, $\text{CH}(\text{CH}_3)_2$), 1.34 (d, 6H, $J_{\text{HH}} = 7$ Hz, $\text{CH}(\text{CH}_3)_2$), 1.29 (dd, 3H, $J_{\text{PH}} = 15$ Hz, $J_{\text{HH}} = 7$ Hz, $\text{CH}(\text{CH}_3)_2$), 1.13 (m, 15H, $\text{CH}(\text{CH}_3)_2$), 1.03 (d, 9H, $J_{\text{PH}} = 10$ Hz, $\text{P}(\text{CH}_3)_3$). $^{13}\text{C}\{^1\text{H}\}$ NMR (C_6D_6): 166.7 (d, $J_{\text{CP}} = 22$ Hz), 157.6 (s), 135.7 (s), 133.8 (s), 131.2 (s), 130.9 (s), 123.3 (d, $J_{\text{CP}} = 7$ Hz), 122.3 (s), 120.3 (dd, $J_{\text{CP}} = 11$ Hz, $J_{\text{CP}} = 4$ Hz), 27.4 (d, $J_{\text{CP}} = 24$ Hz, $\text{CH}(\text{CH}_3)_2$), 24.4 (d, $J_{\text{CP}} = 28$ Hz, $\text{CH}(\text{CH}_3)_2$), 21.3 (Ar CH_3), 20.6 (Ar CH_3), 20.3 (s, $\text{CH}(\text{CH}_3)_2$), 19.9 (d, $J_{\text{CP}} = 13$ Hz, $\text{CH}(\text{CH}_3)_2$), 19.3 (s, $\text{CH}(\text{CH}_3)_2$), 15.5 (d, $J_{\text{CP}} = 30$ Hz, $\text{P}(\text{CH}_3)_3$), 15.3 (s, $\text{CH}(\text{CH}_3)_2$). $^{31}\text{P}\{^1\text{H}\}$ NMR (C_6D_6): δ 74.5 (d, $J_{\text{PP}} = 29$ Hz, $\text{P}(\text{CH}(\text{CH}_3)_2)_2$), -11.2 (d, $J_{\text{PP}} = 29$ Hz, $\text{P}(\text{CH}_3)_3$).

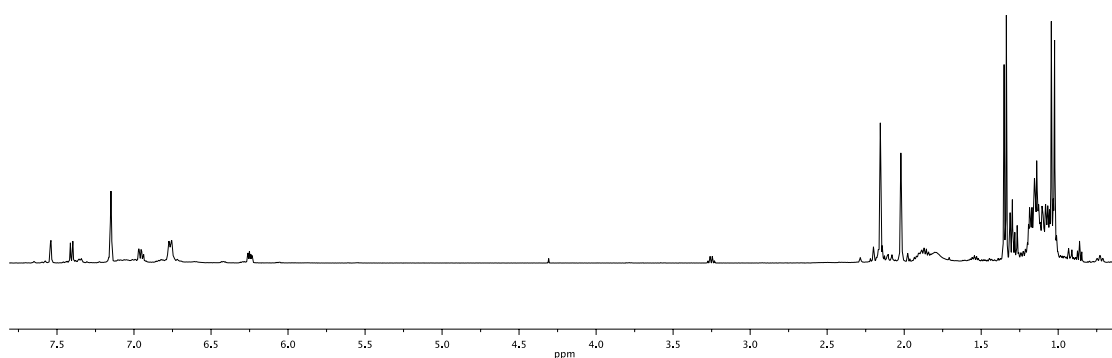


Figure 4.11 ^1H NMR (500 MHz, C_6D_6) of **4-14**. Trace quantities of diethyl ether, dichloromethane, pentane and trimethylphosphine are observed.

4.4.4 X-Ray data collection, solution and refinement

X-Ray data collection, solution and refinement for 4-8. X-ray quality crystals were obtained from a chilled (-35°) pentane solution of **4-8**. This work was done by Dr. Bruce Foxman and Dr. Josh Chen. All operations were performed on a Bruker-Nonius Kappa Apex2 diffractometer, using graphite-monochromated $\text{MoK}\alpha$ radiation. All diffractometer manipulations, including data collection, integration, scaling, and absorption corrections were carried out using the Bruker Apex2 software.¹⁰⁷ Preliminary cell constants were obtained from three sets of 12 frames. Data collection was carried out at 120K, using a frame time of 30 sec and a detector distance of 60 mm. The

optimized strategy used for data collection consisted of six phi and three omega scan sets, with 0.5° steps in phi or omega; completeness was 99.6%. A total of 2767 frames were collected. Final cell constants were obtained from the xyz centroids of 7034 reflections after integration.

From the systematic absences, the observed metric constants and intensity statistics, space group $P\bar{1}$ was chosen initially; subsequent solution and refinement confirmed the correctness of the initial choice. The structures were solved using SIR-92¹⁴⁴ and refined (full-matrix-least squares) using the Oxford University *Crystals for Windows* program.¹⁴⁵ All ordered non-hydrogen atoms were refined using anisotropic displacement parameters. The hydrogen atom attached to the Pd-O-Si oxygen atom, O(1), was refined by using an isotropic displacement parameter. A strong hydrogen bond was observed between the Si-OH group and the unbound carboxylate oxygen atom: O(1)-O(3), 2.423Å; O(1)-H(1)-O(3), 170.5°. Other hydrogen atoms were fixed at calculated geometric positions and allowed to ride on the corresponding carbon atoms.

4-8 refined successfully to $R \approx 6\%$, at which point there were very large unexplainable peaks $\approx 4 \text{ e}^-/\text{Å}^3$ on the ΔF map. ROTAX analysis¹⁵⁵ revealed a twin law -1 0 0/ -0.007 -1 -0.222/ 0.063 -0.001 1.000. Refinement using this twin law led to significant improvement. Reintegration of the data, with consideration of the twin law, using CELL_NOW and TWINABS 2007/5 in the data processing led to a clean ΔF map, with ρ_{max} ca. $0.55 \text{ e}^-/\text{Å}^3$. The scale factors for the two twin components were constrained to sum to 1.0; the value of the major twin component scale was 0.6738(9). The final

least-squares refinement converged to $R_1 = 0.0390$ ($I > 2\sigma(I)$, 6814 data) and $wR_2 = 0.0889$ (F^2 , 7669 data, 321 parameters).

X-Ray data collection, solution and refinement for 4-13. This work was done by Dr. Bruce Foxman and Dr. Josh Chen. Crystals of **4-13** were obtained from slow diffusion of pyridine into a pentane solution stored at -35° . All operations were performed on a Bruker-Nonius Kappa Apex2 diffractometer, using graphite-monochromated $\text{MoK}\alpha$ radiation. All diffractometer manipulations, including data collection, integration, scaling, and absorption corrections were carried out using the Bruker Apex2 software.¹⁰⁷ Preliminary cell constants were obtained from three sets of 12 frames. Data collection was carried out at 120K, using a frame time of 25 sec and a detector distance of 60 mm. The optimized strategy used for data collection consisted of 5 phi and 1 omega scan sets, with 0.5° steps in phi or omega; completeness was 99.8%. A total of 2754 frames were collected. Final cell constants were obtained from the xyz centroids of 9896 reflections after integration.

From the systematic absences, the observed metric constants and intensity statistics, space group $P2_1/n$ was chosen initially; subsequent solution and refinement confirmed the correctness of this choice. The structures were solved using SIR-92,¹⁴⁴ and refined (full-matrix-least squares) using the Oxford University *Crystals for Windows* program.¹⁴⁵ All non-hydrogen atoms were refined using anisotropic displacement parameters; hydrogen atoms were fixed at calculated geometric positions and allowed to ride on the corresponding carbon atoms. The H atom attached to the Si(1)-O(1) unit could not be located on an electron density difference map, nor could its position be inferred from any contacts that might have been associated with hydrogen bonding. The final least-squares refinement converged to $R_1 = 0.0318$ ($I > 2\sigma(I)$, 6732 data) and $wR_2 = 0.0788$ (F^2 , 9049 data, 334 parameters).

CHAPTER V

CONCLUSION

In summary, this dissertation is an overview of the synthesis and characterization of triarylammonium radical cations paired with weakly coordinating carborane anions and novel pincer ligands. Chapter II is an overview of research regarding the synthesis and stabilization of highly oxidizing triarylammonium salts. Triarylammonium oxidants are advantageous since they boast modest oxidation potentials and generate chemically neutral amines upon reduction. Our goal was to expand the scope of triarylammonium oxidants bearing non-coordinating carborane anions. This project was a two part endeavor where we first synthesized new electron-poor triarylamines. These new amines are soluble in non-polar organic solvents making them desirable precursors for the synthesis of triarylammonium radical cations; which in the salt form would be expected to have drastically diminished solubility. In addition, the amines synthesized for this purpose exhibit redox potentials ranging from 1.11 to 1.39 V vs a ferrocene/ferrocenium redox couple; making them suitable precursors to very strong oxidant salts. The second part of this study, the isolation of salts of aminium radical cations, was accomplished by treatment of a neutral amine, Me_3SiX ($\text{X} = \text{OTf}, \text{Cl}$), and $\text{Na}[\text{CRB}_{11}\text{Cl}_{11}]$ ($\text{R} = \text{H}, \text{CH}_3$) with half an equivalent of $\text{PhI}(\text{OAc})_2$.

In Chapters III and IV the synthesis and characterization of new diarylamido based pincer ligands, which incorporate a variety of substituents that change the ligand's stereo and electronic properties, are reported. These ligands fall into four categories: C_{2v} symmetric PNP ligands (two chemically equivalent phosphines), C_s symmetric PNP' ligands (two chemically inequivalent phosphines), C_s symmetric PNN ligands (one phosphine and one imino donor) and finally, C_s symmetric "PNSiO" type ligands. The PN(H)SiO(H) pincer ligand is unique in that it links together phosphine, amine, and silanol donor sites and can also access three different binding modes. Treatment of PN(H)SiO(H) with Pd(acac)₂, (COD)PdCl₂, or Pd(OAc)₂, resulted in the formation of (κ^2 -*P,N*-SiO(H))Pd(acac) (κ^2 -coordination of a monoanionic ligand), (κ^2 -*P,N*(H)-SiO(H))PdCl₂ (κ^2 -coordination of a neutral pincer ligand), and (κ^3 -PNSiO(H))PdOAc (κ^3 -coordination of a monoanionic pincer). In each complex the supporting ligand displayed different degrees of coordination and protonation. The dianionic [PNSiO]²⁺ ligand (κ^3 -coordination of a dianionic pincer) can also be accessed from the reactions of PNSiO(H) with base in the presence of pyridine or PMe₃ to give (κ^3 -PNSiO)Pd(py) and (κ^3 -PNSiO)Pd(PMe₃), respectively.

Unlike the PNSiO(H) ligand, the PNP and PNN type ligands reported in Chapter III, chelate in a monoanionic, meridional, κ^3 -binding mode to group 10 and Rh metal centers. Within the context of the PNP and PNN ligands we were interesting in exploring the relationship between the redox activity of the metal-bound pincer ligand and the electronic effect of the pincer on the metal center. This was accomplished through an analysis of the redox potentials observed for group 10 (pincer)MCl complexes and by

$\nu(\text{CO})$ values in the corresponding (pincer)RhCO complexes. From this study we determined that the oxidation of the (pincer)MCl complexes is consistent with a ligand-based oxidation as it is more affected by substituent changes to the diarylamine backbone, than changes to the identity of the metal center or the donor atoms and their substituents. On the other hand, the $\nu(\text{CO})$ associated with (pincer)RhCO complexes and thus the donor ability of the pincer ligand towards the metal is more strongly affected by the nature of the donors directly attached to the metal. This study also demonstrated that it is not possible to independently change the redox properties of a complex and the donor ability of the ligand to the metal center. However, careful choice of the donor atoms and the nature of their substituents as well as modifications to the diarylamido framework allows for some control of the degree to which the redox activity of the ligand and the electronic effect of the ligand on a metal center are influenced. We hope that this analysis will be used as a guide to these two effects.

REFERENCES

1. Moulton, C. J.; Shaw, B. L. *J. Chem. Soc., Dalton Trans.* **1976**, 1020.
2. (a) Morales-Morales, D.; Jensen, C. G. M. *The Chemistry of Pincer Compounds*; Elsevier: Amsterdam, 2007. (b) Morales-Morales, D. *Rev. Soc. Quím. Méx.* **2004**, *48*, 338. (c) van Koten, G. *J. Organomet. Chem.* **2013**, *730*, 156. (d) van Koten, G.; Milstein, D. *Organometallic Pincer Chemistry*; Springer: Berlin, 2013. (e) Selander, N.; Szabó, K. J. *Chem. Rev.* **2011**, *111*, 2048. (f) Choi, J.; MacArthur, A. H. R.; Brookhart, M.; Goldman, A. S. *Chem. Rev.* **2011**, *111*, 1761. (g) Gunananthan, C.; Milstein, D. *Acc. Chem. Res.* **2011**, *44*, 588.
3. Albrecht, M.; van Koten, G. *Angew. Chem. Int. Ed.* **2001**, *40*, 3750.
4. (a) Fryzuk, M. D. *Can. J. Chem.* **1992**, *70*, 2839. (b) Fryzuk, M. D.; Berg, D. J.; Haddad, T. S. *Coord. Chem. Rev.* **1990**, *99*, 137. (c) Ozerov, O. V.; Watson, L. A.; Pink, M.; Caulton, K. G. *J. Am. Chem. Soc.* **2007**, *129*, 6003. (d) van der Boom, M. E.; Milstein, D. *Chem. Rev.* **2003**, *103*, 1759. (e) Goldman, A. S.; Roy, A. H.; Huang, Z.; Ahuja, R.; Schinski, W.; Brookhart, M. *Science* **2006**, *312*, 257.
5. van Koten, G. *Pure. Appl. Chem.* **1989**, *61*, 1681.
6. Fan, L.; Foxman, B. M.; Ozerov, O. V. *Organometallics* **2004**, *23*, 326.
7. Hermann, W. A.; Kuchler, J. G.; Herdtweck, E. *J. Organomet. Chem.* **1989**, *372*, 371.
8. Langer, R.; Leitus, G.; Ben-David, Y.; Milstein, D. *Angew. Chem. Int. Ed.* **2011**, *50*, 2120.
9. Weng, W.; Chen, C. H.; Foxman, B. M.; Ozerov, O. V. *Organometallics* **2007**, *26*, 3315.
10. (a) Nguyen, A. I.; Blackmore, K. J.; Carter, S. M.; Zarkesh, R. A.; Heyduk, A. F. *J. Am. Chem. Soc.* **2009**, *131*, 3307. (b) Nguyen, A. I.; Zarkesh, R. A.; Lacy, D. C.; Thorson, M. K.; Heyduk, A. F. *Chem. Sci.* **2011**, *2*, 166.
11. Zarkesh, R. A.; Ziller, J. W.; Heyduk, A. F. *Angew. Chem. Int. Ed.* **2008**, *47*.
12. Koller, J.; Sarkar, S.; Abboud, K. A.; Veige, A. S. *Organometallics* **2007**, *26*, 5438.

13. (a) Agapie, T.; Bercaw, J. E. *Organometallics* **2007**, *26*, 2957. (b) Agapie, T.; Day, M. W.; Bercaw, J. E. *Organometallics* **2008**, *27*, 6123. (c) Golisz, S. R.; Bercaw, J. E. *Macromolecules* **2009**, *42*, 8751.
14. (a) Fischer, C.; Fu, G. C. *J. Am. Chem. Soc.* **2005**, *127*, 4594. (b) Arp, F. O.; Fu, G. C. *J. Am. Chem. Soc.* **2005**, *127*, 10482.
15. Jones, G. D.; Martin, J. L.; McFarland, C.; Allen, O. R.; Hall, R. E.; Haley, A. D.; Brandon, R. J.; Konovalova, T.; Desrochers, P. J.; Pulay, P.; Vicic, D. A. *J. Am. Chem. Soc.* **2006**, *128*, 13175.
16. (a) Bedford, R. B.; Yu-Ning, C.; Mairi, F.; McMullin, C. L. *Dalton Trans.* **2011**, *40*, 9034. (b) Feng, J.-J.; Chen, X.-F.; Shi, M.; Duan, W.-L. *J. Am. Chem. Soc.* **2010**, *132*, 5562. (c) Jie, L.; Lutz, M.; Spek, A. L.; van Klink, G. P. M.; van Koten, G.; Gebbink, K.; Robertus, J. M. *J. Organomet. Chem.* **2010**, *695*, 2618. (d) Rubio, M.; Suarez, A.; del Rio, D.; Galindo, A.; Alvarex, E.; Pizzano, A. *Organometallics* **2009**, *28*, 547.
17. (a) Chase, P. A.; Gagliardo, M.; Lutz, M.; Spek, A. L.; Klink, G. P. M.; van Koten, G. *Organometallics* **2005**, *24*, 2016. (b) Adams, J. J.; Lau, A.; Arulsamy, N.; Roddick, D. M. *Inorg. Chem.* **2007**, *46*, 11328. (c) Zhu, Y. J. *Strong Bond Activation with Late Transition-Metal Pincer Complexes as a Foundation for Potential Catalysis*. PhD. Dissertation, Texas A&M University, College Station, TX, 2012. (d) Kossey, E.; Iron, M. A.; Rybtchinski, B.; Ben-David, Y.; Shimon, L. J. W.; Konstantinovski, L.; Martin, J. M. L.; Milstein, D. *Chem. Eur. J.* **2005**, *11*, 2319.
18. Moley, K. G.; Peterson, J. L. *J. Am. Chem. Soc.* **1995**, *117*, 7696.
19. (a) Nakamoto, K. *Infrared and Raman Spectra of Inorganic and Coordination Compounds*; 3rd ed.; Wiley: New York, 1978. (b) Crabtree, R. H. *The Organometallic Chemistry of Transition Metals*; 5th ed.; John Wiley and Sons: Hoboken, 2009.
20. (a) Tolman, C. A. *J. Am. Chem. Soc.* **1970**, *92*, 2953. (b) Tolman, C. A. *Chem. Rev.* **1977**, *77*, 313. (c) Abel, E. W.; Stone, F. G. A. *Q. Chem. Rev.* **1969**, *23*, 325. (d) Strohmeir, W.; Müller, F. J. *Chem. Ber.* **1967**, *100*, 2812.
21. (a) Kossey, E.; Rybtchinski, B.; Diskin-Posner, Y.; Shimon, L. J. W.; Leitun, G.; Milstein, D. *Organometallics* **2009**, *28*, 523. (b) Weng, W.; Guo, C.; Çelenligil-Çetin, C.; Foxman, B. M.; Ozerov, O. V. *Chem. Commun.* **2006**, 197.
22. Anderson, B. G.; Spencer, J. L. *Chem. Eur. J.* **2014**, *20*, 6421.

23. Jørgenson, C. K. *Coord. Chem. Rev.* **1996**, *1*, 164.
24. (a) Billig, E.; Williams, R.; Bernal, I.; Waters, J. H.; Gray, H. B. *Inorg. Chem.* **1964**, *3*, 663. (b) Gray, H. B.; Williams, R.; Bernal, I.; Billig, E. *J. Am. Chem. Soc.* **1962**, *84*, 3596.
25. de Bruin, B. *Eur. J. Inorg. Chem.* **2012**, 340.
26. Chirik, P. J.; Wieghardt, K. *Science* **2010**, *327*, 794.
27. Poverenov, E.; Milstein, D. *Top. Organomet. Chem.* **2013**, *40*, 21.
28. (a) Ben-Ari, E.; Cohen, R.; Gandelman, M.; Shimon, L. J. W.; Martin, J. L.; Milstein, D. *Organometallics* **2006**, *25*, 3190. (b) Schwartzburd, L.; Iron, M. A.; Konstantinovski, L.; Diskin-Posner, Y.; Leitun, G.; Shimon, L. J. W.; Milstein, D. *Organometallics* **2010**, *29*, 3817. (c) Zhang, J.; Leitun, Y.; Ben-David, Y.; Milstein, D. *J. Am. Chem. Soc.* **2005**, *127*, 10840. (d) Gnanaprakasam, B.; Zhang, J.; Milstein, D. *Angew. Chem. Int. Ed.* **2010**, *49*, 1468.
29. Dub, P. A.; Ikariya, T. *J. Am. Chem. Soc.* **2013**, *135*, 2604.
30. (a) Haack, K.-J.; Hashiguchi, S.; Fujii, A.; Ikariya, T.; Noyori, R. *Angew. Chem. Int. Ed. Engl.* **1997**, *26*, 285. (b) Hashiguchi, S.; Fujii, J.; Takehara, J.; Ikariya, T.; Noyori, R. *J. Am. Chem. Soc.* **1995**, *117*, 7562.
31. Fujii, A.; Hashiguchi, S.; Uematsu, N.; Ikariya, T.; Noyori, R. *J. Am. Chem. Soc.* **1996**, *118*, 2521.
32. Khaskin, E.; Iron, M. A.; Shimon, L. J. W.; Zhang, J.; Milstein, D. *J. Am. Chem. Soc.* **2010**, *132*, 8542.
33. Ben-Ari, E.; Gandelman, M.; Rozenberg, H.; Shimon, L. J. W.; Milstein, D. *J. Am. Chem. Soc.* **2003**, *125*, 4714.
34. Milstein, D. *Top. Catal.* **2010**, *51*, 915.
35. Kohl, S. W.; Weiner, L.; Schwartzburd, L.; Konstantinovski, L.; Shimon, L. J. W.; Ben-David, Y.; Iron, M. A.; Milstein, D. *Science* **2009**, *324*, 74.
36. Gunananthan, C.; Milstein, D. *Science* **2007**, *317*, 790.
37. (a) Chirik, P. J. *Inorg. Chem.* **2011**, *50*, 9737. (b) Luca, O. R.; Crabtree, R. H. *Chem. Soc. Rev.* **2013**, *42*, 1440.

38. Eisenberg, R.; Gray, H. B. *Inorg. Chem.* **2011**, *50*, 9741.
39. (a) Hendrickson, D. N.; Pierpont, C. G. *Top. Curr. Chem.* **2005**, *234*, 63. (b) Chaudhuri, P.; Verani, C. N.; Bill, E. B., E.; Weyhermuller, T.; Wieghardt, K. J. *J. Am. Chem. Soc.* **2001**, *123*, 2213.
40. (a) Ringenberg, M. R.; Kokatam, S. L.; Heiden, Z. M.; Rauchfuss, T. B. *J. Am. Chem. Soc.* **2008**, *130*, 788. (b) Ringenberg, M. R.; Rauchfuss, T. B. *Eur. J. Inorg. Chem.* **2012**, 490. (c) Blackmore, K. J.; Lal, N.; Ziller, J. W.; Heyduk, A. F. *Eur. J. Inorg. Chem.* **2009**, 735.
41. (a) Blanchard, S.; Derat, E.; Murr, M.; Fensterbank, L.; Malacria, M.; Mouriès-Mansuy, V. *Eur. J. Inorg. Chem.* **2012**, 376. (b) Vidyaratne, I.; Scott, J.; Gambarotta, S.; Budzelaar, P. H. M. *Inorg. Chem.* **2007**, *46*, 7040. (c) Kapovsky, M.; Dares, C.; Dodsworth, E. S.; Begum, R. A.; Raco, V.; Lever, A. B. P. *Inorg. Chem.* **2013**, *52*, 169.
42. Ciszewski, J. T.; Mikhaylov, D. Y.; Holin, K. V.; Kadirov, M. K.; Budnikova, Y. H.; Sinyashin, O.; Vicic, D. A. *Inorg. Chem.* **2011**, *50*, 8630.
43. Hartwig, J. F. *Organotransition Metal Chemistry: From Bonding to Catalysis*; University Science Books: Sausalito, 2010.
44. van der Vlugt, J. I. *Eur. J. Inorg. Chem.* **2012**, 363.
45. Tondreau, A. M.; Milsmann, C.; Patrick, A. D.; Hoyt, H. M.; Lobkovsky, E.; Wieghardt, K.; Chirik, P. J. *J. Am. Chem. Soc.* **2010**, *132*, 8772.
46. (a) Bouwkamp, M. W.; Cortez, M.-P.; Lobkovsky, E.; Chirik, P. J. *Organometallics* **2006**, *25*, 4269. (b) Russe, S. K.; Lobkovsky, E.; Chirik, P. J. *J. Am. Chem. Soc.* **2011**, *133*, 8858.
47. Sylvester, K. T.; Chirik, P. J. *J. Am. Chem. Soc.* **2009**, *131*, 8772.
48. Bart, S. C.; Lobkovsky, E.; Chirik, P. J. *J. Am. Chem. Soc.* **2004**, *126*, 13794.
49. Tondreau, A. M.; Atienza, C. C. H.; Weller, K. J.; Nye, S. A.; Lewis, K. M.; Delis, J.; Chirik, P. J. *Science* **2012**, *335*, 6068.
50. Bouwkamp, M. W.; Bowman, A. C.; Lobkovsky, E.; Chirik, P. J. *J. Am. Chem. Soc.* **2006**, *128*, 13340.
51. (a) Blackmore, K. J.; Ziller, J. W.; Heyduk, A. F. *Inorg. Chem.* **2005**, *44*, 5559. (b) Blackmore, K. J.; Sly, M. B.; Haneline, M. R.; Ziller, J. W.; Heyduk, A. F. *Inorg.*

- Chem.* **2008**, *47*, 10522. (c) Ketterer, N. A.; Fan, H.; Blackmore, K. J.; Yang, X.; Ziller, J. W.; Baik, M. H.; Heyduk, A. F. *J. Am. Chem. Soc.* **2008**, *130*, 4364. (d) Stanciu, C.; Jones, M. E.; Fanwick, P. E.; Abu-Omar, M. M. *J. Am. Chem. Soc.* **2007**, *129*, 12400.
52. Haneline, M. R.; Heyduk, A. F. *J. Am. Chem. Soc.* **2006**, *128*, 8410.
53. Rosenthal, M. R. *J. Chem. Educ.* **1973**, *50*, 331.
54. Lawrance, G. A. *Chem. Rev.* **1986**, *86*, 17.
55. Honeychuck, R. V.; Hersh, W. H. *Inorg. Chem.* **1989**, *28*, 2869.
56. (a) Gowda, N. M. N.; Naikar, S. B.; Reddy, G. K. N. *Adv. Inorg. Chem. Radiochem.* **1984**, *28*, 255. (b) Beck, W.; Sunkel, K. *Chem. Rev.* **1988**, *88*, 1405.
57. Bihlmeier, A.; Gonsior, M.; Raabe, I.; Trapp, N.; Krossing, I. *Chem. Eur. J.* **2004**, *10*, 5041.
58. Cameron, T. S.; Krossing, I.; Passmore, J. *Inorg. Chem.* **2001**, *40*, 2001.
59. (a) Golden, J. H.; Mutolo, P. F.; Lobrovski, E. B.; DiSalvo, F. J. *Inorg. Chem.* **1994**, *33*, 5374. (b) Fujiki, K.; Ikeda, S.; Kobayashi, H.; Mori, A.; Nagira, A.; Nie, J.; Sonoda, T.; Yagupolskii, Y. *Chem. Lett.* **2000**, *29*, 66.
60. (a) Reed, C. A. *Acc. Chem. Res.* **1998**, *31*, 133. (b) Shelly, K.; Reed, C. A.; Lee, Y. J.; Scheidt, W. R. *J. Am. Chem. Soc.* **1986**, *108*, 3117.
61. Chen, E. Y.-X.; Marks, T. J. *Chem. Rev.* **2000**, *100*, 1391.
62. Kita, F.; Sakata, H.; Kawakami, A.; Kamizori, H.; Sonoda, T.; Nagashima, H.; Pavlenko, N. V.; Yagupolskii, Y. *J. Power Sources* **2001**, *97*, 581.
63. (a) LeSuer, J. J.; Geiger, W. E. *Angew. Chem. Int. Ed.* **2000**, *39*, 248. (b) Camire, N.; Nafady, A.; Geiger, W. E. *J. Am. Chem. Soc.* **2002**, *124*, 7260.
64. (a) Krossing, I.; Raabe, I. *Angew. Chem. Int. Ed.* **2004**, *43*, 2066. (b) Stasko, D.; Reed, C. A. *J. Am. Chem. Soc.* **2002**, *124*, 1148.
65. (a) Kim, K.-C.; Reed, C. A.; Elliot, D. W.; Mueller, L. J.; Tham, F.; Lin, L.; Lambert, J. B. *Science* **2002**, *297*, 825. (b) Reed, C. A. *Chem. Commun.* **2005**, 1669. (c) Kato, T.; Reed, C. A. *Chem. Commun.* **2004**, 2908. (d) Reed, C. A. *Acc. Chem. Res.* **1998**, *31*, 325.

66. (a) Reed, C. A.; Kim, K.-C.; Bolskar, R. D.; Mueller, L. J. *Science* **2000**, *289*, 101. (b) Reed, C. A.; Kim, K.-C.; Stoyonov, D.; Stasko, F. S.; Tham, L. J.; Mueller, P. D.; Boyd, W. *J. Am. Chem. Soc.* **2003**, *125*, 1796.
67. (a) Reed, C. A.; Fackler, N. L. P.; Kim, K.-C.; Stasko, D.; Evans, D. R.; Mueller, L. J.; Boyd, P. D.; Rickard, C. E. F. *J. Am. Chem. Soc.* **1999**, *121*, 6314. (b) Bolskar, R. D.; Mathur, R. S.; Reed, C. A. *J. Am. Chem. Soc.* **1996**, *118*, 13093. (c) Reed, C. A. *Accounts of Chemical Research* **2010**, *43*, 121. (d) Reed, C. A.; Kim, K.-C.; Bolskar, R. D.; Mueller, L. J. *Science* **2000**, *289*, 101.
68. Gu, W.; McCulloch, B. J.; Reibenspies, J. H.; Ozerov, O. V. *Chem. Commun.* **2010**, *46*, 2820.
69. Ivanov, S. V.; Rockwell, J. J.; Polyakov, O. G.; Guadinski, C. M.; Anderson, O. P.; Solntsis, K. A.; Strauss, S. H. *J. Am. Chem. Soc.* **1998**, *120*, 4224.
70. Xie, Z.; Tsang, C.; Sze, E. T.; Yang, Q.; Chan, D. T. W.; Mak, T. C. W. *Inorg. Chem.* **1998**, *37*, 6444.
71. Peymann, T.; Herzog, A.; Knobler, C. B.; Hawthorne, M. F. *Angew. Chem. Int. Ed.* **1999**, *39*, 1061.
72. King, B. T.; Janousek, Z.; Grüner, B.; Trammell, M.; Noll, B. C.; Michl, J. *J. Am. Chem. Soc.* **1996**, *118*, 3313.
73. Fete, M. G. PhD. Dissertation, University of Colorado, Boulder, CO, 2006.
74. Knoth, W. H. *Inorg. Chem.* **1971**, *10*, 598.
75. Ramírez-Contreras, R.; Ozerov, O. V. *Dalton Trans.* **2012**, *41*, 7842.
76. Connelly, N. G.; Geiger, W. E. *Chem. Rev.* **1996**, *96*, 877.
77. Wawzonek, S.; Thelen, P. J. *J. Am. Chem. Soc.* **1950**, *72*, 2118.
78. Jahn, U.; Aussieker, S. *Org. Lett.* **1999**, *1*, 849.
79. Bellville, D. J.; Wirth, D. D.; Bauld, N. L. *J. Am. Chem. Soc.* **1981**, *103*, 718.
80. (a) Yueh, W.; Bauld, N. L. *J. Am. Chem. Soc.* **1995**, *117*, 5671. (b) Dinnocenzo, J. P.; Conlon, D. A. *J. Am. Chem. Soc.* **1988**, *110*, 2324.
81. Lopez, L.; Troisi, L. *Tetrahedron Lett.* **1989**, *30*, 3097.

82. Kim, K.-C.; Hauke, F.; Hirsch, A.; Boyd, P. D.; Carter, E.; Armstrong, R. S.; Lay, P. A.; Reed, C. A. *J. Am. Chem. Soc.* **2003**, *125*, 4024.
83. (a) Nelsen, S. F. *Acc. Chem. Res.* **1987**, *20*, 269. (b) Mirafzal, G. A.; Liu, J.; Bauld, N. L. *J. Am. Chem. Soc.* **1993**, *115*, 6072. (c) Hoffmann, R. W.; Barth, W. *J. Chem. Soc., Chem. Commun.* **1983**, 345. (d) Bauld, N. L.; Bellville, D. J.; Harirchian, B.; Lorenz, K. T.; Pabon, R. A., Jr.; Reynolds, D. W.; Wirth, D. D.; Chiou, H.-S.; Marsh, B. K. *Acc. Chem. Res.* **1987**, *20*, 371. (e) Bauld, N. L. *Tetrahedron* **1989**, *45*, 5307. (f) Mattay, J.; Trampe, G.; Runsink, J. *Chem. Ber.* **1988**, *121*, 1991.
84. (a) Steckhan, S. D. E.; Brinkhaus, K.-H.; Esch, T. *Chem. Ber.* **1991**, *124*, 2557. (b) Schmidt, W.; Steckhan, E. *Chem. Ber.* **1980**, *113*, 577.
85. (a) Douvris, C.; Ozerov, O. V. *Science* **2008**, *321*, 1188. (b) Ramírez-Contreras, R.; Bhuvanesh, N.; Zhou, J.; Ozerov, O. V. *Angew. Chem. Int. Ed.* **2013**, *52*, 10313.
86. Boehm, H.-J.; Banner, D.; Bendels, S.; Kansy, M.; Kuhn, B.; Mueller, K.; Obst-Sander, U.; Stahl, M. *ChemBioChem* **2004**, *5*, 637.
87. (a) Yamamoto, T.; Nishiyama, M.; Koie, Y. *Tetrahedron Lett.* **1998**, *39*, 2367. (b) Shi, W.; Fan, S.; Huang, F.; Yang, W.; Liu, R.; Cao, Y. *J. Mater. Chem.* **2006**, *16*, 2387. (c) Kim, G.; Basarir, F.; Yoon, T.-H. *Synth. Met.* **2011**, *161*, 2092. (d) Zhang, Y.; Yao, Q.; Ma, D. *Org. Lett.* **2012**, *14*, 3056. (e) Tlili, A.; Monnier, F.; Taillefer, M. *Chem. Commun.* **2012**, *48*, 6408. (f) Bedford, R. B. *Chem. Commun.* **2003**, 1787. (g) Hartwig, J. F. *Angew. Chem. Int. Ed.* **1998**, *37*, 2046. (h) Hartwig, J. F. *Acc. Chem. Res.* **1998**, *31*, 852. (i) Wolfe, J. P.; Wagaw, S.; Marcoux, J. F.; Buchwald, S. L. *Acc. Chem. Res.* **1998**, *31*, 805.
88. Surry, D. S.; Buchwald, S. L. *J. Am. Chem. Soc.* **2007**, *129*, 10354.
89. Gritzner, G.; Kuta, J. *Pure. Appl. Chem.* **1984**, *56*, 461.
90. (a) Deprez, N. R.; Sanford, M. S. *Inorg. Chem.* **2007**, *46*, 1924. (b) Kita, Y.; Egi, M.; Okajima, A.; Ohtsubo, M.; Takada, T.; Tohma, H. *Chem. Commun.* **1996**, 1491. (c) Kita, Y.; Tohma, H.; Inagaki, M.; Hatanaka, K.; Yakura, T. *Tetrahedron Lett.* **1991**, *32*, 4321. (d) Kita, Y.; Tohma, H.; Inagaki, M.; Hatanaka, K.; Yakura, T. *J. Am. Chem. Soc.* **1994**, *116*, 3684. (e) Dohi, T.; Ito, M.; Yamaoka, N.; Morimoto, K.; Fujioka, H.; Kita, Y. *Tetrahedron* **2009**, *65*, 10797.
91. (a) Kita, Y.; Egi, M.; Ohtsubo, M.; Saiki, T.; Takada, T.; Tohma, H. *Chem. Commun.* **1996**, 2225. (b) Kita, Y.; Gyoten, M.; Ohtsubo, M.; Tohma, H.; Hatanaka, K.; Takada, T. *Chem. Commun.* **1996**, 1481. (c) Takada, T.; Arisawa,

- M.; Gyoten, M.; Hamada, R.; Tohma, H.; Kita, Y. *J. Org. Chem.* **1998**, *63*, 7698. (d) Arisawa, M.; Utsumi, S.; Nakajima, M.; Ramesh, N. G.; Tohma, H.; Kita, Y. *Chem. Commun.* **1999**, 469. (e) Tohma, H.; Morioka, H.; Takizawa, S.; Arisawa, M.; Kita, Y. *Tetrahedron* **2001**, *57*, 345.
92. Kita, Y.; Watanabe, H.; Egi, M.; Saiki, T.; Fukuoka, Y.; Saiki, T.; Okajima, A.; Takada, T.; Tohma, H. *J. Chem. Soc., Perkin. Trans.* **1998**, *1*, 635.
93. (a) Marcinek, A. *J. Phys. Chem.* **1998**, *102*, 7761. (b) Carter, M. K.; Vincow, G. *J. Chem. Phys.* **1967**, *47*, 302. (c) Bally, T.; Matzinger, S.; Badnarek, P. *J. Am. Chem. Soc.* **2006**, *128*, 7828.
94. (a) Stephens, P. J.; Devlin, F. J.; Chabalowski, C. F.; Frisch, J. *J. Phys. Chem.* **1994**, *98*, 11623. (b) Becke, A. D. *J. Chem. Phys.* **1993**, *98*, 5648. (c) Lee, C.; Yang, W.; Parr, R. G. *Phys. Rev. B*, **1988**, *37*, 785. (d) Vosko, S. H.; Wilk, L.; Nusair, M. *Can. J. Phys.* **1980**, *58*, 1200.
95. Brockway, L. O.; Roberston, J. M. *J. Am. Chem. Soc.* **1939**, *61*, 1324.
96. Kumar, M.; Srivastava, M.; Yadav, R. A. *Spectrochim. Acta* **2013**, *A*, 242.
97. Murahashi, T.; Kurosawa, H. *Coord. Chem. Rev.* **2002**, *231*, 207.
98. (a) Bloom, K. S.; Alexanian, E. J. *J. Am. Chem. Soc.* **2010**, *132*, 12823. (b) Bloom, K. S.; Alexanian, E. J. *J. Am. Chem. Soc.* **2011**, *133*, 20146.
99. Zeller, E.; Schier, A.; Schmidbaur, H. *Z. Naturforsch., B* **1994**, *49*, 1243.
100. Tanaka, M. *Acta. Cryst.* **1992**, *C48*, 739.
101. (a) Seidel, S.; Seppelt, K. *Science* **2000**, *290*, 117. (b) Elder, S. H.; Lucier, G. M.; Hollander, R. J.; Bartlett, N. *J. Am. Chem. Soc.* **1997**, *119*, 1020. (c) Herring, F. G.; Hwang, G.; Lee, K. C.; Mistry, F.; Phillips, P. S.; Willner, H.; Aubke, F. *J. Am. Chem. Soc.* **1992**, *114*, 1271. (d) Blake, A. J.; Gould, R. O.; Greig, J. A.; Holder, A. J.; Hyde, T. I.; Schöder, M. *J. Chem. Soc., Chem. Commun.* **1989**, 876. (e) Greig, J. A.; Holder, A. J.; Hyde, T. I.; Tayler, A.; Schöder, M. *Angew. Chem. Int. Ed.* **1990**, *29*, 197.
102. Sladek, A.; Schmidbaur, H. *Z. Naturforsch., B* **1995**, *50*, 859.
103. POV-Ray-Persistence of Vision Raytracer, available at <http://www.povray.org/>.
104. Farugia, L. J. *J. Appl. Cryst.* **1997**, *30*, 565.

105. (a) Binkley, J. S.; Pople, J. A.; Hehre, W. J. *J. Am. Chem. Soc.* **1980**, *102*, 939. (b) Gordon, M. S.; Binkley, J. S.; Pople, J. A.; Pietro, W. J.; Hehre, W. J. *J. Am. Chem. Soc.* **1982**, *104*, 2797. (c) Dobbs, K. D.; Hehre, W. J. *J. Comput. Chem.* **1986**, *7*, 359. (d) Dobbs, K. D.; Hehre, W. J. *J. Comput. Chem.* **1987**, *8*, 861. (e) Dobbs, K. D.; Hehre, W. J. *J. Comput. Chem.* **1987**, *8*, 880.
106. King, B. T.; Korbe, S. K.; Schreiber, P. J.; Clayton, J.; Němcová, A.; Havlas, Z.; Vyakaranam, K.; Fete, M. G.; Zharov, I.; Ceremuga, J.; Michl, J. *J. Am. Chem. Soc.* **2007**, *129*, 12960.
107. APEX2, Version 2 User Manual, M86-E01078, Bruker Analytical X-ray Systems, Madison, WI, June 2006.
108. Sheldrick, G. M. *Acta. Cryst.* **2008**, *A64*, 112.
109. Heyduk, A. F.; Zarkesh, R. A.; Nguyen, A. I. *Inorg. Chem.* **2011**, *50*, 9849.
110. Radosevich, A. T.; Melnick, J. G.; Stoian, S. A.; Bacciu, D.; Chen, C.-H.; Foxman, B. M.; Ozerov, O. V. *Inorg. Chem.* **2009**, *48*, 9214.
111. Adhikari, D.; Mossin, S.; Basuli, F.; Huffman, J. C.; Szilagi, R. K.; Meyer, K.; Mindiola, D. J. *J. Am. Chem. Soc.* **2008**, *130*, 3676.
112. Madhira, B. N.; Ren, P.; Vechorkin, O.; Hu, X.; Vicic, D. A. *Dalton Trans.* **2012**, *41*, 7915.
113. Kieltsch, I.; Dubinina, G. G.; Hamacher, C.; Kaiser, A.; Torres-Nieto, J.; Hutchinson, J. M.; Klein, A.; Budnikova, Y.; Vicic, D. A. *Organometallics* **2010**, *29*, 1451.
114. (a) Ozerov, O. V.; Guo, C.; Papkov, V. A.; Foxman, B. M. *J. Am. Chem. Soc.* **2004**, *126*, 4792. (b) Ozerov, O. V.; Guo, C.; Fan, L.; Foxman, B. M. *Organometallics* **2004**, *23*, 5573. (c) Fan, L.; Yang, L.; Guo, C.; Foxman, B. M.; Ozerov, O. V. *Organometallics* **2004**, *23*, 4778. (d) Winter, A. M.; Eichele, K.; Mach, H.-G.; Potuznik, S.; Mayer, H. A.; Kaska, W. C. *J. Organomet. Chem.* **2003**, *682*, 142. (e) Liang, L.-C.; Lin, J.-M.; Hung, C.-H. *Organometallics* **2003**, *22*, 3007. (f) Harkins, S. B.; Peters, J. C. *J. Am. Chem. Soc.* **2005**, *127*, 2030. (g) Calimano, E.; Tilley, T. D. *J. Am. Chem. Soc.* **2009**, *131*, 11161. (h) Cantat, T.; Graves, C. R.; Scott, B. L.; Kiplinger, J. L. *Angew. Chem. Int. Ed.* **2009**, *48*, 3681. (i) Whited, M. T.; Grubbs, R. H. *Acc. Chem. Res* **2009**, *42*, 1607.
115. (a) Liang, L.-C. *Coord. Chem. Rev.* **2006**, *250*, 1152. (b) Ozerov, O. V. *The Chemistry of Pincer Compounds*; Morales-Morales, D., Ed.; Elsevier: Amsterdam, 2007, p 287.

116. Harkins, S. B.; Peters, J. C. *J. Am. Chem. Soc.* **2004**, *126*, 2885.
117. (a) Hollas, A. M. G., W.; Bhuvanesh, N.; Ozerov, O. V. *Inorg. Chem.* **2011**, *50*, 3673. (b) Csok, Z.; Vechorkin, O.; Harkins, S. B.; Scopelliti, R.; Hu, X. *J. Am. Chem. Soc.* **2008**, *130*, 8156.
118. (a) Herbert, D. E.; Ozerov, O. V. *Organometallics* **2011**, *30*, 6641. (b) Lansing, R. G.; Goldberg, K. I.; Kemp, R. A. *Dalton Trans.* **2011**, *40*, 8950.
119. Liang, L.-C.; Chien, P.-S.; Lee, P.-Y. *Organometallics* **2008**, *27*, 3082.
120. Huang, M.-H.; Liang, L.-C. *Organometallics* **2004**, *23*, 2813.
121. *NIST Chemistry Handbook*. <http://webbook.nist.gov/chemistry>.
122. Salem, H.; Ben-David, Y.; Shimon, L. J. W.; Milstein, D. *Organometallics* **2006**, *25*, 2292.
123. Crocker, C. E., R. J.; Mrkham, R.; Moulton, C. J.; Odell, K. J.; Shaw, B. L. *J. Am. Chem. Soc.* **1980**, *102*, 4373.
124. Feller, M.; Diskin-Posner, Y.; Shimon, L. J. W.; Ben-Ari, E.; Milstein, D. *Organometallics* **2012**, *31*, 4083.
125. (a) Gusev, D. G. *Organometallics* **2009**, *28*, 6458. (b) Gusev, D. G. *Organometallics* **2009**, *28*, 763.
126. Valyaev, D. A.; Brousses, R.; Lugan, N.; Fernández, I.; Sierra, M. A. *Chem. Eur. J.* **2011**, *17*, 6602.
127. Cooney, K. D.; Cundari, T. R.; Hoffman, N. W.; Pittard, K. A.; Temple, M. D.; Zhao, Y. *J. Am. Chem. Soc.* **2002**, *125*, 4318.
128. (a) Yanagisawa, S.; Sudo, T.; Noyori, R.; Itami, K. *J. Am. Chem. Soc.* **2006**, *128*, 11748. (b) Yanagisawa, S.; Sudo, T.; Noyori, R.; Itami, K. *Tetrahedron* **2008**, *63*, 6073.
129. (a) Esswin, A. J.; Veige, A. S.; Nocera, D. G. *J. Am. Chem. Soc.* **2005**, *127*, 16641. (b) Powers, D. C.; Chambers, M. B.; Teets, T. S.; Elgrishi, N.; Anderson, B. L.; Nocera, D. G. *Chem. Sci.* **2013**, *4*, 2880.
130. Munhá, R. F.; Zarkesh, R. A.; Heyduk, A. F. *Inorg. Chem.* **2013**, *52*, 11244.

131. (a) Mclean, D. A.; Chandler, G. S. *J. Chem. Phys.* **1980**, *72*, 5639. (b) Raghavachari, K.; Binkley, J. S.; Pople, J. A. *J. Chem. Phys.* **1980**, *72*, 650.
132. Frisch, J.; Pople, J. A. *J. Chem. Phys.* **1984**, *72*, 5639.
133. Raghavachari, K.; Binkley, J. S.; Seeger, R.; Pople, J. A. *J. Chem. Phys.* **1980**, *72*, 650.
134. (a) Ditchfield, R.; Hehre, W. J.; Pople, J. A. *J. Chem. Phys.* **1971**, *54*, 724. (b) Hehre, W. J.; Ditchfield, R.; Pople, J. A. *J. Chem. Phys.* **1972**, *56*, 2257. (c) Francl, M. M.; Pietro, W. J.; Hehre, W. J.; Binkley, J. S.; DeFrees, D. J.; Pople, J. A.; Gordon, M. S. *J. Chem. Phys.* **1982**, *77*, 3654. (d) Hariharan, P. C.; Pople, J. A. *Theor. Chem. Acc.* **1973**, *28*, 213. (e) Hariharan, P. C.; Pople, J. A. *Mol. Phys.* **1974**, *27*, 209. (f) Rassolov, V. A.; Pople, J. A.; Ratner, M. A.; Windus, T. L. *J. Chem. Phys.* **1998**, *109*, 1223. (g) Rassolov, V. A.; Ratner, M. A.; Pople, J. A.; Redfern, P. C.; Curtiss, L. A. *J. Comput. Chem.* **2001**, *22*, 976. (h) Gordon, M. S. *Chem. Phys. Lett.* **1980**, *76*, 163. (i) Binning, R. C.; Curtiss, L. A.; Radom, L. *J. Chem. Phys.* **1997**, *107*, 5016.
135. Kuechle, W.; Dolge, M.; Stoll, H.; Preuss, H. *J. Chem. Phys.* **1994**, *100*, 7535.
136. Salomon, O.; Reiher, M.; A., H. B. *J. Chem. Phys.* **2002**, *117*, 4729.
137. Drew, D.; Doyle, J. R. *Inorg. Synth.* **1990**, *28*, 436.
138. Gilman, H.; Zuech, E. A. *J. Org. Chem.* **1961**, *26*, 3481.
139. Hübschle, C. B.; Sheldrick, G. M. *J. Appl. Cryst.* **2011**, *44*, 1281.
140. Spek, A. L. *J. Appl. Cryst.* **2011**, *36*, 7.
141. *FRAMBO, Program for Data Collection on Area Detectors*, v. 4.1.05; BRUKER-Nonius Inc.: Madison, WI.
142. Sheldrick, G. M. *Cell_Now, Program for Obtaining Unit Cell Constants from Single Crystal Data*, version 2008/1; University of Göttingen: Göttingen, Germany, 2008.
143. *SAINT, Program for Data Integration from Area Detector Frames*, Version 7; Bruker-Nonius Inc.: Madison, WI.
144. Altomare, A.; Cascarano, G.; Giacovazzo, G.; Guagliardi, A.; Burla, M. C.; Polidori, G.; Camalli, M. *J. Appl. Cryst.* **1994**, *27*, 435.

145. Betteridge, P. W.; Carruthers, J. R.; Cooper, R. I.; Prout, K.; Watkin, D. J. *J. Appl. Cryst.* **2003**, *36*, 1487.
146. Cooper, R. I.; Thompson, A. L.; Watkin, D. J. *J. Appl. Cryst.* **2010**, *43*, 1100.
147. (a) Spek, A. L. *Acta. Cryst.* **1990**, *A46*, C34. (b) Spek, A. L. "PLATON – A Multipurpose Crystallographic Tool", Utrecht University, Utrecht, The Netherlands, 2006
148. Dolomanov, O. V.; Bourhis, L. J.; Gildea, R. J.; Howard, J. A. K.; Puschmann, H. *J. Appl. Cryst.* **2009**, *42*, 339.
149. (a) Grundy, S. L.; Holmes-Smith, R. D.; Stobart, S. R.; Williams, M. A. *Inorg. Chem.* **1991**, *30*, 3333. (b) Zhou, J.; Stobart, S. R.; Gossage, R. A. *Inorg. Chem.* **1997**, *36*, 3745. (c) MacInnis, M. C.; MacLean, D. F.; Lundgren, R. J.; McDonald, R.; Turculet, L. *Organometallics* **2007**, *26*, 6522. (d) MacLean, D. F.; McDonald, R.; Ferguson, M. J.; Caddell, A. J.; Turculet, L. *Chem. Commun.* **2008**, 5146. (e) Ruddy, A. J.; Mitton, S. J.; McDonald, R.; Turculet, L. *Chem. Commun.* **2012**, *48*, 1159. (f) Li, Y. H.; Ding, X.-H.; Zhang, Y.; He, W.-R.; Huang, W. *Inorg. Chem. Commun.* **2012**, *15*, 194.
150. (a) Dixon, L. S. H.; Hill, A. F.; Sinha, A.; Ward, J. S. *Organometallics* **2014**, *33*, 653. (b) Tilley, T. D.; Sangtrirutnugul, P. *Organometallics* **2008**, *27*, 2223.
151. O'Reilly, M. E.; Ghiviriga, I.; Abboud, K. A.; Veige, A. S. *J. Am. Chem. Soc.* **2012**, *27*, 11185.
152. (a) Stobart, S. R.; Zhou, X.; Cea-Olivares, R.; Toscano, A. *Organometallics* **2001**, *20*, 4766. (b) Korchin, E. E.; Leitus, G.; Shimon, L. J. W.; Konstantinovski, L.; Milstein, D. *Inorg. Chem.* **2008**, *47*, 7177. (c) Garcia-Camprubi, A.; Martin, M.; Sola, E. *Inorg. Chem.* **2010**, *49*, 10649.
153. Yao, W.; Eisenstein, O.; Crabtree, R. H. *Inorg. Chim. Acta* **1997**, *254*, 105.
154. Scharf, A.; Goldberg, I.; Vigalok, A. *Inorg. Chem.* **2014**, *53*, 12.
155. Cooper, R. I.; Gould, R. O.; Parsons, S.; Watkin, D. J. *J. Appl. Cryst.* **2002**, *35*, 168.

APPENDIX A

FIGURES FROM CYCLIC VOLTAMMETRY

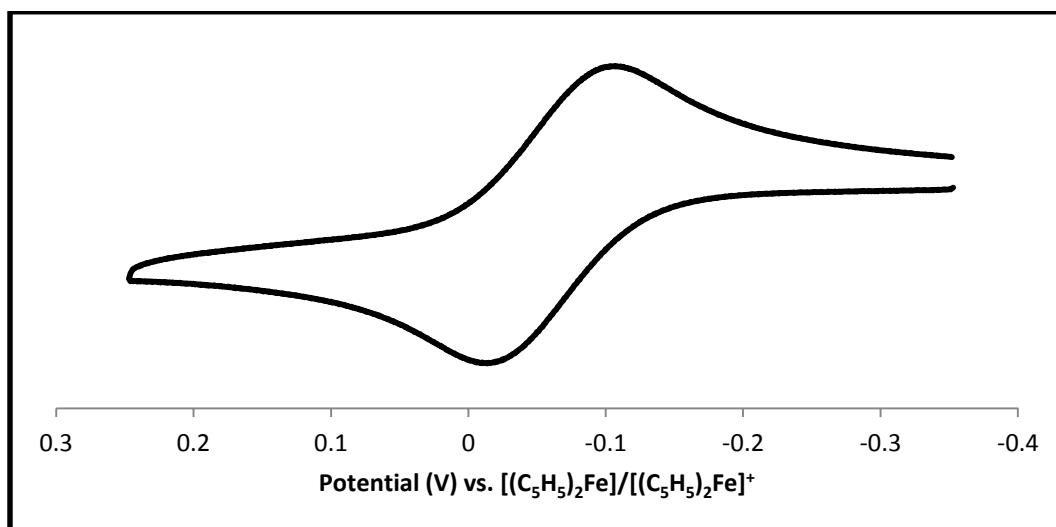


Figure A-1 Cyclic voltammogram of **3-1PdCl** in CH₂Cl₂ at 27 °C. The scan rate was 100 mV/s in the positive direction. The cyclic voltammogram was obtained with 0.3 M [Bu₄N][PF₆] as the supporting electrolyte and resulted in a measured potential ($E_{1/2}$) equal to -0.05 V.

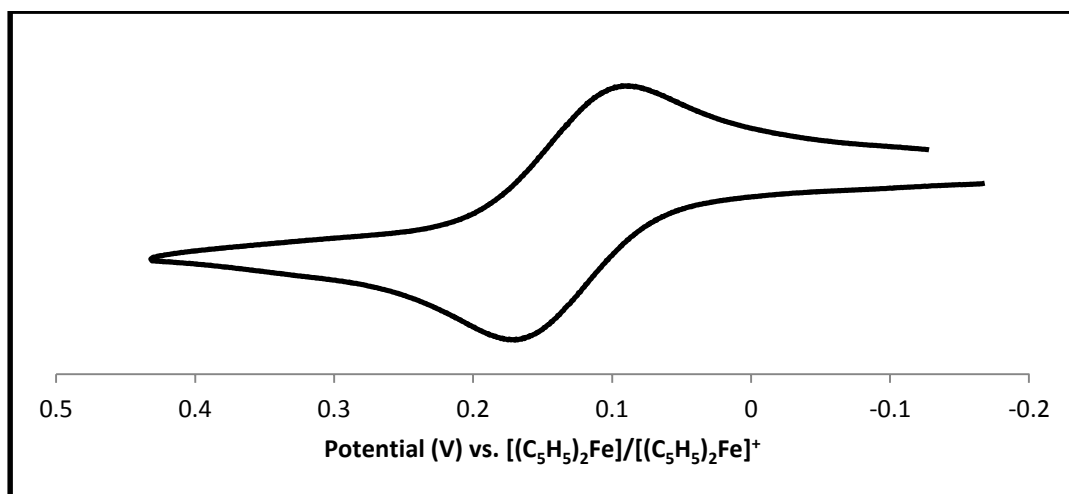


Figure A-2 Cyclic voltammogram of **3-10PdCl** in CH_2Cl_2 at $27\text{ }^\circ\text{C}$. The scan rate was 100 mV/s in the positive direction. The cyclic voltammogram was obtained with 0.3 M $[\text{Bu}_4\text{N}][\text{PF}_6]$ as the supporting electrolyte and resulted in a measured potential ($E_{1/2}$) equal to 0.13 V .

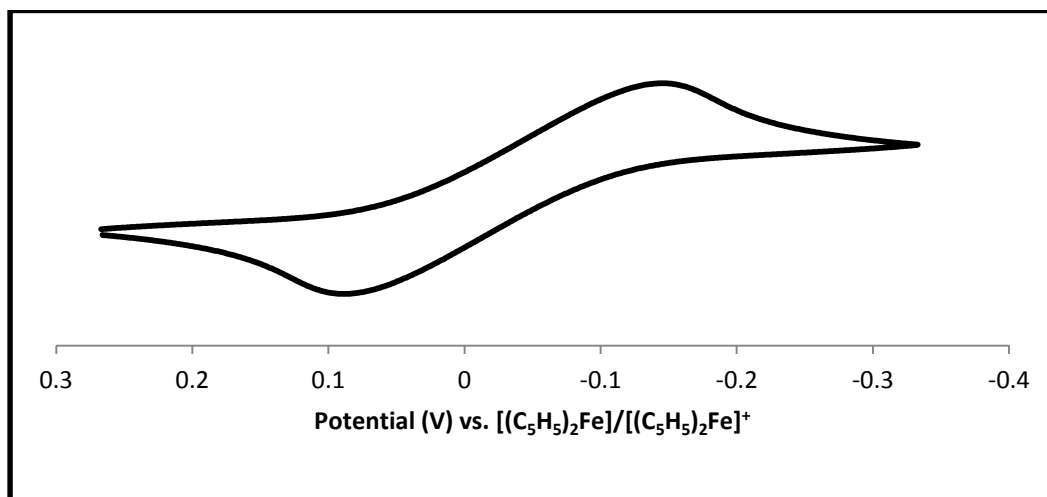


Figure A-3 Cyclic voltammogram of **3-5NiCl** in CH_2Cl_2 at $27\text{ }^\circ\text{C}$. The scan rate was 100 mV/s in the positive direction. The cyclic voltammogram was obtained with 0.3 M $[\text{Bu}_4\text{N}][\text{PF}_6]$ as the supporting electrolyte and resulted in a measured potential ($E_{1/2}$) equal to -0.01 V .

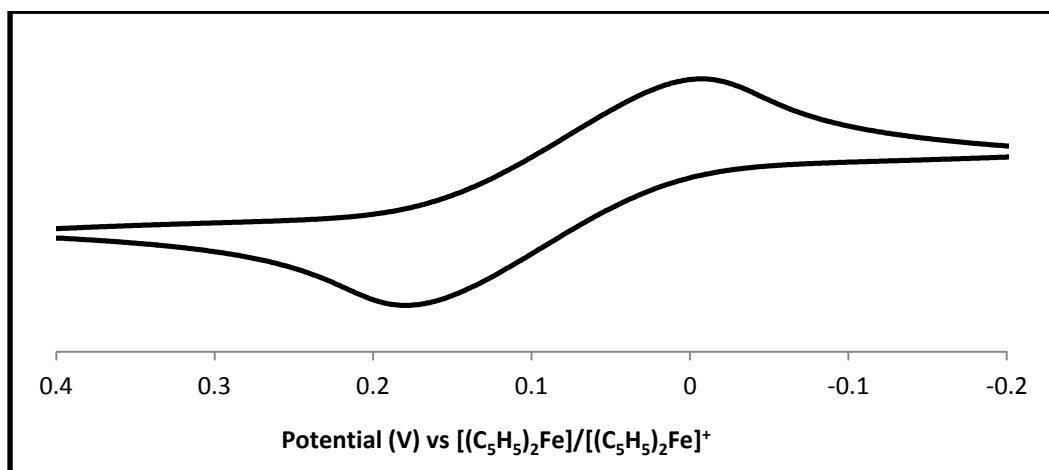


Figure A-4 Cyclic voltammogram of **3-5PdCl** in CH_2Cl_2 at 27°C . The scan rate was 100 mV/s in the positive direction. The cyclic voltammogram was obtained with 0.3 M $[\text{Bu}_4\text{N}][\text{PF}_6]$ as the supporting electrolyte and resulted in a measured potential ($E_{1/2}$) equal to 0.11 V .

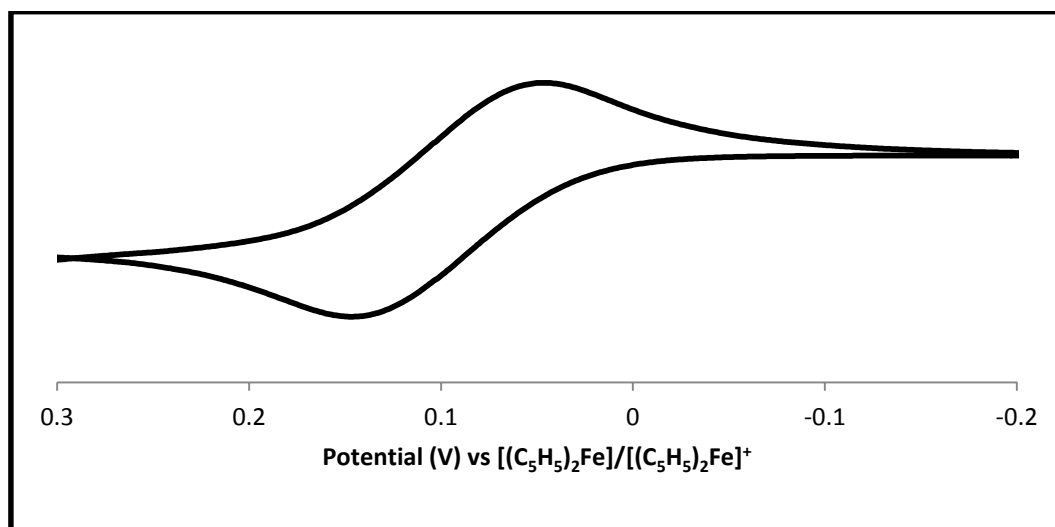


Figure A-5 Cyclic voltammogram of **3-5PtCl** in CH_2Cl_2 at 27°C . The scan rate was 100 mV/s in the positive direction. The cyclic voltammogram was obtained with 0.3 M $[\text{Bu}_4\text{N}][\text{PF}_6]$ as the supporting electrolyte and resulted in a measured potential ($E_{1/2}$) equal to 0.09 V .

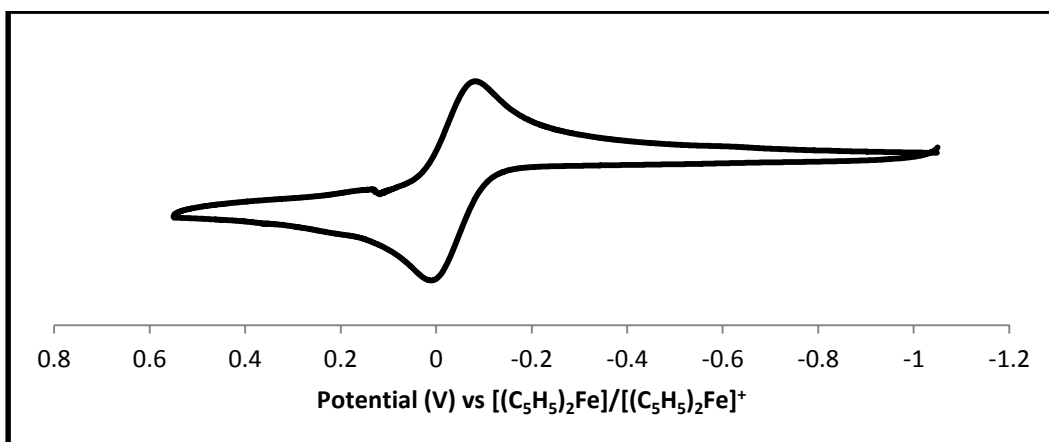


Figure A-6 Cyclic voltammogram of **3-6PdCl** in CH_2Cl_2 at $27\text{ }^\circ\text{C}$. The scan rate was 100 mV/s in the positive direction. The cyclic voltammogram was obtained with 0.3 M $[\text{Bu}_4\text{N}][\text{PF}_6]$ as the supporting electrolyte and resulted in a measured potential ($E_{1/2}$) equal to -0.02 V .

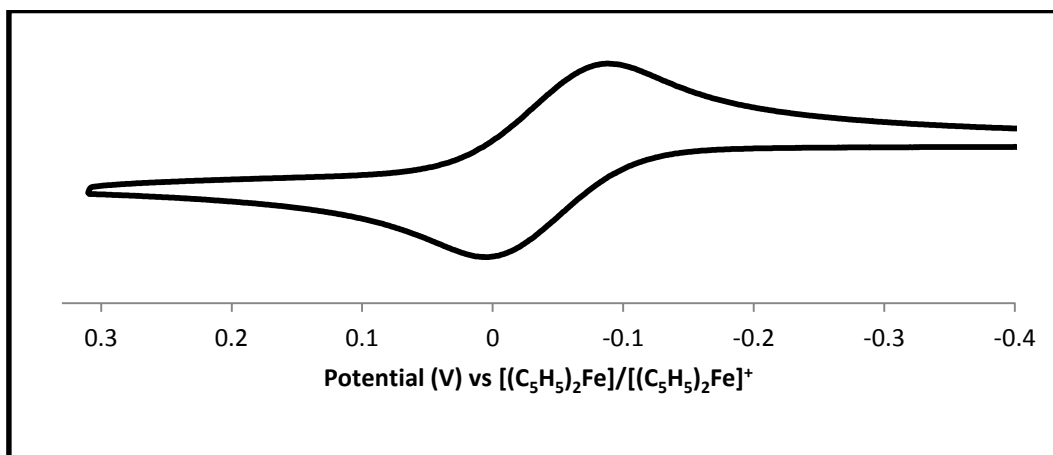


Figure A-7 Cyclic voltammogram of **3-6PtCl** in CH_2Cl_2 at $27\text{ }^\circ\text{C}$. The scan rate was 100 mV/s in the positive direction. The cyclic voltammogram was obtained with 0.3 M $[\text{Bu}_4\text{N}][\text{PF}_6]$ as the supporting electrolyte and resulted in a measured potential ($E_{1/2}$) equal to -0.05 V .

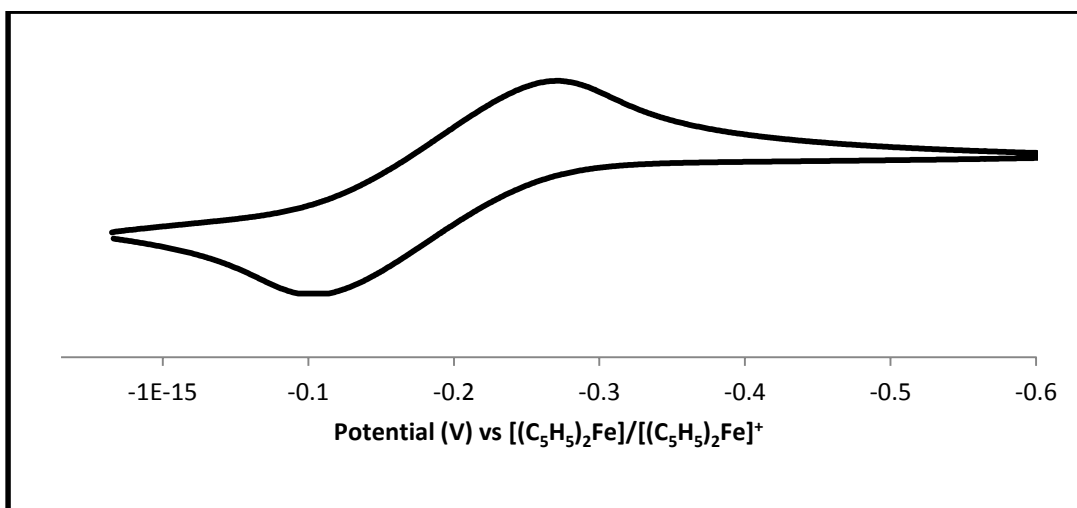


Figure A-8 Cyclic voltammogram of **3-3NiCl** in CH_2Cl_2 at $27\text{ }^\circ\text{C}$. The scan rate was 100 mV/s in the positive direction. The cyclic voltammogram was obtained with 0.3 M $[\text{Bu}_4\text{N}][\text{PF}_6]$ as the supporting electrolyte and resulted in a measured potential ($E_{1/2}$) equal to -0.19 V .

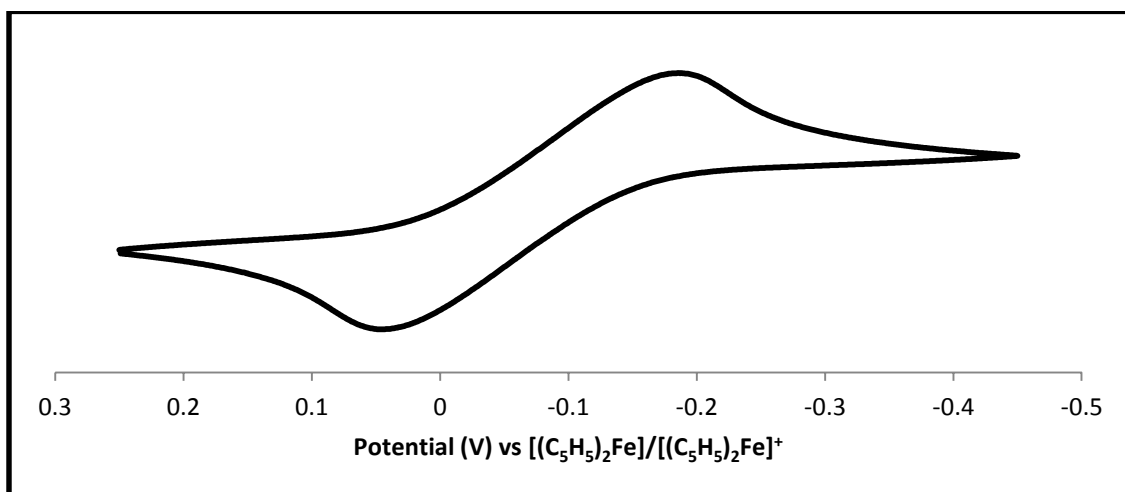


Figure A-9 Cyclic voltammogram of **3-3PdCl** in CH_2Cl_2 at $27\text{ }^\circ\text{C}$. The scan rate was 100 mV/s in the positive direction. The cyclic voltammogram was obtained with 0.3 M $[\text{Bu}_4\text{N}][\text{PF}_6]$ as the supporting electrolyte and resulted in a measured potential ($E_{1/2}$) equal to -0.07 V .

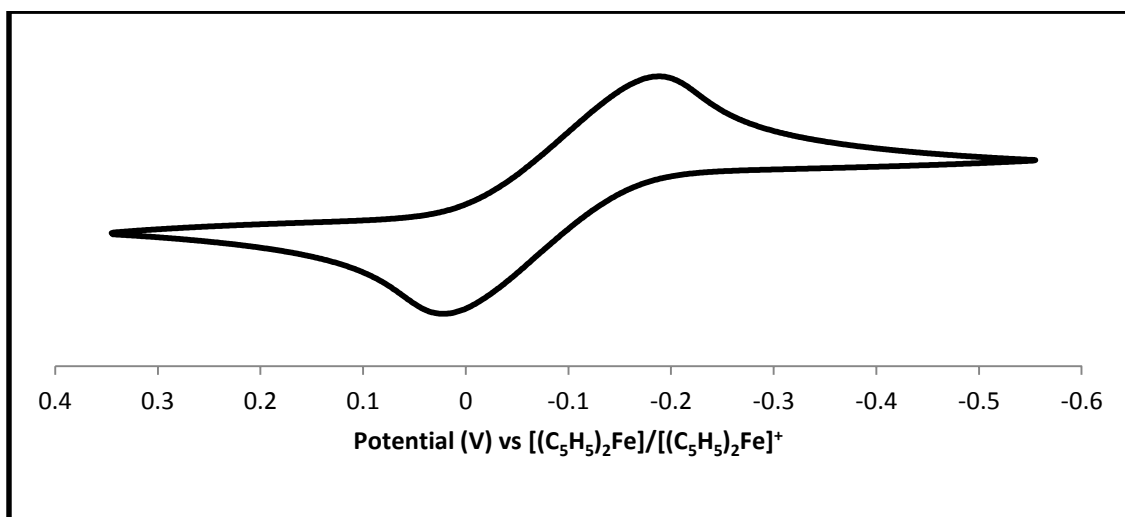


Figure A-10 Cyclic voltammogram of **3-3PtCl** in CH_2Cl_2 at $27\text{ }^\circ\text{C}$. The scan rate was 100 mV/s in the positive direction. The cyclic voltammogram was obtained with 0.3 M $[\text{Bu}_4\text{N}][\text{PF}_6]$ as the supporting electrolyte and resulted in a measured potential ($E_{1/2}$) equal to -0.11 V .

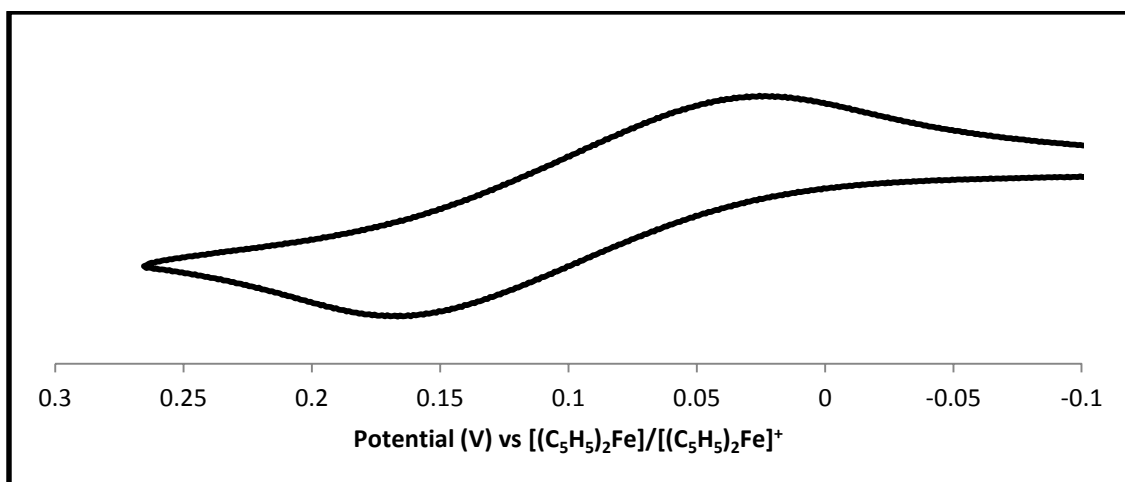


Figure A-11 Cyclic voltammogram of **3-7PdCl** in CH_2Cl_2 at $27\text{ }^\circ\text{C}$. The scan rate was 100 mV/s in the positive direction. The cyclic voltammogram was obtained with 0.3 M $[\text{Bu}_4\text{N}][\text{PF}_6]$ as the supporting electrolyte and resulted in a measured potential ($E_{1/2}$) equal to 0.09 V .

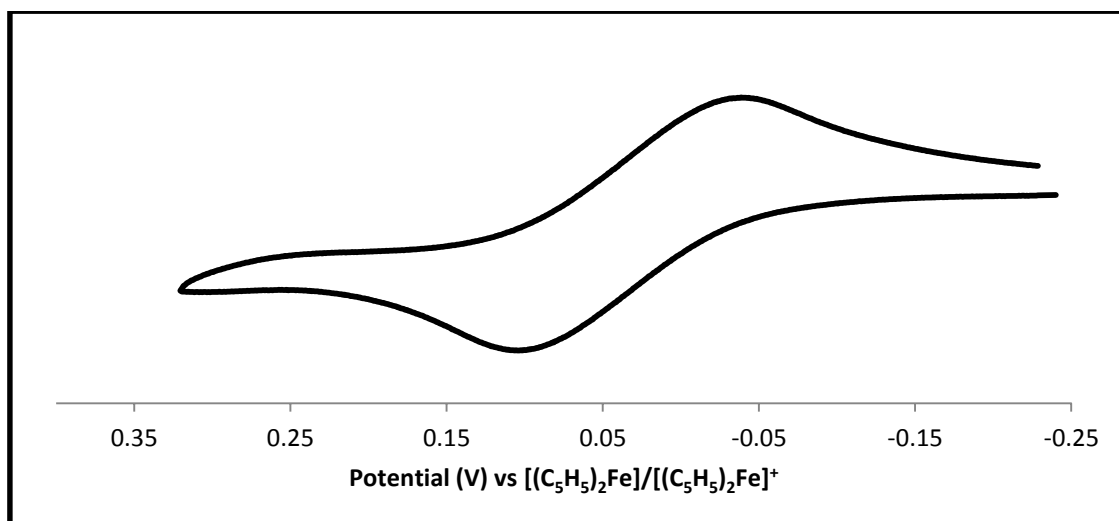


Figure A-12 Cyclic voltammogram of **3-8PdCl** in CH₂Cl₂ at 27 °C. The scan rate was 100 mV/s in the positive direction. The cyclic voltammogram was obtained with 0.3 M [Bu₄N][PF₆]₆ as the supporting electrolyte and resulted in a measured potential ($E_{1/2}$) equal to 0.04 V.

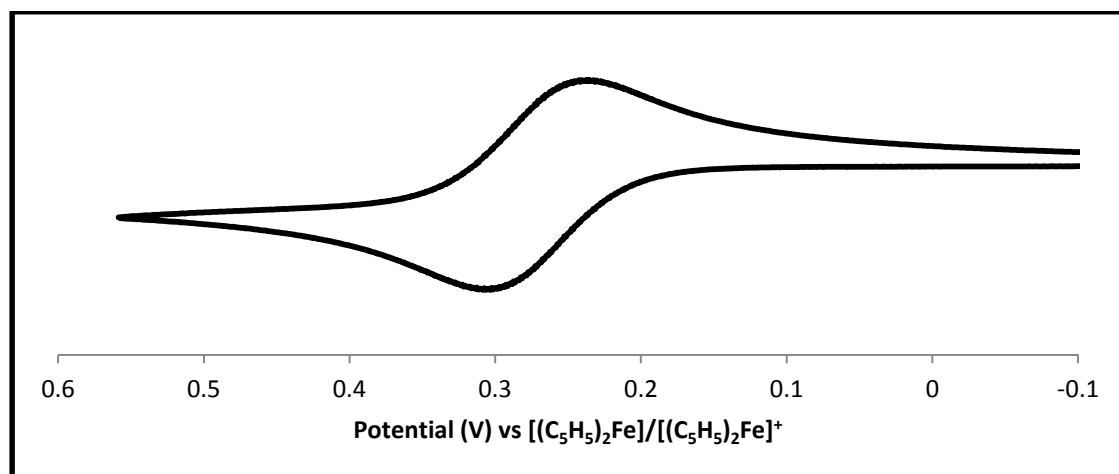


Figure A-13 Cyclic voltammogram of **3-11PdCl** in CH₂Cl₂ at 27 °C. The scan rate was 100 mV/s in the positive direction. The cyclic voltammogram was obtained with 0.3 M [Bu₄N][PF₆] as the supporting electrolyte and resulted in a measured potential ($E_{1/2}$) equal to 0.32 V.

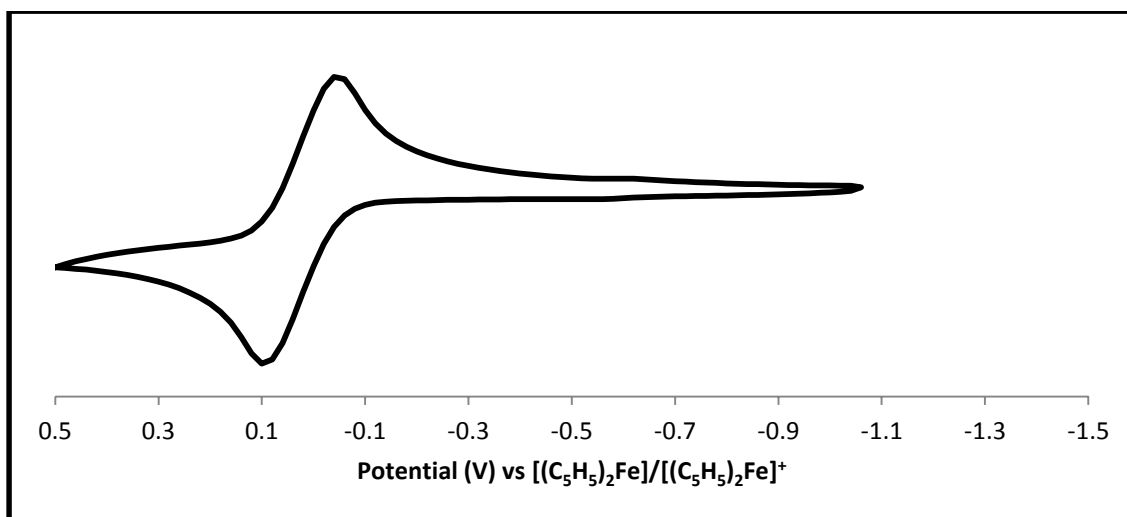


Figure A-14 Cyclic voltammogram of **3-6PdCl** in CH₂Cl₂ at 27 °C. The scan rate was 100 mV/s in the positive direction. The cyclic voltammogram was obtained with 0.3 M [Bu₄N][PF₆] as the supporting electrolyte and resulted in a measured potential ($E_{1/2}$) equal to 0.04 V.

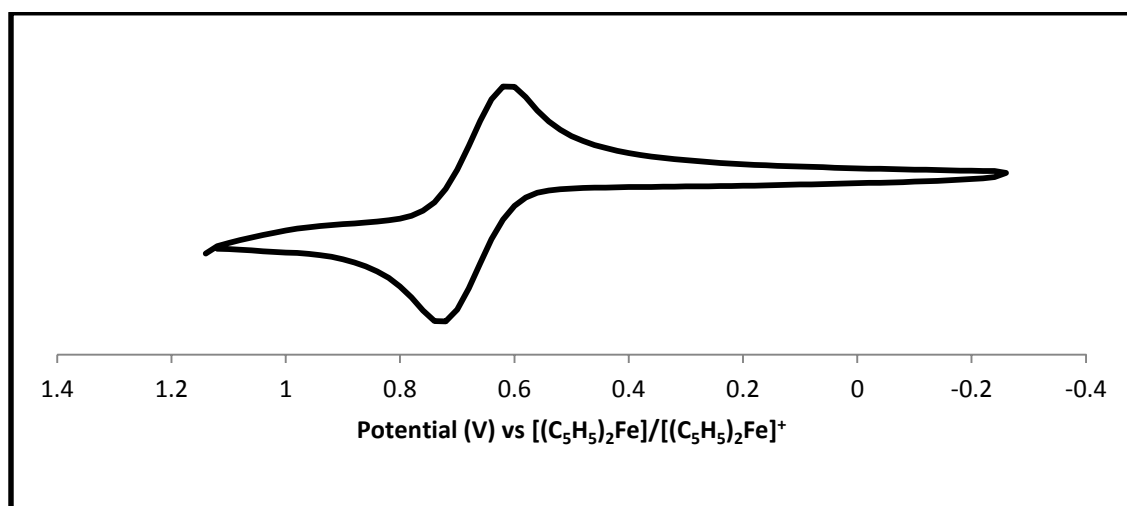


Figure A-15 Cyclic voltammogram of **3-12PdCl** in CH₂Cl₂ at 27 °C. The scan rate was 100 mV/s in the positive direction. The cyclic voltammogram was obtained with 0.3 M [Bu₄N][PF₆] as the supporting electrolyte and resulted in a measured potential ($E_{1/2}$) equal to 0.69 V.

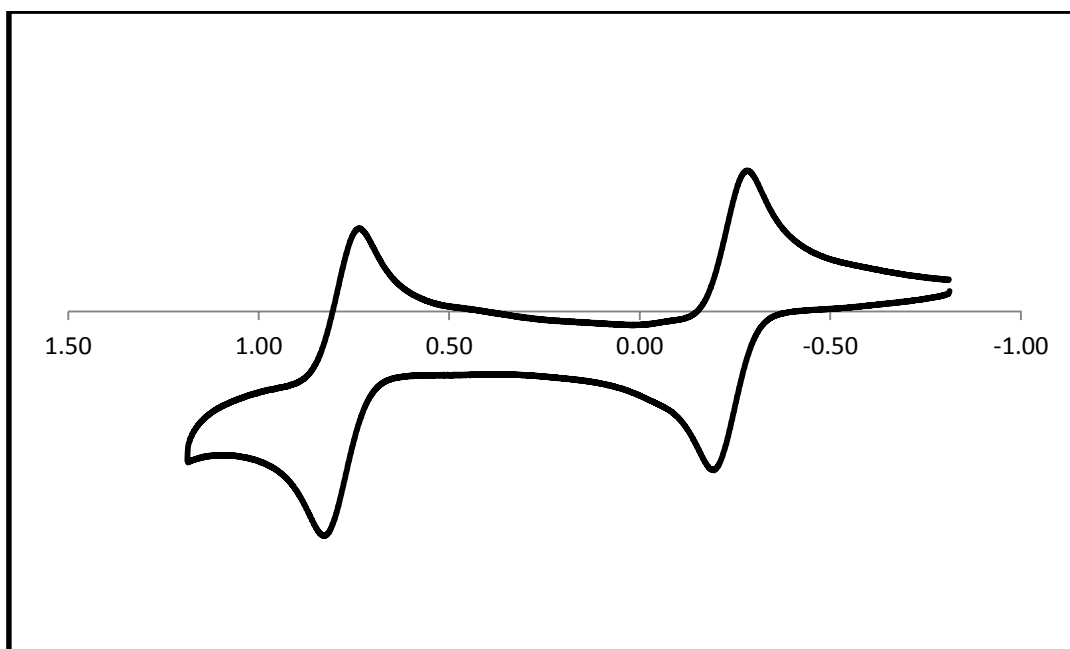


Figure A-16 Cyclic voltammogram of **3-4PdCl** in CH_2Cl_2 at 27 °C. The scan rate was 100 mV/s in the positive direction. The cyclic voltammogram was obtained with 0.3 M $[\text{Bu}_4\text{N}][\text{PF}_6]$ as the supporting electrolyte and resulted in a measured potential ($E_{1/2}$) equal to -0.24V and 0.82 V.

APPENDIX B

UV-Vis Data

Table B.1 Tabulated data regarding UV-Vis spectra of various pincer metal complexes. Each experiment was run in dichloromethane. Individual concentrations of each sample are given as well as the absorbance value at λ_{max} .

Complex	λ_{max} (nm)	ϵ ($\text{cm}^{-1}\text{M}^{-1}$)	A	M (mol/L)
3-5PtCl	375, 460	3492, 4473	1.175, 1.505	3.36×10^{-4}
3-10RhCO	513	107	0.793	2.48×10^{-3}
3-3NiCl	646	297	2.275	7.65×10^{-3}
3-5NiCl	641	NA	NA	1.00×10^{-2}
3-5PdCl	506	977	2.083	2.13×10^{-3}
3-4PdCl	512	1310	2.908	2.22×10^{-3}
3-10PdCl	447, 522	1205, 1150	1.816, 1.733	1.51×10^{-3}
3-6PdOAc	522	1343	2.908	2.17×10^{-3}
3-7PdCl	429, 537	4490, 4403	1.914, 1.877	4.26×10^{-4}
3-2PdOAc	547	718	1.693	2.36×10^{-3}

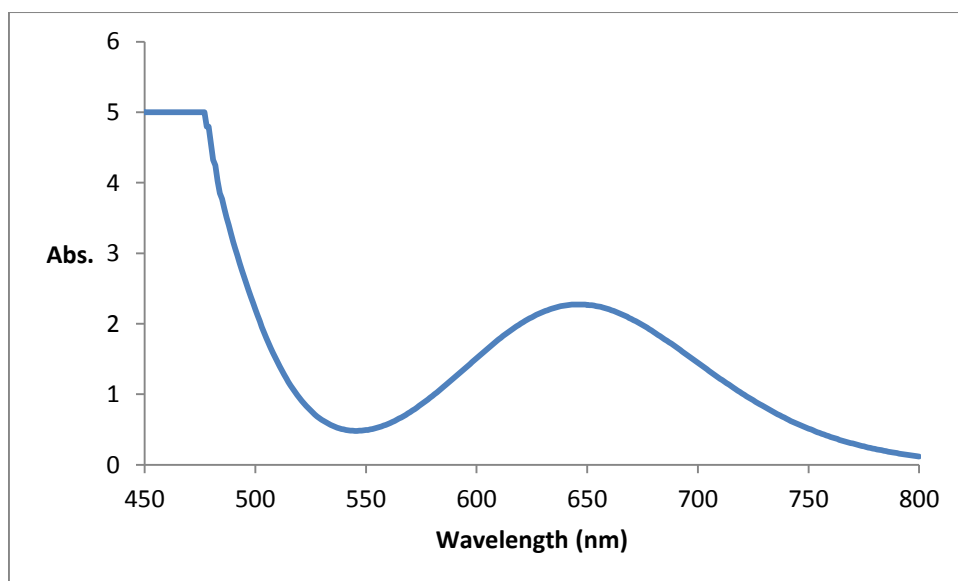


Figure B.1 UV-Vis spectrum of **3-3NiCl**. The spectrum was obtained using a 7.65×10^{-3} M sample of **3-3NiCl** in dichloromethane. λ_{max} was determined to be 646 nm. This corresponds to an ϵ value of $297 \text{ cm}^{-1}\text{M}^{-1}$.

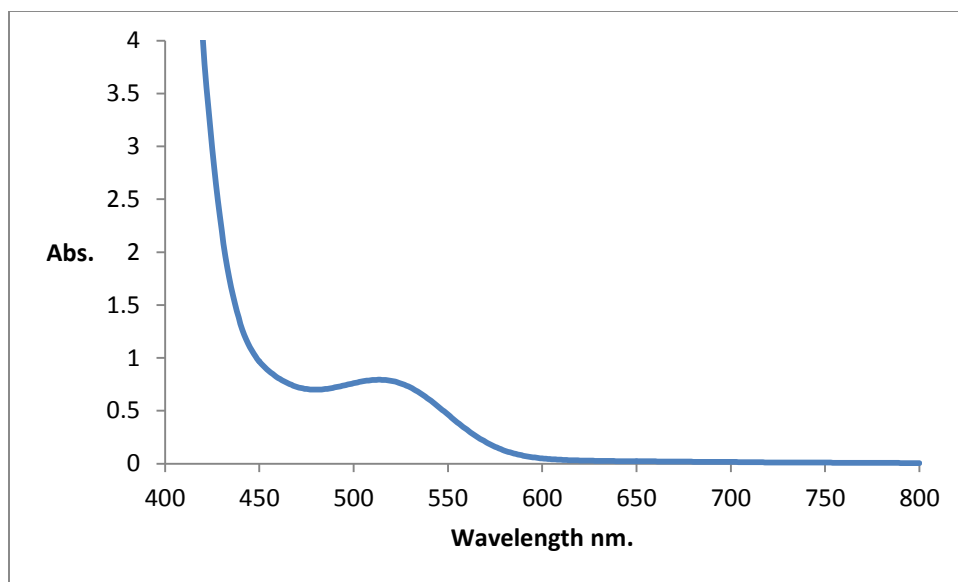


Figure B.2 UV-Vis spectrum of **3-10RhCO**. The spectrum was obtained using a 2.48×10^{-3} M sample of **3-10RhCO** in dichloromethane. λ_{max} was determined to be 513 nm. This corresponds to an ϵ value of $107 \text{ cm}^{-1}\text{M}^{-1}$.

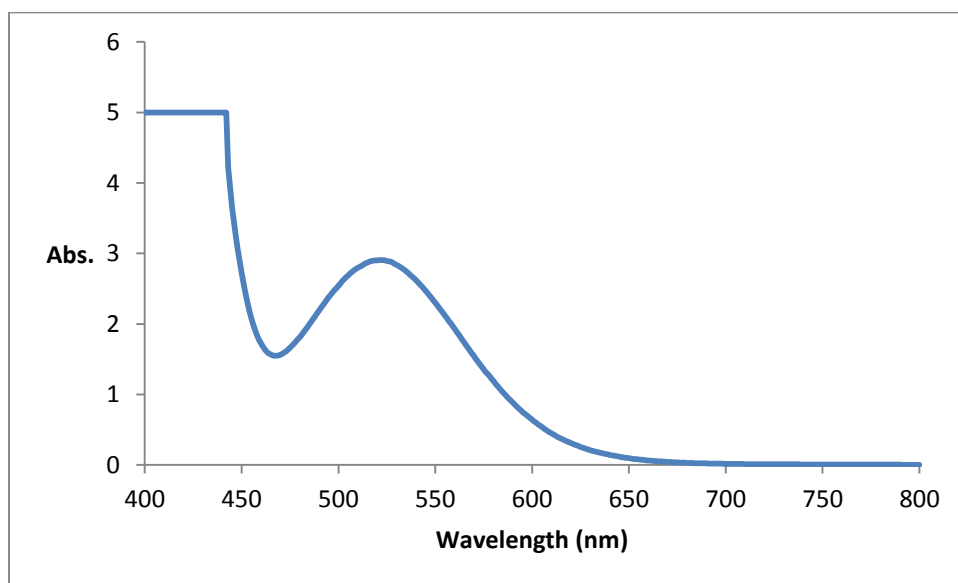


Figure B.3 UV-Vis spectrum of **3-6PdOAc**. The spectrum was obtained using a 2.17×10^{-3} M sample of **3-6PdOAc** in dichloromethane. λ_{max} was determined to be 522 nm. This corresponds to an ϵ value of $1343 \text{ cm}^{-1}\text{M}^{-1}$.

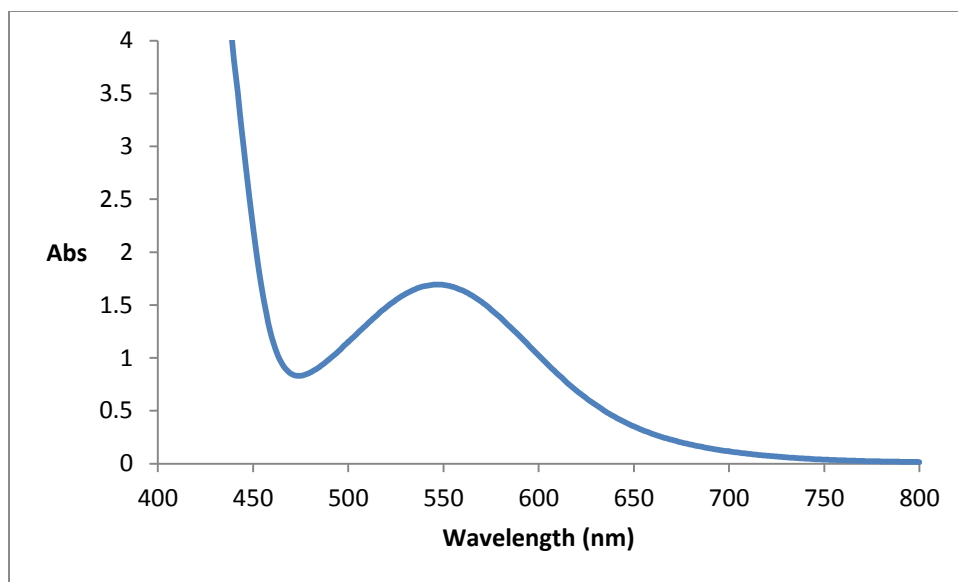


Figure B.4 UV-Vis spectrum of **3-2PdOAc**. The spectrum was obtained using a 2.36×10^{-3} M sample of **3-2PdOAc** in dichloromethane. λ_{max} was determined to be 547 nm. This corresponds to an ϵ value of $718 \text{ cm}^{-1}\text{M}^{-1}$.

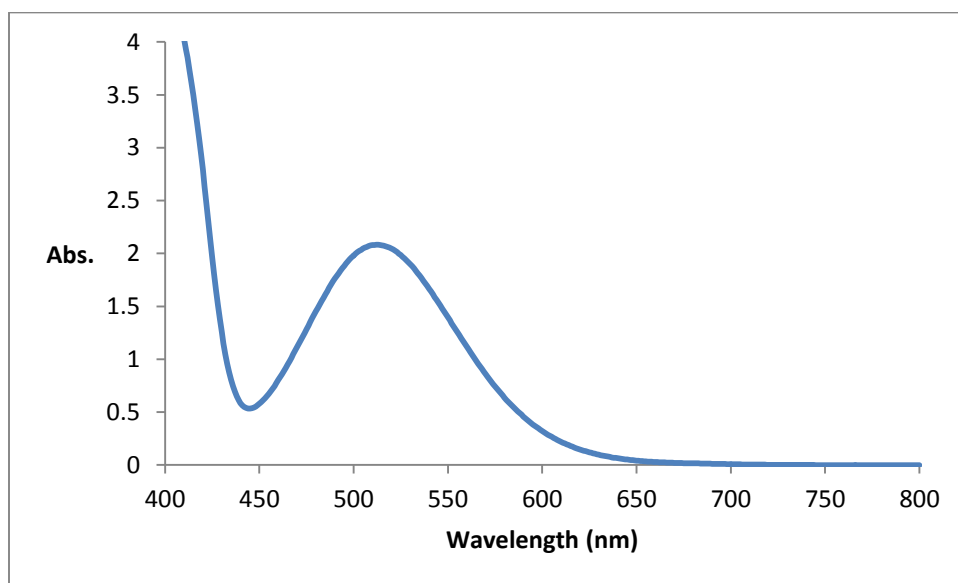


Figure B.5 UV-Vis spectrum of **3-3PdCl**. The spectrum was obtained using a 2.22×10^{-3} M sample of **3-3PdCl** in dichloromethane. λ_{max} was determined to be 512 nm. This corresponds to an ϵ value of $1310 \text{ cm}^{-1}\text{M}^{-1}$.

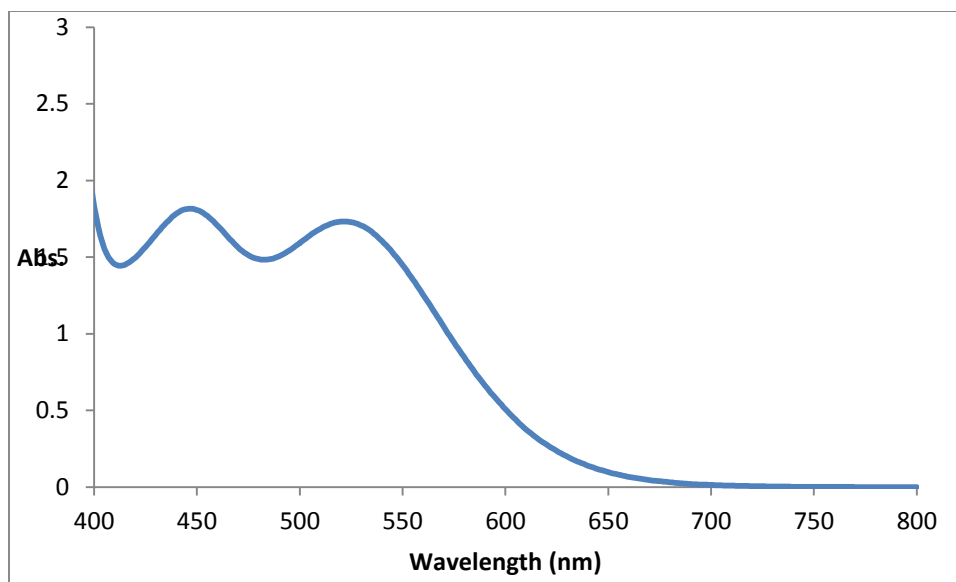


Figure B.6 UV-Vis spectrum of **3-10PdCl**. The spectrum was obtained using a 1.51×10^{-3} M sample of **3-10PdCl** in dichloromethane. λ_{max} was determined to be 447 and 522 nm. These values correspond to ϵ values of 1205 and $1150 \text{ cm}^{-1}\text{M}^{-1}$ respectively.

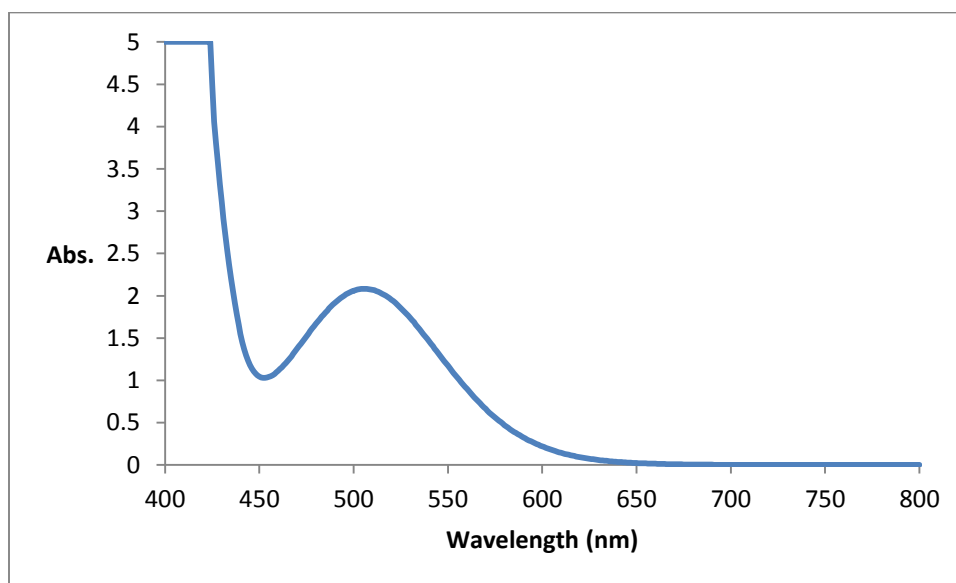


Figure B.7 UV-Vis spectrum of **3-5PdCl**. The spectrum was obtained using a 2.13×10^{-3} M sample of **3-5PdCl** in dichloromethane. λ_{max} was determined to be 506 nm. This corresponds to an ϵ value of $977 \text{ cm}^{-1}\text{M}^{-1}$.

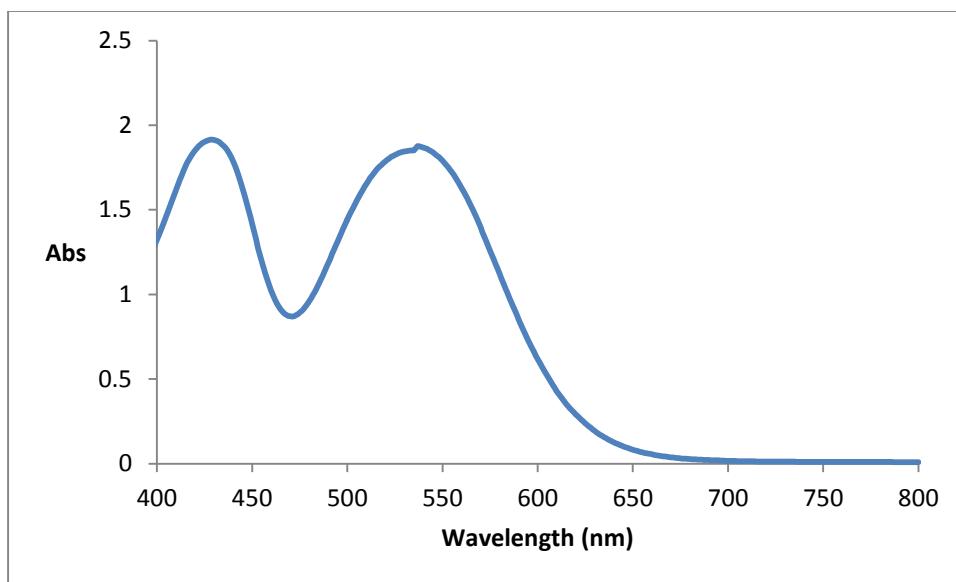


Figure B.8 UV-Vis spectrum of **3-7PdCl**. The spectrum was obtained using a 4.26×10^{-4} M sample of **3-7PdCl** in dichloromethane. λ_{max} was determined to be 429 and 537 nm. These correspond to ϵ values of 429 and 537 $\text{cm}^{-1}\text{M}^{-1}$ respectively.

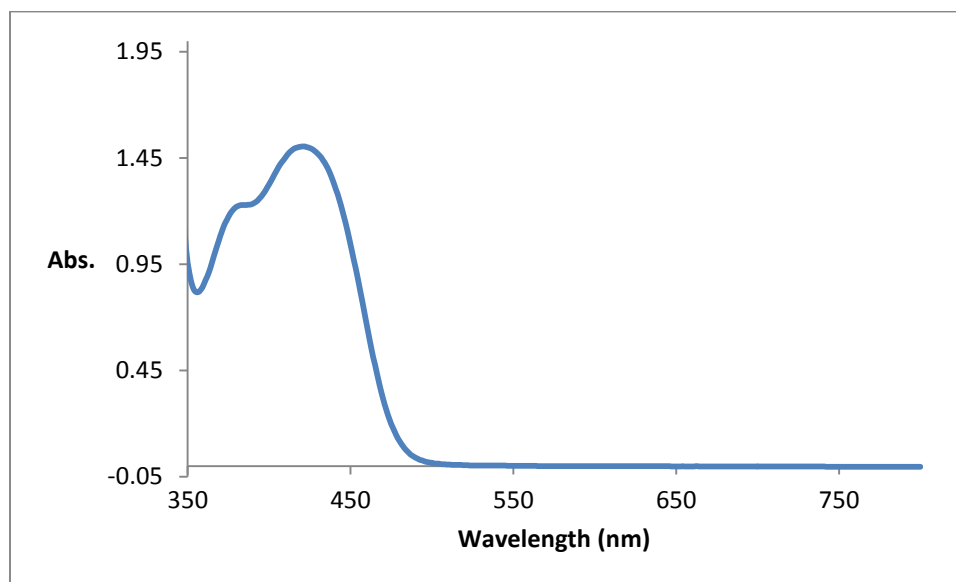


Figure B.9 UV-Vis spectrum of **3-5PtCl**. The spectrum was obtained using a 3.36×10^{-4} M sample of **3-5PtCl** in dichloromethane. λ_{max} was determined to be 375 and 460 nm. These values correspond to ϵ value of 3492 and 4473 $\text{cm}^{-1}\text{M}^{-1}$ respectively.

APPENDIX C

CAMBRIDGE CRYSTALLOGRAPHIC DATA

Compound	CCDC Identifier
4-8 (solved by Dr. Bruce Foxman and Dr. Josh Chen)	999143-999144
4-13 (solved by Dr. Bruce Foxman and Dr. Josh Chen)	999143-999143

*C.1 Crystal data for 2-31[CHB₁₁Cl₁₁]*Table 1. Crystal data and structure refinement for **2-31[CHB₁₁Cl₁₁]**

Identification code	2-31[CHB₁₁Cl₁₁]	
Empirical formula	C _{12.50} H _{27.50} Au _{0.50} B _{5.50} Cl _{5.50} P	
Formula weight	561.73	
Temperature	110.15 K	
Wavelength	0.71073 Å	
Crystal system	Orthorhombic	
Space group	P n m a	
Unit cell dimensions	a = 13.588(4) Å	α = 90°.
	b = 23.600(7) Å	β = 90°.
	c = 14.418(5) Å	γ = 90°.
Volume	4624(2) Å ³	
Z	8	
Density (calculated)	1.614 Mg/m ³	
Absorption coefficient	3.908 mm ⁻¹	
F(000)	2224	
Crystal size	0.32 × 0.2 × 0.1 mm ³	
Theta range for data collection	2.059 to 27.453°.	
Index ranges	-17 ≤ h ≤ 17, -30 ≤ k ≤ 30, -18 ≤ l ≤ 18	
Reflections collected	48524	
Independent reflections	5404 [R(int) = 0.1252]	

Completeness to theta = 25.242°	100.0 %
Absorption correction	Semi-empirical from equivalents
Max. and min. transmission	0.7456 and 0.3886
Refinement method	Full-matrix least-squares on F ²
Data / restraints / parameters	5404 / 0 / 249
Goodness-of-fit on F ²	0.960
Final R indices [I>2sigma(I)]	R1 = 0.0352, wR2 = 0.0936
R indices (all data)	R1 = 0.0466, wR2 = 0.0976
Extinction coefficient	n/a
Largest diff. peak and hole	4.576 and -1.163 e.Å ⁻³

Table 2. Atomic coordinates ($\times 10^4$) and equivalent isotropic displacement parameters ($\text{\AA}^2 \times 10^3$) for **2-31[CHB₁₁Cl₁₁]**. U(eq) is defined as one third of the trace of the orthogonalized U^{ij} tensor.

	x	y	z	U(eq)
Au(1)	5000	5000	5000	15(1)
C(1)	4148(3)	3854(2)	3697(3)	29(1)
P(1)	5899(1)	4457(1)	3943(1)	14(1)
Cl(2)	11248(1)	6745(1)	3503(1)	28(1)
C(2)	7780(3)	3878(2)	4005(3)	31(1)
C(4)	7762(3)	4910(2)	4375(3)	31(1)
C(6)	6788(3)	4621(2)	2148(3)	28(1)
Cl(3)	6958(1)	6740(1)	4277(1)	27(1)
C(13)	7062(3)	4236(2)	5497(3)	30(1)
C(3)	7173(3)	4359(2)	4451(3)	22(1)
Cl(4)	8750(1)	6276(1)	2665(1)	25(1)
Cl(5)	10855(1)	7500	5707(1)	29(1)
Cl(6)	9360(1)	6231(1)	5168(1)	29(1)
Cl(8)	8190(1)	7500	6210(1)	33(1)
Cl(7)	9852(1)	7500	1657(1)	29(1)
C(5)	5266(3)	3747(2)	3786(3)	21(1)
C(7)	5610(3)	3409(2)	2945(3)	32(1)
C(12)	5399(3)	3392(2)	4663(3)	29(1)
C(11)	6150(3)	5482(2)	2996(3)	28(1)
C(10)	4981(3)	4809(2)	2285(3)	29(1)
C(14)	8319(3)	7500	3169(3)	14(1)
C(9)	5973(3)	4847(2)	2802(2)	21(1)
B(1)	10145(3)	7124(2)	3737(3)	16(1)
B(2)	9525(4)	7500	2844(4)	15(1)
B(3)	8066(3)	7123(2)	4161(3)	16(1)
B(4)	9234(3)	6883(2)	4556(3)	17(1)
B(5)	8660(5)	7500	5058(4)	17(1)
B(6)	9955(4)	7500	4806(4)	16(1)

B(7)

8974(3)

6884(2)

3347(3)

15(1)

Table 3. Bond lengths [Å] and angles [°] for **2-31[CHB₁₁Cl₁₁]**.

Au(1)-P(1)#1	2.3361(9)
Au(1)-P(1)	2.3361(9)
C(1)-H(1A)	0.9800
C(1)-H(1B)	0.9800
C(1)-H(1C)	0.9800
C(1)-C(5)	1.546(5)
P(1)-C(3)	1.893(4)
P(1)-C(5)	1.897(4)
P(1)-C(9)	1.889(4)
Cl(2)-B(1)	1.778(4)
C(2)-H(2A)	0.9800
C(2)-H(2B)	0.9800
C(2)-H(2C)	0.9800
C(2)-C(3)	1.542(5)
C(4)-H(4A)	0.9800
C(4)-H(4B)	0.9800
C(4)-H(4C)	0.9800
C(4)-C(3)	1.532(5)
C(6)-H(6A)	0.9800
C(6)-H(6B)	0.9800
C(6)-H(6C)	0.9800
C(6)-C(9)	1.550(5)
Cl(3)-B(3)	1.763(4)
C(13)-H(13A)	0.9800
C(13)-H(13B)	0.9800
C(13)-H(13C)	0.9800
C(13)-C(3)	1.543(5)
Cl(4)-B(7)	1.766(4)
Cl(5)-B(6)	1.783(6)
Cl(6)-B(4)	1.781(4)
Cl(8)-B(5)	1.779(6)

Cl(7)-B(2)	1.767(6)
C(5)-C(7)	1.525(5)
C(5)-C(12)	1.527(5)
C(7)-H(7A)	0.9800
C(7)-H(7B)	0.9800
C(7)-H(7C)	0.9800
C(12)-H(12C)	0.9800
C(12)-H(12B)	0.9800
C(12)-H(12A)	0.9800
C(11)-H(11A)	0.9800
C(11)-H(11B)	0.9800
C(11)-H(11C)	0.9800
C(11)-C(9)	1.543(5)
C(10)-H(10A)	0.9800
C(10)-H(10B)	0.9800
C(10)-H(10C)	0.9800
C(10)-C(9)	1.543(5)
C(14)-H(14)	0.85(6)
C(14)-B(2)	1.705(7)
C(14)-B(3)	1.719(5)
C(14)-B(3)#2	1.719(5)
C(14)-B(7)#2	1.725(5)
C(14)-B(7)	1.725(5)
B(1)-B(1)#2	1.774(8)
B(1)-B(2)	1.776(6)
B(1)-B(4)	1.803(6)
B(1)-B(6)	1.798(7)
B(1)-B(7)	1.779(5)
B(2)-B(1)#2	1.776(6)
B(2)-B(7)#2	1.790(5)
B(2)-B(7)	1.790(5)
B(3)-B(3)#2	1.781(8)
B(3)-B(4)	1.778(5)

B(3)-B(5)	1.765(6)
B(3)-B(7)	1.793(6)
B(4)-B(5)	1.804(5)
B(4)-B(6)	1.792(5)
B(4)-B(7)	1.777(6)
B(5)-B(3)#2	1.765(6)
B(5)-B(4)#2	1.804(5)
B(5)-B(6)	1.797(8)
B(6)-B(1)#2	1.798(7)
B(6)-B(4)#2	1.792(5)
P(1)-Au(1)-P(1)#1	180.00(3)
H(1A)-C(1)-H(1B)	109.5
H(1A)-C(1)-H(1C)	109.5
H(1B)-C(1)-H(1C)	109.5
C(5)-C(1)-H(1A)	109.5
C(5)-C(1)-H(1B)	109.5
C(5)-C(1)-H(1C)	109.5
C(3)-P(1)-Au(1)	107.06(12)
C(3)-P(1)-C(5)	110.62(17)
C(5)-P(1)-Au(1)	108.98(12)
C(9)-P(1)-Au(1)	109.19(12)
C(9)-P(1)-C(3)	110.40(16)
C(9)-P(1)-C(5)	110.52(17)
H(2A)-C(2)-H(2B)	109.5
H(2A)-C(2)-H(2C)	109.5
H(2B)-C(2)-H(2C)	109.5
C(3)-C(2)-H(2A)	109.5
C(3)-C(2)-H(2B)	109.5
C(3)-C(2)-H(2C)	109.5
H(4A)-C(4)-H(4B)	109.5
H(4A)-C(4)-H(4C)	109.5
H(4B)-C(4)-H(4C)	109.5
C(3)-C(4)-H(4A)	109.5

C(3)-C(4)-H(4B)	109.5
C(3)-C(4)-H(4C)	109.5
H(6A)-C(6)-H(6B)	109.5
H(6A)-C(6)-H(6C)	109.5
H(6B)-C(6)-H(6C)	109.5
C(9)-C(6)-H(6A)	109.5
C(9)-C(6)-H(6B)	109.5
C(9)-C(6)-H(6C)	109.5
H(13A)-C(13)-H(13B)	109.5
H(13A)-C(13)-H(13C)	109.5
H(13B)-C(13)-H(13C)	109.5
C(3)-C(13)-H(13A)	109.5
C(3)-C(13)-H(13B)	109.5
C(3)-C(13)-H(13C)	109.5
C(2)-C(3)-P(1)	114.7(3)
C(2)-C(3)-C(13)	108.8(3)
C(4)-C(3)-P(1)	110.2(2)
C(4)-C(3)-C(2)	108.4(3)
C(4)-C(3)-C(13)	106.3(3)
C(13)-C(3)-P(1)	108.2(2)
C(1)-C(5)-P(1)	108.2(2)
C(7)-C(5)-C(1)	108.7(3)
C(7)-C(5)-P(1)	114.7(3)
C(7)-C(5)-C(12)	109.6(3)
C(12)-C(5)-C(1)	105.9(3)
C(12)-C(5)-P(1)	109.4(3)
C(5)-C(7)-H(7A)	109.5
C(5)-C(7)-H(7B)	109.5
C(5)-C(7)-H(7C)	109.5
H(7A)-C(7)-H(7B)	109.5
H(7A)-C(7)-H(7C)	109.5
H(7B)-C(7)-H(7C)	109.5
C(5)-C(12)-H(12C)	109.5

C(5)-C(12)-H(12B)	109.5
C(5)-C(12)-H(12A)	109.5
H(12C)-C(12)-H(12B)	109.5
H(12C)-C(12)-H(12A)	109.5
H(12B)-C(12)-H(12A)	109.5
H(11A)-C(11)-H(11B)	109.5
H(11A)-C(11)-H(11C)	109.5
H(11B)-C(11)-H(11C)	109.5
C(9)-C(11)-H(11A)	109.5
C(9)-C(11)-H(11B)	109.5
C(9)-C(11)-H(11C)	109.5
H(10A)-C(10)-H(10B)	109.5
H(10A)-C(10)-H(10C)	109.5
H(10B)-C(10)-H(10C)	109.5
C(9)-C(10)-H(10A)	109.5
C(9)-C(10)-H(10B)	109.5
C(9)-C(10)-H(10C)	109.5
B(2)-C(14)-H(14)	118(4)
B(2)-C(14)-B(3)	114.9(3)
B(2)-C(14)-B(3)#2	114.9(3)
B(2)-C(14)-B(7)	62.9(2)
B(2)-C(14)-B(7)#2	62.9(2)
B(3)#2-C(14)-H(14)	117(3)
B(3)-C(14)-H(14)	117(3)
B(3)#2-C(14)-B(3)	62.4(3)
B(3)#2-C(14)-B(7)	114.6(3)
B(3)-C(14)-B(7)	62.8(2)
B(3)#2-C(14)-B(7)#2	62.8(2)
B(3)-C(14)-B(7)#2	114.6(3)
B(7)#2-C(14)-H(14)	117.7(11)
B(7)-C(14)-H(14)	117.7(11)
B(7)-C(14)-B(7)#2	115.0(4)
C(6)-C(9)-P(1)	113.6(2)

C(11)-C(9)-P(1)	108.9(3)
C(11)-C(9)-C(6)	109.5(3)
C(10)-C(9)-P(1)	110.2(3)
C(10)-C(9)-C(6)	108.2(3)
C(10)-C(9)-C(11)	106.3(3)
Cl(2)-B(1)-B(4)	122.9(3)
Cl(2)-B(1)-B(6)	122.1(3)
Cl(2)-B(1)-B(7)	122.2(3)
B(1)#2-B(1)-Cl(2)	120.21(13)
B(1)#2-B(1)-B(2)	60.03(16)
B(1)#2-B(1)-B(4)	108.40(18)
B(1)#2-B(1)-B(6)	60.43(17)
B(1)#2-B(1)-B(7)	108.61(18)
B(2)-B(1)-Cl(2)	120.9(3)
B(2)-B(1)-B(4)	107.9(3)
B(2)-B(1)-B(6)	107.9(3)
B(2)-B(1)-B(7)	60.5(2)
B(6)-B(1)-B(4)	59.7(2)
B(7)-B(1)-B(4)	59.5(2)
B(7)-B(1)-B(6)	107.4(3)
Cl(7)-B(2)-B(1)	125.6(3)
Cl(7)-B(2)-B(1)#2	125.6(3)
Cl(7)-B(2)-B(7)	119.9(2)
Cl(7)-B(2)-B(7)#2	119.9(2)
C(14)-B(2)-Cl(7)	120.6(4)
C(14)-B(2)-B(1)	104.8(3)
C(14)-B(2)-B(1)#2	104.8(3)
C(14)-B(2)-B(7)#2	59.1(2)
C(14)-B(2)-B(7)	59.1(2)
B(1)#2-B(2)-B(1)	59.9(3)
B(1)#2-B(2)-B(7)#2	59.9(2)
B(1)-B(2)-B(7)#2	108.1(3)
B(1)-B(2)-B(7)	59.9(2)

B(1)#2-B(2)-B(7)	108.1(3)
B(7)-B(2)-B(7)#2	108.7(4)
Cl(3)-B(3)-B(3)#2	120.78(13)
Cl(3)-B(3)-B(4)	124.7(3)
Cl(3)-B(3)-B(5)	125.4(3)
Cl(3)-B(3)-B(7)	119.2(3)
C(14)-B(3)-Cl(3)	121.0(3)
C(14)-B(3)-B(3)#2	58.79(15)
C(14)-B(3)-B(4)	104.6(3)
C(14)-B(3)-B(5)	104.9(3)
C(14)-B(3)-B(7)	58.8(2)
B(3)#2-B(3)-B(7)	108.35(18)
B(4)-B(3)-B(3)#2	108.56(18)
B(4)-B(3)-B(7)	59.7(2)
B(5)-B(3)-B(3)#2	59.71(15)
B(5)-B(3)-B(4)	61.2(2)
B(5)-B(3)-B(7)	108.9(3)
Cl(6)-B(4)-B(1)	122.1(3)
Cl(6)-B(4)-B(5)	122.6(3)
Cl(6)-B(4)-B(6)	123.3(3)
B(1)-B(4)-B(5)	107.8(3)
B(3)-B(4)-Cl(6)	121.3(3)
B(3)-B(4)-B(1)	107.6(3)
B(3)-B(4)-B(5)	59.0(3)
B(3)-B(4)-B(6)	107.1(3)
B(6)-B(4)-B(1)	60.0(3)
B(6)-B(4)-B(5)	60.0(3)
B(7)-B(4)-Cl(6)	120.4(3)
B(7)-B(4)-B(1)	59.6(2)
B(7)-B(4)-B(3)	60.6(2)
B(7)-B(4)-B(5)	107.9(3)
B(7)-B(4)-B(6)	107.8(3)
Cl(8)-B(5)-B(4)#2	122.0(2)

Cl(8)-B(5)-B(4)	122.0(2)
Cl(8)-B(5)-B(6)	122.7(4)
B(3)-B(5)-Cl(8)	121.3(3)
B(3)#2-B(5)-Cl(8)	121.3(3)
B(3)-B(5)-B(3)#2	60.6(3)
B(3)-B(5)-B(4)	59.8(2)
B(3)#2-B(5)-B(4)	108.1(3)
B(3)-B(5)-B(4)#2	108.1(3)
B(3)#2-B(5)-B(4)#2	59.8(2)
B(3)-B(5)-B(6)	107.4(3)
B(3)#2-B(5)-B(6)	107.4(3)
B(4)#2-B(5)-B(4)	107.7(4)
B(6)-B(5)-B(4)	59.7(2)
B(6)-B(5)-B(4)#2	59.7(2)
Cl(5)-B(6)-B(1)	121.7(3)
Cl(5)-B(6)-B(1)#2	121.7(3)
Cl(5)-B(6)-B(4)#2	121.4(2)
Cl(5)-B(6)-B(4)	121.4(2)
Cl(5)-B(6)-B(5)	121.7(4)
B(1)-B(6)-B(1)#2	59.1(3)
B(4)#2-B(6)-B(1)#2	60.3(2)
B(4)-B(6)-B(1)#2	107.8(4)
B(4)-B(6)-B(1)	60.3(2)
B(4)#2-B(6)-B(1)	107.8(4)
B(4)#2-B(6)-B(4)	108.7(4)
B(4)#2-B(6)-B(5)	60.4(2)
B(4)-B(6)-B(5)	60.4(2)
B(5)-B(6)-B(1)#2	108.3(3)
B(5)-B(6)-B(1)	108.3(3)
Cl(4)-B(7)-B(1)	126.1(3)
Cl(4)-B(7)-B(2)	120.4(3)
Cl(4)-B(7)-B(3)	120.1(3)
Cl(4)-B(7)-B(4)	125.4(3)

C(14)-B(7)-Cl(4)	120.9(3)
C(14)-B(7)-B(1)	103.8(3)
C(14)-B(7)-B(2)	58.0(2)
C(14)-B(7)-B(3)	58.4(2)
C(14)-B(7)-B(4)	104.4(3)
B(1)-B(7)-B(2)	59.7(3)
B(1)-B(7)-B(3)	108.0(3)
B(2)-B(7)-B(3)	107.3(3)
B(4)-B(7)-B(1)	60.9(2)
B(4)-B(7)-B(2)	108.4(3)
B(4)-B(7)-B(3)	59.7(2)

Symmetry transformations used to generate equivalent atoms:

#1 $-x+1, -y+1, -z+1$ #2 $x, -y+3/2, z$

Table 4. Anisotropic displacement parameters ($\text{\AA}^2 \times 10^3$) for **2-31[CHB₁₁Cl₁₁]**. The anisotropic displacement factor exponent takes the form: $-2\pi^2[h^2 a^{*2}U^{11} + \dots + 2 h k a^* b^* U^{12}]$

	U ¹¹	U ²²	U ³³	U ²³	U ¹³	U ¹²
Au(1)	13(1)	20(1)	12(1)	-2(1)	2(1)	3(1)
C(1)	26(2)	32(2)	28(2)	1(2)	2(2)	-10(2)
P(1)	13(1)	18(1)	10(1)	0(1)	1(1)	2(1)
Cl(2)	16(1)	30(1)	38(1)	-5(1)	-1(1)	8(1)
C(2)	19(2)	43(2)	31(2)	2(2)	3(2)	13(2)
C(4)	18(2)	45(3)	31(2)	-4(2)	-4(2)	-2(2)
C(6)	28(2)	45(2)	13(2)	5(2)	5(2)	0(2)
Cl(3)	16(1)	37(1)	29(1)	6(1)	3(1)	-9(1)
C(13)	24(2)	48(2)	18(2)	2(2)	-5(2)	9(2)
C(3)	16(2)	30(2)	19(2)	1(2)	-1(2)	7(2)
Cl(4)	26(1)	24(1)	25(1)	-9(1)	-4(1)	-1(1)
Cl(5)	28(1)	33(1)	26(1)	0	-18(1)	0
Cl(6)	34(1)	25(1)	28(1)	11(1)	-8(1)	-2(1)
Cl(8)	39(1)	49(1)	10(1)	0	6(1)	0
Cl(7)	31(1)	42(1)	13(1)	0	10(1)	0
C(5)	24(2)	22(2)	17(2)	-2(2)	5(2)	-4(2)
C(7)	46(3)	24(2)	27(2)	-9(2)	8(2)	-7(2)
C(12)	34(2)	23(2)	30(2)	7(2)	6(2)	0(2)
C(11)	31(2)	25(2)	29(2)	7(2)	0(2)	-1(2)
C(10)	26(2)	43(2)	19(2)	9(2)	-5(2)	2(2)
C(14)	10(2)	24(3)	7(2)	0	-2(2)	0
C(9)	18(2)	28(2)	15(2)	3(2)	2(2)	1(2)
B(1)	12(2)	19(2)	17(2)	-1(2)	0(2)	0(1)
B(2)	13(3)	21(3)	11(3)	0	2(2)	0
B(3)	15(2)	23(2)	10(2)	2(2)	-2(2)	-1(2)
B(4)	19(2)	19(2)	13(2)	4(2)	-2(2)	2(2)
B(5)	20(3)	23(3)	9(3)	0	1(2)	0
B(6)	14(3)	19(3)	14(3)	0	-5(2)	0

B(7) 14(2) 20(2) 11(2) 0(2) 0(2) 2(2)

Table 5. Hydrogen coordinates ($\times 10^4$) and isotropic displacement parameters ($\text{\AA}^2 \times 10^{-3}$) for **2-31[CHB₁₁Cl₁₁]**.

	x	y	z	U(eq)
H(1A)	3922	4080	4225	43
H(1B)	3800	3490	3691	43
H(1C)	4014	4058	3119	43
H(2A)	7455	3514	4119	47
H(2B)	8441	3873	4277	47
H(2C)	7829	3943	3335	47
H(4A)	7393	5219	4669	46
H(4B)	7871	5001	3719	46
H(4C)	8397	4864	4687	46
H(6A)	7434	4680	2435	42
H(6B)	6760	4823	1555	42
H(6C)	6687	4215	2040	42
H(13A)	6677	4539	5788	45
H(13B)	7715	4219	5785	45
H(13C)	6724	3873	5583	45
H(7A)	5455	3619	2377	49
H(7B)	5274	3042	2933	49
H(7C)	6322	3349	2983	49
H(12C)	5211	3617	5206	44
H(12B)	6089	3277	4719	44
H(12A)	4982	3054	4626	44
H(11A)	5607	5632	3371	42
H(11B)	6183	5689	2408	42
H(11C)	6771	5529	3333	42
H(10A)	4449	4932	2699	44
H(10B)	4864	4417	2091	44
H(10C)	4998	5055	1738	44

H(14)

7890(40)

7500

2750(40)

25

Table 6. Torsion angles [°] for **2-31[CHB₁₁Cl₁₁]**.

Au(1)-P(1)-C(3)-C(2)	163.4(2)
Au(1)-P(1)-C(3)-C(4)	-74.0(3)
Au(1)-P(1)-C(3)-C(13)	41.8(3)
Au(1)-P(1)-C(5)-C(1)	43.6(3)
Au(1)-P(1)-C(5)-C(7)	165.1(3)
Au(1)-P(1)-C(5)-C(12)	-71.3(3)
Au(1)-P(1)-C(9)-C(6)	163.2(2)
Au(1)-P(1)-C(9)-C(11)	40.9(3)
Au(1)-P(1)-C(9)-C(10)	-75.3(3)
Cl(2)-B(1)-B(2)-Cl(7)	5.0(4)
Cl(2)-B(1)-B(2)-C(14)	151.9(2)
Cl(2)-B(1)-B(2)-B(1)#2	-109.4(2)
Cl(2)-B(1)-B(2)-B(7)#2	-146.3(3)
Cl(2)-B(1)-B(2)-B(7)	112.0(3)
Cl(2)-B(1)-B(4)-Cl(6)	-2.0(4)
Cl(2)-B(1)-B(4)-B(3)	-149.3(3)
Cl(2)-B(1)-B(4)-B(5)	148.5(3)
Cl(2)-B(1)-B(4)-B(6)	110.8(3)
Cl(2)-B(1)-B(4)-B(7)	-110.9(3)
Cl(2)-B(1)-B(6)-Cl(5)	-1.4(4)
Cl(2)-B(1)-B(6)-B(1)#2	109.1(2)
Cl(2)-B(1)-B(6)-B(4)	-112.1(3)
Cl(2)-B(1)-B(6)-B(4)#2	146.0(3)
Cl(2)-B(1)-B(6)-B(5)	-150.1(2)
Cl(2)-B(1)-B(7)-Cl(4)	-2.6(5)
Cl(2)-B(1)-B(7)-C(14)	-149.0(3)
Cl(2)-B(1)-B(7)-B(2)	-110.0(3)
Cl(2)-B(1)-B(7)-B(3)	150.1(3)
Cl(2)-B(1)-B(7)-B(4)	112.0(3)
Cl(3)-B(3)-B(4)-Cl(6)	-3.2(5)
Cl(3)-B(3)-B(4)-B(1)	144.4(3)

Cl(3)-B(3)-B(4)-B(5)	-115.0(3)
Cl(3)-B(3)-B(4)-B(6)	-152.4(3)
Cl(3)-B(3)-B(4)-B(7)	106.5(3)
Cl(3)-B(3)-B(5)-Cl(8)	2.6(4)
Cl(3)-B(3)-B(5)-B(3)#2	-108.2(2)
Cl(3)-B(3)-B(5)-B(4)#2	-145.8(3)
Cl(3)-B(3)-B(5)-B(4)	113.9(3)
Cl(3)-B(3)-B(5)-B(6)	151.2(3)
Cl(3)-B(3)-B(7)-Cl(4)	0.6(4)
Cl(3)-B(3)-B(7)-C(14)	110.5(3)
Cl(3)-B(3)-B(7)-B(1)	-154.0(3)
Cl(3)-B(3)-B(7)-B(2)	143.1(3)
Cl(3)-B(3)-B(7)-B(4)	-115.3(3)
C(3)-P(1)-C(5)-C(1)	161.0(2)
C(3)-P(1)-C(5)-C(7)	-77.5(3)
C(3)-P(1)-C(5)-C(12)	46.1(3)
C(3)-P(1)-C(9)-C(6)	45.7(3)
C(3)-P(1)-C(9)-C(11)	-76.6(3)
C(3)-P(1)-C(9)-C(10)	167.2(3)
Cl(6)-B(4)-B(5)-Cl(8)	0.7(6)
Cl(6)-B(4)-B(5)-B(3)#2	-147.5(3)
Cl(6)-B(4)-B(5)-B(3)	-109.5(3)
Cl(6)-B(4)-B(5)-B(4)#2	149.4(2)
Cl(6)-B(4)-B(5)-B(6)	112.5(4)
Cl(6)-B(4)-B(6)-Cl(5)	-0.4(5)
Cl(6)-B(4)-B(6)-B(1)	110.8(3)
Cl(6)-B(4)-B(6)-B(1)#2	147.2(3)
Cl(6)-B(4)-B(6)-B(4)#2	-148.9(2)
Cl(6)-B(4)-B(6)-B(5)	-111.4(3)
Cl(6)-B(4)-B(7)-Cl(4)	3.8(4)
Cl(6)-B(4)-B(7)-C(14)	150.2(3)
Cl(6)-B(4)-B(7)-B(1)	-111.7(3)
Cl(6)-B(4)-B(7)-B(2)	-149.2(3)

Cl(6)-B(4)-B(7)-B(3)	111.1(3)
Cl(8)-B(5)-B(6)-Cl(5)	0.000(1)
Cl(8)-B(5)-B(6)-B(1)	148.7(2)
Cl(8)-B(5)-B(6)-B(1)#2	-148.7(2)
Cl(8)-B(5)-B(6)-B(4)	110.7(2)
Cl(8)-B(5)-B(6)-B(4)#2	-110.7(2)
Cl(7)-B(2)-B(7)-Cl(4)	-0.3(5)
Cl(7)-B(2)-B(7)-C(14)	-109.9(4)
Cl(7)-B(2)-B(7)-B(1)	116.3(4)
Cl(7)-B(2)-B(7)-B(3)	-142.6(3)
Cl(7)-B(2)-B(7)-B(4)	154.3(3)
C(5)-P(1)-C(3)-C(2)	44.8(3)
C(5)-P(1)-C(3)-C(4)	167.4(3)
C(5)-P(1)-C(3)-C(13)	-76.8(3)
C(5)-P(1)-C(9)-C(6)	-77.0(3)
C(5)-P(1)-C(9)-C(11)	160.7(2)
C(5)-P(1)-C(9)-C(10)	44.5(3)
C(14)-B(2)-B(7)-Cl(4)	109.6(3)
C(14)-B(2)-B(7)-B(1)	-133.8(3)
C(14)-B(2)-B(7)-B(3)	-32.8(3)
C(14)-B(2)-B(7)-B(4)	-95.8(3)
C(14)-B(3)-B(4)-Cl(6)	-149.0(2)
C(14)-B(3)-B(4)-B(1)	-1.4(3)
C(14)-B(3)-B(4)-B(5)	99.2(3)
C(14)-B(3)-B(4)-B(6)	61.8(4)
C(14)-B(3)-B(4)-B(7)	-39.4(2)
C(14)-B(3)-B(5)-Cl(8)	149.9(2)
C(14)-B(3)-B(5)-B(3)#2	39.1(3)
C(14)-B(3)-B(5)-B(4)	-98.8(3)
C(14)-B(3)-B(5)-B(4)#2	1.5(4)
C(14)-B(3)-B(5)-B(6)	-61.5(3)
C(14)-B(3)-B(7)-Cl(4)	-109.9(3)
C(14)-B(3)-B(7)-B(1)	95.5(3)

C(14)-B(3)-B(7)-B(2)	32.6(3)
C(14)-B(3)-B(7)-B(4)	134.2(3)
C(9)-P(1)-C(3)-C(2)	-77.9(3)
C(9)-P(1)-C(3)-C(4)	44.7(3)
C(9)-P(1)-C(3)-C(13)	160.5(2)
C(9)-P(1)-C(5)-C(1)	-76.4(3)
C(9)-P(1)-C(5)-C(7)	45.1(3)
C(9)-P(1)-C(5)-C(12)	168.7(3)
B(1)#2-B(1)-B(2)-Cl(7)	114.4(3)
B(1)#2-B(1)-B(2)-C(14)	-98.8(2)
B(1)#2-B(1)-B(2)-B(7)	-138.6(2)
B(1)#2-B(1)-B(2)-B(7)#2	-36.98(18)
B(1)#2-B(1)-B(4)-Cl(6)	-149.9(2)
B(1)#2-B(1)-B(4)-B(3)	62.8(3)
B(1)#2-B(1)-B(4)-B(5)	0.5(3)
B(1)#2-B(1)-B(4)-B(6)	-37.2(2)
B(1)#2-B(1)-B(4)-B(7)	101.20(19)
B(1)#2-B(1)-B(6)-Cl(5)	-110.5(3)
B(1)#2-B(1)-B(6)-B(4)#2	36.96(18)
B(1)#2-B(1)-B(6)-B(4)	138.8(2)
B(1)#2-B(1)-B(6)-B(5)	100.8(2)
B(1)#2-B(1)-B(7)-Cl(4)	144.6(2)
B(1)#2-B(1)-B(7)-C(14)	-1.9(3)
B(1)#2-B(1)-B(7)-B(2)	37.2(2)
B(1)#2-B(1)-B(7)-B(3)	-62.7(2)
B(1)#2-B(1)-B(7)-B(4)	-100.85(19)
B(1)#2-B(2)-B(7)-Cl(4)	-153.6(3)
B(1)-B(2)-B(7)-Cl(4)	-116.6(3)
B(1)#2-B(2)-B(7)-C(14)	96.8(3)
B(1)-B(2)-B(7)-C(14)	133.8(3)
B(1)#2-B(2)-B(7)-B(1)	-37.0(3)
B(1)-B(2)-B(7)-B(3)	101.1(3)
B(1)#2-B(2)-B(7)-B(3)	64.1(4)

B(1)-B(2)-B(7)-B(4)	38.0(3)
B(1)#2-B(2)-B(7)-B(4)	1.0(4)
B(1)-B(4)-B(5)-Cl(8)	-149.5(3)
B(1)-B(4)-B(5)-B(3)#2	62.3(4)
B(1)-B(4)-B(5)-B(3)	100.3(3)
B(1)-B(4)-B(5)-B(4)#2	-0.8(5)
B(1)-B(4)-B(5)-B(6)	-37.7(3)
B(1)-B(4)-B(6)-Cl(5)	-111.2(4)
B(1)-B(4)-B(6)-B(1)#2	36.5(3)
B(1)-B(4)-B(6)-B(4)#2	100.3(4)
B(1)-B(4)-B(6)-B(5)	137.8(3)
B(1)-B(4)-B(7)-Cl(4)	115.5(3)
B(1)-B(4)-B(7)-C(14)	-98.0(3)
B(1)-B(4)-B(7)-B(2)	-37.4(3)
B(1)-B(4)-B(7)-B(3)	-137.2(3)
B(2)-C(14)-B(3)-Cl(3)	-144.1(3)
B(2)-C(14)-B(3)-B(3)#2	106.3(3)
B(2)-C(14)-B(3)-B(4)	3.3(3)
B(2)-C(14)-B(3)-B(5)	66.8(3)
B(2)-C(14)-B(3)-B(7)	-36.5(2)
B(2)-C(14)-B(7)-Cl(4)	-108.7(3)
B(2)-C(14)-B(7)-B(1)	39.9(3)
B(2)-C(14)-B(7)-B(3)	142.7(3)
B(2)-C(14)-B(7)-B(4)	102.9(3)
B(2)-B(1)-B(4)-Cl(6)	146.6(3)
B(2)-B(1)-B(4)-B(3)	-0.7(3)
B(2)-B(1)-B(4)-B(5)	-63.0(4)
B(2)-B(1)-B(4)-B(6)	-100.7(3)
B(2)-B(1)-B(4)-B(7)	37.7(2)
B(2)-B(1)-B(6)-Cl(5)	-148.6(2)
B(2)-B(1)-B(6)-B(1)#2	-38.1(3)
B(2)-B(1)-B(6)-B(4)#2	-1.2(4)
B(2)-B(1)-B(6)-B(4)	100.7(3)

B(2)-B(1)-B(6)-B(5)	62.7(3)
B(2)-B(1)-B(7)-Cl(4)	107.4(3)
B(2)-B(1)-B(7)-C(14)	-39.0(3)
B(2)-B(1)-B(7)-B(3)	-99.9(3)
B(2)-B(1)-B(7)-B(4)	-138.0(3)
B(3)#2-C(14)-B(2)-Cl(7)	-145.2(2)
B(3)-C(14)-B(2)-Cl(7)	145.2(2)
B(3)-C(14)-B(2)-B(1)	-3.7(3)
B(3)#2-C(14)-B(2)-B(1)	66.0(2)
B(3)#2-C(14)-B(2)-B(1)#2	3.7(3)
B(3)-C(14)-B(2)-B(1)#2	-66.0(2)
B(3)#2-C(14)-B(2)-B(7)#2	-36.5(3)
B(3)-C(14)-B(2)-B(7)#2	-106.2(3)
B(3)-C(14)-B(2)-B(7)	36.5(3)
B(3)#2-C(14)-B(2)-B(7)	106.2(3)
B(3)#2-C(14)-B(3)-Cl(3)	109.5(2)
B(3)#2-C(14)-B(3)-B(4)	-103.1(2)
B(3)#2-C(14)-B(3)-B(5)	-39.5(3)
B(3)#2-C(14)-B(3)-B(7)	-142.9(2)
B(3)-C(14)-B(7)-Cl(4)	108.6(3)
B(3)#2-C(14)-B(7)-Cl(4)	144.6(3)
B(3)#2-C(14)-B(7)-B(1)	-66.8(4)
B(3)-C(14)-B(7)-B(1)	-102.8(3)
B(3)-C(14)-B(7)-B(2)	-142.7(3)
B(3)#2-C(14)-B(7)-B(2)	-106.6(4)
B(3)#2-C(14)-B(7)-B(3)	36.0(3)
B(3)-C(14)-B(7)-B(4)	-39.8(3)
B(3)#2-C(14)-B(7)-B(4)	-3.7(4)
B(3)#2-B(3)-B(4)-Cl(6)	149.5(2)
B(3)#2-B(3)-B(4)-B(1)	-62.9(3)
B(3)#2-B(3)-B(4)-B(5)	37.7(2)
B(3)#2-B(3)-B(4)-B(6)	0.3(3)
B(3)#2-B(3)-B(4)-B(7)	-100.86(19)

B(3)#2-B(3)-B(5)-Cl(8)	110.8(3)
B(3)#2-B(3)-B(5)-B(4)	-137.9(2)
B(3)#2-B(3)-B(5)-B(4)#2	-37.57(19)
B(3)#2-B(3)-B(5)-B(6)	-100.6(2)
B(3)#2-B(3)-B(7)-Cl(4)	-142.82(19)
B(3)#2-B(3)-B(7)-C(14)	-32.9(2)
B(3)#2-B(3)-B(7)-B(1)	62.6(2)
B(3)#2-B(3)-B(7)-B(2)	-0.4(3)
B(3)#2-B(3)-B(7)-B(4)	101.21(19)
B(3)-B(4)-B(5)-Cl(8)	110.2(4)
B(3)-B(4)-B(5)-B(3)#2	-37.9(3)
B(3)-B(4)-B(5)-B(4)#2	-101.1(4)
B(3)-B(4)-B(5)-B(6)	-138.0(3)
B(3)-B(4)-B(6)-Cl(5)	148.0(3)
B(3)-B(4)-B(6)-B(1)	-100.8(3)
B(3)-B(4)-B(6)-B(1)#2	-64.4(4)
B(3)-B(4)-B(6)-B(4)#2	-0.5(5)
B(3)-B(4)-B(6)-B(5)	36.9(3)
B(3)-B(4)-B(7)-Cl(4)	-107.3(3)
B(3)-B(4)-B(7)-C(14)	39.1(3)
B(3)-B(4)-B(7)-B(1)	137.2(3)
B(3)-B(4)-B(7)-B(2)	99.7(3)
B(3)-B(5)-B(6)-Cl(5)	-148.08(18)
B(3)#2-B(5)-B(6)-Cl(5)	148.08(18)
B(3)#2-B(5)-B(6)-B(1)	-63.2(2)
B(3)-B(5)-B(6)-B(1)	0.6(3)
B(3)-B(5)-B(6)-B(1)#2	63.2(2)
B(3)#2-B(5)-B(6)-B(1)#2	-0.6(3)
B(3)-B(5)-B(6)-B(4)	-37.3(2)
B(3)#2-B(5)-B(6)-B(4)	-101.2(3)
B(3)#2-B(5)-B(6)-B(4)#2	37.3(2)
B(3)-B(5)-B(6)-B(4)#2	101.2(3)
B(4)-B(1)-B(2)-Cl(7)	-144.3(3)

B(4)-B(1)-B(2)-C(14)	2.6(3)
B(4)-B(1)-B(2)-B(1)#2	101.3(2)
B(4)-B(1)-B(2)-B(7)#2	64.4(3)
B(4)-B(1)-B(2)-B(7)	-37.2(3)
B(4)-B(1)-B(6)-Cl(5)	110.7(3)
B(4)-B(1)-B(6)-B(1)#2	-138.8(2)
B(4)-B(1)-B(6)-B(4)#2	-101.8(4)
B(4)-B(1)-B(6)-B(5)	-38.0(2)
B(4)-B(1)-B(7)-Cl(4)	-114.6(3)
B(4)-B(1)-B(7)-C(14)	99.0(3)
B(4)-B(1)-B(7)-B(2)	138.0(3)
B(4)-B(1)-B(7)-B(3)	38.1(3)
B(4)-B(3)-B(5)-Cl(8)	-111.3(3)
B(4)-B(3)-B(5)-B(3)#2	137.9(2)
B(4)-B(3)-B(5)-B(4)#2	100.3(4)
B(4)-B(3)-B(5)-B(6)	37.3(2)
B(4)-B(3)-B(7)-Cl(4)	116.0(3)
B(4)-B(3)-B(7)-C(14)	-134.2(3)
B(4)-B(3)-B(7)-B(1)	-38.7(3)
B(4)-B(3)-B(7)-B(2)	-101.6(3)
B(4)-B(5)-B(6)-Cl(5)	-110.7(2)
B(4)#2-B(5)-B(6)-Cl(5)	110.7(2)
B(4)#2-B(5)-B(6)-B(1)	-100.6(3)
B(4)-B(5)-B(6)-B(1)#2	100.6(3)
B(4)#2-B(5)-B(6)-B(1)#2	-37.9(2)
B(4)-B(5)-B(6)-B(1)	37.9(2)
B(4)#2-B(5)-B(6)-B(4)	-138.5(4)
B(4)-B(5)-B(6)-B(4)#2	138.5(4)
B(5)-B(3)-B(4)-Cl(6)	111.8(3)
B(5)-B(3)-B(4)-B(1)	-100.5(3)
B(5)-B(3)-B(4)-B(6)	-37.3(3)
B(5)-B(3)-B(4)-B(7)	-138.5(3)
B(5)-B(3)-B(7)-Cl(4)	153.8(2)

B(5)-B(3)-B(7)-C(14)	-96.3(3)
B(5)-B(3)-B(7)-B(1)	-0.8(3)
B(5)-B(3)-B(7)-B(2)	-63.7(3)
B(5)-B(3)-B(7)-B(4)	37.8(2)
B(5)-B(4)-B(6)-Cl(5)	111.1(4)
B(5)-B(4)-B(6)-B(1)	-137.8(3)
B(5)-B(4)-B(6)-B(1)#2	-101.3(3)
B(5)-B(4)-B(6)-B(4)#2	-37.5(4)
B(5)-B(4)-B(7)-Cl(4)	-143.9(3)
B(5)-B(4)-B(7)-C(14)	2.5(4)
B(5)-B(4)-B(7)-B(1)	100.5(3)
B(5)-B(4)-B(7)-B(2)	63.1(4)
B(5)-B(4)-B(7)-B(3)	-36.6(3)
B(6)-B(1)-B(2)-Cl(7)	152.7(2)
B(6)-B(1)-B(2)-C(14)	-60.5(3)
B(6)-B(1)-B(2)-B(1)#2	38.3(3)
B(6)-B(1)-B(2)-B(7)#2	1.3(4)
B(6)-B(1)-B(2)-B(7)	-100.3(3)
B(6)-B(1)-B(4)-Cl(6)	-112.7(3)
B(6)-B(1)-B(4)-B(3)	99.9(3)
B(6)-B(1)-B(4)-B(5)	37.7(3)
B(6)-B(1)-B(4)-B(7)	138.4(3)
B(6)-B(1)-B(7)-Cl(4)	-151.5(3)
B(6)-B(1)-B(7)-C(14)	62.0(3)
B(6)-B(1)-B(7)-B(2)	101.1(3)
B(6)-B(1)-B(7)-B(3)	1.2(3)
B(6)-B(1)-B(7)-B(4)	-37.0(2)
B(6)-B(4)-B(5)-Cl(8)	-111.8(5)
B(6)-B(4)-B(5)-B(3)#2	100.0(4)
B(6)-B(4)-B(5)-B(3)	138.0(3)
B(6)-B(4)-B(5)-B(4)#2	36.9(4)
B(6)-B(4)-B(7)-Cl(4)	152.7(3)
B(6)-B(4)-B(7)-C(14)	-60.8(3)

B(6)-B(4)-B(7)-B(1)	37.2(3)
B(6)-B(4)-B(7)-B(2)	-0.3(4)
B(6)-B(4)-B(7)-B(3)	-100.0(3)
B(7)-C(14)-B(2)-Cl(7)	108.69(19)
B(7)#2-C(14)-B(2)-Cl(7)	-108.69(19)
B(7)#2-C(14)-B(2)-B(1)#2	40.2(2)
B(7)-C(14)-B(2)-B(1)	-40.2(2)
B(7)-C(14)-B(2)-B(1)#2	-102.4(3)
B(7)#2-C(14)-B(2)-B(1)	102.4(3)
B(7)-C(14)-B(2)-B(7)#2	-142.6(4)
B(7)#2-C(14)-B(2)-B(7)	142.6(4)
B(7)#2-C(14)-B(3)-Cl(3)	145.7(3)
B(7)-C(14)-B(3)-Cl(3)	-107.6(3)
B(7)#2-C(14)-B(3)-B(3)#2	36.18(19)
B(7)-C(14)-B(3)-B(3)#2	142.9(2)
B(7)#2-C(14)-B(3)-B(4)	-66.9(3)
B(7)-C(14)-B(3)-B(4)	39.8(2)
B(7)#2-C(14)-B(3)-B(5)	-3.4(4)
B(7)-C(14)-B(3)-B(5)	103.3(3)
B(7)#2-C(14)-B(3)-B(7)	-106.7(4)
B(7)#2-C(14)-B(7)-Cl(4)	-145.4(2)
B(7)#2-C(14)-B(7)-B(1)	3.3(5)
B(7)#2-C(14)-B(7)-B(2)	-36.6(4)
B(7)#2-C(14)-B(7)-B(3)	106.1(4)
B(7)#2-C(14)-B(7)-B(4)	66.3(4)
B(7)-B(1)-B(2)-Cl(7)	-107.0(3)
B(7)-B(1)-B(2)-C(14)	39.8(2)
B(7)-B(1)-B(2)-B(1)#2	138.6(2)
B(7)-B(1)-B(2)-B(7)#2	101.6(4)
B(7)-B(1)-B(4)-Cl(6)	108.9(3)
B(7)-B(1)-B(4)-B(3)	-38.4(3)
B(7)-B(1)-B(4)-B(5)	-100.7(3)
B(7)-B(1)-B(4)-B(6)	-138.4(3)

B(7)-B(1)-B(6)-Cl(5)	147.6(3)
B(7)-B(1)-B(6)-B(1)#2	-101.9(2)
B(7)-B(1)-B(6)-B(4)	36.9(3)
B(7)-B(1)-B(6)-B(4)#2	-65.0(3)
B(7)-B(1)-B(6)-B(5)	-1.1(3)
B(7)#2-B(2)-B(7)-Cl(4)	142.9(2)
B(7)#2-B(2)-B(7)-C(14)	33.4(3)
B(7)#2-B(2)-B(7)-B(1)	-100.5(4)
B(7)#2-B(2)-B(7)-B(3)	0.6(5)
B(7)#2-B(2)-B(7)-B(4)	-62.5(4)
B(7)-B(3)-B(4)-Cl(6)	-109.7(3)
B(7)-B(3)-B(4)-B(1)	38.0(3)
B(7)-B(3)-B(4)-B(5)	138.5(3)
B(7)-B(3)-B(4)-B(6)	101.2(3)
B(7)-B(3)-B(5)-Cl(8)	-148.5(3)
B(7)-B(3)-B(5)-B(3)#2	100.7(2)
B(7)-B(3)-B(5)-B(4)#2	63.1(4)
B(7)-B(3)-B(5)-B(4)	-37.2(3)
B(7)-B(3)-B(5)-B(6)	0.1(3)
B(7)-B(4)-B(5)-Cl(8)	147.5(3)
B(7)-B(4)-B(5)-B(3)#2	-0.6(4)
B(7)-B(4)-B(5)-B(3)	37.3(3)
B(7)-B(4)-B(5)-B(4)#2	-63.8(4)
B(7)-B(4)-B(5)-B(6)	-100.6(3)
B(7)-B(4)-B(6)-Cl(5)	-148.2(3)
B(7)-B(4)-B(6)-B(1)	-37.0(3)
B(7)-B(4)-B(6)-B(1)#2	-0.6(4)
B(7)-B(4)-B(6)-B(4)#2	63.3(4)
B(7)-B(4)-B(6)-B(5)	100.8(3)

Symmetry transformations used to generate equivalent atoms:

#1 -x+1,-y+1,-z+1 #2 x,-y+3/2,z